ACS SYMPOSIUM SERIES 1067

Environmental Chemistry of Explosives and Propellant Compounds in Soils and Marine Systems: Distributed Source Characterization and Remedial Technologies

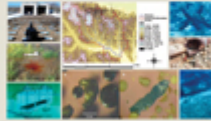

EDITED BY
Mark A. Chappell, Cynthia L. Price,
and Robert D. George

Environmental Chemistry of Explosives and Propellant Compounds in Soils and Marine Systems: Distributed Source Characterization and Remedial Technologies

ACS SYMPOSIUM SERIES **1069**

Environmental Chemistry of Explosives and Propellant Compounds in Soils and Marine Systems: Distributed Source Characterization and Remedial Technologies

Mark A. Chappell, Editor
US Army Corps of Engineers, Environmental Research and Development Center

Cynthia L. Price, Editor
US Army Corps of Engineers, Environmental Research and Development Center

Robert D. George, Editor
Space and Naval Warfare Systems Center Pacific

Sponsored by the
ACS Division of Environmental Chemistry

American Chemical Society, Washington, DC

Distributed in print by Oxford University Press, Inc.

Library of Congress Cataloging-in-Publication Data

Environmental chemistry of explosives and propellant compounds in soils and marine systems : distributed source characterization and remedial technologies / Mark A. Chappell, Cynthia L. Price, Robert D. George, editor[s] ; sponsored by the ACS Division of Environmental Chemistry.
p. cm. -- (ACS symposium series ; 1069)
Includes bibliographical references and index.
ISBN 978-0-8412-2632-6 (alk. paper)
1. Organic compounds--Environmental aspects. 2. Propellants. 3. Soil pollution. 4. Marine sediments. 5. Soil absorption and adsorption. I. Chappell, Mark A. (Mark Allen) II. Price, Cynthia L. III. George, Robert D. IV. American Chemical Society. Division of Environmental Chemistry.
TD879.O73E575 2011
628.4'2--dc23
2011033530

The paper used in this publication meets the minimum requirements of American National Standard for Information Sciences—Permanence of Paper for Printed Library Materials, ANSI Z39.48n1984.

Distributed in print by Oxford University Press, Inc.

PRINTED IN THE UNITED STATES OF AMERICA

Foreword

The ACS Symposium Series was first published in 1974 to provide a mechanism for publishing symposia quickly in book form. The purpose of the series is to publish timely, comprehensive books developed from the ACS sponsored symposia based on current scientific research. Occasionally, books are developed from symposia sponsored by other organizations when the topic is of keen interest to the chemistry audience.

Before agreeing to publish a book, the proposed table of contents is reviewed for appropriate and comprehensive coverage and for interest to the audience. Some papers may be excluded to better focus the book; others may be added to provide comprehensiveness. When appropriate, overview or introductory chapters are added. Drafts of chapters are peer-reviewed prior to final acceptance or rejection, and manuscripts are prepared in camera-ready format.

As a rule, only original research papers and original review papers are included in the volumes. Verbatim reproductions of previous published papers are not accepted.

ACS Books Department

Preface

Active military operations throughout the world, coupled with continuing war-fighter training, depends heavily on the use and distribution of particular explosive and propellant compounds into the environment. The United States Department of Defense (DoD) and the different armed services contained within its structure have established specific guidelines aimed at promoting compliance with national and international environmental regulatory requirements in all of its operations. In addition, the DoD is actively incorporating policies that include considerations of environmental risk as part of overall decisions on operational sustainability. Yet, in spite of these policies, the DoD faces considerable challenges in meeting these goals, particularly in view of potential post-conflict decontamination and clean-up from ongoing active military operations, as well as decommissioned training and manufacturing sites where legacy explosives and propellant contaminations in soil and groundwater are being actively investigated. The scope of the problem now, and in the foreseeable future, emphasizes the need for reliable, scientifically verifiable models for predicting the environmental fate of munition compounds.

The most commonly employed energetic formulations typically contain combinations of three main explosive compounds, TNT, RDX, and HMX. Munitions that detonate properly (termed high-order detonation) leave virtually no residue of these toxic munition constituents (MC) in the environment. However, munitions do, at times, malfunction, producing either low-order detonations or "duds". Low-order detonations, representing either incomplete or sub-optimal detonation, typically result in the deposition of explosive residue released from the broken shell casing on soil. In the case of duds, munition constituents remain contained unless the shell casing is breached either through physical impact or by corrosion. On the other hand, propellant compounds may be found widely distributed wherever munitions are used, both from traces due to weapons firing (e.g., mortars, etc.) to trails of propellant compounds that have been reported along the entire pathway to the target (e.g., rocket propelled weapons). Common propellant compounds include perchlorate, nitroglycerin, and 2,4-DNT. Attempts to model the behavior of these compounds are limited by the poor understanding of the fate of these contaminants under relevant field conditions, both in terms of their release and persistence once deposited into the environment.

The purpose of this book is to present the latest knowledge regarding the environmental chemistry and fate of explosive and propellant compounds. This book is largely based on a symposium organized for the 22-25 March 2009 American Chemical Society meetings entitled, "Environmental Distribution, Degradation, and Mobility of Explosive and Propellant Compounds", held in

Salt Lake City, UT. The purpose of this symposium was to bring together an international body of government and academic experts to share information regarding the environmental fate of these contaminants, with an emphasis on assessing and/or supporting the environmental sustainability of military training activities. In particular, presentations focused on the use of this information to inform assessment and management actions. For example, it was anticipated that information would be presented toward improved capabilities for post-conflict cleanup and assessment of MC. Given the growing body of work in this area, additional chapters from particular experts and scientists regarding important topics not covered in the original 2009 symposium were included in this book. In short, the expanded content of this book is designed to address three main topics with respect to explosive and propellant compounds: (i) new and summary chemistry information regarding the sorption, degradation (abiotic and biotic), mobility, and overall environmental fate of these compounds in soil; (ii) techniques for statistically reliable detection and field-deployable remote sensing of munition constituents, and (iii) technologies for targeted remediation of MC-contaminated soils and sediments.

We envision the book to be of primary interest to researchers, project officers, range managers, and contractors to the federal defense agencies who are tasked with improving the sustainability of military training and activities by mitigating the off-site transport of these contaminants from training ranges. Also, this book will be of interest to federal defense agency practioners tasked with directed cleanup of contaminated sites, formerly used defense sites (FUDS), and base-realignment (BRAC) activities. Finally, this information will be important to training range managers tasked with designing ranges that are safe and effective for warfighter readiness, while at the same time, limiting the environmental risk from off-site migration.

In terms of future needs, the contents of this book are designed to be of significant interest to decision makers in expected post-conflict cleanup activities. With rapid mobility and deployment of troops and equipment, there is often inadequate time to conduct baseline land surveys of occupied areas, which include, among other details, an environmental assessment. Thus, the need for specific tools that allow for retroactive modeling of contaminants in order to reconstruct a reasonable baseline survey for determining pre-conflict contaminant levels. The principles included in this book, and in particular, one chapter directly addresses such concerns.

While the contents of this book focus mainly on terrestrial systems, current knowledge and considerations with respect to the fate of explosives and propellant compounds under coastal and marine environments are also discussed. Providing a consolidated source of information on this topic is very important as governments around the world are under increasing public pressure to ascertain, and if necessary, attenuate the environmental impacts to the ocean systems due to wide-scale dumping of unexploded ordnance (UXO) following World Wars I and II, and other 20th century conflicts. Currently, there is limited information on the fate of UXO in marine environments – a subject being actively pursued by a number of international government and research agencies.

Acknowledgments

We express appreciation for the support of Drs. John Cullinane and Elizabeth Ferguson, past and present Technical Directors of the U.S. Army Environmental Quality and Installations research program within the Environmental Laboratory, U.S. Army Engineer Research & Development Center (ERDC), Vicksburg, MS, for providing funding for a number of the research efforts described in this book. The editors also acknowledge the efforts of numerous reviewers for their expert comments and suggestions, particularly Mr. Christian McGrath (ERDC, Vicksburg, MS), who provided thorough and helpful reviews of several chapters. The editors also acknowledge Dr. Souhail Al-Abed, U.S. Environmental Protection Agency-ORD, Cincinnati, OH, who served as the 2009 Chair of the Environmental Division within the American Chemical Society, for his support in organizing this symposium, and the subsequent efforts leading up to publication of this book. We also express our gratitude to Ms. Beth Porter for formatting much of the text in this book in preparation for publication.

Mark A. Chappell

U.S. Army Engineer Research & Development Center
3909 Halls Ferry Rd.
Vicksburg, MS 39180
mark.a.chappell@usace.army.mil (e-mail)

Cynthia L. Price

U.S. Army Engineer Research & Development Center
3909 Halls Ferry Rd.
Vicksburg, MS 39180
cynthia.l.price@usace.army.mil (e-mail)

Robert D. George

Environmental Sciences - Code 71752
SPAWARSYSCEN PACIFIC
53475 Strothe Road
San Diego, CA 92152-6325
robert.george@navy.mil (e-mail)

Chapter 1

Solid-Phase Considerations for the Environmental Fate of TNT and RDX in Soil

Mark A. Chappell*

Soil and Sediment GeochemistryTeam Lead, Environmental Laboratory, U.S. Army Engineer Research and Development Center, (ERDC), 3909 Halls Ferry Road, Vicksburg, MS
***mark.a.chappell@usace.army.mil**

This chapter provides a basic review of the environmental fate of the two most common munition constituents used by the DoD, TNT and RDX. Here is reviewed the basic scientific literature of nitroaromatic and tirazine sorption, with specific data that is available for TNT and RDX. In general, the behavior of these munition constituents (MC) in soils and sediments is generally well described by the available information for nitroaromatic and triazine compounds, with notable differences attributed to the ready reduction of MC nitro groups to amine derivatives. In general, the environmental fate of TNT is much better described in the scientific literature, emphasizing a remaining need for more research elucidating the behavior of RDX in soil and sediments. Here, we summarize trends in reported partitioning coefficients describing sorption of MC with soil/sediment cation exchange capacity (CEC), extractable Fe, and exchangeable Ca. New concepts in terms of fugacity-based quantity-intensity theory are introduced for more detailed descriptions of sorption behavior. Also, we expand on classical considerations of soil biological degradation potentials to include agricultural concepts of soil tilth for predicting the long-term fate of MC in soil.

This review focuses on the sorption processes of two important MCs in soils and sediments, 1,3,5-trinitrotoluene (TNT) and hexahydro-1,3,5-trinitro-1,3,5-triazine (RDX, Fig.

1). One of the more difficult aspects of understanding the environmental fate of these contaminants lies in their relatively weak interactions with soil. As noncharged organics with limited water solubility, these compounds do not interact with strongly charged soil surfaces like exchangeable cation species, but are limited to interactions with micro-scale hydrophobic or noncharged mineral domains, and the flexible, often surfactant-like humic polymers. The principles and challenges of understanding the sorption and transport of MC and nitrobenzene and triazine compounds in general are discussed here.

Introduction

Equilibrim Models Applied for MC Sorption

The distribution of a solute between the soil solid phase and liquid phase is commonly described using three types of sorption models: partitioning, Freundlich, and Langmuir sorption. Each of these models is represented by a particular sorption coefficient, a purely empirical representation of the solute equilibrium state. The simplest and most common type of sorption coefficient is the distribution coefficient (K_D), which implies description of solute partitioning as:

$$K_D = C_S / C_e \quad [1]$$

where C_S = the concentration of solute sorbed on the solid phase and C_e = the concentration of solute in the equilibrium solution. Here K_D represents the slope of data plotted as C_e vs. C_s. The sorption coefficient represents the relative solute affinity term – the higher the coefficient, the higher the selectivity. Yet, the parameter is limited in that direct measure of selectivity is only impolied and not quantified by this parameter.As a purely empirical parameter, K_D values are easy to generate, yet it is important to realize that the values possess no relevant thermodynamic information.

MC sorption is commonly represented by the Freundlich sorption model, which is:

$$C_s = K_F C_e^n \quad [2]$$

where K_F = the Freundlich sorption coefficient and n represents the unitless coefficient of linearity. An n value < 1 implies the solute undergoes L-type sorption; n = 1 implies C-type, linear sorption, and K_F essentially represents K_D (analogous to an octanol-water partitioning coefficient, K_{ow}); n > 1 (concave upward) implies S-type or cooperative sorption of solutes (*1*).

The Langmuir sorption model is less commonly applied to MCs. The equation for the Langmuir-type sorption is:

$$C_s = \frac{K_L C_s^{\max} C_e}{1 + K_L C_e} \quad [3]$$

where K_L = Langmuir sorption coefficient and C_s^{max} = maximum number of adsorption sites available to MC. The Langmuir model describes sorption in terms of the relative saturation of the sorbent, a behavior typically exhibited by high-loading solutes. For example, Eriksson and Skyllberg (*2*) demonstrated Langmuir (L-type) sorption of TNT on dissolved and particulate soil organic matter. Interestingly, Eriksson et al. (*3*) derived a combined Langmuir and partioning sorption model in order to simultaneously account for particulate matter through the simple summation of Equations 1 and 3.

A Solid-Phase Buffering Approach

Chappell et al. (*4*) recently proposed a new scheme for quantifying MC sorption by considering soil/sediment potential buffering capacity (PBC) for the solute utilizing a modified Quantity-Intensity approach. The potential buffering capacity describes the ability of sediment to replace a quantity of dissolved MC. Here, MC is assumed to have been instantaneously removed from solution (such as by microbial degradation). MC is replenished into solution through desorption of sorbed solute in an attempt to restore system equilibrium. The classical definition of potential buffering capacity (PBC) is reserved for ion constituents where the chemical potential of the system is described in terms of single ion activities or ion activity ratios (*5*, *6*). Since MC is noncharged, we modified the classical PBC, describing solute chemical potential in terms of fugacity. A solute's fugacity describes the "escaping tendency" to move from a defined phase (*7*).

While the concept of fugacity is traditionally reserved for characterizing the non-ideality of gases, Mackay and other authors utilized the fugacity concept to describe the distribution of solutes among different phases (*8–10*). In this paper, we employ this convention as follows: For a solute in water,

$$C_w = f_w Z_w \quad [4]$$

where f_w = solute fugacity (in units of pressure, Pa), C_w = solute concentration (mol m^{-3}), and Z_w = fugacity capacity, or quantity representing the capacity of the phase for fugacity (mol m^{-3} Pa^{-1}).

For a given fugacity (f_w), a lower Z_w requires a higher C_w to enable the solute to "escape" from its phase, such as by volatilization or solid-phase partitioning. For dissolved solutes, f is also related to the solute's Henry constant as $f_w = HC_w$, where $Z_w = 1/H$ (*9*).

For a solid, fugacity is also defined as $C_s = f_s Z_s$. We can calculate solute distribution between two phases (K_{sw}) by assuming at equilibrium, the solute fugacities are equal ($f_w = f_s$). Substituting, $C_w/Z_w = C_s/Z_s$ and rearranging, we show

$$Z_s/Z_w = C_s/C_w = K_{sw} \quad [5]$$

where K_{sw} is unitless.

Solute fugacity can also be calculated from a typical sorption isotherm, which for many nonpolar and weakly polar organic compounds, can be described by a linear sorption as

$$X_s \text{ (mol kg}^{-1}) = K_D C_w \quad [6]$$

where K_D = partitioning coefficient between solid and liquid phases. To match units between X_s and C_w, we multiply X_s by sediment bulk density (ρ_b) to give X_s' in units of mol m^{-3} (*10*). Thus,

$$X_s' = K_D' C_w \quad [7]$$

where $K_D' = K_{sw}$ and is unitless. Therefore, $K_D' = Z_s/Z_w = Z_s H$. If we apply the Q/I concept, then the instantaneous loss of solute in solution results in a change in sorbed munition constituents as

$$\Delta X_S^{'} = \Delta X_{S-final}^{'} \pm \Delta X_{S-initial}^{'} \quad [8]$$

where the slope of a plot of C_w vs. $\Delta X_s'$ is

$$\partial(\Delta X_s')/\partial C_w = Z_s H \pm X_s'. \quad [9]$$

As $C_w \rightarrow 0$, then $\pm X_s'$ = the y-intercept, or $X_s'^{\circ}$ (Fig. 1) while as $\Delta X_S' \rightarrow 0$, the x-intercept represents $C_{W\,MC}^{\circ}$, and $Z_s H$ is considered equivalent to PBC.

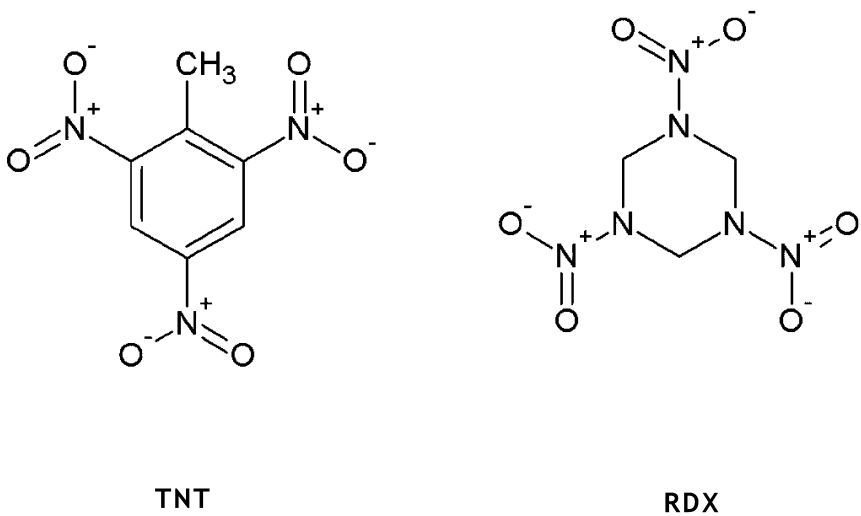

Figure 1. Molecular structure of TNT and RDX

The modified Q/I theory is depicted graphically in Fig. 2. Potential buffering capacity is represented as the derivative (and therefore more dynamic) of the distribution coefficient (K_D, which is equal to K_D'/ρ_s). This is commonly used to

describe the partitioning of MC in sediments. The Q/I plot shows that an increase in solution concentration of MC beyond the C_{w-MC}^0 results in MC sorption on the surface (thus, the + change in sorbed MC). A reduction in solution MC below C_{w-MC}^0 results in release of sorbed MC (thus, the - change in sorbed MC). This tendency for MC release is influenced by the Z_s. Sediments exhibiting a high Z_s possess a relatively abundant pool of sorbed MC that may be released when dissolved MC concentration decreases. Thus, the $X'_{s-MC}{}^0$ represents what we would term the lower boundary of the environmentally relevant concentration, as it represents the extent of labile MC that is readily released. The upper boundary of environmentally relevant MC concentrations is represented by $X'_{s-MC}s^0$, representing MC tightly bound to the surface, and generally unavailable for release. Thus, the Q/I approach provides information with respect to Z_S and the dynamic nature in which the sediment responds to temperature.

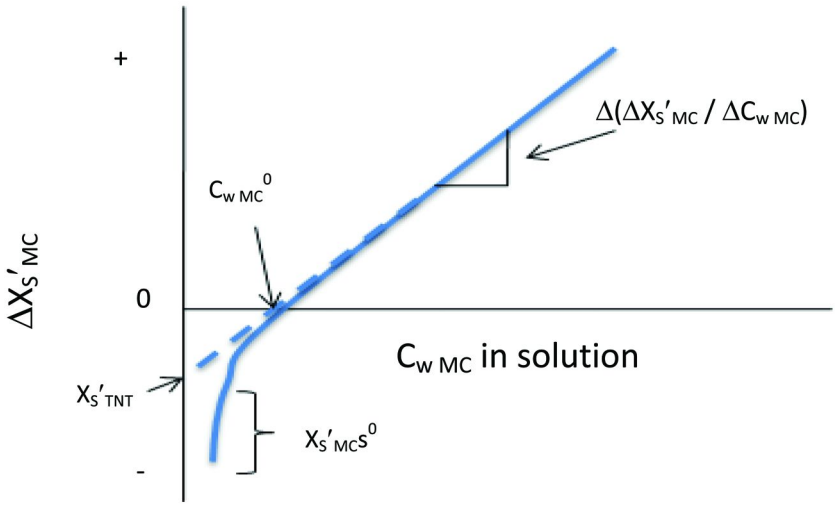

Figure 2. Fugacity-modified quantity-intensity (Q/I) plot showing the theoretical solid-liquid interactivity controlling changes in dissolved MC concentration. Parameters in the plot are defined as the quantity (Q) factor, $\Delta X'_{s-MC}$ = change in sorbed MC concentration; the intensity (I) factor, C_{w-MC} = the concentration of MC in solution at equilibrium; $C_{w\,MC}°$ = x-intercept of the Q-I plot; $X_s'{}_{MC}°$ = labile (or releasable) MC, which is the y-intercept of the Q/I plot; $X'_{s-MC}\,s°$ = irreversibly sorbed MC (causing the nonlinear deviation in the plot). Z_s is determined by the slope of the Q/I plot.

Note that the convenience of this theory lies in the fact that the sorption model included in Eq. 6 can be substituted for a more appropriate model, such as the Freundlich or Langmuir equation, if needed, and the appropriate equation derived for describing PBC.

General Observations Regarding MC Sorption Behavior

TNT and RDX are generally observed to exhibit relatively weak sorption behavior to soils and sediments, yielding low K_D values. Typically, K_D values for TNT are on the order of 10^1 L kg^{-1} while RDX K_D values are on the order of 10^{-1} L kg^{-1} in soils. However, much information has been shown demonstrating that these munitions do offer high sorption potentials on particular soil fractions. For example, soil organic carbon or humic materials have long been known to exhibit high K_D values for sorption (*11–16*), a behavior long attributed to hydrophobic partitioning. MC also have been shown to exhibit high affinities for clay minerals, particular 2:1-type swelling clays (*17–27*). Yet, the natural combination or "formulation" of organic matter and clay appears to serve in often blocking MC access to potential sorption sites (*14*, *28*). MCs appear to exhibit negligible sorption on quartz, silts, and most types of iron oxides (*22*, *29*).

Aside from hydrophobic partitioning on organic matter, much work has been done elucidating the sorption complex of MC with clays. Haderlein et al (*18*) proposed that the presence of NO_2 electron-withdrawing substituents left the pi system of the aromatic ring electron deficient. Thus, sorption of TNT and other nitroaromatic compounds (NACs) on clays was proposed to occur via the formation of electron donor-acceptor (EDA) complexes between the solute and the clay surface. However, quantum mechanical calculations presented by Boyd et al. (*30*) predicted that the electron environment of the aromatic ring remained virtually unchanged by the presence of electron donating/withdrawing substituents. Similarly, Pelmenschikov and Leszczynski (*31*) modeled high-afinity TNT interaction on a model silozane surface as attributed to both columbic and van der Waals forces between the surface and planar structure of the solute, and not electron withdrawing/donating (i.e., EDA complexation) mechanisms. Using oriented clay films and computational modeling, evidence was presented that nitroaromatic and triazine solutes are oriented during sorption generally parallel to the basal plane in smectitic clays (*32*, *33*). Data has shown that NACs and triazine compounds compete with hydration water at the clay surface as evidenced by collapse in basal spacings (*34*, *35*). In this position, these compounds interact with the hydration sphere of the exchangeable cations, which in theory, should have a lower dielectric constant than bulk water, and thus, a more favorable environment for the solute. Thus, cations with lower hydration energy should have a smaller hydration sphere containing lower dielectric water.

Using Sorption Coefficients To Predict MC Interaction in Soil/Sediment

The purpose of applying these sorption models is to provide some measure of predicting MC behavior in the environment. The most common approach involves establishing trends in sorption coefficients for MC as a function of specific soil properties. For example, K_D values obtained from the scientific literature describing TNT sorption on soils, sediments, and aquifer materials were plotted against cation exchange capacity (CEC), total organic carbon (TOC), and percent clay using data summarized by Brannon and Pennington ((*36*); Tables 4

and 11; Fig. 3). Figure 3 shows a linear trend in the K_D values for TNT (linear trend is also visually apparent for RDX – data not shown), while R^2 values for the regressions were far too poor to be used as predictors, indicating that the regression predicts the trend in K_D values no better than the simple mean K_D value of 2.9 L kg^{-1}. Thus, K_D values describing TNT sorption cannot be readily correlated to any single soil property. A similar trend was observed for RDX (data not shown), giving a mean K_D value of 0.99 L kg^{-1}. It is of particular note that TOC, which is considered a controlling factor in MC sorption (*11*, *12*, *15*, *16*) cannot be used as a sole predictor for the sorption K_D value.

Employing a multi-linear regression analysis from the data contained in Brannon and Pennington (*36*), and additional information from the original papers cited in that publication (including pH, EC, and extractable elemental concentrations), Chappell et al. (*37*) demonstrated that TNT sorption K_D can be predicted based on a linear combination of different soil and sediment properties (Fig. 4, Table 1). This analysis showed that the sorption K_D for TNT was directly related to soil CEC and extractable soil Fe content, while inversely related to exchangeable soil Ca content. The direct relationship to extractable Fe suggests that TNT experienced microbial degradation over the reported equilibrium period (whether the authors were aware of it or not), as release of Fe(II) from Fe(III) reduction (*38–40*). Pennington and Patrick (*41*) reported statistically significant correlations (i.e., R values) among K_D for TNT with oxalate-extractable Fe, soil CEC, and percent clay. Note that in this analysis, K_D values were again not correlated with TOC, in spite of its importance in MC sorption. Tucker et al. (*42*) showed a similarly poor predictable relationship between organic carbon and sorption K_D. Pennington and Patrick's (*41*) data also showed a nonsignificant coefficient of correlation ($R^2 = 0.16$) between the K_D TNT and TOC.

The relationships between CEC and extractable (ie., exchangeable) Ca, on the other hand, are linked to particulars associated with soil/sediment properties. These are discussed in detail below.

Effect of Soil/Sediment Properties on the MC Sorption and Mobility

If we assume sorption of the neutral, non-charged MC species, then relationship between K_D and CEC is opposite of the expected trend. Laird et al (*21*) showed an indirect relationship between the sorption K_F of the similarly weakly polar molecule, atrazine, and clay surface charge density. Sheng et al. (*43*) showed that reduction for the clay charge greatly enhanced the sorption of the nitroaromatic dionseb on a smectite clay. In both cases, reduction of charge equated to a reduction in CEC. Lee et al. (*44*) showed an inverse relationship between the sorption of aromatic compounds from aqueous systems and the layer charge of organically modified smectites (saturated with tetramethyl ammonium ions. Yet, a simple analysis of the data from Weissmahr et al, (*25*) suggests a linear relationship between sorbed 1,3,5-trinitrobenzene (TNB), the final d-spacing following sorption ($R^2 = 0.7389$), and the total surface area ($R^2 = 0.7663$) of the clay rather than its surface charge density.

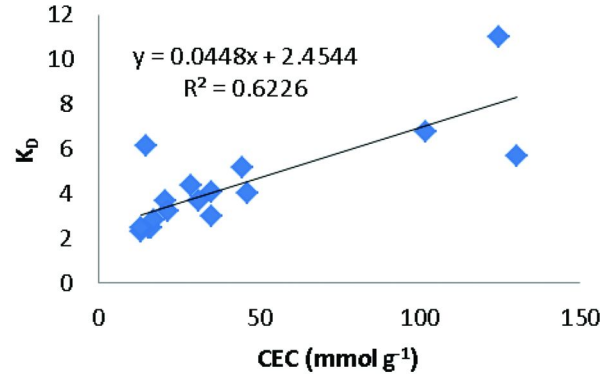

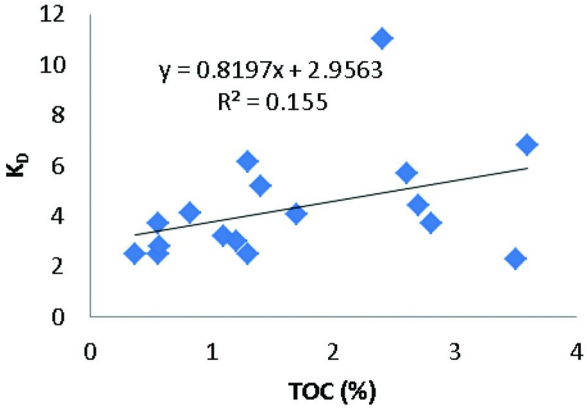

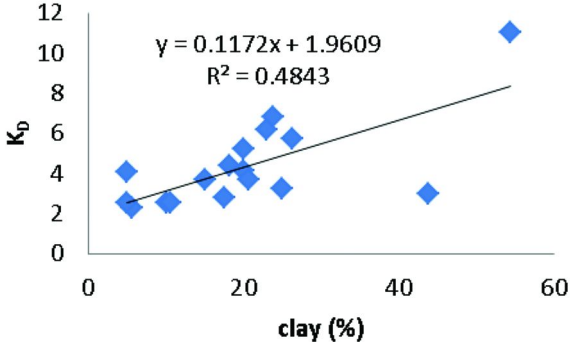

Figure 3. Plots comparing K_D values describing the sorption of TNT with respect to CEC, TOC and clay contents fitted to a linear model. Similar plots for RDX sorption (not shown) also possessed very poor fits (R^2 for $K_{D\ RDX}$ was 0.332 and 0.327 when regressed against TOC and CEC, respectively), and poor predictability. Data obtained from Brannon and Pennington (2002).

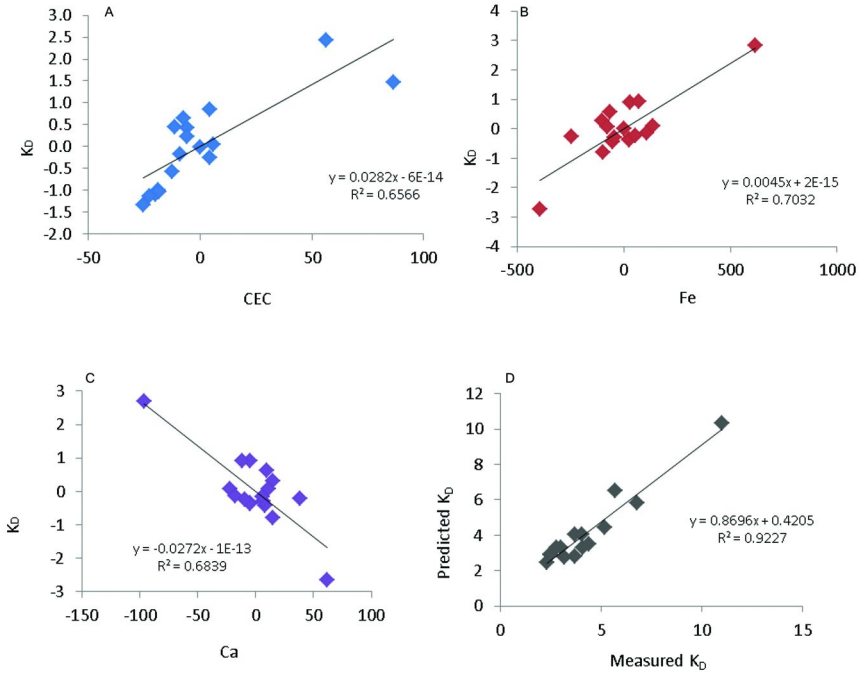

Figure 4. (A-C) Multi-linear regression of soil partitioning coefficients (K_D) for TNT, collected and published by Brannon and Pennington (2002) and (D) resultant prediction of K_D values based on the multivariate analysis.

The results of the multi-linear regression, predicting K_D as directly related to the CEC, is consistent with the general message contained in the scientific literature for TNT sorption. For example, Price et al. (*45*) showed a similarly linear trend in TNT sorption in low carbon and clay materials. Here, the authors assumed that this trend indicated that TNT was readily adsorbed at "easily accessible surfaces on clay minerals" - its quantity indicated by the magnitude of the CEC. This relationships points to the tendency for TNT to transform to reduced aminonitrotoluene derivatives (*46–49*), including 2-amino-4,6-dinitrotoluene (2ADNT), 4-amino-2,6-dinitrotoluene (4ADNT), 2,4-diaminonitrotoluene (2,4DANT), and 2,6-diaminonitrotoluene (2,6DANT). As positively charged ammoniuimmolecules, these are expected to exhibit strong adsorption potentials for soils (particularly 2:1 clays) as well as long-term stability in soils, similar to ammoniated amino acids, such as lysine (*50*, *51*).

Table 1. Results from multi-linear regression of K_D values for TNT from Brannon and Pennington (2002).

R^2	R	Adj. R^2	S.E. of Estimate
0.927	0.963	0.910	0.658

ANOVA

Source	*Sum Sq.*	*D.F.*	*Mean Sq.*	*F*	*Prob.*
Regression	71.423	3	23.808	54.940	0.000
Residual	5.633	13	0.433		
Total	77.057	16			

Regression Coefficients

Source	*Coefficient*	*Std Error*	*Std Beta*	*-95% C.I.*	*+95% C.I.*	*t*	*Prob.*
Intercept	1.842	0.255		1.292	2.392	7.23	6.608E-06
CEC	0.028	0.006	0.497	0.016	0.040	4.96	2.492E-04
Fe	0.004	0.001	8.447	0.003	0.006	5.55	9.380E-05
Ca	-0.027	0.005	-8.125	-0.038	-0.016	-5.3	1.431E-04

It is commonly observed that organic matter enhances the CEC of a soil. In part, the linear relationship between soil/sediment TOC and sorption K_D was poor. It is reasonable to hypothesize that the poor linear correlation between K_D values and TOC arises from the fact that humic materials are highly variable both in composition and properties in soils. As a case in point: Laird et al. (*52*, *53*) demonstrated significant chemical and physical differences among the humic fractions of different soil clay fractions isolated by physical particle size separations. Humics associated with the coarse clay fraction (0.2—2 μm particle size) were composed of discrete particles, high in organic carbon but with low C:N ratios, relatively resistant to microbial mineralization, and estimated as several centuries old (via $_{13}C/_{12}C$ ratios). On the other hand, humics separated with the fine clay fraction (< 0.02 μm) were film like in appearance, highly labile, and dated as modern carbon. Solid-state NMR evidence concluded that the humics in the coarse clay fraction were dominated by pyrogenically formed, aromatic, condensed carbon phases (such as black carbon or chars) while the fine clay fraction represented more biopolymeric rich organic material. It is interesting to note that the total CEC values associated with these fractions were 65 and 102 cmol(+) kg^{-1} for the coarse and fine clay fractions, respectively. Thus, shifts in sorption K_D values vary with the proportion of biogenic to pyrogenic carbon in soil. This conclusion is consistent with the results of Eriksson et al. (*3*), who demonstrated the difference in sorption of TNT on organic matter extracted from an organic-rich Gleysol. Utilizing the combined sorption relationship, the authors demonstrated that the dissolved organic matter (DOM) fraction exhibited

more Langmuir-type sorption while the particulate organic matter (POM) fraction had two to three times greater aromatic content, and exhibited hydrophobic partitioning behavior that was approximately one order of magnitude greater than the DOM. The greater partitioning behavior was attributed to the fact that the POM possessed 2-3 times greater density of hydrophobic moieties. Laird et al (*22*) showed that K_D value for atrazine was one order of magnitude larger on the coarse clay fraction than the fine clay fraction in a smectitic soil.

Sample Handling: Cation Saturation and Sample Handling

Cation Saturation

The scientific literature shows that sorption K_D values are affected by the type of cation dominating the exchange phase of soils and clays. Singh et al. (*54*) tested the effect of cation saturation on the sorption of TNT on a sandy loam and sitly clay soil. Their results showed that K-saturation of the exchange phase enhanced the modeled Freundlich sorption coefficient (Sandy loam: K_F = 22.1, n = 1.01; silty clay: K_F = 43, n = 0.52) while NH_4, Ca, and Al-saturating the soils generally decreased sorption (sandy loam: K_F ranging from 1.86-3.64, n ranging from 0.68-0.94; silty clay: K_F ranging from 9.67-23.97, n ranging from 0.67-0.81) below the control soil (sandy loam: K_F = 5.82, n = 0.56; silty clay: K_F = 31.44, n = 0.35). Price et al. (*45*) showed that sorption of TNT was increased when a low-carbon aquifer material was K-saturated relative to Ca-saturation. Fractional loading of the exchange phase with K^+ appeared to nominally affect total sorption. The enhanced sorption was only realized at saturation. Chappell et al. (*55*) reported enhanced sorption of atrazine (a chlorinated triazine) in batch experiments when the background electrolyte was switched from 10 mM $CaCl_2$ to 20 mM KCl (charge equivalent background electrolyte concentrations). Charles et al. (*28*) reported the contribution of K-saturating clays from smectitic soils to NAC sorption was far greater than the contribution of soil organic matter.

Numerous studies have shown the effect of cation saturation on both MC, as well as a wide array of NAC and triazine compounds. Haderlein and Schwarzerbach (*56*) showed the effect of the hydration energy of the saturation cation on the NAC sorption. The authors demonstrated large increases in K_D values describing NAC sorption with saturation of cations with decreasing energy of hydration. Most these studies in the published literature have focused on the effects of the saturation cation type on the sorption of NACs and triazine compounds on smectite clays. Such an approach has been particularly fruitful for the information gained describing the chemical properties of the smectite interlayer in a collapsed (e.g., K-saturated) vs. an expanded (e.g., Ca-saturated) interlayer state. This information has provided new insights into possible remediation strategeies ((*26*); (*57*); (*58*) and references therein), such as the targeted delivery of long-chained alkyl-ammonium cations polymers to the smectite interlayer for enhanced capture of NACs.

In terms of clays, there is an apparent paradox between clay colloid size and interlayer spacings in these clays. Pils et al. (*59*) showed that smectite clays loaded with exchange phase concentration ratios ($CR_X = X^+/(Ca^{2+})^{1/2}$, where X

= Na, K, and NH_4 ions) ranging from 0 (i.e., Ca-saturated) to 9, dramatically increased the Stokes settling times of the clay particles, presumably due the decrease in colloid size (inhibited aggregation). Yet, the size of the basal spacing was largely a function of the clay's ion selectivity. At low ionic strength (I = 0.004 M), clay particles generally remained as quasicrystals in suspension, containing 3 - 4 hydration layers in the interlayer. At higher ionic strength (I = 0.04 M), basal spacings decreased at much lower CR_X values than the low ionic strength system due to the increase in the monovalent cation selectivity. Li et al. (*34*) similarly showed that inspite of being K-saturated, the smectites exhibited expanded interlayer spacings at low electrolyte concentration (0.01 M KCl). With increasing KCl electrolyte background, clay basal spacings decreased along with the colloid size, as inferred from optical density measurements. Li et al. (*60*) also showed that total sorption of 1,3-dinitrobenzene (DNB) was increased by approximately 15,000 mg kg^{-1}. This implies an effect of particle surface area on sorption where the larger surface area is exhibited by the smaller colloids. Thus, the inverse trend between Ca concentration and K_D values can be attributed to both (1) specific effects associated with MC complexes (and potentially co-sorption) (*61*) with exchangeable cations and (2) colloidal size and resultant surface area for sorption.

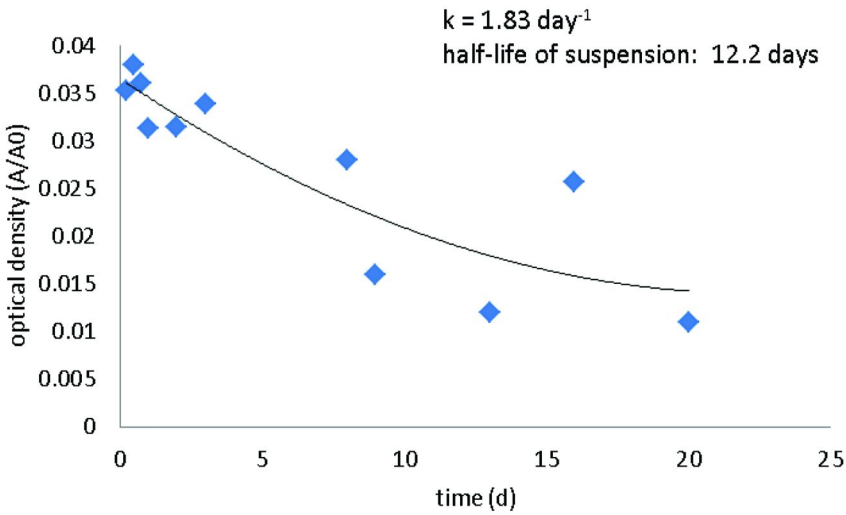

Figure 5. Kinetic data showing the particle aggregation of a silver colloidal dispersion in 1 mM $NaNO_3$ under constant agitation. Data was fit to a second-order decay model.

In terms of the colloidal phase, it is important to realize that the state of the dispersion can change significantly over the equilibrium time of a batch study. If so, then a change in the total surface area for interaction with the solid also changes over the equilibrium time. In simple terms, this occurs by way of colloidal flocculation processes, which can be represented as (*62*):

$$\frac{dN}{dt} = \frac{k N_o^2}{W} \qquad [10]$$

where, N represents the number density of colloids or particles (m^{-3}), W = stability ratio of the particles, a result of the electrostatic repulsive interactions and attractive van der Waals forces, N_o = the initial number density of colloids at time = 0, and k = the second order rate constant for flocculation. This equation emphasizes the point that the state of a suspension is not constant but in flux. For example, Fig. 5 shows a colloidal silver suspension that even under constant agitation (by shaking) shows evidence of settling behavior. An important aspect of Eq. 10 is the relationship between settling rate and suspension concentration or, in other terms, the solid-to-solution ratio. Eq. 10 predicts that the rate of settling is directly proportional to the square of particle density.

Sample Handling

While exchange-phase homogenization (i.e., Ca saturation) can have irreversible effects on the sorption behavior of soil clays (*63*), there is some information to show that preparation of soil and clay samples can also impact measured K_D values. It is a common laboratory practice to air-dry soil samples as part of processing to reduce sample heterogeneity. While soils regularly cycle through seasonal periods of wetting and drying, rarely are soils ever desiccated in nature to the extent they are in the lab during pre-processing. Chappell et al. (*55*) showed that smectitic soils that were previously air-dried exhibited higher partitioning coefficients for atrazine than soils that were kept at field moisture. Experiments showed that this effect was in part related to the slow kinetics of soil rehydration. Also, studies with a K-saturated bentonite clay showed that the interlayer was never able to recover its hydration status following air-drying. It was hypothesized that as a one to two-layer hydrate, the interlayer exhibited a more favorable dielectric for sorbing atrazine than the three-layer hydrate measured in the non-dried K-saturated clay. Currently, no information exists showing how air-drying affects sorption behavior of munition constituents, but it is reasonable to expect that sorption to follow similar trends.

Solid to Solution Ratios

The importance of the solid-to-solution (s/s) ratio for determining sorption K_D values can be demonstrated from a statistical point of view. Using propagation-of-error theory, McDonald and Evangelou (*64*) showed relationships between the standard deviation of K_D and the s/s of the system (Fig. 6). The minima of the curve represents the s/s where the K_D has the lowest standard deviation (since some

parameters were arbitrarily assigned equal to 1, comparisons are only relative, not absolute, called relative standard deviation or RSD). Note that the curve minima shifts with the value of K_D, making the optimal s/s approximately $K_D/1.2$ or 55 % sorption. Thus, K_D values may possess a large potential uncertainty depending on the s/s used in the experiments. Data points on Fig. 6 represent s/s ratios commonly used in sorption experiments for nitroaromatic compounds, assuming K_D values were 1, 10, or 100 L kg^{-1}.

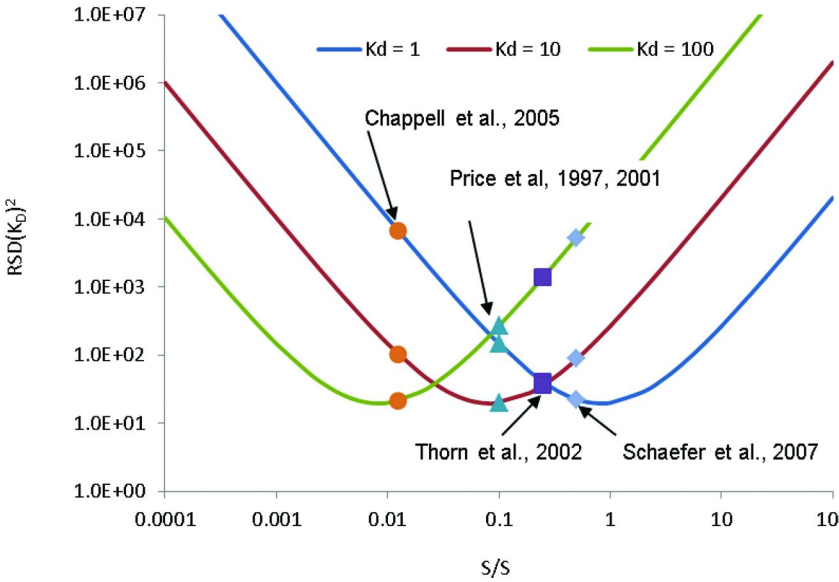

Figure 6. The effect of solid-to-solution ratio (g/mL) on the relative standard deviation (RSD) for three different values of K_D. Plotted points represent common solid-to-solution ratios used in batch experiments: (○) 0.0125, (△) 0.1, (□) 0.25, and (◇) 0.5. (Adapted from McDonald and Evangelou, 1997). (see color insert)

MC Hysteresis, Humification, and Mobility in Soils

MC K_D values are influenced by the magnitude of sorption hysteresis. Sorption reactions are primarily studied in the form of the "forward" sorption reaction but, as in all reactions, sorption processes also possess a backward desorption reaction that is rarely considered in most models. Neglecting the desorption reaction is justified if the sorption reaction is fully reversible. Yet, nearly all solutes exhibit some degree of irreversibility in sorption.

Sorption hysteresis can be exhibited in two forms: (i) sorbates that transform on the surface will exhibit hysteresis due to the reduction in concentration and (ii) sorbates that are stable on the surface will exhibit hysteresis due to soil pore deformation. In the latter case, thermal motion of incoming solute molecules create new internal surface area in soil solids by expanding the pore openings (*65*).

Thus, in this "conditioned" state, the soil may actually exhibit a higher preference for the solute, resulting in a higher apparent K_D. For example, long-term, batch studies determined that sediments exhibiting high potential for TNT sorption also reduced its extractability under abiotic conditions (*4*). This conditioning may occur due to the introduction of an individual solute (such as trichloromethane) or by sample preparation effects such as cation saturation and air-drying.

Sorption hysteresis for TNT appears to primarily occur due to rapid transformations discussed earlier. These degradation products exhibit considerable stability in soil and sediment with little evidence of microbial mineralization to CO_2 (*66–68*). Here, TNT is considered to undergo humification (*69*, *70*). Similar to TNT, RDX typically degrades in soil via a step-wise reduction of NO_2 substitutents, forming a variety of nitroso metabolites, including hexahydro-1-nitroso-3,5-dinitro-1,3,5-triazine (MNX), hexahydro-1,3-dinitroso-5-nitro-1,3,5-triazine (DNX), and hexahydro-1,3,5-trinitroso-1,3,5-triazine (TNX). RDX typically degrades very slowly in aerobic soil (*71*, *72*) which contributes to its fate as a groundwater contaminant. Hysteresis of RDX sorption-desorption is usually less than that of TNT, but is significant (*73*, *74*).

Because of their high nitrogen content, TNT and RDX may potentially serve as good nitrogen sources (electron acceptors) for microorganisms provided there are soil microorganisms possessing the appropriate enzyme "sets" to degrade the molecules and that the proper external conditions can be met. Pure culture studies have demonstrated the direct use of these munitions by microorganisms as a nitrogen source (*38*, *75*, *76*), however the direct viability of this behavior continues to be investigated. Yet, this may serve as a useful model for considering the environmental fate of organic compounds in soils in terms classical consideration of soil fertility. Current knowledge with respect to the environmental fate of organics employs evidence of solute partitioning and soil properties (e.g., soil organic carbon content), considering soil components in terms of categories, etc. A more holistic approach employed successfully in agriculture links the chemical, physical, and nutritional state of the soil, called soil "tilth", to biological activity in a soil, i.e., plant growth to reach maximum yields, where in this case, the "yield" is represented by the maximum activity of MC degrading microorganisms in soil. The term soil tilth goes beyond simple consideration of C:N ratios in soil, but refers to the total nutritional balance and external conditions (e.g., water, temperature) within a soil that allows for soil biology to thrive.

Theoretically, the basis for predicting munition persistence or residence time can be presented based on definitions of soil tilth. The concept of soil tilth couples theories for soil contaminant transport with the factors controlling contaminant degradation. In the most general sense, "retention" of contaminants from the solution phase is described through the use of a partitioning or distribution coefficient (K_D).The relationship of K_D to the transport of a solute is (*77*)

$$\frac{\partial c}{\partial t} + \frac{\rho_b}{\theta}\frac{\partial (K_D c)}{\partial t} = D_e \frac{\partial^2 c}{\partial z^2} - v\frac{\partial c}{\partial z} \qquad [11]$$

where c = solute concentration, ρ_b = soil bulk density, θ = soil volumetric content, D_e = diffusion-dispersion coefficient, v = solution velocity, t = time, and z=

distance. If we expand the definition of K_D to include all processes that alter the mobility of the solute through the soil (i.e., degradation, diffusion, sorption, etc.), then we can redefine K_D as K_D'. Here, we set K_D' equal to the steady state constant describing the total kinetics of the system, (modified from Chappell et al.) (*4*):

$$K_D{}' = k_{total} = k_{transport} + k_{sorption} + k_{\deg radation} \quad [12]$$

Under water-saturated conditions, a retardation factor (R) can be defined as

$$R = 1 + \frac{\rho_b}{\theta} K_D{}' \quad [13]$$

In this case, R serves as a relative measure of solute retention. For $t \rightarrow \infty$, R represents mean residence time relative to the time required for water to move distance z in a soil profile.

Understanding the conditions that promote MC degradation in soil require focus on the limiting factors for microbial activity. Various factors that "limit" MC mobility include soil fertility, water status, and temperature. The presence of multiple limiting factors suggests that there is a combination of these factors required to optimize K_D'. Utilizing Mitscherlich-Baule relationship, we propose describing the interaction of these parameters as (*78*)

$$\frac{K_D{}'}{K'_{D\max}} = \left(1 - e^{c_{NPK}(NPK - NPK_{\max})}\right)\left(1 - e^{c_\theta(\theta - \theta_{\max})}\right)\left(1 - e^{c_T(T - T_{\max})}\right) \quad [14]$$

where $K'_{D\,max}$ = maximum K_D' obtainable for that particular soil, c_i = the efficiency coefficient, θ = volumetric water content, and NPK refers to the nutritional status with respect to the major macronutrients. According to Eq. 14, the parameters subscripted as "max" represent the optimum quantity of that factor so that its particular interaction reduces to 1 if the soil concentration is close to max.

Assuming favorable temperature and water conditions, it can be theorized that MC residence times are related to the soil nutritional or fertility status. Soils possessing naturally high fertility exhibit abundant microbiological activity, while soils with poor fertility, possess microorganisms in a more "feast or famine" mode. In agriculture, proper establishment of crop plants depends on successful rhizosphere microbiological interactions that provide the proper fertility to the growing plant. Often, the success of this relationship and its ability to support plant growth depends on maintaining the proper balance between nutrient inputs. For example, this is best demonstrated in manipulating the soil C:N ratio. If the C:N ratio is too high, microorganisms will be nitrogen limited, and thus, will seek to immobilize most nitrogen sources, and thus, promote nitrogen deficiencies in plants. On the other hand, successful fertility management, such as nitrogen amendments, keeps the C:N ratio sufficiently low to promote microbiological mineralization of nitrogen sources, and thus improving plant availability of the nutrient. Yet, all of this is coupled with the consideration that all other macro-and micro-nutrients are in abundant supply and that the external conditions, such as pH, EC, and temperature, are non-limiting.

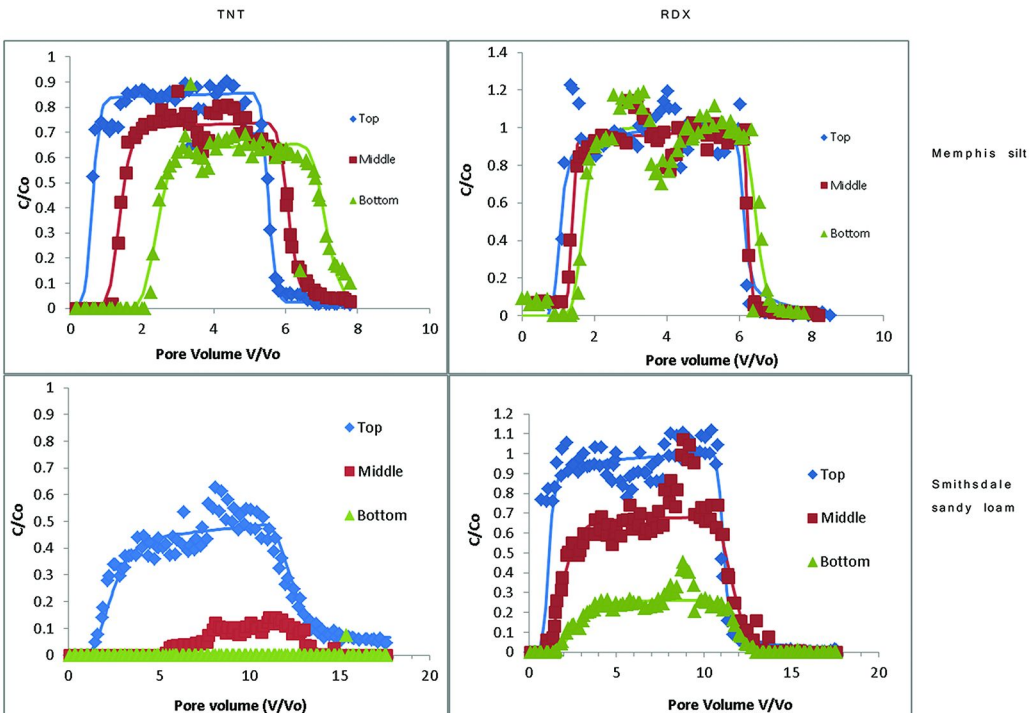

Figure 7. Breakthrough curves for TNT and RDX through a Memphis silt and Camp Shelby (Smithdale sandy loam) soils under water-saturated conditions. Solid lines represent fitted transport model. (see color insert)

This line of thinking may be helpful for considering how soil microorganisms will respond to inputs of organic chemicals, particularly those that contain nitrogen. Figure 7 shows data for the mobility of TNT and RDX through two soils: a Smithdale sandy loam soil (Fine-loamy, siliceous, subactive, thermic Typic Hapludults), an Ultisol of poor fertility, and a Memphis silt (Fine-silty, mixed, active, thermic Typic Hapludalfs) soil of good fertility. Both TNT and RDX showed much greater retention factors (R) and K_D values for the less fertile Smithdale soil (*37*). Note that the calculated high K_D values in Table 2 attributed to TNT and RDX mobility include the breakdown and degradation of the munitions in the soil. It is interesting to point out that the Smithdale soil texture is dominated by its sand composition, thus the soil is expected to exhibit to a higher hydraulic conductivity than the Memphis silt material. In the absence of degradation processes, the MC solutes would be expected to move readily through the Ultisol soil. With its poor fertility, the Smithdale soil is particularly low in soil nitrogen, while the Memphis silt contains moderate levels of nitrogen. Thus, we hypothesize that the slow mobility of the munition constituents in the Smithdale soil is related to the action of opportunistic microorganisms within the soil, while in the more fertile Memphis silt, reactive utilization of munition constituents was less important to the soil bacteria.

Table 2. Fitted solute transport parameters for TNT and RDX breakthrough curves.

		TNT		***RDX***	
Soil	*Sample position*	R_{fac}	K_D	R_{fac}	K_D
Memphis silt	Top	7.5	2.4	1.2	0.1
	Middle	17.0	5.8	1.6	0.22
	Bottom	24.2	8.5	1.7	0.26
Camp Shelby	Top	40.8	11.67	1.4	1.1
	Middle	-	-	39.8	11.38
	Bottom	-	-	300.7	87.89

Water Unsaturated Conditions and Transient Water Flow in Cell

It is important to caveat the above discussion in terms of the degree to which water-saturated batch suspensions represent actual soil conditions. With some exceptions in inundated areas, most soils are rarely water-saturated Maximum average matric potentials typically range from -0.1 to -0.3 bar at "field capacity" or less (*79*)). Here, the proportion of solid phase greatly dominates the proportion of liquid phase, which gives way to a very different s/s than batch systems. This difference is typically borne out in the literature as resulting in relatively

rapid transformation rates. For example, Price et al. (*46*) showed that under water-saturated batch conditions, TNT disappeared from the solution phase following one day of incubating the aqueous suspension under anaerobic (Eh = -150 mV) conditions while it required approximately four days for complete TNT removal from solution under aerobic (Eh = +500 mV) conditions. Similarly, RDX concentrations reduced by approximately 80 % after a 15-day incubation period under anaerobic (Eh = -150 mV) conditions in aqueous suspension systems while < 10 % was reduced under aerobic (Eh = +500 mV) conditions. In general, TNT and HMX exhibit degradation half-lives ($t_{1/2}$) on the order of 10^{1} h^{-1} under water-saturated batch conditions while RDX $t_{1/2}$ is approx. 10^{-1} h^{-1} under the same conditions (*46*, *49*, *72*). While useful in the general sense for comparing the degradation potentials of different organic compounds, the absolute K_D values are generally not useful under field conditions where degradation proceeds at much slower rates (*69*, *71*, *74*, *80*). For example, predictive models of MC fate in high-sand soils using degradation parameters obtained from batch studies produced errors on the order of thousands of percent (*81*), providing biases on the order of hundreds to millions of days. Dortch et al. (*82*) further emphasized this point showing that the fate models more accurately predicted RDX degradation in soil when $t_{1/2}$ was arbitrarily set at approx. 100 years or 10^{-6} h^{-1} - a difference of five orders of magnitude from $t_{1/2}$ predicted in batch studies. Values obtained from batch isotherm studies clearly fail to provide adequate predictions because soils are rarely water saturated. Thus, MC degradation kinetics needs to be evaluated in terms of water-unsaturated conditions.

Conclusions

This chapter reviews some basic mechanisms described in the scientific literature controlling the sorption and fate of munition constituents in soil and sediment. The literature indicates that much of MC behavior can be patterned after what is generally understood regarding nitroaromatic and triazine compounds in general, in terms of sorption by organic matter and soil clays, and their resulting environmental formulations.

The limitations of predictions based solely on equilibrium batch experiments are discussed, particularly in terms of solute transport considerations. After years of study, the scientific literature contains a well-rounded picture of the environmental fate of TNT. However, our understanding of the environmental fate of RDX is much less well developed. Yet, there are indications that RDX behaves more similar to some of the classical nitroaromatic and triazine compounds, but undergoes a less-specific interaction with soil because of its apparent greater resistance to degradation processes. Therefore, some of the novel remedial options developed for migrating organic compounds may be feasible, such as clay charge reductions through K-saturated “barriers” or use of organically modified clays.

Specific mechanisms with respect to how a soil sample is handled and prepared for sorption experiments, as well as the sorption experiments themselves, are discussed briefly to point out that there must be uniformity in the way K_D

values are measured as this contributes to the often wide variance of the data. Such uniformity in approach is important as the sorption coefficients are empirical in nature and operational defined. For this reason, we introduced a new theoretical treatment for considering MC behavior in soil by simultaneously addressing a soil's sorption affinity and buffering capacity for the solute. Inherently, this approach is more descriptive providing both soil preference and action at the soil surface, while at the same time, incorporating fugacity concepts to introduce thermodynamic validity to these relationships.

This review also theoretically addressed the subject of expanding considerations of soil properties to the concept of soil tilth for predicting MC long-term residence.

References

1. Giles, C. H.; Mac Ewan, T. H.; Nakhwa, S. N.; Smith, D. Studies in adsorption. Part XI. A system of classification of solution adsorption isotherms, and its use in diagnosis of adsorption mechanisms and in measurement of specific surface areas of solids. *J. Chem. Soc.* **1960**, *1960*, 3973–3993.
2. Eriksson, J.; Skyllberg, U. Binding of 2,4,6-trinitrotoluene and its degradation products in a soil organic matter two-phase system. *J. Environ. Qual.* **2001**, *30*, 2053–2061.
3. Eriksson, J.; Frankki, S.; Shchukarev, A.; Skyllberg, U. Binding of 2,4,6-trinitrotoluene, aniline, and nitrobenzene to dissolved and particulate soil organic matter. *Environ. Sci. Technol.* **2004**, *38*, 3074–3080.
4. Chappell, M. A.; Price, C. L.; Porter, B. E.; Pettway, B. A.; George, R. D. Dependence of Abiotic and Biotic Processes Controlling the Environmental Fate of TNT in Simulated Marine Systems. *Mar. Pollut. Bull.* **2011**, *62*, 1736–1743.
5. Beckett, P. H. T. Studies on soil potassium. I. Confirmation of the Ratio Law: Measurement of potassium potential. *J. Soil Sci.* **1964**, *15*, 1–8.
6. Oertli, J. J. The use of chemical potentials to express nutrient availabilities. *Geoderma* **1973**, *9*, 81–95.
7. Atkins, P. *Physical Chemistry*; 6th ed.; W.H. Freeman and Company: New York, 1997.
8. Connolly, J. P.; Pederson, C. J. A thermodynamic-based evaulation of organic chemical accumulation in aquatic organisms. *Environ. Sci. Technol.* **1988**, *22*, 99–103.
9. Mackay, D. Finding fugacity feasible. *Environ. Sci. Technol.* **1979**, *13*, 1218–1223.
10. Mackay, D.; Paterson, S. Calculating fugacity. *Environ. Sci. Technol.* **1981**, *15*, 1006–1014.
11. Chiou, C. T.; Peters, L. J.; Freed, V. H. A physical concept of soil-water equilibria for nonionic organic compounds. *Science* **1979**, *206*, 831–832.

12. Chiou, C. T.; Porter, P. E.; Schmedding, D. W. Partition equilibria of nonionic organic compounds between soil organic-matter and water. *Environ. Sci. Technol.* **1983**, *17*, 227–231.
13. Chiou, C. T.; Kile, D. E.; Rutherford, D. W. Sorption of selected organic compounds from water to a peat soil and its humic-acid and humin fractions: Potential sources of the sorption nonlinearity. *Environ. Sci. Technol.* **2000**, *34*, 1254–1258.
14. Karickhoff, S. W. On sorption of neutral organic solutes in soils. *J. Agric. Food Chem.* **1981**, *29*, 424–425.
15. Karickhoff, S. W.; Brown, D. S.; Scott, T. A. Sorption of hydrophobic pollutants on natural sediments. *J. Hydraulic Eng.* **1979**, *110*, 707–735.
16. Pignatello, J. J.; Xing, B. Mechanisms of slow sorption of organic chemicals to natural particles. *Environ. Sci. Technol.* **1996**, *30*, 1–11.
17. Barriuso, E.; Laird, D. A.; Koskinen, W. C.; Dowdy, R. H. Atrazine desorption from smectites. *Soil Sci. Soc. Am. J.* **1994**, *28*, 1632–1638.
18. Haderlein, S. B.; Weissmahr, K. W.; Schwarzenbach, R. P. Specific adsorption of nitroaromatic explosives and pesticides to clay minerals. *Environ. Sci. Technol.* **1996**, *30*, 612–622.
19. Jaynes, W. F.; Boyd, S. A. Hydrophobicity of siloxane surfaces in smectites as revealed by aromatic hydrocarbon adsorption from water. *Clays Clay Miner.* **1991**, *39*, 428–436.
20. Laird, D. A.; Sawhney, B. L.. Reactions of pesticides with soil minerals In *Soil Mineralogy with Environmental Applications*; Dixon, J. B., Schulze, D. G., Eds.; Soil Science Society of America, Inc.: Madison, WI, 2002; pp 765−793.
21. Laird, D. A.; Barriuso, E.; Dowdy, R. H.; Koskinen, W. C. Adsorption of atrazine on smectites. *Soil Sci. Soc. Am. J.* **1992**, *56*, 62–67.
22. Laird, D. A.; Yen, P. Y.; Koskinen, W. C.; Steinhelmer, T. R.; Dowdy, R. H. Sorption of atrazine on soil clay components. *Environ. Sci. Technol.* **1994**, *28*, 1054–1061.
23. Sheng, G.; Xu, S.; Boyd, S. A. Mechanism(s) controlling sorption of neutral organic contaminants by surfactant-derived and natural organic matter. *Environ. Sci. Technol.* **1996**, *30*, 1553–1557.
24. Sheng, G.; Johnston, C. T.; Teppen, B. J.; Boyd, S. A. Potential contributions of smectite clays and organic matter to pesticide retention in soils. *J. Agric. Food Chem.* **2001**, *49*, 2899–2907.
25. Weissmahr, K. W.; Haderlein, S. B.; Schwarzenbach, R. P. *In situ* spectroscopic investigations of adsorption mechanisms of nitroaromatic compounds at clay minerals. *Environ. Sci. Technol.* **1997**, *31*, 240–247.
26. Weissmahr, K. W.; Hildenbrand, M.; Schwarzenbach, R. P.; Haderlein, S. B. Laboratory and field scale evaluation of geochemical controls on groundwater transport of nitroaromatic ammunition residues. *Environ. Sci. Technol.* **1999**, *33*, 2593–2600.
27. Xue-Kun, Z.; Yang, G.-P.; Gao, X.-C. Studies on the sorption behaviors of nitrobenzene on marine sediments. *Chemosphere* **2003**, *52*, 917–925.

28. Charles, S.; Teppen, B. J.; Li, H.; Laird, D. A.; Boyd, S. A. Exchangeable cation hydration properties strongly influence soil sorption of nitroaromatic compounds. *Soil Sci. Soc. Am. J.* **2006**, *70*, 1470–1479.
29. Nefso, E. K.; Burns, S. E.; McGrath, C. J. Degradation kinetics of TNT in the presence of six mineral surfaces and ferrous iron. *J. Hazard. Mater.* **2005**, *B123*, 79–88.
30. Boyd, S. A.; Sheng, G.; Teppen, B. J.; Johnston, C. T. Mechanisms for the adsorption of substituted nitrobenzenes by smectite clays. *Environ. Sci. Technol.* **2001**, *35*, 4227–4234.
31. Pelmenschikov, A.; Leszczynski, J. Adsorption of 1,3,5-trinitrotoluene on the siloxane sites of clay minerals: Ab initio calculations of molecular models. *J. Phys. Chem. B* **1999**, *103*, 6886–6890.
32. Johnston, C. T.; Oliveria, M. F. D.; Teppen, B. J.; Sheng, G.; Boyd, S. A. Spectroscopic study of nitroaromatic-smectite sorption mechanisms. *Environ. Sci. Technol.* **2001**, *35*, 4767–4772.
33. Sheng, G.; Johnston, C. T.; Teppen, B. J.; Boyd, S. A. Adsorption of dinitrophenol herbicides from water by montmorillonites. *Clays Clay Miner.* **2002**, *50*, 25–34.
34. Li, H.; Pereira, T. R.; Teppen, B. J.; Laird, D. A.; Johnston, C. T.; Boyd, S. A. Ionic strength-induced formation of smectite quasicrystals enhances nitroaromatic compound sorption. *Environ. Sci. Technol.* **2007**, *41*, 1251–1256.
35. Pereira, T. R.; Laird, D. A.; Thompson, M. L.; Johnston, C. T.; Teppen, B. J.; Li, H.; Boyd, S. A. Role of smectite quasicrystal dynamics in adsorption of dinitrophenol. *Soil Sci. Soc. Am. J.* **2008**, *72*, 347–354.
36. Brannon, J. M.; Pennington, J. C. *Environmental fate and transport process descriptors for explosives*; ERDC/EL TR-02-10; U.S. Army Corps of Engineers: Vicksburg, MS, 2002.
37. Chappell, M. A.; Price, C. L.; Miller, L. F. Solid-phase considerations for the environmental fate of nitrobenzene and triazine munition constituents in soil. *Appl. Geochem.* **2011**, *26*, S330–S333.
38. Esteve-Nunez, A.; Caballero, A.; Ramos, J. L. Biological degradation of 2,4,6-trinitrotoluene. *Microbiol. Mol. Biol. Rev.* **2001**, *65*, 335–352.
39. Hofstetter, T. B.; Schwarzenbach, R. P.; Haderlein, S. B. Reactivity of Fe(II) species associated with clay minerals. *Environ. Sci. Technol.* **2003**, *37*, 519–528.
40. Hofstetter, T. B.; Heijman, C. G.; Haderlein, S. B.; Holliger, C.; Schwarzenbach, R. P. Complete reduction of TNT and other (poly)nitroaromatic compounds under iron-reducing subsurface conditions. *Environ. Sci. Technol.* **1999**, *33*, 1479–1487.
41. Pennington, J. C.; Patrick, W. H., Jr. Adsorption and desorption of 2,4,6-trinitrotoluene by soils. *J. Environ. Qual.* **1990**, *19*, 559–567.
42. Tucker, W. A.; Murphy, G. J.; Arenberg, E. D. Adsorption of RDX to soil with low organic carbon: Laboratory results, field observations, remedial implications. *Soil Sediment Contam.* **2002**, *11*, 809–826.

43. Sheng, G.; Johnston, C. T.; Teppen, B. J.; Boyd, S. A. Adsorption of dinitrophenol herbicides from water by montmorillonites. *Clays Clay Miner.* **2002**, *50*, 25–34.
44. Lee, J. F.; Mortland, M. M.; Chiou, C. T.; Kile, D. E.; Boyd, S. A. Adsorption of benzene, toluene, and xylene by two tetramethylammonium-smectites having different charge densities. *Clays Clay Miner.* **1990**, *38*, 113–120.
45. Price, C. L.; Brannon, J. M.; Yost, S. L.; Hayes, C. A. *Adsorption and transformation of explosives in low-carbon aquifer soils*; U.S Army Corps of Engineers, 2000.
46. Price, C. B.; Brannon, J. M.; Hayes, C. A. Effect of redox potential and pH on TNT transformation in soil-water slurries. *J. Environ. Eng.* **1997**, *123*, 988–992.
47. Thorn, K. A.; Kennedy, K. R. ^{15}N NMR investigation of the covalent binding of reduced TNT amines to soil humic acid, model compounds, and lignocellulose. *Environ. Sci. Technol.* **2002**, *36*, 3878–3796.
48. Thorn, K. A.; Pennington, J. C.; Hayes, C. A. ^{15}N NMR investigation of the reduction and binding of TNT in an aerobic bench scale reactor simulating windrow composting. *Environ. Sci. Technol.* **2002**, *36*, 3797–3805.
49. Yost, S. L.; Pennington, J. C.; Brannon, J. M.; Price, C. B. Environmental process descriptors for TNT, TNT-related compounds and picric acid in marine sediment slurries. *Mar. Pollut. Bull.* **2007**, *54*, 1262–1266.
50. Gonzalez, J. M.; Laird, D. A. Carbon sequestration in clay mineral fractions from ^{14}C-labeled plant residues. *Soil Sci. Soc. Am. J.* **2003**, *67*, 1715–1720.
51. Gonzalez, J. M.; Laird, D. A. Role of smectites and A1-substituted goethites in the catalytic condensation of arginine and glucose. *Clays Clay Min.* **2004**, *52*, 443–450.
52. Laird, D. A.; Martens, D. A.; Kingery, W. L. Nature of clay-humic complexes in an agricultural soil: I. Chemical, biochemical, and spectroscopic analyses. *Soil Sci. Soc. Am. J.* **2001**, *65*, 1413–1418.
53. Laird, D. A.; Chappell, M. A.; Martens, D. A.; Wershaw, R. L.; Thompson, M. L. Distinguishing black carbon from biogenic humic substances in soil clay fractions. *Geoderma* **2008**, *143*, 115–122.
54. Singh, N.; Hennecke, D.; Hoerner, J.; Koerdel, W.; Schaeffer, A. Sorption-desorption of trinitrotoluene in soils: Effect of saturating metal cations. *Bull Environ. Contam. Toxicol.* **2008**, *80*, 443–446.
55. Chappell, M. A.; Laird, D. A.; Thompson, M. L.; Li, H.; Aggarwal, V.; Teppen, B. J.; Johnston, C. T.; Boyd, S. A. Influence of smectite hydration and swelling on atrazine sorption behavior. *Environ. Sci. Technol.* **2005**, *39*, 3150–3156.
56. Haderlein, S. B.; Schwarzenbach, R. P. Adsorption of substituted nitrobenzenes and nitrophenols to mineral surfaces. *Environ. Sci. Technol.* **1993**, *27*, 316–326.
57. Li, H.; Teppen, B. J.; Laird, D. A.; Johnston, C. T.; Boyd, S. A. Geochemical modulations of pesticide sorption on smectite clay. *Environ. Sci. Technol.* **2004b**, *38*, 5393–5399.
58. Roberts, M. G.; Li, H.; Teppen, B. J.; Boyd, S. A. Sorption of nitroaromatics by ammonium- and organic ammonium-exchanged smectite shifts from

adsorption/complexation to a partition-dominated process. *Clays Clay Miner.* **2006**, *54*, 426–434.
59. Pils, J. R. V.; Laird, D. A.; Evangelou, V. P. Role of cation demixing and quasicrystal formation and breakup on the stability of smectitic colloids. *Appl. Clay Sci.* **2007**, *35*, 201–211.
60. Li, H.; Teppen, B. J.; Johnston, C. T.; Boyd, S. A. Thermodynamics of nitroaromatic compound adsorption from water by smectite clay. *Environ. Sci. Technol.* **2004**, *38*, 5433–5442.
61. Pereira, T. R.; Laird, D. A.; Johnston, C. T.; Teppen, B. J.; Boyd, S. A. Mechanism of dinitrophenol herbicide sorption by smectites in aqueous suspensions by varying pH. *Soil Sci. Soc. Am. J.* **2007**, *71*, 1476–1481.
62. Ottewill, R. H. Colloidal properties of latex particles. In *Scientific Methods for the Study of Polymer Colloids and their Applications*; Candau ,F., Ottewill, R. H., Eds.; Kluwer Academic Publishers: Amsterdam, The Netherlands, 1990; pp 129−157.
63. Laird, D. A.; Shang, C. Relationship between cation exchange selectivity and crystalline swelling in expanding 2:1 phyllosilicates. *Clays Clay Miner.* **1997**, *45*, 681–689.
64. McDonald, L. M., Jr.; Evangelou, V. P. Optimal solid-to-solution ratios for organic chemical sorption experiments. *Soil Sci. Soc. Am. J.* **1997**, *61*, 1655–1659.
65. Lu, Y.; Pignatello, J. J. Demonstration of the "conditioning effect" in soil organic matter in support of a pore deformation mechanism for sorption hysteresis. *Environ. Sci. Technol.* **2002**, *36*, 4553–4561.
66. Bradley, P. M.; Chapelle, F. H. Factors affected microbial 2,4,6-trinitrotoluene mineralizatin in contaminated soil. *Environ. Sci. Technol.* **1995**, *29*, 802–806.
67. Elovitz, M. S.; Weber, J. B. Sediment-mediated reduction of 2,4,6-trinitrotoluene and fate of the resulting aromatic (poly)amines. *Environ. Sci. Technol.* **1999**, *33*, 2617–2625.
68. Lewis, T. A.; Ederer, M. M.; Crawford, R. L.; Crawford, D. L. Microbial transformation of 2,4,6-trinitrotoluene. *J. Ind. Microbiol. Biotechnol.* **1997**, *18*, 89–96.
69. Hundal, L. S.; Shea, P. J.; Comfort, S. D.; Powers, W. L.; Singh, J. Long-term TNT sorption and bound residue formation in soil. *J. Environ. Qual.* **1997**, *26*, 869–904.
70. Robertson, B. K.; Jjemba, P. K. Enhanced bioavailability of sorbed 2,4,6-trinitrotoluene (TNT) by a bacterial consortium. *Chemosphere* **2005**, *58*, 263–270.
71. Dontsova, K. M.; Hayes, C. A.; Pennington, J. C.; Porter, B. E. Sorption of high explosives to water-dispersible clay: Influence of organic carbon, aluminosilicate clay, and extractable iron. *J. Environ. Qual.* **2009**, *38*, 1458–1456.
72. Price, C. B.; Brannon, J. M.; Yost, S. L.; Hayes, C. A. Relationship between redox potential and pH on RDX transformation in soil-water slurries. *J. Environ. Eng.* **2001**, *127*, 26–31.

73. Sheremata, T. W.; Halasz, A.; Paquet, L.; Thiboutot, S.; Ampleman, G.; Hawari, J. The fate of the cyclic nitramine explosive RDX in natural soil. *Environ. Sci. Technol.* **2001**, *35*, 1037–1040.
74. Yamamato, H.; Morley, M. C.; Speitel, G. E., Jr.; Clausen, J. Fate and transport of high explosives in a sandy soil: Adsorption and desorption. *Soil Sediment Contam.* **2004**, *13*, 361–379.
75. Binks, P. R.; Nicklin, S.; Bruce, N. C. Degradation of hexahydro-1,3,5-trinitro-1,3,5-trazine (RDX) by *Stenotrophomonas maltophilia* PB1. *Appl. Environ. Microbiol.* **1995**, *61*, 1318–1322.
76. Thompson, K. T.; Crocker, F. H.; Fredrickson, H. L. Mineralization of the cyclic nitramine explosive hexahydro-1,3,5-trinitro-1,3,5-triazine by *Gordonia* and *Williamsia* spp. *Appl. Environ. Microbiol* **2005**, *71*, 8265–8272.
77. Radcliffe, D. E.; Simunek, J. *Soil Physics with HYDRUS: Modeling and Applications*; CRC Press: Boca Raton, FL, 2010.
78. Hosaini, Y.; Homaee, M.; Karimian, N. A.; Saadat, S. Modeling vegetative stage response of canola (Brassica napus L.) to combined salinity and boron stresses. *Int. J. Plant Prod.* **2009**, *3*.
79. Brady, N. C. *The nature and properties of soils*, 10th Ed.; MacMillian Publishing Company: New York, 1990.
80. Comfort, S. D.; Shea, P. J.; Hundal, L. S.; Li, Z.; Woodbury, B. L.; Martin, J. L.; Powers, W. L. TNT transport and fate in contaminated soil. *J. Environ. Qual.* **1995**, *24*, 1174–1182.
81. Dortch, M., Zakikhani, M.; Furey, J.; Meyer, R.; Fant, S.; Gerald, J.; Qasim, M.; Fredrickson, H.; Honea, P.; H. Bausum, Walker, K.; Johnson; M. *Data gap analysis and database expansion of parameters for munitions constituents*; US Army Engineering and Research Development Center: Vicksburg, MS, 2005.
82. Dortch, M. S.; Fant, S.; Gerald, J. A. Modeling fate of RDX at demolition area 2 of the Massachusetts Military Reservation. *Soil Sediment Contam.* **2007**, *16*, 617–635.

Chapter 2

Environmental Assessment of Small Arms Live Firing: Study of Gaseous and Particulate Residues

S. Brochu,[1,*] I. Poulin,[1] D. Faucher,[1] E. Diaz,[1] and M. R. Walsh[2]

[1]Defence R&D Canada – Valcartier, 2459 Pie-XI Blvd North, Quebec (Qc) G3J 1X5, Canada
[2]U.S. Army Engineer Research and Development Center, Cold Regions Research and Engineering Laboratory, 72, Lyme Road, Hanover, NH 03755-1290, USA
[*]sylvie.brochu@drdc-rddc.gc.ca

Small arms training is an important military activity of the Canadian Forces and the U.S. Army, and contributes to the accumulation of residues on the training areas. In the present work, the amount of unburned energetic residues deposited per round was estimated for five calibers (9 mm, 7.62 mm, 5.56 mm, 0.50 and 0.338) and nine weapons (Browning and Sig Sauer pistols, rifle C7, carbine C8, machine guns C6, C9 and M2HB, and rifles McMillan and Timberwolf). Samples were collected in aluminum containers located on the soil in front of weapons, and three air samples were collected using pumps, monitoring cassettes and sorbent tubes. The percentage of unburned Nitroglycerin (NG) per round varied between 0.001% and 3.90%, and up to 2.03 mg NG per round was deposited. Detectable concentrations of cyanide and acrolein were found in the gaseous emissions of 7.62- and 5.56-mm cartridges. Most particles collected during air sampling were smaller than 1 μm and made mainly of lead or copper. It is important to note that the reported concentrations are not representative of the soldiers' exposure because the sample was not collected in the breathing zone. These results indicate that the burning efficiency of most small arms is better than mortars, but worse than some artillery rounds, and that the accumulation of NG

in the environment is cumulative over years, and probably decades.

Introduction

The small arms (SA) training represents a huge portion of military activities, since all service personnel must be qualified in the handling of a personal weapon. In this context, SA training ranges are being used extensively, which contributes to the escalation of residue accumulation on site. It is well known that heavy metals such as lead, copper, zinc and antimony accumulate in and near the stop berms in concentrations high enough to affect the soil, biomass, surface water, or even groundwater (*1*, *2*).

A large number of small arms ranges have been characterized in Canada and the United States to assess propellant residue accumulation in near-surface soils at firing point areas. Jenkins et al. (*3*) have shown that residues coming from the incomplete combustion of gun propellant accumulate as solid particulates in front of the firing positions of SA ranges. Major constituents of concern are 2,4-dinitrotoluene (2,4-DNT) and nitroglycerin (NG), which are part of single and double base propellants, respectively.

However, little is known about the amount and distribution of residues emitted per types of rounds and weapons, or about the parameters controlling the combustion of gun propellant in small arms. The combustion efficiency is thought to be influenced by the type of calibrer propellant and weapon used, as well as weather conditions. However, from range characterization data, the evaluation of the extent of contamination associated with a specific ammunition/weapon system is impossible. Indeed, none of these ranges is used for a single munition, and information on the historic use of a range is limited and sometimes inaccurate. Moreover, the soil of these ranges is often contaminated from unknown past activities. Not only is there a lack of information on the build-up of propellant residues on the ground, but also there is little information on the gaseous emissions resulting from the live-fire of the weapons. There is a need to better understand the gun propellant combustion and the parameters having an influence on the propellant efficiency.

In addition, the firing of a weapon produces an aerial plume composed of various gases and particles. Previous work was conducted in the United States by the U.S. Army Environmental Center to develop emission factors based on firing point emissions for various types of range operations, such as weapons firing, smoke and pyrotechnic devices, and exploding ordnances. The work, conducted with the United States Environmental Protection Agency (U.S. EPA), used different munitions test facilities, such as test chambers, blast spheres and bangboxes at the Aberdeen Test Center, Maryland, to sample and analyze emitted products. The results of theses tests led to the calculation of emission factors that were published in the U.S. EPA Compilation of Air Pollutant Emission Factors (AP-42) (*4*). An emission factor is a representative value that attempts to relate the quantity of a pollutant released to the atmosphere with an activity associated with the release of that pollutant. These factors are usually expressed

as the weight of pollutant divided by a unit weight, volume, distance, or duration of the activity emitting the pollutant (e.g., kilograms of particulate emitted per megagram of coal burned). However, little is known about the composition of the aerial plume and the particulate matter that can stay in suspension several minutes around the shooter of a small arms weapon.

This study had two objectives. The first was to characterize the behaviour of various types of small calibre weapons and ammunitions and the distribution of gun propellant residues on the training range using the most common weapons under realistic training conditions. The second objective was to assess the nature of gaseous species and characterize solid particles emitted in the vicinity of the gun during the live firings.

Materials and Methods

A study was thus undertaken to estimate the amount of unburned energetic residues deposited per round fired. As shown in Table 1, five calibers (9 mm, 7.62 mm, 5.56 mm, 0.50 and 0.338) and nine weapons (Browning and Sig Sauer pistols, rifle C7, carbine C8, machine guns C6, C9 and M2HB, and rifles McMillan and Timberwolf) were selected for this study. A more thorough description of the weapons and ammunition can be found in Faucher et al. (*5*). Weapons were fired remotely from a fixed mount.

Several trials were done in duplicate and one was done in triplicate. Some trials could not be performed more than once because of operational time constraints. For all trials, samples were collected in aluminum containers strategically located on the ground in front of the gun. Air samples were also collected for three ammunition/weapons systems, commonly used in the Canadian Forces, using an enclosure bag when possible to minimize dilution. All samples were analyzed for NG and 2,4-DNT. In addition, gas samples were analyzed for polycyclic aromatic hydrocarbons (PAH), total cyanides, the BTEX suite (benzene, toluene, ethylbenzene and xylenes), aldehydes, and nitric acid.

Propellant Residues

Aluminum containers (Set-up is in Figure 1) were used to collect propellant residues. The sampling area was based on the results of Walsh *et al*. (*6*) for similar trials on snow. The calculations are based on the assumption that 100% of the plume was contained within the sampled area. Solvent was put in the containers to prevent any loss of particles. After a test, the contents of all particle traps at the same distance from the weapon were combined in a single sample. Propellant residues were extracted and analyzed by an in-house HPLC method derived from the current EPA analysis Method 8330b (*7*). One result of NG concentration (or mass) is thus obtained for each of the selected distances from the gun (1, 2, 3, 4, 5, 7.5, 10, 12.5, 15, 20 and 25 m). Then, a piece-wise linear concentration distribution was integrated in the axial direction to give the total mass of NG. The complete sample processing and calculations are reported in Faucher et al. (*5*).

Table 1. Description of ammunitions and weapons used for each trial.

Ammunition		*Weapon*			
Cartridge	*Type*	*Type*	*Max Weapon Length cm*	*Max Barrel Length cm*	*Muzzle Velocity m/s*
9 mm	MK1 ball Luger 115 FMJ Frangible	Browing pistol (*10*) Sig Sauer pistol (*11*)	19.7 17.8	12.4 9.8	365 357
7.62 mm	C21/C19 4B1T[1] Link C24 blank link	C6 Machine gun (*12*)	127	67	840
5.56 mm	C77 ball clip C77/C78 4B1T[1] Link C79A1 blank link Frangible	C7A1 Automatic rifle (*13*) C8 Automatic carbine (*14*) C9A1 Light machine gun (*15*)	103 84 104	51 40 53	915[2] 910[2] 962
.50 cal	M2/M17 4B1T[1] Link AAA750 Hodgdon H50BMG 225 gr	Browning heavy machine gun (*16*) McMillan rifle (*17*)	166 144	114 74	860 818
.338 cal	Lapua Magnum	Timberwolf (*18*)	125	66	823

[1] Sequence of 4 ball and 1 tracer in a link belt. [2] Velocity at 24 m.

Figure 1. Stop berms and sampling layout.

Gases and Airborne Particles

Gases and airborne particles were sampled using sorbent tubes and filters for three weapons: 1) Browning pistol, 9 mm MK1 ball (500 rounds); 2) machine gun C6, 7.62 mm link C21/C19 ball (880 rounds) and; 3) automatic rifle C7, 5.56 mm C77 ball (450 rounds). As shown in Figure 2, the sampling media were strategically positioned at two locations: close to the muzzle of the gun and near the upper receiver. For the C6 machine gun and the C7 automatic rifle, an enclosure bag was placed around the gun in order to minimize the gas and particle dispersion. Details of sampling are reported in Faucher et al. (*5*). Sampling tubes were analyzed by the Institut de recherche Robert-Sauvé en santé et en sécurité du travail (IRSST, Montreal, Canada). Particle size distribution, morphology, and chemical composition were studied at Université Laval (Quebec, Canada) by scanning electron microscopy (SEM) with a JEOL JSM-840A microscope equipped with a NORAN energy dispersive X-ray spectrometer.

Figure 2. Browning pistol surrounded by air-monitoring cassettes and sorbent tubes.

Results

Gun Propellant Residues

The dispersion of NG per calibreris shown in Figure 3. For simplicity of presentation, NG concentrations are reported in mg per 1000 rounds, per area sampled. Table 2 gives a summary for each ammunition/weapon. The results of NG dispersion show that most of the rounds and weapons that were tested deposited a mass of NG below 0.09 mg/round or that the percentage of unburned NG/round is lower than 0.06%. Exceptions are the following:

- Cartridges 9 mm, which deposited between 0.74 and 2.03 mg NG/round (1.39 to 3.90% of unburned NG per round). The dispersion seemed to be worse when the Sig Sauer pistol was used.
- Cartridges 7.62 mm, both C21/C19, ball, linked and C24, blank, linked, fired with the C6 machine gun, which were found to deposit approximately 0.98 and 0.16 mg NG per cartridge, corresponding to 0.3% (theoretical calculation) and 0.11% of unburned NG per round, respectively.
- Cartridges 5.56 mm, C77/C78, ball, fired with the C7 automatic rifle, that deposited 0.30 mg/round (0.19% of unburned NG per round).

- Frangible cartridges 5.56 mm fired with the C7 automatic rifle, which led to an amount of 1.06 mg NG/round (0.62% of unburned NG per round).

The results indicate that cartridges 9 mm deposited a larger amount of unburned NG on the soil and had a lower burning efficiency. The burning efficiency seems to increase as the amount of propellant in the round increases, with the exception of cartridges 7.62 mm, for which more gun propellant residues were emitted for cartridges ball and blank, as compared to 5.56-mm cartridges. Blank cartridges had a burning efficiency similar to that of ball cartridges, but since less propellant was present, smaller amounts of NG (0.01-0.02 mg, as compared to 0.05-0.30 mg) were deposited per round fired.

The results also confirmed that either the weapon and/or the primer had a significant effect on the burning efficiency because very different values were obtained for the 9 mm fired with the same propellant (WPR 289), but using different pistols and primers (0.74 and 2.03 mg NG). The results for the frangible cartridges 9 mm and 5.56 mm should be verified in a subsequent study because the contamination associated with those two rounds was unusually high. These findings suggest that the lead-free primer may not be as effective as current formulations to ignite the gun propellant.

The cartridges 5.56 mm were fired with the same propellant (PRB SS 109), but using three weapons with different barrel lengths (C7, 67 cm; C8, 40 cm; C9, 52 cm); the precision of the results was not high enough because of the wind. It was not possible to see any clear tendency of the effect of the barrel length or firing mechanism. The calibrer.50 cartridge had a high burning efficiency, but because of the larger amount of propellant in the round, each shot deposited a larger amount of NG (0.25 mg) into the environment. And lastly, considering the large amount of propellant in the Lapua Magnum, the release of NG by the Timberwolf sniper rifle was quite small (0.03 mg) compared to the other small arms.

The percentages of unburned NG per round were within an order of magnitude to those of Walsh et al. (*6*, *8*), who obtained 1.1% of unburned NG for the cartridges 5.56 mm fired from a rifle (as opposed to 0.2-0.6% in this study), 0.56% for the cartridges 7.62 mm fired from a machine gun (as opposed to 1.36% in this study), 5.4% for the cartridges 9 mm (as compared to 1.39 to 3.90% in this study) and 0.73% for the calibre .50 cartridges (as compared to 0.02% in this study). Nevertheless, dispersion patterns for all of the rounds were similar.

A certain number of reasons can be invoked to explain the differences between the trials of Walsh et al. (*6*, *8*), and those of this study. One of them is certainly the trial set-up. Walsh's trial was conducted on snow, with the weapon located just high enough (approximately 30 cm) from the surface to minimize the effect of the muzzle blast. For our study, the trial was done in the spring, at temperatures approximately 30°C higher than those of Walsh; samples were recovered in aluminum containers filled with solvent, and weapons were much farther from the ground (1 m). The effect of the wind, which was more significant during some of our trials with the cartridges 5.56 mm and the calibrer.50 cartridges, cannot be ruled out. Another important point is that the Canadian and the U.S. Armed Forces do not use the same weapons, and often not the same gun propellants and primers. This could contribute to significant

differences, as shown from our results for the cartridges 9 mm fired with Sig Sauer and a lead-free primer (2.03 mg NG, 3.90% of unburned NG) and the Browning pistol with a traditional primer (0.74 mg NG, 1.39% of unburned NG per round). Also, the manufacturer's data are often imprecise, inaccurate, or hard to obtain; in-house analysis of the gun propellant used for a given experiment should always be obtained to allow for more accurate estimates of burning efficiencies.

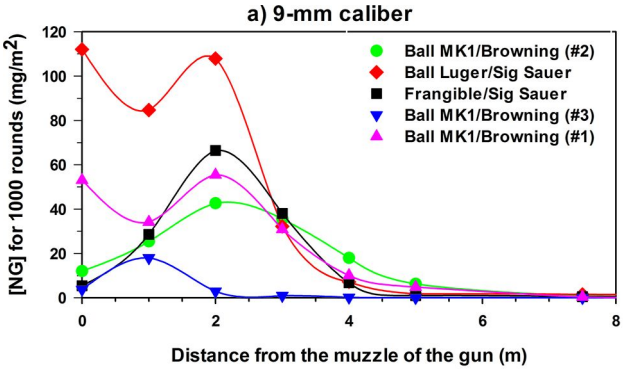

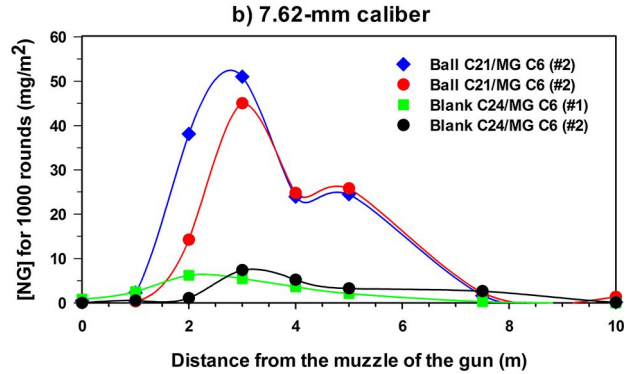

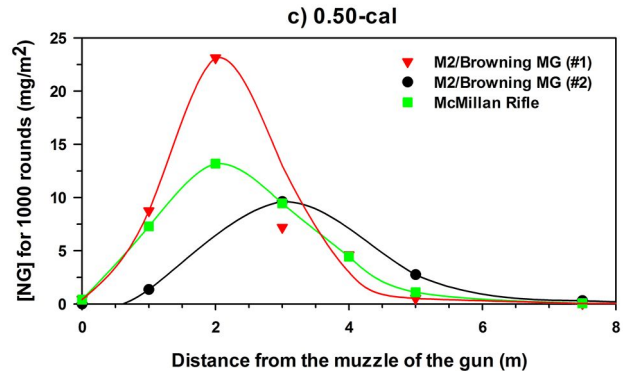

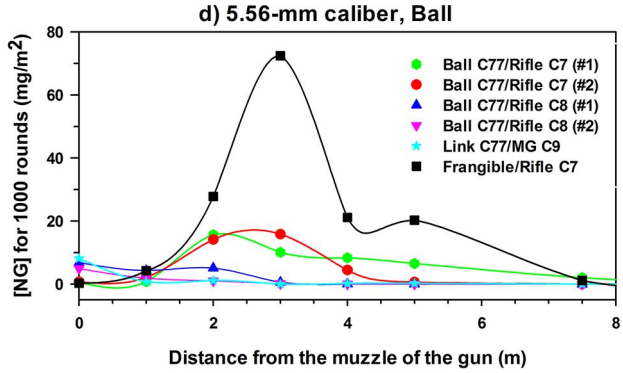

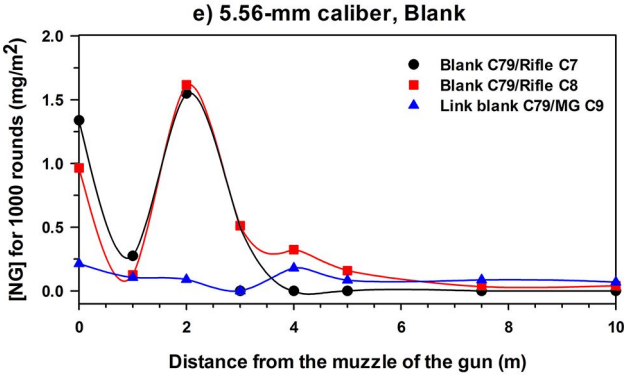

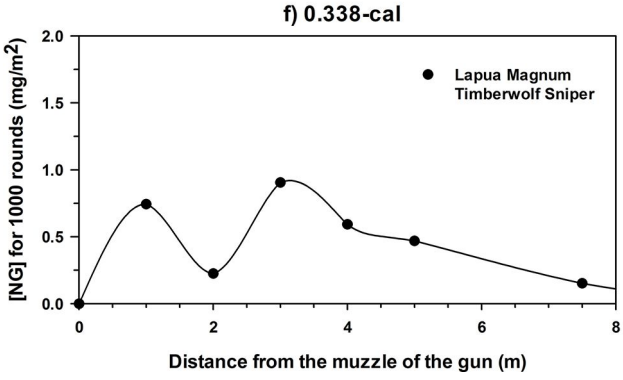

Figure 3. Dispersion of NG on the ground after 1000 rounds, a) 9-mm caliber, b) 7.62-mm caliber, c) 5.56-mm caliber, d) 0.50-cal, e) 0.338-cal. (see color insert)

Table 2. NG residues per cartridge/weapon

Calibre	*Weapon*	*Cartridge*	*Propellant Type*[1]	*NG/round*	
				mg	*%*
9 mm	Browning pistol	MK1, ball	WPR 289	0.74	1.39
	Sig Sauer	Frangible	PCL 2595	0.95	1.97
	Sig Sauer	Luger 115 FMJ ball	WPR 289	2.03	3.90
7.62 mm	C6 Machine gun	C21/C19, 4B1T	WC 846	0.98	0.3[2]
	C6 Machine gun	C24, blank	Unique no. 20	0.16	0.11
5.56 mm	C7 Automatic rifle	Frangible	WC 747	1.06	0.62
	C7 Automatic rifle	C77, ball	PRB SS 109	0.30	0.19
	C7 Automatic rifle	C79A1, blank	NA	0.02	0.05
	C8 Automatic carbine	C77, ball	PRB SS 109	0.07	0.04
	C8 Automatic carbine	C79A1, blank	NA	0.02	0.06
	C9 Light machine gun	C77/C78, 4B1T	PRB SS 109	0.05	0.03
	C9 Light machine gun	C79A1, blank	XPRO-11GO	0.01	0.01
.50 cal	Browning machine gun	M2/M17, 4B1T	WC 860 (M2) IMR 5013 (M17)	0.25	0.02
	McMillan rifle	AAA750 Hodgdon H50BMG	NA	0.27	0.02
.338 cal	Sniper Rifle (Timberwolf)	Match B406	RP15/LAPUA	0.03	0.001

[1] NA: not available. [2] Based on a mean percentage of 10% NG in the C21 (*19*).

Gas Residues

During combustion of the gun propellant, gases and particulate matter are produced at the gun muzzle and at the upper receiver. Gas analyses are shown in Table 3. Only a few of the selected gaseous compounds (polycyclic aromatic hydrocarbons, benzene, toluene, ethylbenzene, xylenes, total cyanides, nitrates, and aldehydes) were detected. For the 9-mm pistol, none of the selected gases were detected. In the case of the C6 machine gun, cyanide, acrolein, 2,4-DNT, and benzene were detected. A similar situation was observed for the C7 rifle: cyanide, acetaldehyde, and acrolein were detected.

Table 3. Gas analysis of air samples collected at the muzzle and the upper receiver of the gun

Weapon/cartridge	*Position*	*Compound detected*	*Concentration mg/m³*
Browning pistol 9 mm, MK1, ball	Muzzle of the gun	None	---
	Upper receiver	None	---
C6 Machine gun 7.62 mm, C21/C19, ball	Muzzle of the gun	Total cyanide	0.13
		Acrolein	0.002
		2,4-DNT	6×10^{-6}
	Upper receiver	Total cyanide	0.89
		Benzene	0.11
		Acrolein	0.004
C7 Automatic rifle 5.56 mm, C77, ball	Muzzle of the gun	None	---
	Upper receiver	Total cyanide	2.4
		Acetaldehyde	0.035
		Acrolein	0.023

Airborne Solid Residues

Monitoring cassettes with filters were inspected visually in order to make a qualitative evaluation of the particles collection. As seen in Figure 4a, the monitoring cassettes after the firing of the 500 cartridges 9 mm MK1 ball, with the Browning pistol have a very different appearance if they were positioned at the muzzle of the gun (Figure 4a, left) or at the upper receiver (Figure 4a, right). The filter at the muzzle of the gun is of light grey color while the filter at the upper receiver is still white. Obviously, the number of particles collected at the muzzle is higher. Figure 4b shows the monitoring cassettes after the firing of 800 7.62-mm cartridges, C21/C19, with the C6 machine gun, and Figure 4c shows the filters after the firing of 450 5.56-mm cartridges, C77, with the C7 automatic rifle. In both cases, the number of particles was higher at the upper receiver (cassettes

on the right hand side) than at the muzzle of the gun (cassettes on the left hand side). The presence of the enclosure bag was certainly the cause of this efficient collection of particles. The lower number of particles for the 9-mm pistol trial can be explained by the absence of the enclosure bag, and also by the fact that the ammunition used contained a lower mass of propellant.

All of the filters from the monitoring cassettes located at the muzzle and at the upper receiver of the guns were analyzed by SEM. The results of all calibersare summarized in Table 4. Figures 5 and 6 show typical micrographs of particles obtained at the muzzle and the upper receiver for the calibrer9 mm. The analysis of the particles emitted from the cartridges 9 mm fired with the Browning Pistol indicate that lead was the main component of the particles smaller than 1 μm (both sampling positions). Most particles collected after the firing with the C6 were also smaller than 1 μm and composed of copper and lead. The particle analysis showed that copper was the main component of particles sampled near the muzzle, while at the upper receiver, it was lead. A similar situation was observed for the cartridges 5.56 mm C77 fired with the rifle C7.

Discussion

At first glance, the reported amounts of unburned NG per round can be seen as low, and the burning efficiency, pretty high. However, artillery rounds generally have higher burning efficiencies (0.0005 to 0.08% of unburned NG per bullet) than small arms (*6*); the burning efficiency of mortars (1.4 to 3.5% of unburned NG per round) is either similar to or lower than that of small arms. Moreover, the large number of bullets fired on small arms ranges has to be taken into account to evaluate the impact on the environment. For example, on a small arms range, on which were fired approximately 0.5M cartridges 5.56 mm (ball) per year since 1996, the calculated amount of NG deposited on the soil surface is 150 g per year. With the hypothesis that all of the rounds were fired from the 100-m berm to the 400-m berm in a 75 000-m^2 area, and using a soil density of 1.7 g/cm^3, the concentration of NG on the top 2-cm of surface soil should be approximately 0.06 mg/kg. Reported concentrations on the 100-yard firing berm were three orders of magnitude higher than those of Jenkins et al. (*3*), but they tended to decrease after 15 m. Nevertheless, none of the results went below 0.1 mg/kg up to 40 m in front of the firing point, and the mean NG concentration was 8.8 mg/kg. Instead, if Walsh's values of 1.1% per cartridge and a 1-cm sampling depth are used, the loading rate is 0.7 mg/kg/yr, which is closer but still lower than the reported concentrations of NG. Of course, other munitions were also fired on that range, but they amounted to less than 4% of the total number of rounds fired, including cartridges 7.62 mm (1.4%), cartridges 5.56 mm, linked (1.4%) and cartridges 9 mm (0.3%). The results thus tend to indicate that NG has a significant cumulative effect. However, care has to be taken when interpreting these soil surface characterization results because only 12% of the entire surface was sampled, and no depth sampling was done.

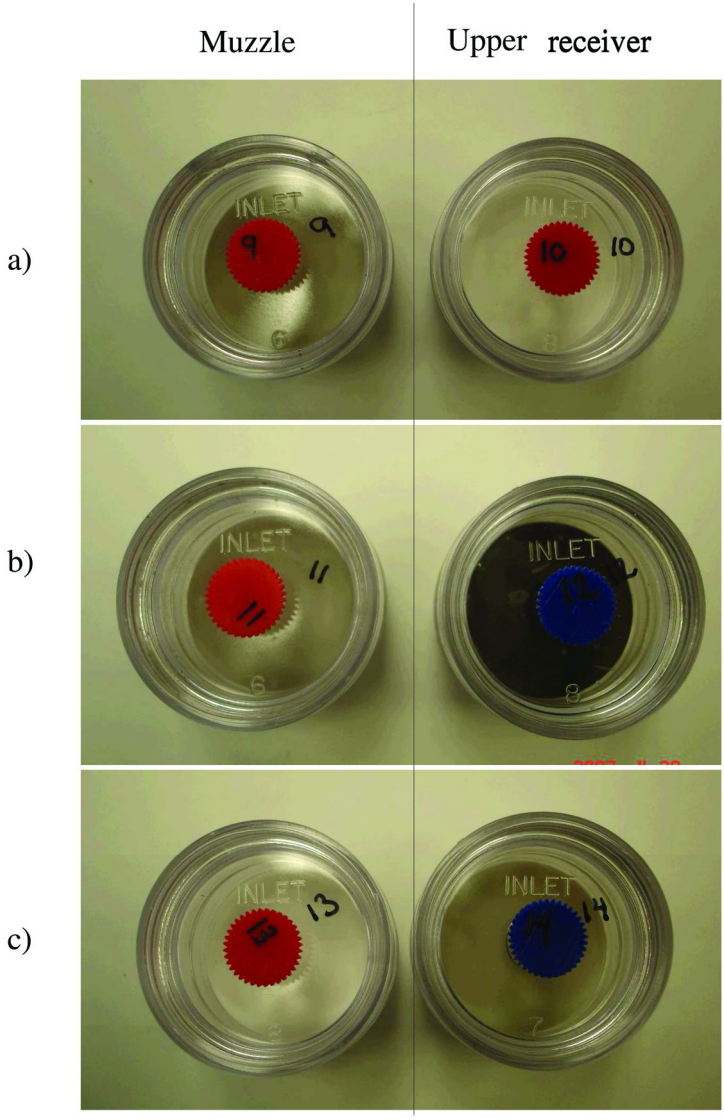

Figure 4. Monitoring cassettes (left: muzzle of the gun, right: upper receiver) a) After sampling 500 9-mm cartridges, MK1, ball, with the Browning pistol; b) After sampling 880 7.62-mm cartridges, C21/C19, ball, with the C6 machine gun; c) After sampling 450 5.56-mm cartridges, C77, ball, with the C7 automatic rifle. (see color insert)

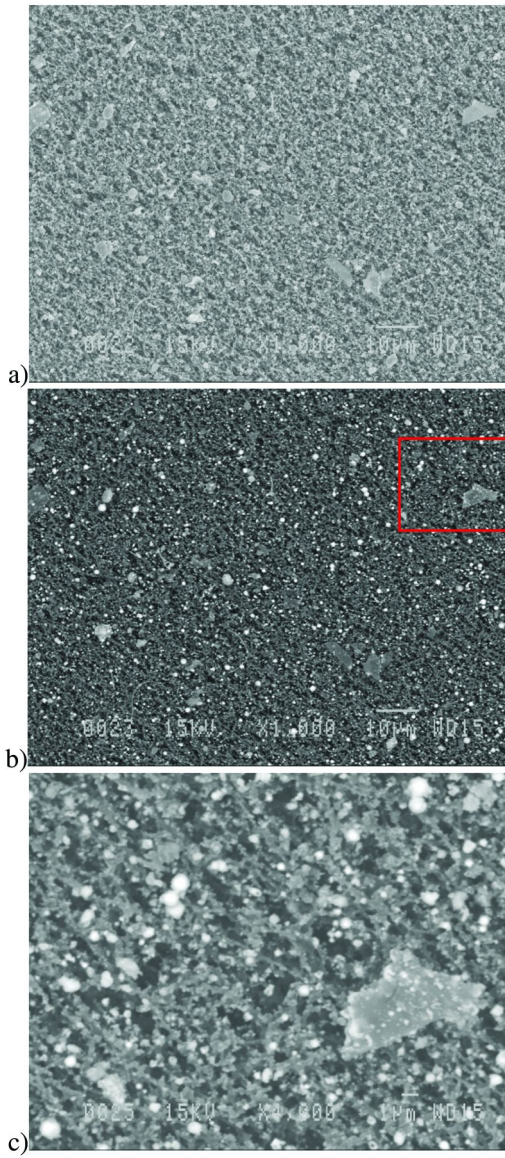

Figure 5. Micrographs of particles collected on filter #9 (muzzle of the 9-mm pistol); a) SE 1000x magnification, b) BEI 1000x, c) BEI 4000x, zoom of the red-squared region.

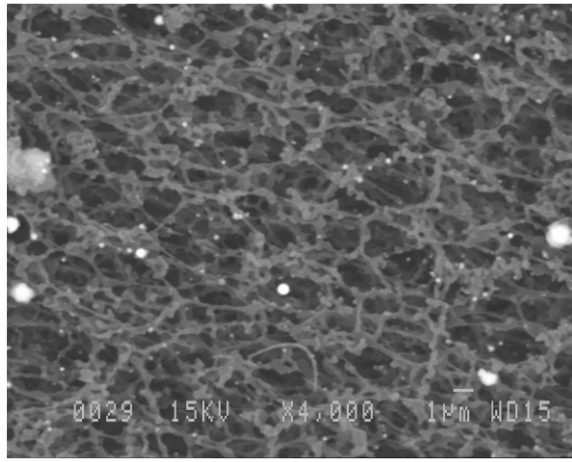

Figure 6. Micrograph of particles collected on filter #10 (upper receiver of the 9-mm pistol) (BEI 4000x magnification).

The same calculation was applied to another small arms range. This time, the entire surface of the range was sampled using the multi-increment approach as described in EPA Method 8330b (*7*) because of it small size (1250 m^2). The calculated loading from the amount of unburned NG per round using an average of 70,000 cartridges 9 mm fired each year led to a deposit of 52 g NG on the soil each year. However the estimated loading from surface soil characterization of the top 2cm gives an amount of NG that is slightly over 1 kg, which corresponds to a 20-year accumulation. This does not take into account the contaminants below the soil surface, because no depth profiling was done. So, either the amount of unburned NG per round is grossly underestimated, or there is a significant cumulative effect of NG in the environment. Although the amount of NG is certainly slightly underestimated, the long-term persistency of NG is not unexpected, because it is embedded in a nitrocellulose (NC) matrix, which is insoluble in water and does not degrade. NC can thus stay a very long time on the surface of the soil, and is probably trapping NG (*9*).

Another discrepancy between soil surface characterization and the results of this study is worth noting. Indeed, energetic residues were detected up to 40 m in front of the firing points, while in this study residues do not get farther than 12 m from the muzzle of the gun. Several hypotheses could explain this phenomenon. This could be the result of a multi-decade use that allowed the NG concentrations to build-up until high enough for detection. It could also be the result of runoff water carrying particles far from their ejection point, or be due to dominant wind that could blow in a direction that is parallel to the firing lanes. The hypothesis of soldiers firing between berms is considered improbable because this has not been the usual military practice for the last three decades, except for the 100-m berm. Older military practices are unknown.

Table 4. Comparison of the particulate matter collected with the monitoring cassettes for different weapons/cartridges

Weapon/cartridge	*Sampling position*	*Proportion*	*Particle Size*	*Composition*	*Morphology*	*Source*
Browning Pistol #2, cartridges 9 mm, MK1, ball	Muzzle of the gun	Majority	< 3 µm, majority < 1 µm	Pb	Spherical	Pb: vaporization of the primer, followed by its solidification as small particles
		Minority	3-10 µm	C and Pb	Irregular and fractured (probably soot)	
	Upper receiver	Majority	≤ 1µm	Pb	Spherical	Pb: vaporization of the primer, followed by its solidification in small particles
Machine gun C6, cartridges 7.62 mm, C21, ball (weapon enclosure bag)	Muzzle of the gun	Majority	100 nm - 3 µm	Cu (+ traces of Sr and Pb)	Spherical	Cu: erosion of the cartridge inside the gun Sr: tracer composition
		Minority	5 µm	C and O	Flaky and irregular (probably soot)	Cu: erosion of the cartridge case inside the barrel of the gun
	Upper receiver	Majority	< 1 µm	Pb (+ traces of Sb, Cu, Ca, K, C and O)	Spherical	Sb and Pb: priming composition (Type C) Cu: erosion of the cartridge inside the gun K: propellant composition
		Minority	1-5 µm		Flaky and irregular	

The particle analysis for the three calibers under study showed that copper was the main component at the muzzle, while at the upper receiver, it was lead. It is not believed that the bullet can liberate any lead during its propulsion out of the gun because it is covered with a copper/zinc jacket. Rather, the main source for lead on the filters was probably the primer: lead was vaporized during the firing and was condensed shortly afterward in small particles. These particles may be carried by the winds, spreading lead in areas other than the firing point. This assumption has to be confirmed by further studies. At the upper receiver, particles collected are from the combustion of the primer. The main source of copper is probably the erosion of the cartridge inside the barrel. As these particles (created by the melting of the metal followed by its subsequent condensation on cooling), were following the trajectory of the bullet, it is normal that they are mainly ejected at the muzzle of the gun. The erosion of the cartridge seemed to become significant enough that particles of copper are found for longer barrels (C6 machine gun and C7 automatic rifle).

Conclusion

In this study, 23 trials were performed with 15 different calibers/weapons (including duplicate and triplicate), and three of them were air-sampled to measure selected airborne gases and particles. The results indicated that up to 2.03 mg NG/round was deposited. This makes the burning efficiency of most SA better than that of mortars, but less than that of artillery. Although the amount of dispersed NG per bullet seems low, the large amount of small calibre ammunition used in training can lead to significant accumulation on the surface of the soil, especially since SA ranges are small.

Only a few of the selected gaseous compounds were detected. Cyanide and acrolein were detected for both the 7.62- and 5.56-mm rounds. The use of an enclosure bag over the weapon improved the efficiency of particles and gases collection by reducing the dilution with the surrounding air, especially when winds were present. Most airborne particles collected were smaller than 1 μm and made of Pb (lead) and Cu (Copper). The concentrations reported are not representative of the soldier exposure since the sample collection was not made in the breathing zone.

The study of these results will lead to a better understanding of the burning mechanisms for a specific propellant under various conditions. This will help decision-makers in developing improved management tools for outdoor military training ranges.

References

1. ITRC Small Arms Firing Range Team. *Characterization and Remediation of Soils at Closed Small Arms Firing Ranges*; Interstate Technology and Regulatory Council, 2003 http://www.itrcweb.org/gd_smart.asp.

2. ITRC Small Arms Firing Range Team. *Environmental Management at Operating Outdoor Small Arms Firing Range*; Interstate Technology and Regulatory Council, 2005. http://www.itrcweb.org/gd_smart.asp.
3. Jenkins, T. F.; Hewitt, A. D.; Walsh, M. R.; Walsh, M. E.; Bailey, R. N.; Ramsey, C. A.; Bigl, S. R.; Lambert, D. J.; Brochu, S.; Diaz, E.; Lapointe, M.-C.; Poulin, I.; Faucher, D. *Chapter 8: Accumulation of Propellant Residues at Small Arms Firing Points, in Characterization and Fate of Gun and Rocket Propellant Residues on Testing and Training Ranges: Final Report*; ERDC TR-08-1; U.S. Army Engineer Research and Development Center, Cold Regions Research and Engineering Laboratory, 2008.
4. Bach, J. C.; Conway, B. E.; Mulligan, S. B.; Watts, K. A. U.S. Army Environmental Center's Development of AP-42 Emission Factors for Munition Use. *15th International Emission Inventory Conference - Reinventing Inventories - New Ideas in New Orleans*; New Orleans, 2006.
5. Faucher, D.; Brochu, S.; Poulin, I.; Walsh, M. R. *Chapter 5: Assessment of Gaseous and Particulate Propellant Residues Resulting from Small Arms Live Firing, in Characterization and Fate of Gun and Rocket Propellant Residues on Testing and Training Ranges: Final Report*; ERDC TR-08-1; U.S. Army Engineer Research and Development Center, Cold Regions Research and Engineering Laboratory, 2008.
6. Walsh, M. R.; Walsh, M. E.; Bigl, S. R.; Perron, N. M.; Lambert, D. J.; Hewitt, A. D. *Chapter 3: Propellant Residues Deposition from Small Arms Munitions, in Characterization and Fate of Gun and Rocket Propellant Residues on Testing and Training Ranges: Final Report*; ERDC TR-08-1; U.S. Army Engineer Research and Development Center, Cold Regions Research and Engineering Laboratory, 2008.
7. U.S. Environmental Protection Agency. *Nitroaromatics and Nitramines by High Performance Liquid Chromatography (HPLC)*; SW-846 Method 8330B; 2006 http://www.epa.gov/epaoswer/hazwaste/test/pdfs/8330b.pdf.
8. Walsh, M. R.; Walsh, M. E.; Bigl, S. R.; Perron, N. M.; Lambert, D. J.; Hewitt, A. D. *Propellant Residues Deposition from Small Arms Munitions*; ERDC/CRREL TR-07-17; U.S. Army Engineer Research and Development Center, Cold Regions Research and Engineering Laboratory, 2007.
9. Thiboutot, S.; Ampleman, G.; Gagnon, A.; Marois, A.; Martel, R.; Bordeleau, G. *Persistence and Fate of Nitroglycerin in Legacy Antitank Range*; Unclassified, DRDC Valcartier Report, TR 2010-059, June 2010.
10. DND. Data Summary, Pistol, 9 mm, Browning FN, HP, No 2 MK 1, CFTO C-71-107-000/MA-000, 2000.
11. DND. Data Summary, Pistol, 9 mm, Sig Sauer, Model P225, CFTO C-71-318-000/MA-000, 1999.
12. DND. Data Summary, Machine gun, GMPG, 7.62mm, C6, C-71-267-000/MA-000, 2003.
13. DND. Data Summary, Rifle, 5.56 mm, Automatic, C7 and C7A1, C-71-295-000/MA-000, 1998.
14. DND. Data Summary, Carbine, 5.56 mm, Automatic, C8, C-71-294-000/MA-000, 1998.

15. DND. Data Summary, Machine-gun, Light, 5.56 mm, C9 and C9A1, C-71-296-000/MA-000, 2003.
16. DND. Data Summary, Machine-gun, Heavy, Flexible, .50 Calibre, M2HB, QCB, C-71-159-000/MA-000, 2001.
17. DND. Rifle, Sniper, .50 Calibre, McMillan, Tactical, C-71-348-000/MA-001, 2005.
18. PGW Defence Technologies Inc. http://pgwdti.com.
19. DND. Cartridge 7.62 mm. All Types, C-74-305-NA0/TA-000, 1985.

Chapter 3

Canadian Approach to the Environmental Characterization and Risk Assessment of Military Training

S. Brochu,[1,*] S. Thiboutot,[1] G. Ampleman,[1] E. Diaz,[1] I. Poulin,[1] and R. Martel[2]

[1]Defense R&D Canada – Valcartier, 2459 Pie-XI Blvd North, Quebec (Qc) G3J 1X5, Canada
[2]Institut National de la recherche scientifique, Centre - Eau Terre Environnement, 490, rue de la Couronne, Québec (Québec) G1K 9A9, Canada
[*]Sylvie.brochu@drdc-rddc.gc.ca

The main goal of Canada's sustainable military training program is to maintain force generation and environmentally-friendly defense activities in order to ensure the long-term usage of military training areas. This paper will describe Canada's approach to the characterization of ranges and training areas, and also to perform appropriate risk assessments.

Literature Review

The Canadian sustainable military training R&D program, in agreement with the Sustainable Development Strategy promulgated by the Department of National Defence (DND) (*1*), is aimed at maintaining both military readiness and environmentally-friendly defence activities in order to ensure the long-term usage of military training areas. Moreover, as with many other countries, Canada has to deal with growing public concerns about environmental issues and is facing more stringent environmental laws. Indeed, the Fisheries Act (*2*) prohibits *any work or undertaking that could result in the harmful alteration, disruption or destruction of the fish habitat* by introducing deleterious substances in water, while the Canadian Environmental Protection Act (*3*) is concerned with pollution prevention and toxic substances releases. In addition, several compounds commonly found in military training areas are regulated by the

Canadian Council of Ministers of the Environment (CCME) guidelines (*4*). Some of these compounds are also on the list of priority substances of the ARET program (Accelerated Reduction/Elimination of Toxics) that promulgates the voluntary reduction or near-elimination of the release of some of the most persistent, bioaccumulative and toxic substances in the environment (*5*). The U.S. Department of Defence (DoD), together with the Environmental Council of the States (ECOS) Sustainability Working Group and the Environmental Protection Agency (EPA), is also closely monitoring some emerging contaminants on military sites that could have a significant impact on DoD personnel and activities (*6*).

Within this context, Defence R&D Canada – Valcartier (DRDC Valcartier) initiated in the mid 90's a research program for the environmental assessment of the main ranges and training areas (RTAs) of the Canadian Forces (CF). Many studies, supported by Director Land Environment (DLE) Canada and Director General Environment (DGE) Canada have been conducted since then to better understand the nature and extent of contamination in RTAs (*7–38*).

In 2000, a six-year research project (ER-1155) was initiated by the U.S. Army Engineer Research and Development Center, Cold Regions Research Engineering Laboratory (CRREL, Hanover, U.S.) in collaboration with DRDC Valcartier under the Strategic Environmental Research and Development Programme (SERDP, Arlington, VA). The aim of this project was to study the deposition, accumulation, and fate of residues of energetic compounds at live-fire training ranges to determine the source terms for energetic contaminants. SERDP project ER-1155 was focussed on impact areas where cyclo-1,3,5-trimethylene-2,4,6-trinitramine (RDX) was deposited and thus where the potential for groundwater contamination was the largest. A significant part of this work was performed in Canadian RTAs. SERDP project ER-1155 allowed the development of transport processes descriptors for the current explosives and their main transformation products (*39–65*). A protocol for the characterization of sites contaminated with energetic materials was written in 2003 under the umbrella of The Technical Cooperation Program (TTCP) (*66*). In 2009, EPA method SW-846 8330, used for the analysis of energetic materials, was updated to include sampling and processing methods (*67*), leading to EPA method 8330b (*68*).

Finally, SERDP project ER-1481 was initiated in 2006 to better understand the fate and transport of propellant residues at firing points (*69*, *70*). Several studies have been performed on DoD and DND RTAs to better define the distribution and fate of propellant residues associated with live-fire training with munitions (*71–91*).

Background Information

Contaminants of Concern

Accurately detecting the type and quantity of contamination of munitions materials and their breakdown products in water, soil, sediment and biomass is vital to assessing the extent of contamination and ultimately the risk to human and ecological receptors. The contaminants of concern that might be dispersed

in the environment following live fire training are energetic materials, their decomposition products and metals.

Energetic Materials

Conventional weapons use energetic materials (EM) in the form of propellants, explosives, and pyrotechnics. A brief description of each type of EM is given below.

Explosives are classified as 'primary' or 'secondary' based on their susceptibility to initiation. Primary explosives, which include lead azide, lead styphnate, and mercury fulminate, are highly susceptible to ignition and are often referred to as initiating explosives, since they can be used to ignite secondary explosives.

Secondary explosives are much more prevalent on military sites than primary explosives. They include trinitrotoluene (TNT), 1,3,5-hexahydro-1,3,5-trinitrotriazine or research development explosive (RDX), octrahydro-1,3,5,7-tetranitro-1,3,5,7-tetrazocine or high melting explosive (HMX), and 2,4,6-trinitro-phenylmethylnitramine or tetryl. Since they are formulated to detonate under specific circumstances, secondary explosives are often used as main charges or boosting explosives.

Secondary explosives fall into two main categories: (1) melt-cast explosives, based primarily on TNT, and (2) plastic-bonded explosives (PBX), which consist of a polymer matrix filled with a crystalline explosive such as RDX. Secondary explosives can also be classified according to their chemical structure. For example, TNT and trinitrobenzene are classified as nitroaromatics, whereas RDX and HMX are nitramines. The major classes of EM used by the military personnel throughout the world as well as their physical and chemical properties are reported in (*66*).

Propellants include both rocket and gun propellants. Most rocket propellants consist of a rubbery binder filled with an ammonium perchlorate (AP) oxidizer and sometimes powdered aluminum as fuel. Propellants may also be based on a nitrate ester, usually nitroglycerine (NG), nitrocellulose (NC), or a nitramine such as RDX or HMX. Gun propellants are usually single base (e.g., NC), double base (e.g., NC and NG), or triple base (e.g., NC, NG, and nitroguanidine (NQ)). Single-based propellants may also contain 2,4-dinitrotoluene (2,4-DNT) as an energetic plasticizer.

Pyrotechnic compositions are usually homogenized mixtures of small particles of fuels and oxidizers. High burning rates are obtained with particles of high surface area or high oxidizer content. Binders are sometimes used to turn the powder into a solid material. Typical fuels are based on metal or metalloid powders. Common fuels include metals (aluminum, magnesium, iron, zirconium, titanium, manganese, zinc, copper, tungsten, antimony, arsenic, etc), organic materials and polymers. Oxidizers are usually made of perchlorates, chlorates or nitrates. Several addititives, both organic and inorganic, also act as opacifiers, colorants, flame suppressants, catalysts, stabilizers, anticaking agents, binders, plasticizers, curing or bonding agents.

Metals

The metallic composition of the shells and fusing system is generally proprietary information, and therefore little information is known about the proportion of heavy metal in a given munition. Most shells are made of steel, which is an alloy of iron and carbon, with several other metals added to modify their mechanical properties. Grenade shells are generally made of brass, an alloy of zinc and copper. Small arms bullets are made of a lead-antimony core contained in a brass jacket. However, other types of ammunition are made of several other metals, as shown by the large variety of metallic species detected in RTAs.

Issues and Sources of Munitions-Related Residues

Energetic Materials

It is now well known that normally functioning munitions (i.e. high order detonation) only spread about 0.001% of their explosive content in their surrounding environment (*59–65*). Therefore, most of the contamination in impact areas comes from UXOs that are cracked open by the detonation of an incoming round, by incomplete (low-order) detonations, by the destruction of duds using blow-in-place options, or by the corrosion of UXOs. In addition, UXOs pose a safety problem for troops, both in domestic training and in operations. A regular surface clearance of RTAs is often needed to get rid of surface UXOs. Additional UXO-related issues arise at the closure or decomissionning of RTAs, such as safety problems for the civilian population, huge costs of UXO detection and clearance operations, as well as government liability.

The most widespread compound of concern in impact areas is unexploded or deflagrated RDX, a common explosive found in Composition B and C4. RDX does not degrade in soil and, because of its solubility in water, has the potential to migrate easily to groundwater and outside the boundaries of military bases. This could trigger a serious environmental problem and even become a public health concern if the groundwater is used for crop irrigation or as drinking water.

Another ecological issue arises from the incomplete combustion of gun propellant in weapons and from the expedient burning of excess gun propellant bags on the soil at firing positions. Propellants contain significant amounts of carcinogenic and toxic components, some of which have recently been forbidden in Europe. Gun propellant residues, mainly nitroglycerin and 2,4-dinitrotoluene, are routinely detected at several firing positions of small, medium and large calibre ammunition.

Metals

Unlike energetic materials, metals are not destroyed during the detonation process. During the detonation, each component of the fuzing system and the projectile are disintegrated into fragments of various sizes and dispersed in the environment. Usually, the higher the order of detonation, the smaller the

fragments. Small fragments have a high surface area and are much more prone to be transported away from the impact area through corrosion and dissolution or dispersion in water, or by wind erosion. Consequently, small fragments are those that have the potential to cause the greatest effect on the environment.

Impacted Sites

The most contaminated ranges are usually the smallest sites (demolition, small arms, grenade and anti-tank ranges, and firing positions), on which an accumulation of contaminants can occur. However, artillery impact areas also represent a significant challenge from the perspective of contamination, characterization and remediation. Demolition ranges, on which obsolete ammunition is destroyed by open burning or open detonation and where various demolition activities are practiced, are usually highly contaminated with explosive and propellant residues along with heavy metals. The small arms ranges contain high concentrations of lead, antimony, copper and zinc in the bullet stop berms, and of propellant residues at the firing positions. The grenade ranges are typically characterized by a mixed contamination of explosive residues, copper and zinc. HMX accumulates around targets in the impact area of anti-tank ranges, while propellant residues are preferentially located at firing positions. References (*69–87*) report the proportion of gun propellant that does not burn completely in the guns during the live firing of specific military ammunitions.

Environmental Fate

A thorough knowledge of the bioavailability, degradation pathways, toxicity and transport properties of munitions-related residues and of their metabolites is crucial to understand their environmental fate and to design appropriate remediation strategies.

Energetic Materials

The environmental fate of energetic materials is mainly related to their water solubility, their adsorption to soil particles and their biotic and abiotic transformations. For instance, TNT is more soluble and dissolves more rapidly in water than RDX or HMX (HMX being the least soluble) (*92*). In addition, TNT tends to degrade by photolysis, while RDX and HMX do not. The metabolites of TNT all have various solubilities and toxicities. For example, the aminodinitrotoluenes that result from the photolysis or biodegradation of TNT are much more soluble than the parent compound, but they can covalently bind to humic acid. Therefore, these metabolites are stabilized by the formation of an amide with the organic content of the soil. Moreover, in soils that contain clays, the sorption mechanisms are stronger with TNT and its metabolites than for RDX and HMX, which adsorb very poorly to clay minerals. Therefore the relative rates of soil leaching of these three explosives can be explained in terms of the relative water solubilities and adsorption strengths: TNT and its metabolites are more

soluble than RDX, but their migration is inhibited by strong bonding interactions with soil constituents. Therefore, RDX leaches out faster than TNT, which in turn leaches out faster than HMX. However, HMX has a tendency to remain at the surface of the soils, because it is almost insoluble in water.

Interactions with the soil are also important factors to consider when characterizing munitions-related residues in terms of bioavailability and extractability. TNT is particularly difficult to characterize because it is easily reduced to amino degradation products, namely 2- and 4-amino-dinitrotoluene (ADNT), 2,4- and 2,6-diamino-nitrotoluene (DANT), and, under anaerobic conditions, 2,4,6-triaminotoluene (2,4,6-TAT).

The characterization of the degradation products of energetic materials is important in establishing their overall toxicity, remediation, transport, and extractability. The adsorption and desorption characteristics of TNT and its metabolites are important physical factors to consider when assessing the availability of the compounds to microbial degradation and physical analysis.

Metals

The fate and transport of heavy metals in the environment depends strongly on their solubility in water and their bioavailability, i.e. their capacity to bind to the soil constituents. A compound with a high solubility and a low binding capacity has a higher mobility and presents a larger potential for leaching in groundwater and/or travel far away from the range. However, a compound having a low solubility will most probably stay on the surface of the soil, and a compound with strong binding affinities will most probably stay either on the surface or in the subsurface, where a specific bonding agent is encountered.

The water solubility of heavy metals in their elemental state is generally low. However, heavy metals do not generally remain in their elemental form when they are exposed to weathering and water. They are easily oxidized in their ionic form and will form various oxides and salts with soil constituents, each having a different solubility and bioavailability.

As a general rule, nitrates, chlorides, bromides and acetates are readily soluble in water, and sulphides are considered to be insoluble. However, the solubility of hydroxides, sulphates, phosphates, and carbonates will vary depending on the heavy metal component, and on the pH of the water. The lowest solubilities are generally observed in neutral pH water (6.5 to 7.5). Acidic water ($pH < 6.5$) tends to increase the solubility of most metals salts, while basic water ($pH > 7.5$) will either induce the precipitation and immobilisation of an insoluble heavy metal compound, or increase its solubility, depending on the heavy metal. Thus, extreme caution must be exercised when trying to decrease the leaching of soils containing multiple heavy metals by controlling the pH of the soil, because the solubility of some heavy metal compounds may increase when exposed to basic pH.

Key parameters governing the bioavailability of a given heavy metal compound are (1)the composition (organic matter, metallic constituents) and pH of the soil, (2)the particle size distribution, and (3)the contact time between water and the heavy metal compound. These parameters govern in turn measurable

macroscopic parameters, such as the type of soil (sand, silt, clay, etc.), the cation exchange capacity (CEC), and the reduction-oxidation (redox) potential.

The binding capacity tends to increase with the decrease in size of soil particles. For example, absorption in clay is much higher than in sand because the groundwater movement in clay is slower, and also because of the high surface area of soil particles to which heavy metal compounds can bind. In consequence, sandy soils present the highest leaching potential.

The contact time between water and the heavy metal compounds is controlled by the amount of annual precipitation and intensity of the rainfall . The adsorption of several heavy metal compounds to soil components also tends to increase with the cation exchange capacity. The redox potential will affect the type of heavy metal compound that is stable in a given area. The bioavailability of heavy metals and factors affecting it is a very complex subject, and a thorough review is beyond the scope of this document. Interested readers may consult appropriate references for more information.

The mobility of heavy metals is also affected by external physical factors, such as the topographic slope and the intensity of wind. Particles of heavy metal compounds or dissolved heavy metals can be moved by storm water runoff. The ability of water to transport lead is influenced by two factors: velocity of the water and weight or size of the lead fragment. Water's capacity to carry small particles is proportional to the square of the water's velocity (*92*). Clear water moving at a velocity of 100 feet per minute can carry a lead particle 10,000 times heavier than water, moving the particle at a velocity of 10 feet per minute. Muddy water can carry even larger particles. A shallow groundwater table is indicative of potentially higher risk for mobilized heavy metals to reach the groundwater. The shorter the distance traveled, the greater the risk of migration of heavy metals into the environment.

Characterization Approach

The characterization of munitions-related residues poses a significant challenge because of the local and distributional heterogeneity of the distribution of contaminants, and also because of the large diversity of military activities. The large sizes of RTAs (impact areas can reach 10 to 20 km^2, and bombing areas are much larger than that) also pose a significant challenge for the characterization. It is indeed not possible to obtain samples that are representative of the mean concentration of a whole area.

The characterization approach developed by DRDC Valcartier is to perform the soil surface study concurrently with a detailed hydrogeological study of the site. This approach is carried out as part of a collaborative effort with the *Institut national de la recherche scientifique - Centre Eau, Terre et Environnement* (INRS-ETE). Soil sampling is performed using a multi-increment composite sampling strategy and a systematic/random sampling design specifically adapted to each range, depending on the type of activity occurring on the site. This approach is illustrated in Figure 1; more details can be found in (*66*).

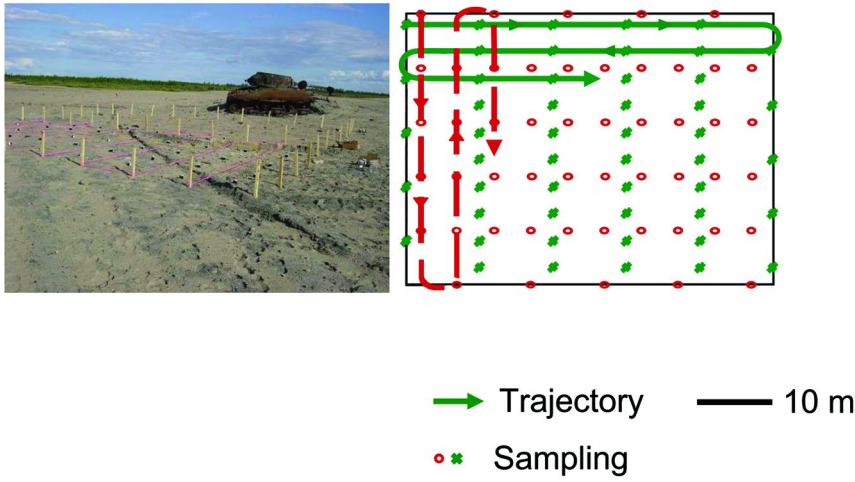

Figure 1. Soil sampling strategy illustrating a systematic sampling design. (see color insert)

Hydrogeology typically provides detailed information on the quality and flow direction of surface water and groundwater, on the water table depth and on the various types of soil on which the ranges are built. The hydrogeological data collected lead to the preparation of several thematic maps (piezometric, surficial geology, etc.), two of which are shown in Figures 2 and 3. The following step is the modeling of groundwater flow. This step is generally performed using a numerical model, such as FEFLOW, which uses input parameters such as piezometry, hydraulic conductivity of the various stratigraphic units, recharge with the HELP model, 3D geological model, etc. This model allows the reproduction of the behaviour of the groundwater at regional and local scales, and the prediction of the transport of contaminants. This is a parameter extremely important to have in order to perform risk analyses of the ecological and human receptors surrounding RTAs. A conceptual model is then built following the 3D geological model and from the knowledge of the environmental fate of energetic materials in the environment. Several monitoring wells are necessary to build a precise conceptual model, to validate this model, and to adequately follow potential contamination in the groundwater. Canada, which has installed several hundreds of monitoring wells in its RTAs, has developed a very proactive military site assessment approach and acts as a world leader in this domain.

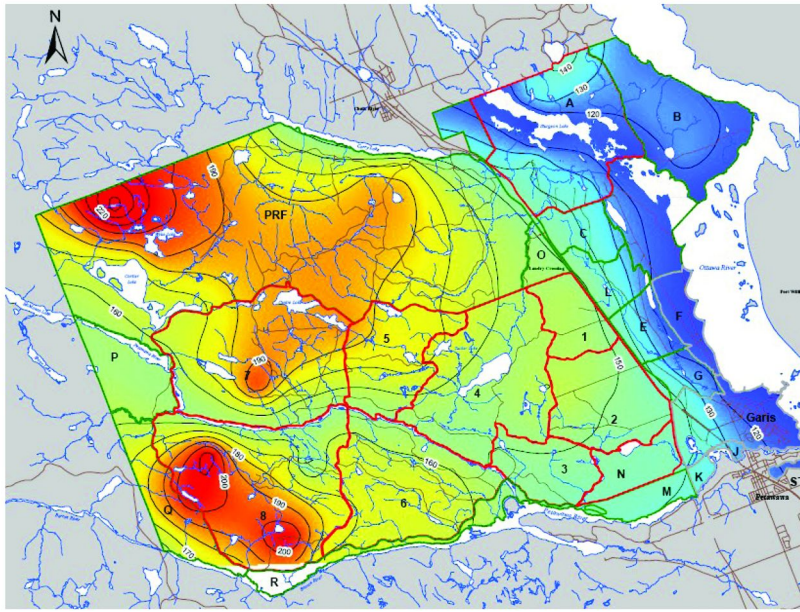

Figure 2. Piezometric map. (see color insert)

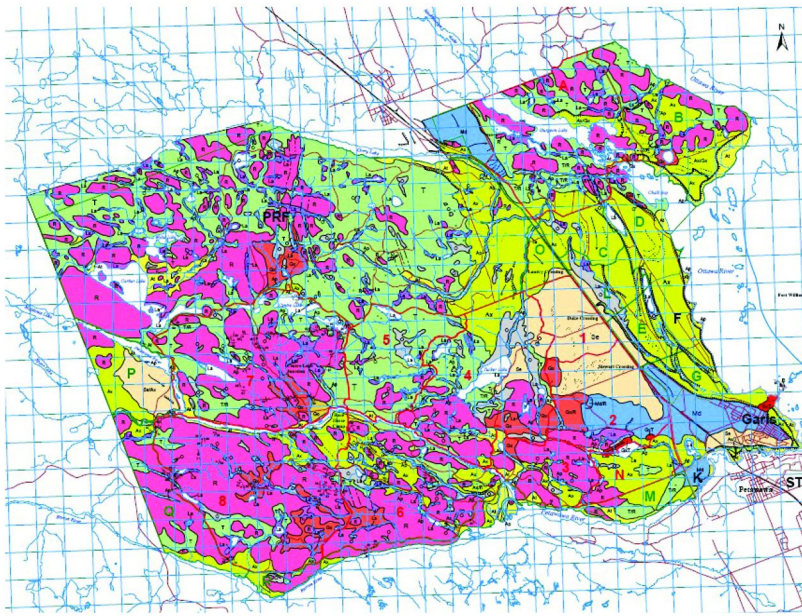

Figure 3. Surficial geology map. (see color insert)

Ecological Risk Assessment

Risk is defined as the probability of an adverse event due to disturbances in the environment:

Risk = Severity of event (Hazard) x Exposure

The Ecological Risk Assessment (ERA) of RTAs will attempt to estimate and, where possible, quantify risk posed to the environment and its non-human inhabitants by the presence of munitions-related residues concentrations. It is a complex process involving the participation of a team of professionals with expertise in various disciplines (chemists, munitions specialists, toxicologists, ecologists, hydrogeologists, environmental fate and transport modeling specialists). This ambitious R&D program has been realized by a long-term partnership of DRDC Valcartier, INRS-ETE, and the Biotechnology Research Institute (BRI) of the Canadian National Research Council. The ERA of RTAs involves the following steps:

- Receptor Characterization
- Exposure Assessment
- Hazard Assessment
- Risk Characterization

The Receptor Characterization attempts to identify the ecological (non-human) receptors of concern, the effects against which it is desirable to protect those receptors, and the means or pathways specific to each receptor by which it may come into contact with contaminants (*93*). This part of the process is carried out by BRI which performs state-of-the-art R&D to evaluate the effect of energetic materials on terrestrial plants, terrestrial animals, soil microorganisms and aquatic species (*94–157*). BRI also studies the degradation of energetic materials through biotic and abiotic pathways, phytolysis, and chemical degradation. One significant output of their R&D program was the development of the first worldwide ecotoxicological criteria specifically developed for a military scenario (*151*).

The Exposure Assessment, defined as the evaluation of the potential exposure of the receptors to munitions-related residues, is dealt with using vulnerability maps which reflect the vulnerability of a given aquifer-to- surface contamination and the risks related to soil contamination by residues of energetic materials.

Aquifer vulnerability can be assessed with a method that uses the hydrogeologic properties of the area (infiltration, porosity, permeability, etc.) obtained through the 3D geologic modeling, to estimate the downward advective time (DAT) of travel for infiltration water in the vadose zone from the surface to the water table of the first aquifer.

Vulnerability maps describe the relative ease with which dissolved contaminants reach the upper boundary of an aquifer from land surface by vertical transport/migration, advection, non-retarded, non-reactive transport. It is basically the time it takes a drop of water to travel from the surface of the soil

to the groundwater table. The output is translated into vulnerability maps, an example of which is shown in Figure 4.

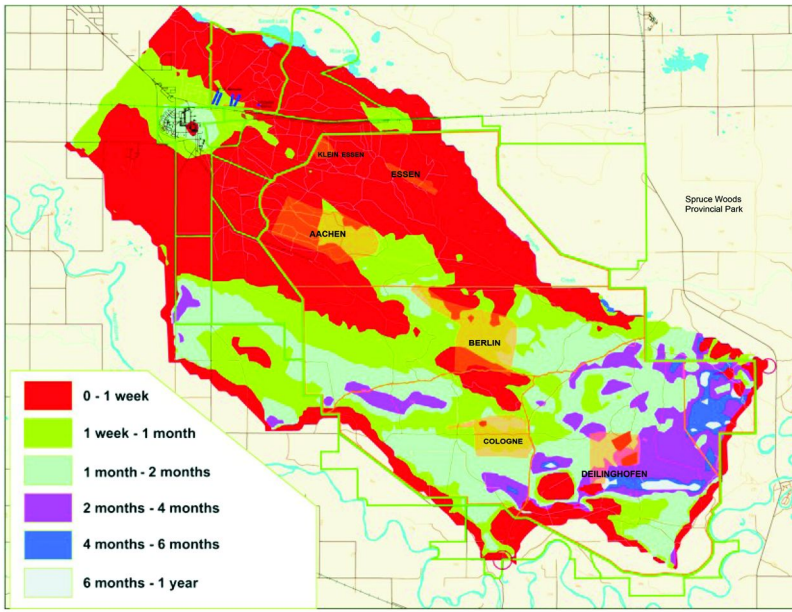

Figure 4. Vulnerability map. (see color insert)

Hazard Assessment is the process of determining the potential for munitions-related residues to cause adverse effects in exposed individuals or populations, and of estimating the relationship between the extent of exposure and the severity of effects. The evaluation of the risk of environmental contamination associated with military activities is performed with an index system specifically developed for military training areas (*158*) using parameters such as firing frequency, quantity of energetic materials deposited on the training area, solubility and persistence of the contaminants associated with each munitions type, and spatial extent of the contamination. These data are used to generate hazard maps, as shown in Figure 5.

Risk Characterization is the integration of information derived from receptor characterization, exposure assessment and hazard assessment. It gives an estimate of the degree of risk that is present from specified contaminants to the receptors of a given site. Practically, the analysis of the risk of aquifer contamination associated with military training activities is conducted by combining the vulnerability map defined using the DAT approach and the hazard map, taking into account the type of munitions used. The final result is a risk map, as shown in Figure 6.

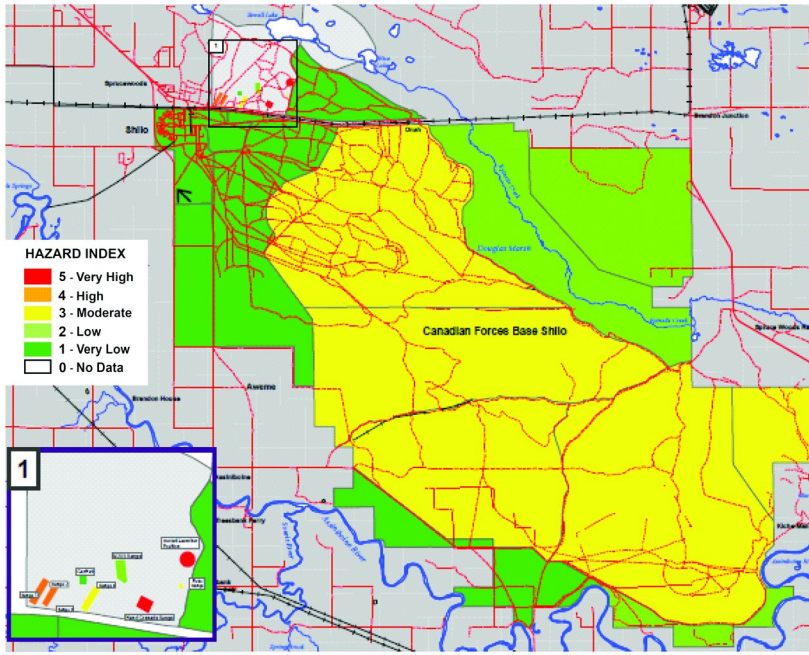

Figure 5. Hazard map. (see color insert)

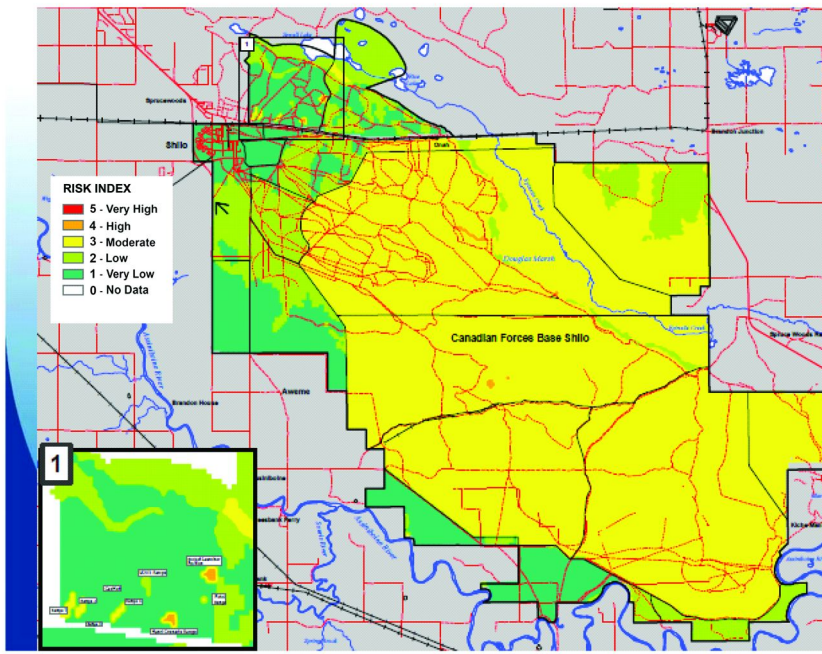

Figure 6. Risk map. (see color insert)

Conclusions

A thorough knowledge of the bioavailability, degradation pathways, toxicity and transport properties of munitions-related residues and of their metabolites is crucial to the understanding of their environmental fate and to design appropriate remediation strategies. Canada is currently developing management tools that will be extremely useful to manage RTAs in a sustainable manner and to reduce the risk associated with military training. The use of vulnerability, hazard and risk maps will enable stakeholders to assess the impacts of military training activities in RTAs. These maps will also help in performing appropriate risk assessments and implementing suitable mitigation and remediation measures from the standpoint of potential for groundwater and surface water contamination. They also represent an invaluable tool to assist in the selection of suitable locations for future training activities and to the establishment of yearly sampling plans for soils, groundwater and surface water. Environmentally-friendly defence activities will help Canada ensure the long-term usage of RTAs that will guarantee military readiness.

Acknowledgments

Director Land Environment and Director General Environment of the Department of National Defence Canada, the Sustain Thrust of DRDC, and SERDP are gratefully acknowledged for their vision and financial support throughout this entire R&D program.

References

1. Environment Canada's Sustainable Development Strategy 2004-2006, Environment Canada, Ottawa, Canada. http://www.ec.gc.ca/sd-dd_consult/SDS2004/index_e.cfm.
2. Fisheries Act Department of Justice, Ottawa, Canada, 1985. http://laws.justice.gc.ca/en/showtdm/cs/F-14.
3. Canadian Environmental Protection Act Department of Justice, Ottawa, Canada, 1999. http://laws.justice.gc.ca/en/c-15.31/.
4. Canadian Council of Ministers of the Environment, Canadian Environmental Quality Guidelines, Ottawa, Canada. http://documents.ccme.ca.
5. Accelerated Reduction /Elimination of Toxics (ARET), Environment Canada, Ottawa, Canada. http://www.ec.gc.ca/nopp/aret/en/index.cfm.
6. Defense Environmental Network & Information Exchange (online), Office of the Under Secretary Deputy of Defense Installations and Environment, USA. http://www.denix.osd.mil/.
7. Thiboutot, S.; Ampleman, G.; Gagnon, A.; Marois, A.; Jenkins, T. F.; Walsh, M. E.; Thorne, P. G.; Ranney, T. A. *Characterization of Antitank Firing Ranges at CFB Valcartier, WATC Wainwright and CFAD Dundurn*; DREV R-9809; Defence Research Establishment Valcartier, Quebec, Canada, 1998.
8. Martel, R.; Hebert, A.; Lefebvre, R.; Ampleman, G.; Thiboutot, S. *Complementary Soil and Groundwater Characterization Study at the OB/OD*

Site CFAD Dundurn (Saskatchewan); Report 1998-05; INRS Georessources: University of Quebec, Quebec, Canada, 1998.
9. Ampleman, G.; Thiboutot, S.; Gagnon, A.; Marois, A.; Martel, R.; Lefebvre, R. *Study of the Impacts of OB/OD Activity on Soils and Groundwater at the Destruction Area in CFAD Dundurn*; DREV R-9827; Defence Research Establishment Valcartier, Quebec, Canada, 1998.
10. Thiboutot, S.; Ampleman, G.; Lewis, J.; Brochu, S. *Evaluation of Heavy Metals Contamination at CFAD Dundurn Resulting from Small-Arms Ammunition Incineration*; DREV TR-2001-127; Defence Research Establishment Valcartier, Quebec, Canada, 2001.
11. Dubé, P.; Ampleman, G.; Thiboutot, S.; Gagnon, A.; Marois, A. *Characterization of Potentially Explosives-Contaminated Sites at CFB Gagetown, 14 Wing Greenwood and CFAD Bedford*; DREV TR-1999-137; Defence Research Establishment Valcartier, Quebec, Canada, 1999.
12. Ampleman, G.; Thiboutot, S.; Désilets, S.; Gagnon, A.; Marois, A. *Evaluation of the Soils Contamination by Explosives at CFB Chilliwack and CFAD Rocky Point*; DREV TR-2000-103; Defence Research Establishment Valcartier, Val-Bélair, Canada, 2000.
13. Thiboutot, S.; Ampleman, G.; Gagnon, A.; Marois, A. *Characterization of an Unexploded Ordnance Contaminated Range (Tracadie Range) for Potential Contamination by Energetic Materials*; DREV TR 2000-102; Defence Research Establishment Valcartier, Quebec, Canada, 2000.
14. Thiboutot, S.; Ampleman, G.; Martel, R.; Paradis, D.; Lefebvre, R.*Environmental Characterization of Canadian Forces Base Shilo Training Area (Battleruns) Following GATES Closure*; DREV TR 2001-126; Defence Research Establishment Valcartier, Quebec, Canada, 2001.
15. Ampleman, G.; Thiboutot, S.; Martel, R.; Lefebvre, R.; Ranney. T.; Jenkins, T. F.; Pennington, J. *Evaluation of the Impacts of Live Fire Training at CFB Shilo (Final Report)*; DREV TR 2003-066; Defence Research Establishment Valcartier, Quebec, Canada, 2003.
16. Thiboutot, S.; Ampleman, G.; Hamel, A.; Ballard, J. M.; Martel, R.; Lefebvre, R.; Downe S. *Research on the Environmental Conditions of Groundwater and Surface Water Prevailing in the Training Area at CFB Gagetown, New Brunswick*; DRDC Valcartier TR 2003-016; Defence Research and Development Canada – Valcartier, Québec, Canada, 2003.
17. Thiboutot, S.; Ampleman, Lewis, J.; Faucher, D. Marois, A.; Martel, R.; Ballard, J. M.; Downe S.; Jenkins, T.; Hewitt, A. *Environmental Conditions of Surface Soils and Biomass Prevailing in the Training Area at CFB Gagetown, New Brunswick*; DRDC Valcartier TR 2003-152; Defence Research and Development Canada – Valcartier, Québec, Canada, 2003.
18. Thiboutot, S.; Ampleman, G.; Marois, A.; Gagnon, A.; Bouchard, M.; Hewitt, A.; Jenkins, T.; Walsh, M. E.; Bjella, K. *Environmental Condition of Surface Soils, CFB Gagetown Training Area: Delineation of the Presence of Munitions Related Residues (Phase III, Final Report)*; DRDC Valcartier TR 2004-205; Defence Research and Development Canada – Valcartier, Québec, Canada, 2004.

19. Lewis, J.; Thiboutot, S.; Ampleman, G.; Martel, R.; Ait-Ssi, L.; Ballard, J. M.; Parent, M.; Downe, S. *Research on the Environmental Conditions of Ground and Surface Water Prevailing in the Training Area at CFB Gagetown, New Brunswick-Part II*; DRDC Valcartier TR 2004-456; Defence Research and Development Canada – Valcartier, Québec, Canada, 2005.
20. Marois, A.; Gagnon, A.; Thiboutot, S.; Ampleman, G. *Caractérisation des sites de destruction d'explosifs, Base des Forces Aériennes de Bagotville*; DRDC Valcartier TR 2003-028, Recherche et développement pour la défense Canada – Valcartier, Québec, Canada, 2003.
21. Ampleman, G.; Thiboutot, S.; Lewis, J.; Marois, A.; Jean, S.; Gagnon, A.; Bouchard, M.; Jenkins, T. F.; Hewitt, A. D.; Pennington, J. C.; Ranney, T. A. *Evaluation of the Contamination by Explosives in Soils, Biomass and Surface Water at Cold Lake Air Weapons Range (CLAWR), Alberta, Phase 1*; DRDC-Valcartier TR 2003-208; Defence Research and Development Canada – Valcartier, Québec, Canada, 2003.
22. Ampleman, G.; Thiboutot, S.; Lewis, J.; Marois, A.; Gagnon, A.; Bouchard, M.; Jenkins, T. F.; Ranney, T. A.; Pennington, J. C. *Evaluation of the Contamination by Explosives and Metals in Soils, Vegetation, Surface Water and Sediment at Cold Lake Air Weapons Range (CLAWR), Alberta, Phase II Final Report*; DRDC Valcartier TR 2004-204; Defence Research and Development Canada – Valcartier, Québec, Canada, 2004.
23. Martel, R.; Calderhead, A.; Lewis, J.; Ampleman, G.; Thiboutot, S. *Groundwater and Surface Water Study for Potential Contamination by Energetic Material, Metals and Related Compounds at the Cold Lake Air Weapon Range (CLAWR) – Phase I*; INRS-ETE Report R 746, Institut national de la recherche scientifique – Centre Eau, Terre et Environnement, University of Quebec, Quebec, Canada, 2004.
24. Martel, R.; Ait-Ssi, L.; Bordeleau, G.; Cloutier, V.; Gabriel, U.; Lewis, J.; Ross, M.; Ampleman, G.; Thiboutot, S. *Groundwater and Surface Water Study for Potential Contamination by Energetic Material, Metals and Related Compounds at the Cold Lake Air Weapon Range (CLAWR)-Phase II Report*; INRS-ETE Report R-000237, Institut national de la recherche scientifique – Centre Eau, Terre et Environnement, University of Quebec, Quebec, Canada, 2005.
25. Martel, R.; Bordeleau, G.; Lahcen A.-S., Ross, M.; Comeau, G.; Lewis, J.; Ampleman, G.; Thiboutot, S. *Groundwater and Surface Water Study for Potential Contamination by Energetic Materials. Metals and Related Compounds at the Cold Lake Air Weapons Range (CLAWR)*; INRS Final report R-746-F, Institut national de la recherche scientifique – Centre Eau, terre et environnement, University of Quebec, Quebec, Canada, 2007.
26. Bordeleau, G.; Martel, R.; Schäfer, D.; Ampleman, G.; Thiboutot, S. Groundwater Flow and Contaminant Transport Modeling at an Air Weapon Range. *Environ. Geol.* **2008**, *55* (2), 385–396.
27. Bordeleau, G.; Savard, M.; Martel, R.; Ampleman, G.; Thiboutot, S. Determination of the Origin of Groundwater Nitrate at an Air Weapons Range Using the Dual Isotope Approach. *Contaminant Hydrogeology J.* **2008**, *98* (3−4), 97–105.

28. Bordeleau, G.; Martel, R.; Ampleman, G.; Thiboutot, S.; Jenkins, T. F. Environmental Impacts of Training Activities at an Air Weapons Range. *J. Environ. Qual.* **2008**, *37*, 308–317.
29. Martel, R.; Mailloux, M.; Lefebvre, R.; Michaud, Y.; Parent, M.; Ampleman, G.; Thiboutot, S.; Jean, S.; Roy, N. *Energetic Materials Behaviour in Groundwater at the Arnhem Anti-Tank Range*; CFB Valcartier, Québec, Canada, Report 1999-02, INRS Georessources, University of Quebec, Quebec, Canada, 1999.
30. Marois, A.; Gagnon, A.; Thiboutot, S.; Ampleman, G. *Caractérisation des sols de surface dans les secteurs d'entraînement, Base des Forces Canadiennes, Valcartier*; DRDC TR 2004-206, Recherche et Développement pour la Défense Canada – Valcartier, Québec, Canada, 2004.
31. Thiboutot, S.; Marois, A.; Gagnon, A.; Gamache, T.; Roy, N.; Tremblay, C.; Ampleman, G. *Caractérisation de la dispersion de résidus de munitions dans les sols de surface d'un secteur d'essai*; DRDC Valcartier TR 2007-110, Recherche et développement pour la défense Canada – Valcartier, Québec, Canada, 2007.
32. Thiboutot, S.; Ampleman, G.; Marois, A.; Gagnon, A. *Caractérisation des sols de surface du champ de tir et secteurs d'entraînement de la Garnison Valcartier*; DRDC Valcartier TR 2008-190, Recherche et développement pour la défense Canada – Valcartier, Québec, Canada, 2008.
33. Mailloux, M.; Martel, R.; Gabriel, U.; Lefebvre, R.; Thiboutot, S.; Ampleman, G. Hydrogeological Study of an Antitank Range. *J. Environ. Qual.* **2008**, *37*, 1468–1476.
34. Martel, R.; Mailloux, M.; Gabriel, U.; Lefebvre, R.; Thiboutot, S.; Ampleman, G. Behavior of Energetic Materials in Groundwater and an Anti-Tank Range. *J. Environ. Qual.* **2009**, *38*, 75–92.
35. Diaz, E.; Brochu, S.; Thiboutot, S.; Ampleman, G.; Marois, A.; Gagnon, A. 2007*Energetic Materials and Metals Contamination at CFB/ASU Wainwright, Alberta – Phase I*; DRDC Valcartier TR 2007-385; Defence Research and Development Canada – Valcartier, Québec, Canada.
36. Martel, R.; Robertson, T.; Lewis, J.; Parent, M.; Ampleman, G.; Thiboutot, S.; Ross, M.; Clairet-Baril, G. *Evaluation of Surface and Groundwater Quality and Environmental Conditions at the WATC Wainright, Alberta*; Report R-739, Institut national de la recherche scientifique – Centre Eau, Terre et Environnement, University of Quebec, Quebec, Canada, 2004.
37. Martel, R.; Ait-Ssi, L.; Ross, M.; Gabriel, U.; Parent, M.; Lewis, J.; Diaz, E.; Brochu, S.; Ampleman, G.; Thiboutot, S.; Michaud, Y. *Evaluation of Surface and Groundwater Quality at the WATC, Wainwright, Alberta, Phase II Report*; Report R-739, Institut national de la recherche scientifique – Centre Eau, Terre et Environnement, University of Quebec, Quebec, Canada, 2005.
38. Ampleman, G.; Thiboutot, S.; Marois, A.; Gagnon, A. *Evaluation of Soil Contamination by Explosives and Metals at the Land Force Central Area Training Centre (LFCA TC) Meaford, Ontario (Phase I)*; DRDC Valcartier TR 2008-390; Defence Research and Development Canada – Valcartier, Québec, Canada, 2009.

39. Martel, R.; Nadeau, V.; Bordeleau, G.; Comeau, G.; Ballard, J. M.; Guay, C.; Ross, M.; Parent, M.; Brochu, S. *Groundwater And Surface Water Study for Potential Contamination by Energetic Materials, Metals and Related Compounds at the Canadian Force Base Petawawa (Ontario) Phase II and III Report*; Report No. R-966, Institut national de la recherche scientifique – Centre Eau, Terre et Environnement, University of Quebec, Quebec, Canada, 2007.
40. Martel, R.; Nadeau, R.; Ross, M.; Cloutier, V.; Trépanier, L.; Ait-Ssi, L.; Lewis, J.; Gabriel, U.; Brochu, S.; Ampleman, G.; Thiboutot, S.; Diaz, E. *Groundwater and Surface Water Study for Potential Contamination by Energetic Materials, Metals and Related Compounds at the Canadian Force Base Petawawa (Ontario): Phase 1 Report*; CR-2006-042, Report R-842, Institut national de la recherche scientifique – Centre Eau, Terre et Environnement, University of Quebec, Quebec, Canada, 2006.
41. Brochu, S.; Diaz, E.; Thiboutot, S.; Ampleman, G.; Marois, A.; Gagnon, A.; Hewitt, A. D.; Bigl, S. R.; Walsh, M. E.; Walsh, M. R.; Bjella, K.; Ramsey, C. A.; Taylor, S.; Wingfors, H.; Qvarfort, U.; Karlsson, R.-M.; Ahlberg, M. *Environmental Assessment of 100 Years of Military Training at Canadian Forces Base Petawawa: Phase 1 - Study of the Presence of Munitions-Related Residues in Soils and Vegetation of Main Ranges and Training Areas*; DRDC Valcartier TR 2008-118; Defence Research and Development Canada – Valcartier, Québec, Canada, 2009.
42. Ampleman, G.; Thiboutot, S.; Marois, A.; Gagnon, A. *Evaluation of the Contamination by Explosives and Metals in Soils at the Land Forces Central Area Training Centre (LFCATC) Meaford, Ontario (Phase I)*; DRDC Valcartier TR 2008-390; Defence Research and Development Canada – Valcartier, Québec, Canada, 2009.
43. Ampleman, G.; Thiboutot, S.; Marois, A.; Gagnon, A. *Surface Soil Characterization of Explosive and Metals at the Land Force Central Area Training Centre (LFCA TC) Meaford, Ontario (Phase II) Final report*; DRDC Valcartier TR 2009-218; Defence Research and Development Canada – Valcartier, Québec, Canada, 2009.
44. Jenkins, T. F.; Walsh, M. E.; Thorne, P. G.; Thiboutot, S.; Ampleman, G.; Ranney, T. A.; Grant, C. L. *Assessment of Sampling Error Associated with Collection and Analysis of Soil Samples at a Firing Range Contaminated with HMX*; CRREL Special Report # 97-22; U.S. Army Engineer Research and Development Center, Cold Regions Research and Engineering Laboratory, Hanover, NH, 1997.
45. Jenkins, T. F.; Grant, C. L.; Brar, G. S.; Thorne, P. G.; Schumacher, P. W.; Ranney, T. A. Assessment of Sampling Error Associated with the Collection and Analysis of Soil Samples at Explosives Contaminated Sites. *Field Anal. Chem. Technol.* **1997**, *1*, 151–163.
46. Jenkins, T. F.; Walsh, M. E.; Thorne, P. G.; Miyares, P. H.; Ranney, T. A.; Grant, C. L.; Esparza, J. *Site Characterization for Explosives Contamination at a Military Firing Range Impact Area*; CRREL Special Report 98-9; U.S. Army Cold Regions Research and Engineering Laboratory, Hanover, NH, 1998.

47. Jenkins, T. F.; Grant, C. L.; Walsh, M. E.; Thorne, P. G.; Thiboutot, S.; Ampleman, G.; Ranney, T. A. Coping with Spatial Heterogeneity Effects on Sampling and Analysis at an HMX - Contaminated Antitank Firing Range. *Field Anal. Chem. Technol.* **1999**, *3* (1), 19–28.
48. Jenkins, T. F.; Pennington, J. C.; Ranney, T. A.; Berry, T. E., Jr.; Miyares, P. H.; Walsh, M. E.; Hewitt, A. D.; Perron, N.; Parker, L. V.; Hayes, C. A.; Wahlgren, Maj. E. *Characterization of Explosives Contamination at Military Firing Ranges*; ERDC Technical Report TR-01-05; U.S. Army Engineer Research and Development Center, Cold Regions Research and Engineering Laboratory, Hanover, NH, 2001.
49. Walsh, M. E.; Ramsey, C. A.; Jenkins, T. F. The Effect of Particle Size Reduction by Grinding on Sub-Sampling Variance for Explosives Residues in Soil. *Chemosphere* **2002**, *49*, 1267–1273.
50. Hewitt, A. D.; Walsh, M. E. *On-site Processing and Subsampling of Surface Soils Samples for the Analysis of Explosives*; ERDC TR-03-14; U.S. Army Engineer Research and Development Center, Cold Regions Research and Engineering Laboratory, Hanover, NH, 2003.
51. Walsh, M. E.; Collins, C. M.; Hewitt, A. D.; Walsh, M. R.; Jenkins, T. F.; Stark, J.; Gelvin, A.; Douglas, T. S.; Perron, N.; Lambert, D.; Bailey, R.; Myers, K. *Range Characterization Studies at Donnelly Training Area, Alaska: 2001 and 2002*; ERDC/CRREL TR-04-3; U.S. Army Engineer Research and Development Center, Cold Regions Research and Engineering Laboratory, Hanover, NH, 2004.
52. Jenkins, T. F.; Ranney, T. A.; Hewitt, A. D.; Walsh, M. E.; Bjella, K. L. *Representative Sampling for Energetic Compounds at an Antitank Firing Range*; ERDC/CRREL TR-04-7; U.S. Army Engineer Research and Development Center, Cold Regions Research and Engineering Laboratory, Hanover, NH, 2004.
53. Walsh, M. E.; Collins, C. M.; Hewitt, A. D.; Walsh, M. R.; Jenkins, T. F.; Stark, J.; Gelvin, A.; Douglas, T.; Perron, N. M.; Lambert, D.; Bailey, R.; Myers, K. *Range Characterization Studies at Donnelly Training Area, Alaska 2001 and 2002*; ERDC/CRREL TR-04-3; U.S. Army Engineer Research and Development Center, Cold Regions Research and Engineering Laboratory, Hanover, NH, 2004.
54. Walsh, M. E.; Ramsey, C. A.; Collins, C. M.; Hewitt, A. D.; Walsh, M. R.; Bjella, K. L.; Lambert, D. J.; Perron, N. M.*Collection Methods and Laboratory Processing of Samples from Donnelly Training Area Firing Points, Alaska (2003)*; ERDC/CRREL TR-05-6; U.S. Army Engineer Research and Development Center, Cold Regions Research and Engineering Laboratory, Hanover, NH, 2005.
55. Jenkins, T. F.; Thiboutot, S.; Ampleman, G.; Hewitt, A. D.; Walsh, M. E.; Ranney, T. A.; Ramsey, C. A.; Grant, C. L.; Collins, C. M.; Brochu, S.; Bigl, S. R.; Pennington, J. C. *Identity and Distribution of Residues of Energetic Compounds at Military Live-Fire Training Ranges*; ERDC/CRREL TR-05-10; U.S. Army Engineer Research and Development Center, Cold Regions Research and Engineering Laboratory, Hanover, NH, 2005.

56. Jenkins, T. F.; Hewitt, A. D.; Grant, C. L.; Thiboutot, S.; Ampleman, G.; Walsh, M. E.; Ranney, T. A.; Ramsey, C. A.; Palazzo, A. J.; Pennington, J. C. Identity and Distribution of Residues of Energetic Compounds at Army Live-Fire Training Ranges. *Chemosphere* **2006**, *63*, 1280–1290.
57. Hewitt, A.; Bigl, S.; Walsh, M. E.; Brochu, S.; Bjella, K.; Lambert D. *Processing of Training Range Soils for the Analysis of Energetic Compounds*; ERDC/CRREL TR-07-15; U.S. Army Engineer Research and Development Center, Cold Regions Research and Engineering Laboratory, Hanover, NH, 2007.
58. Ragnvaldsson, D.; Brochu, S.; Wingfors, H. Pressurized Liquid Extraction with Water as a Tool for Chemical and Toxicological Screening of Soil Samples at Army Live-Fire Training Ranges. *J. Hazard. Mater.* **2007**, *142* (1−2), 418–424.
59. Pennington, J. C.; Jenkins, T. F.; Brannon, J. M.; Lynch, J.; Ranney, T. A.; Berry, J.; Thomas E.; Hayes, C. A.; Miyares, P. H.; Walsh, M. E.; Hewitt, A. D.; Perron, N.; Delfino, J. J. *Distribution and Fate of Energetics on DoD Test and Training Ranges: Interim Report 1*; ERDC TR-01-13; U.S. Army Engineer Research and Development Center, Vicksburg, MS, 2001.
60. Pennington, J. C.; Jenkins, T. F.; Ampleman, G.; Thiboutot, S.; Brannon, J. M. Lynch, J.; Ranney, T. A.; Stark, J. A.; Walsh, M. E.; Lewis, J.; Hayes, C. A.; Mirecki, J. E. Hewitt, A. D.; Perron, N.; Clausen, J.; Delfino, J. J. *Distribution and Fate of Energetics on DoD Test and Training Ranges: Interim Report 2*; ERDC TR-02-8; U.S. Army Engineer Research and Development Center, Environmental Laboratory, Vicksburg, MS, 2002.
61. Pennington, J. C.; Jenkins, T. F.; Ampleman, G.; Thiboutot, S.; Brannon, J. M.; Lewis, J.; Delaney, J. E.; Clausen, J.; Hewitt, A. D.; Hollander, M. A.; Hayes, C. A.; Stark, J. A.; Marois, A.; Brochu, S.; Dinh, H. Q.; Lambert, D.; Martel, R.; Brousseau, P.; Perron, N. M.; Lefebvre, R.; Davis, W.; Ranney, T. A.; Gauthier, C.; Taylor, S.; Ballard, J. M. *Distribution and Fate of Energetics on DoD Test and Training Ranges: Interim Report 3*; ERDC TR-03-02; U.S. Army Engineer Research and Development Center, Environmental Laboratory, Vicksburg, MS, 2003.
62. Pennington, J. C.; Jenkins, T. F.; Thiboutot, S.; Ampleman, G.; Clausen, J.; Hewitt, A. D.; Lewis, J.; Walsh, M. R.; Walsh, M. E.; Ranney, T. A.; Silverblatt, B.; Marois, A.; Gagnon, A.; Brousseau, P.; Zufelt, J. E.; Poe, K.; Bouchard, M.; Martel, R.; Walker, D. D.; Ramsey, C. A.; Hayes, C.; Yost, S. L.; Bjella, K. L.; Trépanier, L.; Berry, T. E.; Lambert, D.; Dubé, P.; Perron, N. M. *Distribution and Fate of Energetics on DoD Test and Training Ranges: Interim Report 5*; ERDC TR-05-2; U.S. Army Engineer Research and Development Center, Vicksburg, MS, 2005.
63. Pennington, J. C.; Jenkins, T. F.; Ampleman, G.; Thiboutot, S.; Brannon, J.; Clausen, J.; Hewitt, A. D.; Brochu, S.; Dube, P.; Lewis, J.; Ranney, T.; Faucher, D.; Gagnon, A.; Stark, J.; Brousseau, P.; Price, C.; Lambert, D.; Marois, A.; Bouchard, M.; Walsh, M.; Yost, S.; Perron, M.; Martel, R.; Jean, S.; Taylor, S.; Hayes, C.; Ballard, J.; Walsh, M. E.; Mirecki, J.; Downe, S.; Collins, N.; Porter, B.; Richard, K. *Distribution and Fate of Energetics on*

DoD Test and Training Ranges: Interim Report 4; ERDC/EL TR-04-4; U.S. Army Engineer Research and Development Center, Vicksburg, MS, 2004.

64. Pennington, J. C.; Jenkins, T. F.; Ampleman, G.; Thiboutot, S.; Hewitt, A. D.; Brochu, S.; Robb, J.; Diaz, E.; Lewis, J.; Colby, H.; Martel, R.; Poe, K.; Groff, K.; Bjella, K.; Ramsey, C. A.; Hayes, C. A.; Yost, S.; Marois, A.; Gagnon, A.; Silverblatt, B.; Crutcher, T.; Harriz, K.; Heisen, K.; Bigl, S. R.; Berry, J.; Thomas E.; Muzzin, J.; Lambert, D. J.; Bishop, M. J.; Rice, B.; Wojtas, M.; Walsh, M. E.; Walsh, M. R.; Taylor, S. *Distribution and Fate of Energetics on DoD Test and Training Ranges: Interim Report 6*; ERDC TR-06-12; U.S. Army Engineer Research and Development Center, Vicksburg, MS, 2006.
65. Pennington, J. C.; Jenkins, T. F.; Ampleman, G.; Thiboutot, S.; Brannon, J. M.; Hewitt, A. D.; Lewis, J.; Brochu, S.; Diaz, E.; walsh, M. R.; Walsh, M. E.; Taylor, S.; Lynch, J. C.; Clausen, J.; Ranney, T. A.; Ramsey, C. A.; Hayes, C. A.; Grant, C. L.; Collins, C. M.; Bigl, S. R.; Yost, S.; Dontsova, K. *Distribution and Fate of Energetics on DoD Test and Training Ranges: Final Report*; ERDC TR-06-13; U.S. Army Engineer Research and Development Center, Vicksburg, MS, 2006.
66. Thiboutot S.; Ampleman G.; Brochu S.; Martel R.; Sunahara, G.; Hawari, J.; Nicklin, S.; Provotas, A.; Pennington, J. C.; Jenkins, T. F.; Hewitt, A. *Protocol for Energetic Materials-Contaminated Sites Characterization, Volume 2*; Final Report TTCP WPN-4 KTA 4-28, 2003. http://www.em-guidelines.org.
67. United States Environmental Protection Agency. Method 8330b, Nitroaromatics, nitramines and nitrate esters by High Performance Liquid Chromatography (HPLC). http://www.epa.gov/osw/hazard/testmethods/pdfs/8330b.pdf.
68. Hewitt, A. D.; Jenkins, T. F.; Walsh, M. E.; Brochu, S. *Environmental Security Technology Certification Program - Project ER-0628, Validation of Sampling Protocol and the Promulgation of Method Modifications for the Characterization of Energetic Residues on Military Testing and Training Ranges*; ERDC/CRREL TR-09-6; U.S. Army Engineer Research and Development Center, Cold Regions Research and Engineering Laboratory, Hanover, NH, 2009.
69. Jenkins, T. F.; Pennington, J. C.; Ampleman, G.; Thiboutot, S.; Walsh, M. R.; Diaz, E.; Dontsova, K.; Hewitt, A. D.; Walsh, M. E.; Bigl, S. R.; Taylor, S.; MacMillan, D. K.; Clausen, J. L.; Lambert, D. J.; Perron, N. M.; Lapointe, M.-C., Brochu, S.; Brassard, M.; Stowe, R.; Farinaccio, R.; Gagnon, A.; Marois, A.; Gilbert, D.; Faucher, D.; Yost, S.; Hayes, C.; Ramsey, C. A.; Rachow, R. J.; Zufelt, J. E.; Collins, C. M.; Gelvin, A. B.; Saari, S. P. *Characterization and Fate of Gun and Rocket Propellant Residues on Testing and Training Ranges: Interim Report 1*; ERDC TR-07-1; U.S. Army Engineering Research and Development Center, Vicksburg, MS, 2007.
70. Jenkins, T. F.; Bigl, S. R.; Taylor, S.; Walsh, M. R.; Walsh, M. E.; Hewitt, A. D.; Fadden, J. L.; Perron, N. M.; Moors, V.; Lambert, D.; Bayley, R. N.; Dontsova, K. M.; Chappel, M. A.; Pennington, J. C.; Ampleman, G.; Thiboutot, S.; Faucher, D.; Poulin, I.; Brochu, S.; Diaz, E.; Marois,

A.; Fifield, L. N. R.; Gagnon, A.; Gamache, T.; Gilbert, D.; Tanguya, V.; Melanson, L.; Lapointe, M.; Martel, R.; Comeau, G.; Ramsey, C. A.; Quémerais, B.; Simunek, J. *Characterization and Fate of Gun and Rocket Propellant Residues on Testing and Training Ranges: Final Report*; ERDC TR-08-1; U.S. Army Engineer Research and Development Center, Cold Regions Research and Engineering Laboratory, Hanover, NH, 2008.

71. Quémerais, B.; Melanson, L.; Ampleman, G.; Thiboutot, S.; Poulin, I.; Diaz, E. *Characterization of Atmospheric Emissions During Live Gun Firing at the Muffler Installation in Nicolet, Lac St. Pierre, Canada: Test on Howitzer 105 mm*; DRDC Toronto TR 2007-060; Defence Research and Development Canada – Toronto, Toronto, Canada, 2007.
72. Thiboutot, S.; Ampleman, G.; Marois, A.; Gagnon, A.; Fifield, R. *Preliminary Assessment of the Dispersion of Propellant Residues from Naval Live-Fire Training*; DRDC Valcartier TR 2007-264; Defence Research and Development Canada – Valcartier, Québec, Canada, 2007.
73. Quémerais, B.; Diaz, E.; Poulin, I.; Marois, A. *Characterization of Atmospheric Emission Produced by Live Gun Firing: Test on the M777 155-mm Howitzer*; DRDC Toronto TR 2007-102, Toronto, Canada, 2007.
74. Walsh, M. R.; Walsh, M. E.; Bigl, S. R.; Perron, N. M.; Lambert, D. J.; Hewitt, A. D. *Propellant Residues Deposition from Small Arms Munitions*; ERDC/CRREL TR-07-17; U.S. Army Engineer Research and Development Center, Cold Regions Research and Engineering Laboratory, Hanover, NH, 2007.
75. Thiboutot, S.; Ampleman, G.; Marois, A.; Gagnon, A.; Gilbert, D.; Tanguay, V.; Poulin, I. *Deposition of Gun Propellant Residues from 84-mm Carl Gustav Rocket Firing*; DRDC Valcartier TR 2007-408; Defence Research and Development Canada – Valcartier, Québec, Canada, 2008.
76. Ampleman, G.; Thiboutot, S.; Marois, A.; Gagnon, A.; Gilbert D. *Evaluation of the Propellant Residues Emitted During 105-mm Leopard Tank Live Firing and Sampling of Demolition Ranges at CFB Gagetown, Canada*; DRDC Valcartier TR 2007-515; Defence Research and Development Canada – Valcartier, Québec, Canada, 2008.
77. Poulin, I.; Diaz, E. *Airborne Particulate Matter Emissions During Live Firing of LG1 Mark II 105-mm Howitzer*; DRDC Valcartier TM 2007-297; Defence Research and Development Canada – Valcartier, Québec, Canada, 2008.
78. Ampleman, G.; Thiboutot, S.; Marois, A.; Gamache, T.; Poulin, I.; Quémerais, B.; Melanson, L. *Analysis of Propellant Residues Emitted During 105-mm Howitzer Live Firing at the Muffler Installation in Nicolet, Lac St-Pierre, Canada*; DRDC Valcartier TR 2007-514; Defence Research and Development Canada – Valcartier, Québec, Canada, 2008.
79. Quémerais, B.; Diaz, E.; Poulin, I.; Marois, A. *Characterization of Atmospheric Emission Produced by Live Gun Firing : Test on the Carl Gustav Anti-Tank, 84-mm Weapon*; DRDC Toronto TR 2007-103; Defence Research and Development Canada – Valcartier, Toronto, Canada, 2008.
80. Martel, R.; Bellavance-Godin, A.; Thiboutot, S.; Ampleman, G. 2008*Environmental Fate and Transport of Propellant Residues at Firing*

Positions in the Unsaturated Zone; INRS Report -991, Institut national de la recherché scientifique – Centre Eau, Terre et Environnement, University of Quebec, Quebec, Canada.

81. Thiboutot, S.; Ampleman, G.; Lapointe, M. C.; Brochu, S.; Brassard, M.; Stowe, R.; Farinaccio, R.; Gagnon, A.; Marois, A.; Gamache, T. *Study of the Dispersion of Ammonium Perchlorate Following the Static Firing of MK-58 Rocket Motors*; DRDC Valcartier TR 2008-240; Defence Research and Development Canada – Valcartier, Québec, Canada, 2008.
82. Poulin, I.; Diaz., E.; Quémerais, B. *Particulate Matter Emitted from the M777 Howitzer During Live Firing*; DRDC Valcartier TR 2008-215; Defence Research and Development Canada – Valcartier, Québec, Canada, 2008.
83. Poulin, I.; Diaz, E.; Quémerais, B. *Airborne Contaminants in Two Anti-Tank Weapons Back Blast Plume : Carl Gustav 84-mm and M72 66-mm*; DRDC Valcartier TR 2008-242; Defence Research and Development Canada – Valcartier, Québec, Canada, 2008.
84. Thiboutot, S.; Ampleman, G.; Marois, A.; Gagnon, A.; Gilbert, D. *Nitroglycerine Deposition from M-72 Antitank Rocket Firing*; DRDC TR 2009-003; Defence Research and Development Canada – Valcartier, Québec, Canada, 2009.
85. Poulin, I.; Nadeau, G.; Gagnon, A. *Development of a Remediation Strategy for Surface Soils Contaminated with Energetic Materials by Thermal Processes*; Phases 1, 2 and 3; DRDC Valcartier TR 2009-150; Defence Research and Development Canada – Valcartier, Québec, Canada, 2009.
86. Poulin, I.; Diaz, E. *Air Quality Measurements from Live-Firing of the 105-mm Leopard Tank*; Study of the Gaseous and Particulate Matter Emissions Inside and Outside a Leopard Tank; DRDC Valcartier TR 2009-225; Defence Research and Development Canada – Valcartier, Québec, Canada, 2009.
87. Ampleman, G.; Thiboutot, S.; Marois, A.; Gagnon, A.; Gilbert, D.; Walsh, M. R.; Walsh, M. E.; Woods, P. *Evaluation of the Propellant Residues Emitted During 105-mm Leopard Tank Live Firing at CFB Valcartier, Canada*; DRDC Valcartier TR 2009-420; Defence Research and Development Canada – Valcartier, Québec, Canada, 2009.
88. Poulin, I.; Thiboutot, S.; Brochu, S. *Production of Dioxins and Furans from the Burning of Excess Gun Propellant*; DRDC Valcartier TR 2009-365; Defence Research and Development Canada – Valcartier, Québec, Canada, 2009.
89. Martel, R.; Lange, S.; Coté, S.; Ampleman, G.; Thiboutot, S. *Fate and Behaviour of Energetic Material Residues in the Unsaturated Zone: Sand Columns and Dissolution Tests*; INRS Report R-1161, Institut national de la recherche scientifique – Centre Eau, Terre et Environnement, University of Quebec, Quebec, Canada, 2010.
90. Martel, R.; Bordeleau, G.; Trépanier, L.; Thiboutot, S.; Ampleman, G.; Gagnon, A.; Marois, A. *The Environmental Fate of Nitroglycerine (NG) from Double Base Propellant Residues*; INRS Report R 1130, Institut national de la recherché scientifique – Centre Eau, Terre et Environnement, University of Quebec, Quebec, Canada, 2010.

91. Ampleman, G. Thiboutot, S.; Marois, A.; Gagnon, A.; Woods, P.; Walsh, M. R.; Walsh, M. E.; Ramsey C.; Archambault, P. *Evaluation of the Propellant Residues Emitted During the Live Firing of Triple Base Ammunition Using a British 155mm Howitzer Gun at CFB Suffield, Canada*; Defence Research and Development Canada – Valcartier, Québec, Canada, in press.
92. ITRC. *Environmental Management at Operating Outdoor Small Arms Firing Ranges - Smart-2*; The Interstate Technology & Regulatory Council, Small Arms Firing Range Team, 2005. www.itrcweb.org.
93. Guidance on Sampling and Analytical Methods for Use at Contaminated Sites in Ontario. *Ontario Ministry of Environment and Energy*; Standards Development Branch, 1996
94. Sunahara, G.; Lotufo, G.; Kuperman, R.; Hawari, J. Thiboutot, S.; Ampleman, G. *Ecotoxicology of Explosives*; CRC Press, Taylor and Francis Group, 2009.
95. Jones, A. M.; Labelle, S.; Paquet, L.; Hawari, J.; Rho, D.; Samson, R.; Greer, C.; Lavigne, J.; Thiboutot, S.; Ampleman, G. Assessment of the Aerobic Biodegradation Potential of RDX, TNT, GAP, and NC. In *Environmental Biotechnology: Principles and Practice*; Moo-Young, M.; Anderson, W. A., Charabarty, A. M., Eds.; Kluwer Academic Publishers: Dordrecht, 1996; pp 368−381.
96. Jones, A.; Greer, C.; Ampleman, G.; Thiboutot, S.; Lavigne, J.; Hawari, J. Biodegradability of Selected Highly Energetic Pollutants under Aerobic Conditions; In *Bioremediation of Recalcitrant Organics*; Hinche, R. E., Anderson, D. B., Hoeppel, R. E., Eds.; 1995; pp 251−257.
97. Greer, C. W.; Godbout, J.; Zilber, B.; Labelle, S.; Sunahara, G.; Hawari, J.; Ampleman, G.; Thiboutot, S. Bioremediation of RDX-Contaminated Soil: From Flask to Field. In *In-situ and Ex-situ Bioremediation*; Hinchee, R., Hoeppel, R. E., Anderson, D. B., Eds.; Batelle Press: Columbus, Richmond, USA, 1997, Vol. 4, issue 5, pp 393−398.
98. Hawari, J.; Greer, C.; Jones, A.; Shen, C. F.; Guiot, S. R.; Sunahara, G.; Thiboutot, S.; Ampleman, G. In Soil Contaminated With Explosives: A Search for Remediation Technologies; In *Challenges in Propellants and Combustion 100 Years After Nobel*; Ed Kenneth, K. K.; Bagell House Inc. Publishers: New York; pp 135−144, 1997.
99. Cattaneo, M.; Masson, C.; Hawari, J.; Sunahara, G.; Thiboutot, S.; Ampleman, G.; Greer, C. W. Natural Attenuation of TNT in Soil Columns. In *In-situ and Ex-situ Bioremediation*; Hinchee, R.; Hoeppel, R. E.; Anderson, D. B., Ed.; Batelle Press: Columbus, Richmond, USA, 1997; Vol. 4, issue 2, pp 3−8.
100. Sunahara, G. I.; Dodard, S.; Sarrazin, M.; Paquet, L.; Ampleman, G.; Thiboutot, S.; Hawari, J.; Renoux, A. Development of a Soil Extraction Procedure for Ecotoxicity Characterization of Energetic Compounds. *Ecotoxicol. Environ. Saf.* **1998**, *39*, 185.
101. Shen, C. F.; Guiot, S. R.; Hawari, J.; Thiboutot, S.; Ampleman, G. Fate of RDX and TNT in Bioslurry Reactor Processes. *Biodegradation* **1998**, *8*, 339.

102. Hawari, J.; Spencer, B.; Halasz, A.; Thiboutot, S.; Ampleman, G. Biotransformation of TNT with Anaerobic Sludge: The Role of Triaminotoluene. *Appl. Environ. Microbiol.* **1998**, *64* (6), 2200.
103. Rocheleau, S.; Cimpoia, R.; Paquet, L.; Van Koppen, I.; Guiot, S. R.; Ampleman, G.; Thiboutot, S.; Hawari, J.; Sunahara, G. Ecotoxicological Evaluation of a Bench-Scale Bioslurry Process Treating Explosives-Spiked Soil. *Bioremediation J.* **1999**, *3* (3), 233–245.
104. Guiot S. R.; Shen, C. F.; Paquet, L.; Breton, J.; Hawari, J.; Ampleman, G.; Thiboutot, S., Pilot-Scale Anaerobic Bioslurry Remediation of Highly RDX- and HMX-Contaminated Soils; In *Bioremediation Series, Bioremediation of Nitroaromatic and Haloaromatic compounds*; Alleman, B. C.; Leeson, A., Eds.; Battelle Press: Columbus, OH, 1999; Vol. 5, issue 7, pp 15−20.
105. Lachance, B.; Robidoux, P. Y.; Hawari, J.; Ampleman, G.; Thiboutot, S.; Sunahara, G. I. Cytotoxic and Genotoxic Effects of Energetic Compounds on Bacterial and Mammalian Cells in Vitro. *Mutat. Res., Genet. Toxicol. Environ. Mutagen.* **1999**, *444* (1), 25–39.
106. Robidoux, P. Y.; Hawari, J.; Thiboutot, S.; Ampleman, G.; Sunahara, G. Acute Toxicity of 2,4,6-Trinitrotoluene (TNT) in The Earthworm (Eisenia Andrei). *Ecotoxicol. Environ. Saf.* **1999**, *44*, 311.
107. Jenkins, T. F.; Grant, C. L.; Walsh, M. E.; Thorne, P. G.; Thiboutot, S.; Ampleman, G.; Ranney, T. A. Coping with Spatial Heterogeneity Effects on Sampling and Analysis at an HMX - Contaminated Antitank Firing Range. *Field Anal. Chem. Technol.* **1999**, *3* (1), 19–28.
108. Dodard, S.; Renoux, A. Y.; Hawari, J.; Ampleman, G.; Thiboutot, S.; Sunahara, G. I. Ecotoxicity Characterization of Dinitrotoluenes and Some of Their Reduced Metabolites. *Chemosphere* **1999**, *38* (9), 2071–2079.
109. Sunahara, G.; Dodard, S.; Sarrazin, M.; Paquet, L.; Hawari, J.; Greer, C. W.; Ampleman, G.; Thiboutot, S.; Renoux, A. Y. Ecotoxicological Characterization of Energetic Substances Using a Soil Extraction Procedure. *Ecotoxicol. Environ. Saf.* **1999**, *43*, 138–148.
110. Hawari, J.; Halasz, A.; Beaudet, S.; Paquet, L.; Ampleman, G.; Thiboutot, S. Biotransformation of 2,4,6-Trinitrotoluene with Phanerochaete Chrysosporium in Agitated Cultures at pH 4.5. *Appl. Environ. Microbiol.* **1999**, *65* (7), 2977–2986.
111. Sheremata, T. W.; Thiboutot, S.; Ampleman, G.; Paquet, L.; Halasz, A.; Hawari, J. Fate of 2,4,6-Trinitrotoluene and Its Metabolites in Natural and Model Soil Systems. *Environ. Sci. Technol.* **1999**, *33*, 4002–4008.
112. Gong, P.; Gasparrini, P.; Rho, D.; Hawari, J.; Thiboutot, S.; Ampleman, G.; Sunahara, G. I. An *In Situ* Respirometric Technique to Measure Pollution-Induced Microbial Community Tolerance in Soils Contaminated with 2,4,6 Trinitrotoluene. *Ecotoxicol. Environ. Saf.* **2000**, *47*, 96–103.
113. Shen, C. F.; Hawari, J.; Ampleman, G.; Thiboutot, S.; Guiot, S. R. Enhanced Biodegradation and Fate of Hexahydro-1,3,5-Trinitro-1,3,5-Triazine (RDX) and Octahydro-1,3,5,7-Tetranitro-1,3,5,7-Tetrazocine (HMX) in Anaerobic Soil Slurry Bioprocess. *Bioremediation J.* **2000**, *4* (1), 27–39.

114. Hodgson, J.; Rho, D.; Guiot, S.; Ampleman, G.; Thiboutot, S.; Hawari, J. Tween 80 Enhanced TNT Mineralization by Phanerochaete Chrysosporium. *Can. J. Microbiol.* **2000**, *46*, 110–118.
115. Shen, C. F.; Hawari, J.; Ampleman, G.; Thiboutot, S.; Guiot, S. R. Origin of p-Cresol in The Anaerobic Degradation of Trinitrotoluene. *Can. J. Microbiol.* **2000**, *46*, 119–124.
116. Robidoux, P. Y.; Svendsen, C.; Caumartin, J.; Hawari, J.; Ampleman, G.; Thiboutot, S.; Weeks, J. M.; Sunahara, G. I. Chronic Toxicity of Energetic Compounds in Soils Determined Using the Earthworm (Eisenia Andrei) Reproduction Test. *Environ. Toxicol. Chem.* **2000**, *19* (7), 1764–1773.
117. Hawari, J.; Halasz, A.; Beaudet, S.; Groom, C.; Paquet, L.; Rhofir, C.; Ampleman, G.; Thiboutot, S. Characterization of Metabolites and End Products During Biodegradation of Hexahydro-1,3,5-Trinitro-1,3,5-Triazine (RDX) with Municipal Sludge. *Appl. Environ. Microbiol.* **2000**, *66* (6), 2652–2657.
118. Hawari, J.; Beaudet, S.; Halasz, A.; Thiboutot, S.; Ampleman, G. Microbial Degradation of Explosives: Biotransformation versus Mineralization. *Appl. Microbiol. Biotechnol.* **2000**, *54*, 605–618.
119. Hawari, J.; Shen, C. F.; Guiot, S. R.; Greer, C. W.; Rho, D.; Sunahara, G.; Ampleman, G.; Thiboutot, S. Bioremediation of Highly Energetic Compounds: A Search for Remediation Technologies. *Water Sci. Technol.* **2000**, *42* (5−6), 385–394.
120. Robidoux, P. Y.; Hawari, J.; Thiboutot, S.; Ampleman, G.; Sunahara, G. I. Chronic Toxicity of Octahydro-1,3,5,7-Tetranitro-1,3,5,7-Tetrazocine (HMX) in Soil Determined Using the Earthworm (Eisenia Andrei) Reproduction Test. *Environ. Pollut.* **2001**, *111*, 283–292.
121. Rho, D.; Hodgson, J.; Thiboutot, S.; Ampleman, G.; Hawari, J. Transformation of 2,4,6-Trinitrotoluene (TNT) by Immobilized Phanerochaete Chrysosporium Under Fed-Batch and Continuous TNT Feeding Conditions. *Biotechnol. Bioeng.* **2001**, *73* (4), 271–281.
122. Sunahara, G. I.; Robidoux, P. Y.; Gong, P.; Lachance, B.; Rocheleau, S.; Dodard, S. G.; Sarrazin, M.; Hawari, J.; Thiboutot, S.; Ampleman, G.; Renoux, A. Y. Laboratory and Field Approaches to Characterize the Soil Exotoxicology of Polynitro Explosives; *Environmental Toxicology and Risk Assessment: Science, Policy and Standardization-Implications for Environmental Decisions: Tenth Volume*; ASTM STP 1403; Greenberg, B. M., Hull, R. N., Roberts, M. H., Jr., Gensemer, R. W., Eds.; American Society for Testing and Materials: West Conshohocken, PA, 2001; pp 293−312.
123. Hawari, J.; Halasz, A.; Beaudet, S.; Paquet, L.; Ampleman, G.; Thiboutot, S. Biotransformation of Octahydro-1,3,5,7-Tetranitro-1,3,5,7-Tetrazocine by Municipal Anaerobic Sludge. *Environ. Sci. Technol.* **2001**, *35*, 70–75.
124. Sheremata, T. W.; Halasz, A.; Paquet, L.; Thiboutot, S.; Ampleman, G.; Hawari, J. The Fate of the Cyclic Nitramine Explosive RDX in Natural Soil. *Environ. Sci. Technol.* **2001**, *35*, 1037–1040.

125. Gong, P.; Hawari, J.; Thiboutot, S.; Ampleman, G.; Sunahara, G. I. Ecotoxicological Effects of Hexahydro-1,3,5-Trinitro-1,3,5-Triazine on Soil Microbial Activities. *Environ. Toxicol. Chem.* **2001**, *20* (5), 947–951.
126. Renoux, A.; Caumartin, J.; Thiboutot, S.; Ampleman, G.; Sunahara, G. I. Derivation of Environmental Soil Quality Guidelines for 2,4,6 Trinitrotoluene: CCME Approach. *Hum. Ecol. Risk Assess.* **2001**, *27* (6), 1715–1735.
127. Gong, P.; Hawari, J.; Thiboutot, S.; Ampleman, G.; Sunahara, G. I. Microbial Toxicity of Octahydro-1,3,5,7-Tetranitro-1,3,5,7-Tetrazocine (HMX) in Soil. *Bull. Environ. Toxicol. Chem.* **2001**, *20* (5), 947–951.
128. Gong, P.; Hawari, J.; Thiboutot, S.; Ampleman, G.; Sunahara, G. I. Ecotoxicological Effects of Hexahydro-1,3,5-Trinitro-1,3,5-Triazine (RDX) on Soil Microbial Activities. *Environ. Toxicol. Chem.* **2001**, *20* (5), 947–951.
129. Robidoux, P. Y.; Hawari, J.; Bardai, G.; Paquet, L.; Ampleman, G.; Thiboutot, S.; Sunahara, G. I. TNT, RDX and HMX Decrease Earthworm (Eisenia Andrei) Life-Cycle Responses in a Spiked Natural Forest Soil. *Arch. Environ. Contam. Toxicol.* **2002**, *43* (4), 379–388.
130. Robidoux, P. Y.; Svendsen, C.; Sarrazin, S.; Hawari, J.; Thiboutot, S.; Ampleman, G.; Weeks, J. M.; Sunahara, G. I. Evaluation of Tissue and Cellular Biomarkers to Assess 2,4,6-Trinitrotoluene (TNT) Exposure in Earthworms - Effects Based Assessment in Laboratory Studies Using Eisenia Andrei. *Biomarkers* **2002**, *7* (4), 306–321.
131. Bhushan, B.; Halasz, A.; Spain, J.; Thiboutot, S.; Ampleman, G.; Hawari, J. Biotransformation of Hexahydro-1,3,5 trinitro-1,3,5 triazine (RDX) Catalyzed by a NAD(P)H: Nitrate Oxydoreductase from Aspergillus Niger. *Environ. Sci. Technol.* **2002**, *36* (14), 3104–3108.
132. Halasz, A.; Groom; Zhou, E. C.; Paquet, L.; Beaulieu, C.; Deschamps, S.; Corriveau, A.; Thiboutot, S.; Ampleman, G.; Dubois, C.; Hawari, J. Detection of Explosives and Their Degradation Products in Soil Environments. *J. Chromatogr., A* **2002**, *963*, 411–418.
133. Zhao, J. S.; Fournier, D.; Thiboutot, S.; Ampleman, G.; Hawari, J., Biodegradation and Bioremediation of Explosives; *Soil Biology: Bioremediation, Phytoremediation and Natural Attenuation*; Singh, A., Ward, O., Ed.; Springer : 2003.
134. Robidoux, P. Y.; Bardai, G.; Paquet, L.; Ampleman, G.; Thiboutot, S.; Hawari, J.; Sunahara, G. I. Phytotoxicity of 2,4,6-Trinitrotoluene (TNT) and Octahydro-1,3,5,7-Tetranitro-1,3,5,7-Tetrazocine (HMX) in Spiked Artificial and Natural Forest Soils. *Arch. Environ. Contam. Toxicol.* **2003**, *44*, 198–209.
135. Monteil-Rivera, F.; Halasz, A.; Groom, C.; Zhao, J. S.; Thiboutot, S.; Ampleman, G.; Hawari, J. Fate and Transport of Explosives in the Environment: A Chemist's View; *Ecotoxicology of Explosives and Unexploded Ordnance*; EET series text book; CRC Press, 2004.
136. Kuperman, R.; Checkai, R. T.; Sunahara, G.; Robidoux, P. Y.; Thiboutot, S.; Ampleman, G. *Ecological Risk Assessment of Soil Contamination with Explosives in North America*; CRC Press, 2004; Chapter 13.

137. Robidoux, P. Y.; Svendsen, C.; Sarrazin, M.; Thiboutot, S.; Ampleman, G.; Hawari, J.; Weeks, J. M.; Sunahara, G. I. Assessment of a 2,4,6-Trinitrotoluene–Contaminated Site Using Aporrectodea Rosea and Eisenia Andrei in Mesocosms. *Arch. Environ. Contam. Toxicol.* **2004**, *48*, 56–67.
138. Zhao, J.-S.; Fournier, D.; Thiboutot, S.; Ampleman, G.; Hawari, J. Biodegradation and Bioremediation of Explosives. In *Soil Biology, Bioremediation, Phytoremediation and Natural Attenuation*; Singh, A., Ward, O., ,Eds.; Springer-Verlag, 2004; Vol. 1, pp 55−80.
139. Bhushan, B.; Halasz, A.; Thiboutot, S.; Ampleman, G.; Hawari, J. Chemotaxis-Mediated Biodegradation of Cyclic Nitramine Explosives RDX, HMX and CL-20 by Clostridium sp. EDB2. *Biochem. Biophys. Res. Commun.* **2004**, *316*, 816–821.
140. Zhao, J.-S.; Greer, C. W.; Thiboutot, S.; Ampleman, G.; Hawari, J. Biodegradation of the nitramime explosive hexahydro-1,3-5-trinitro-1,3,5-triazine and octahydro-1, 3,5,7-tetranitro-1,3,5,7-tetrazocine in cold marine sediment under anaerobobic and oligottrophic conditions. *Can. J. Microbiol.* **2004**, *50*, 91–96.
141. Zhao, J.-S.; Spain, J.; Thiboutot, S.; Ampleman, G.; Greer, C. W.; Hawari, J. Phylogeny of Cyclic Nitramine-Degrading Psychrophilic Bacteria in Marine Sediment and Their Potential Role in the Natural Attenuation of Explosives. *FEMS Microbiol. Ecol.* **2004**, *49*, 349–3574.
142. Fournier, D.; Halasz, A.; Thiboutot, S.; Ampleman, G.; Manno, D.; Hawari, J. Biodegradation of Octahydro-1,3,5,7-tetranitro-1,3,5,7-tetrazocine (HMX) by Phanerochaete Chrysosporium: New Insight into the Degradation Pathway. *Environ. Sci. Technol.* **2004**, *38*, 4130–4133.
143. Groom, C. A.; Halasz, A.; Paquette, L.; Thiboutot, S.; Ampleman, G.; Hawari, J. Detection of Nitroaromatic and Cyclic Nitramine Compounds by Cyclodextrin Assisted Capillary Electrophoresis Quadrupole Ion Trap Mass Spectrometry. *J. Chromatogr., A* **2005**, *1072*, 73–82.
144. Doddard, S.; Sunahara, G.; Kuperman, R. G.; Sarrazin, M.; Gong, P.; Ampleman, G.; Thiboutot, S.; Hawari, J. Survival and Reproduction of Enchytraeid Worms, Oligochaeta, in Different Soil Types Amended with Energetic Cyclic Nitramines. *Environ. Toxicol. Chem.* **2005**, *24* (10), 2579–2587.
145. Robertson, T. J.; Martel, R.; Quan, D. M.; Ampleman, G.; Thiboutot, S.; Jenkins, T.; Provatas, A. Fate and Transport of 2,4,6-Trinitrotoluene in Loams at a Former Explosives Factory. *Soil Sediment Contam.* **2007**, *16*, 159–179.
146. Zhao, J. S.; Manno, D.; Thiboutot, S.; Ampleman, G.; Hawari, J. Shewanella Canadensis Sp. Nov. and Shewanella Atlantica Sp. Nov., two Novel Manganese Dioxide - and Hexahydro-1,3,5-Trinitro-1,3,5-1,3,5-Triazine Reducing Psychrophilic Species of Marine Bacteria. *Int. J. Syst. Evol. Microbiol.* **2007**, *57*, 2155–2162.
147. Lazar, C.; Halasz, A.; Beaulieu, C.; Thiboutot, S.; Ampleman, G.; Hawari, J. Phototransformation of Perchlorate to Chloride in the Presence of Polysilanes. *Aust. J. Chem.* **2007**, *60* (11), 857–861.
148. Kuperman, R. G.; Checkai, R.; Johnson, M.; Robidoux, P. Y.; Lachance, B.; Thiboutot, S.; Ampleman, G. *Ecological Risk Assessment of Soil*

Contamination with Explosives in North America; CRC Press, 2007; Chapter 14, pp 1−58.
149. Naja, G.; Halasz, A.; Thiboutot, S.; Ampleman, G.; Hawari, J. Degradation of Hexahydro-1,3,5-trinitro-1,3,5-triazine (RDX) Using Zerovalent Iron Nanoparticles. *Environ. Sci. Technol.* **2008**, *42* (12), 4364–4370.
150. Rocheleau, S.; Lachance, B.; Kuperman, R. G.; Hawari, J.; Thiboutot, S.; Ampleman, G.; Sunahara, G. Toxicity and Uptake of Cyclic Nitramine Explosives in Ryegrass Lolium Perenne. *Environ. Pollut.* **2008**, *156* (1), 199–206.
151. Lachance, B.; Bergeron, P.-M., Bérubé, V.; Sunahara, G. I.; Robidoux, P.-Y., *Validation of Environmental Military Threshold Values for Explosives in Soil*; NRC # 49926, National Research Council Canada, Biotechnology Research Institute, Montreal, Canada.
152. Monteil-Rivera, F.; Halasz, A.; Mannoa, D.; Kuperman, R. B.; Thiboutot, S.; Ampleman, G.; Hawari, J. Fate of CL-20 in Sandy Soils: Degradation Products as Potential Markers of Natural Attenuation. *Environ. Pollut.* **2009**, *157* (1), 77–85.
153. Rocheleau, S.; Kuperman, R. G.; Simini, M.; Hawari, J.; Checkai, R. T.; Thiboutot, S.; Ampleman, G.; Sunahara, G. Toxicity of 2,4-Dinitrotoluene to Terrestrial Plants in Natural Soils. *Sci. Total Environ.* **2010**, *408* (16), 3193–3199.
154. Sunahara, G.; Lotufo, G.; Kuperman, R.; Hawari, J. Thiboutot, S.; Ampleman, G. *Ecotoxicology of Explosives*, CRC Press, Taylor and Francis Group, ISBN 978-0-8493-2839-8, 2009.
155. Sarrazin, M.; Doddard, S. G.; Savard, K.; Lachance, B.; Robidoux, P. Y.; Kuperman, R.; Hawari, J.; Ampleman, G.; Thiboutot, S.; Sunahara, G. Accumulation of Hexahydro-1,3,5-Trinitro-1,3,5-Triazine by the Earthworm Eisenia Andrei in a Sandy Loam Soil. *Environ. Toxicol. Chem.* **2009**, *28* (10), 2125–2133.
156. Halasz, A.; Thiboutot, S.; Ampleman, G.; Hawari, J. Microwave-Assisted Hydrolysis of Nitroglycerin (NG) Under Mild Alkaline Conditions: New Insight into the Degradation Pathway. *Chemosphere* **2010**, *79*, 228–232.
157. Monteil-Rivera, F.; Deschamps, S.; Ampleman, G.; Thiboutot, S.; Hawari, J. Dissolution of a New Explosive Formulation Containing TNT and HMX: Comparison with Octol. *J. Hazard. Mater.* **2010**, *174*, 281–288.
158. Parent, G. *Gestion des secteurs d'entraînement de la base militaire de Wainwright (AB) à partir de la vulnérabilité des aquifers et du risque de contamination par les résidus de munitions*; Mémoire INRS-ETE, Institut national de la recherche scientifique – Centre Eau, Terre et Environnement, Université du Québec, Québec, Canada, 2008.

Chapter 4

The Use of Conventional and Surface Enhanced Raman Spectroscopy to Evaluate Chemistries for the Detection and/or Remediation of Pechlorate in Aqueous Systems

P. A. Mosier-Boss*

SPAWAR Systems Center Pacific, Code 71730, San Diego, CA 92152
***pam.boss@navy.mil**

Perchlorate is highly soluble and non-reactive with soil sediments. As a result perchlorate is exceedingly mobile in aqueous systems. Because of its resistance to react with other available constituents, perchlorate can persist for many decades under typical ground and surface water conditions. Detection and remediation of perchlorate often rely on the use of resins and coatings to selectively extract/concentrate perchlorate from its aqueous environment. In this chapter, the use of both conventional (normal) Raman spectroscopy and surface enhanced Raman spectroscopy (SERS) to evaluate the effectiveness of the chemistries used in the resins and coatings to selectively extract perchlorate will be discussed. Specifically SERS has been used to evaluate the selectivity of cationic self assembled monolayers (SAMs) for anions and conventional Raman spectroscopy has been used to compare the performance of two similar bifunctional resins, Purolite A-530 and Amberlite PWA-2.

Introduction

The most commonly used methods to detect and remediate perchlorate rely on the use of coatings and/or ionophores to selectively extract perchlorate from an aqueous medium. The Thermo Orion perchlorate ion selective electrode uses a membrane with tris (substituted 1,10-phenanthroline) iron (II) ion exchanger

dissolved in *p*-nitrocymene to create a non-water soluble ion-exchanging liquid (*1*). The ion exchange resins used in drinking water and wastewater treatment use quaternary amines to remove perchlorate. However, both the membranes and resins used to detect/remediate perchlorate are not specific for perchlorate. Although they do interact with other anions, the interaction with perchlorate is stronger. Consequently, the selectivitity of the membranes and resins for perchlorate need to be evaluated to develop a better understanding of the underlying molecular interactions. Such information can later be used to design membranes and resins that exhibit greater selectivity for perchlorate.

In the case of the ion selective electrode (ISE), the selectivity is determinied by measuring the potential of a series of solutions in which the concentration of perchlorate is varied in the presence of a constant background level of the ionic interferent. Both perchlorate and the interfering ion contribute to the measured potential, *E*. The relationship that describes the response of the ISE for both species is given by the following relationship:

$$E = C + \frac{RT}{z_i F} \ln \left[a_i + \sum K_{ij} a_j^{(z_i / z_j)} \right] \quad (1)$$

where *C* is a constant, a_i is the activity of the primary ion with charge z_i, a_j is the activity of the interfering ion with charge z_j, and K_{ij} is the selectivity ratio. However, in order to correct for the potential contribution due to the interfering ions, their identities must be known. Alternatively, some interferences may be eliminated by adding masking agents to complex the interfering species thereby preventing them from interacting with the membrane of the ISE.

To evaluate the performance of ion exchange resins, the sorption of the primary species *i* is measured by mixing *m* amount of resin with known quantities of primary species (*i*) and interfering species (*j*) (*2*). After allowing time (*t*) to equilibrate, the concentration of the ions in the supernatant are measured. The distribution coefficient for species *i*, K_d, is then calculated using the following relationship:

$$K_d = \frac{(C_0 - C)m^{-1}}{C} \quad (2)$$

where C_0 is the concentration of species *i* added to the resin and *C* is the concentrations of species *i* in the supernatant after sample equilibration. For a given resin, K_d varies as a function of equilibration time and background electrolyte concentration.

The methods used to evaluate resins and sensing membranes do not directly measure the anion interaction with the ionophore. In this chapter, the use of conventional Raman spectroscopy (hereafter referred to as Raman) and SERS to evaluate the effectiveness of resins and coatings to selectively extract perchlorate (*3*, *4*) is discussed. The advantages of Raman/SERS for this application are: (i) all polyatomic species exhibit a characteristic Raman/SERS spectrum, (ii) the Raman/SERS spectral lines are narrow which allows simultaneous detection of

multiple polyatomic species, (iii) SERS can result in a 10^5–10^{10} enhancement of the Raman signal, (iv) water is a very poor Raman scatterer and does not interfere, and (v) both the resin and coatings will also exhibit Raman/SERS lines that can be used as internal standards. In these investigations, SERS has been used to evaluate the selectivity of cationic SAMs for anions and Raman spectroscopy has been used to compare the performance of two similar bifunctional resins, Purolite A-530 and Amberlite PWA-2.

Results and Discussion

Evaluation of Ion Exchange Resins Using Raman Spectroscopy

The selectivity of ion exchange resins for perchlorate depends upon the polymeric backbone (acrylic versus styrenic) and the quaternary ammonium group. It has been shown that styrenic resins exhibit greater selectivity for perchlorate than acrylic (*3*). Recently, quaternary, strong-base anion exchange resins were investigated for the sorption of perchlorate from aqueous solution (*2*). While the resins selected for this study had the same polystyrenic backbone structure and similar bead size, they had different trialkyl ammonium functional groups grafted onto the benzyl groups of the resin backbone. This study showed that the resin with two quaternary ammonium groups, $-N(n\text{-}C_6H_{15})_3^+$ and $-N(C_2H_5)_3^+$, exhibited the highest selectivity for perchlorate and optimum adsorption kinetics. It is believed that the long chains of the trihexylammonium (THA) group enhances selectivity for perchlorate, while the triethylammonium (TEA) group reduces congestion (steric considerations) thereby improving sorption kinetics.

This bifunctional anion exchange resin can be obtained from either Purolite (A-530) or Rohm and Haas (Amberlite PWA-2). Upon visible inspection, these two resins look quite different. The Purolite A-530 resin beads are pearly white in color and opaque. In contrast, the Rohm and Haas Amberlite PWA2 resin beads are transparent and golden brown in color. The technical literature available for these resins does not specify the TEA/THA composition of the resins nor does it indicate the degree of cross-linking. It was therefore of interest to determine if Raman spectroscopy could be used to ascertain the TEA/THA composition of the resins, the degree of cross-linking, as well as the details of their interaction with anions (*4*).

Figure 1a shows Raman spectra obtained for an Amberlite PWA-2 resin bead, TEA, and THA. The arrows in the Raman spectrum of the resin bead indicate the CH_2 /CH_3 out-of-phase and in-phase deformation modes of the trialkylamines at 1459 and 1325 cm^{-1}, respectively. The trialkylamine groups bind to the benzyl moieties of the resin though their nitrogen atoms. Therefore, it is expected that the binding of the trialkylamine groups to the benzyl groups will not affect the intensities of the peaks due to the trialkylamine CH_2 /CH_3 out-of-phase and in-phase deformation modes. Consequently, the ratio of the intensity of the 1325 cm^{-1} peak to the 1459 cm^{-1} peak can be used to estimate the TEA/THA composition of the resin using the following relationship:

$$R_{resin} = xR_{THA} + (1-x)R_{TEA} \quad (3)$$

where R_{resin}, R_{THA}, and R_{TEA} are the ratios of the 1325 cm^{-1} peak to the 1459 cm^{-1} peak for the resin, THA, and TEA respectively and x is the fractional amount of the resin that is THA. Using this relationship, the composition of the Amberlite PWA-2 resin was found to be 25% TEA / 75% THA while it was found to be 41% TEA/ 59% THA for Purolite A-530 (*4*).

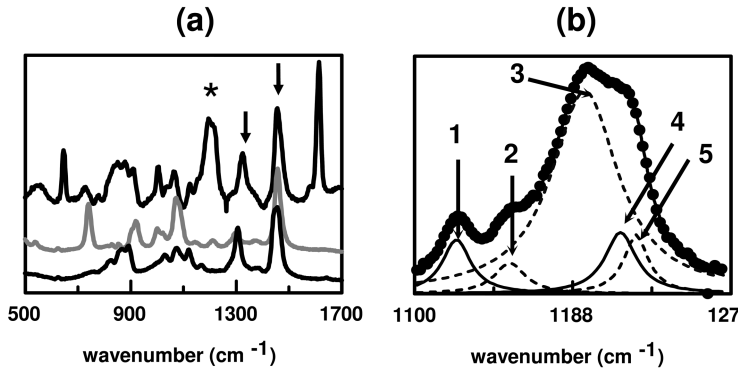

Figure 1. (a) Raman spectra obtained for (top) the Amberlite PWA-2 resin bead, (middle) TEA, and (bottom) THA. The arrows indicate the CH_2 /CH_3 in-phase deformation modes of the trialkyl amines at 1324 cm^{-1} and the CH_2 /CH_3 out-of-phase deformation modes of the trialkyl amines at 1459 cm^{-1}. The asterisk indicates the broad band beween 1100 and 1300 cm^{-1} due to the ring modes for the benzyl group and the divinylbenzene cross-linker. (b) Results of deconvolution of the Amberlite PWA-2 resin Raman band beween 1100 and 1275 cm^{-1} into five Lorentzian peaks. For the Raman band, • represents the experimental data and — , which connects the measured data points, is the sum of the five calculated Lorentzian peaks showing the goodness of fit. The five Lorentzian peaks are numbered. Reprinted with permission from Applied Spectroscopy (4).

To determine the degree of cross-linking of the resins, the Raman band between 1100 and 1300 cm^{-1}, indicated by the asterisk in Figure 1a, was analyzed (*4*). This band is attributed to the ring modes of the benzyl groups, onto which the trialkylamine moeties are grafted, and the divinyl benzene cross-linker. Figure 1b shows the results of deconvoluting this Raman band, as measured for the Amberlite PWA-2 resin, into five Lorentzian peaks centered at 1124, 1152, 1194, 1213, and 1223 cm^{-1}. These same five peaks were also obtained upon deconvolution of the 1100-1300 cm^{-1} Raman band observed for the Purolite A-530 resin. Peak 1 in Figure 1b is centered at 1124 cm^{-1} and is attributed to

THA. For the Amberlite PWA-2 resin this peak is larger than that observed for the the Purolite A-530 resin. This is not surprising as the PWA-2 resin has a higher THA content than the A-530 resin. The large 1194 cm^{-1} peak, peak 3 in Figure 1b, is assigned to the ring mode of the polyvinylbenzyl backbone onto which the triaklyamines are grafted. In both resins, the 1152, 1213, and 1223 cm^{-1} peaks (peaks 2, 4, and 5 in Figure 1b) exhibit the same peak ratios, relative to each other, which indicates that they are due to the same species. These peaks are assigned to the divinylbenzene cross-linker. These peaks are larger in the A-530 resin than they are in the PWA-2. This indicates that the A-530 resin contains more divinyl benzene than the PWA-2 resin and is therefore more cross-linked than the PWA-2 resin.

As received from the manufacturer, the positively charged surface functional groups of the resin contain sorbed chloride ions. When exposed to a solution containing anions other than chloride, the anions will enter the pores of the resin and replace chloride ions (*2*). As shown in Figure 2a, if the anion is polyatomic, this exchange can be monitored using Raman spectroscopy (*4*). Figure 2a shows Raman spectra of the Amberlite PWA-2 resin bead obtained before and after immersion of the resin bead in a 50 ppm perchlorate solution overnight. New peaks, at 460, 630, and 935 cm^{-1} due to perchlorate, can be seen after the bead had been immersed in the perchlorate solution. Spectra were obtained for resin beads immersed in a series of aqueous solutions with varied perchlorate concentration from 5 to 500 ppm. The concentration response is shown in Figure 2b. The area of the 935 cm^{-1} perchlorate peak was normalized to the area of the 1613 cm^{-1} peak of the resin bead to account for bead-to-bead variation. This resin peak is indicated by an arrow in Figure 2a. As shown in Figure 2b, at low perchlorate concentrations, the normalized area of the perchlorate peak rapidly increases with concentration. At higher perchlorate concentrations, the measured response levels off as the adsorption sites on the substrate become fully occupied by perchlorate. It was found that the observed concentration response can be described by a Frumkin isotherm:

$$\theta = \frac{CKe^{2g\theta}}{1+CKe^{2g\theta}}$$

where θ is the fractional coverage of perchlorate on the resin bead, K is the ion pair constant between perchlorate and the resin bead, C is the solution concentration of perchlorate (in M), and g is the Frumkin parameter. The Frumkin parameter takes into account interactions between adsorbed perchlorate ions. The K and g values measured for the Purolte A-530 and Amberlite PWA-2 resins for perchlorate and other polyatomic anions are summarized in Table I.

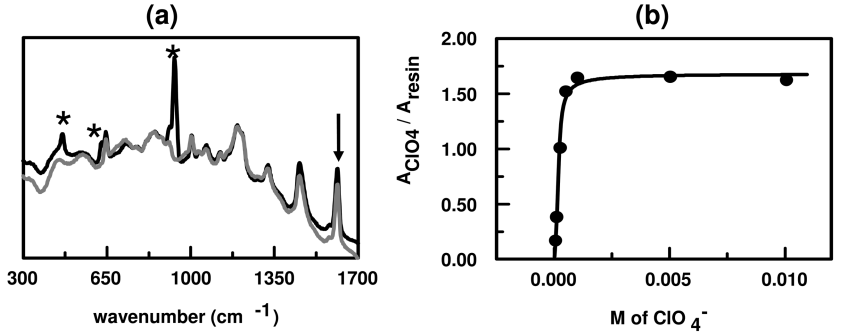

Figure 2. (a) Raman spectra obtained for the Amberlite PWA-2 rein bead in the presence (black) and absence (gray) of 50 ppm perchlorate. Asterisks indicate peaks due to perchlorate.(b) Plot of the 935 cm^{-1} perchlorate peak area normalized to the 1613 cm^{-1} resin peak area (peak indicated by an arrow in Figure 1a) as a function of perchlorate concentration in M.In this plot, • is the experimental data and — is the results of computer analysis fitting the experimental data to a Frumkin isotherm.

Table I. Summary of the ion pair constants and Frumkin parameters for the anion-resin interactions (*4*). No interactions were observed between both resins and HPO_4^{2-} or $H_2PO_4^-$

Purolite A-530		
anion	***K (M^{-1})***	***g***
Perchlorate	1960 ± 410	1.69 ± 0.16
Nitrate	3360 ± 320	0.918 ± 0.090
Sulfate	53800 ± 5300	-0.440 ± 0.089
Chromate	2180 ± 270	1.48 ± 0.19
Chloride	35 ± 10	0.918 ± 0.090
Amberlite PWA-2		
anion	***K (M^{-1})***	***g***
Perchlorate	1530 ± 350	1.23 ± 0.22
Nitrate	2200 ± 250	0.63 ± 0.11
Sulfate	14200 ± 2200	0.07 ±0.15
Chromate	1820 ± 250	1.05 ± 0.12
Chloride	19 ±10	0.63 ± 0.11

Chloride ion does not have a Raman active mode. To determine the value of *K* for chloride ion, a competitive complexation approach is used (*5*). In this method, the concentration of an anion exhibiting a Raman active mode (the probe ion) is kept constant while the concentration of the chloride ion is varied. Both the probe ions and chloride ions will compete for sites on the resin. The change in the peak area due to the probe ion is then measured as a function of chloride

ion concentration. The results of the competitive analysis are summarized in Figure 3 as well as the equations that describe the interaction of the two ions as they compete for sites on the resin. From previous experiments, the values of K_{ClO4} and g_{ClO4} are known, see Table I. As a result of the competive complexation experiment, summarized in Figure 3, C_{ClO4} is known and κ can be determined. While the value of g_{Cl} is not known, because chloride and nitrate ions have the same net charge and are close in ionic size (*5*), have similar solvation properties in water (*5*), similar conductances in formamide (*6*), similar ionic mobilities in hexamethylphosphorotriamide (*7*), and are next to each other in the Hofmeister series (*8*), it is reasonable to assume that the value of the Frumkin parameter will be similar for both nitrate and chloride ions. With this assumption, the value of K_{Cl} can be calculated for both resins and these values are tabulated in Table I.

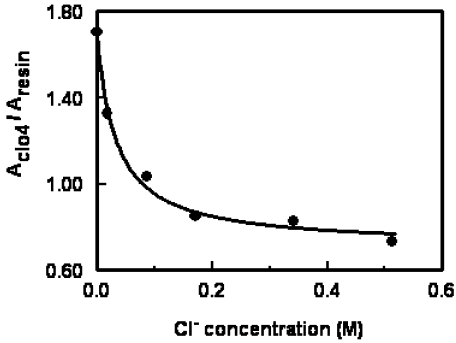

$$\Delta A_{ClO4} = \frac{VC_{Cl}}{\kappa + C_{Cl}} = A_0 - A_{Cl}$$

where $V = \alpha\theta_0$ and

$$\kappa = \frac{1 + C_{ClO4} K_{ClO4}[\exp(2g_{ClO4}\theta_0)]}{K_{Cl}[\exp(2g_{Cl}\theta_0)]}$$

Figure 3. Results of the competitive complexation analysis to evaluate the chloride ion interaction with the Purolite A-530 resin. The plot shows the normalized perchlorate peak area as a function of chloride ion concentration. Perchlorate ion concentration is 50 ppm. The equations on the right hand side describe the interaction of the two ions with the resin where A_0 and A_{Cl} are the normalized areas of the perchlorate peak in the absence and presence of chloride; C_{Cl} and C_{ClO4} are the solution concentrations, in M, of chloride and perchlorate; K_{Cl} and K_{ClO4} are the ion pair constants of chloride and perchlorate; g_{Cl} and g_{ClO4} are the Frumkin parameters for chloride and perchlorate; and α is a proportionality constant. Plot reprinted with permission from Applied Spectroscopy (4).

Examining Table I, it can be seen that for both resins, the ion pair constants are $SO_4^{2-} >> NO_3^- > CrO_4^{2-} > ClO_4^- >> Cl^-$. If selectivity of the resin is determined solely by the ion pair constant, then one would expect the resins to be more selective for both sulfate and nitrate, not perchlorate. However, field testing of these resins show that the resins preferentially sorb perchlorate in the presence of competing anions such as sulfate, chloride, and bicarbonate (*2*). Furthermore these competing anions usually exist in relatively high concentrations, compared to perchlorate, in groundwater and surface water. Figure 4 summarizes Raman results obtained by placing Purolite A-530 and Amberlite PWA-2 resin beads in

aqueous solutions of (a) 7.5 ppm perchlorate and 200 ppm sulfate and (b) 7.5 ppm perchlorate and 100 ppm nitrate. The results shown in Figure 4 indicate that for both resins, the perchlorate interaction is stronger than the nitrate and sulfate interactions, even though the nitrate and sulfate concentrations were more than ten times greater than that of perchlorate. The Raman results also show that the actual selectivity of both resins for the anions is ClO_4^- > NO_3^- > SO_4^{2-}. These observations indicate that the ion pair constant alone does not reliably predict the selectivity of the resins. As shown in Eq. 4, the Frumkin isotherm has another parameter, *g*, referred to as the Frumkin parameter. The importance of the Frumkin parameter on resin selectivity has not been previously investigated. According to the literature, the Frumkin parameter takes into account interactions between anions adsorbed on the resin. A negative value of *g* is indicative of repulsive forces between species adsorbed on a substrate while a positive value is indicative of attractive forces. Nothing has been said about the magnitude of the Frumkin parameter and its role on the overall selectivity of the resin for a given species has been largely ignored. However, it is interesting to note that, for both resins, the magnitude of the Frumkin parameter decreases in the order ClO_4^- > NO_3^- > SO_4^{2-}, which mirrors the observed selectivity of the resins for these anions. Additional work needs to be done to show whether or not the Frumkin parameter can be useful to predict selectivities.

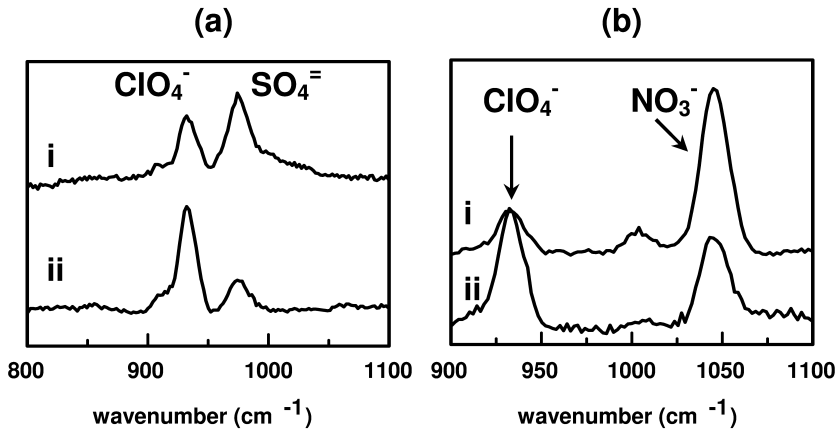

Figure 4. (a) Raman spectra obtained for (i) Amberlite PWA-2 and (ii) Purolite A-530 resin beads immersed in solutions of 7.5 ppm perchlorate and 200 ppm sulfate. (b)) Raman spectra obtained for (i) Amberlite PWA-2 and (ii) Purolite A-530 resin beads immersed in solutions of 7.5 ppm perchlorate and 100 ppm nitrate. Reprinted with permission from Applied Spectroscopy (4).

The results in Figure 4 also indicate that Purolite A-530 exhibits greater selectivity for perchlorate than the Amberlite PWA-2. As discussed *vide supra*, Raman spectroscopic measurements showed that PWA-2 has a higher THA content compared to A-530 and that A-530 is more cross-linked than PWA-2. Greater cross-linking translates into a more hydrophobic/lipophilic environment. Perchlorate, being lipophilic, will preferentially partition into substrate that is more hydrophobic/lipophilic.

Evaluation of Ionophores Using Surface Enhanced Raman Spectroscopy (SERS)

There are commercially available cationic thiols that can be used as ionophores in the detection of anions, including perchlorate. These thiols can be classified as either cysteamine derivatives, cysteine derivatives, or aromatic. The cysteamine derivatives include cysteamine hydrochloride (CY), dimethylaminoethanethiol hydrochloride (DMA), and diethylaminoethanethiol hydrochloride (DEA). The cysteine derivatives that were investigated were L-cysteine hydrochloride (CYS), L-cysteine methyl ester hydrochloride (CYSM), and L-cysteine ethyl ester hydrochloride (CYSE). The aromatic cationic thiols were 4-(2-mercaptoethyl) pyridinium hydrochloride (MEP), 2-amino-4-trifluoromethyl benzenethiol hydrochloride (ATB), and 2-mercapto-4-methylpyrimidine hydrochloride (MMP).

The cationic thiols bind to a SERS-active surface, through the thiol group, to form a self-assembled monolayer (SAM). The interaction of anions with these SAMs is typically instantaneous. For multi-atomic anionic species the interaction with the cationic coating is followed by monitoring the SERS response of the anion with increasing anion concentration (*9*). Figure 5a shows SERS spectra obtained for Ag/CY in the presence of 0, 25, and 7500 ppm perchlorate. The large CY peaks at 633 and 719 cm^{-1} are due to the C-S stretching modes of the *gauche* and *trans* conformers of CY, respectively. When exposed to perchlorate, a new peak at 935 cm^{-1} is observed, Figure 5a. This peak due to the symmetric Cl-O stretching mode of perchlorate (*10*). When the spectral contributions of the coating are subtracted out, two additional small peaks, due to perchlorate, are observed at 460 and 630 cm^{-1}, Figure 5b. These peaks are due to the O-Cl-O bending modes (*10*). The peak due to the asymmetric Cl-O stretching mode, which would have occurred at ~1100 cm^{-1}, is not Raman active and is, therefore, not observed.

Figure 5c shows a plot of perchlorate peak area as a function of perchlorate concentration for the Ag SERS substrate. At low perchlorate concentration, the perchlorate peak area increases linearly with concentration. At higher solution concentrations of perchlorate, the perchlorate peak area levels off as the adsorption sites on the AG/CY substrate become fully occupied. As with the bifunctional resins, the adsorption of perchlorate on the Ag/CY substrate can also be described by the Frumkin isotherm, Eq. 4. The values of the ion pair constant, K, and the Frumkin parameter, g, for the perchlorate interaction with CY are shown in Table II.

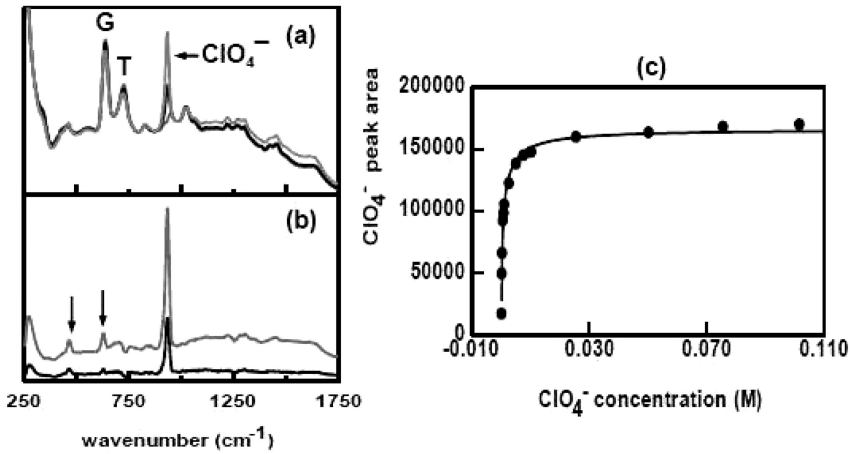

Figure 5. (a) SERS spectra obtained for Ag/CY exposed to 0, 25, and 7500 ppm perchlorate. G and T refer to the gauche and trans conformers of CY, respectively. The perchlorate peak is indicated. (b) SERS spectra for the Ag/CY exposed to 25 and 7500 ppm perchlorate in which the spectral contributions of the CY coating have been subtracted out.Arrows indicate the small perchlorate peaks at 460 and 630 cm-1. (c) Perchlorate peak area plotted as a function of perchlorate concentration for Ag/CY. Reprinted with permission from Applied Spectroscopy (9).

Using SERS, the interaction of other multiatomic anions with thiolated cationic ionophores was also examined. Table II summarizes the ion pair constants and Frumkin parameters for these interactions. As chloride ion does not have a Raman active mode, the ion pair constant for the chloride ion interaction with the cationic thiols was determined using the competitive complexation method described *vide supra*.

The cysteamine derivatives are CY, DMA, and DEA. These derivatives interacted with chloride, nitrate, sulfate, and pechlorate. No interaction was observed between these cationic coatings and either dihydrogen phosphate or monohydrogen phosphate. These coatings formed thioesters when exposed to either chromate or dichromate (*9*). Recently, Gu *et al.* evaluated the selectivity of DMA for perchlorate (*11*) and showed that they were able to detect perchlorate in the presence of 2-5 orders of magnitude concentrations of background ionic species (nitrate, sulfate, phosphate, and chloride). If selectivity was only determined by the ion pair constant, it would be expected that the DMA coating would interact preferentially with sulfate ion. This was not observed by Gu *et al.* However, as shown in Table II, the Frumkin parameter for DMA decreases in the order ClO_4^- > SO_4^{2-} > NO_3^-, Cl^-. This agrees with the observed selectivity of DMA for these anions as reported by Gu *et al*. and provides further evidence that the Frumkin parameter may be useful in predicting selectivities.

Table II. Summary of ion pair constants and Frumkin parameters for the anion-cationic thiol interactions (*9*)[a,b]

cationic thiol	*perchlorate*	*nitrate*	*sulfate*	*chloride*
CY	K= 6150±830 g=-1.10±0.15	K= 382±60 g=-0.30±0.25	K= 1620±320 g=-0.37 ±0.23	K= 146±32 g= -0.30±0.25
DMA	K=404±59 g=-0.64±0.21	K= 301±78 g= -2.3±1.1	K= 972±85 g= -1.14±0.13	K= 310±180 g= -2.3±1.1
DEA	K= 4950±250 g=-2.42±0.10	K= 228±29 g=-1.22±0.30	K= 770±100 g= -0.07±0.12	K= 107±20 g= -1.22±0.30
CYS	No interaction	No interaction	No interaction	No interaction
CYSM	K= 7380±450 g=-2.71±0.10	K= 307±15 g=-1.20±0.11	No interaction	K= 36600±6800 g= -1.20±0.11
CYSE	K= 4650±500 g=-2.14±0.18	K= 513±85 g=-2.06±0.44	No interaction	K= 1190±260 g= -2.06±0.44
MMP	K= 1163±56 g=-2.51±0.21	K= 2370±200 g=-2.58±0.15	Peaks overlap	K= 596±77 g=-2.58 ±0.15
MEP	K= 38±11 g= 1.35±0.24	No interaction	No interaction	K= 92±22 g= 1.35±0.24

[a] These cationic coatings did not ion pair with either HPO_4^{2-} or $H_2PO_4^-$. [b] ATB did not form ion pairs with any anion.

The cationic thiols CYS, CYSM, and CYSE are cysteine derivatives. CYS did not form an ion pair with nitrate, sulfate, or perchlorate. This indicates that the carboxylate group of CYS repels these anions. It was shown that CYS does form thioesters with chromate and dichromate (*9*). CYSM and CYSE are esters of CYS. It was observed that CYSM and CYSE form ion pairs with nitrate, sulfate, and perchlorate and that they form thioesters with chromate and dichromate (*9*). Both the magnitudes of the ion pair constant and Frumkin parameter indicate that CYSM is selective for chloride ion. Molecular modeling indicated that the high selectivity of CYSM for chloride is due to hydrogen bonding between the chloride ion and hydrogen of the CH_3 moieties of adjacent ester groups (*12*).

The aromatic cationic thiols are MEP, ATB, and MMP. There was no observed interaction between the anions and ATB (*9*). This lack of interaction is related primarily to steric hindrance. When ATB adsorbs onto the SERS active surface through its sulfur atom, the amine group is in close proximity to the SERS surface. As a result the amine group of ATB is not in the proper orientation to form ion pairs with the anions.

MMP has two nitrogen atoms in its aromatic ring. The thiol group is on the ring carbon between the two nitrogen atoms. The spectral changes observed in the SERS spectrum of MMP upon adsorption onto a SERS-active substrate indicated that the three heteroatoms of MMP bond to the surface. As a result, MMP has a flat orientation on the SERS surface (*13*). Using SERS, it was shown that MMP

forms an ion pair with chromate with a *K* of 2760±150 and *g* of -2.80 ±0.18 (*9*). Table II summarizes the *K* and *g* values for the interaction of MMP with nitrate, perchlorate, and chloride. For these anions, the *g* values are approximately the same. Therefore, the selectivity of MMP for these anions is determined by *K*. Consequently, the selectivity of MMP follows the order $CrO_4^{=} > NO_3^{-} > ClO_4^{-} > Cl^{-}$.

MEP has a protonated pyridine ring. Table II summarizes the *K* and *g* values for the interaction of MEP with perchlorate and chloride. The interaction of MEP with these anions was very weak. No interaction was observed to occur between MEP and either sulfate or nitrate. SERS showed that MEP formed an ion pair with chromate with a *K* of 142800±7700 and *g* of -2.068±0.063 (*6*). The SERS results do indicate that MEP is selective for chromate. When Turyan and Mandler used MEP to form a SAM on gold electrodes (*14*), they were able to use it to detect chromate by square wave voltammetry. It was shown that chloride, nitrate, and perchlorate did not interfere in the detection of chromate. They suggested that the high selectivity of MEP for chromate was due to hydrogen bonding. This conclusion is supported by changes in the SERS spectra of the coating in the presence of chromate (*13*).

Conclusions

For the bifunctional resins Purolite A-530 and Amberlite PWA-2, Raman spectroscopy proved useful in determining proprietary information about the resins, in particular the THA/TEA compositions and degree of cross-linking of the resins. It was shown that the Raman and SERS techniques provide a means to directly probe the interaction of anions with cationic resins and coatings. Using the Raman/SERS techniques, it was possible to measure the adsorption isotherms of the anion interactions with the cationic resins and SAMs. It was determined that the concentration responses of the anions with the resin and SAMs can both be described by Frumkin isotherms. In the Frumkin isotherm, the ion pair constant, *K*, describes the strength of interaction between the cationic moiety of the resin/SAM and the anion. The Frumkin parameter, *g*, is proportional to the strength and nature of the interactions between anions adsorbed on the resin. It was also shown that the selectivity of the resins/SAMs for a given anion was consistent with the sign and magnitude of the Frumkin parameter.

Acknowledgments

These efforts were funded by the SPAWAR Systems Center San Diego ILIR program, the Strategic Environmental Research and Development Program (SERDP) and the Navy's Environmental Sustainability Development to Integration (NESDI) Program.

References

1. Janata, J. *Principles of Chemical Sensors*; Plenum Press: New York, NY, 1989.
2. Gu, B.; Brown, G. M. Recent Advances in Ion Exchange for Perchlorate Treatment, Recovery and Destruction. In *Perchlorate: Environmental Occurrence, Interactions and Treatment*; Gu, B., Coates, J. D., Eds.; Springer: New York, NY, 2006.
3. Boodoo, F. POU/POE Removal of Perchlorate. *Water Conditioning and Purification* **2003**, *45*, 1–4.
4. Mosier-Boss, P. A. Use of Raman Spectroscopy to Evaluate the Selectivity of Bifunctional Anion Exchange Resins for Perchlorate. *Appl. Spectrosc.* **2008**, *62*, 157–165.
5. Mosier-Boss, P. A.; Boss, R. D.; Lieberman, S. H. Determination of the Ion-Pair Constant between Chloride Ion and Cationic-Coated, Silver SERS Substrates Using Competitive Complexation. *Langmuir* **2000**, *16*, 5441–5448.
6. Notley, J. M.; Spiro, M. Tranference Numbers and Ionic Conductances in Formamide at 25°. *J. Phys. Chem.* **1966**, *70*, 1502–1510.
7. Hanna, E. M.; Pethybridge, A. D; Prue, J. E.; Spiers, D. J. Electrolyte Conductivity of Salts in Hexamethylphosphotriamide. *J. Solution Chem.* **1974**, *3*, 563–583.
8. Roberts, J. M.; Diaz, A. R.; Fortin, D. T.; Friedle, J. M.; Piper, S. D. Influence of the Hofmeister Series on the Retention of Amines in Reversed-Phase Liquid Chromatography. *Anal. Chem.* **2002**, *74*, 4927–4932.
9. Mosier-Boss, P. A.; Lieberman, S. H. Detection of Anions by Normal Raman Spectroscopy and Surface-Enhanced Raman Spectroscopy of Cationic-Coated Substrates. *Appl. Spectrosc.* **2003**, *57*, 1129–1137.
10. Nakamoto, N. *Infrared Spectra of Inorganic and Coordination Compounds*; John Wiley and Sons: New York, NY, 1963.
11. Gu, B.; Ruan, C.; Wang, W. Perchlorate Detection at Nanomolar Concentrations by Surface-Enhanced Raman Scattering. *Appl. Spectrosc.* **2009**, *63*, 98–102.
12. Mosier-Boss, P. A.; Lieberman, S. H. The Role of Hydrogen Bonding in the Selectivity of L-Cysteine Methyl Ester (CYSM) and L-Cysteine Ethyl Ester (CYSE) for Chloride Ion. *Spectrochim. Acta, Part A* **2005**, *61*, 845–854.
13. Mosier-Boss, P. A.; Lieberman, S. H. Surface-Enhanced Raman Spectroscopy (SERS) and Molecular Modeling of the Chromate Interaction with 4-(2-Mercaptoethyl)Pyridinium. *Langmuir* **2003**, *19*, 6826–6836.
14. Turyan, I.; Mandler, D. Selective Determination of Cr(VI) by a Self-Assembled Monolayer-Based Electrode. *Anal. Chem.* **1997**, *69*, 894–897.

Chapter 5

Assessing Sample Processing and Sampling Uncertainty for Energetic Residues on Military Training Ranges: Method 8330B

Marianne E. Walsh,[1,*] Alan D. Hewitt,[2] Thomas F. Jenkins,[3] Charles A. Ramsey,[4] Michael R. Walsh,[1] Susan R. Bigl,[1] Charles M. Collins,[1] and Mark A. Chappell[5]

[1]U.S. Army Engineer Research and Development Center, Cold Regions Research and Engineering Laboratory (ERDC/CRREL), 72 Lyme Road, Hanover, NH 03755
[2]Deceased, formerly of ERDC/CRREL
[3]Retired, formerly of ERDC/CRREL
[4]Envirostat, Inc., PO Box 636, Fort Collins, CO 80522
[5]U.S. Army Engineer Research and Development Center, Environmental Laboratory, 3909 Halls Ferry Road, Vicksburg, MS 39180
[*]Marianne.E.Walsh@usace.army.mil

The standard analytical method to determine explosives in soils (EPA SW-846 Method 8330) was developed in the late 1980s to support efforts to remediate Army ammunition plants and depots where wastewater from munitions production was released onto the soil. Subsequently, the characterization of energetic residues on military training ranges required the development of field sampling and laboratory processing methods suitable for the unique nature of the explosives and propellants dispersed by live-firing exercises. The revised method is based on research at more than 50 training ranges and addresses the uncertainty due to the heterogeneity in the physical form and the spatial distribution of these potentially hazardous constituents. The revised method (8330B) provides guidance for sampling and processing of soil samples. Proper sampling involves collecting an adequate number of evenly spaced increments from throughout a decision unit to reduce uncertainty due to distributional heterogeneity and enough

mass to reduce uncertainty due to compositional heterogeneity. Soil samples may be several kilograms, and the entire sample must be processed to maintain representativeness.

Introduction

Energetic residues are deposited on military training ranges as irregular fibers (*1*) or pieces of propellants (*2*, *3*) and as particles of solid explosives (*4*, *5*). These energetic residue particles accumulate on the soil surface of firing points and where ordnance has partially detonated or ruptured. In addition, energetic residues are found in areas where unexploded ordnance (UXO) has been "blown-in-place" during a range clearance or training activity (*6–9*).

Protocols used for initial investigations on military training ranges included the collection of discrete samples or a five- to seven-increment sample (*10*) that was subsampled in the field and only a small soil aliquot used for determination of energetic concentrations. The Environmental Security Technology Certification Program (ESTCP) Environmental Restoration ER-0628 program recognized that use of different sampling and sample-processing protocols would impact the data used to estimate mass loading of energetic residues on Department of Defense (DoD) training and testing ranges. This project examined the uncertainties associated with estimates of the mean concentration of energetics in soil obtained using commonly used strategies and compared them to a revised approach based on the unique nature of energetic residues. Sampling error was examined using soils collected from a firing point, an impact area, and a demolition area. This paper briefly describes the technology demonstrated during ER-0628 and summarizes some of the more important findings. A detailed description of the demonstration sites, sampling activities, experimental design, and data evaluation were published elsewhere (*11*). The objective is to reduce the uncertainty associated with estimating the mean concentration of energetic compounds within a decision unit by using appropriate sample collection and processing methods.

Experimental Design

Field Sites

Three training areas on Fort Richardson, Alaska were chosen based on the known presence of energetic residues at concentrations that would be detectable by the standard analytical method (SW846 8330). Method 8330 (*12*) uses high performance liquid chromatography and an ultraviolet detector that provides reporting limits around 0.04 mg/kg. The field sites were also selected to represent different types of training ranges: an impact area, a demolition training range, and a mortar firing point.

Impact Area

The Eagle River Flats impact area is used for live-fire training with mortars and howitzers. Within the central impact area, we chose a location that contained residues from a partial detonation of a 120-mm mortar projectile. The projectile was filled with Composition B (60% RDX, 40% TNT) and solid chunks of the explosive filler were scattered over a 380-m^2 area (*5*). We marked a 20 × 20-m area that encompassed the Comp B pieces and the crater. In addition to RDX and TNT, the analytes of interest included HMX that exists as an impurity in RDX, 2,4-DNT and 2,6-DNT that exist as an impurity in TNT, and 2-Am-DNT and 4-Am-DNT that are reduction products of TNT. The surface of the impact area was a mudflat composed of glacially derived silts and clays that are saturated for most of the year.

Demolition Range

Demo Range III is used for heavy demolition training, most with C4 (91% RDX, 9% nonexplosive plasticizers). We chose a 30 × 30-m area that encompassed an area that we sampled the previous year and found RDX from the C4 demolition charges and other energetic residues (HMX, TNT and 2,4-DNT). The surface of this area was gravel; pieces of C4 were scattered throughout the 30 × 30-m area.

Firing Point

Firing Point Fox is a mortar firing point where we had previously found 10 mg/kg of NG, an ingredient in double-base propellant, in an 800-m^2 portion of the 4,422 m_2 firing point (*13*). We established a 40 × 40-m area in the center of the firing point. The surface of the firing point was vegetated loess that was underlain with sand and gravel. In addition to firing of mortars, excess propellant was burned at the firing point.

Field Sampling Strategies

Three conventional sampling strategies, known as discrete, box and the wheel, were used. Discrete samples were collected within each decision unit and were 150 to 200 g of field-moist soil or sediment. The locations for the discrete samples at the demolition range and firing point were randomly selected from a table of random numbers or from the roll of a pair of dice. The discrete samples from the impact area were positioned systematically at 2-m intervals from a random starting point. For the box sampling design, five increments, each equal in mass to a discrete sample, were combined to form one bulk sample. The increments were collected at the center and at 5-m distances from the center, moving in the four cardinal directions (Figure 1a). In the wheel sampling design, seven increments, each equal in mass to a discrete sample, were combined to form one bulk sample, with increments from a location at the center and at six equally spaced locations on the perimeter of a circle with a 0.6-m radius (Figure 1b). Locations for the center

points of the box and wheel samples were from random locations selected based on the roll of a pair of dice, with the constraint that the increments be within the area marked for sampling. At the demolition range and firing point, 100 discrete, five box, and five wheel samples were collected. At the impact area, two sets of 100 discrete samples along with five box and five wheel samples.

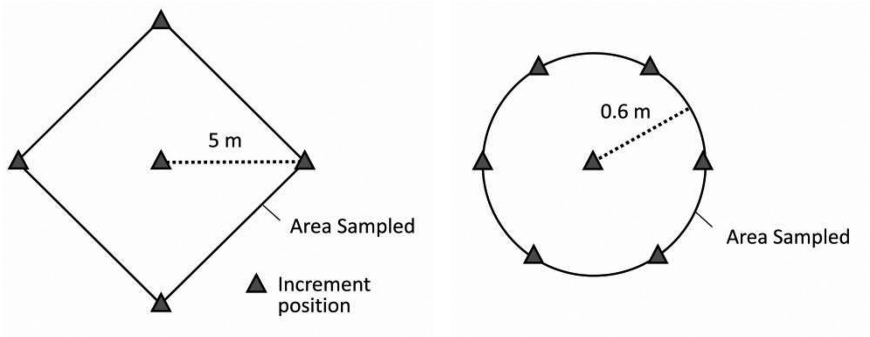

a. Five-increment 50-m^2 box. *b. Seven-increment 0.6-m radius wheel.*

Figure 1. The two conventional sampling designs used.

Method 8330B uses a field sampling strategy called multi-increment where 100 soil increments are collected at evenly spaced intervals throughout each decision unit to form one sample (Figure 2). We collected ten multi-increment samples from each decision unit. The starting point for each multi-increment sample was a random point near one corner of each decision unit.

All samples were collected to a depth of 2.5 cm. The discrete, box and the wheel samples were collected with stainless steel scoops. The multi-increment samples were collected with a 3-cm diameter corer (*14*).

Field Processing and Subsampling of Soil Samples

The conventional practice is to perform a mass reduction step in the field to minimize the mass of soil that is sent to an analytical lab. We examined the error introduced by this procedure. In the field, the box and wheel samples were thoroughly mixed in a stainless steel bowl and subsamples were transferred to 250-mL jars with a large spoon. At each field site, one of the box and one of the wheel samples were completely divided in the field into five or seven jars, respectively (Figure 3). These and all other samples were chilled to 4°C and shipped to our laboratory in Hanover, NH.

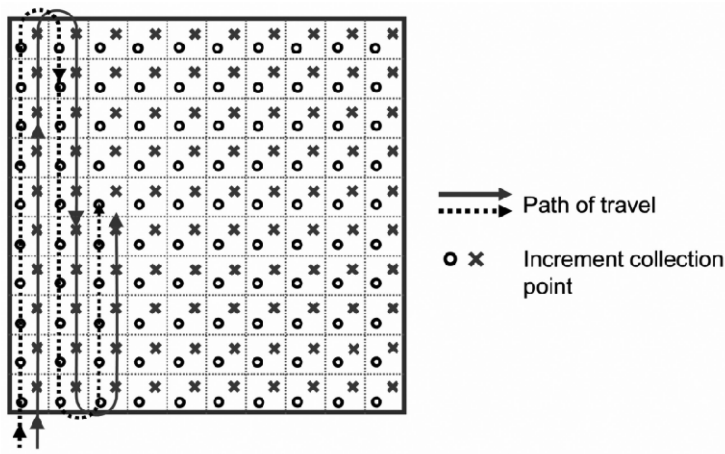

Figure 2. Illustration of multi increment sampling designs for collecting two separate samples.

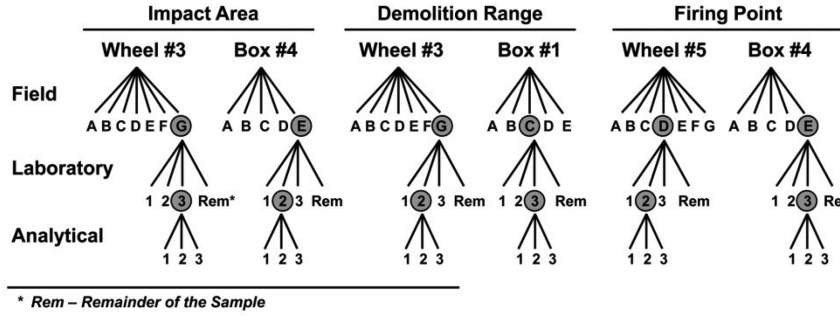

Figure 3. Study design to evaluate uncertainties associated with conventional sample splitting method.

Laboratory Processing of Soil Samples

Laboratory Subsampling Prior to Processing

Another conventional practice once soil samples arrive at an analytical laboratory is to remove a small portion of an undried field sample for analysis and then archive or dispose of the rest of the sample. We measured the uncertainty associated with this practice using samples from the box and wheel designs from each field site (Figure 3). The selected samples, which were in 250-mL jars, were stirred, and then triplicate 20-g subsamples were removed off the top of the unprocessed soil with a stainless steel spatula. The subsamples were air-dried then passed through a 10-mesh sieve. A 10.0-g portion of each less than 2-mm

fraction was combined with 20 mL of acetonitrile in 60-mL amber wide-mouth glass bottles with Teflon-lined lids. Any soil that remained after subsampling was returned to the original 250 mL jar that was sent from the field site and contained the rest the unprocessed sample.

Samples Solvent-Extracted without Subsampling

The bulk samples from the step above and all other discrete, box, and wheel samples were air-dried and passed through a 10-mesh sieve. Each <2-mm fraction was combined with a volume (mL) of acetonitrile equal to twice the sample mass (g) in individual wide mouth jars.

Sample Processing and Laboratory Subsampling Following Method 8330B

Multi-increment samples were air-dried at room temperature, weighed, then passed through a 10-mesh (2-mm) sieve; both fractions were weighed. The <2-mm fraction of each multi-increment sample was ground in aliquots not exceeding 500 g in a Lab TechEssa LM2 puck mill grinder. The samples from the impact area were ground for 90 seconds (*15*) and the samples from the other two sites were ground for 5 × 60-second cycles, with a 60-second cool-down period between each grinding cycle (*1*).

After grinding, each sample was spread to a thickness not exceeding 1 cm on a large sheet of aluminum foil in a hood. Subsamples of 10.0 g were obtained by combining at least 30 increments taken at evenly spaced intervals from the ground sample. Each 10.0-g subsample was combined with 20.0 mL of acetonitrile in a 60-mL amber wide-mouth glass bottle with Teflon-lined lid. Triplicate subsamples were taken for every fifth multi-increment sample to determine laboratory-subsampling uncertainty.

To compare the concentration estimates from 10-g subsamples to those obtained from the remaining bulk sample, an additional set of triplicate subsamples were collected using the same procedure as above. Then, these subsamples and the remainder of each of bulk multi-increment sample were extracted with acetone at the same time. This experiment was done using one multi-increment sample from each site. New sets of triplicate subsamples were removed because this experiment was performed following 3–5 months of storage at room temperature. Acetone was used as a solvent instead of acetonitrile because of the large solvent volume required.

Analytical Method

The revised Method 8330B was used to determine energetic concentrations. The revision of the original Method 8330 included use of a platform shaker instead of a sonic bath for solvent extraction, improved chromatographic separations, and

the use of a dual wavelength detector. The specific instruments and procedures that we used are briefly described here.

Energetic compounds were solvent-extracted from all soil samples using a platform shaker for 18 hours at 150 rpm. Filtered extracts were mixed 1/3 v/v with water prior to injection into the HPLC. The HPLC was a modular system composed of a SpectraSYSTEM® Model P1000 isocratic pump with a 100 µL sample loop, a SpectraSYSTEM UV2000 dual wavelength UV/Vis absorbance detector set at 210 and 254 nm (1 cm cell path), and a SpectraSYSTEM AS3000 auto-sampler. The primary separation was made on a 15-cm × 3.9-mm (4-µm) NovaPak C-8 column maintained at 28°C and eluted with 15:85 isopropanol/water (v/v) at 1.4 mL/min. Secondary (confirmation) separation was made on a 25-cm × 4.6-mm (5-µm) Supelcosil Liquid Chromatograph-Cyanoproply (LC-CN) column (Supelco) and eluted with 65:25:10 water, methanol, and acetonitrile (v/v) at 1.3 mL/min. Concentrations were estimated from peak height measurements compared to commercial (Restek Corp.) multi-analyte and single analyte standards. Procedures for quality control/quality assurance are give in detail elsewhere (*11*). These procedures included an initial five-point method calibration over the range 0.05 to 40 mg/L, method detection limit determination, matrix spikes/matrix spike duplicates, confirmation by dual column analysis and by an independent commercial laboratory, laboratory control samples, performance evaluation samples, and laboratory processing blanks.

Triplicate analysis of a subset of sample extracts was used to assess the analytical uncertainty associated with the analytical method.

Results

Uncertainties from Field Subsampling, Laboratory Subsampling of Unprocessed and Processed Samples, and Analytical Method

Field Subsampling of Soil Samples

The uncertainty associated with a mass reduction step in the field was examined by taking replicate field subsamples of bulk samples such that the entire bulk sample was used. At each of the three field sites, one box sample was divided into five jars, and one wheel sample was divided into seven jars. Complete data tables are found in Hewitt et al., 2009 (*11*) and are summarized here. The data for RDX at the impact area and demolition range and for NG at the firing point are shown schematically in Figure 4 and are typical of each analyte detected. Uncertainty is expressed in Table I as the ratio between the high concentration and the low concentration and the number of field subsamples that yielded concentration estimates that are less than the bulk sample. The data are not normally distributed, so means and variances are not presented.

The ratios of high to low concentrations ranged from 2 to 18 (Table I) for the field subsamples. The results for RDX in the impact area Wheel 3 field subsamples are illustrative (Figure 4a). The RDX concentrations range was 15 to 166 mg/kg in the seven field subsamples. The RDX concentration in the bulk sample, calculated from the total mass of RDX divided by the total mass of soil, was 65 mg/kg. Five out of the seven field subsamples underestimated the concentration in the bulk sample. In 12 of the 14 results listed in Table I, most of the field subsamples underestimated the concentration in the bulk sample.

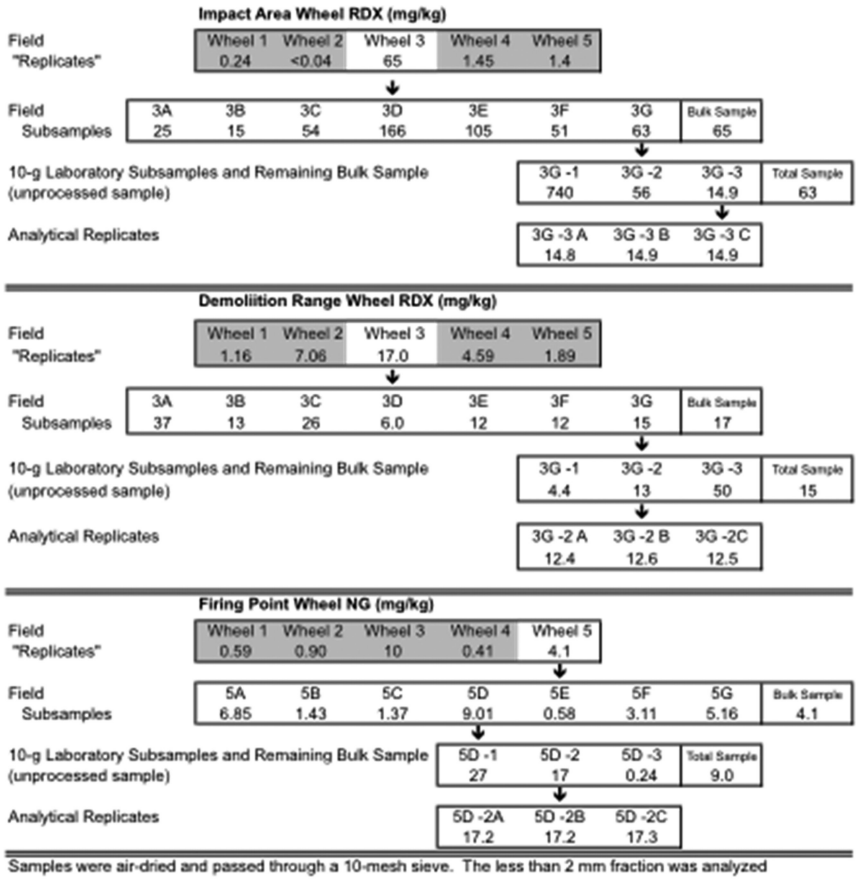

a. Results from wheel samples.

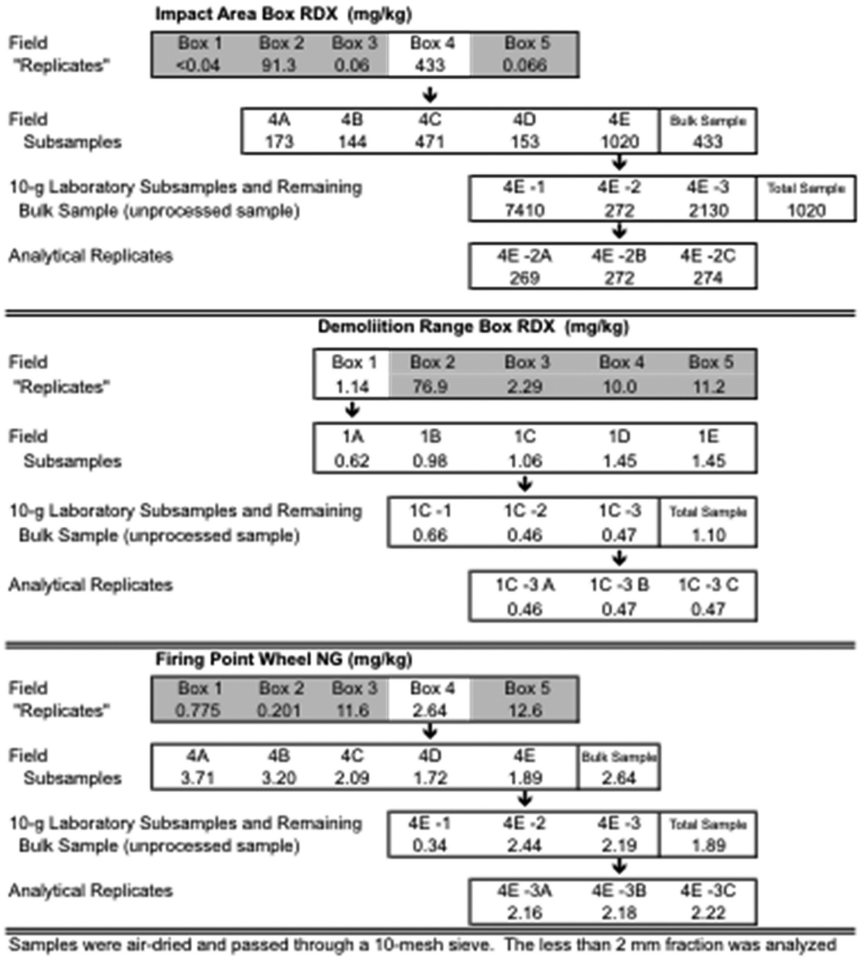

b. Results from box samples.

Figure 4. Concentrations in samples split, subsampled, and analyzed by conventional methods.

Laboratory Subsampling of Field Samples Prior to Processing

The uncertainty associated with removing a subsample off the top of a field sample prior to processing is summarized in Table II and shown schematically in Figure 4. Looking again at the results for the impact area Wheel 3 (Figure 4a), the laboratory subsamples for split G range from 15 to 740, a ratio of 49, while the concentration in the total sample was 63. In the most aberrant case (impact area Wheel 3G), TNT concentrations determined for the three laboratory subsamples ranged over three orders of magnitude (<0.035 to 262 mg/kg). For only one sample (demolition range Box 1C) did the ratio of high to low approach the ideal value

Table I. Field subsampling uncertainty expressed as the ratio of high concentration to low concentration and the number of subsamples that underestimated the concentration of the total bulk sample

Site	*Sample*	*Analyte*	*High/Low*	*Field Subsamples with Concentration less than Bulk Field Sample*
Impact Area	Wheel 3	HMX	7	5 out of 7
		RDX	11	5 out of 7
		TNT	17	5 out of 7
	Box 4	HMX	5	3 out of 5
		RDX	7	3 out of 5
		TNT	18	3 out of 5
Demo Range	Wheel 3	HMX	3	5 out of 7
		RDX	6	5 out of 7
		2,4-DNT	2	3 out of 7
	Box 1	HMX	3	2 out of 5
		RDX	2	3 out of 5
		2,4-DNT	3	3 out of 5
Firing Point	Wheel 5	NG	16	4 out of 7
	Box 4	NG	2	3 out of 5

of one. However, for both analytes (HMX and RDX) all three subsamples yielded concentrations less than the total sample.

Analytical Uncertainty

Triplicate analysis of a subset of soils extracts showed that the analytical uncertainty was insignificant (Analytical Replicates in Figure 4).

Sample Processing and Subsampling Using Method 8330B

There were six multi-increment samples processed according to Method 8330B. Triplicate 10-g subsamples from each sample were analyzed. The data set from these analyses yielded of 15 sets of concentration estimates that were above the estimated reporting limits (Table III). The relative standard deviations for the 15 triplicate estimates were almost all less than 5%. Unlike the results for the triplicate subsamples from unprocessed samples, none of the data sets contained values both above and below the estimated reported limit.

Table II. Laboratory subsampling of unprocessed soil samples. Uncertainty expressed as the ratio of high concentration to low concentration and the number of subsamples that underestimated the concentration of the total sample

Site	*Sample*	*Analyte*	*High/Low*	*Subsamples[1] with Concentration less than Total Sample*
Impact Area	Wheel 3G	HMX	46	2
		RDX	49	2
		TNT	>7000	2
	Box 4E	HMX	22	1
		RDX	28	1
		TNT	77	1
Demo Range	Wheel 3G	HMX	7	2
		RDX	11	2
		2,4-DNT	5	2
	Box 1C	HMX	1	3
		RDX	1	3
		2,4-DNT	5	2
Firing Point	Wheel 5D	NG	113	1
	Box 4E	NG	7	1

[1] Triplicate subsamples were taken from each unprocessed soil sample.

To determine if a multi-increment field sample was represented by a subsample that was less than 1% of the total mass, triplicate 10-g subsamples were taken from three multi-increment samples that weighed between 1200 and 1800 g. After subsampling, the entire remaining mass of each field sample was solvent-extracted to obtain the concentration in the bulk sample. For the three samples, the concentration estimates in the 10-g subsamples were essentially identical to each other and to the remaining multi-increment sample (Table IV).

Field Sampling Strategies

For each of the field sites, none of the field sampling strategies produced normally distributed data (*11*). Therefore the arithmetic means are not valid measure of the central tendency of the data.

A grand mean concentration for each site was calculated from the total mass of soil collected and the total mass of analyte (e.g., RDX or NG) determined. Each grand mean represents our best estimate of the true mean concentration at each site. For the impact area, demolition range, and firing point, the total sample masses

Table III. Concentrations (mg/kg) and Relative Standard Deviations (%) for triplicate 10.0 g subsamples from multi-increment samples processed according to Method 8330B

Location	*Sample ID*	*HMX*	*RDX*	*TNT*	*2,4-DNT*	*NG*
Impact Area	MI-5	2.19 (2.6%)	13.0 (2.8%)	1.14 (3.5%)		
	MI-10	6.67 (1.42%)	50.5 (0.4%)	25.5 (0.45%)		
Demo Range	MI-5	1.66 (5.3%)	7.20 (2.8%)		6.37 (4.8%)	
	MI-10	2.59 (1.6%)	11.9 (2.7%)	0.06 (11%)	6.15 (4.12%)	
Firing Point	MI-5					62.8 (3.4%)
	MI-10					4.99 (3.1%)

Table IV. Comparison of concentrations (mg/kg) found in triplicate 10-g subsamples to the concentration in the remaining sample. Samples were processed according to Method 8330B

Location	*Field Sample (Mass)*	*Analyte*	*Mean (RSD) in Triplicate 10-g Subsamples*	*Remaining Sample*
Impact Area	MI-5 (1300 g)	HMX	2.68 (1.26%)	2.76
		RDX	14.0 (0.89%)	14.3
		TNT	1.61 (1.0%)	1.56
Demo Range	MI-9 (1800 g)	HMX	1.99 (0.48%)	2.02
		RDX	11.7 (0.77%)	11.9
		2,4-DNT	4.97 (6.5%)	4.81
Firing Point	MI-10 (1200 g)	NG	4.37 (13%)	4.21

were 38, 30, and 21 kg. For RDX at the impact area and the demolition range, the grand means were 49 and 21 mg/kg, respectively. For NG at the firing point, the grand mean was 10 mg/kg.

To evaluate the uncertainties associated with each field sampling strategy, the individual concentration estimates from the different sampling strategies were plotted in percentile plots (Figure 5). The bottom and top of each rectangle in the plots represent the fifth and 95th percentiles, respectively. The median is the solid line and the dotted lines are 25th and 75th percentiles. The heavy solid line is the estimated grand mean.

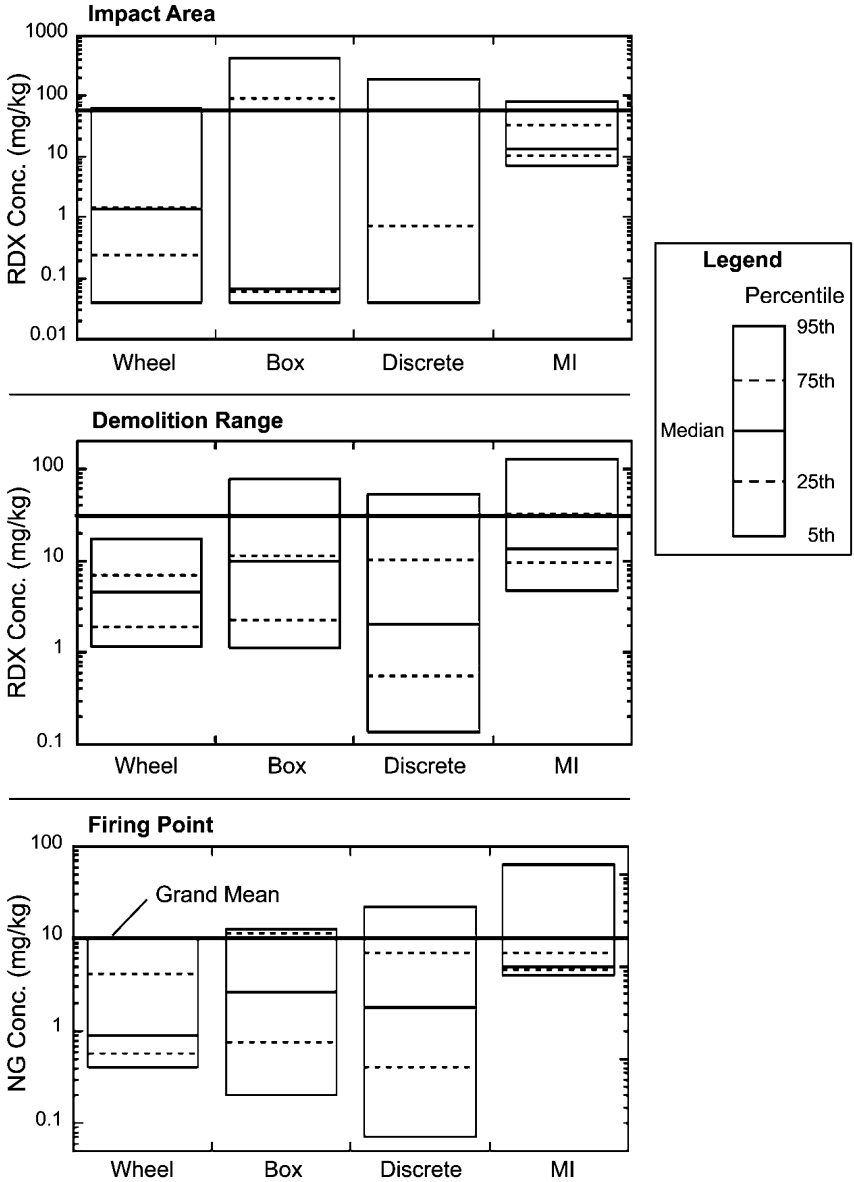

Figure 5. Percentile plots for field samples using the four sampling strategies. Heavy solid horizontal line represents the estimated grand mean.

Discussion

Estimates of the mean concentration of energetics can be biased by inadequate sample collection and by improper sample preparation. This study documented the uncertainties associated with various sample handling and collection procedures. The first issue addressed was the inability to adequately subsample a bulk 1- to 2-kg sample in the field. The results obtained using

conventional field mass reduction procedures showed that the masses of the field subsamples were inadequate to represent the proportion of analytes to the proportion of soil. In almost all cases, the concentration estimates in field subsamples underestimated the concentration in the bulk sample. Therefore, field subsampling is not recommended. The second issue examined was the common laboratory practice of removing only a small portion of a field sample for analysis. Consistent with the field subsampling results, laboratory subsampling of unprocessed soil introduced large uncertainties. In contrast, subsampling uncertainty was insignificant for samples that were processed by air-drying, sieving, and grinding according to Method 8330B. Likewise the uncertainty associated with the analytical determination of energetics by HPLC-UV was insignificant.

Estimating the mean concentration of energetic compounds at training ranges remains a difficult challenge. Field sampling strategies must address both the large heterogeneities associated with the complex composition of the soil matrix and the sporadic distribution of the energetic particles. In the typical sampling scenario, where only a few wheel, box or discrete samples may be collected to represent a given decision unit, underestimation of the mean is the most likely result. In this study, the results for the multi increment samples bracketed the estimated grand mean; however, more mass and more increments were needed to reduce the sample variance and improve the estimations of the mean for each of these sites. Uncertainties were greatest for discrete sample sets, where non-detect values were typical, and least for multi-increment samples. The box and wheel strategies do not have a sufficient number of increments or sample mass to represent the proportion of energetics within a decision unit.

A similar study was conducted at by the National Defense Center for Energy and the Environment (*16*) where the wheel, box, discrete and multi-increment sampling strategies were compared. The two sites sampled were a bombing range and an anti-tank rocket firing point where the analytes of interest were TNT and NG, respectively. Concentrations of these analytes were much higher (>1000 mg/kg) than the three sites we studied, and the multi-increment approach produced normally distributed data. The means and relative standard deviations of the mean were 1,580 (29%) mg/kg and 1,870 (9%) for TNT and NG, respectively. The uncertainties associated with the wheel, box, discrete samples were much greater than for the multi-increment samples. For example, TNT for the wheel samples ranged from 0.6 to 21,000 mg/kg, which is a strong indication of insufficient mass and number of increments.

Conclusions

The objective of this project was to document the sources of uncertainty for estimating energetics residues in soils at military training ranges. Improper sampling procedures include the failure to collect sufficient soil mass and number of increments from the decision unit followed by field subsampling and laboratory subsampling of unprocessed samples. Improper methods will typically result in underestimation of the mean concentration and replicate estimates that may differ

by orders of magnitude. Proper sampling involves collecting an adequate number of evenly spaced increments from throughout a decision unit to reduce uncertainty due to distributional heterogeneity and enough mass to reduce uncertainty due to compositional heterogeneity. For the three training ranges described in this study, 100-increment samples weighing one to two kilograms provided data with less uncertainty than conventional sampling methods, but more increments and sample mass would be needed to generate normally distributed data. Once a representative sample is collected, laboratory processing of the sample according to Method 8330B provided repeatable concentration estimates that maintained the representativeness of the field samples.

Acknowledgments

The authors gratefully acknowledge support provided under project ER-0628 by the Environmental Security Technology Certification Program, Dr. Jeffrey Marqusee, Director, and Dr. Andrea Leeson, Cleanup Program Manager. We thank Gary Larsen and the U.S. Army Garrison Alaska for supporting this research on Alaskan military training ranges.

References

1. Walsh, M. E.; Ramsey, C. A.; Taylor, S.; Hewitt, A. D.; Bjella, K.; Collins, C. M. *Soil Sediment Contam.* **2007**, *16* (5), 459–472.
2. Walsh, M. R.; Walsh, M. E.; Thiboutot, S.; Ampleman, G. *Propellant residues deposition from firing of AT4 rockets*; ERDC/CRREL Technical Report TR-09-13; Cold Regions Research and Engineering Laboratory: Hanover, NH, 2009.
3. Jenkins, T. F.; Ampleman, G.; Thiboutot, S.; et al. *Characterization and fate of gun and rocket propellant residues on testing and training ranges; Final report*; ERDC/CRREL Technical Report TR-08-1; Cold Regions Research and Engineering Laboratory: Hanover, NH, 2008.
4. Jenkins, T. F; Hewitt, A. D.; Grant, C. L.; Thiboutot, S.; Ampleman, G.; Walsh, M. E.; Ranney, T.; Ramsey, C. A.; Palazzo, A.; Pennington, J. *Chemosphere* **2006**, *63*, 1280–1290.
5. Walsh, M. E.; Taylor, S.; Hewitt, A. D.; Walsh, M. R.; Ramsey, C. A.; Collins, C. M. *Chemosphere* **2010**, *78*, 467–473.
6. Hewitt, A. D.; Jenkins, T. F; Taylor, S. *Chemosphere* **2005**, *61*, 888–894.
7. Walsh, M. R. *Explosives residues resulting from the detonation of common military munitions: 2002-2006*; ERDC/CRREL Technical Report TR-07-2; Cold Regions Research and Engineering Laboratory: Hanover, NH, 2007.
8. Taylor, S.; Lever, J. H.; Campbell, E.; Perovich, L.; Pennington, J. *Chemosphere* **2006**, *65*, 1405–1413.
9. Taylor, S.; Hewitt, A.; Lever, J.; Hayes, C.; Perovich, L.; Thorne, P.; Daghlian, C. *Chemosphere* **2004**, *55*, 357–367.
10. Clausen, J. L. *Federal Facilities Environmental Journal* **2005**, *16* (2), 49–62.

11. Hewitt, A. D; Jenkins, T. F.; Walsh, M. E.; Bigl, S.; Brochu, S. *Validation of Sampling Protocol and the Promulgation of Method Modifications for the Characterization of Energetic Residues on Military Testing and Training Ranges*; ERDC/CRREL TR-09-06; Cold Regions Research and Engineering Laboratory: Hanover, NH, 2009.
12. United States Environmental Protection Agency. *SW-846 Method 8330B Nitroaromatics, nitramines, nitrate esters by high performance liquid chromatography (HPLC)*; U. S. Environmental Protection Agency Office of Solid Waste: Washington, DC, 2006.
13. Walsh, M. E.; Collins, C. M.; Walsh, M. R.; Ramsey, C. A.; Taylor, S. *Energetic residues and crater geometries from the firing of 120-mm high-explosive mortar projectiles into Eagle River Flats, June 2007*; ERDC/CRREL Technical Report TR-08-10; Cold Regions Research and Engineering Laboratory: Hanover, NH, 2008.
14. Walsh, M. R. *User's manual for the CRREL multi-increment sampling tool*; ERDC/CRREL Technical Report SR-09-1; Cold Regions Research and Engineering Laboratory: Hanover, NH, 2009.
15. Walsh, M. E.; Ramsey, C. A.; Jenkins, T. F. *Chemosphere* **2002**, *49*, 1267–1273.
16. Roote, D.; Tomljanovic, C.; Bryant, S. *FY08 Environmental Technology Integrated Process Team Projects: Appendix A3 – Large-Scale Chemical Characterization of Contamination Sources on Military Training Ranges*; NDCEE-CR-2010-099; National Defense Center for Energy and Environment: Johnstown, PA, 2010.

Chapter 6

Energetic Residue Observations for Operational Ranges

J. L. Clausen*

US Army Corps of Engineers, Engineer Research and Development Center, Cold Regions Research and Engineering Laboratory, 72 Lyme Road, Hanover, NH 03257

***jay.l.clausen@us.army.mil**

Over the past 20 years the US Army Corps of Engineers (USACE) Engineer Research and Development Center (ERDC) Cold Regions Research and Engineering Laboratory (CRREL), USACE – ERDC – Environmental Laboratory (EL), US Army Public Health Command, Defense Research Establishment Valcartier - Canada, and various contractors have been engaged in the assessment of operational military ranges in the US and Canada to understand the extent of energetic residues derived from training. Surface soil sampling conducted at over 30 military installations has been the primary means of assessing the ranges. In addition to surface soil sampling, other media types have been assessed to a lesser degree including subsurface soil, surface water (including snow), storm water runoff, vadose zone pore-water, and groundwater. The primary focus of previous assessments has been on Army ranges; however a number of Air Force and Navy ranges have been studied. Samples were collected at open burn/open detonatiom (OB/OD) areas, firing points, and impact areas. Ranges were further subdivided depending on the type of weapon system being trained with, such as artillery, mortar, rocket, bombs, grenade, and small arms. The research has led to the identification of several energetic compounds typically present on operational ranges including 2,4,6-trinitrotoluene (TNT), hexahydro-1,3,5-trinitro-1,3,5-triazine (RDX), octahydro-1,3,5,7-tetranitro-1,3,5,7-tetrazocine (HMX), perchlorate, dinitrotoluene (DNT), nitroglycerin (NG),

pentaerythritol tetranite (PETN) and associated transformation products of TNT.

Introduction

Military testing and training ranges are vital for preparing military troops for combat and maintaining readiness. In the late 1990s, energetic residues in soil and groundwater were found at Camp Edwards, MA. One of the questions raised was whether the presence of the energetic compounds at Camp Edwards was the norm or an atypical occurrence. The question is important because the Army, Navy and Air Force use munitions on an annual basis that collectively contain millions of pounds of RDX, HMX, TNT, and perchlorate (*1*). Prior to the 1990s, the assumption based on physical and chemical models was that greater than 99.999% of the energetic material used in munitions was consumed in the firing or detonation process.

Sudies over the past two decades at military ranges demonstrate the presence of energetic compounds in surface soils (*2–11*). Further, these studies confirmed that under ideal conditions a large percentage of the energetic material is consumed during detonation. However, these studies also demonstrated field conditions are not always ideal and consequently not all munitions undergo a high-order detonation, thereby consuming the explosive material. In fact, a percentage of munitions undergo a partial detonation or loworder detonation, whereby only a portion of the energetic material is consumed in the detonation reaction. The remainder of the energetic material is scattered in the environment as particulate residues (*3*, *12–14*) in an extremely heterogeneous manner (*15–18*). The percentage of low- order detonations is dependent on the ordnance type as well as environmental and human factors during training. It is also recognized that undetonated ordnance items on military ranges, unexploded ordnance (UXO), can be sympathetically detonated when a high- order detonation occurs nearby.

In addition, burning of excess propellant for artillery and mortar weapons systems is an inefficient combustion process resulting in a large amount of propellant residue deposited into the environment. Consequently, open burn/open detonation (OB/OD) sites can have some of the highest concentrations of propellant residues. Additionally, open detonation of UXO or training activities with high explosives can result in very high concentration of explosive compounds.

The types of energetic compounds present on military ranges and their associated fate and transport properties are important to the Department of Defense (DoD) because DoD has responsibility for 1,400 sites across the US where munitions containing energetic compounds have been used (*19*). Energetic residues may be a persistent source of soil and groundwater contamination and thus their presence is a potential concern for the DoD (*10*). Consequently, over the past several decades CRREL has been involved with the study of energetic compounds to determine what constituents are present and the concentration levels for specific types of training ranges. To date, studies have been conducted at over 30 different military installations (Army, Air Force, and Navy) in the US

and Canada (Figure 1). These studies have involved assessments at both firing points and impact areas for bombing, artillery/mortar, anti-tank rocket, tank, rifle-grenade, grenade, small arms, and demolition ranges. Limited subsurface soil sampling has been conducted as well as vadose zone monitoring with tension lysimeters.

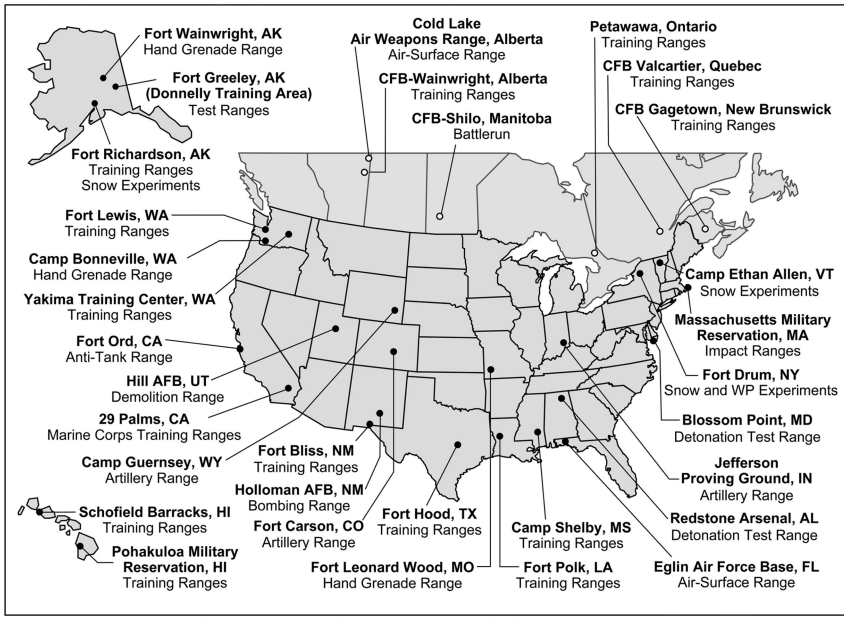

Figure 1. Training and test ranges studied in the US and Canada by CRREL.

Firing Points

Military training involves the firing of weapon systems that utilize energetic materials, such as solid propellants, to propel a projectile toward the target. There are three classes of propellants; single-base, double-base, and triple-base. The typical propellant formulations include a double-base formulation with nitrocellulose (NC) and either nitroglycerin (NG), DNT, or triple-base with NC, nitroguanidine (NQ), and NG (Table I). Single-base propellant consists of NC with DNT in some formulations.

Historically, NG and DNTs were not considered threats to groundwater because they were believed to be too unstable to leach significantly. However, the regulators overseeing the actives at Camp Edwards, MA continue to demonstrate a high level of concern regarding NG and the DNTs. This concern has persisted because these compounds have been detected in surface soils at small arms ranges, artillery and mortar, and anti-tank firing positions. Interest in the migration of NG and the DNTs also has increased because recent field studies have found higher concentrations than previously measured (*3*, *20*, *21*) and have described NG as being "mobile in soil environments" (*22*). Concentrations up to 242 mg/kg

have been reported in the Central Impact Area at Camp Edwards, MA and more than 1 mg/kg has been found on various other MMR (Massachusetts Military Reservation) training ranges. At Canadian Forces Base (CFB) Valcartier Arnhem, anti-tank rocket range surface soils had NG concentrations of nearly 2,000 mg/kg 5 m behind the rocket firing line and over 100 mg/kg 25 m behind the firing line (*23*). A rocket firing range at CFB Gagetown was described as having NG concentrations over 1% near the firing location (*23*). Another study reported NG in all composite, and in several discrete samples, collected near the target area of an anti-tank range (*11*).

Other constituents possibly present in the environment are burn rate modifiers, binders, plasticizers, and stabilizers. Two of the stabilizers used in propellant formulations are energetic materials and these include ethyl centralite (diethyl diphenyl urea) and akardites (methyl diphenyl urea). One of the plasticizers, diethylene glycol dinitrate (DEGDN) is also an energetic compound. The primary energetic compounds, oxidizers, and energetic binders constitute the largest mass in the propellant (60 to 90 percent by weight) followed by 5 to 25 percent for the plasticizers and binders, with stabilizers and other compounds making less than 5 percent (*24*).

Solid propellants used in rocket fuel may have an oxidizer, such as ammonium perchlorate, HMX, a metal, and binder. The exact propellant formulation is dependent upon the weapon system and ordnance being used. Single base propellants are used with many artillery, tank, and small-arms nunitions. Double-base is the predominant class used in most ordnance. Triple-base is used with some of the larger artillery and tank weapons systems. Most ordnance utilizes a primer and two of the energetic compounds commonly used are pentaerythritol tetranitrate (PETN) and diazodinitrophenol (DDNP). In general, the firing points can be separated by use of the following types of weapon systems utilized; artillery and mortar, anti-tank rocket, rifle- grenade, and small arms.

Artillery and Mortar

Artillery and mortar firing positions are located around the periphery of an impact area and can vary in size from less than an acre to several acres or more. The firing location is typically cleared of trees and small vegetation and depending on the level of training the soil can be highly disturbed.

At artillery and mortar firing positions, two sources of propellant materials exist; residue generated from the firing of the weapon system and residue from the burning of excess propellant charges on the ground surface. Following training with artillery and mortar weapon systems, there is often a large quantity of unused propellant remaining resulting from the lack of need for the full propellant charge supplied. The general practice is to destroy this unused material in the field by piling up the material or laying it in a line on top of the soil and igniting it. Sometimes it may be collected and burned in a burning pan.

The principal propellants used with artillery and mortar munitions are types M1, M2, and M3 which contain some mixture of NC, NG, or DNT. Nitrocellulose is the primary constituent, with 0 to 43 percent of NG by weight as the secondary constituent.

Table I. Propellant classes with common formulations

Propellant Type	*Uses*	*Examples*	*Principal ingredients*
Single base	Small arms to cannons	M1 M6 M10	NC, 2,4-DNT NC, 2,4-DNT NC, diphenylamine
Double base	Multiple applications	M2 M5 M8	NC, NG, ethyl centralite NC, NG, ethyl centralite NC, NG, diethyl phthalate
Triple base	Large caliber guns	M30 M31	NC, NG, NQ, ethyl centralite NC, NG, NQ, ethyl centralite
Composite	Rockets and missiles	Class 1.3	Ammonium perchlorate, Al, HTPB[a]
CMDB[b]	Rockets and missiles	Class 1.1	NC, NG, Ammonium perchlorate, Al, HMX, HTPB

[a] HTPB – hydroxyl-terminated polybutadiene [b] CMDB – composite modified double base

Numerous characterization efforts conducted at a variety of ranges demonstrate that propellants are not completely consumed during live-fire training exercises and result in surface soil contamination (*3*, *10*, *11*, *25–34*). The mass of residue deposited by artillery and mortar weapon system has been measured (*20*, *35–45*) and this material can be significant (*40*, *45*). Significant levels of propellant residues are also produced during open burning of excess propellant (*44*, *46*). The levels observed were in excess of those resulting from fallout from the firing of the weapon system.

The principal energetics introduced to the environment during artillery and mortar training are 2,4-DNT, 2,6-DNT, and NG. The levels of these compounds observed in surface soil range from concentrations near the analytical detection limit (using EPA Method 8330B) to thousands of mg/kg (Table II). The higher NG and DNT concentrations were observed at sites where excess propellant burning occurred. In general, the concentrations of NG and DNT observed at artillery and mortar firing points is less than that observed at anti-tank firing points.

Nitroguanidine (NQ) is only used in triple-based propellants, which also contain NC and NG. The M30 propellant mixture for the 105-mm projectile is a triple-based propellant. This mixture is intended for firing the projectile over long distances. Many of the military ranges in the US have limited space, therefore NQ is not widely utilized. Although NQ presence has only been assessed at a small number of sites it has been detected in surface soil. The detections shown in Table II occurred at 2 of the 11 sites studied. These were the only two sites with triple-base propellant use.

Table II. Energetic residues (mg/kg) detected in surface soil at artillery and mortar firing points studied from 2000 to 2010 by CRREL

Analyte	*HMX*	*RDX*	*TNT*	*2,4-DNT*	*2,6-DNT*	*Tetryl*	*NG*	*NQ*
Min	0.017	0.009	0.004	0.0007	0.04	10	0	880
Max	302	186	5,600	237,000	4,840	24	11,290,000	2,350
Mean	118	34	0.049	0.87	102	18	11	1,940
Median	133	43	88	6,691	370	17	135,393	1,861
Detections	21	9	155	415	62	5	89	27
# Samples	577	577	577	577	577	577	577	577
# Installations	11	11	11	11	11	11	11	11

Depending on the activities performed at the firing point, it is possible to have non-propellant material present. For example, Table II shows that RDX, HMX, TNT, and tetryl have been detected on occasion at firing points, suggesting that artillery and mortar firing was not the only activity to have occurred at these sites. In this particular example, all of the detections were observed at a single military installation suggesting the presence of explosives at the firing point is atypical. The HMX, RDX, and TNT detections occurred at a military installation where a "shoot and scoot" type of training activity occurred, i.e. non-fixed firing points. At these sites, firing occurs in the impact area and so there are both propellant residues from firing, and explosives from the detonation of ordnance.

Tetryl (2,4,6-trinitro-phenylmethylnitramine) was used in some munitions but was discontinued in the 1950s. Tetryl is typically subject to rapid transformation in the environment. Thus, the presence of tetryl likely is limited to sites where training occurred prior to the 1960s and also in an arid environment.

In addition to the extensive CRREL studies, more than 1,300 soil samples were collected and analyzed for propellants at artillery and mortar positions at Camp Edwards (*47*). More than 500 samples were analyzed for other energetic compounds as well. Overall, 2,4-DNT was detected in four percent of these samples, approximately four times more often than 2,6-DNT. The majority (twenty-nine) of the detections were in samples collected 0 to 0.3 m in depth. Overall, the soil findings at the artillery and mortar firing positions at Camp Edwards are consistent with the CRREL observations from the 11 other installations studied.

The only extensive study of groundwater beneath artillery and mortar firing points in the US has been at Camp Edwards, MA. These studies did not reveal the presence of propellant compounds (NG and DNT) in the groundwater (*48*), which is consistent with their fate and transport properties, i.e. slowly dissolved, highly sorbed to soil, and rapid transformation. Nitroglycerin found in surface soil samples at an artillery/mortar firing position did not have a corresponding presence in shallow vadose zone water (*20*). Apparently, leaching from surfaces and edges of the propellant residue cause an initial burst of contaminant transport, which quickly ceases because of rentention of NG and DNT within the NC matrix (*68*, *69*).

Anti-Tank

Anti-tank weapons systems consist of rockets fired in line-of-site to the target. Nitroglycerine and NC are the primary propellants for the anti-tank rockets and resiudes are found in surface soil at firing positions (*6*, *9–11*, *21*, *23*, *29*, *31*, *49–51*). As shown in Table III, NG surface soil concentrations are the highest of the energetic compounds observed. The deposition pattern consists of NG residue distributed up to 10 to 20 m in front of the firing position and up to 50 m behind (*20*, *52*). The highest concentration of NG is found behind the firing position and can approach percent levels.

At Camp Edwards, NG was the most widespread energetic compound detected (*49*, *50*). Consistent with the CRREL studies NG was most prevalent at the firing positions at Camp Edwards and was likely deposited as ejected gasses

and particles from firing the rocket. The distribution of NG in soil (highest concentrations at or near the surface and decreasing with depth) at the firing points is consistent with the presumed airborne deposition of propellant compounds. Nitroglycerine was detected in 22 out of 215 samples collected between 0 to 0.8 meters in depth at Camp Edwards (*49*, *50*), but in none of the six samples collected from greater than 0.8 meters (*49*, *50*). Detected concentrations ranged from an estimated high of 130 mg/kg in a discrete sample collected at the surface, to an estimated 2.9 mg/kg in the composite sample collected from a back-blast grid at a former 90 mm rocket firing point (*34*, *49*, *50*).

The presence of other chemical constituents may be associated with activities unrelated to anti-tank training. For example, some anti-tank ranges also are used for small arms training and DNT is contained in small arms propellant. This explains the occasional observation of DNT. Although not typical, RDX, HMX, and TNT may be found at the anti-tank firing point and may be associated with a misfire. Also, the LAW rocket uses a booster propellant charge, which contains RDX. The compounds HMX and TNT are the principal explosives used in anti-tank rockets .

The mass of propellant deposited was determined for several different anti-tank weapon systems (*36*, *52*) and found to be the highest of any type of firing position, with the exception of excess propellant bag burning at the artillery and mortar firing positions. Despite these high mass loading rates, a study of the anti-tank ranges at Camp Edwards, MA did not reveal the presence of NG or DNT in groundwater (*47*, *48*, *53*, *54*).

Table III. Energetic residues (mg/kg) detected in surface soil at Anti-Tank firing points studied from 2000 to 2010 by CRREL

Analytes	*HMX*	*RDX*	*TNT*	*2,4-DNT*	*2,6-DNT*	*NG*
Min	0.008	0.004	0.002	0.01	0.048	0.002
Max	1,920	262	778	4520	126	1,380,000
Mean	0.078	0.047	0.004	0.23	4.0	0.5
Median	61	75	22	884	20	15,900
Detections	63	12	36	12	13	297
# Samples	300	300	300	300	300	300
# Installations	3	3	3	3	3	3

Rifle-Grenade

Consistent with their use, the propellants NG and 2,4-DNT are found in surface soils where rifle-grenades have been fired (Table IV). Nitroglycerin is the principal propellant in rifle-grenades. Typically, these types of ranges also include small arms training and these types of projectiles contain DNT in the propellant. The NG and DNT concentrations observed at rifle-grenade ranges are less than

found at other types of firing positions. RDX and TNT are constituents present in the rifle-grenade warhead so their presence, although unusual is possible.

Table IV. Energetic residues (mg/kg) detected in surface soil at Rifle-grenade firing points studied from 2000 to 2010 by CRREL

Analyte	*RDX*	*TNT*	*2,4-DNT*	*NG*
Min	0.004	70	0.014	0.012
Max	0.004	78	58	36,400
Mean	0.004	74	0.021	3.6
Median	0.004	74	15	9,430
Detections	1	2	4	10
# Samples	20	20	20	20
# Installations	2	2	2	2

Small Arms Ranges

The configuration of a small arms range consists of a firing position from which a soldier fires the weapon over the range floor toward a target. The small arms ranges are typically oriented around the periphery of an artillery/mortar impact area. In some configurations, targets are located in a line spanning the width of the range at a fixed distance with a primary backstop berm originally installed for safety purposes, but now also serving an environmental function by concentrating bullet residue. The berm, usually constructed with native soil material, can vary from a few meters up to 10 m in height. Sometimes a trough to collect surface water runoff is located at the base. Other configurations include targets at varying downrange distances, often with a small berm, <1 m, located immediately behind the target.

Most of the ammunition firing on military SARs is with high-velocity automaticweapons. The projectiles typically consist of a steel penetrator followed by a lead/antimony slug, which is jacketed with a copper alloy consisting of copper, zinc, and lead (*24*). A brass cartridge holds the projectile, the propellant, and an ignition cap. Military small arms typically refer to pistol, shotgun, rifle, and machine gun weapon systems. The predominant ammunition (5.56, 7.62, and 9mm as well as 0.5 cal) consists of a lead slug that is fired using propellant.

Double-base smokeless powders used in small arms ammunition typically contain NC, NG, stabilizing agents, and filler compounds. Double-base propellants used within newer small-arms ammunition typically contain up to 84% NC, with 10% NG, a stabilizer, and up to 6% filler compounds (*24*). During the manufacturing process, dinitroglycerin and mononitroglycerin are produced as impurities, and DNT is often added as a flash suppressor.

Studies conducted to date confirm the presence of 2,4-DNT and NG in surface soils in the immediate vicinity of the small arms firing point (Table V). NG and

DNT are deposited as a component of NC particles. The amount of accumulation is clearly a function of the number of rounds fired. M. R. Walsh et al. (*42*) estimated 99% of the residue from small arms is deposited within 5 m of the firing line for pistols, 10 m for rifles and small machine guns, and 20 m for 50-caliber machine guns. This study quantified the mass of residue deposited by munition type (5.56, 7.62, 9, 12.7-mm) using snow as the sampled media with NG introduced at the firing point ranging from 0.00042 to 0.1 grams per-round.

Observed soil concentrations at small arms firing ranges are much lower than other types of firing ranges, consistent with the much lower mass of propellant. Although, the small size of the propellant grains may enhance leaching to some extent. In contrast to other types of weapons systems used in training, a large quantity of small arms are fired from a fixed location. Further, these fixed firing positions are often used for decades or more with the ranges being frequently graded thereby moving and burying the residues. Thus, for small arms firing ranges used for an extended period, the buildup of propellant residue levels is possible.

Impact Areas

Impact areas are locations where targets are set up and ordnance is fired into from the firing points. Firing positions are often arranged around the perimeter of the range with firing fans, likelyhood of projectile impact, leading into the impact areas. The explosive compounds used in the warhead formulation vary depending on the weapon system (Table VI). The two predominant formulations are Composition B (Comp B) a 60:40 mixture of RDX and TNT (*14*) and Octol a 70:30 mixture of HMX and TNT. Comp B can also contain HMX as an impurity up to 10 percent by weight (*56*). Both 2,4-DNT and 2,6-DNT are by products in the manufacturing process of TNT and typically are found in a 4:1 mass ratio of 2,4 to 2,6-DNT. Composition B is typically used in artillery and mortar ordnance and Octol is typically used in anti-tank rockets. These formulations can also be used in primers, fuses, and ignition and propellant charges.

Detonation of a warhead can function in three ways depending on the yield. First, a projectile can be a dud where no detonation occurs resulting in an UXO, i.e. the projectile is intact with the explosive formulation protected from the environment by the casing material. Second, a projectile can undergo a low-order detonation where only a portion of the explosive detonates leaving chunks and particles of explosive compounds on the range surface. Finally, a projectile can undergo a high-order detonation where nearly 100 percent of the explosive material is consumed in the detonation. Depending on the munitions, up to 4.4 % of the rounds may be duds and 0.22% low order detonations (*3*). Although, field observations for some munitions are much higher – as high as 20 percent for the (M888) 60-mm projectiles (*43*). Repeated low-order detonations over time within an impact area can result in the accumulation of explosive residue. A general rule-of-thumb is 10,000 to 100,000 high-order detonations are needed to yield the equivalent residue mass from a single low-order detonation.

Table V. Energetic residues (mg/kg) detected in surface soil at a selection of small arms range firing points studied by CRREL[a]

				NG			*2,4-DNT*		
Military Installation	***Range***	***Type***	***n***	***Min***	***Max***	***Mean***	***Min***	***Max***	***Mean***
Fort Lewis, WA	6A	Varied	2	47	67	57	0.19	0.48	0.31
Camp Edwards, MA	Bravo	Varied	9	7.5	22	11	0.04	0.14	0.06
	Charlie	Varied	3	12	16	14	0.09	.017	0.13
	India	Varied	1	27	27	27	0.16	0.16	0.16
	Juliet[b]	Varied	3	2.9	3.0	3.0	0.08	0.11	0.10
	Echo[b]	Varied	3	0.06	0.43	0.25	<0.014	<0.014	<0.014
	Kilo[b]	Varied	3	1.4	70	38	<0.014	1.5	0.52
Fort Benning, GA	Malone 9	Varied	7	2.2	2.3	2.3	ND	ND	ND
	Malone 11	Varied	2	31	48	40	0.3	0.42	0.36
	Malone 17	Varied	2	ND	0.12	-	ND	ND	ND
	Coursen West	Varied	2	65	67	66	0.46	0.48	0.47
29 Palms, CA	Range 2[c]	9-mm Pistol	4	80	124	110	<0.04	<0.04	<0.04
	Range 5/5A[c]		11	23	42	29	<0.04	<0.04	<0.04
	Range 113[c]	MG	7	84	101	93	<0.28	0.46	0.35
Fort Richardson, AK	Oates[c]	MG	39	0.24	627	162	<0.04	17	4.3
	Sports[c]	Varied	57	7.1	231	59	<0.04	3.7	0.79

Continued on next page.

Table V. (Continued). Energetic residues (mg/kg) detected in surface soil at a selection of small arms range firing points studied by CRREL[a]

				NG			*2,4-DNT*		
Military Installation	***Range***	***Type***	***n***	***Min***	***Max***	***Mean***	***Min***	***Max***	***Mean***
CFB Petawa, Canada	B Range	Rifle	44	0.09	139	22	<0.04	2.3	0.41
	C Range	Rifle	8	5.5	20	12	0.04	0.36	0.26
	D Range	Rifle	12	2.4	18	7.1	<0.04	0.33	0.18
	E Range	Pistol	6	0.76	36	7.7	<0.04	0.13	NA
	Q Range	Pistol	12	4.5	29	17	<0.04	0.08	0.04
	Y Range	Rifle	26	0.15	104	15	ND	0.92	0.24
CFB ASU Wainwright,Canada	Range 4	Rifle	3	0.6	40	21	<0.04	0.10	NA
	Range 5	Rifle	3	<0.01	23	13	NA	NA	NA
	Range 6	Rifle	16	ND	3.1	0.6	ND	0.4	0.2
	Range 9	Zeroing	7	1.0	7.4	3.3	ND	0.1	NA

[a] CFB – Canadian Forces Base, MG – machine gun, n – number of samples, NA – not applicable, ND – non detect [b] Clausen et al. 2010 (*55*) [c] Jenkins et al. 2008 (*36*)

Table VI. Explosive constituents present in military explosive formulations

Compound	*Uses*	*Chemical Ingredients*
Composition A	Demolition explosive	91% Military-grade RDX 9% wax
Composition B	Artillery; mortar	60% Military-grade RDX (Contains ≤10% HMX) 39% Military-grade TNT (Contains ≤ 1% other TNTisomers and DNTs); 1 % wax
Composition C4	Demolition explosive	91% Military-grade RDX
Tritonal	Air Force bombs	Military-grade TNT, aluminum
Composition A4	40-mm grenades	Military-grade RDX
TNT	Artillery	Military-grade TNT
Composition H-6	Navy and Air Force bombs	Military-grade RDX and TNT, aluminum
Octol	Anti-tank rockets	70% Military-grade HMX 30% Military-grade TNT
Explosive D	Naval projectiles	Ammonium Picrate
PB XN-109	Naval projectiles	64% Military-grad RDX 20% Aluminum 16% HTPB[a] 7.3% dioctyl adipate 1% Other[b]
LX-14	Naval projectiles	95.5% Military-grade HMX 4.5% Estane
PB XN-5	Naval projectiles	95% Military-grade HMX 5% Viton A

[a] HTPB: Hydroxyl terminated polybutadiene [b] Other compounds at less than 1% include N N2-hydroxethyl, 2-2-methylenebis, and triphenylbismuth

Artillery and Mortar

Artillery ranges are the largest training ranges used by the Army, covering areas of hundreds of square kilometers throughout the US (*19*). In the past, fixed firing points were used; with modern mobile artillery, firing activities have become more de-centralized as training has changed to support a "shoot and scoot" strategy. Once fired, artillery and mortar rounds can travel up to a few kilometers before impacting and detonating in the vicinity of targets forming a crater.

The explosive compounds RDX, and TNT are the principal compounds in Comp B, although HMX can be present as well. These materials are the high explosive filler used in most artillery and mortar munitions. Energetic residues primarily identified in soil at the various impact areas include RDX, HMX, TNT and TNT transformation products such as 2-amino-4,6-dinitrotolune (2a-DNT) and 4-amino-2,6-dinitrotolune (4a-DNT) (*10*, *11*, *27*, *29*, *31*, *48*, *57*). As shown in Table VII other explosive compounds such as tetryl and the

propellant compounds 2,4-DNT, NG, and NQ are observed in surface soil at some impact ranges. Other constituents observed infrequently and not shown in Table VII include 1,3,5-trinitrobenzene (TNB), nitrobenzene (NB), 2,6-DNT, PETN, and 4-nitrotoluene (4-NT). The RDX transformation products such as dinitroso-hexahydro-1,3,5-triazine (DNX), nitroso-dinitro-hexahydro-1,3,5-triazine (MNX), and tri-nitroso-hexahydro-1,3,5-triazine (TNX) have not been observed in surface soil samples but have been observed in some groundwater samples (*58*).

The concentration of RDX, HMX, and TNT in surface soil is typically tens of mg/kg or less. The statistical summary values in Table VII are skewed by the collection of samples immediately beneath or adjacent to a low-order detonation or locations where a soil sample was collected after a blow-in-place operation. When UXO is discovered and needs to be removed but cannot be moved due to safety concerns, it is typically detonated using a donor charge of C4, block of TNT, or a RDX shape charge. If the UXO item undergoes a low-order detonation a large mass of RDX and TNT can be deposited on the soil surface.

Perchlorate is used in the spotting charge for artillery and mortar weapons systems and thus can be introduced into the environment. Unlike, RDX, HMX, and TNT, perchlorate is highly soluble and does not persist in surface soils when significant precipitation is present.

Explosive residues exist in near-surface soils close to the range targets and have contributed to groundwater contamination (*10*). In addition, not all ordnance items hit their intended target so the potential exists for explosive residues and UXO some distance away from the targets. Because low-order detonations are random and unpredictable, the distribution of residues and UXO can be extremely variable throughout an impact area. Although, typically the residue mass and UXO are more concentrated near the targets. In general, detectable energetic residues are found in the top 5 cm of soil and concentrations decrease rapidly with depth and distance from the targets (*6*, *10*, *15*, *16*, *58*).

Groundwater sampling at Camp Edwards showed HMX, RDX, TNT, TNT transformation products, and perchlorate in the aquifer indicating the mobility of these compounds. A plume of groundwater contamination consisting of HMX, RDX, and perchlorate is evident within the impact area (*54*). Trinitrotoluene and its transformation products are evident in groundwater near some of the targets but become undetectable a short distance in the downgradient direction. These observations are fully consistent with the fate-and-transport properties of these compounds. HMX, RDX, and perchlorate undergo dissolution to varying degrees and once in solution are recalcitrant. In contrast, TNT and its transformation products adsorb to a greater degree to soil and are susceptible to transformation processes limiting their mobility.

Table VII. Energetic residues (mg/kg) detected in surface soil at artillery and mortar impact areas studied from 2000 to 2010

Analyte	*HMX*	*RDX*	*TNT*	*2,4-DNT*	*2a-DNT*	*4a-DNT*	*Tetryl*	*NG*	*NQ*
Min	0.006	0.002	0.002	0.000	0.004	0.004	0.022	0.005	0
Max	11,451,000	1,132,000	15,100,000	40,100	21	14	4,800	44,600	28,741,000
Mean	2.2	8.0	18	25	0.12	0.10	6.0	1126	744
Median	66,832	5,010	97,469	708	0.79	0.72	137	5,848	227,819
Detections	468	559	492	109	119	118	41	86	131
# Samples	1,020	1,020	1,020	1,020	1,020	1,020	1,020	1,020	10,20
# Installations	15	15	15	15	15	15	15	15	15

Aerial Bombing Ranges

Bombing ranges can cover 1,000 to 10,000s of acres and are typically employed for a variety of training activities. The majority of bombs used in training are inert and typically filled with concrete to simulate the payload of an explosive-filled bomb. However, bombs containing explosive filler are used on occasion. The predominant explosive filler is Tritonal, which is a mixture of TNT and aluminum powder. Although, HMX and RDX are used as explosive fillers for some types of ordnance.

The Navy also uses coastal bombing ranges for both aircraft and naval vessel training. In addition to bombs being dropped from aircraft, naval guns are used to fire projectiles into the impact area. The Navy's primary explosives are Explosive D, which consists primarily of ammonium picrate, and H-6 which is a mixture of RDX, TNT, and aluminum.

The data shown in Table VIII is from Air Force bombing ranges and one inland Marine training range. The Marine range employs the shoot and scoot form of training with artillery, mortar, tanks, and small arms as well as the dropping of bombs from aircraft. All of the major explosives HMX, RDX, TNT were detected along with the transformation products of TNT: 2a-DNT and 4a-DNT. In addition to the explosive constituents, propellant compounds of 2,4-DNT and NQ were detected. The compounds infrequently detected on bombing ranges, and not shown in Table VIII, include NB, 2,6-DNT, tetryl, NG, 2-nitrotoluen (2-NT), 3-nitrotoluene (3-NT), and 4-NT.

Surface soil samples collected at Air Force bombing ranges indicate high concentrations of TNT (hundreds of mg/kg) in the immediate vicinity of low-order bombs that contain Tritonal, but soil concentrations elsewhere are much lower (*5*, *59*, *60*). Mono-amino transformation products of TNT (2a-DNT and 4a-DNT) are also present but at much lower concentrations. RDX has been detected at low concentrations (generally less than 0.1 mg/kg) and its presence may be due to the C4 demolition explosive (91% RDX) used to destroy duds.

Hewitt and co-workers (*61*) sampled a range where H-6 bombs were dropped. At least one bomb had apparently undergone a low-order detonation. In this area, H-6 chunks were observed and the mean concentrations of RDX, TNT, and HMX in a 100 × 100-m area just down slope of where the largest mass of explosive was located were 9.4, 1.4, and 1.3 mg/kg, respectively.

Anti-Tank Rocket Ranges

Anti-tank rocket ranges are direct fire ranges and are typically several hundred acres in size. Due to the necessity of maintaining a line of sight for training, they are typically maintained to promote low-growing vegetation. Targets are often derelict armored vehicles placed downrange at distances of 100 m or more from the firing points. The predominant weapon system used in training are the 66-mm M72 light anti-armor weapon (LAW) and the 84-mm AT4 rocket. Except for the AT4, whichuses gunpowder as propellant these ordnance items contain M7 double-base propellant with Octol in the warhead and RDX in the booster charge. The M7 propellant contains 54.6% NC, 35.5% NG, 7.8% potassium perchlorate, 0.9%

ethyl centralite, and 1.2% carbon black (*24*). Octol is composed of 70% HMX and 30% TNT. At some ranges practice rounds are fired that contain propellant but do not contain Octol.

Field experiments have been conducted at seven active anti-tank ranges. The primary residue detected at anti-tank rocket impact areas is HMX where concentrations in surface soils adjacent to targets are generally in the hundreds of mg/kg (Table IX). Even though 30% TNT is present in Octol, it is generally only present at about 1/100th of the HMX level in the soil at these ranges. The primary reason for this is TNT's susceptibility to transformation processes. Also present at detectable levels are RDX and two environmental transformation products of TNT (2a-DNT and 4a-DNT), but the concentrations are always several orders of magnitude lower than HMX. The level of HMX in the soil declines as the distance from the target increases. At Camp Edwards the findings at the anti-tank rocket range were similar to those observed by CRREL (*49*, *50*). The highest residue concentrations were found in the upper six inches of soil, consistent with the presumed surface deposition. These findings are also consistent with other anti-tank rocket range impact areas studied (*6*).

The mode of contaminant deposition at a rocket range is different from the areas previously discussed. At the target locations, rockets that hit the target but do not detonate will often shear apart due to their thin aluminum casing. Therefore, explosive residues along with chunks of material can be expected primarily in front of the target. Lower levels of munitions' constituents are found on either side of the target with minimal levels behind the target. If the rocket misses the target it will continue down range until its propellant is exhausted. Consequently, anti-tank rocket ranges are typically located around the periphery of an artillery and mortar impact area.

Many anti-tank rockets are propelled all the way to the target with fuel remaining. Consequently, propellants can still be present when these rockets detonate upon impact. Small pieces of propellant are thereby spread over the soil surface in the area surrounding the targets. These residues are often visible and NG has been detected at the impact areas at concentrations as high as 23 mg/kg. This is due to the poor burn characteristics of the propellant, which, ideally is fully-consumed before the projectile leaves the launcher.

Hand Grenade

Hand grenade ranges are only a few acres in size and because of the large number of individual detonations in a small area, the surface is usually bare or poorly vegetated. These ranges often have several training bays from which soldiers throw grenades. Most of the detonation craters lie at distances between 15 and 35 m from the throwing pits. Compared with other types of ranges, only a very small area is subject to residue deposition. The most commonly used item at these ranges is the M67 fragmentation grenade. Its explosive charge is 185 g of Composition B. This means that compounds expected include RDX, TNT, HMX, and wax (Table I), along with a few other isomers of TNT and DNT (*62*).

Table VIII. Energetic residues (mg/kg) detected in surface soil at bombing range impact areas studied from 2000 to 2010 by CRREL

Analyte	*HMX*	*RDX*	*TNT*	*TNB*	*2,4-DNT*	*2a-DNT*	*4a-DNT*	*NQ*
Min	0.002	0.001	0.002	0.002	0.001	0.002	0.002	0.000
Max	88,000	560,000	572,000	1.6	7,590	2.4	2.1	21,000
Mean	20	6.0	22	0.13	0.11	0.69	0.62	1,603
Median	2,334	12,139	12,317	0.16	103	0.72	0.64	1,610
Detections	167	214	385	111	238	175	216	151
# Samples	466	466	466	466	466	466	466	466
# Installations	5	5	5	5	5	5	5	5

Table IX. Energetic residues (mg/kg) detected in surface soil at anti-tank impact areas studied from 2000 to 2010 by CRREL

Analyte	*HMX*	*RDX*	*TNT*	*TNB*	*2,4-DNT*	*2A-DNT*	*4A-DNT*	*Tetryl*	*NG*
Min	0.029	0.046	0.042	0.038	0.040	0.050	0.042	0.068	0.040
Max	75,000	4,220	4,660	54	32	3.4	3.7	0.36	630
Mean	183	0.52	2.0	0.04	0.40	0.31	0.29	0.12	4.8
Median	599	62	30	14	3.0	0.48	0.47	0.19	22
Detections	336	119	238	4	26	79	77	7	159
# Samples	385	385	385	385	385	385	385	385	385
# Installations	4	4	4	4	4	4	4	4	4

Table X. Summary of results for energetic compounds detected in surface soils at hand grenade ranges

Installation	*Year sampled*	*Samples analyzed*[a,b,c]	*Mean concentration (mg/kg)*					
			HMX	***RDX***	***TNT***	***TNB***	***4ADNT***	***2ADNT***
Fort Lewis, WA[d]	2000	23[a]	1.8	7.5	9.3	0.05	0.15	0.13
	2001	5[b] [50]	1.0	4.4	1.5	ND[c]	ND	ND
Fort Richardson, AK[d]	2000	27[a]	0.02	0.08	0.03	ND	0.01	0.01
Fort Leonard Wood, MO	2001	18[b] [30]	0.19	0.45	<0.01	<0.01	<0.01	<0.01
CFB-Shilo, Manitoba[e]	2001	15[b] [20]	0.05	0.71	0.06	<0.01	0.02	0.02
Fort Wainwright, AK	2002	25[b] [1,5,10,20,40]	2	11	1.2	0.15	ND	ND
Schofield Barracks, HI	2002	3[b] [30]	9.1	51	36	0.28	0.40	0.03
Pohakuloa Training Center, HI	2002	7[b] [30]	0.53	5.6	0.78	<0.01	<0.01	<0.01
CFB-Gagetown, New Brunswick								
New Castle Range[f]	2002	5[b] [30]	<0.01	<0.01	<0.01	<0.01	<0.01	<0.01
New Castle Range[g]	2003	15[b] [25]	<0.01	<0.01	<0.01	<0.01	<0.01	<0.01
Fort Polk, LA	2003	2[b] [30]	<0.01	0.01	<0.01	<0.01	<0.01	<0.01
CFB-Petawawa, Ontario	2004	9[b] [25,100]	0.18	0.65	0.16	<0.01	<0.01	<0.01

[a] Discrete samples [b] Multi-increment samples with (n) increments per sample [c] ND – Not determined [d] Jenkins et al. 2001 (*3*) [e] Ampleman et al. 2003 (*4*) [f] Thiboutot et al. 2003 (*9*) [g] Thiboutot et al. 2004 (*51*)

Soil samples were collected at 11 active ranges (Table X). The concentrations of the major residue chemicals (RDX, TNT, and HMX) fell into two groups: one had concentrations generally less than 0.12 mg/kg and the other had concentrations generally above 1 mg/kg (*63*). Live-fire studies indicate grenades that detonate high-order do not deposit sufficient residues to account for the ranges with higher residue concentrations. However, remnants of grenades that did not completely detonate were found at these ranges. These grenades either had undergone partial (low-order) detonations or had been duds that did not fully detonate. These UXO items were the detonated in place.

Rifle-Grenade

A rifle-grenade is a form of anti-tank round used until the end of the Vietnam War. These munitions have largely been replaced by the anti-tank rockets. However, there are still active ranges where these devices were used and the ranges are now used to train with the newer anti-tank rockets. The explosive filler used in rifle-grenades was largely Comp B and therefore the constituents to be found are similar to those found on anti-tank ranges. Table XI presents results for two ranges where rifle-grenades were utilized. As expected, RDX and TNT were detected along with the propellants 2,4-DNT and NG. The observed concentrations are lower than observed at anti-tank ranges but could be due to the length of time since training with these munitions.

Table XI. Energetic residues (mg/kg) detected in surface soil at rifle-grenade impact areas studied from 2000 to 2010 by CRREL

Analyte	*RDX*	*TNT*	*2,4-DNT*	*NG*
Min	0.058	0.004	0.006	0.004
Max	8.7	53	0.05	0.25
Mean	0.5	0.40	0.01	0.04
Median	2.0	7.5	0.02	0.08
Detections	5	8	4	10
# Samples	12	12	12	12
# Installations	2	2	2	2

Open Burn/Open Detonation

Open Burn/Open Detonation sites typically are used for the burning of propellant or the detonation of UXO. Typically, these sites are relatively small, tens of acres, resulting in focused activities. Because a concentrated activity is being conducted in a small space, the expectation is of higher soil contaminant concentrations. The potential for energetic compounds to reach groundwater also is increased. The detonation of ordnance typically involves the use of TNT,

Composition C4 (C4), shape charges, or detonation cord. The C4 formulation is predominantly RDX with a plasticizer and a similar formulation is used for non military shape charges. Unfortunately, C$, when used in this manner, has proven inefficient, often resulting in propellant scattered about the site. Detonation cord contains dinitrotoluene and PETN. Because of the varied activities that occur at OB/OD sites a variety of energetic compounds are possible. Low-order detonations of UXO are common and propellant burning is also a potentially dirty process. The use and incomplete detonation of C4 and TNT blocks results in the random distribution of chunks as well as fine particulates of explosives. Pennington (*64*) and Hewitt (*13*) and co-workers documented mg levels of RDX residue deposited from blow-in-place operation of UXO using C4. Energetic compounds of interest at OB/OD sites include perchlorate, HMX, RDX, TNT, 2a-DNT, and 4a-DNT. Depending on the munitions detonated, some propellants such as 2,4-DNT, 2,6-DNT, and NG may be present.

The energetic compounds TNT, 2a-DNT, 4a-DNT, RDX, HMX, 2,4-DNT, and perchlorate have been detected in soil as well as groundwater at several OB/OD sites (*11*, *54*, *65–70*). For example, OB/OD activities conducted at the Demolition 1 site at Camp Edwards over several decades has resulted in the deposition of RDX, HMX, TNT, 2,4-DNT, 2,6-DNT, and perchlorate (*71*). Table XII indicates similar observations for the OB/OD sites studied by CRREL. Although not reported in Table XII, infrequent detections of TNB, 2a-DNT, 4a-DNT, and tetryl were observed.

Table XII. Energetic residues (mg/kg) detected in surface soil at open burn open detonation areas studied from 2000 to 2010 by CRREL

Analyte	*HMX*	*RDX*	*TNT*	*2,4-DNT*	*2,6-DNT*	*NG*
Min	0.017	0.007	0.004	0.004	0.004	0.021
Max	11,100	60,200	11,600	31,600	530	10,500
Mean	0.09	0.16	0.06	1.5	0.12	0.30
Median	2,314	5,601	750	2,203	82	477
Detections	15	34	31	39	19	25
# Samples	49	49	49	49	49	49
# Installations	6	6	6	6	6	6

Conclusions

In summary, a variety of energetic compounds can be expected at firing points and impact areas depending on the type of ordnance used (Table XIII). In impact areas, RDX, HMX, and TNT are expected with elevated concentrations associated with low-order detonations. In artillery and mortar impact areas where spotting charges have been used, the presence of perchlorate is probable at arid sites. Where training occurs in a humid environment, perchlorate may no longer be present in

the surface soil due to transport. Depending on the weapons system being used, the presence of propellants in the impact area cannot be completely ruled out, e.g. anti-tank rocket ranges. At firing positions, the propellants NC, NG, DNT, can be expected. Nitroguanidine is likely only at firing positions with large impact areas where artillery is being fired over long distances. The explosive, PETN, has only been detected in artillery and mortar impact areas where PETN-containing detonation cord has been used. The energetic constituents infrequently detected include NB, tetryl, 2-NT, 3-NT, and 4-NT. Several energetic constituents have never been detected in any studies to date and include DNB, 2-DANT, 4-DANT, picric acid, and 3,5-dinitro-toluene—an isomer of DNT.

Table XIII. Energetic residues expected at military ranges by training activity

Training Area	*Type of Range*	*Expected Energetic Compounds*
Firing Point	Artillery and Mortar	2,4-DNT, 2,6-DNT, NC
	Anti-Tank	NG, NC
	Small Arms	2,4-DNT, NG, NC
Impact Area	Artillery and Mortar	HMX, RDX, TNT, Perchlorate Transformation products for TNT and RDX
	Anti-Tank	HMX, RDX, TNT Transformation products for TNT and RDX
	Aerial Bombing Ranges	HMX, RDX, TNT Transformation products for TNT and RDX
Other	Grenade Courts	HMX, RDX, TNT Transformation products for TNT and RDX
	OB/OD	HMX, RDX, TNT, 2,4-DNT, 2,6-DNT, NG, NC Transformation products for TNT and RDX

References

1. Clausen, J. L.; Scott, C. L.; Cramer, R. J. *Development of Environmental Data for Navy, Air Force, and Marine Munitions*; ERDC-CRREL TR-07-07; US Army Corps of Engineers, Cold Regions Research and Engineering Laboratory: Hanover, NH, 2007.
2. Jenkins, T. F.; Walsh, M. E.; Thorne, P. G.; Miyares, P. H.; Ranney, T. A.; Grant, C. L.; Esparza, J. R. *Site Characterization for Explosives Contamination at a Military Firing Range Impact Area*; CRREL Special Report 98-9; US Army Corps of Engineers, Cold Regions Research and Engineering Laboratory: Hanover, NH, 1998.
3. Jenkins, T. F.; Pennington, J. C.; Ranney, T. A.; Berry, T. E.; Miyares, P. H.; Walsh, M. E.; Hewitt, A. D.; Perron, N. M.; Parker, L. V.; Hayes, C. A.; Wahlgren, E. G. *Characterization of Explosives Contamination at Military*

Firing Range; ERDC TR-01-5; US Army Corps of Engineers, Cold Regions Research and Engineering Laboratory: Hanover, NH, 2001.
4. Ampleman, G.; Thiboutot, S.; Lewis, J.; Marois, A.; Jean, S.; Gagnon, A.; Brouchard, M.; Martel, R.; Lefebvre, R.; Gauthier, C.; Ballard, J. M.; Ranney, T. A.; Jenkins, T. F. *Evaluation of the Impacts of Live Fire Training at CFB Shilo*; TR-2003-066; Defence Research Establishment – Valcartier: Valcartier, Quebec, Canada, 2003.
5. Ampleman, G.; Thiboutot, S.; Lewis, J.; Marois, A.; Jean, S.; Gagnon, A.; Brouchard, M.; Jenkins, T.; Hewitt, A.; Pennington, J. C.; Ranney, T. A. *Evaluation of the Contamination by Explosives in Soils, Biomass and Surface Water at Cold Lake Air Weapons Range (CLAWR), Alberta, Phase 1 Report*; DRDC-Valcartier-TR-2003-208-Annex; Defence Research Establishment – Valcartier: Valcartier, Quebec, Canada, 2003.
6. Thiboutot, S.; Ampleman, G.; Gagnon, A.; Marois, A.; Jenkins, T. F.; Walsh, M. E.; Thorne, P. G.; Ranney, T. A. *Characterization of Anti-tank Firing Ranges at CFB Valcartier, WATC Wainwright and CFAD Dundurn*; Defence Research Establishment – Valcartier: Valcartier, Quebec, Canada, 1998.
7. Thiboutot, S.; Ampleman, G.; Gagnon, A.; Marois, A. *Characterization of an Unexploded Ordinance Contaminated Range (Tracadie Range) for Potential Contamination by Energetic Materials*; DREV-TR-2000-102; Defence Research Establishment – Valcartier: Valcartier, Quebec, Canada, 2000.
8. Thiboutot, S.; Ampleman, G.; Dube, P.; Dubois, C.; Martel, R.; Lefebvre, R.; Mailloux, M.; Sunahara, G.; Roubidoux, P. Y.; Hawari, J. *Characterization of DND Training Ranges Including Anti-Tank Firing Ranges and Ecotoxicological Assessment*; Defence Research Establishment – Valcartier: Valcartier, Quebec, Canada, 2000.
9. Thiboutot, S.; Ampleman, G.; Lewis, J.; Faucher, D.; Marois, A.; Martel, R.; Ballard, J. M.; Downe, S.; Jenkins, T. F.; Hewitt, A. *Environmental Conditions of Surface Soils and Biomass Prevailing in the Training Area at CFB Gagetown, New Brunswick*; DREV-TR-2003-152; Defence Research Establishment – Valcartier: Valcartier, Quebec, Canada, 2003.
10. Clausen, J. L.; Robb, J.; Curry, D.; Korte, N. *Environ. Pollut.* **2004**, *129*, 13–21.
11. Pennington, J. C.; Jenkins, T. F.; Hewitt, A. D.; Stark, J. A.; Lambert, D.; Perron, N. M.; Taylor, S.; Ampleman, G.; Thiboutot, S.; Lewis, J.; Marois, A.; Gauthier, C.; Brousseau, P.; Martel, R.; Lefebvre, R.; Ballard, J.; Brochu, S.; Clausen, J.; Delaney, J. E.; Hollander, M. A.; Dinh, H. Q.; Davis, I.; Ranney, T. A.; Hayes, C. A. *Distribution and Fate of Energetics on DoD Test and Training Ranges: Interim Report 4*; ERDC TR-04-4; Strategic Environmental Research and Development Program: Arlington, VA, 2005.
12. Taylor, S.; Hewitt, A.; Hayes, C.; Perovich, L.; Thorne, P.; Daghlian, C. *Chemosphere* **2004**, *55*, 357–367.
13. Hewitt, A. D.; Jenkins, T. F.; Ranney, T. A.; Stark, J.; Walsh, M. E.; Taylor, S.; Walsh, M.; Lambert, D.; Perron, N.; Collins, N. *Estimates for Explosives Residue Deposition from the Detonation of Army Munitions*; ERDC/CRREL

TR-03-16; US Army Corps of Engineers, Cold Regions Research and Engineering Laboratory: Hanover, NH, 2003.
14. Jenkins, T. F.; Walsh, M. E.; Miyares, P. H.; Hewitt, A. D.; Collins, N. H.; Ranney, T. A. *Thermochim. Acta* **2002**, *384*, 173–185.
15. Jenkins, T. F.; Grant, C. L; Brar, G. S.; Thorne, P. G.; Ranney, T. A.; Schumacher, P. W. *Assessment of sampling error associated with collection and analysis of soil samples at explosives-contaminated sites*; CRREL Special Report 96-15; US Army Corps of Engineers, Cold Regions Research and Engineering Laboratory: Hanover, NH, 1996.
16. Jenkins, T. F.; Walsh, M. E.; Thorne, P. G.; Thiboutot, S.; Ampleman, G.; Ranney, T. A.; Grant, C. L. *Assessment of Sampling Error Associated with the Collection and Analysis of Soil Samples at a Firing Range Contaminated with HMX*; CRREL Special Report 97-22; US Army Corps of Engineers, Cold Regions Research and Engineering Laboratory: Hanover, NH, 1997.
17. Jenkins, T. F.; Grant, C. L.; Brar, G. S.; Thorne, P. G.; Schumacher, P. W.; Ranney, T. A. *Field Anal. Chem. Technol.* **1997**, *1*, 151–163.
18. Jenkins, T. F.; Grant, C. L.; Walsh, M. E.; Thorne, P. G.; Thiboutot, S.; Ampleman, G.; Ranney, T. A. *Field Anal. Chem. Technol.* **1999**, *3*, 19–28.
19. DSB. *Report of the Defense Science Board Task Force on Unexploded Ordnance*; Office of the Under Secretary of Defense for Acquisition and Technology, Defense Science Board: Washington, DC, 2003.
20. Jenkins, T. F.; Pennington, J.; Ampleman, G.; Thiboutot, S.; Walsh, M. E.; Dontsova, K.; Diaz, E.; Bigl, S.; Hewitt, A.; Clausen, J.; Lambert, D.; Perron, N.; Yost, S.; Brannon, J.; Lapointe, M. C.; Brochu, S.; Brassard, M.; Stowe, M.; Fainaccio, R.; Gagon, A.; Moris, A.; Gamche, T.; Gilbert, G.; Faucher, D.; Walsh, M. E.; Ramsey, C.; Rachow, R.; Zufelt, J.; Collins, C.; Gelvin, A.; Sarri, S. *Characterization and fate of gun and rocket propellant residues on testing and training ranges: Interim report 1*; ERDC TR-07-1; US Army Corps of Engineers, Cold Regions Research and Engineering Laboratory: Hanover, NH, 2007.
21. Brochu, S.; Diaz, E.; Thiboutot, S.; Ampleman, G.; Marois, A.; Gagnon, A.; Hewitt, A. D.; Bigl, S. R.; Walsh, M. E.; Walsh, M. R.; Bjella, K.; Ramsey, C.; Taylor, S.; Wingfors, H.; Qvarfort, U.; Karlsson, R.-M.; Ahlberg, M.; Creemers, A.; van Ham, N. *Environmental Assessment of 100 Years of Military Training at Canadian Forces Base Petawawa; Phase I - Study of the Presence of Munitions-Related Residues in Soils and Vegetation of Main Range and Training Areas*; TR 2008-118; Defence Research Establishment – Valcartier: Valcartier, Quebec, Canada, 2009.
22. Mirecki, J. E.; Porter, B.; Weiss, C. A., Jr. *Environmental Transport and Fate Process Descriptors for Propellant Compounds*; ERDC/EL TR-06-7; Army Engineer, Research and Development Center: Vicksburg, MS, 2006.
23. Jenkins, T. F.; Ranney, T. A.; Hewitt, A. D.; Walsh, M. E.; Bjella, K. *Representative Sampling for Energetic Compounds at an Anti-tank Firing Range*; ERDC-TR-04-7; US Army Corps of Engineers, Cold Regions Research and Engineering Laboratory: Hanover, NH, 2004.
24. MIDAS. *Munition item disposition action system*; U.S. Army Defense Ammunition Center: McAlester, OK, 2010. https://midas.dac.army.mil.

25. Thiboutot, S.; Ampleman, G.; Marois, A.; Gagnon, A.; Gilbert, D.; Tanguay, V.; Poulin, I. *Deposition of gun propellant residues from 84-mm Carl Gustav rocket firing*; TR 2007-408; Defence Research Establishment – Valcartier: Valcartier, Quebec, Canada, 2007.
26. Dubé, P.; Thiboutot, S.; Ampleman, G.; Marois, A.; Bouchard, M. *Preliminary assessment of the dispersion of propellant residues from the static live firing of 105 mm howitzer*; TM 2005-284; Defence Research Establishment – Valcartier: Valcartier, Quebec, Canada, 2006.
27. Walsh, M. E.; Collins, C. M.; Hewitt, A. D.; Walsh, M. R.; Jenkins, T. F.; Stark, J.; Gelvin, A.; Douglas, T. S.; Perron, N.; Lambert, D.; Bailey, R.; Meyers, K. *Range characterization studies at Donnelly Training Area, Alaska: 2001 and 2002*; ERDC/CRREL TR-04-3; US Army Corps of Engineers, Cold Regions Research and Engineering Laboratory: Hanover, NH, 2004.
28. Walsh, M. E.; Collins, C. M.; Ramsey, C. A.; Douglas, T. A.; Bailey, R. N.; Walsh, M. R.; Hewitt, A. D.; Clausen, J. L. *Energetic Residues on Alaskan Training Ranges*; ERDC/CRREL TR-07-9; US Army Corps of Engineers, Cold Regions Research and Engineering Laboratory: Hanover, NH, 2007.
29. Jenkins, T. F.; Thiboutot, S.; Ampleman, G.; Hewitt, A. D.; Walsh, M. E.; Ranney, T. A.; Ramsey, C. A.; Grant, C. L.; Collins, C. M.; Brochu, S.; Bigl, S. R.; Pennington, J. C. *Identity and Distribution of Residues of Energetic Compounds at Military Live-Fire Training Ranges*; ERDC TR-05-10; US Army Corps of Engineers, Cold Regions Research and Engineering Laboratory: Hanover, NH, 2005.
30. Hewitt, A. D. *Analysis of Nitroglycerine in Soils and on Mortar Fins Using GC-TID*; CRREL Report TR-02-03; US Army Corps of Engineers, Cold Regions Research and Engineering Laboratory: Hanover, NH, 2002.
31. AMEC. *Draft IAGWSP Technical Team Memorandum 01-13 Central Impact Area Soil Report for the Camp Edwards Impact Area Groundwater Quality Study, Massachusetts Military Reservation, Cape Cod, MA*; MMR.3915; AMEC Earth and Environmental: Westford, MA, 2001.
32. AMEC. *Revised Draft IAGWSP Technical Team Memorandum 01-14 Gun and Mortar Firing Positions Volume I of II for the Camp Edwards Impact Area Groundwater Quality Study, Massachusetts Military Reservation, Cape Cod, MA*; MMR-4425; AMEC Earth and Environmental: Westford, MA, 2001.
33. CHPPM. *Training range site characterization and risk screening, Camp Shelby, MS*; Geohydrologic Study No. 38-EH-8879-99; Center for Health Promotion and Preventive Medicine: Aberdeen Proving Ground, MD, 2000.
34. Ogden. *Final IAGS Technical Team Memorandum 00-3: Evaluation of gun and mortar firing positions for the Camp Edwards impact area groundwater quality study, Massachusetts Military reservation, Cape Cod, MA*; Ogden Environmental and Energy Services: Westford, MA, 2000.
35. Ampleman, G.; Thiboutot, S.; Marois, A.; Gagnon, A.; Gilbert, D.; Walsh, M. R.; Walsh, M. E.; Woods, P. *Evaluation of the Propellant, Residues Emitted During 105-mm Leopard Tank Live Firing at CFB Valcartier,*

Canada; TR 2009-420; Defence Research Establishment – Valcartier: Valcartier, Quebec, Canada, 2009.
36. Jenkins, T. F.; Ampleman, G.; Thiboutot, S.; Bigl, S. R. *Characterization and Fate of Gun and Rocket Propellant Residues on Testing and Training Ranges: Final Report*; ERDC TR-08-1; US Army Corps of Engineers, Cold Regions Research and Engineering Laboratory: Hanover, NH, 2008.
37. Walsh, M. E.; Ramsey, C. A.; Collins, C. M.; Hewitt, A. D.; Walsh, M. R.; Bjella, K. L.; Lambert, D. J.; Perron, N. M. *Collection methods and laboratory processing of samples from Donnelly Training Area Firing Points, Alaska, 2003*; ERDC/CRREL TR-05-6; US Army Corps of Engineers, Cold Regions Research and Engineering Laboratory: Hanover, NH, 2005.
38. Walsh, M. R.; Walsh, M. E.; Collins, C. M.; Saari, S. P.; Zufelt, J. E.; Gelvin, A. B.; Hug, J. W. *Energetic residues from Live-fire detonations of 120-mm mortar rounds*; ERDC/CRREL TR-05-15; US Army Corps of Engineers, Cold Regions Research and Engineering Laboratory: Hanover, NH, 2005.
39. Walsh, M. E.; Lambert, D. J. *Extracting kinetics of energetic compounds from training range and army ammunition plant soils*; ERDC/CRREL TR-06-6; US Army Corps of Engineers, Cold Regions Research and Engineering Laboratory: Hanover, NH, 2006.
40. Walsh, M. E.; Ramsey, C. A.; Taylor, S.; Hewitt, A. D.; Bjella, K.; Collins, C. M. *Soil Sediment Contam.* **2007**, *16* (5), 459–472.
41. Walsh, M. R.; Taylor, S.; Walsh, M. E.; Bigl, S.; Bjella, K.; Douglas, T.; Gelvin, A.; Lambert, D.; Perron, N.; Saari, S. *Residues from Live Fire Detonations of 155-mm Howitzer Rounds*; ERDC/CRREL TR-05-14; US Army Corps of Engineers, Cold Regions Research and Engineering Laboratory: Hanover, NH, 2005.
42. Walsh, M. R.; Walsh, M. E., Bigl. S. R.; Perron, N. M.; Lambert, D. J.; Hewitt, A. D. *Propellant residues deposition from small arms munitions*; ERDC/CRREL-TR-07-17; US Army Corps of Engineers, Cold Regions Research and Engineering Laboratory: Hanover, NH, 2007.
43. Walsh, M. R.; Walsh, M. E.; Ramsey, C. A.; Rachow, R. J.; Zufelt, J. E.; Collins, C. M.; Gelvin, A. B.; Perron, N. M.; Saari, S. P. *Energetic residues from a 60-mm and 81-mm live fire exercise*; ERDC/CRREL TR-06-10; US Army Corps of Engineers, Cold Regions Research and Engineering Laboratory: Hanover, NH, 2006.
44. Walsh, M. R.; Walsh, M. E.; Hewitt, A. D. *Energetic Residues from the Expedient Disposal of Artillery Propellants*; ERDC/CRREL TR-09-8; US Army Corps of Engineers, Cold Regions Research and Engineering Laboratory: Hanover, NH, 2009.
45. Walsh, M. R.; Hewitt, A. D.; Taylor, S. Determination of explosives residues from winter live-fire exercises; ERDC/CRREL MP-04-6305; *Proceedings of the conference on Sustainable range management*; Battelle Press: Columbus, OH, 2004.
46. Walsh, M. R.; Walsh, M. E.; Hewitt, A. D. *J. Hazard. Mater.* **2010**, *173*, 115–122.
47. AMEC. *Revised Draft IAGWSP Technical Team Memorandum 01-14 Gun and Mortar Firing Positions Volume I of II for the Camp Edwards Impact*

Area Groundwater Quality Study, Massachusetts Military Reservation, Cape Cod, MA; MMR-4342; AMEC Earth and Environmental: Westford, MA, 2001.
48. AMEC. *Draft IAGWSP Technical Team Memorandum 01-13 Central Impact Area Soil Report for the Camp Edwards Impact Area Groundwater Quality Study, Massachusetts Military Reservation, Cape Cod, MA*; MMR-3915; AMEC Earth and Environmental: Westford, MA, 2001.
49. Ogden. *Final IAGS Technical Team Memorandum 99-1 KD & U Ranges for the Camp Edwards Impact Area Groundwater Quality Study, Massachusetts Military Reservation Cape Cod, MA*; MMR-2071; Ogden Environmental and Energy Services: Westford, MA, 2000.
50. Ogden. *Final Phase I Initial Site Investigation Report KD Range, RTN 4-15033 for the Camp Edwards Impact Area Groundwater Quality Study, Massachusetts Military Reservation Cape Cod, MA*; MMR-2384; Ogden Environmental and Energy Services: Westford, MA, 2000.
51. Thiboutot, S.; Ampleman, G.; Marois, A.; Gagnon, A.; Bouchard, M.; Hewitt, A.; Jenkins, T.; Walsh, M.; Bjella, K. *Environmental condition of surface soils, CFB Gagetown Training Area: Delineation of the presence of munitions-related residues (Phase III, Final Report)*; TR 2004-205; Defence Research Establishment – Valcartier: Valcartier, Quebec, Canada, 2004.
52. Walsh, M. R.; Walsh, M. E.; Thiboutot, S.; Ampleman, G.; Bryant, J. *Propellant Residue Deposition from Firing of AT4 Rockets*; ERDC/CRREL TR-09-13; US Army Corps of Engineers, Cold Regions Research and Engineering Laboratory: Hanover, NH, 2009.
53. AMEC. *Final IAGS Technical Team Memorandum 99-1 KD & U Ranges for the Camp Edwards Impact Area Groundwater Quality Study*; MMR-2071; AMEC Earth and Environmental: Westford, MA, 2000.
54. AMEC. *Draft Addendum to Final IAGWSP Technical Team Memorandum TM 01-6 Central Impact Area Groundwater Report, Camp Edwards Impact Area Groundwater Study Program Massachusetts Military Reservation, Cape Cod, MA*; MMR-8334; AMEC Earth and Environmental: Westford, MA, 2004.
55. Clausen, J. L.; Scott, C.; Mulherin, N.; Bigl, S.; Gooch, G.; Douglas, T.; Osgerby, I.; Palm, B. *Sorption/Desorption Measurements of Nitroglycerin and Dinitrotoluene in Camp Edwards, Massachusetts Soil*; ERDC-CRREL TR-10-1; US Army Corps of Engineers, Cold Regions Research and Engineering Laboratory: Hanover, NH, 2010.
56. Phelan, J. M.; Romero, J. V.; Barnett, J. L.; Parker, D. R. *Solubility and Dissolution Kinetics of Composition B Explosive in Water*; SAND2002-2420; Sandia National Laboratories: Albuquerque, NM, 2002.
57. CHPPM. *Range Site Characterization and Risk Screening Regional Range Study, Jefferson Proving Ground, Madison, IN*; Report No. 38-EH-8220-03; Center for Health Promotion and Preventive Medicine *Training:* Aberdeen Proving Ground, MD, 2003.
58. Clausen, J. L.; Korte, N.; Dodson, M.; Robb, J.; Rieven, S. *Conceptual Model for the Transport of Energetic Residues from Surface Soil to Groundwater by*

Range Activities; ERDC-CRREL TR-06-18; US Army Corps of Engineers, Cold Regions Research and Engineering Laboratory: Hanover, NH, 2007.
59. Ampleman, G.; Thiboutot, S.; Lewis, J.; Marois, A.; Gagnon, A.; Bouchard, M.; Jenkins, T.; Ranney, T. A.; Pennington, J. C. *Evaluation of the Contamination by Explosives and Metals in Soils, Vegetation, Surface Water, and Sediment at Cold Lake Air Weapons Range (CLAWR), Alberta, Phase II Final Report*; TR 2004-204; Defence Research Establishment – Valcartier: Valcartier, Quebec, Canada, 2004.
60. Jenkins, T. F.; Hewitt, A. D.; Ramsey, C. A.; Bjella, K.; Bigl, S. R.; Lambert, D. J. *Sampling studies at an air force live-fire bombing range impact area*; ERDC/CRREL TR-06-2; US Army Corps of Engineers, Cold Regions Research and Engineering Laboratory: Hanover, NH, 2006.
61. Hewitt, A. D.; Jenkins, T. F.; Ramsey, C. A.; Bjella, K. L.; Ranney, T. A.; Perron, N. M. *Estimating energetic residue loading on military artillery ranges: Large decision units*; ERDC/CRREL TR-05-7; US Army Corps of Engineers, Cold Regions Research and Engineering Laboratory: Hanover, NH, 2005.
62. Leggett, D. C.; Jenkins, T. F.; Murrmann, R. P. *Composition of Vapors Evolved from Military TNT as Influenced by Temperature Solid Composition, Age, and Source*; CRREL Report 77-16; US Army Corps of Engineers, Cold Regions Research and Engineering Laboratory: Hanover, NH, 1977.
63. Jenkins, T. F.; Hewitt, A. D.; Grant, C. L.; Thiboutot, S.; Ampleman, G.; Walsh, M. E.; Ranney, T. A.; Ramsey, C. A.; Palazzo, A.; Pennington, J. C. *Chemosphere* **2006**, *63*, 1280–1290.
64. Pennington, J. C.; Jenkins, T. F.; Ampleman, G.; Thiboutot, S. *Distribution and Fate of Energetics on DoD Test and Training Ranges: Final Report*; TR-06-13; US Army Engineer Research and Development Center: Vicksburg, MS, 2006.
65. AMEC. *Final IAGWSP Technical Team Memorandum 01-6 Central Impact Area Groundwater Report for the Camp Edwards Impact Area Groundwater Quality Study, Massachusetts Military Reservation, Cape Cod, MA*; MMR-3757; AMEC Earth and Environmental: Westford, MA, 2001.
66. Ampleman, G.; Thiboutot, S.; Gagnon, A.; Marois, A.; Martel, R.; Lefebvre, R. 1998. *Study of the Impacts of OB/OD Activity on Soils and Groundwater at the Destruction Area in CFAD Dundurn*; DREV-R-9827; Defence Research Establishment – Valcartier: Valcartier, Quebec, Canada, 1998.
67. Ampleman, G.; Thiboutot, S.; Desilets, S.; Gagnon, A.; Marois, A. *Evaluation of the Soils Contamination by Explosives at CFB Chilliwack and CFAD Rocky Point*; DREV-TR-2000-102; Defence Research Establishment – Valcartier: Valcartier, Quebec, Canada, 2000.
68. Martel, R.; Lefebvre, R.; Martel, K.; Roy, N. *Preliminary Soil and Groundwater Characterization Study at the CFAD Dundurn Explosives Facility (Saskatchewan)*; INRS-Georesources, Sainte-Foy, Quebec. Defence Research Establishment – Valcartier: Valcartier, Quebec, Canada, 1996.
69. Martel, R.; Hebert, A.; Lefebvre, R. *Complementary Soil and Groundwater Characterization Study at the Open Burning/Open Detonation Site CFAD*

Dundurn (Saskatchewan); Univerite du Quebec; Defence Research Establishment – Valcartier: Valcartier, Quebec, Canada, 1998.
70. ESE. *1995/1996 Hydrogeological Investigation/Monitoring Results North Post 40 Complex Camp Grayling Training Facility Grayling, MI*; ESE # 47-95076 & 47-95078; Environmental Science and Engineering: Cadillac, MI, 1997.
71. AMEC. *Draft Demo 1 Groundwater Report Addendum to TM 01-2, Camp Edwards, Massachusetts Military Reservation, Cape Cod, MA*; MMR-7702; AMEC Earth and Environmental: Westford, MA, 2003.

Chapter 7

Dissolution of High Explosives on Range Soils

Susan Taylor,[1,*] James H. Lever,[1] Jennifer Fadden,[1] Susan R. Bigl,[1] Nancy M. Perron,[1] Kathleen F. Jones,[1] and Bonnie Packer[2]

[1]Cold Regions Research and Engineering Laboratory, 72 Lyme Road, Hanover, NH 03755.
[2]Strata-Geo, 4024 Shallow Brook Lane, Olney, MD 20832.
[*]Susan.Taylor@usace.army.mil

High explosives (HE) are deposited onto military range soils by live-fire training. A critical problem facing range managers is how to determine if explosives from training activities are likely to migrate off base, an outcome that might trigger federal regulatory actions able to close the base or restrict the type of training permitted. Partial detonations scatter most of the HE mass available for dissolution onto range soils as mm- to cm-sized particles. These particles are dissolved by contact with precipitation such as rain or snow, and the dissolved HE is transported to groundwater that can migrate off base. Our laboratory and outdoor tests mimic rainfall-driven dissolution of HE. We can model the effluent concentration given the starting mass of the HE particle and the rainfall record. Our tests revealed that photo-transformation and particle breakage, processes inherent to outdoor dissolution, greatly influence the amount of HE dissolved and hence the HE influx to soil.

Introduction

Many high explosives comprise a class of organic chemicals that undergo rapid chemical reaction and are able to sustain a shock wave, a process called detonation. These compounds are used in military munitions and, when detonated, send fragments of the casing at high velocity outward from the impact point. Two commonly used high explosives are 2,4,6-trinitrotoluene (TNT) and 1,3,5-hexahydro-1,3,5-trinitrotriazine (RDX). Both have low drinking-water screening levels: 2.2 $\mu g L^{-1}$ for TNT and 0.6 $\mu g L^{-1}$ for RDX (*1*, *2*).

When fired, munitions will experience one of many possible fates (Figure 1). Taylor et al (*3*) estimated the probabilities for these various fates using available data such as that from the Ammunition Stockpile Reliability Program (*4*). Generally, rounds will detonate high-order as intended. However, they may also partially detonate (low-order), break open, or not detonate and become an unexploded ordnance (UXO). Whether they come to rest on the surface or underground, a UXO will eventually be: 1) intentionally blown-in-place (partial or high-order), 2) detonated by a nearby exploding round (partial or high order), 3) have its shell pierced by a nearby detonation(s) (Figure 2a), or 4) corroded through to the explosive fill (Figure 2b). Partial detonations and broken rounds are thought to be the main source of contamination on ranges today (*3*, *5*). Although the cm- to mm- sized pieces are not an explosive hazard, the gram to kilogram quantities of HE pieces deposited can contaminate large volumes of water. For example ten kg of dissolved RDX can contaminate 10^{10} L of water above the drinking water standard.

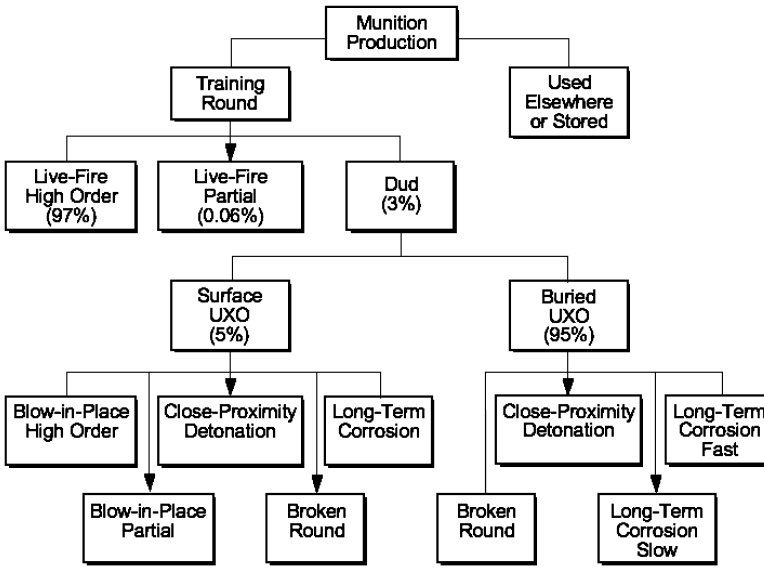

Figure 1. Possible fates of a fired round (3).

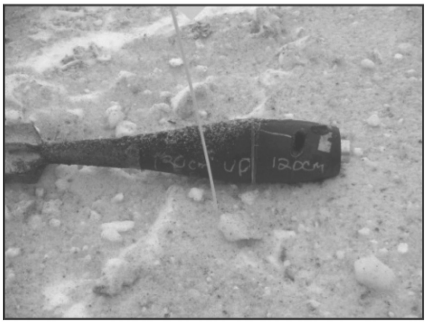

a. 81-mm round pierced by a fragment from a high-order detonation

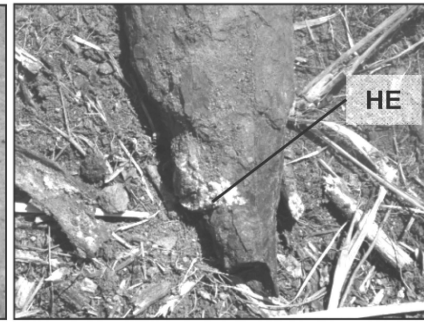

b. Exposed HE on a corroded 60-mm UXO

Figure 2. Examples of damaged and corroded unexploded ordnance.

High order detonations generally deposit explosive-free carbon particles and consume more than 99.99% of the explosive originally in the round (*6*). Partial detonations can scatter most of their fill (*7*, *8*) onto the soil surface as mm- to cm-sized pieces (*9*, *10*) and deposit 10,000 to 100,000 times more HE on a per-round basis than high-order detonations. Rounds broken open during impact or pierced through to their explosive fill can over time release 100% of their HE fill to the environment. Munitions experiencing these fates release HE that is immediately available for dissolution and transport.

Intact UXOs do not release explosives immediately, but UXOs do not stay intact forever. The corrosion rate of low carbon steel, the most commonly used steel in military munitions, is about 0.025 mm yr^{-1}, with a factor of 5 variation attributable to soil chemical conditions and the composition of the casing alloy (*3*). This suggests that most UXOs, with wall thicknesses between 2 and 10 mm, will corrode within 80 to 400 years under normal aerated soil conditions. Under reducing conditions, similar to those encountered in wetlands and other anaerobic environments, sulfide production accelerates corrosion by about a factor of 10, resulting in perforation of the round after approximately 10–40 years (*3*). Although corrosion is a relatively slow process, the high density of surface and near surface UXOs on ranges make it possible that fragments from high-order detonations will crack or breach these rounds. A field test where 34, 81-mm rounds were set 1.2 m or less from a high-order detonation of another 81-mm found that 17% remained intact, 39% were pierced, 30% partially detonated, 4% detonated high-order and the fate of 9% is unknown (*11*).

The area over which HE residue is deposited from a fired round varies for these different fates. High order detonations distribute mainly carbon and metal residues for 100s of meters. Partial detonations scatter cm-sized HE particles to distances of 30 meters whereas mm-sized pieces are deposited within a few meters of the detonation point (*9*, *10*). Rounds that are broken open and corroded UXOs spill their HE within a meter of the round (Figure 2). Because the depositional areas are so different for these different fates, the HE concentrations in impact range soils are heterogeneous over short distance scales.

Although many studies have mapped HE concentrations and distributions in range soils (e.g. Table I) only a few studies have measured the persistence of HE in the field. Radtke et al. (*12*) sampled surface soils at an explosives testing area that had not been used for 50 years and found explosives only in the >3mm size fraction suggesting that smaller particles had dissolved. In a different study, powdered explosives were mixed in with soils at Los Alamos National Laboratory, NM (*13*). After 20 years the RDX, HMX, and PETN concentrations were similar to starting values while concentrations of explosives containing TNT, barium nitrate or boric acid had dramatically decreased in the soils. Walsh M.E. et al. (*14*) documented the total disaggregation, over just three years, of Composition B chunks scattered by partial detonations in an Alaskan impact range. This range is located in a salt water marsh and the chunks were subjected to submersion, drying and freezing which accelerated their breakdown over similar sizes chunks studied in less extreme environments (*15*).

Table I. Variability of soil concentrations among multi-increment samples collected from grids at different ranges.

Installation	*Range type*[a]	*No Samples (Increments)*	*Grid Side (m)*	*Analyte*	*Concentration (mg/kg)*			
					Max	*Min*	*Mean*	*Std. Dev.*
Donnelly Training Area (AK) (*25*)	Artillery FP	10 (30)	10	2,4-DNT	1.35	0.60	0.94	0.24
Holloman AFB (NM) (*26*)	Bombing IA	3 (100)	10	TNT	17.2	12.5	14.4	2.45
Ft. Polk (LA) (*27*)	Mortar IA	10 (25)	10	RDX	290	4.6	54	86
29 Palms (CA) (*28*)	Artillery IA	6 (100)	100	RDX	9.4	3.9	5.6	2.1
Hill AFB (UT) (*29*)	TTA	3 (100)	100	HMX	4.26	3.96	4.13	0.15

[a] Firing point (FP), Impact Area (IA), or Thermal Treatment Area (TTA).

Once deposited on the soil, HE can be transported off the range by wind, by surface water or by ground water. Although transport of energetic particles by wind or by surface water is possible, wind cannot entrain mm-sized particles for long distances, and only the small fraction of land abutting a river could contribute HE particles by overland flow. Furthermore, oxygen isotope studies show that groundwater dominates a river's hydrograph indicating that most water reaches a river via groundwater (*16*). Dissolution and aqueous transport to groundwater is

probably the major mechanism for transporting energetic compounds off of the range (*17*).

Biotransformation and biodegradation for HE compounds is thought to occur once they are in aqueous solution. Partitioning coefficients have been measured between dissolved explosives and soils (e.g. (*18*, *19*)). During transit through the vadose zone, energetic compounds interact with soil in a variety of ways: they can bind to soil, and break down chemically or biologically while in solution. Research has found RDX to be persistent and mobile in comparison with TNT, which photo-degrades rapidly and is aerobically bio-transformed to 2-Am-DNT and 4-Am-DNT (*20*). The amino DNT compounds can be detected in soils after TNT is no longer present.

Although there are documented cases of groundwater contamination below Army ammunition plants, groundwater has not been sampled under very many impact ranges. To date, RDX has been found in groundwater at Fort Lewis WA (*6*), Massachusetts Military Reservation (*4*) and at three Canadian installations (*21–24*).

Range managers need an estimate of the aqueous HE influx into soils at their sites. Three pieces of information are needed: the total mass of HE deposited onto a range soil (the load), the particle size distribution of the HE, and the dissolution rate as a function of particle size and weather conditions. Although we will discuss all three factors, our work focused on the dissolution of explosives because this process was poorly understood yet initiates aqueous-phase HE transport.

The HE Load and Size Distribution of HE Particles

The amount of HE deposited onto range soils has been estimated in two ways. The HE can be calculated from the average soil concentration, which has been measured for a number of areas at different types of ranges using multi-increment samples (e.g. Table I). These types of studies have found HE in surface soils at all military impact areas sampled (*4*, *6*, *8*, *30–32*).

Alternatively, the amount of HE could be estimated using range records (number and type of rounds fired), their detonation probabilities (high-order, partial detonation or dud) (Figure 1) and the average mass of HE deposited by each type of outcome. This estimate can rarely be made because although the HE mass deposited by high-order detonations of individual rounds has been measured for some of the most commonly used munitions (*7*, *30*, *33*), range records are rarely available and the detonation probabilities for many types of munitions are still unknown.

Taylor et al. (*9*, *34*) measured particle size distributions for partial detonations for two Composition B and two TNT filled rounds. The partial detonations produced a wide range of particles that ranged from cm-sized crystalline chunks to mm-sized partially or totally melted beads as shown in Figure 3 (*9*). Although the number of tests is small, the tail slopes of these particle distributions suggest that Comp B-filled rounds may produce more narrowly distributed particles than TNT-filled rounds (Figure 4).

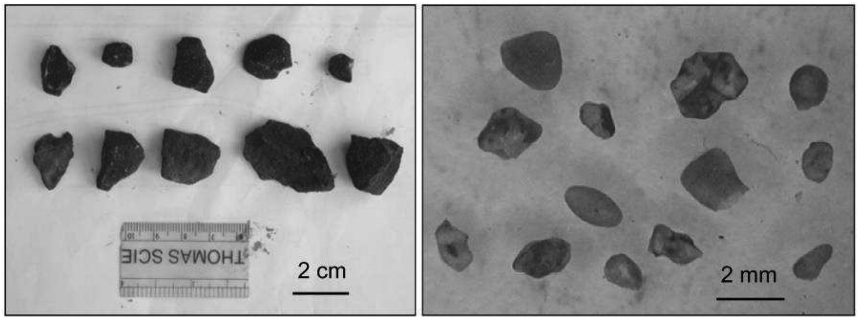

Figure 3. Centimeter and mm-sized TNT pieces from a partial detonation.

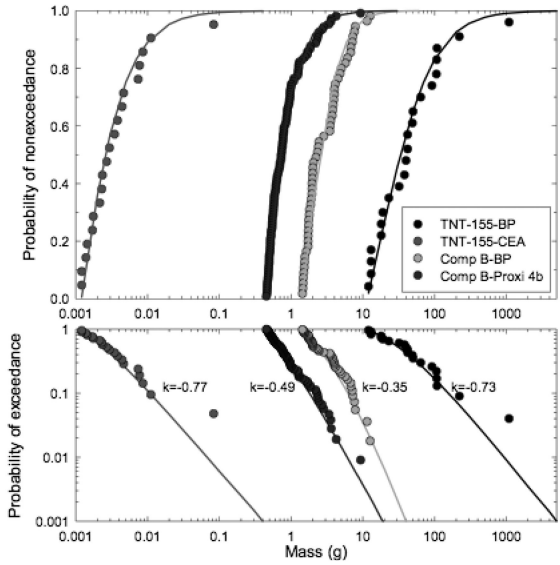

Figure 4. Particle mass distributions for low-order detonations. The largest 10% of the pieces were fitted using a generalized Pareto distribution. The tail slopes of these distributions suggest the TNT filled rounds (k=-0.77 and -0.73) produce a wider range of particles than do Comp B filled rounds (k=-0.49 and -0.35).

Dissolution Tests

Although the solubilities of pure explosives have been measured (e.g. (*35*)), it is the dissolution rate as a function of particle size that is needed to predict aqueous influx of explosive compounds on ranges. Researchers have measured the dissolution of explosive particles in laboratory settings, using stirring experiments and column studies (*36–39*), experimental approaches that do not directly relate to what occurs on range soils, namely dissolution of HE particles scattered onto soil.

We designed our experiments to mimic rainfall-driven dissolution of HE residues on surface soils. We used HE residues collected from detonations,

tracked changes in individual particles as dissolution proceeded, and modeled the data using the 'drop-impingement' dissolution model. The model was developed using laboratory data (*17*, *40*) and validated using outdoor test data (*15*, *17*), which we discuss in this paper. The model assumes that raindrops intercepted by HE particles drip off fully saturated in HE. Particle size, HE type, annual rainfall and average temperature are the key input parameters. The processes that we measured and modeled apply directly to processes occurring on military ranges.

We measured dissolution of cm-sized chunks of TNT, Composition B, Tritonal, and C4 exposed to natural weather conditions (*15*). TNT, Comp B, Tritonal, and C4 were selected because they are widely used high explosives. TNT is a single compound, whereas Comp B is a 60-39% mixture of RDX-TNT, Tritonal is an 80-20 TNT-aluminum mix and C4 is a plastic explosive primarily composed of RDX (92%) with added plasticizers (8%).

We placed 11 TNT, five Tritonal, 12 Comp B and six C4 chunks outside in 4-cm-diameter Buchner funnels (Figure 5). The funnels were attached to 1-liter bottles with a rubber stopper fitted with two holes – one for the funnel stem and the other for air exchange. The bottles fit snuggly into an insulated wooden box that kept them in the dark and from tipping over and moderated the temperatures experienced by the samples. Rainwater or snowmelt interacting with the HE collected in the bottles and the volume and concentration of these samples were measured every other week. Monthly we photographed the pieces of HE in situ to document changes in their appearance and size.

Figure 5. Outdoor tests showing Buchner funnels used to hold the HE pieces. Any precipitation landing in the funnel moves through the glass frit and into 1-L glass bottles in the wooden boxes.

This set-up exposed the explosives to conditions similar to those they experience on a range, where rain, snow, sun and freeze thaw cycles weather the HE, while allowing us to collect and analyze the dissolved HE and monitor changes in their appearance. Because the dissolution rate of a particle depends on its surface area (particle size), we sought insight into this factor by intentionally crushing three of the HE chunks and returning the pieces to their outdoor funnels to measure the dissolution rate of known populations of HE particles.

We also documented natural splitting, cracking and spalling of HE chunks during the three-year experiment to estimate the frequency of these particle size population-changing processes.

The cumulative mass loss for the TNT, Comp B, Tritonal and C4 chunks measured by High Performance Liquid Chromatography (HPLC) are shown in Figure 6. The shapes of the cumulative mass loss curves are similar among all the chunks except for increased dissolution for the chunks that split naturally or where crushed experimentally. During the three-year test, HE chunks which initially weighed over 1 g lost less than 5% of their mass while those that were less than 1 g lost up to 15% of their initial mass.

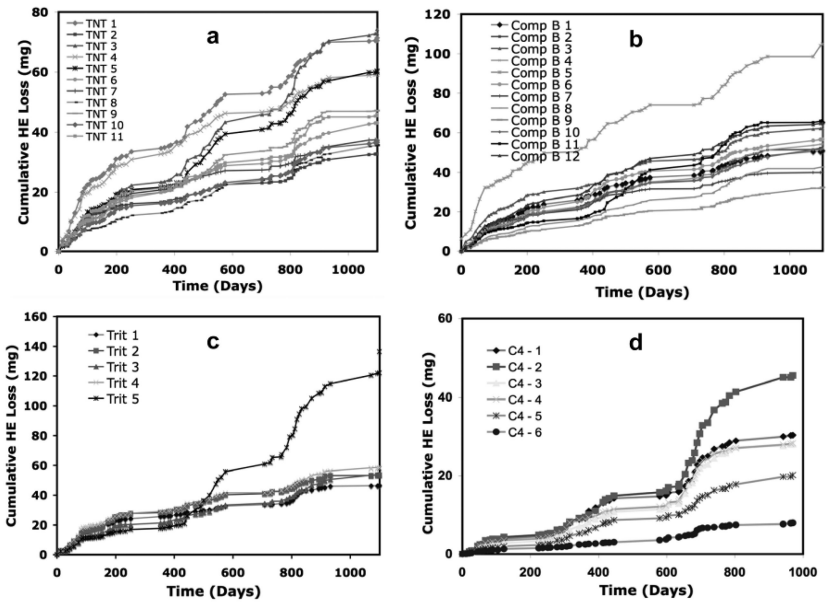

Figure 6. Cumulative mass loss (mg) versus time for a) TNT, b) Comp B, c) Tritonal and d) C4.

We used the drop impingement model along with the HE chunk masses and rainfall and temperature records to model the outdoor dissolution data (*15*, *40*). Model results for two TNT and Tritonal chunks are shown in Figure 7. The complete data set can be found in Taylor et al. (*15*). The drop-impingement model predicts the TNT dissolved-mass time-series with remarkably low root mean square prediction errors (12–13%) for both TNT and Tritonal chunks. The model has a simple physical interpretation: all rainfall captured by the particle flows off it fully saturated in HE. A nearly linear relationship exists between dissolution rate and rainfall rate, which makes it possible to link average annual HE influx to average annual rainfall. This linear approximation can be applied easily to ranges across the country using readily available rainfall and temperature climatology

(Figure 8). We predict that, in the absence of breakage and disaggregation, 1–10 g pieces should last 100 – 300 years (*17*). As the data were collected in an area with a ~100 cm/yr rainfall rate, the dissolution would be higher at wetter sites and lower at drier sites.

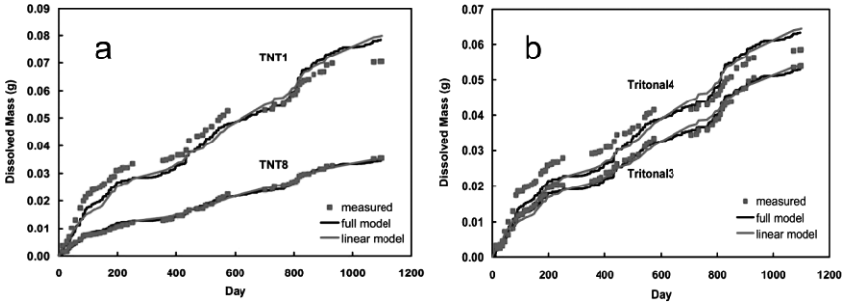

Figure 7. Dissolved TNT mass measured for a) TNT-1 and TNT-8 and b) Tritonal-3 and Tritonal-4 along with predictions from full and linear drop impingement models.

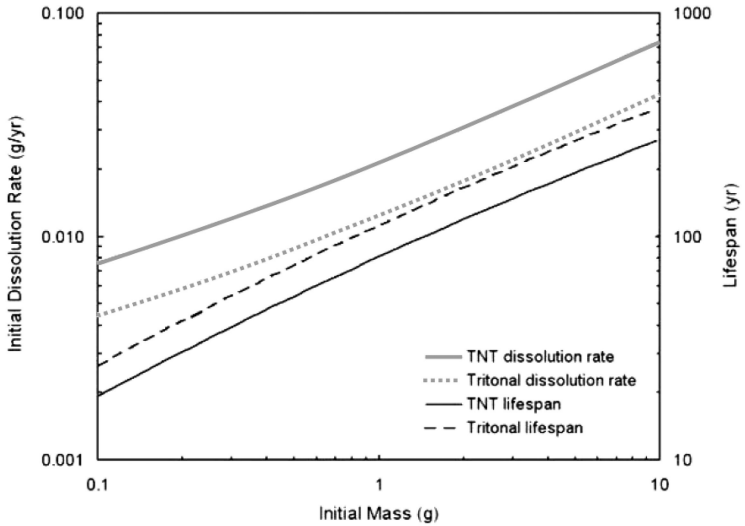

Figure 8. Predicted dissolution rate and particle lifespan versus the initial mass of a TNT or Tritonal particle. Curves were generated using the linear drop-impingement model (17), an average annual rainfall of 100 cm/yr and an average annual temperature of 11 °C.

Although we can model the concentration of explosives in the effluent samples, given their sizes and range climatology, two factors strongly affect the uncertainty of our dissolution results: photo-transformation of the HE and fracture of the HE pieces to create additional surface area. These uncertainties

are small compared with the huge uncertainty in the amount of HE on range soils. We discuss each of these factors in turn. Because we sought to document changes in the appearance of HE chunks and to check for mass balance, we periodically photographed and weighed them. This revealed an important finding: dissolved TNT mass, measured by HPLC, accounted for only about one-third of the mass lost from the TNT and Tritonal chunks, and dissolved RDX mass was about one-half of the RDX mass lost from Comp B and C4chunks. Mass losses measured with the balance were larger than dissolved masses and grew with time (Figure 9). Since both measurement methods (HPLC and balance) have low uncertainties, and we had very good mass balances for TNT, Tritonal and Comp B in the laboratory tests (*17*, *41*), we investigated other mass-loss pathways. Water did not pool in, or overflow from, the Buchner funnels and the 6 cm distance between the top of the funnels and the location of the HE chunks on the frits precluded wind or raindrops from bouncing pieces out of the funnels. We found that aqueous-phase transformation in sample bottles, sublimation of HE, handling of chunks when we weighed them all negligibly influenced the mass balances. We conclude that photo-transformation of the explosives to compounds not quantified by Method 8330B (*42*) accounts for these discrepancies.

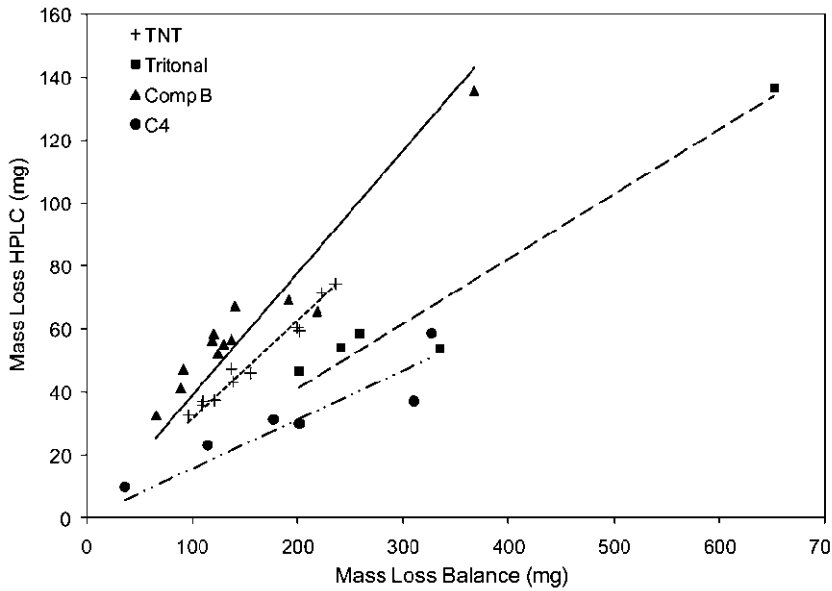

Figure 9. Dissolved mass loss, measured by HPLC was far less than mass loss by electronic balance for TNT, Tritonal, Comp B and C4 samples.

It has long been noted that TNT in solution turns red when exposed to sunlight and that the TNT concentrations decrease rapidly (e.g. (*43*)). The surfaces of TNT solids also turn red and Bedford et al. (*44*) reported photo-trans-formation of solid RDX. The formation, dissolution and transport of photo-transformation products

are processes inherent to outdoor exposure of explosives. As yet we do not know if these products occur solely due to radiation or are mediated by moisture on the particle surface. The identities of these products are also unknown as are their stability in soils (*15*), and their health risks, if any. However, the influx of these products into range soils may exceed that for the explosive itself and thus clearly warrants more attention.

Dissolution rate depends on surface area so it will increase as more surface area is exposed by weathering. During the three years of outdoor exposure, four of the HE chunks split naturally (Figure 10), and cracks developed in four TNT, two Tritonal, and three Comp B chunks. On multiple occasions small particles (> 1 mm across) broke off from the HE pieces—eight from TNT, two from Tritonal, and three from Comp B chunks. Over the three years, the TNT generated more small <1mm flakes than either the Tritonal or Comp B chunks. As we saw splitting, spalling and cracking of our test particles over a three-year period, these processes are probably common during the decades-long lifespans for gram chunks of HE and would significantly accelerate dissolution by increasing surface area exposed to rainfall.

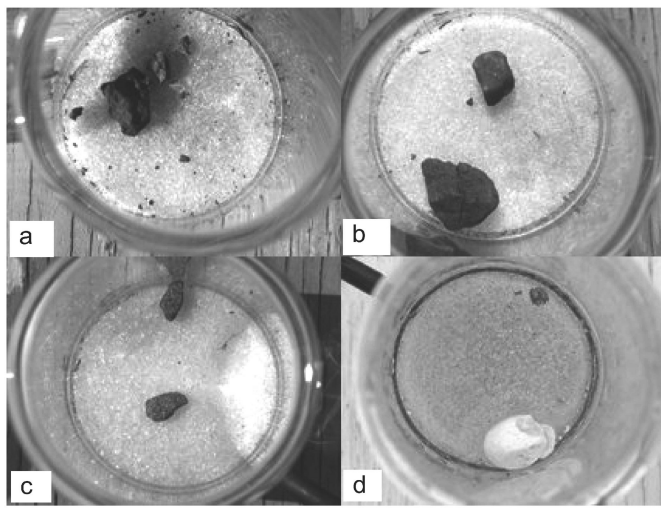

Figure 10. During the three years of outdoor exposure, four of the HE chunks split naturally a) TNT-3, b) TNT-11, c) Comp B-6 and d) C4-5.

To estimate the magnitude of this accelerated dissolution we crushed TNT-5, Tritonal-5 and Comp B-11. We weighed all the resulting particles to obtain the daughter particle size distribution for each chunk (Figure 11). We then returned the daughter particles to the outdoor funnels. As expected we observed an increase in the amount of HE dissolved for these samples (Figure 12). Both TNT and Composition B dissolution increased by about 60% over similarly sized chunks that were not crushed and Tritonal, which produced more daughter

particles, increased by 150%. We used the measured size distributions of TNT-5 and Tritonal-5 as input to model their dissolution after they were crushed. Figure 13 shows that the drop impingement model was able to predict the dissolution of a split chunk extremely well given the size distribution of the daughter particles (*15*, *40*).

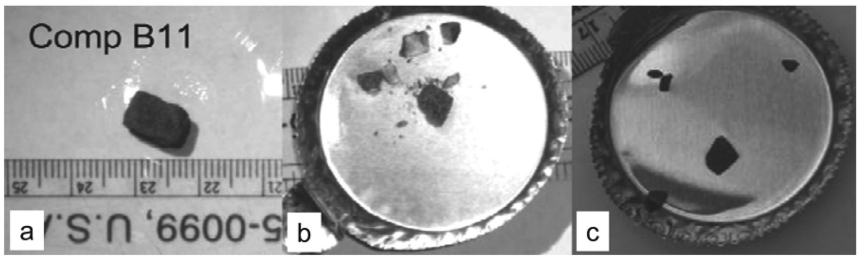

Figure 11. Appearance of Comp B11 a) before crushing, b) after crushing and c) after two years of outdoor exposure.

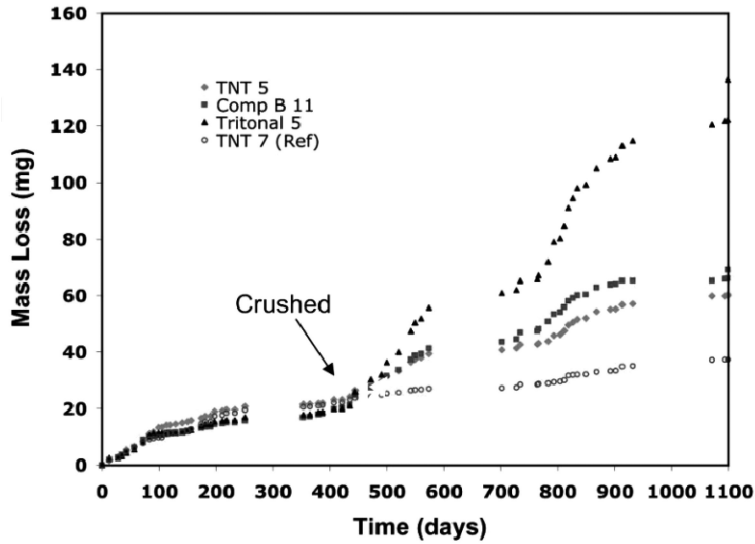

Figure 12. Cumulative HE mass loss as a function of time for TNT-5, Trit-5 and Comp B-11 that were crushed on day 436 of the test. TNT-7 was not crushed and is shown as a reference.

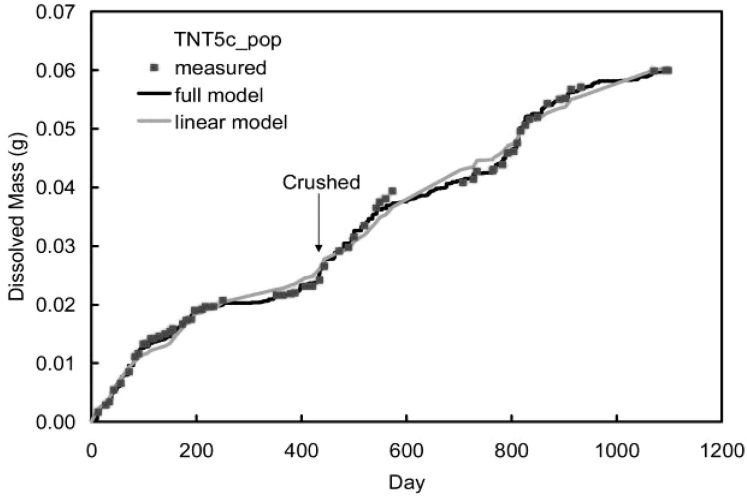

Figure 13. Measured and predicted dissolution for TNT 5. The post- crushing predictions used the measured-size distribution of the daughter particles.

At the end of the dissolution tests, we measured the masses of the remaining daughter particles from the crushed Comp B, TNT and Tritonal pieces. The slope of the distribution should flatten if large pieces split into many smaller ones and steepen if small particles are preferentially dissolved. Differences between their pre- and post- weathering mass distributions suggest that for the TNT and Tritonal samples the distributions became steeper, indicating that dissolution is the dominant process (Figure 14). The net change in the shape and magnitude of the mass distribution will depend on the relative rates of dissolution versus splitting.

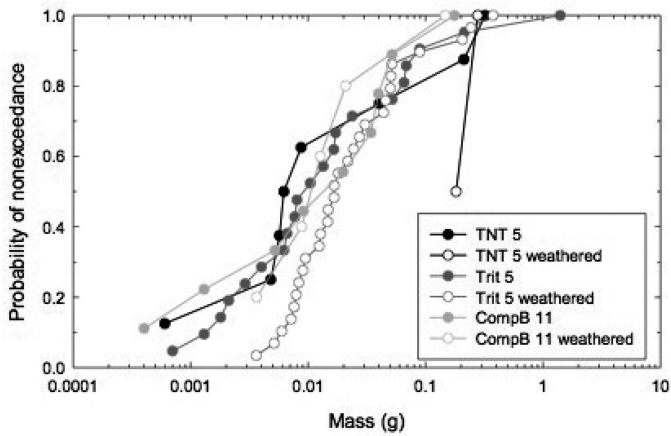

Figure 14. Change in mass distributions for crushed pieces of TNT, Tritonal and Comp B after 22 months of outdoor dissolution (15).

Summary

Transport of HE off military ranges can occur when substantial quantities of HE are deposited on the soils, precipitation is high, and the transit time for water to reach groundwater is short (shallow groundwater or very permeable soils). Researchers have measured the mass of high explosives in range soils and measured how dissolved explosives behave in different types of soils. We focused our research on the dissolution of explosives exposed to rainfall because rates of HE dissolution were poorly understood yet initiated aqueous-phase HE transport. Given the initial size distribution of HE pieces on the soil, the drop impingement model offers a simple and accurate method to predict aqueous dissolution of HE. However, factor-of-two uncertainties can result if the HE chunks photo-transform or if they fracture to create additional surface area. Additional work is needed to quantify the photo-formation products, their toxicities (if any) and their dissolution rates. Also we cannot yet predict splitting rates of HE particles exposed outdoors. Both photo-transformation and splitting are inherent to outdoor dissolution.

Much larger uncertainties result because the initial mass distribution of HE particles on ranges is poorly known. Mass distributions are difficult to measure and can introduce order-of-magnitude uncertainties into forecasts of the dissolved mass influx to soils. Possibly, the uncertainty could be reduced by using the HE concentrations measured in soils along with cumulative mass distributions measured from partially detonated rounds to estimate initial mass distributions. Given an HE mass distribution the drop impingement model could calculate the aqueous influx for the site, a value that could be input to vadose transport models, to make first-order estimates of the HE mass reaching groundwater. Although such values would have large uncertainties they, nevertheless, could help range managers assess the risk to groundwater and would provide a time frame over which mitigation measures could be implemented.

References

1. ATSDR. *Toxicological profile for 2,4,6-trinitrotoluene and RDX*; U.S. Department of Health and Human Services, Public Health Service, Agency for Toxic Substances and Disease Registry: Atlanta, GA, 1995.
2. U.S. Environmental Protection Agency (US EPA). Region 6 Human Health Medium - Specific Screening Levels. www.epa.gov/Region6/6pd/rcra_c/pd-n/screen.htm, 2008.
3. Taylor, S.; Lever, J. H.; Bostick, B.; Walsh, M. R.; Walsh, M. E.; Packer, B. *Underground UXO: Are they a significant source of explosives in soil compared to military training on ranges?* ERDC/CRREL Technical Report TR-04-23; Cold Regions Research and Engineering Laboratory: Hanover, NH, 2004.
4. Dauphin, L.; Doyle, C. *Study of ammunition dud and low-order detonation rates*; US Army Environmental Center Report SFIM-ACE-ET-CR-200049; Aberdeen Proving Ground: MD, 2000.

5. Jenkins, T. F.; Hewitt, A. D.; Grant, C. L.; Thiboutot, S.; Ampleman, G.; Walsh, M. E.; Ranney, T. A.; Ramsey, C. A.; Palazzo, A. J.; Pennington, J. C. *Chemosphere* **2006**, *63*, 1280–1290.
6. Jenkins, T. J.; Pennington, J. C.; Ranney, T. A.; Berry, T. E., Jr.; Miyares, P. H.; Walsh, M. E.; Hewitt, A. D.; Perron, N. M.; Parker, L. V.; Hayes, C. A.; Wahlgren, E. G. *Characterization of explosives contamination at military firing ranges*; ERDC/CRREL Technical Report TR-01-5, 2001.
7. Pennington, J. C.; Jenkins, T. F.; Ampleman, G.; Thiboutot, S.; et al. *Distribution and fate of energetics on DoD test and training ranges: Interim Report 3*; ERDC Technical Report ERDC TR-03-2; Engineer Research and Development Center: Vicksburg, MS, 2003.
8. Pennington, J. C.; Jenkins, T. F.; Ampleman, G.; Thiboutot, S.; Brannon, J. M.; et al. *Distribution and fate of energetics on DoD test and training ranges: final report*; ERDC Technical Report TR-06-13, 2006.
9. Taylor, S.; Hewitt, A.; Lever, J.; Hayes, C.; Perovich, L.; Thorne, P.; Daghlian, C. *Chemosphere* **2004**, *55*, 357–367.
10. Taylor, S.; Campbell, E.; Perovich, L.; Lever, J.; Pennington, J. *Chemosphere* **2006**, *65*, 1405–1413.
11. Poulin, I., Taylor, S.; Walsh, M. R.; Bigl, S.; Walsh, M. E.; Wagner A. In preparation. *Production of breached UXOs by proximity detonations: A study of the damage to the breached projectile and HE particle deposition.*
12. Radtke, C. W.; Gianotto, D.; Roberto, F. F. *Chemosphere* **2002**, *46*, 3–9.
13. DuBois, F. W; Baytos, J. F. *Weathering of Explosives for Twenty Years*; Los Alamos Report LA-11931; Los Alamos National Lab.: NM, 1991.
14. Walsh, M. E.; Taylor, S.; Hewitt, A. D.; Walsh, M. R.; Ramsey, C. A.; Collins, C. M. *Chemosphere* **2010**, *78*, 467–473.
15. Taylor, S.; Lever, J. H.; Walsh, M. E., Fadden, J.; Perron, N.; Bigl, S.; Spanggord, R.; Curnow, M.; Packer, B. *Dissolution rate, weathering mechanics, and friability of TNT, Comp B, Tritonal and Octol*; ERDC/CRREL Technical Report TR-10-2, 2010.
16. Buttle, J. M. *Prog. Phys. Geog.* **1994**, *18*, 16–41.
17. Lever, J.; Taylor, S.; Perovich, L.; Bjella, K.; Packer, B. *Environ. Sci. Technol.* **2005**, *39*, 8803–8811.
18. Morley, M. C.; Yamamoto, H.; Speitel, G. E.; Clausen, J. *J. Contam. Hydrol.* **2006**, *85*, 141–158.
19. Dontosava, K. M.; Yost, S. L.; Simunek, J.; Pennington, J. C.; Williford, C. W. *J. Environ. Qual.* **2006**, *35*, 2043–2054.
20. McCormick, N. G.; Feeherry, F. E.; Levinson, H. S. *Appl. Environ. Microbiol.* **1976**, *31*, 1357–1374.
21. Martel, R.; Mailoux, M.; Gabriel, U.; Lafebvre, R.; Thiboutot, S.; Ampleman, G. *J. Environ. Qual.* **2009**, *38*, 75–92.
22. Martel, R.; Mailloux, M.; Lefebvre, R.; Michaud, Y.; Parent, M.; Ampleman, G.; Thiboutot, S.; Jean, S.; Roy, N. *Energetic materials behavior in groundwater at the Arnhem Anti-Tank Range, CFB Valcartier, Quebec, Canada*; INRS- Georesources Report 1999-02; INRS- Georesources: Sainte-Foy, Quebec, Canada, 1999.

23. Bordeleau, G.; Martel, R.; Ampleman, G.; Thiboutot, S. *J. Environ. Qual.* **2008**, *37*, 308–317.
24. Bordeleau, G.; Martel, R.; Schafer, D.; Ampleman, G.; Thiboutot, S. *Environ. Geol.* **2008**, *55* (2), 385–396.
25. Walsh, M. E.; Collins, C. M.; Hewitt, A. D.; Walsh, M. R.; Jenkins, T. F.; Stark, J.; Gelvin, A.; Douglas, T. S.; Perron, N.; Lambert, D.; Bailey, R.; Myers, K. *Range characterization studies at Donnelly Training Area, Alaska: 2001 and 2002*; ERDC/CRREL Technical Report TR-04-3, 2004.
26. Jenkins, T. F.; Hewitt, A. D.; Ramsey, C. A.; Bjella, K. L.; Bigl, S. R.; Lambert, D. J. *Sampling studies at an air force live-fire bombing range impact area*; ERDC/CRREL Technical Report TR-06-2, 2006.
27. Jenkins, T. F.; Hewitt, A. D.; Ranney, T. A.; Ramsey, C. A.; Lambert, D. J.; Bjella, K. L.; Perron, N. M. *Sampling strategies near a low-order detonation and a target at an artillery impact area*; ERDC/CRREL Technical Report TR-04-14, 2004.
28. Hewitt, A. D.; Jenkins, T. F.; Ramsey, C. A.; Bjella, K. L.; Ranney, T. A.; Perron, N. M. *Estimating energetic residue loading on military artillery ranges: Large decision units*; ERDC/CRREL Technical Report TR-05-7, 2005.
29. Nieman, K. Select Engineering Services, 75 CEG/CEVC, Hill Air Force Base, UT. Personal communication, 2007.
30. Hewitt, A. D.; Jenkins, T. F.; Ranney, T.; Stark, J.; Walsh, M. E.; Taylor, S.; Walsh, M. R.; Lambert, D.; Perron, N.; Collins, C. M.; Karn, R. *Estimates for Explosive Residue Deposition from the Detonation of Army Munitions*; ERDC/CRREL Technical Report TR-03-16, 2003.
31. Thiboutot, S.; Ampleman, G.; Gagnon, A.; Marois, A.; Jenkins, T. F.; Walsh, M. E.; Thorne, P. G.; Ranney, T. A. *Characterization of antitank firing ranges at CFB Valcartier, WATC Wainwright and CFAD Dundurn*; Report # DREV-R-9809; Defence Research Establishment Valcartier: Val-Belair, Quebec, Canada, 1998.
32. Ampleman, G.; Thiboutot, S.; Lewis, J.; Marois, A.; Gagnon, A.; Gagnon, M.; Jean, S.; Jenkins, T. F.; Hewitt, A.; Pennington, J. C.; Ranney, T. A. *Evaluation of the contamination by explosives in soils, biomass and surface water at Cold Lake Air Weapons Range (CLAWR), Alberta, Phase I Report*; Report # DRDC-TR-2003-208; Defence R&D Canada–Valcartier: Val-Belair, Quebec, Canada, 2003.
33. Jenkins, T. J.; Ranney, T. A.; Miyares, P. H.; Collins, C. M.; Hewitt, A. D. *Use of surface snow sampling to estimate the quantity of explosive residues resulting from land mine detonations*; ERDC/CRREL Technical Report TR-00-12, 2000.
34. Taylor, S.; Lever, J. H.; Perovich, L.; Campbell E.; Pennington, J. A study of Composition B particles from 81-mm mortar detonations; Conference on Sustainable Range Management; New Orleans, Louisiana, 2004.
35. Ro, K. S.; Venugopal, A.; Adrian, D. D.; Constant, D.; Qaisi, K.; Valsaraj, K. T.; Thibodeaux, L. J.; Roy, D. *J. Chem. Eng. Data* **1996**, *41*, 758–761.
36. Lynch, J. C.; Brannon, J. M.; Delfino, J. J. *J. Chem. Eng. Data* **2002**, *47*, 542–549.

37. Lynch, J. C.; Brannon, J. M.; Delfino, J. J. *Chemosphere* **2002**, *47*, 725–734.
38. Phelan, J. M.; Webb, S. W.; Romero, J. V.; Barnett, J. L.; Griffin, F.; Eliassi, M. *Measurement and Modeling of Energetic Material Mass transfer to Soil Pore Water- Project CP-1227*; Sandia Report 2003-0153; Sandia National Laboratories: Albuquerque, NM, 2003.
39. Lynch, J. C.; Brannon, J. M.; Hatfield, K.; Delfino, J. J. *J. Contam. Hydrol.* **2003**, *66* (3−4), 147–159.
40. Taylor, S.; Lever, J.; Fadden, J.; Collins, P.; Perron, N.; Packer, B. *Chemosphere* **2009**, *77*, 1338–1345.
41. Taylor, S.; Lever, J. H.; Fadden, J.; Perron, N.; Packer, B. *Chemosphere* **2009**, *75*, 1074–1081.
42. US EPA. Method 8330B: Nitroaromatics, nitramines, nitrate esters by high performance liquid chromatography (HPLC). In *Test Methods for Evaluating Solid Waste, Physical/Chemical Methods*; Office of Solid Waste and Emergency Response, SW-846; Washington, DC, 2006. http://www.epa.gov/waste/hazard/testmethods/pdfs/8330b.pdf.
43. Spanggord, R. J.; Mill, T.; Chou, T-W.; Mabey, W. R.; Smith, J. H.; Lee, S. Environmental fate studies on certain munition wastewater constituents-Phase 1 and 11; Contract Report to U.S. Army Medical Research and Development Center, 1980.
44. Bedford, C. D.; Carpenter, P. S.; Nadler, M. P. *Solid-State Photo-decomposition of Energetic Nitramines (RDX and HMX)*; NAWCWPNS TP 8271; Naval Air Warefare Center Weapons Division: China Lake, CA, 1996.

Chapter 8

Photolysis of 2,4,6-Trinitrotoluene in Seawater: Effect of Salinity and Nitrate Concentration

Daniel W. O'Sullivan,* Jeffrey R. Denzel, and Dianne J. Luning Prak

Department of Chemistry, United States Naval Academy, 572 Holloway Road, Annapolis, MD 21402
***osulliva@usna.edu**

The photolysis rate of 2,4,6-trinitrotoluene (TNT) was examined in a variety of natural waters from pure water to a seawater end member. Photolysis experiments were performed using a Suntest CPS+® solar simulator equipped with an optical cell holder with eight positions for long-pass cutoff filters ranging from 295 to 495 nm. The rate of disappearance of TNT followed first order kinetics in all water types examined, and occurred at wavelengths less than 320 nm, but not significantly at wavelengths above 395 nm. The rate of photolysis decreased in the order seawater > estuarine water > fresh water > pure water, with the photolysis half-life for each water type at wavelengths less than 320 nm of 70, 120, 200 and 700 minutes, respectively. Changes in ionic strength from fresh to seawater do not account for the observed differences. Photolysis rates of TNT were not affected by the concentration of nitrate over the range expected in natural waters.

Introduction

Nitrogenous energetic materials are widely used in an extensive array of military ordnance, and a number of the nitroaromatic explosive compounds are toxic. Environmental transformation products of many nitrogenous energetic compounds (NECs) such as azoxy- and azo-compounds are equal to or more toxic than the parent compound. Nitroaromatic explosive compounds can enter the marine environment through a breach in the casing of discarded unexploded ordnance (UXO) or from run-off at coastal ranges. The most

abundant and frequently used military explosive is 2,4,6-trinitrotolunene (TNT). TNT has been used in combination with hexahydro-1,3,5-trinitro-1,3,5-triazine (RDX) and octahydro-1,3,5,7-tetranitro-1,3,5,7-tetrazocine (HMX) in bombs, armor-piercing shells, and torpedoes. A detailed understanding of the kinetics of NEC transformation in marine waters will aid the Department of the Navy (DON) in developing and implementing environmental management and mitigation programs for these coastal sites. Although SERDP, Army and Air Force have sponsored much work on energetic transformation in industrial waste streams and terrestrial and groundwater systems (*1–4*), very little information is available on rates of attenuation of energetic materials in coastal aquatic systems (*5*). In marine systems the complex mixture of salts can significantly alter the chemical behavior of trace constituents.

Photochemical transformation (i.e., photolysis or photooxidation) of TNT in aqueous solutions has been investigated as a treatment strategy for contaminated soils, slurries, and waters—particularly in conjunction with catalysts, such as TiO_2 (*6*, *7*), or with additions of peroxide and ozone (*3*), borohydride (*8*), H_2O_2 (*9*), and Fenton's reagent (H_2O_2 and Fe^{2+}) (*10*). Collectively known as advanced oxidation processes (AOPs), these techniques employ reactive oxidizing species such as hydroxyl radical ($OH\cdot$) and superoxide to facilitate the opening of aromatic rings and the ultimate mineralization of organic pollutants to CO_2 and H_2O (*3*). Because both $OH\cdot$ and superoxide ion are very effective oxidants for organic compounds, they hold much promise for *in situ* chemical oxidations of organic pollutants. Zero-valent iron (ZVI) has also been used to enhance contaminant degradation, which results in the reduction of the contaminant, generating a suite of reaction products (*11–13*).

As sunlight (or artificial UV light) decomposes TNT, it is converted into a variety of aromatic photolysis products including the nitroamine compounds and azoxydimers (*14*). Direct photolysis of ^{14}C-labelled TNT by high energy UV for a period of six days was reported to partially cleave the ring and degrade 17% of labeled TNT to $^{14}CO_2$ (*14*). Under natural light conditions, TNT half lives are reportedly as short as 10 min for sunlit Holston River water, 20 min for Searsville Pond water, 90 min for Waconda Bay water or as long as 11-22 hours for distilled water (*15*, *16*). Recently, Liou et al. (*17*) has determined that TNT degradation follows first order kinetics and has deduced the steps of degradation for the photo-Fenton process in distilled water. Characterization of the reaction products via each oxidation pathway in natural estuarine waters is critical to ensure that any mitigation strategy does not produce a more persistent compound of greater toxicity (i.e., azo, azoxy and nitroso compounds), as enhanced toxicity in bioassays has been observed during the photodegradation of TNT (*18*).

The efficacy of photochemical degradation and the associated mechanistic pathways is fundamentally related to the aquatic system in which the degradation is taking place. Freshwater ecosystems at mid-latitudes, such as surface water disposal lagoons, are likely poor environments for substantial degradation of nitrogenous energetic compounds (NEC) by photochemical degradation. These aquatic ecosystems often have high concentrations of chromophoric dissolved organic matter (CDOM), effectively limiting the photic zone where photochemical reactions may occur (less than 1 cm to several meters). Atmospheric conditions

(clouds, chemistry) and seasonal variations in solar radiation reaching surface waters, may also limit the photon efficiency for photolysis. At mid-latitudes, this means that strong seasonal variation in the efficiency of photochemical reactions is expected. In contrast, marine ecosystems at subtropical latitudes (Hawaii, Puerto Rico, and the Bahamas) have very low amounts of particles and CDOM, thus the photic zone may extend much deeper and insolation is much greater than freshwater ecosystems. For example, we have measured very low sunlight attenuation off the coast of Oahu, HI, such that the effective photic zone depth may extend to depths of 40 m (the limit of detection of our radiometer) and perhaps greater depths where there may be substantial photochemical degradation. The photochemical degradation of TNT produces biologically-important inorganic N (nitrate, ammonium ion) from the denitration of nitro groups on TNT (and its derivatives) and the deamination of amino groups of RDX and HMX. Thus photochemistry may be an important process for fueling increased production in aquatic ecosystems and therefore enhanced TNT degradation via biological pathways.

Research to determine the influence of various natural water constituents on photolysis rates suggests that dissolved ions can influence those rates (*19–21*). Nitrate has been found to increase the rate of photolysis of several organic compounds (*19*, *20*), while the presence of chloride has been found to increase or decrease the photolysis rate depending on the compound being photolyzed (*22–24*). The presence of inorganic ions has also been shown to lower the solubility of nitroaromatic compounds relative to pure water, a process called "salting out" (*25–28*). Lower solubility values should be included in any modeling efforts. For solutions such as seawater that are a complex mixture of salts, the salting-out effect has been quantified using a version of the Setschenow equation, which relates organic compound solubility to solution ionic strength, I (mol L^{-1}) (*25–30*):

$$\log (S_w/S) = K_s' I \tag{1}$$

where S_w is the solute solubility in pure water (mg L^{-1}), S is the solute solubility in the salt solution (mg L^{-1}), and K_s' is a salting-out parameter (L mol^{-1}). The ionic strength, I, is defined by

$$I = \frac{1}{2} \sum_{i} C_i Z_i^2 \tag{2}$$

where C_i is the concentration of ion i (mol L^{-1}) and Z_i is the charge on ion i. Values of K_s' in seawater for several nitroaromatic compounds have been reported to be between 0.08 and 0.16 (*25–28*).

In addition to the effect of media composition on the solubility, the media has an influence on the photolysis rate of TNT in marine waters. The increase in photolysis rate in marine waters may be due to enhanced absorption by TNT in marine waters, the presence of an additional photo-transformation pathway, or an increase in efficiency of the photo-transformation pathway present in pure waters. Fully characterizing which of the possibilities is producing the enhanced photo-

transformation rate observed in marine waters is necessary to facilitate developing the best remediation site models possible.

This work examined the photolysis kinetics of 2,4,6-trinitrotoluene in surface seawater and several other surface waters in a solar simulator. The influence of salinity and nitrate concentration on the rate of photolysis was determined.

Experimental Methods

Materials

2,4,6-Trinitrotoluene (Eastman Chemical Co., >97%) was used without further purification. A stock solution of TNT was prepared in HPLC grade acetonitrile (Aldrich Co.) and stored in an amber borosilicate vial at 4°C in the dark. Working solutions of 5 to 25 mg TNT L^{-1} were prepared by dilution with the appropriate media, pure water, freshwater or seawater. Pure water with a conductivity of 18 MΩ cm^{-1} was obtained from a Milli-Q UV-Plus® water system (Millipore Inc.). Freshwater from the Susquahanna river, the head waters of the Chesapeake Bay, estuarine water from the middle of the Chesapeake Bay, and seawater from the Mid Atlantic Bight were sequentially filtered through 0.45 and 0.22 μm 142 mm cellulose ester membrane filters (Advantec MFS, Inc.) and stored at room temperature before use. Sodium chloride and sodium nitrate (Fisher, ACS Reagent Grade) were used as received. Acetonitrile and methanol (Sigma−Aldrich, Chromosolv® Plus, for HPLC) were used as received.

Laboratory Photolysis Experiments

The photolysis experiments were performed using a Suntest CPS+® Solar Simulator. The solar simulator's spectrum is similar to the solar spectrum at the sea surface, but the intensity was about 2.5 to 3 times the intensity of clear sky conditions at noon at 39° N. Thirty mL aqueous samples containing dissolved energetics, typically 2.2 to 25 mg TNT L^{-1}, were placed in 10-cm quartz cuvettes (Helma Cells, Inc.). The optical cells were housed in a specially designed, thermostated optical cell holder which was inserted into the solar simulator irradiation chamber. Prior to exposure the absorption spectrum for each solution in each optical cell was determined using a Cary 3C spectrophotometer (200 to 700 nm). The optical cell holder has eight positions for 2" square optical cutoff filters. Long-pass cutoff filters (Edmund Industrial Optics, Inc.) with wavelengths of 295, 305, 320, 395, 420, 455, and 495 nm were used to isolate different portions of the solar spectrum during different irradiation experiments. The optical cell holder has positions for 16 10-cm path length quartz optical cells, two optical cells were oriented vertically below each 2" square cutoff filter, allowing for duplicates of each optical treatment. For all irradiations one filter position was blacked out and the solutions below this filter were used as controls, and for many irradiation experiments at least two positions had identical cutoff filters to generate quadruplicate exposures. For some experiments all the filter positions contained the same wavelength cutoff filter, usually 295 nm, and the optical cells contained solutions with varying concentrations of DOC, nitrate, salinity or pH

etc. The optical cell holder was thermostated at 20.0 ± 1.0°C by continuously circulating Milli-Q water using a thermocirculator (Neslab RTE 7, Thermo Inc.). The design of the cell holder is patterned after Johannessen and Miller (*31*).

Analysis of TNT

One-mL aliquots were taken from each optical cell after the exposure time and analyzed for TNT. TNT was quantified using an Agilent 1100 Series high performance liquid chromotograph (HPLC) with a C-18 column (Platinum, 100A, 5 mm, 150 mm x 4.6 mm; Alltech) and variable wavelength detector set to 254 nm, following the procedures established in EPA method 8330. Samples (10 µL) were injected into an eluent (50% MeOH: 50 % water) for isocratic separation with a flow rate of 0.5 mL min^{-1}. Duplicate analyses were performed on replicate samples for each exposure treatment of the solar spectrum. The detection limit was 0.05 mg TNT L^{-1} in both pure water and seawater media. The technique was linear from 0.1 to 25 mg TNT L^{-1}.

Analysis of Nitrate

A direct spectrophotometric method for the quantitative determination of nitrate in seawater was used for both the seawater and pure water experiments (*32*). The method involves the nitration of resorcinol in acidified seawater, forming a colored product that absorbs at 505 nm with a molar absorptivity of 1.7 x 10^4 L mol^{-1} cm^{-1}. A 2% (w/v) resorcinol (Sigma-Aldrich, >98% purity) stock solution was prepared daily, and a 0.6 mL aliquot was reacted with 2 mL of concentrated sulfuric acid and 1.0 mL of the sample. For non-seawater solutions, 0.5 mL of a 1.0 M solution of trace metal grade HCl was used as the chloride ion source. All solutions were diluted to total volume of 5.0 mL with Milli-Q water. The absorbance of each sample was measured at 505 nm in a 1.0-cm cuvette on a Cary 3C UV-Vis spectrophotometer, samples with an absorbance in excess of 1.5 were diluted with Milli-Q water to within the range of the calibration curve. A calibration curve was prepared from sodium nitrate. Different volumes of a 0.05 M stock solution of NO_3^- were added to produce varying concentrations of nitrate for the calibration curve, and irradiation experiment solutions with 5 ppm 2,4,6-trinitrotoluene with either a pure water matrix or using seawater.

Results and Discussion

TNT added to seawater and irradiated with simulated sunlight rapidly decreased (Figure 1). The loss of TNT fit first order kinetics with $r^2 > 0.90$, for nearly all experiments over two or three half-lives and in all water types (Figure 2). Mabey et al. (*33*) observed an increase in the photolysis rate after three hours of irradiation in pure water. The pure water photolysis rate observed in this work did not exhibit an increase in rate with up to six hours of irradiation. The rate of photolysis decreased in the order seawater > estuarine water > fresh water > pure water (Table 1). The photolysis rate at wavelengths greater than 395 nm was very

small (Table 1). The transformation was largely driven by wavelengths less than 320 nm with some photochemical transformation occurring in the wavelength range from 320 to 395 nm. Photolysis of TNT in ultrapure water, 18 MΩ cm^{-1} Milli-Q water, had a half-life ($t_{1/2}$) of 770 minutes when exposed to sunlight with wavelengths greater than 295 nm. The pure water photolysis rate constant of 1.66 ± 0.33 x 10^{-5} s^{-1} determined here is in excellent agreement with the air-saturated pure water value of 1.7 ± 0.2 x 10^{-5} s^{-1} found by Mabey et al (*33*). In freshwaters under the same conditions the half-life was 210 minutes, for estuarine water $t_{1/2}$ was 115 minutes, and in seawater $t_{1/2}$ was 69 minutes. Mabey et al (*33*) observed enhanced photolysis rates for TNT in pond and river water relative to pure water. Simmons and Zepp (*34*) examined the direct and indirect photolysis of a number of substituted nitroaromatic compounds in fresh and pure water. They also observed enhanced photolysis rates for TNT in fresh waters.

The direct photolysis of TNT in a dilute aqueous solution can be described by the following equation:

$$\frac{-d[TNT]}{dt} = k_{obs}[TNT] = 2.303\phi_\lambda I_{o\lambda}\epsilon_\lambda l[TNT] \qquad (3)$$

where $\emptyset_\lambda$ is the quantum yield, $I_{o\lambda}$ is the incident light intensity, ε_λ is the molar absorptivity and l is the path length. Nitroaromatic compounds (TNT, DNT) absorb electromagnetic radiation in the ultraviolet (UV) range of 200 nm and 400 nm (*35*). The absorption spectra are exponential, thus the absorption in the environmentally-relevant UV (290 to 400 nm) is much less than at wavelengths <290 nm (Figure 3). The increased photolysis rate of TNT in seawater may be due to an increase in the molar absorptivity of TNT in seawater media. The molar absorptivity of TNT in pure water was determined to be 1450 +/- 30 M^{-1} cm^{-1} at 300 nm. This is somewhat less than the value reported by Mabey et al. (*33*) of 1600 M^{-1} cm^{-1} at 300 nm in a 90% water: 10% acetonitrile solution. The molar absorptivity determination in aqueous media in the absence of acetonitrile is likely more environmentally relevant. The influence of ionic strength on the molar absorptivity was examined by preparing known concentrations of TNT in sodium chloride solutions of known composition. Sodium chloride concentrations of 10, 20 and 40 ppt correspond to ionic strengths of 0.17, 0.34, and 0.68 m. Seawater consists of a complex mixture of salts with and ionic strength of 0.68 at a salinity of 34. The molar absorptivity of TNT decreases with increasing ionic strength at all wavelength examined, and at 300 nm the molar absorptivity decreases to 1290 M^{-1} cm^{-1} at ionic strengths similar to seawater, Figure 4. The decrease in molar absorptivity of about 12% from pure water to seawater ionic strengths would reduce the photolysis rate. Consequently the change in molar absorptivity does not account for the faster photolysis rates observed in seawater. Although the observed change in molar absorptivity does not account for the enhanced photolysis rates, the absorption spectrum in seawater with the largest molar absorptivities at wavelengths less than 380 nm is consistent with greater photolysis rates in filter treatments with incident radiation of wavelengths less than 340 nm.

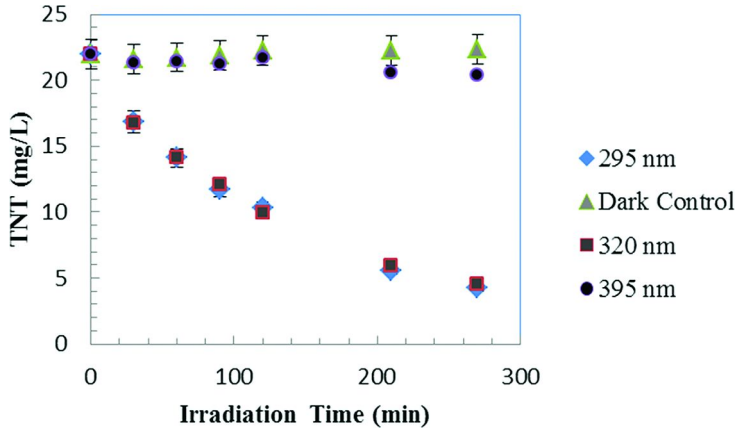

Figure 1. Degradation of TNT as a function of irradiation time in mid salinity Chesapeake Bay seawater, S = 17 ‰ with several long pass cut-off filters and the dark control.

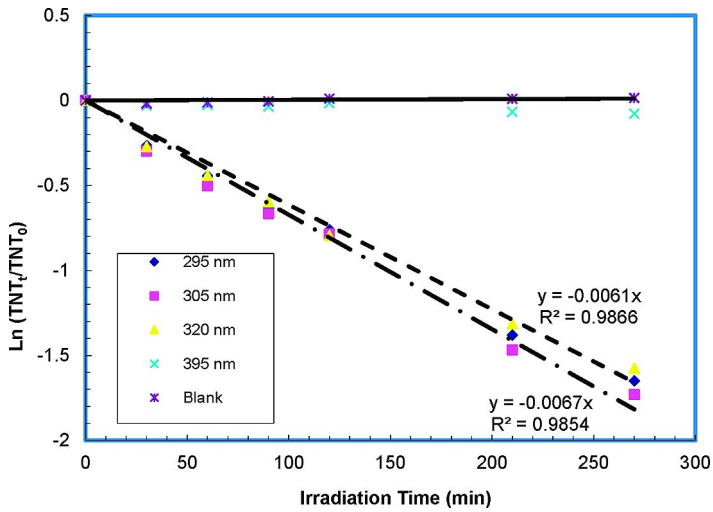

Figure 2. Fit of the loss of TNT as a function of irradiation time in mid salinity Chesapeake Bay seawater, S = 17 ‰ to a first order loss equation. Results from a number of long pass cut-off filter treatments and the dark control are shown.

Table 1. Summary table of solar simulator experiments

Media	*Initial [TNT] (mg/L)*	*Final [TNT] (mg/L)*	*Total Irradiation Time (hr)*	*Sample Frequency (min)*	k_{obs} *295 nm* (min^{-1})	k_{obs} *320 nm* (min^{-1})	k_{obs} *395 nm* (min^{-1})
Pure Water [a], Milli-Q	24	16	6	60, 120	0.0009	0.0010	0.0007
Freshwater	21	15.3	1.75	15, 30	0.0033	0.0034	0.0003
Estuarine water	21	10.6	1.75	15, 30	0.0060	0.0057	0.0007
50% Station M Seawater	22	3.7	5	30, 60	0.0064	0.0061	0.0003
Station M seawater	23	1.0	8	60, 120	0.0100	0.0098	0.0007

[a] Irradiation intensity was 500 W/m^2, all other experiments used 750 W/m^2.

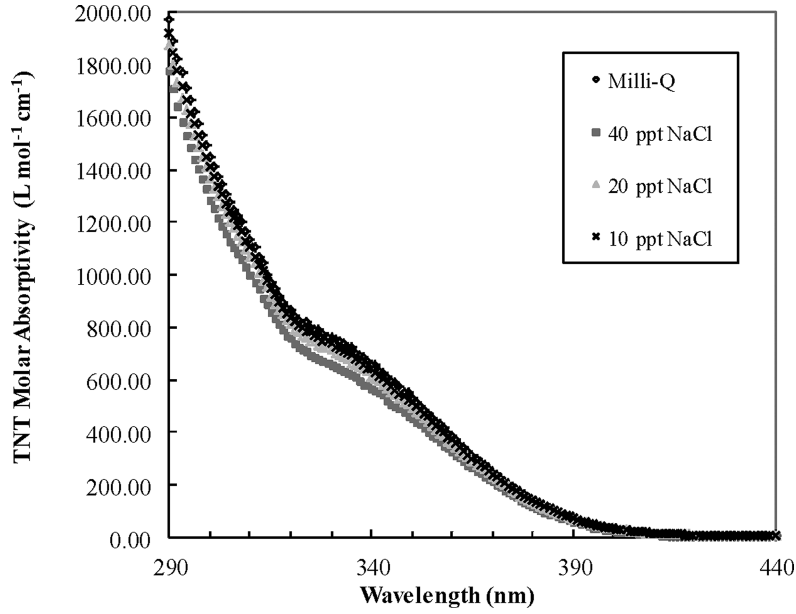

Figure 3. The molar absorptivity of TNT at different ionic strengths from 290 nm to 440 nm.

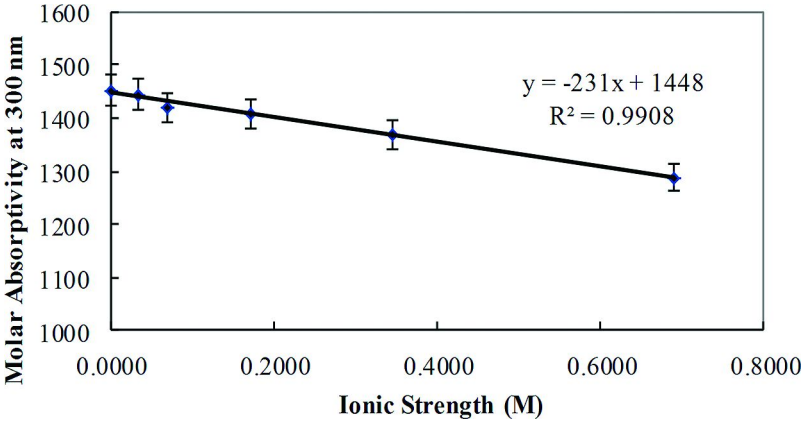

Figure 4. The decrease in the molar absorptivity of TNT at 300 nm with increasing ionic strength in sodium chloride solutions.

The combination of increasing molar absorptivity at shorter wavelengths coupled to the decrease in the photonic flux at short wavelengths means that natural sunlight is often too weak to cause much direct photolysis deep within an estuarine water column, but research has shown that the presence of oxidizing agents and catalysts may facilitate complete degradation of TNT with natural sunlight through secondary photochemical processes. These agents and catalysts may already be present in the water column under certain environmental conditions.

Effect of Nitrate Ion on the Photolysis of TNT in Seawater

The photolysis of nitrobenzene in pure water has been shown to increase by nearly an order of magnitude in the presence of dissolved nitrate ion (*20*). In pure water solutions with up to 4 mM added nitrate ion, Zepp et al. (*20*) observed an increase in the photolysis rate of nitrobenzene by nearly an order of magnitude. Direct photolysis of nitrate ion generates hydroxyl radical which provided a second reaction path for the removal of nitrobenzene. We examined the influence of nitrate ion concentration on the photolysis of TNT in seawater and pure water. The photolysis rate for TNT in pure water increased by a factor of three in the presence of up to 4 mmol NO_3^- L^{-1} (Table 2). In pure water the observed first order rate constant was 0.0012 min^{-1} which is similar to the value determined by Zepp et al. (*20*) of 0.0003 min^{-1} for nitrobenzene. The addition of nitrate to pure water to achieve a concentration of 4 mmol NO_3^- L^{-1} increased the rate constant to 0.0037 ± 0.0004 min^{-1} which is nearly identical to the value obtained by Zepp et al. (*20*) of 0.0033 min^{-1} at similar nitrate concentrations. In both pure water and seawater systems with added nitrate, the photolysis of TNT was not significant at wavelengths greater than 395 nm (Table 2). The photolysis rate of TNT in seawater was not affected by nitrate concentrations from 0 to 600 µmol NO_3^- L^{-1} (Table 2). The lower concentration of nitrate used in the seawater experiments, greatly exceeded typical concentrations of nitrate in surface seawater from 0.5 to 30 µmol NO_3^- L^{-1}. These results indicate that the direct photolysis of TNT in seawater is sufficiently fast that NO_3^- photolysis does not enhance the rate significantly.

Conclusions

TNT added to seawater and irradiated with simulated sunlight rapidly degraded. The loss of TNT was modeled with first order kinetics over two or three half-lives. The pure water photolysis rate observed in this work did not exhibit an increase in rate with up to six hours of irradiation. First-order rate constants were determined for all water types. The rate of photolysis decreased in the order seawater > estuarine water > fresh water > pure water (Table 1). The photolysis rate at wavelengths greater than 395 nm was very small (Table 1). The transformation was largely driven by wavelengths less than 320 nm with some photochemical transformation occurring in the wavelength range from 320 to 395 nm. Photolysis of TNT in ultrapure water, 18 MΩ cm^{-1} Milli-Q water, had a half-life ($t_{1/2}$) of 770 minutes when exposed to sunlight with wavelengths greater than 295 nm. In freshwaters under the same conditions the half-life was 210 minutes, for estuarine water $t_{1/2}$ was 120 minutes, and in seawater $t_{1/2}$ was 70 minutes. The addition of nitrate ion up to 4 mM in pure water increased the photolysis rate. Addition of nitrate ion up to 600 µM in seawater did not change the photolysis half-life.

Table 2. Photolysis rates of 5 ppm TNT in seawater and pure water with added nitrate

		Photolysis Rate Constant by Cut off filter (min^{-1})				
Water Type	***Conc. NO_3^-***	***295 nm***	***305 nm***	***320 nm***	***395 nm***	***Dark Control***
Milli-Q	0 mM[a]	0.0012		0.0013	0.00007	
	2 mM	0.0031 ± 0.0006	0.0039 ± 0.0006	0.0019 ± 0.0003	0.00005 ± 0.00002	0.00004 ± 0.00002
	4 mM	0.0037 ± 0.0004	0.0045 ± 0.0005	0.0023 ± 0.0004	0.00003 ± 0.00004	0.00005 ± 0.00003
Sea Water	0 μM	0.0124 ± 0.0007	0.0125 ± 0.0004			NC
		0.0123 ± 0.0007	0.0084 ± 0.0021			NC
	150 μM	0.0130 ± 0.0007	0.0139 ± 0.0007	0.0122 ± 0.0004	NC	
		0.0123 ± 0.0007	0.0130 ± 0.0009	0.0126 ± 0.0003	NC	
	450 μM	0.0108 ± 0.0011	0.0129 ± 0.0008	0.0115 ± 0.0013	NC	NC
			0.0121 ± 0.0010			
	600 μM	0.0124 ± 0.0010	0.0132 ± 0.0015	0.0118 ± 0.0009	NC	NC
		0.0116 ± 0.0007	0.0141 ± 0.0014			

[a] Initial [TNT] 24 mg/L.; NC – no observed change

Acknowledgments

Funding was provided by the Strategic Environmental Research and Development Program (SERDP), ER-1431.

References

1. Alnaizy, R.; Akgerman, A. *Water Res.* **1999**, *33*, 2021–2030.
2. Garcia Einschlag, F. S.; Lopez, J.; Carlos, L.; Capparelli, A. L. *Environ. Sci. Technol.* **2002**, *36*, 3936–3944.
3. Rodgers, J. D.; Bunce, N. J. *Water Res.* **2001**, *35*, 2101–2111.
4. Spain, J. C., Hughes, J. B., Knackmuss, H. J., Eds. *Biodegradation of Nitroaromatic Compounds and Explosives*; Lewis Publishers: New York, 2000.
5. Zhao, J.-S.; Greer, C. W.; Thiboutot, S.; Ampleman, G.; Hawari, J. *Can. J. Microbiol.* **2004**, *50*, 91–96.
6. Schmelling, D. C.; Gray, K. A.; Kamat, P. V. *Environ. Sci. Technol.* **1996**, *30*, 2547–2555.
7. Son, H. S.; Lee, S. J.; Cho, I. H.; Zoh, K. D. *Chemosphere* **2004**, *57*, 309–17.
8. Larson, R. A.; Miller, P. L.; Crowley, T. O. *Environ. Sci. Technol.* **1996**, *30*, 1192–1197.
9. Ho, P. C. *Environ. Sci. Technol.* **1986**, *20*, 260–267.
10. Liou, M.-J.; Lu, M.-C.; Chen, J.-N. *Chemosphere* **2004**, *57*, 1107–1114.
11. Agrawal, A.; Tratnyek, P. G. *Environ. Sci. Technol.* **1996**, *30*, 153–160.
12. Oh, S. Y.; Cha, D. K.; Chiu, P. C.; Kim, B. J. *Water Sci. Technol.* **2003**, *47*, 93–99.
13. Bandstra, J. Z.; Miehr, R. M.; Tratnyek, P. G. *Environ. Sci. Technol.* **2005**, *39*, 230–238.
14. Andrews, C. C.; Osmon. J. L. Rep. No. WQEC/C 75-197 (AD-B008175). Naval Weapons Support Center, Crane, IN, 1975.
15. Spanggord, R. L.; Mabey, W.-R.; Mill, T.; Chou, T. W.; Smith, J. H.; Less, S.; Robert, D.. LSU-7934, AD-A138550, SRI International, Menlo Park, CA, 1983
16. Talmage, S. S.; Opresko, D. M.; Maxwell, C. J.; Welsh, C. J. E.; Cretella, F. M.; Reno, P. H.; Daniel, F. B. *Rev. Environ. Contam. Toxicol.* **1999**, *161*, 1–156.
17. Liou, M.-J.; Lu, M.-C.; Chen, J.-N. *Chemosphere* **2004**, *57*, 1107–1117.
18. Davenport, R.; Johnson, L. R.; Schaffer, D. J.; Balbach, H. *Ecotox. Environ. Safety* **1994**, *27*, 14–22.
19. Brezonik, P.; Fulkerson-Brekken, J. *Environ. Sci. Technol.* **1998**, *32*, 3004–3010.
20. Zepp, R. G.; Holgne, J.; Bader, H. *Environ. Sci. Technol.* **1987**, *21*, 433–450.
21. O'Sullivan, D. W.; Denzel, J. R.; Luning Prak, D. J. *Aquat. Geochem.* **2010**, *16*, 491–505.
22. Chiron, S.; Minero, C.; Vione, D. *Environ. Sci. Technol.* **2006**, *40*, 5977–5983.

23. Mateus, M. C. D. A.; Da Silva, A. M.; Burrow, H. D. *Water Res.* **2000**, *23*, 1119–1126.
24. Mihas, O.; Kalogerakis, N.; Psillakis, E. *J. Hazard. Mater.* **2007**, *146*, 535–539.
25. Luning Prak, D. J.; O'Sullivan, D. W. *J. Chem. Eng. Data* **2006**, *51*, 448–450.
26. Luning Prak, D. J.; O'Sullivan, D. W. *J. Chem. Eng. Data* **2007**, *52*, 2446–2450.
27. Luning Prak, D. J.; Moran, P. J. *J. Chem. Eng. Data* **2008**, *53*, 586–587.
28. Luning Prak, D. J.; O'Sullivan, D. W. *J. Chem. Eng. Data* **2009**, *54*, 1231–1235.
29. Sada, E.; Kito, S.; Ito, Y. *J. Chem. Ref. Data* **1975**, *20*, 373–375.
30. Hashimoto, A.; Sakino, H.; Kojima, T.; Yamagami, E.; Tateishi, S.; Akiyama, T. *Water Res.* **1984**, *16*, 891–897.
31. Johannnessen, S. C.; Miller, W. L. *Mar. Chem.* **2001**, *76*, 271–283.
32. Zhang, J-Z.; Fisher, C. J. *Mar. Chem.* **2006**, *99*, 220–226.
33. Mabey, W. R.; Tse, D.; Baraze, A.; Mill, T. *Chemosphere* **1983**, *12*, 3–16.
34. Simmons, M. S.; Zepp, R. G. *Water Res.* **1986**, *20*, 899–904.
35. Bartolo, B. D.; Pacheco, D. P.; Shultz, J. *Spectroscopic Investigations of Energetic Materials and Associated Impurities*; Boston College, Boston, MA, 1979.

Chapter 9

2,4,6-Trinitrotoluene Mineralization and Incorporation by Natural Bacterial Assemblages in Coastal Ecosystems

Michael T. Montgomery,[1,*] Thomas J. Boyd,[1] Joseph P. Smith,[2] Shelby E. Walker,[3] and Christopher L. Osburn[4]

[1]Naval Research Laboratory, Washington, DC 20375
[2]US Naval Academy, Annapolis, MD 21402
[3]National Oceanic and Atmospheric Administration, Silver Spring, MD 20910
[4]North Carolina State University, Raleigh, NC 27695
[*]michael.montgomery@nrl.navy.mil

Because of logistical and technical challenges to studying energetics in coastal environments, lab and terrestrial data are often extrapolated to aquatic field sites. We found measurable TNT mineralization rates from natural microbial assemblages in several coastal ecosystems unlikely to have a history of exposure to energetics. During nine sampling events in coastal waterways from 2002 to 2010, we measured TNT mineralization rates in surface sediment and water samples that were often the same order of magnitude as the rate of total heterotrophic bacterial metabolism. These rates were often similar to those of other organic compounds that are transient in natural ecosystems such as petroleum hydrocarbons and amino acids - due to their use in bacterial metabolism.

Research Challenges

Relative to other organic (e.g. PAHs, PCBs, TCE, BTEX) and inorganic (e.g. metals, radionuclides) contaminants, our understanding of the ecological fate of energetics is limited (see reviews by (*1*, *2*)). There has been relatively sparse funding for basic research on energetics as they are seen as DoD-specific

contaminants and outside the scientific interests of the EPA or NSF. Burdensome regulations for handling energetics at DoD and academic facilities has greatly limited the number of labs participating in this research area. It has also led to the use of analog compounds in place of energetics and these analogs are likely to behave differently in natural environments. Most of the previous research has been focused on terrestrial and groundwater systems (e.g. shore-side ranges) and applied laboratory work (e.g. flask biotreatability studies) in lieu of field studies of coastal ecosystems (*3*). As seen with virtually all contaminants, the application of laboratory studies to bioremediation at field sites has been problematic for both DoD and industry as laboratory-cultured bacteria tend to poorly represent natural bacterial assemblages (*4*).

There are additional technical challenges to studying fate and transport of energetics in the field. Environmental studies that empirically determine energetic concentrations in coastal waters and sediment are greatly hampered by limited access to DoD sites. It is also difficult, if not impossible, for ecological scientists to collect samples using their standard equipment (e.g. benthic grab in a underwater UXO field) and processing the sample in an ecologically relevant period (i.e. minutes to hours). Because of relatively limited available information, results of published studies tend to have reduced replication, to be extrapolated to ecosystems where there is even less information (e.g. freshwater data extrapolated to marine, estuarine sites), and are more prone to misapplication to applied problems, such as environmental cleanup and determination of environmental risk.

Reports of slow TNT degradation in flask-based studies along with known large input of energetic compounds to shore side ranges suggest that these sites have the potential to impact adjacent coastal waters. These impacts can include toxicity to coastal fauna (i.e. ecotoxicity), as well as, pose a risk to human health. Energetic bioaccumulation into fish and shellfish is the primary proposed pathway for human health risk, though actual supporting evidence is limited ((*5*), see also review by (*6*)). In the laboratory, toxicity studies with marine organisms have proven difficult to perform as TNT concentrations rapidly decrease in incubation chamber seawater over the course typical for such study (e.g. 28 days; (*7*, *8*)) and much of the toxicity may be associated with reduced TNT products rather than the parent compound (e.g. (*9*)). Such studies with other energetics, like 1,3,5-Trinitroperhydro-1,3,5-triazine (RDX), are confounded by the use of formaldehyde in its preparation (*10*) which complicates data interpretation in both toxicity and biodegradation studies (especially at higher energetic concentration). Field collection and measurement of energetics in marine organisms are further hampered by lack of standardized methods for tissue extraction (e.g. sediment methods often used) and the use of energetic detection methods that are prone to false positives (e.g. overlapping peaks with GC/FID for fish tissue extracts).

In addition to difficulty assessing ecological and human health risks associated with long-term exposure to energetics, *in situ* evidence to substantiate energetics' long residence time in coastal environments is also lacking. Some of this lack of evidence has to do with the paucity of data collected from these environments. Though even when energetic analyses are performed on field samples, significant concentrations are rarely found in coastal ranges (e.g. Vieques Island; (*11*, *12*)) or

offshore dumpsites (Oahu; (*13*)) indirectly suggesting that energetic compounds may be more labile in saline waters and sediment at these field sites than would be suggested based on the previous laboratory studies.

TNT Transformation

TNT transformation typically refers to alteration of its chemical structure to reduced dead end metabolites or intermediates. Transformation includes catabolic processes, such as mineralization and incorporation into microbial biomass, but most energetic literature documents TNT reduction to aminotoluenes and related intermediates with subsequent binding to organic matter (humification) or dimerization. TNT is transformed by many naturally occurring abiotic processes, such as photolysis and chemical hydrolysis, as well as biological processes involving bacteria, microalgae, fungi, and higher plants (cf. (*3*, *14*)). Transformation rates vary based on *in situ* environmental conditions but, in general, photolysis > microbial metabolism > chemical hydrolysis rate for TNT under typical conditions in coastal surface waters (*13*). Although there are differences in interpretation of published data on the relative degree of TNT transformation, commonality can be found amongst most work if it is segregated according to relative importance of nitrogen to the TNT transformation process being studied; specifically, nitrogen-independent (abiotic), not nitrogen-limited (biotic), and nitrogen-limited conditions (biotic; Figure 1). Nitrogen is often a limiting nutrient for microbial growth (*15*) in estuarine and marine ecosystems, while the terrestrial and freshwater environments that form the basis of much of our current understanding of TNT metabolism are generally phosphorus-limited.

Nitrogen-Independent (Abiotic) Conditions

Nitrogen-independent (abiotic) conditions include systems where photolysis and chemical hydrolysis predominate and where presence of energetics (as a nitrogen source for microbiota) would have little impact. Research papers involving these abiotic processes most often reported production of reduced products from TNT transformation (e.g. aminotoluenes; (*16*)). These products would bind to humic particles and aggregates (if present) or form dimers in solution. Some papers report the photolytic (*17*), alkaline hydrolytic (*18*), or gamma irradiation-induced mineralization of TNT to CO_2 as part of a treatment system process (*19*). In seawater, photo-Fenton type reactions involving the photochemical redox cycling of iron (Fe) represent natural, in-situ advanced oxidation processes (AOP, see review by (*20*)) that are the likely photochemical removal mechanism for energetics and liberation of nitrogen as the aromatic ring is oxidized.

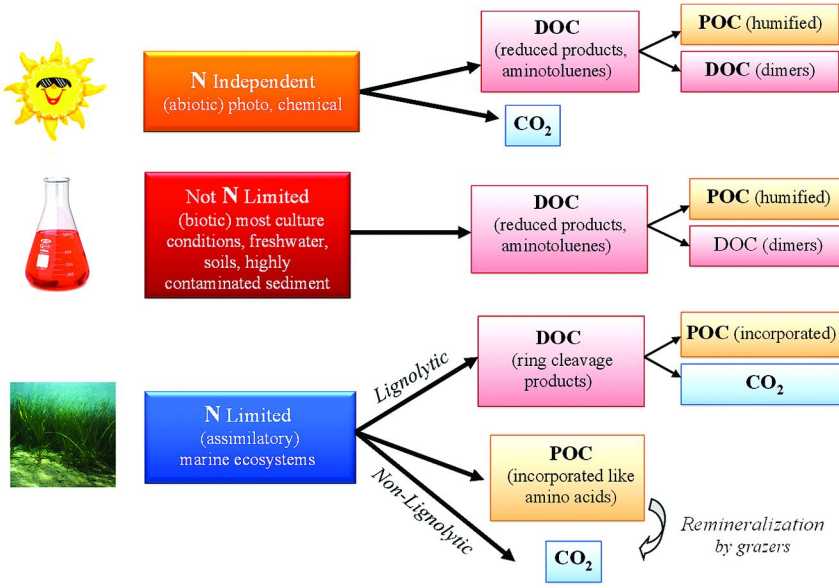

Figure 1. Production of dissolved organic carbon (DOC), particulate organic carbon (POC), or CO_2 can result from TNT transformation or metabolism depending on whether or not the process is abiotic or biotic and limited by nitrogen (N). TNT metabolism of ring C includes mineralization to CO_2 and incorporation into bacterial macromolecules (e.g. DNA, proteins). Relative size of the product boxes approximates the relative mass of each product. (see color insert)

Non Nitrogen-Limited (Biotic) Conditions

Non nitrogen-limited (biotic) conditions include most laboratory culture scenarios, freshwater and groundwater environments, soils and some highly contaminated sediment where nitrogen species would be subject to dissimilatory processes for microbial energy production (e.g. reduction of nitrate to ammonia). Reported products for systems that were not nitrogen limited but biotic were very similar to those for abiotic processes (e.g. aminotoluene; (*21*)). Amount of mineralization (usually reported as a percentage of starting material rather than rate) is usually low (< 2%; (*22*)) as denitration products (nitrate) are not subsequently incorporated into bacterial macromolecules (e.g proteins, DNA), but rather, used as electron acceptors.

Nitrogen-Limited (Biotic) Conditions

Nitrogen-limited (biotic) conditions include most marine and estuarine systems where organic nitrogen would be subject to assimilatory processes for new

biomass production (e.g. protein synthesis). Heterotrophic metabolism in nitrogen limited systems could result in substantially different proportions of CO_2 produced from available organic matter as organisms balance their need for energy and both carbon and nitrogen to build biomass. Due to nitrogen limitation, it is typical for organic nitrogen sources to be incorporated into microbial biomass with higher efficiency in marine systems (i.e. $(N_{incorporated}/(N_{incorporated}+N_{mineralized})*100\%$; TCA precipitation method, (*32*)). Incorporated efficiencies calculated from literature values for mixed microbial assemblages in differing environments range from 49-99.5% though most values are >90% (Table 2). Generally, in marine systems, organic nitrogen is incorporated into heterotrophic bacterial biomass with mineralization occurring only under unusual circumstances (carbon limitation). However, it would be expected that protozoan grazers would mineralize some proportion of bacterial macromolecules (remineralization of incorporated ^{14}C-TNT to $^{14}CO_2$). Under lignolytic conditions in marine environments, fungi and bacteria use extracellular lignases (and associated enzymes) to hydrolyze the ring carbon of many aromatic organic contaminants, such as TNT, and subsequently mineralize substantial amounts of TNT to CO_2 (e.g. 30%, see Table 1, and reviews by (*22*, *33*)). In addition to using TNT for energy (i.e., mineralizing TNT to CO_2), some of the ring carbon is incorporated into the carbon skeleton of fungal macromolecules (i.e. new biomass; (*34*, *35*)).

TNT Mineralization

There are scattered reports on microbial TNT metabolism by natural freshwater assemblages (*42–44*), and more recently by natural estuarine or marine assemblages (*45*). A common observation from studies on TNT metabolism by bacterial isolates is that relatively small amounts of the parent compound are mineralized to CO_2 (typically < 2 %). Among the numerous explanations is that bacterial enzymes are unable to attack the aromatic ring of TNT because of the presence of nitro groups (*22*, *46*). These nitro groups can often be reduced to form aminotoluenes, which are then purported to bind to humic matter present in the sample rather than become incorporated into bacterial biomass (*47*, *48*). In nature, however, degradation of recalcitrant carbon and nitrogen sources routinely occurs via complex interactions within microbial assemblages. Because natural degradation pathways are difficult to deconvolute with standard laboratory methods, microbial biogeochemists tend to focus on process rates in nature rather than identifying enzymatic pathways.

One important tool that biogeochemists use for following the flow of carbon and nitrogen though complex microbial assemblages involves isotopically labeled substrates. Gallagher et al. (*49*) used stable isotope probing methods (SIP; (*50*)) with ^{13}C-TNT (ring labeled) and ^{15}N-TNT to determine that estuarine bacterial assemblages can catabolize TNT ring carbon and incorporate it into bacterial biomass. This elegant technique not only establishes that TNT is not recalcitrant among natural estuarine assemblages but also identifies the involved bacterial genotypes as the ring carbon (and nitrogen) is incorporated into bacterial DNA that is then sequenced. The 'heavier' ^{13}C-DNA can be physically separated (via high-speed centrifugation) from that of strains that are not incorporating

the ^{13}C-TNT or ^{15}N-TNT. Although the rate of TNT metabolism is difficult to determine using this method, it does contradict the paradigm developed for freshwaters and derived from lab culture work that TNT is recalcitrant to enzymatic attack by bacterial enzymes.

We found measurable rates of TNT mineralization to CO_2 from natural microbial assemblages taken from several coastal ecosystems unlikely to have a history of exposure to energetics (*13*, *45*, *51*, *52*). During nine sampling events in coastal waterways from 2002 to 2010, we measured TNT mineralization rates in surface sediment and water samples that were often the same as, or within one order of magnitude of, the rate of total heterotrophic bacterial metabolism. These rates were often similar to those of other organic compounds that are transient in natural ecosystems due to their use in bacterial metabolism, such as petroleum hydrocarbons and amino acids (*53*). At first, these findings appear to conflict with those interpretations widely reported in the literature. However, our rates are very similar to many of those reports once those values are normalized to rate measurement units more typical of ecological studies of organic metabolism (μg C L^{-1} d^{-1} for aqueous samples (Table 1) or μg C kg^{-1} d^{-1} for sediment (Table 2)).

Table 1. TNT mineralization (as a rate, μg C L^{-1} d^{-1}; % of added) and incorporation efficiency (%) calculated from data provided in the literature for microbial assemblages in aqueous media. The associated rates of heterotrophic bacterial metabolism (μg C L^{-1} d^{-1}) are rarely reported.

Microbial Assemblage Type (Aqueous)	TNT Mineralization		Incorporation Efficiency (%)	Bacterial Metabolism (μg C L^{-1} d^{-1})	Reference
	Rate (μg C L^{-1} d^{-1})	% of added TNT			
wastewater	20 - 140	0.7	97	1.88 g L^{-1}	Kroger et al. 2004
Phanerochaete (fungi)	18	10	ND	ND	Spiker et al. 1992
Phanerochaete (fungi, lignolytic conditions)	27	30	ND	ND	Michels and Gottschalk 1994
Actinomyces (soil isolates)	33	2	96	ND	Pasti-Grigsby et al. 1996
Klebsiella (TNT enriched sludge)	41	6	99	500 (mg protein L^{-1})	Kim et al. 2002
Phanerochaete (fungi)	65	30	ND	ND	Fernando et al. 1990
Rhizobia (soil isolate)	89	< 2	ND	ND	Labidi et al. 2001
Irpex (fungi)	198	30	2	ND	Kim and Song 2003
Pseudomonas (TNT impacted soil)	< 1000	< 2	98	ND	Oh et al. 2003
Chesapeake Bay water	3	3	90	ND	THIS STUDY (2005)
Pearl Harbor water	5	3	97	1.7 – 3.4	THIS STUDY (2005)
Kahana Bay water	0.14 – 0.8	3	79 - 100	1.7 – 6.8	THIS STUDY (2006)
Kahana Bay water	0.35 - 3	3	93 - 100	24 – 71	THIS STUDY (2007)

Table 2. TNT mineralization (as a rate, µg C kg^{-1} d^{-1}; % of added; and % d^{-1}) and incorporation efficiency (%) calculated from data provided in the literature for soil and sediment slurries of mixed assemblages along with bacterial metabolism (µg C kg^{-1} d^{-1}).

Microbial Assemblage Type (Slurry)	TNT Mineralization		Incorporation Efficiency %	Bacterial Metabolism (µg C kg^{-1} d^{-1})	Reference
	Rate (µg kg^{-1} d^{-1})	% of added TNT			
soil	1	8	84-92	190 (nm CO_2 g^{-1} d^{-1})	Bradley et al. (1994)
freshwater sediment	3	0.5	99.5	10^5 (CFU d^{-1})	Wilstrom et al. (2000)
soil	20	0.5	ND	ND	Funk et al. (1993)
soil	30	8	92	ND	Gunnison et al. (1999)
soil	330	0.3	95	ND	Shen et al. (1998)
TNT impacted soil	400	30	66	5×10^6 (CFU d^{-1})	Robertson et al. (2005)
TNT impacted soil	12500	23.5	49	1×10^6 (CFU d^{-1})	Clark and Boopathy (2009)
Chesapeake Bay sediment	13 - 114	3	ND	1 - 29	THIS STUDY (2002)
Pearl Harbor sediment	2 - 47	3	ND	1 - 18	THIS STUDY (2002)
San Francisco Bay sediment	0.05 - 1	3	ND	3 - 62	THIS STUDY (2003)
Chesapeake Bay sediment	4 - 146	3	ND	13 - 327	THIS STUDY (2004)
Chesapeake Bay sediment	0.3 - 69	3	ND	4 - 62	THIS STUDY (2005)
Kahana Bay sediment	9 - 50	3	ND	42 - 122	THIS STUDY (2007)

TNT Incorporation

Due to metabolic costs in synthesizing organic molecules, organic nitrogen sources are typically incorporated into marine bacterial macromolecules (e.g. proteins, DNA) in preference to inorganic nitrogen species ((*54*), and references herein). Though organic nitrogen sources would likely be incorporated into bacterial biomass, incorporation rates for TNT are rarely reported in the literature. Some of this under reporting may have to do with the lack of recognition in the bioremediation community that bacterial metabolism of organic contaminants should include incorporation into bacterial biomass. This may be because their focus is on the complete detoxification of the organic contaminant to 'harmless' CO_2 rather than the metabolic fate of the contaminant carbon. Instead of being recognized as incorporated, this fraction is often reported as being associated with humic material, because ^{14}C-labelled organic compounds that are incorporated into bacterial macromolecules would typically co-precipitate in this analytical fraction (cf. (*55*, *56*)).

^{14}C-TNT incorporation rate into microbial biomass was measured in coastal water samples using the TCA precipitation method (*32*) and found to be one to two orders of magnitude more rapid than the TNT mineralization rate (*13*). More specifically, 80-99% of ^{14}C-TNT that is fully metabolized by the microbial assemblage is incorporated into biomass rather than being respired for energy (Table 1; (*13*)). Incorporation rates and efficiencies were often highest at low salinity and decreased towards the marine stations (higher salinity) though occasionally the highest were at mid salinity (i.e. 10 PSU at a frontal boundary; (*13*)).

In freshwater systems, lignolytic fungi dominate nitroaromatic degradation. Therefore, the elevated mineralization and incorporation rates for TNT measured by Montgomery et al. (*13*) may be attributable to lignolytic marine fungi, rather than bacteria. However, there is little precedence for fungi outcompeting bacteria for organic matter in marine environments. Lignolytic bacteria comprise a large component of the marine assemblage (*57–60*), and outcompete fungi as the predominant degraders of lignocellulosic detritus in marine ecosystems (*61*, *62*). Thus, TNT metabolism and mineralization in coastal waters is more likely due to the natural bacterial assemblage rather than fungal assemblage, as observed for freshwaters. Incorporation of TNT ring carbon and nitrogen into bacterial nucleic acids is further evidence that TNT is metabolized by components of natural bacterial assemblages in coastal ecosystems (*49*). It follows that in areas of the ecosystem where lignin is rapidly metabolized by the microbial assemblage, TNT may also be rapidly metabolized.

There is some evidence of this relationship between TNT and lignin degradation from our work examining sediment from the Chesapeake Bay system. The Patuxent River mouth appears to be a catchment that receives large amounts of agricultural runoff containing lignocellulose and nitrogenous pesticides, including simazine ((*63*, *64*) and references therein). Labile organic components of agricultural waste should be microbially metabolized upstream as lignocellulosic material migrates downstream to intermediate salinity prior to degradation (*65*). In addition, McConnell and coworkers (*64*) found rapid pesticide (also a nitrogenous aromatic organic) degradation rates at a site in the Patuxent River. As part of our Chesapeake Bay system surveys in 2004 and 2005, we found sediment at this Patuxent River location (salinity = 12) to have the highest rates of TNT mineralization relative to total bacterial heterotrophic production (one to two orders of magnitude higher than all but one other river mouth station (Rappahannock; (*13*)). Confluences between fresh and saline water masses may trap otherwise recalcitrant aromatic organics and provide an environment of positive selection for bacterial assemblages that metabolize these compounds (e.g. lignin, TNT, PAHs, pesticides).

Transition Zones

Transition zones between fresh and saline water masses in coastal environments often provide conditions of enhanced organic metabolism by providing steady supply of nutrients and rapidly removing built up waste products. One side of the front can provide organic matter, nutrients (e.g. nitrogen, iron) or conditions (e.g. light, temperature) that are limiting to microbial growth on the other side (*66*). They can also inhibit lateral transport of organic particles and sediment which traps these materials and deposits them to the underlying sediment ((*67*) and references therein). These transition or mixing zones enhance bacterial production (*68*), remineralization of nutrients by zooplankton (*66*), nitrogen cycling (*69*), and phytoplankton growth (*70*). Not only are these fronts important regulators of organic matter processing in the water column, but tidal fronts moving back and forth in the water column can strongly influence and enhance organic matter processing in the sediment underlying the region of the

passing front (*71*). By these mechanisms, we hypothesize that transition zones create the biogeochemical conditions that enhance overall heterotrophic bacterial metabolism of recalcitrant aromatic organic matter and, by extension, may create the conditions of enhanced TNT metabolism.

On the macro scale, these transition zones typically occur between water masses stratified by density differences due to salinity and/or temperature and include tidal fronts (vertically stratified; e.g. salt wedges) and zones of convergence (horizontally stratified; e.g. Gulf Stream rings) between rivers and higher salinity estuarine water. On the micro scale, which may be equally as relevant to biogeochemical functioning of the natural microbial assemblage, these transition zones may occur wherever there is input of freshwater or rain runoff into estuarine or marine coastal ecosystems.

Conclusions

We found that rates of TNT incorporation into microbial biomass and mineralization to CO_2 might be rapid enough to account for loss of range source material across the salinity gradient in estuarine systems (these rates were also used in an estuarine model; (*72*)). There may be some relationship between microbial TNT metabolism and salinity but the trend is not universal amongst the ecosystems studied for all times of the year. This may be because aromatic organic matter, like TNT, may be most rapidly metabolized at frontal boundaries that occur between water masses along the estuarine gradient (e.g. tidal fronts, salt wedges, and zones of confluence) and not a simple function of salinity. These frontal boundaries can be relatively narrow areas and may only randomly fall into the typical survey of estuarine salinity gradient (or avoided entirely as being atypical of the surrounding water).

Application to Sites

In many cases, remedial program managers (RPMs) know that UXO are present is a coastal estuarine environment but are reluctant to sample the sediment for energetics for a variety of reasons including discovery, danger to divers (ecorisk verses human health risk), and financial expense. The finding that natural microbial assemblages mineralize and incorporate TNT at rates similar to other common organic matter provides the RPM with a scientific basis for a site conceptual model involving rapid attenuation of energetics as they migrate through a coastal ecosystem. It may also explain the paucity of detectable measurements of energetics across near shore sediment (e.g. active ranges, historic dumpsites).

By coupling energetic metabolism rate range (mineralization and incorporation) with models of contaminant migration, RPMs and regulators may be able to determine whether an energetic would likely accumulate in sediment adjacent to an active shore side range and then expose benthic organisms to ecological risk at UXO dumpsites. Empirical measurements of energetic degradation rates using site water and sediment (as part of a seasonal sampling

regime) would make the model estimates more robust and reduce the likelihood of excavating a submerged area (with concomitant destruction of habitat) that posed little to no ecorisk. Conversely, a more robust model would lessen the chance of leaving in place sediment that was contaminated and harbored substantial risk to the environment.

Coastal ecosystems that feature estuarine transition zones may be more likely to attenuate energetics migrating from terrestrial environments or into surface waters from underlying sediment. This may be due, in part, to natural aromatic OM delivered to coastal water via runoff and sustaining microbial populations capable of metabolizing aromatic energetics. Co-variability of the fluxes of energetics with fluxes of natural OM (e.g., humics, lignin) should be investigated, as the latter affords a means of tracking and prediction, through scalable detection technologies (e.g., OM fluorescence). At some scale, these transitions zones will be characteristic of any DoD range or UXO impacted area adjacent to an estuarine or marine ecosystem. Specific examples of where these processes may be applied to UXO-impacted sites where freshwater creeks and rainfall runoff (0 PSU salinity) input to adjacent estuarine or marine systems include Jackson Park to Ostrich Bay, WA (14-31 PSU; (*73*)), Moffett Field marsh to lower San Francisco Bay, CA (14-33 PSU; (*74*)), Concord Naval Weapons Station to Suisun Bay, CA (mixing area between freshwater and seawater; (*75*)), and Live Impact Area of VNTR to BahAa Salina del Sur, Vieques, Puerto Rico (33 PSU; (*11*)).

As with all organic contaminants, TNT metabolism at a specific site over a specific time frame is more likely to be regulated by general biogeochemical constraints that regulate overall heterotrophic organic carbon and nitrogen processing rather than regulated by something specific to TNT itself (e.g. rules derived from chemical structure and lab based flask studies). For instance, large boluses of organic carbon (regardless of its relative lability; e.g. sugar, oil, TNT, plant agricultural waste) into a relatively unmixed, unaerated, static ecosystem (holding pond, subsurface groundwater reservoir) are going to have a long residence times. Whereas that same organic carbon or nitrogen substrate added to a well mixed ecosystem (e.g. wastewater treatment trickling filter, intertidal wave zone, bioturbated sediment, frontal mixing zone) will have relatively short residence times (high turnover rate). Thus, understanding seasonal and other climate related influences on these constraining biogeochemical parameters may be very important in modeling the fate of energetics in coastal ecosystems.

Acknowledgments

Financial support for this research was provided by the Strategic Environmental Research and Development Program (SERDP ER-2124, ER-1431 and CU-1209; Andrea Leeson, Program Manager), Office of Naval Research (POC: Linda Chrisey), and the Naval Facilities Engineering Command N45 (POC: Andy Del Collo).

References

1. Brar, S. K.; Verma, M.; Surampalli, R. Y.; Misra, K.; Tyagi, R. D.; Meunier, N.; Blais, J. F. *Pract. Periodical Hazard, Toxic, Radioactive Waste Manage.* **2006**, *10* (2), 59–72.
2. Stenuit, B. A.; Agathos, S. N. *Appl. Microbiol. Biotechnol.* 2010, *88,* 1043–1064; DOI 10.1007/s00253-010-2830-x.
3. Spain, J. C., Hughes J. B., Knackmuss, H. J., Eds.; *Biodegradation of Nitroaromatic Compounds and Explosives*; Lewis Publishers: New York, 2000; p 434.
4. Rappé, M. S.; Giovannoni, S. J. *Annu. Rev. Microbiol.* **2003**, *57*, 369–394.
5. Kilian, P. H.; Skrzypek, S.; Becker, N.; Havemann, K. *Leuk. Res.* **2001**, *25* (10), 839–845.
6. Lewis, T. A.; Newcombe, D. A.; Crawford, R. L. J. *Environ. Manage.* **2004**, *70*, 291–307.
7. Belden, J. B.; Ownby, D. R.; Lotufo, G. R.; Lydy, M. J. *Chemosphere* **2005**, *58* (9), 1161–1168.
8. Conder, J. *Disappearing Doses: Fate and toxicity of TNT in sediment toxicity tests over time*. Presentation at the 23rd Annual Meeting of the Society of Environmental Toxicology and Chemistry, Salt Lake City, UT, 2002, November 16−20.
9. Blumer, J. L.; Friedman, A.; Meyer, L. W.; Fairchild, E.; Webster, L. T.; Speck, W. T. *Cancer Res.* **1980**, *40*, 4599–4605.
10. Ampleman, G.; Marois, A.; Thiboutot, S.; Hawari, J.; Greer, C. W.; Godbout, J.; Sunahara, G. I.; Shen, C. F.; Guiot, S. R. *Canadien Defense Research Establishment publication (UNCLASSIFIED)*; DREV-TR-1999-199, 2000. http://www.dtic.mil/cgi-bin/GetTRDoc?AD=ADA373448&Location=U2&doc =GetTRDoc.pdf.
11. CH2M HILL. Response to comments on Time Critical Removal Action (TCRA) of unexploded munitions in the former Vieques Naval Training Range (VNTR). Memorandum, 28 March, 2006. http://public.lantops-ir.org/sites/public/vieques/Site_Files_/Public%20Review/MR%20Contract%20Reference%20Documents/Final_TCRA_WP_amend.pdf (verified 16 September 2010).
12. Simmons, C. C.; Carvalho-Knighton, K. M.; Pyrtle, A. J. *Small scale characterization of the presence of the explosive octahydro-1,3,5,7-tetranitro-1,3,5,7 tetrazocine (HMX) near former naval sites on Vieques Island, Puerto Rico*; American Geophysical Union, Fall Meeting, abstract #OS31B-0409, 2007. http://adsabs.harvard.edu/abs/2007AGUFMOS31B0409S (verified 16 September 2010).
13. Montgomery, M. T.; Walker, S. W.; Osburn, C. L.; Hamdan, L. J.; Boyd, T. J.; Furukawa, Y.; Hawari, J.; Monteil-Rivera, F.; O'Sullivan, D. W.; Luning-Prak, D.; Paerl, H. W.; Li, Q. X. *Biotic and abiotic attenuation of nitrogenous energetic compounds (NEC) in coastal waters and sediments: final report (ER-1431)*; Strategic Environmental Research and Development Program, 2008. http://www.serdp.org/content/download/6351/84945/file/ER-1431-FR.pdf (verified 16 September 2010).

14. Rylott, E. L.; Bruce, N. C. *Trends Biotechnol.* **2009**, *27* (2), 73–81.
15. Pomeroy, L. R. *Annu. Rev. Ecol. Syst.* **1970**, *1*, 171–190.
16. Larson, S. L.; Martin, W. A.; Escalon, B. L.; Thompson, M. *Environ. Sci. Technol.* **2008**, *42*, 786–792.
17. Yardin, G.; Chiron, S. *Chemosphere* **2006**, *62*, 1395–1402.
18. Felt, D. R.; Nestler, C. C.; Davis, J. L.; Larson, S. L. *Potential for Biodegradation of the Alkaline Hydrolysis End Products of TNT and RDX*; Engineer Research and Development Center, Vicksburg, MS, 2007, Final Report. http://handle.dtic.mil/100.2/ADA469989.
19. Lee, B.; Jeong, S.-W. *J. Hazard. Mater.* **2009**, *165*, 435–440.
20. Ayoub, K.; van Hullebusch, E. D.; Cassir, M.; Bermon, A. *J. Hazard. Mater.* **2010**, *178* (1−3), 10−20; DOI:10.1016/j.jhazmat.2010.02.042.
21. Roldan, M. D.; Perez-Reinado, E.; Castillo, F.; Moreno-Vivian, C. *FEMS Microbiol. Rev.* **2008**, *32*, 474–500.
22. Hawari, J.; Beaudet, S.; Halasz, A.; Thiboutot, S.; Ampleman, G. *Appl. Microbiol. Biotechnol.* **2000**, *54*, 605–618.
23. Kroger, M.; Schumacher, M. E.; Risse, H.; Fels, G. *Biodegradation* **2004**, *15*, 241–248.
24. Spiker, J. K.; Crawford, D. L.; Crawford, R. L. *Appl. Environ. Microbiol.* **1992**, *58* (9), 3199–3202.
25. Michels, J.; Gottschalk, G. *Appl. Environ. Microbiol.* **1994**, *60*, 187–194.
26. Pasti-Grigsby, M. B.; Lewis, T. A.; Crawford, D. L.; Crawford, R. L. *Appl. Environ. Microbiol.* **1996**, *62* (3), 1120–1123.
27. Kim, H. Y.; Bennett, G. N.; Song, H. G. *Biotechnol. Lett.* **2002**, *24*, 2023–2028.
28. Fernando, T.; Bumpus, J. A.; Aust, S. D. *Appl. Environ. Microbiol.* **1990**, *56* (6), 1666–1671.
29. Labidi, M.; Ahmad, D.; Halasz, A.; Hawari, J. *Can. J. Microbiol.* **2001**, *47* (6), 559–566.
30. Kim, H. Y.; Song, H. G. *Appl. Microbiol. Biotechnol.* **2003**, *61*, 150–156.
31. Oh, S. Y.; Cha, D. K.; Chiu, P. C.; Kim, B. *J. Water Sci. Technol.* **2003**, *47*, 93–99.
32. Kirchman, D. L.; K'nees, E.; Hodson, R. *Appl. Env. Microbiol.* **1985**, *49*, 599–607.
33. Boopathy, R. In *Soil biology: advances in applied bioremediation*; Singh, A., Kuhad, R. C., Ward, O. P., Eds.; Springer-Verlad: Berlin, 2009; pp 151−172.
34. Van Aken, B.; Hofrichter, M.; Scheibner, K.; Hatakka, A. I.; Naveau, H.; Agathos, S. N. *Biodegradation* **1999**, *10*, 83–91.
35. Van Aken, B.; Godefroid, L. M.; Peres, C. M.; Naveau, H.; Agathos, S. N. *J. Biotechnol.* **1999**, *68*, 159–169.
36. Bradley, P. M.; Chapelle, F. H.; Landmeyer, J. E.; Schumacher, J. G. *Appl. Environ. Microbiol.* **1994**, *60* (6), 2170–2175.
37. Wikstrom, P.; Andersson, A. -C.; Nygren, Y.; Sjostrom, J. M. *J. Appl. Microbiol.* **2000**, *89*, 302–308.
38. Funk, S. B.; Roberts, D. J.; Crawford, D. L.; Crawford, R. L. *Appl. Environ. Microbiol.* **1993**, *59* (7), 2171–2177.

39. Gunnison, D.; Fredrickson, H.; Ringelberg, D.; Felt, D. R.; Hayes, C. H.; Richmond, M.; O'Neal, B.; Porter, B. E. In *Explosives Conjugation Products in Remediation Matrices: Interim Report 2*; Technical Report SERDP-98-12; Pennington, J. C., Thorn, K. A., Gunnison, D., McFarland, V. A., Thorne, P. G., Inouye, L. S., Fredrickson, H., Leggett, D. C., Ringelberg, D., Jarvis, A. S., Felt, D. R., Lutz, C. H., Hayes, C. H., Clarke, J. U., Richmond, M., O'Neal, B., Porter, B. E., Eds.; U.S. Army Corps of Engineers Waterways Experiment Station: Vicksburg, MS, pp 53−72.
40. Shen, C. F.; Guiot, S. R.; Thiboutot, S.; Ampleman, G.; Hawari, J. *Biodegradation* **1998**, *8*, 339–347.
41. Robertson, B. K.; Jjemba, P. K. *Chemosphere* **2005**, *58*, 263–270.
42. Clark, B.; Boopathy, R. *J. Hazard. Mater.* **2007**, *143*, 643–648.
43. Travis, E. R.; Bruce, N. C.; Rosser, S. J. *Environ. Pollut.* **2008**, *153*, 119–126.
44. Zheng, W.; Lichwa, J.; D'Alessio, M.; Ray, C. *Chemosphere* **2009**, *76*, 1167–1177.
45. Montgomery, M. T.; Coffin, R. B.; Boyd, T. J.; Hamdan, L. J.; Smith, J. P.; Plummer, R. B.; Walker, S. E.; Dittel, A.; Masutani, S.; Li, Q. X.; Osburn, C. L. *Bacterial production and contaminant mineralization in sediments of the Ala Wai Canal, Oahu, Hawai'i*; US Naval Research Laboratory Technical Memorandum, NRL/MR/6110-09-9212, 2009.
46. Qasim, M.; Gorb, L.; Magers, D.; Honead, P.; Leszczynskia, J.; Moore, B.; Taylor, L.; Middleton, M. *J. Hazard. Mater.* **2009**, *167* (1−3), 154–163.
47. Myers, T. E.; Brannon, J. M.; Pennington, J. C.; Davis, W. M.; Myers, K. F.; Townsend, D. M.; Ochman, M. K.; Hayes, C. A. *Laboratory studies of soil sorption/transformation of TNT, RDX, and HMX*; Technical Report IRRP-98-8; U.S. Army Engineer Waterways Experiment Station: Vicksburg, MS, 1998. http://libweb.wes.army.mil/uhtbin/hyperion/TR-IRRP-98-8.pdf (verified 16 September 2010).
48. Thorn, K. A.; Kennedy, K. R. *Environ. Sci. Technol.* **2002**, *36* (17), 3787–3796.
49. Gallagher, E. M.; Young, L. Y.; McGuinness, L. M.; Kerkhof, L. *J. Appl. Environ. Microbiol.* **2010**, *76* (5), 1695−1698; DOI:10.1128/AEM.02274-09.
50. Radajewski, S.; Philip-Ineson, P.; Parekh, N. R.; Murrell, J. C. *Nature* **2000**, *403*, 646–649.
51. Montgomery, M. T.; Boyd, T. J.; Osburn, C. L.; Smith, D. C. *Biodegradation* **2010**, *21* (2), 257−266; DOI:10.1007/s10532-009-9298-3.
52. Montgomery, M. T.; Coffin, R. B.; Boyd, T. J.; Smith, J. P.; Plummer, R. E.; Walker, S. E.; Osburn, C. L. *Environ. Pollut.* **2011**, accepted 20 January 2011.
53. Boyd, T. J.; Smith, D. C.; Apple, J. K.; Hamdan, L. J.; Osburn, C. L.; Montgomery, M. T. In *Microbial ecology research trends*; Van Dijk, T., Ed.; NOVA Science Publishers, Inc.: Hauppauge, NY, 2008; pp 1−41.
54. Kirchman, D. L. *Microb. Ecol.* **1994**, *28* (2), 255–271.
55. Nam, K.; Chung, N.; Alexander, M. *Environ. Sci. Technol.* **1998**, *32* (23), 3785–3788.

56. Singh, N.; Hennecke, D.; Hoerner, J.; Koerdel, W.; Schaeffer, A. *J. Environ. Sci. Health, Part A: Toxic/Hazard. Subst. Environ. Eng.* **2008**, *43* (4), 348–356.
57. González, J.; Moran, M. *Appl. Environ. Microbiol.* **1997**, *63*, 4237–4242.
58. Buchan, A.; Collier, L. S.; Neidle, E. L.; Moran, M. A. *Appl. Environ. Microbiol.* **2000**, *66*, 4662–4672.
59. Buchan, A.; González, J. M.; Moran, M. A. *Appl. Environ. Microbiol.* **2005**, *71* (10), 5665–5677; DOI:10.1128/AEM.71.10.5665-5677.2005.PMCID: PMC1265941.
60. Buchan, A.; Neidle, E. L.; Moran, M. A. *Appl. Environ. Microbiol.* **2001**, *67*, 5801–5809.
61. Benner, R.; Moran, M. A.; Hodson, R. E. *Limnol. Oceanogr.* **1986**, *31* (1), 89–100.
62. Benner, R.; Newell, S. Y.; Maccubbin, A. E.; Hodson, R. E. *Appl. Environ. Microbiol.* **1984**, *48* (1), 36–40.
63. Harman-Fetcho, J. A.; McConnell, L. L.; Baker, J. E. *J. Environ. Qual.* **1999**, *28*, 928–938.
64. McConnell, L. L.; Harman-Fetcho, J. A.; Hagy, J. D. *J. Environ. Qual.* **2004**, *33*, 594–604.
65. Louchouarn, P.; Lucotte, M.; Canuel, R.; Gagne, J.-P.; Richard, L.-F. *Mar. Chem.* **1997**, *58* (1-2), 3–26.
66. Floodgate, G. D.; Fogg, G. E.; Jones, D. A.; Lochte, K.; Turley, C. M. *Nature* **1981**, *290*, 133–136.
67. Neill, S. P. *Estuarine, Coastal Shelf Sci.* **2009**, *81*, 345–352.
68. Borsheim, K. Y. *Deep-Sea Res.* **1990**, *37* (8), 1297–1309.
69. Fogg, G. E.; Egan, B.; Floodgate, G. D.; Jones, D. A.; Kassab, J. Y.; Lochte, K.; Rees, E. I. S.; Scrope-Howe, S.; Turley, C. M. *Philos. Trans. R. Soc. London, Ser. B* **1985**, *310* (1146), 555–571.
70. Hyun, J.-H.; Kim, K.-H. *Mar. Ecol.: Prog. Ser.* **2003**, *252*, 77–88.
71. Josefson, A. B.; Conley, D. J. *Mar. Ecol.: Prog. Ser.* **1997**, *147*, 49–62.
72. Wang P. -F.; Liao, Q.; George, R.; Wild, W. *(ER-1453) Defining munition constituent (MC) source terms in aquatic environments on DoD ranges*; (Phase II) Draft Technical Report provided for Strategic Environmental Research and Development Program, 2009.
73. Carr, R. S.; Nipper, M.; Biedenbach, J. M.; Hooten, R. L.; Miller, K.; Saepoff, S. *Arch. Environ. Contam. Toxicol.* **2001**, *41*, 298–307.
74. U.S.G.S., 2007. http://sfbay.wr.usgs.gov/hydroclimate/sal_variations/index.html.
75. Gross, E. S.; Koseff, J. R.; Monismith, S. G. *J. Hydraul. Eng.* **1999**, *125* (11), 1199–1209.

Chapter 10

TNT, RDX, and HMX Association with Organic Fractions of Marine Sediments and Bioavailability Implications

Judith C. Pennington,[1] Guilherme Lotufo,[1] Charolett A. Hayes,[2] Beth Porter,[2] and Robert D. George[3,*]

[1]U.S. Army Engineer Research and Development Center, 3909 Halls Ferry Road, Vicksburg, MS 39180 US
[2]SpecPro, 4815 Bradford Dr., Suite 201, Huntsville, AL 35805
[3]Space and Naval Warfare Systems Center Pacific, Environmental Sciences - Code 71750, San Diego, CA 92152
[*]robert.george@navy.mil

Explosives may enter marine environments from unexploded ordnance, thus the potential for marine sediments to act as a sink for released explosives was evaluated. Relative distributions of TNT, RDX, and HMX in volatile, overlying water, pore water and sediment compartments were quantified, and their respective partitioning behaviors into various components of organic matter in marine sediments were determined. Marine sediments were incubated with radiolabeled explosives, held at 15°C for periods varying from 1 to 90 days and fractionated to the solvent extractable, cellulose, fulvic acid (FA), humic acid (HA), and humin organic carbon sediment pools. Studies of incubated sediment systems designed to trap CO_2 and volatile organic compounds were also performed. For TNT and RDX, sediment is the principal sink, whereas for HMX, mineralization to CO_2 is important. Mineralization is negligible for TNT, but significant for RDX. Contact time with sediment had a decreasing effect on the bioavailability of TNT, RDX, and HMX.

Introduction

Release of explosives such as 2,4,6-trinitrotoluene (TNT), hexahydro-1,3,5-trinitro-1,3,5-triazine (RDX), and octahydro-1,3,5,7-tetranitro-1,3,5,7-tetrazocine (HMX) into marine environments is a concern where live ordnance has been used in training and where ocean dumping of discarded ordnance has occurred. The fate of these compounds in marine sediments is of particular interest because the sediment may serve as a sink, reducing bioavailability and exposure potential by removing freely dissolved compounds from the aqueous media. TNT in its reduced form has been demonstrated to react by covalent bonding to functional groups on organic matter (*1–3*). In the latter study (*3*), it was shown that different types of mechanisms are responsible for the binding of TNT and its degradation products to soil organic matter. Both physical partitioning and chemical/electrostatic interactions between contaminant and organic matter results in contaminant sorption. The hydrophobic partitioning reaction occurs mainly between non-polar organic contaminants and non-polar moieties of soil organic matter and gives linear adsorption isotherms. Electrostatic interactions/covalent bond formation reactions occur between functional groups in the organic contaminant and soil organic matter. These reactions are very specific, unlike hydrophobic partitioning, which is non-specific in nature. Adsorption isotherms obtained due to specific interaction leads to non-linear isotherms. Soil organic matter has very complex structure with both a hydrophobic backbone and numerous different types of reactive functional groups. Thus, both specific and non-specific adsorption mechanism are possible in TNT/metabolite and soil organic matter. Achtnich, et al (*4*), Bruns-Nagel, et al (*5*), and Thorn, et al (*2*), each studied binding of TNT in soil organic matter using ^{15}N-labeled TNT with nuclear magnetic resonance spectroscopy. The results indicated that reduced degradation products of TNT (diaminonitrotoluene and triaminotoluenes) undergo 1,2-nucleophilic addition reactions with carbonyl groups or quinones, resulting in a covalent bonding to soil organic matter such as that observed by Thorn and Kennedy (*1*).

Specific molecular interactions between explosives compounds and marine sediments have not been defined, whereas for soils, numerous studies have characterized the interactions of soils with TNT and related degradation products (*1–5*). Most notably, degradation products related to or comprised of aromatic amines have been the subject of an investigation, in which Thorn et al (*6*) evaluated the environmental fate of nitrogen containing aromatic chemical species using aniline as a model compound suitable for mechanistic studies using ^{15}N NMR. Results for aniline were consistent with, and contributed to, interpretations of ^{15}N NMR data from later studies concerned with covalent bond formation between TNT degradation products and soil organic matter, as described above (*1*). In all of these types of investigations, where a variety of soil types were evaluated, one of the important underlying requirements is to evaluate and understand the relative partitioning processes occurring in the various soil organic matter components. This can typically be performed as an initial study, prior to initiating targeted investigations focused on interactions of contaminants with soil fraction chemistries. Similarly, the objective of this study was to

determine the relative partitioning capabilities of TNT, RDX, and HMX into the various organic components of marine sediments, prior to initiating focused follow-on studies related to chemical interactions with sediment components, bioavailability, toxicity, and bioconcentration. Marine sediments that had been spiked with TNT, RDX, and HMX were incubated, sampled at increasing time intervals, and fractionated to define associations between the explosives and various components of the organic carbon pool of the sediments, i.e., solvent extractable, cellulose, fulvic acid, humic acid, and humin fractions. In addition to fractionation, bioavailability was asssed by measuring bioaccumulation in a benthic invertebrate exposed to the sediment (*7*). This paper presents results of the fractionations of a marine sediment incubated with TNT, RDX, or HMX. While this was the main objective of the study reported here, a second objective was to determine mass balance of the explosives in volatile, overlying water, pore water and sediment compartments. In these experiments radiolabeled compounds were incubated with sediment systems designed to trap CO_2 and VOCs. Subsequently, the sediment, overlying and pore water compartments were assayed for radioactivity.

Materials and Methods

An uncontaminated marine sediment from Sequim Bay, WA, (total organic carbon, 3.6 mg kg^{-1}; cation exchange capacity, 49 meq $100g^{-1}$; and pH, 7.6) was spiked with radiolabeled and unlabelled TNT, RDX and HMX. TNT treatments received 50 mg kg^{-1} TNT (71,511 dpm [^{14}C]TNT per g dry sediment, specific activity 35.0 mCi $mmol^{-1}$, Sigma-Aldrich Radiochemicals, St. Louis, MO). RDX treatments received 50 mg kg^{-1} RDX (19,900 [^{14}C]RDX per g dry sediment, specific activity 20 mCi $mmol^{-1}$, Perkin Elmer Life Science, Boston, MA). HMX treatments received 0.0815 mg kg^{-1} HMX (117,564 dpm [^{14}C]HMX per g dry sediment, specific activity 8.2 mCi $mmol^{-1}$, Sigma-Aldrich Radiochemicals). The general experimental approach in these studies is shown in Figure 1. Methanol solutions of the explosives were sprayed on to dry quartz sand and allowed to dry. The amended sand was added to the sediment and mixed vigorously with an impeller mixer at 1000 rpm for two hours. Sediment concentration was checked by complete combustion of sediment subsamples in a sample oxidizer (Packard Sample Oxidizer, Model 307, Packard Instruments, Meridan, CT). Oxidized carbon was trapped as CO_2 and counted by liquid scintillation (Packard Liquid Scintillation Counter, Model 2500 TR, Packard Instruments).

For each explosive compound the amended sediment was split into five portions, one for each sampling time, 0, 1, 7, 28, and 90 days. All samples were placed into beakers in a water bath at 15^{o}C in the dark until sampled. HMX-spiked sediment was incubated at 23^{o}C to accommodate unrelated experiments. For each explosive, one beaker was removed from incubation for immediate use in fractionation procedures and for bioavailability assessment.

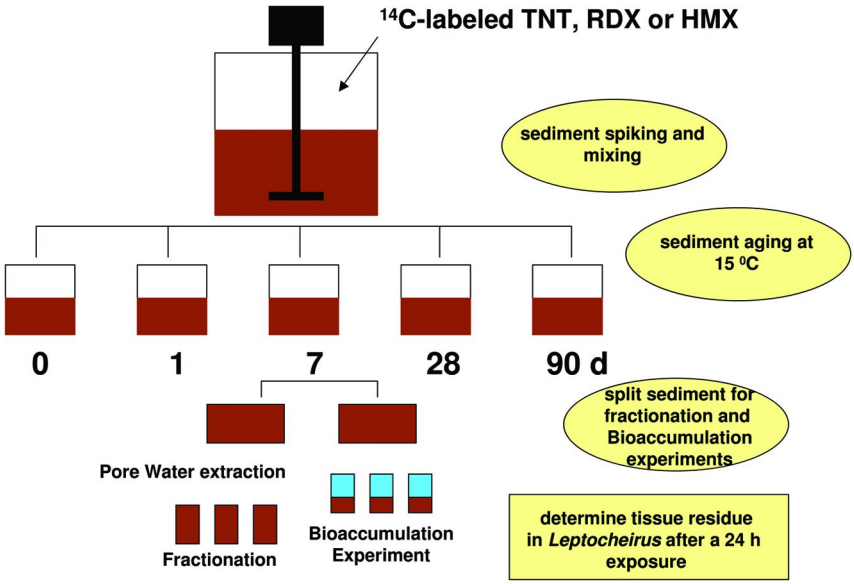

Figure 1. Experimental approach for evaluating fractionation of radiolabelled explosives in marine sediment.

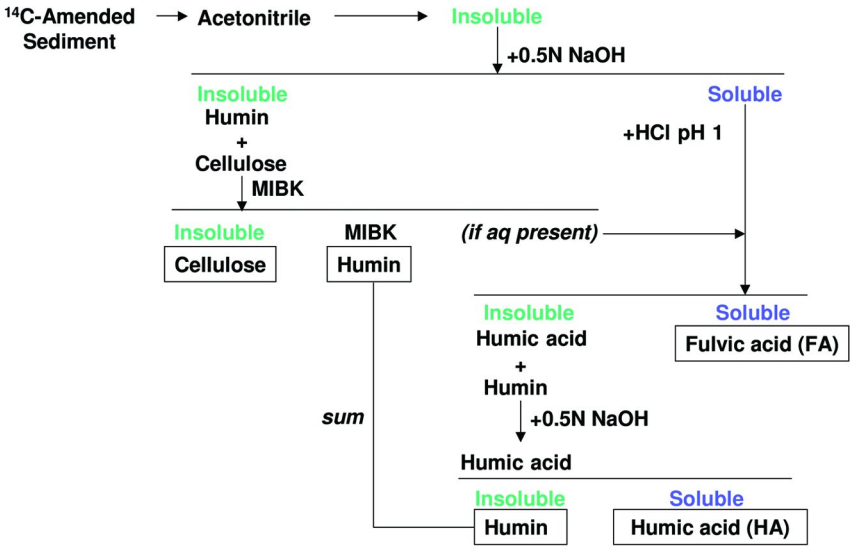

Figure 2. Fractionation procedure for radiolabelled explosives in marine sediment, following Stevenson (8) as modified by Pennington et al. (9).

Three replicates of 30-g subsamples of each sediment treatment were centrifuged for 30 min at 2,000 RCF to remove excess water. Sediments were fractionated according to procedures of Stevenson (*8*) as modified by Pennington et al. (*9*) (Figure 2). The solvent-extractable fraction was generated by extracting the sediment twice with 50 ml of acetonitrile for 18 h on a reciprocating shaker. The two supernatants, recovered by centrifugation for 30 min at 2,000 RCF, were combined and three 1-ml portions were counted to obtain the solvent-extractable fraction.

The remaining insoluble material was air dried and extracted twice with 50 mL of 0.5 N NaOH by shaking for 24 hours for the first extraction, and for 4 hours for the second extraction. The NaOH supernatants from the first and second extractions, which contained fulvic and humic acid and humin, were combined and retained. The insoluble material was washed with 50 mL of distilled deionized water by shaking 1 h. The sides of the bottle were rinsed with 10 more mls of water before centrifuging at 2,000 RCF. The supernatants from the water rinses were added to the NaOH supernatants.

The insoluble fraction containing humin and cellulose was air dried and extracted with 40 mL methyl isobutyl ketone (MBIK) for 24 h. Following phase separation by centrifugation, the supernatant containing humin, was removed and three 1-ml portions were counted. The remaining insoluble cellulose fraction was burned in the sample oxidizer and counted.

The NaOH supernatants retained earlier were acidified with 50-percent HCl to pH 1. Samples were allowed to settle overnight, and then centrifuged to separate phases. The supernatant containing soluble fulvic acid was removed. The insoluble material was re-dissolved in 15 mL 0.5 N NaOH and place on a shaker for 4 hours, after which it was re-acidified with HCl. After settling overnight, samples were centrifuged and the supernatants were combined and counted for the fulvic acid fraction.

The remaining insoluble humin/humic acid material was re-dissolved with 15 ml 0.5 N NaOH, placed on a shaker for 24 hours then centrifuged for 30 minutes. The supernatant containing the humic acid was removed and the procedure was repeated with 10 ml NaOH. Supernatants were combined and counted for the humic acid fraction. The remaining insoluble material, humin, was burned on the oxidizer and counted. These counts were added to those from the MIBK extraction.

Occasionally, during this procedure an aqueous phase separates from the MIBK extract. Although this did not occur in this set of fractionations, such a phase can be combined with the NAOH soluble fraction and continued through the process (Figure 2).

Mass balance was conducted on separate tests of the Day 0 amended sediments. Three 100-g replicates were placed into flasks to which 100 ml of 20 ppt (2.0 % by mass) seawater was overlaid. The flasks, which were equipped with a center well containing 1 ml of 1N KOH to trap CO_2, were incubated in a 15^{o}C water bath for 12 days. The KOH was replaced and assayed daily by counting 0.5 mL. After 12 days the overlying water was removed, measured and 1 mL counted. The sediment was centrifuged at 2,000 RCF. The pore water was removed, measured, and counted. The sediment was assayed by counting after combustion.

Poor mass balance for HMX treatments led to speculation that volatile organic compounds (VOCs) may have been produced. Therefore, all mass balance tests were repeated using a flow-through system in which air was passed over the water and through 10 mL of KOH and 2.5 grams of granular activated charcoal. The KOH was changed and assayed daily as previously described. VOC traps were extracted after the 12-day incubation by sonicating the charcoal with 10 mL of acetonitrile overnight and counting the extract.

Statistical analysis of treatment results were conducted using analysis of variance (ANOVA) on replicate means unless the test for normality failed. In those cases the Kruskal-Wallis One Way ANOVA on ranks was used. Mean separations were achieved with Holm-Sidak All Pairwise Multiple Comparison Procedures. Median values from the Kruskal-Wallis ANOVA were separated with Dunn's All Pairwise Multiple Comparison Procedures.

Results and Discussion

Fractionations

The acetonitrile fraction decreased rapidly in all treatments as the sediments aged (Figures 3-5). For TNT and RDX the decrease was from 73.43 to 3.07 percent and from 55.9 to 1.46 percent over the 90-day incubation, respectively. For HMX the drop was from 56.6 to 2.99 percent over 28 days. (At this point the HMX test was terminated because most values were near detection limits.) The recovery of TNT, RDX and HMX in the acetonitrile fraction at each sampling time did not differ ($P=0.470$, ANOVA on means). Results suggest that these compounds were increasingly binding to organic matter in the sediments over time, which removed them from the acetonitrile-extractable pool. Some of the decrease may be attributable to mineralization to CO_2, especially in RDX and HMX treatments (see Mass Balance results below). Compounds that are unextractable with acetonitrile are likely to be unavailable to marine organisms in the overlying or pore water. Concurrently with declines in the acetonitrile fraction, an increase in FA and HA fractions occurred. The amount of TNT was significantly greater than the amounts of RDX and HMX associated with these fractions. TNT and RDX associated with the cellulose fraction did not differ significantly, but both exceeded HMX associated with cellulose. The greatest amount of recovered radioactivity in RDX treatments was in the cellulose fraction after 7 days. Since cellulose is subject to long-term degradation, release of compounds associated with cellulose over time is possible. Humin was relatively stable at a very low percentage of the total initial radioactivity; however, TNT exceeded RDX and HMX ($P<0.001$, Kruskal-Wallis ANOVA on ranks). This fraction is a very slow-forming fraction, representing the culmination of the humification process. Ninety days is probably an insufficient time for achieving significant quantities of humin. This may be related to observations by Singh et al (*3*), where different soil organic matter fractions were shown to have different structural compositions for carbon (termed relative structural carbon percent, RSCP). These soil organic matter fractions with varying RSCP would have differential affinity for nitroaromatic contaminants. Thus, the structural chemistry

of soil or sediment organic matter can play an important role in the sorption of nitroaromatic compounds. It was also noted that the non-specific sorption of both TNT and 2,4-DNT in soil fractions was mainly controlled by the aliphatic fraction of sediment organic matter, where the order of nitroaromatic sorption in the different components was: humic acid-commercial > humic acid compost > humin~lignin.

Mass Balance

Results of mass balance studies of TNT indicated that 87 % of the added radioactivity was associated with the sediment after 12 days, which was significantly greater than radioactivity recovered from any of the other compartments in the TNT treatments (P= 0.056). The recovered radioactivity from overlying water, pore water and as CO_2 did not differ significantly (P = 0.05) (Figure 6). Mass balance profiles for RDX and HMX were similar, but both were significantly different from the TNT profile (Figures 7 and 8). The distribution of radioactivity recovered from RDX and HMX were different only in the overlying water where RDX was higher than HMX (P <0.001). No VOCs were detected in any treatments.

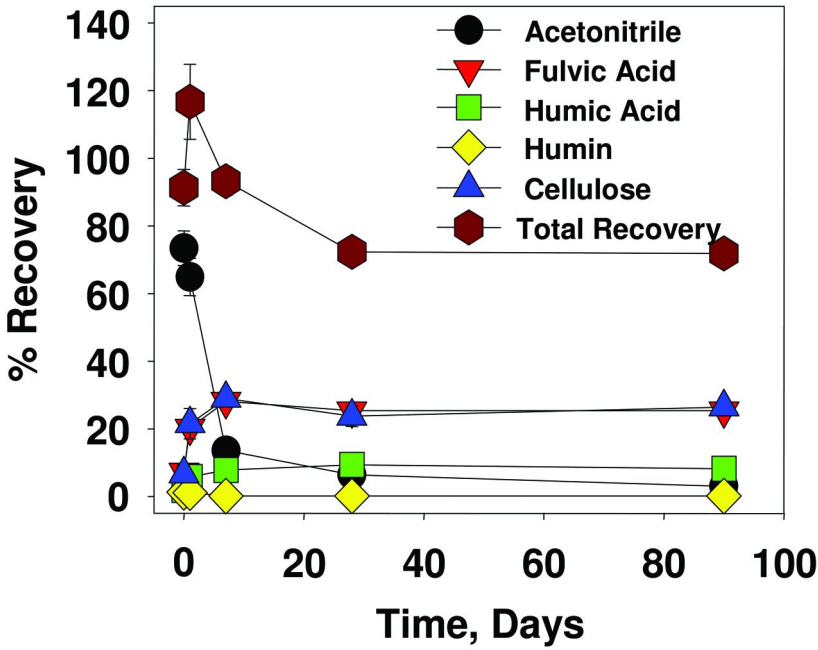

Figure 3. Fraction of organic matter with which radioactivity became associated over time for [^{14}C]TNT. Error bars are standard deviations of three replicates.

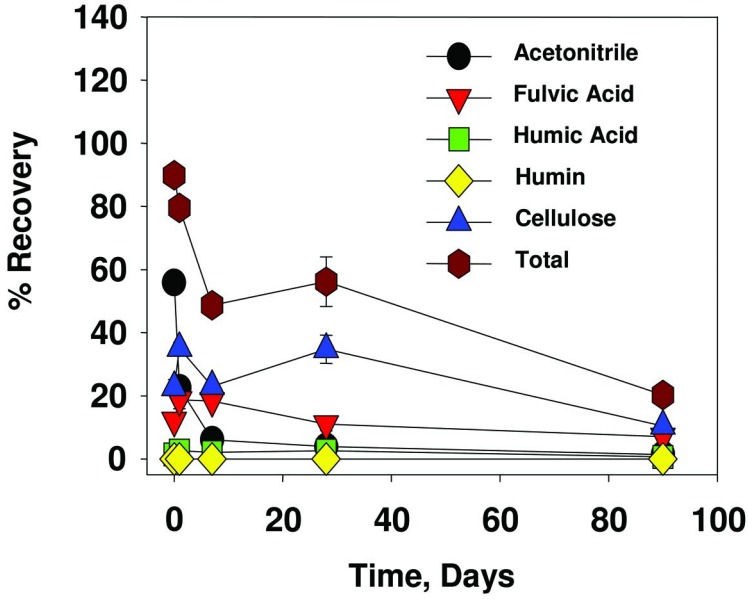

Figure 4. Fraction of organic matter with which radioactivity became associated over time for [^{14}C]RDX. Error bars are standard deviations of three replicates.

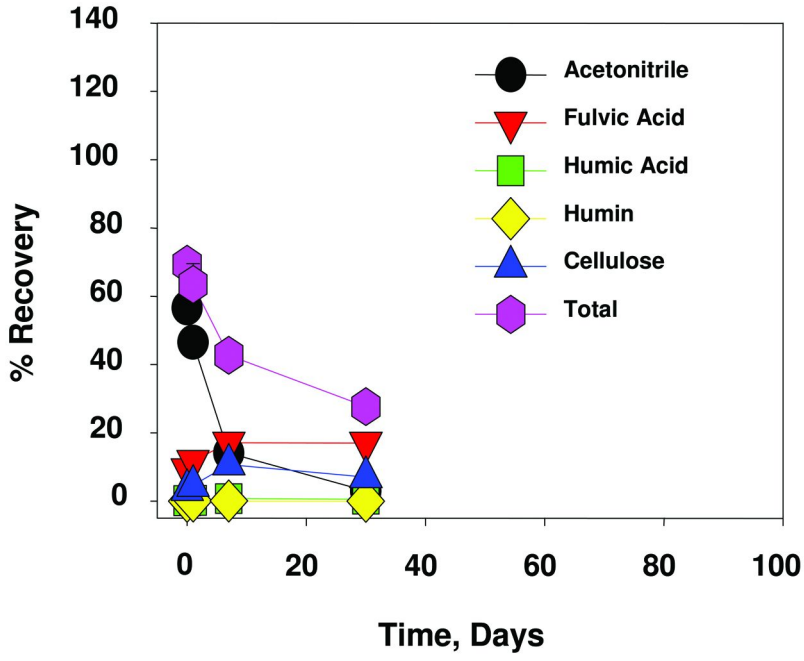

Figure 5. Fraction of organic matter with which radioactivity became associated over time for [^{14}C]HMX. Error bars are standard deviations of three replicates.

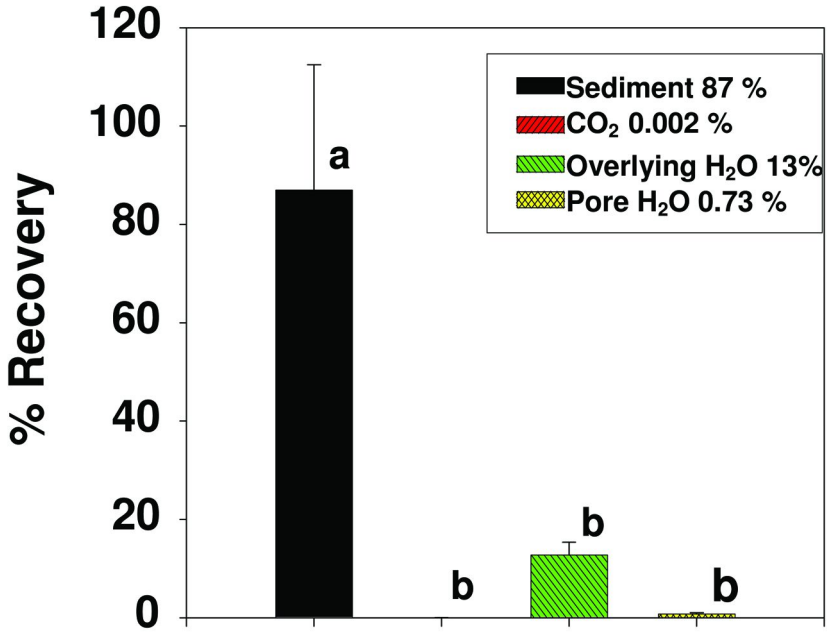

Figure 6. Mass balance of [^{14}C]TNT. Error bars represent standard deviations for three replicates. Total recovery was 100.4 %; incubation was 12 days. Bars showing the same letters are not significantly different (P <0.001, Holm-Sidak All Pairwise Multiple Comparison Procedures).

These results suggest that the sediment serves as a sink for TNT, but much less so for RDX and HMX. The small amount of recovered radioactivity in the pore water and overlying water suggests limited bioavailability of TNT. The barely detectable CO_2 evolution demonstrates that TNT is not readily mineralized. The large recovery in the sediment indicates that TNT is attenuated in the sediment, perhaps by mechanisms of covalent bonding described by Thorn and Kennedy (*1*) and Singh et al (*3*). The parallel bioavailability assessment experiment revealed a decrease in benthic bioaccumulation potential with increasing incubation time (*7*).

The sediment was the largest compartment in RDX treatments suggesting that it will serve as a significant sink for RDX. The sediment was also a sink for HMX, but the recovered radioactivity did not differ significantly from recovery as CO_2. The mineralization of RDX and HMX are likely to be significant fate processes (31 and 27.1 % for RDX and HMX, respectively). Recoveries in overlying water for both compounds suggest significant bioavailability to marine organisms. Although significantly less than other compartments, pore water recoveries represented approximately 10 % of added radioactivity. Therefore, pore water may be a limited source of RDX and HMX for sediment-dwelling organisms.

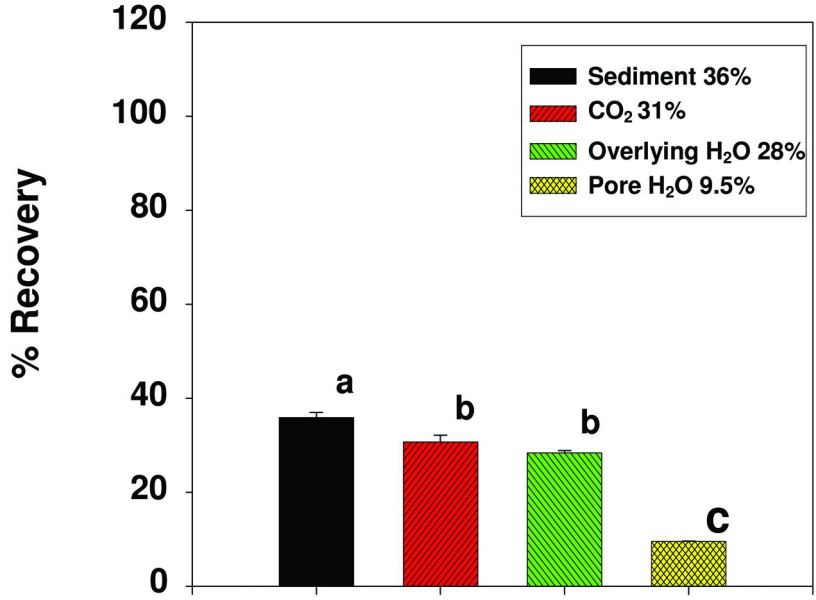

Figure 7. Mass balance of [^{14}C]RDX. Error bars represent standard deviations. Total recovery was 104.5 %; incubation was 12 days. Bars showing the same letters are not significantly different (P <0.001, Holm-Sidak All Pairwise Multiple Comparison Procedures.

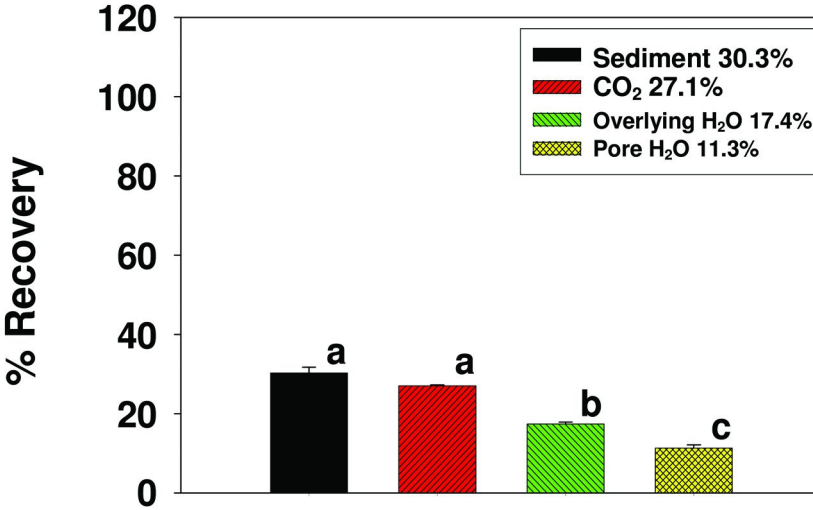

Figure 8. Mass balance of [^{14}C]HMX. Error bars represent standard deviations. Total recovery was 86.1 %; incubation was 12 days. Bars showing the same letters are not significantly different (P <0.001, Holm-Sidak All Pairwise Multiple Comparison Procedures).

Conclusions

Results of these studies illustrate the associations formed by TNT, RDX, and HMX with various components of marine sediment organic matter. The sediment serves as a sink for TNT, but much less so for RDX and HMX. Results of fractionation studies demonstrate removal of these compounds from the solvent-extractable pool over time with a concurrent increase in their associations with the cellulose, HA, and FA pools. Therefore, these compounds are participants in the humification processes occurring in the marine sediment organic matter. Mineralization of TNT was barely detectable; therefore, rather than leaving the system as CO_2, TNT is attenuated in the sediment. Further evidence is the relatively small recoveries of radioactivity in the overlying and pore water of TNT treatments. Mineralization of RDX and HMX are potentially significant fate processes in marine sediments. Therefore, given sufficient time and conditions, both of these compounds may be degraded. No VOCs were generated from TNT, RDX or HMX treatments. Only small recoveries of radioactivity from TNT and HMX treatments were obtained in overlying water, but substantial recoveries were obtained from RDX treatments. Therefore, RDX will be more readily available to water-dwelling organisms than TNT and HMX. Recoveries of radioactivity in pore water suggest limited availability of these compounds to sediment-dwelling organisms.

References

1. Thorn, K. A.; Kennedy, K. R. *Environ. Sci. Technol.* **2002**, *36*, 3787–3796.
2. Thorn, K. A.; Pennington, J. C.; Hayes, C. A. *Environ. Sci. Technol.* **2002**, *36*, 3797–3805.
3. Singh, N.; Berns, A. E.; Hennecke, D.; Hoerner, J.; Koerdel, W.; Schaeffer, A. *J. Hazard. Mater.* **2010**, *173* (1−3), 343–348.
4. Achtnich, C.; Fernandes, E.; Bollag, J. M.; Knackmuss, H. J.; Lenke, H. *Environ. Sci. Technol.* **1999**, *33* (24), 4448–4456.
5. Bruns-Nagel, D.; Knicker, H.; Drzyzga, O.; Butehorn, U.; Steinbach, K.; Gemsa, D.; von Low, E. *Environ. Sci. Technol.* **2000**, *34* (8), 1549–1556.
6. Thorn, K. A.; Goldenberg, W. S.; Younger, S. J.; Weber, E. J. *Humic and Fulvic Acids, Isolation, Structure, and Environmental Role*; Gaffney, J. S., Marley, N. A., Clark, S. B., Eds.; ACS Symposium Series 651; American Chemical Society: Washington, DC, 1996; Chapter 19, pp 299−326.
7. Lotufo, G. U.S. Army Engineer Research and Development Center, unpublished.
8. Stevenson, F. J. *Humus Chemistry: Genesis, Composition, Reactions*; Wiley-Interscience Publication, John Wiley and Sons: New York, 1989.
9. Pennington, J. C.; Hayes, C. A.; Myers, K. F.; Ochman, M.; Gunnison, D.; Felt, D. R.; McCormick, E. F. *Chemosphere* **1995**, *30*, 429–438.

Chapter 11

The Fate of Nitroaromatic (TNT) and Nitramine (RDX and HMX) Explosive Residues in the Presence of Pure Metal Oxides

Thomas A. Douglas,[1,*] Marianne E. Walsh,[2] Christian J. McGrath,[3] Charles A. Weiss, Jr.,[4] Ashley Marie Jaramillo,[1,5] and Thomas P. Trainor[5]

[1]U.S. Army Engineer Research and Development Center, Cold Regions Research and Engineering Laboratory, P.O. Box 35170, Fort Wainwright, Alaska 99703, USA

[2]U.S. Army Engineer Research and Development Center, Cold Regions Research and Engineering Laboratory, 72 Lyme Road, Hanover, New Hampshire 03755, USA

[3]U.S. Army Engineer Research and Development Center, Environmental Laboratory, 3909 Halls Ferry Road, Vicksburg, Mississippi 39180, USA

[4]U.S. Army Engineer Research and Development Center, Geotechnical and Structures Laboratory, 3909 Halls Ferry Road, Vicksburg, Mississippi 39180, USA

[5]University of Alaska Fairbanks, Department of Chemistry, Fairbanks, Alaska 99707, USA

[*]Thomas.A.Douglas@usace.army.mil

Packed beds of six different, granular, pure, metal oxide phases were loaded with explosives through controlled proximal detonation of Composition B. Composition B contains the commonly used explosives 2,4,6-trinitrotoluene (TNT), hexahydro-1,3,5-trinitro-1,3,5-triazine (RDX), and octahydro 1,3,5,7-tetranitro-1,3,5,7-tetrazocine (HMX). The metal oxides examined include magnetite (Fe_3O_4; Fe[II] and 2Fe[III]), two different hematites (Fe_2O_3; Fe[III]), manganese oxide (MnO; Mn[II]), pyrolusite (MnO_2; Mn[IV]), and aluminum oxide (Al_2O_3; Al[III]). These metal oxides were selected because of their potential to promote reductive transformation of explosive compounds. Following detonation subsamples of surficial

and bulk metal oxides were mixed in aqueous batches using ultraclean water and monitored for TNT, RDX, HMX, 2ADNT, and 4ADNT concentrations for 149 days.

Our results suggest that, even with highly controlled detonations, the explosive residues are heterogeneously loaded to the pure mineral phases. A logarithmic equation provides the best-fit description of the temporal trends in explosive analyte concentrations in the aqueous batches. RDX behaves more conservatively than TNT but does exhibit some loss from solution over time. Batches containing detonated magnetite and manganese oxide yielded the greatest loss of TNT, RDX, and HMX from solution and the highest 2ADNT and 4ADNT concentrations in the mineral material at the end of the batch experiments. These two batches also yielded the highest concentrations of the nitroso transformation products of RDX. This result suggests that reduced valence Fe and Mn metals promote explosive compound transformation, likely serving as a source of electrons for reductive transformation.

Introduction

One of the inevitable effects of military training is the deposition of explosive compounds and associated detonation residues to range soil systems. These compounds most commonly include nitroaromatics such as 2,4,6-trinitrotoluene (TNT) and nitramines like hexahydro-1,3,5-trinitro-1,3,5-triazine (RDX) and octahydro-1,3,5,7-tetranitro-1,3,5,7-tetrazocine (HMX). These explosive compounds are known toxicants (*1*, *2*). It is well established that TNT sorbs to soil minerals (*3*). Further, soil organic matter (*4–6*), and microbes (*7*, *8*) are associated with the transformation of TNT to 2-amino-4,6-dinitrotoluene (2ADNT) and 4-amino-2,6-dinitrotoluene (4ADNT). However, RDX and HMX are generally considered less reactive than TNT in training range soils (*9–11*).

Training range soils are comprised of complex and heterogeneous mixtures of crystalline and amorphous minerals and organic materials. Thus, any attempt to predict the fate and transport of explosive compounds in soils requires an understanding of the fundamental processes affecting contaminant dissolution, sorption-desorption, and transformation biogeochemically heterogeneous soil systems. If specific mineral phases are identified that promote the retention (i.e., sorption) or beneficial transformation (i.e., to less toxic compounds) of explosive compounds, it may be possible to augment impact areas, hand grenade ranges or storage areas with these materials to reduce the potential risk of off-site migration of explosive compounds.

Numerous studies guide our understanding of the interactions between explosive compounds and soil mineral phases. These include investigations of the fate of explosive compounds in clays (*3*, *12–15*), sandy soils (*9*), and mixed soils (*16–18*). Surficial ferrous iron has been known to promote the reductive transformation of TNT (*12*, *13*, *19*, *20*). However, there have been fewer studies of the role that metals (with their varied oxidation states) play in promoting explosive compound transformation (*21*, *22*).

The aforementioned studies rely on the aqueous addition of solutions spiked with explosive compounds to load explosive compounds to soils and minerals. This is appropriate in considering the fate of dissolved explosives following their released into the environment from burn pits or legacy manufacturing or packing facilities. However, detonation processes on training ranges load substrates with residues and undetonated particles of varying mass, size, and surface area (*23–26*). The present investigation was designed to increase our understanding of the fate of these particular explosive compounds and their residues in the presence of pure metal oxides. Understanding the interactions of explosives with these ideal, pure mineral phases serves as a basis for expanded examination of more biogeochemically complex soil systems. Samples were exposed to detonation under controlled conditions and batch reactors were constructed by adding ultrapure water to the detonated oxide samples. Aqueous samples were extracted over a period of 149 days and analyzed for concentrations of TNT, RDX, HMX , TNT transformation products 2ADNT and 4ADNT, and RDX transformation products hexahydro-1-nitroso-3,5-dinitro-1,3,5-triazine (MNX) and hexahydro-1,3-dinitroso-5-nitro-1,3,5-triazine (DNX) over time.

Materials and Methods

Ten kilograms of six different pure metal oxide minerals were procured from suppliers (Table 1). The detonations in conducted within a 2-meter cubic detonation chamber, constructed of 8-cm thick steel that was open to air at the top. A three meter length of military Detonation Cord with an Uli knot tied in one end was placed into a paper cup containing 120 g of Composition B flakes (0.5-cm thick and less than 3 cm in length or width). The cup of Composition B was placed at the bottom of a 20-cm wide by 40-cm high by 50-cm long steel can. Five kg of each sample was loaded on top of their respective explosive charge. The sample material filled the container to height of 15 cm. The detonation cord was then initiated with a M21 shock tube initiator from location 100 meters away.

Two different types of samples were collected from each container. The surface sample was collected with a PTFE (Teflon) scoop and consisted of the upper 0.5 cm of the detonated sample. This generally consisted of small (1 to 5 mm) clumps of the original mineral particles with a dark gray to black coating. The bulk sample consisted of the remaining material in the container. Since the cup of Composition B was located below the sample the surface sample represents material that was furthest away from the explosive blast.

Table 1. Elemental and speciation information, descriptions and manufacturer's grain size information for the pure metal oxides investigated in this study.

Sample	*Metal*	*Name*	*Description*	*Source*	*Mesh size*	*Particle diameter in mm.*
Fe_2O_3	Fe^{3+}	Hematite	Reddish powder	Fisher Scientific (Fairlawn, NJ)	<325	<0.04
Fe_2O_3	Fe^{3+}	Hematite	Reddish powder	Strem Chemicals (Newburyport, MA)	<325	<0.04
Fe_3O_4	Fe^{2+}, Fe^{3+}	Magnetite	Silver granules	Greg Crocco (Albuquerque, NM)	<80	<0.18
MnO	Mn^{2+}	Manganese oxide	Green granules	Alfa Aesar (Ward Hill, MA)	<100	<0.15
MnO_2	Mn^{4+}	Pyrolusite	Gray granules	Alfa Aesar (Ward Hill, MA)	<100	<0.15
Al_2O_3	Al^{3+}	Aluminum oxide	White powder	Fisher Scientific (Fairlawn, NJ)	<325	<0.04

All batch slurries were prepared in duplicate. Mineral samples (3 to 15 g) were placed into an amber glass bottle containing 500 mL of 18 MΩ water leaving minimal headspace. The mass of explosive compound residues in each batch was calculated to be below the solubility of RDX (46.6 mg/L; (*27*)) by multiplying the acetonitrile-extractable explosive compound concentration following detonation (details below) by the mass of sample in each batch and dividing by the amount of ultrapure water added to each batch. As a consequence, we were able to estimate the maximum expected concentration of each analyte once each batch reactor was mixed. The glass bottles were capped and placed on a platform shaker and shaken continuously at 200 rpm in the dark at 25°C for five months. One (1.00) mL of each aqueous sample was collected from the batches at the following elapsed times: 1, 3, 7, 12, 23, 37, 52, 78, 100, 129, and 149 days and pipetted into a 7-mL amber glass vial with 2.0 mL deionized water and 1.0 mL acetonitrile. A total volume of only 10 mL (2%) was removed for analysis prior to termination of the batch experiments and acetonitrile extraction.

At day 149 water was decanted from the batch slurries which were placed in a convection oven at 25°C until they were dried (two days). Twenty mL of HPLC-grade acetonitrile was added to the dried mineral samples (3-15 g) and the mixture was capped and placed on a platform shaker for 24 hours. The sample vials were centrifuged at 200 rpm for 10 minutes. The acetonitrile extracts were diluted with HPLC grade acetonitrile in order to be within the calibration range of the HPLC-UV detector, and 1.00 mL of the diluted extract was mixed with 3.00 mL of deionized water into a 7-mL amber glass vial. These samples represent the acetonitrile-extractable explosive compound concentrations in the minerals at the end of the batch experiments.

Concentrations of TNT, RDX, HMX, 2ADNT, and 4ADNT were determined in the batch aqueous and acetonitrile extracted samples following SW846 Method 8330B (*28*). Peaks and concentrations were identified for MNX and DNX. However, the concentrations were consistently low and MNX and DNX are transient so we do not report the concentration values here. Our method could not quantify HMX transformation products. Samples were filtered through a Millex-FH PTFE (Teflon) 0.45-µm filter unit prior to analysis. Explosive compound concentrations in aqueous solutions were determined on a Finnigan Spectra- SYSTEM P4000 (Thermo Electron Corporation, Waltham, MA) consisting of a pump and a Finnigan SpectraSYSTEM UV2000 dual wavelength UV/VS absorbance detector at 254 nm (cell path 1 cm). A 100-µL sample loop was used and the column was a 15 cm X 3.9-mm (4 µm) NovaPak C8 held at 28°C and eluted with 1.4 mL/min of 15:85 isopropanol/water (v/v).

Calibration standards were prepared from 8095 Calibration Mix A (Restek Corporation Bellefonte, PA) at 1, 10, and 40 mg/mL in acetonitrile of TNT, RDX, 2ADNT, and 4ADNT. The percent relative standard deviation of the explosive compound concentration measurements was less than 2% based on numerous analyses of laboratory standards.

Results and Discussion

Following detonation the samples exhibited an irregular grayish black sheen and there was some evidence of agglomeration of detonated materials into clumped aggregates roughly 1cm in diameter and smaller (Figure 1). The lightly cemented particles are presumably attributable to the heat and pressures associated with the detonation events and the grayish coating on the mineral grains and their aggregates is most likely composed of explosive residues and/or detonation residuals (*25*, *26*, *29*, *30*). This material was not present prior to detonation.

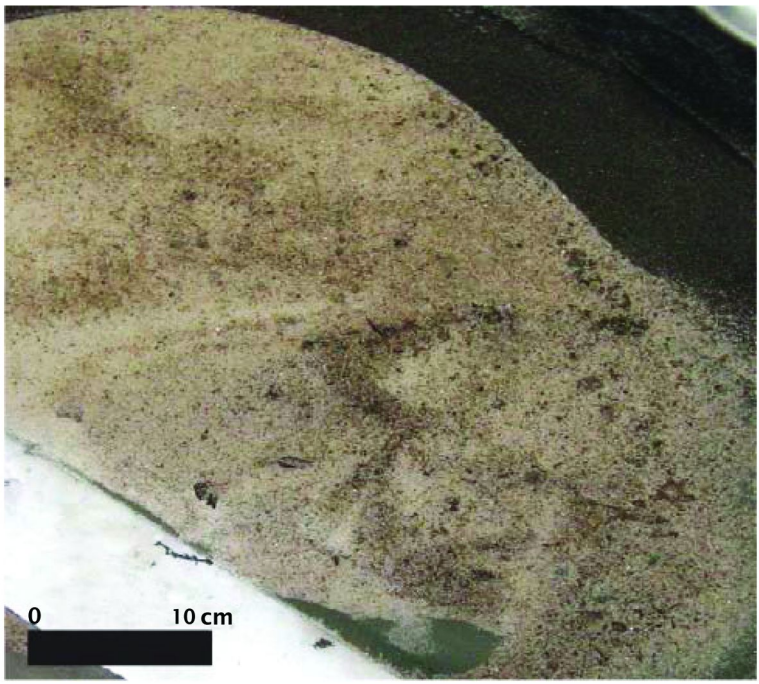

Figure 1. A photograph of the surface residue on the aluminum oxide sample following detonation.

The explosive compound concentrations measured from the batch reactor aqueous samples and the mineral sample acetonitrile extractions at day 149 are summarized in Tables 2 and 3. In all of the samples the aqueous apparent equilibrium concentration − defined here as the mean concentration of each analyte measured from the batches from day 37 onward − is greater than the maximum expected concentration. The reasons for this counterintuitive trend are unclear but some of the differences could be ascribed to the inherent heterogeneity associated with explosive compound loading to detonated samples (*26*). However, the "a" and "b" batches, representing duplicate batch reactors, generally yield similar results in all sample types for all analytes.

Table 2. Best fit parameters for 2,4,6-trinitrotoluene (TNT) over time from the results of the eighteen batch reactors. Aqueous-apparent equilibrium concentrations are calculated by taking the mean concentration of each analyte measured from the batches, day 37 and onward. Expected concentrations are those calculated based on combining ultraclean water with the detonated minerals. Final mineral concentrations are the acetonitrile-extractable explosive compound concentrations.

Sample	*TNT*							*2ADNT*	*4ADNT*
	Equation	r^2	*pH at day 1*	*pH at day 149*	*Aqueous apparent equilibrium (mg/L)*	*Aqueous expected concentration at day 149 (mg/L)*	*Acetonitrile-extractable concentration at day 149 (mg/kg)*	*Acetonitrile-extractable concentration at day 149 (mg/kg)*	*Acetonitrile-extractable concentration at day 149 (mg/kg)*
Hematite Fisher surface a	C= -0.5 ln(t) + 24.4	0	4.3	6.9	47	20.6	52.5	0.00	0.00
Hematite Fisher surface b	C= -0.01 ln(t) + 16.5	0	4.2	6.6	28.5	20.6	95.6	0.00	0.00
Hematite Fisher bulk a	C= 1.4ln(t) + 14.2	0.05	4.6	5.8	23.3	20.5	252.7	0.00	0.00
Hematite Fisher bulk b	C= 1.1 ln(t) + 15.8	0.11	4.3	5.8	29.1	20.4	62.7	0.13	0.17
Hematite Strem surface a	C= 2.3 ln(t) + 14.0	0.35	7.9	8.8	27.7	22.1	44.4	0.14	0.12
Hematite Strem surface b	C= -0.02 ln(t) + 18.8	0	8.7	8.8	25.9	21.7	29.7	0.23	0.09
Hematite Strem bulk a	C= -2.2 ln(t) + 25.35	0.04	8.4	8.3	25.3	19.2	93.9	0.00	0.00

Continued on next page.

Table 2. (Continued). Best fit parameters for 2,4,6-trinitrotoluene (TNT) over time from the results of the eighteen batch reactors. Aqueous-apparent equilibrium concentrations are calculated by taking the mean concentration of each analyte measured from the batches, day 37 and onward. Expected concentrations are those calculated based on combining ultraclean water with the detonated minerals. Final mineral concentrations are the acetonitrile-extractable explosive compound concentrations.

Sample	*TNT*							*2ADNT*	*4ADNT*
	Equation	r^2	*pH at day 1*	*pH at day 149*	*Aqueous apparent equilibrium (mg/L)*	*Aqueous expected concentration at day 149 (mg/L)*	*Acetonitrile-extractable concentration at day 149 (mg/kg)*	*Acetonitrile-extractable concentration at day 149 (mg/kg)*	*Acetonitrile-extractable concentration at day 149 (mg/kg)*
Hematite Strem bulk b	C= -1.2 ln(t) + 18.6	0.23	8.4	8.4	26.4	19.2	75. 3	0.24	0.00
Magnetite sand bulk a	C= 2.0 ln(t) + 13.8	0.15	7.9	8.3	30.8	14.6	0.33	0.61	1.03
Magnetite sand bulk b	C= 2.1 ln(t) + 12.6	0.23	7.9	8.3	30.2	14.5	0.48	0.67	1.25
MnO surface a	C= -0.7 ln(t) + 16.3	0.01	7.3	7.8	25.2	19.2	68.7	1.90	1.69
MnO surface b	C= -1.7 ln(t) + 19.5	0.08	7.0	7.6	25.1	18.9	73.4	2.15	2.21
MnO bulk a	C= 0.47 ln(t) + 17.2	0.02	6.7	9.6	26	17.7	0.18	0.00	0.00
MnO bulk b	C= 1.3 ln(t) + 14.4	0.16	6.6	9.5	27.4	17.9	0.26	0.00	0.00

Sample	*TNT*							*2ADNT*	*4ADNT*
	Equation	r^2	*pH at day 1*	*pH at day 149*	*Aqueous apparent equilibrium (mg/L)*	*Aqueous expected concentration at day 149 (mg/L)*	*Acetonitrile-extractable concentration at day 149 (mg/kg)*	*Acetonitrile-extractable concentration at day 149 (mg/kg)*	*Acetonitrile-extractable concentration at day 149 (mg/kg)*
MnO_2 surface a	C= 4.1 ln(t) + 4.9	0.41	5.1	6.6	28.1	20.4	52.9	0.00	0.00
MnO_2 surface b	C= 4.5 ln(t) + 3.2	0.23	5.1	6.8	30.3	20.4	14.3	0.00	0.00
Aluminum oxide surface a	C= 4.6 ln(t) -3.2	0.52	7.1	7.2	30.3	24.5	10.6	0.17	0.12
Aluminum oxide surface b	C= 2.5 ln(t) -1.0	0.2	7.1	7.4	26.5	24.6	4.29	0.07	0.09

Table 3. Best fit parameters for hexahydro-1,3,5-trinitro-1,3,5-triazine (RDX) over time from the results of the eighteen batch reactors. Aqueous-apparent equilibrium concentrations are calculated by taking the mean concentration of each analyte measured from the batches, day 37 and onward. Expected concentrations are those calculated based on combining ultraclean water with the detonated minerals. Final mineral concentrations are the acetonitrile-extractable explosive compound concentrations.

Sample	*RDX*				
	Equation	r^2	*Aqueous Apparent Equilibrium (mg/L)*	*Aqueous Expected concentration at day 149 (mg/L)*	*Acetonitrile-extractable concentration at day 149 (mg/kg)*
Hematite Fisher surface a	C= 2.3 ln(t) + 19.1	0.08	41.7	31.8	257
Hematite Fisher surface b	C= 2.1 ln(t) + 16.0	0.07	41.3	31.8	674
Hematite Fisher bulk a	C= 4.0 ln(t) + 10.1	0.29	26.3	30.5	1287
Hematite Fisher bulk b	C= 3.8 ln(t) + 12.6	0.58	32	30.3	133
Hematite Strem surface a	C= 6.1 ln(t) + 8.3	0.81	39.6	33.1	195
Hematite Strem surface b	C= 4.7 ln(t) + 11.7	0.43	36.2	32.5	73.6
Hematite Strem bulk a	C= 0.3 ln(t) + 26.4	0	42.3	30.0	399
Hematite Strem bulk b	C= 3.4 ln(t) + 21.1	0.3	30.5	30.0	381
Magnetite sand bulk a	C= 4.6 ln(t) + 12.8	0.64	32.4	22.9	13.7
Magnetite sand bulk b	C= 4.8 ln(t) + 11.2	0.7	32.5	22.9	14.4
MnO surface a	C= 0.1 ln(t) + 23.2	0	29.1	30.0	121
MnO surface b	C= -0.51 ln(t) + 26.5	0.01	29.1	29.8	147

Sample	*RDX*				
	Equation	r^2	*Aqueous Apparent Equilibrium (mg/L)*	*Aqueous Expected concentration at day 149 (mg/L)*	*Acetonitrile-extractable concentration at day 149 (mg/kg)*
MnO bulk a	C= 3.6 ln(t) + 15.1	0.39	32.9	29.3	0.04
MnO bulk b	C= 3.9 ln(t) + 14.7	0.49	36.3	29.5	0.13
MnO_2 surface a	C= 6.8 ln(t) + 3.7	0.67	39.5	30.7	205
MnO_2 surface b	C= 6.4 ln(t) + 3.2	0.45	33.8	30.7	132
Aluminum oxide surface a	C= 6.3 ln(t) -2.9	0.53	40.3	38.6	94.8
Aluminum oxide surface b	C= 5.1 ln(t) -3.3	0.4	37.8	38.9	46.5

For most of the batches the acetonitrile-extractable explosive compound concentrations recovered from the metal oxides at day 149 are greater than either the aqueous apparent equilibrium or the expected maximum concentration. This is to be expected as the batches were constructed by adding between 3 and 15 grams of detonated minerals to roughly 500 mL of ultraclean water so the final mineral acetonitrile-extractable concentrations should be greater than the apparent equilibrium or expected concentration values. However, magnetite and some of the MnO samples yielded unexpectedly low TNT, RDX, and HMX (not shown) inthe acetonitrile-extractable final mineral concentrations. Aluminum oxide yielded an unexpectedly low final mineral TNT concentration. These results suggest that transformation and/or partitioning to solution have occurred in these batches.

Figures 2 and 3 include plots of TNT, RDX, HMX, and TNT transformation products 2ADNT and 4ADNT measured over time from eight of the batch reactors. All of the batches were constructed in duplicate ("a" and "b"). The differences between the "a" and "b" analyses for any given sampling day and analyte were typically within 5%. This suggests that the evolution of explosive concentration values over time in the batches is consistent among a given sample type. Only the "a" samples are presented in Figures 2 and 3 for consistency. Explosive compounds were measured each sampling day from randomly selected triplicate samples; the percent relative standard deviation for these samples was typically within 5%.

TNT has been shown to undergo transformation in a variety of aqueous reactors containing soils (*16–18*) and pure mineral phases (*3*, *10*). In the magnetite sand and manganese oxide batches the TNT concentrations generally increase initially and then decrease over time. The 2ADNT and 4ADNT monoamines first begin to exceed detection limits after roughly 10 to 30 days in most batches. This is commonly around the time that TNT has reached maximum concentrations associated with dissolution and desorption processes of the explosive residues and any undetonated Composition B (*23*). The TNT transformation products were not present in the Composition B used to detonate the pure minerals (*25*) or in the initial acetonitrile extractions following detonation so their presence in the batches is most likely attributed to the reductive transformation of TNT (*32*, *33*) during the batch experiments.

In most of the batch reactors the TNT concentrations maintain an apparent equilibrium concentration or decrease slightly around day 100 or 129. After a few weeks, 2ADNT and 4ADNT begin to be detected and in almost all of the batches at concentrations that increase and then decrease with time. This loss of 2ADNT and 4ADNT from solution could be attributed either to adsorption of these monoamines onto the metal oxide mineral surfaces or to the transformation of these compounds to phenolic derivatives (*8*, *25*, *34*). Although we did not measure the phenolic derivatives only a few of the minerals yielded detectable 2ADNT or 4ADNT in the acetonitrile-extracted samples at day 149 (Strem Fe_2O_3, magnetite sand, MnO, and Al_2O_3). This suggests that in these samples some of the 2ADNT and 4ADNT is lost from solution by sorbing onto the metal oxides. However, the acetonitrile-extractable 2ADNT and 4ADNT concentrations are 2 mg/kg or lower so they can only account for a very small fraction of the TNT

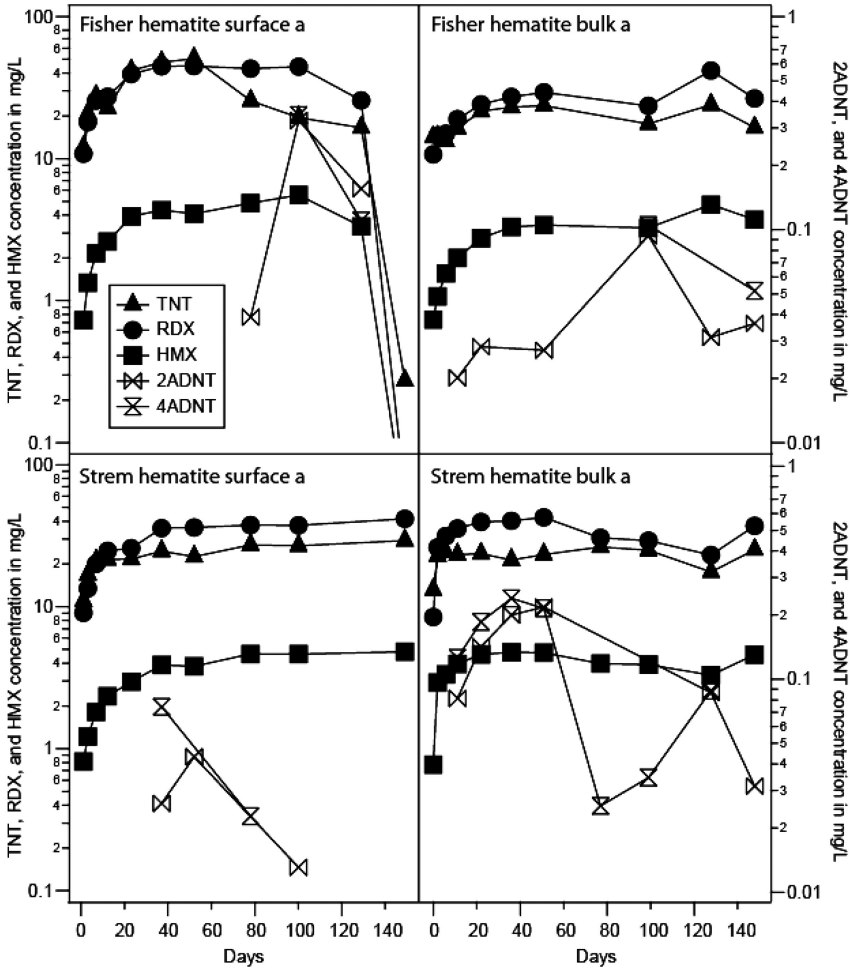

Figure 2. A plot of explosive compounds in four of the hematite batch slurries over time.

initially present as a residue on the detonated metals. In addition, the samples that yielded acetonitrile-extractable 2ADNT and 4ADNT have the lowest acetonitrile extractable TNT, RDX, and HMX concentrations so these minerals are not likely effective adsorbents for 2ADNT and 4ADNT and we can only suspect the 2ADNT and 4ADNT are transformed (*8*, *14*, *26*).

All of the batch RDX and HMX concentrations exhibit the same general trends for the first 30 days: the initial samples yield values of 5 to 15 mg/L and over the course of the next 20 to 30 days they reach an "apparent equilibrium" where adsorption-desorption and dissolution processes are approaching equilibrium (*26*). The explosive compound values generally remain relatively stable (primarily for RDX and HMX) for the remaining 100 days.

The acetonitrile-extractable concentrations of RDX and HMX in most of the metal oxide samples at the end of the batch experiments were greater than their

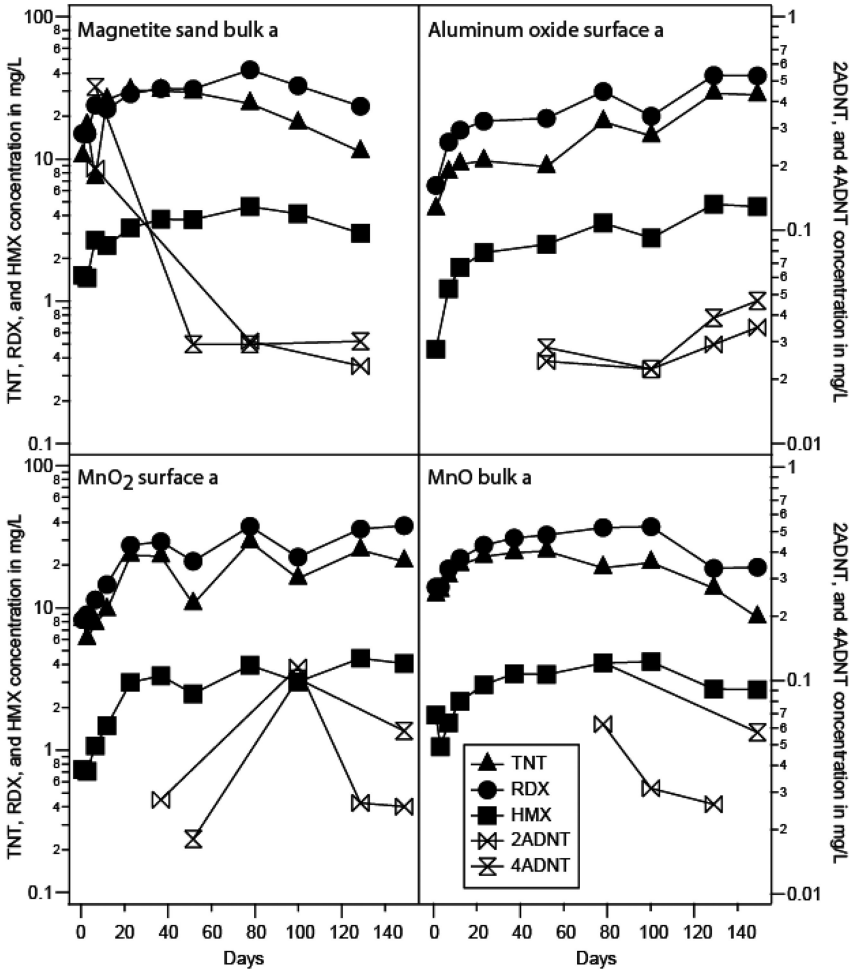

Figure 3. A plot of explosive compounds in magnetite sand, aluminum oxide, MnO and MnO_2 batch slurries over time.

concentrations in solution at any time. This implies the nitramines are readily sorbed to the metal oxides. However, RDX and HMX concentrations in the magnetite sand and manganese oxide bulk samples at day 149 were far lower than the initial RDX and HMX concentrations (compare the aqueous expected concentration at day 149 with the acetonitrile-extractable concentration at day 149 in Table 3). This might indicate these nitramines are undergoing transformation in the presence of these metal oxides. For reasons thus far undetermined, the MnO surface samples do not exhibit the same trend of lower acetonitrile-extractable concentrations at day 149 than was expected.

We identified the RDX nitroso reduction reaction products MNX and DNX in the HPLC chromatograms from all of the batch reactors. The nitroso compounds are transient intermediates in the transformation of RDX to formaldehyde, nitrous oxide gas and ammonium (*30*, *31*). MNX concentrations were almost always

greater than DNX. MNX and DNX were detected in the initial samples of all the batches but their concentrations generally decreased to values below detection limits within 10 days. The magnetite sand and MnO top batches were the only ones for which MNX and DNX were detected in all aqueous samples. For both sample types the nitroso values peaked within 10 days and then steadily decreased to values of roughly 0.1 mg/L at day 149. The presence of these nitroso analytes in the batches signifies the transformation of RDX which was likely greatest in the magnetite sand and MnO bulk batch reactors. Our method could not quantify HMX transformation products but we speculate that the loss of HMX from solution is attributable to transformation and/or sorption.

Best fit analyses were performed for the concentration trends in RDX, HMX and TNT from the batch samples. The logarithmic fit (Tables 2 and 3) yielded the best coefficient of determination values among linear (2nd, 3rd, or 4th order), power, or exponential curve fittings. This is similar to the results from a study investigating the fate of explosive compounds in batches constructed of detonated soils (*26*) that provided the following equation for the logarithmic best fit of the explosive compound concentrations:

$$C=k_1 \ln(t)+k_2$$

where C is the concentration in mg/L, t is the time in days, and k_1 and k_2 are fitting parameters.

It is apparent from the coefficient of determination (r^2) values for the logarithmic best fit equations (Tables 2 and 3) that TNT values are less well approximated by the logarithmic best fit equation than RDX. This can be attributed to the fact that TNT is more susceptible to transformation or adsorption than RDX or HMX (*11*, *14*, *35–37*). However, RDX does not consistently exhibit high coefficient of determination values which suggests that the dissolution and sorption-desorption processes for RDX are not at an equilibrium after 149 days, that some sorption is occurring between RDX and the metal oxides, and/or that RDX is undergoing transformation to compounds other than those measured.

In almost all of the batches the expected maximum concentrations are lower than the apparent equilibrium concentrations resulting from the logarithmic fit equations. The values are not markedly different but the reasons for this are unclear. The higher apparent equilibrium values could be explained by the limits of the logarithmic fit parameterization, by the heterogeneous loading of explosives to the detonated materials, and/or by some aspect of the desorption processes occurring in acetonitrile versus water.

The objective of this study was to determine whether pure metal oxides provide substrates that transform explosive compound residues under isothermal, aerobic, abiotic conditions in mixed batch suspensions. Metals of varying oxidation states have been shown to promote the transformation of nitroaromatic and nitramine explosive compounds, especially ferrous iron (FeII). For example, surficial structural ferrous iron on Fe^{2+}-bearing clays has been found to promote the reductive transformation of TNT (*13*, *38–40*). Iron in powdered pyrite (FeS_2; Fe[II]) and magnetite (Fe_3O_4; Fe[II and III]) has also been shown to promote the

reductive transformation of TNT, RDX, and nitroglycerin in aqueous batches (*21*, *22*).

Conclusions

Three important conclusions can be made from this study that build on previous efforts. First, results from the batch experiments suggest that the dissolution, adsorption-desorption, and transformation processes commonly believed to occur in aqueous solutions containing explosive compounds and mineral phases appear to occur abiotically in the presence of metal oxides as well. It takes roughly 20 to 30 days to reach an apparent equilibrium and some of the explosive compounds eventually decrease in concentration. None of this is surprising but some of the mineral species evaluated here have not been evaluated previously for detonation effects or for the fate of explosive compounds in their presence.

Second, it is apparent that TNT undergoes transformation to 2ADNT and 4ADNT in the presence of all the metal oxide mineral phases regardless of their oxidation state. The mineral phases we utilized were pure phases that we believe do not contain the humic or other organic materials common in natural soils. In three of the sample types (magnetite, manganese oxide, and aluminum oxide) the 2ADNT and 4ADNT undergo transformation and exhibit minor sorption to the metal oxides.

Third, magnetite and manganese oxide are associated with the loss of RDX and HMX from solution and with the greatest TNT sorption of all the metal oxide substrates. We identified the RDX transformation products MNX and DNX in the HPLC chromatograms from all of the batches. However, the loss of RDX and HMX only occurred in the batch solutions containing magnetite and MnO. Due to their ability to transform TNT, RDX, and perhaps HMX the magnetite and MnO provide the optimal substrates to promote the transformation of TNT and the loss of nitramine compounds from solution. Based on previous research it is likely that the Fe[II] and Mn[II] present in magnetite and MnO, respectively, may serve as electron donors to promote chemical reduction transformations in explosive compounds (*21*, *22*). Though ferrous iron minerals have been shown to provide a promising remediation component, there has been little research in using manganese as a remediation tool.

The specific surface area was not measured for of any of the present oxide samples. This parameter could be a major factor in quantifying the amount of reactive substrate available to provide a medium for explosive residue transformation or sorption. However, some inferences can be made based on the particle size information. The transformation of TNT and the loss of 2ADNT and 4ADNT from solution do not appear to correlate with any particular substrate particle size. However, the two substrates that were associated with the most RDX transformation (the magnetite sand and the manganese oxide) contained the largest particle diameters (and thus the lowest specific surface areas) of our sample set. The hematite and aluminum oxide samples had much smaller particle sizes and yet these two substrates were not associated with the same degree of

RDX transformation. One reasonable next step for this investigation would be to detonate sets of pure metal oxides (and other common soil minerals) with a range of specific surface areas for each substrate and then quantify the fate of explosive residues over time.

Acknowledgments

Charles Collins, Tom Jenkins, Terry Sobecki, Susan Taylor, Dave Ringelberg, Karen Foley, Mike Reynolds, Jay Clausen, and Alan Hewitt provided insightful comments throughout the incubation and development of this project. The tests described and the resulting data presented herein, unless otherwise noted, were obtained from research conducted under the U.S. Army Environmental Quality Technology Basic Research Program by the U.S. Army Engineer Research and Development Center. The use of trade, product, or firm names in this paper is for descriptive purposes only and does not imply endorsement by the U.S. Government. Permission was granted by the Chief of Engineers to publish this information.

References

1. Rickert, D. E. E. *Toxicity of Nitroaromatic Compounds*; Hemisphere: Washington, DC, 1985.
2. Weissmahr, K. W.; Haderlein, S. B.; Schwarzenbach, R. P. *Environ. Sci. Technol.* **1997**, *31*, 240–247.
3. Larson, S.; Martin, W.; Escalon, B.; Thompson, M. *Environ. Sci. Technol.* **2008**, *42*, 786–792.
4. Tucker, W. A.; Murphy, G. J.; Arenberg, E. D. *Soil Sediment Contam.* **2002**, *11*, 809–826.
5. Eriksson, J.; Frankki, S.; Shchukarev, A.; Skyllberg, U. *Environ. Sci. Technol.* **2004**, *38*, 3074–3080.
6. Crocker, F. H.; Thompson, K. T.; Szecsody, J. E.; Frekrickson, H. L. *J. Environ. Qual.* **2005**, *34*, 2208–2216.
7. Hallas, L. E.; Alexander, M. *Appl. Environ. Microbiol.* **1983**, *45*, 1234–1241.
8. Hawari, J.; Beaudet, S.; Halasz, A.; Thiboutot, S.; Ampleman, G. *Appl. Microbiol. Biotechnol.* **2000**, *54*, 605–618.
9. Yamamoto, H.; Morley, M.; Speitel, G.; Clausen, J. *Soil Sediment Contam.: Int. J.* **2004**, *13*, 361–379.
10. Dontsova, K. M.; Hayes, C.; Pennington, J. C.; Porter, B. *J. Environ. Qual.* **2009**, *38*, 1458–1465.
11. Douglas, T. A.; Johnson, L.; Walsh, M. E.; Collins, C. *Chemosphere* **2009**, *76*, 1–8.
12. Weissmahr, K.; Haderlein, S.; Schwarzenbach, R. *Soil Sci. Soc. Am. J.* **1998**, *62*, 369–378.
13. Hofstetter, T.; Neumann, A.; Schwarzenbach, R. *Environ. Sci. Technol.* **2006**, *40*, 235–242.

14. Douglas, T. A.; Walsh, M. E.; McGrath, C. J.; Weiss, C. A. *J. Environ. Qual.* **2009**, *38* (6), 1–10.
15. Jaramillo, A. M.; Douglas, T. A.; Walsh, M. E.; Trainor, T. P. *Chemosphere* **2011**, *84* (8), 1058–1065.
16. Pennington, J. C.; Patrick, W. H., Jr. *J. Environ. Qual.* **1990**, *19*, 559–567.
17. Xue, S. K.; Selim, H. M.; Iskandar, I. K. *Soil Sci.* **1995**, *160* (5), 317–327.
18. Comfort, S. D.; Shea, P. J.; Hundal, L. S.; Li, Z.; Woodbury, B. L.; Martin, J. L.; Powers, W. L. *J. Environ. Qual.* **1995**, *24*, 1174–1182.
19. Zilberberg, I.; Pelmenschikov, A.; McGrath, C. J.; Davis, W. M.; Leszczynska, D.; Leszczynski, J. *Int. J. Mol. Sci.* **2002**, *3*, 801–813.
20. Monteil-Rivera, F.; Paquet, L.; Halasz, A.; Montgomery, M. T.; Hawari, J. *Environ. Sci. Technol.* **2005**, *39*, 9725–9731.
21. Nefso, E. K.; Burns, S. E.; McGrath, C. J. *J. Hazard. Mater.* **2005**, *B123*, 79–88.
22. Oh, S.-Y.; Chiu, P. C.; Cha, D. K. *J. Hazard. Mater.* **2008**, *158* (2−3), 652–655.
23. Ro, K.; Venugopal, A.; Adrian, D.; Constant, D.; Qaisi, K.; Valsaraj, K.; Thibodeaux, L.; Roy, D. *J. Chem. Eng. Data* **1996**, *41*, 758–761.
24. Lynch, J.; Brannon, J.; Delfino, J. *Chemosphere* **2002**, *47*, 725–734.
25. Pantea, D.; Brochu, S.; Thiboutot, S.; Ampleman, G.; Scholz, G. *Chemosphere* **2006**, *65*, 821–831.
26. Douglas, T. A.; Walsh, M. E.; McGrath, C. J.; Weiss, C. W., Jr.; Jaramillo, A. M.; Trainor, T. P. *Environ. Toxicol. Chem.* **2010**, *30* (2), 345–353.
27. Monteil-Rivera, F.; Paquet, L.; Deschamps, S.; Balakrishan, V. K.; Beaulieu, C.; Hawari, J. *J. Chromatogr., A* **2004**, *1025*, 125–132.
28. United States Environmental Protection Agency, (USEPA). *SW846 Method 8330B USEPA Office of Solid Waste Standard Methods of Analysis Test Methods for Evaluating Solid Waste, Physical/Chemical Methods*; Office of Solid Waste: Washington, DC, 2006.
29. Hewitt, A. D.; Jenkins, T. F.; Walsh, M. E.; Walsh, M. R.; Taylor, S. *Chemosphere* **2005**, *61*, 888–894.
30. Boparai, H. K.; Comfort, S. D.; Satapanajaru, T.; Szecsody, J. E.; Grossi, P. R.; Shea, P. J. *Chemosphere* **2010**, *79*, 865–872.
31. Larese-Casanova, P.; Scherer, M. M. *Environ. Sci. Technol.* **2008**, *42*, 3975–3981.
32. Jenkins, T.; Hewitt, A.; Grant, C.; Thiboutot, S.; Ampleman, G.; Walsh, M.; Ranney, T.; Ramsey, C.; Palazzo, A.; Pennington, J. *Chemosphere* **2006**, *63*, 1280–1290.
33. Thorn, K. A.; Kennedy, K. R. *Environ. Sci. Technol.* **2002**, *36*, 3787–3796.
34. Kaplan, D. L.; Kaplan, A. M. *Appl. Environ. Microbiol.* **1982**, *44*, 757–760.
35. Haderlein, S. B.; Weissmahr, K. W.; Schwarzenbach, R. P. *Environ. Sci. Technol.* **1996**, *30*, 612–622.
36. Li, H.; Teppen, B. J.; Johnston, C. T.; Boyd, S. A. *Environ. Sci. Technol.* **2004**, *38*, 5433–5442.
37. Charles, S.; Teppen, B.; Li, H.; Laird, D.; Boyd, S. *Soil Sci. Soc. Am. J.* **2006**, *70*, 1470.

38. Hofstetter, T. B.; Schwarzenbach, R. P.; Haderlein, S. B. *Environ. Sci. Technol.* **2003**, *37*, 519–528.
39. Jaisi, D. P.; Dong, H.; Liu, C. *Geochim. Cosmochim. Acta* **2007**, *71*, 1145–1158.
40. Gregory, K. B.; Larese-Casanova, P.; Parkin, G. F.; Scherer, M. M. *Environ. Sci. Technol.* **2004**, *38*, 1408–1414.

Chapter 12

Soil Vadose Zone Chemistry of TNT and RDX Under Water-Saturated Conditions

Mark A. Chappell,[1,*] Cynthia L. Price,[1] Gerald G. Bourne,[2] Brad A. Pettway,[2] and Beth E. Porter[2]

[1]U.S. Army Engineer Research and Development Center, (ERDC), 3909 Halls Ferry Road, Vicksburg, MS
[2]SpecPro, Inc., 4815 Bradford Drive, Huntsville, AL 35805
[*]mark.a.chappell@usace.army.mil

Here, we describe experiments investigating the mobility and fate of TNT and RDX in elongated soil columns in order to simulate potential reactions as these munition constituents move down through the soil profile. Plexiglas columns (24 x 8 in) were dry-packed with a Memphis silt soil to a bulk density of 1.18 g cm^{-3} and leached at a constant rate with a proportional mixture of TNT and RDX representing the explosive formulation, Composition B. Samples were collected with time from three sampling ports (labeled top, middle, and bottom) located down the height of the soil column using rhizome samplers. Solute breakthrough data was determined and modeled using a two-site non-equilibrium adsorption model. TNT was shown to become increasingly partitioned to the soil immobile phase with depth, which was attributed to the degradation and subsequent humification of ammonium-based degradation products. On the other hand, RDX was largely unaffected by its interaction with this soil. The KD value of RDX determined for the mobility experiments was similar to that determined in batch sorption isotherms. This study demonstrates the potential opportunities for transformation of munition constituents as the solutes traverse the soil profile.

Introduction

During military training, munitions that malfunction result in low-order detonations. These detonations deposit fragments of munition constituents (MC) on the soil surface. Typical MC compounds include TNT, RDX, and HMX, which exhibit ecological toxicity in areas where these materials accumulate (*1*). These molecules are weakly polar but MC are fairly soluble (*2*). Thus, particulates are slowly dissolved with precipitation events, allowing for movement into the soil profile.

In general, MC undergo weak interactions with the dominant soil domains (e.g., cation exchange capacity) because of functional group incompatibility. Therefore, molecules of this type require long time periods to reach full equilibrium with soil (*3*), commonly on the order of 300 h. In spite of this interaction, MC mobility in soil is commonly described in terms of an empirical partitioning coefficient, based on standard 24-48 h batch sorption isotherm determinations. But, studies continually reveal that the sorption K_D values possess limited ability for accurate extrapolation to other soils, particularly with similar textural and organic carbon characteristics. However, recent multi-linear regression analysis (*4*) using data included in the review by Brannon and Pennington (*5*) showed some evidence for K_D predictability based on soil constituents and properties (see Chapter 1).

While it seems clear that K_D values for soils may be matched to a soil by adding a function that accounts for soil properties, still these K_D values typically over-predict the transport of MC through the soil profile – the exception being high sand soils. We hypothesize that the consistency of over-prediction speaks to the prolonged interaction of MC with the soil surface and the variation of K_D with respect to soil properties with continued permeation through the profile. This prolonged interaction has implications both in terms of abiotic and biotic processes controlling the fate of munition constituents.

Soil Transport Considerations

The mobility of dissolved solute is regulated by the potential of soil to conduct water and the potential of the solute to react with soil constituents. Assuming water flow through the soil is constant, nonreactive solutes will move through the soil at the same rate as water. However, if solutes are reactive, they will be less mobile through the soil than water (*6*). A thorough review on solute transport is given by Dane and Topp (*7*). For the case that a soil column is leached with a solution containing a dissolved solute not presently found in the soil, solute transport results from the combination of three different types of flow: convective or bulk flow, hydrodynamic dispersion, and molecular or ionic diffusion. Convective flow refers to the passive transport of a solute occurring solely by the velocity of the flowing water. Convective flow, J_C is expressed as:

$$J_C = qC \qquad [1]$$

Where q = the rate of water flow and C represents the influent concentration of the dissolved solute in water. Actually, Eq. 1 does not fully represent the total convective solute flow thorugh porous medium because it fails to describe the extra motion through the tortuous flow paths (*8*). The differing shapes and sizes of soil pores create variations in flow according to its velocity distribution. This type of motion is known as hydrodynamic dispersion flux (J_h) and is expressed as

$$J_h = -\theta D_{h\,i} \frac{\delta C}{\delta x} \qquad [2]$$

where θ = volumetric water content ($cm^3\ cm^{-3}$), $D_{h\,i}$ = hydrodynamic dispersion coefficient of chemical species i, and $\delta C/\delta x$ is the concentration gradient over distance x.

Solute movement resulting from Browniam motion or diffusive flow (J_d) is defined, according to Fick's law as the diffusional solute flux:

$$J_d = -\theta D_{d\,i} \frac{\delta C}{\delta x} \qquad [3]$$

Where $D_{d\,I}$ is the diffusion coefficient of the dissolved solute i in the porous medium (soil in this case). The minus sign in Eq. 3 indicates that the net direction of species *i* diffusional flow occurs toward the lower concentrations of species i.

Because of the similarity of the effect, not the mechanisms, of diffusion and dispersion (*9*), the hydrodynamic dispersion coefficient and the diffusion coefficient are combined as

$$D_i = D_{h\,i} + D_{d\,i} \qquad [4]$$

Where D_i = the diffusion-dispersion coefficient of species i. Therefore, the combined forces driving solute flow (J_S) is expressed as

$$J_{S\,i} = -\theta D \frac{\delta C}{\delta x} + qC\,. \qquad [5]$$

For reactive solutes, Eq. 5 falls short as it does not consider adsorption processes that occur on the soil surface. For this, Eq. 5 can be substituted into the equation for continuity (*8*) to give,

$$\frac{\rho_b}{\theta}\frac{\delta S}{\delta t} + \frac{\delta C}{\delta t} = D\frac{\partial^2 C}{\partial x^2} - V\frac{\delta C}{\delta x} \qquad [6]$$

Where S = sorbed concentration of species I, ρ_b = soil bulk density, V = the pore water velocity, and t = time. The distribution of a solute between the solid and solution phases is described by the distribution coefficient (K_D) as

$$K_D = \frac{S_i}{C_i}\,. \qquad [7]$$

In a homogenous soil column under steady-state water flow, Eq. 6 reduces to

$$R_i \frac{\delta C}{\delta t} = D \frac{\partial^2 C}{\partial x^2} - V \frac{\delta C}{\delta x} \quad [8]$$

Where R_i = the retention factor of the solute. The retention factor describes the "slower" movement of an adsorbing solute relative to the movement of a nonreactive solute. The relationship between the retention factor of a solute and K_D under water-saturated conditions is given by (*8*)

$$R = 1 + \frac{\rho_b}{\theta} K_D . \quad [9]$$

Eq. 9 shows how the K_D of species i can retard the flux of the solute through the soil. For nonreactive solutes, where $K_D = 0$, $R = 1$. In negatively charged soils, chloride (Cl^-) tracers are generally considered nonreactive solutes (except for some anion exclusion) and are used to delineate the source, direction, and velocity of the wetting front (*6*). Retention factors greater than 1 indicate that the solute is adsorbed by the soil and its mobility is less than the flow of the solvent.

In real practice, however, the R value can actually indicate retention of the solute due to degradation processes in addition to abiotic retention processes, unless special precautions are undertaken to limit biotic degradation of the solute. In this case, the K_D value represent more of an "apparent" K_D, where both abiotic and biotic processes are combined, and perhaps a more representative measure of the actual environmental fate of the solute. A common approach is to attempt separating these processes, assigning abiotic K_D values obtained from batch isotherms and then allowing the model to calculate degradation rates based on any additional solute retention. However, for this work, we will consider the K_D value as representative of both abiotic and biotic processes, and make no attempt to separate them in our measurements. Instead, we will interpret K_D value using a two-site non-equilibrium adsorption model, where solute retention or adsorption is modeled as the combination of two terms, β = the partitioning coefficient (for non-equilibrium modeling) and ω, the mass transfer coefficient indicating the rate of exchange between the mobile (dynamic) and immobile (stagnant) soil-water domains (*10*). The equations for these parameters are as follows:

$$\beta = \frac{R_m}{R} \quad [10]$$

and

$$\omega = \alpha(1-\beta)RL / v \quad [11]$$

where, R_m = the retention factor for the dynamic soil region, α = mass transfer coefficient between the two phases in the absence of adsorption, L = column length, and v = porewater velocity.

Materials and Methods

Batch sorption isotherms for TNT and RDX were constructed using a Memphis silt soil (Fine-silty, mixed, active, thermic Typic Hapludalfs) collected from Vicksburg, MS. Approx. 3 g of soil was added to glass centrifuge tubes containing approx. 20 mL of 100 mM $CaCl_2$. Tubes were then capped and shaken for 24 h to rehydrate the previously air-dried soil, as our previous work demonstrated the effect of incomplete rehydration on the sorption coefficient (*11*). After shaking, tubes were reopened and spiked with different aliquots of solution from either a stock TNT (50 mg L^{-1}) or RDX (30 mg L^{-1}) solution. Initial TNT concentrations ranged from 0-25 mg L^{-1} while for RDX ranged from 0-20 mg L^{-1}. Afterwards, the centrifuge tubes were recapped and shaken for another 24 h. After this second shaking period, tubes were centrifuged at 9500 rpm for 10 min. The supernatant was sampled and analyzed for TNT, RDX, and degradation products as described by EPA Method 8330 B (*12*). Sorbed munition constituents and their degradation products were extracted using methods described in EPA Method 8330 (*12*). Acetonitrile was added at a ratio of 1:5 soil to acetonitrile. The samples were sonicated overnight and syringe filtered (0.45um) and analyzed via HPLC. The solute distribution coefficient (K_D) was quantified from the slope of the linear fit of the data.

Column mobility experiments were performed by dry-packing the Memphis silt soil to a bulk density of 1.18 g cm^{-3} in duplicate 24-in x 8 in (diameter) Plexiglas columns (schematically presented in Fig. 1). Columns were first presaturated by leaching with a dilute $CaCl_2$ solution to stabilize the soils and prevent dispersion due to continuous leaching. Afterward, a solution containing 20 mg L^{-1} TNT and RDX (with residual HMX) with dilute $CaBr_2$ background was continuously leached at a flow rate of 2.5 ml min^{-1}. Leachate was collected via sampling ports positioned at three different intervals along the height of the column. Leachates were collected using micro-rhizome samplers manufactured by Rhisosphere Research Products, The Netherlands, and analyzed for MC and degradation products via HPLC (*12*). MC breakthrough was followed until dissolved MC concentration reached steady state. Afterwards, the columns were leached with only a dilute $CaBr_2$ solution and the depletion of MC was followed with time. Dissolved Br concentration was measured using Accumet ion-specific electrodes manufactured by Cole-Palmer Instrument Company, Vernon Hills, IL, the Br breakthrough curve (BTC) serving as the non-interactive tracer for the mobile solutes. Tracer BTCs were modeled using the models CFITM (*13*), a simplified equilibrium model included in the STANMOD software package (*14*) that provides an analytical solution to steady state transport problems. Solute dispersivities (D) were calculated from the dimensionless Peclet (Pe) number as, $Pe = vL/D$, where v = solute velocity, L = sample collection height, and t = time, R was calculated from Eq. 9 and a dimensionless pulse time (T_0) was also used. Since accurate measures of pore volume could only be obtained from the bottom sampling point, tracer curves were fitted at the bottom sampling point to obtain the solute R value. The tracer BTCs for the middle and top sampling points were then adjusted by modifying the pore volumes to represent that these curves exhibited the same R values. Adjusted BTCs were then inversed modeled

to confirm this in the R values. These adjusted pore volume values were then used in modeling the BTCs of the other solute curves.

TNT and RDX BTCs were modeled using CFITIM (*13*), a simplified non-equilibrium model also included in the STANMOD software package that provides analytical solution to steady-state transport problems. In addition to accounting for solute dispersivities (D), retention factors (R), and pulse time (T_0), this model includes two other terms: β = a nonequilibrium partitioning coefficient and ω for a mass transfer coefficient determining the rate of exchange between the mobile and immobile phases (*13*). For this modeling, ω was set at an initial value of 0.5.

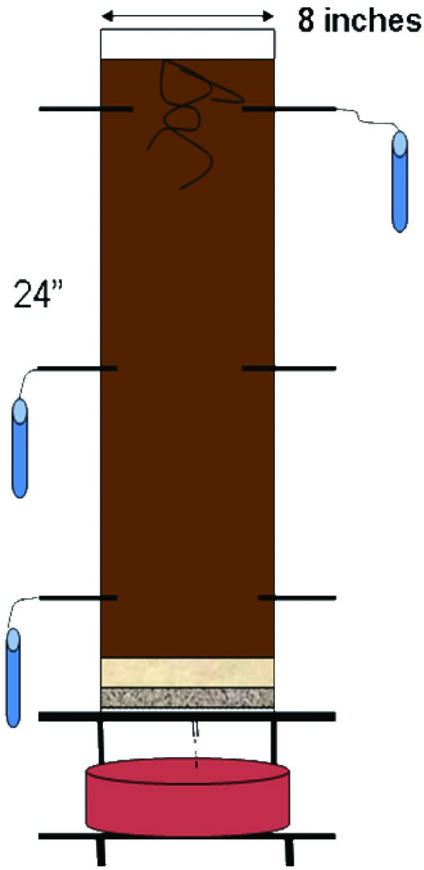

Figure 1. Schematic of the soil column for the mobility studies. (see color insert)

Results and Discussion

Sorption isotherms for TNT and RDX (Fig. 2) show relatively low sorption of the munitions on the silty Memphis soil. The sorption curves for both MCs are well described by the linear model, but the evidence of slight curvature in the TNT sorption curve (evidence of L-type sorption, Chapter 1) suggests that a Freundlich model may be appropriate as well. However, the linear sorption model is sufficient for our purposes here in this paper. The data shows that the Memphis silt soil exhibits a very weak preference for TNT and RDX. The KD value for TNT is virtually equivalent to straight partitioning. For RDX, the fitted KD values, indicated by the slope of the lines in Fig. 2, are comparable to what is commonly observed in the scientific literature, however, for TNT, KD value appears to be somewhat smaller than that typically observed. We attribute this, in part, to the sorption method detailed above, where the soil was allowed to rehydrate for 24 h before adding TNT. Chappell et al. (*11*) showed significant decrease in measured sorption coefficients for the triazine molecule atrazine with extended rehydration times of soils prior to sorption experiemtns. We assume that this rehydration effect, a product of sample handling, is responsible for the lower KD value. This effect (explained in more detail in Chapter 1) may also be related to the lack of detecting TNT degradation products from the extracted soils after conducting the isotherm.

Breakthrough curves for TNT and RDX are shown in Figure 3. For TNT, note that the BTC is shifted in pore volume (e.g., to the right with increasing depth) indicating increasing retention as the solute moves through the column profile. In addition, note that the maximum value for C/Co also decreases with depth in the column, beginning at approximately 0.9 for the top sampling port to approx. 0.6 for the bottom sampling port. Also, note the appearance of increased tailing of the BTCs as moving from the top to the bottom sampling ports. Since the adjustments of the Br tracer for the top and middle sampling ports were verified with modeling, we assume the shift in TNT breakthrough to be real, and indicative of reactions within the column. is associated with the microbial breakdown of the solute as it penetrates down the column into ammonium derivatives. Higher KD values for overall retention (increasing from 2.48 - 11.28 from top to bottom sampling ports, Table 1) were modeled. According to the model, the increase in KD is attributed to a decreased portioning to the soil mobile (dynamic) phase (e.g., decreasing β value) and an increased movement of solute in the immobile (stagnant) soil phase. Thus, this increase in KD value suggests TNT is being actively degraded in the column – increased retention and tailing with overall reduction of the maximum C/Co are likely attributed to the breakdown of the solute into ammonium-derivatives, which are expected to be highly adsorbing to the soil surface.

For RDX, the BTC for the top sampling port passed through maximum C/C_o = 0.8, which appears to be a result of the high error in the that plateau part of the curve. The BTCs for the middle and bottom sampling ports passed through a maximum of C/C_o of approx. 1, but appear progressively shifted to the right of the BTC for the top sampling port with depth of penetration. Modeling of the BTC curves show that R values were close to 1, with KD values increasing from 0.1 to 0.4 with increasing depth of the column. These values are actually similar to the KD value calculated from the sorption isotherms, suggesting that

RDX underwent minimal transformations/degradation reactions as it permeated through the column. Modeling shows reduction in dynamic RDX mobility (β) decreased only in the bottom sampling port, yet, this change was not captured in the differential distribution of solute to the immobile phase.

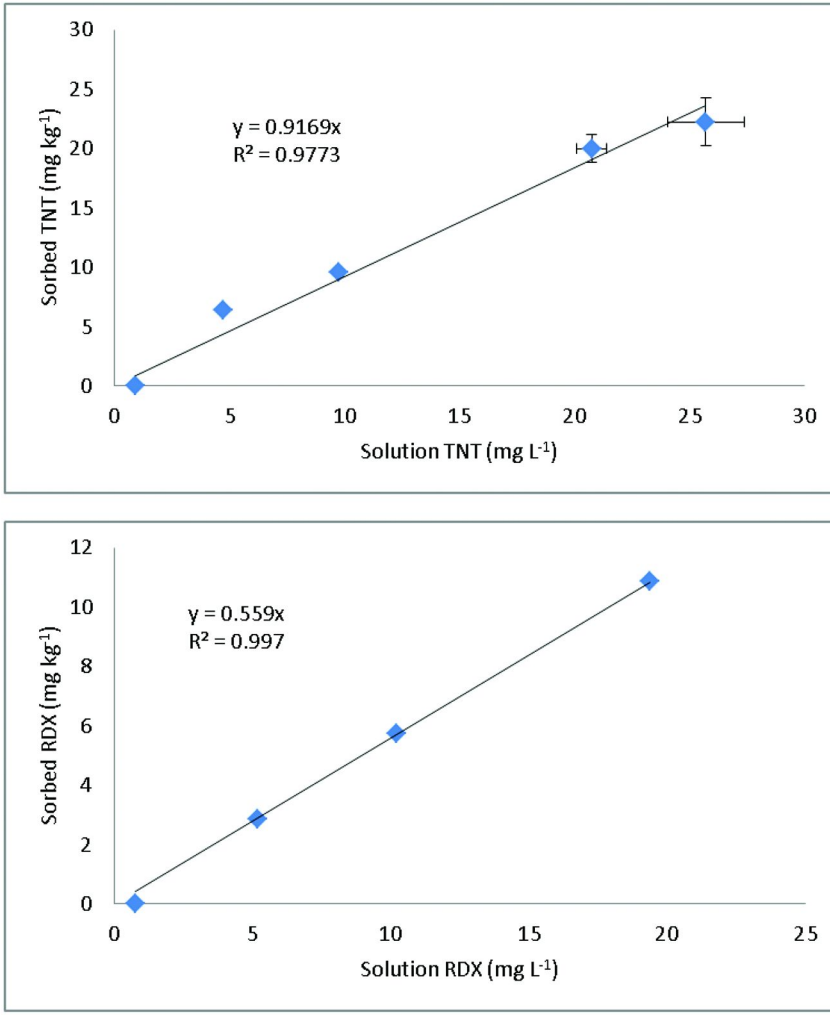

Figure 2. Sorption isotherms for TNT (top) and RDX (bottom) on Memphis silt soil. K_D values are indicated by the slope of the fitted line.

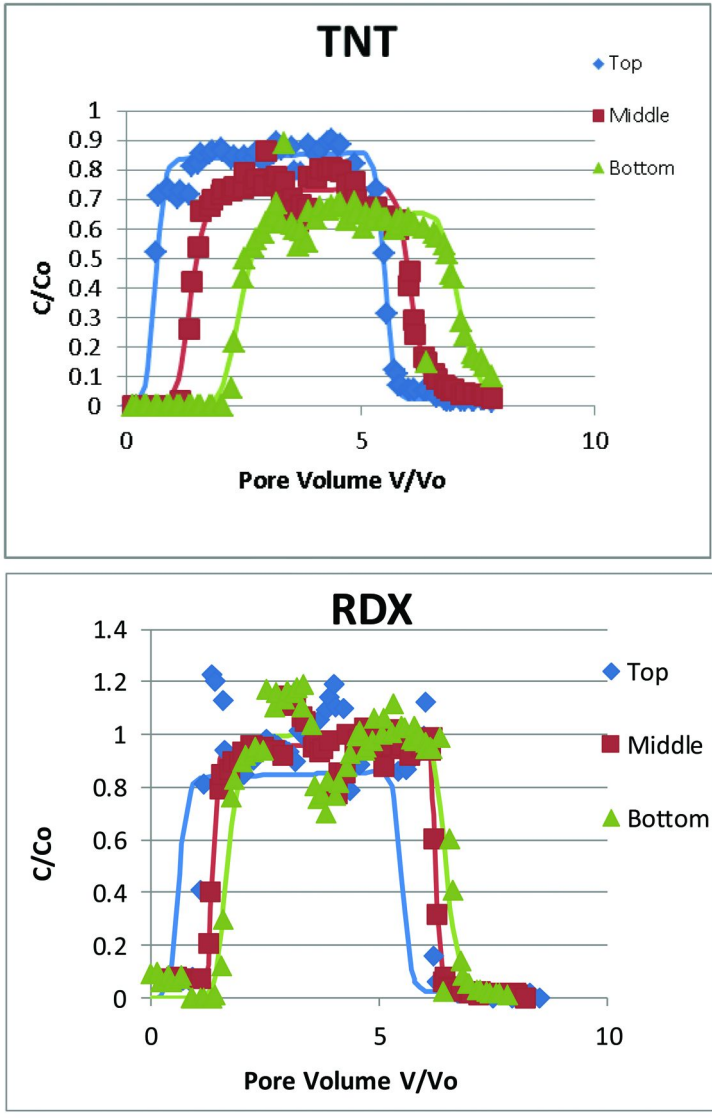

Figure 3. TNT and RDX breakthrough curves through duplicate columns dry-packed with Memphis silt soil and leached under water-saturated conditions (4). (see color insert)

Table 1. Fitted parameters from modeling of the TNT and RDX breakthrough curves (*4*).

Solute	*Position, L (cm)*	*D (cm^2 day^{-1})*	*R*	*β*	*ω*	T_0	K_D
TNT	Top (10.5)	137.0	5.5	0.26	0.23	4.82	2.45
	Middle (26)	1008.6	12.1	0.16	0.33	4.57	6.12
	Bottom (46.5)	1089.5	21.5	0.13	0.52	4.57	11.28
RDX	Top (10.5)	27.6	1.2	0.94	0.27	4.96	0.10
	Middle (26)	125.5	1.4	0.92	0.28	4.85	0.22
	Bottom (46.5)	870.1	1.7	0.52	0.28	4.76	0.39

The data in this chapter demonstrates changes in TNT and RDX mobility with increased depth of penetration in a soil column. For TNT, the data suggests the solute is actively degraded, and degradation products retained within the soil. On the other hand, RDX was virtually unaffected by movement through the soil column, exhibiting non-equilibrium partitioning coefficients similar to sorption coefficients determined in batch.

References

1. Rosen, G.; Lotufo, G. R. Toxicity and fate of two munition constituents in spiked sediment exposures with the marine amphipod *Eohasustorius estuarius*. *Environ. Toxicol. Chem.* **2005**, *24*, 2887–2897.
2. Lynch, J. C.; Brannon, J. M.; Delfino, J. J. Dissolution rates of three high explosive compounds: TNT, RDX, and HMX. *Chemosphere* **2002**, *47*, 725–734.
3. Borisover, M.; Graber, E. R. Relationship between strength of organic sorbate interactions in NOM and hydration effect on sorption. *Environ. Sci. Technol.* **2002**, *36*, 4570–4577.
4. Chappell, M. A.; Price, C. L.; Miller, L. F. Solid-phase considerations for the environmental fate of nitrobenzene and triazine munition constituents in soil. *Appl. Geochem.* **2011**, *26*, S330–S333.
5. Brannon, J. M.; Pennington, J. C. *Environmental fate and transport process descriptors for explosives*; ERDC/EL TR-02-10; U.S. Army Corps of Engineers, Vicksburg, MS, 2002.
6. Biggar, J. W.; Nielson, D. R. Miscible displacement: II. Behavior of tracers. *Soil Sci. Soc. Proc.* **1961**, *26*, 125–128.
7. Dane, J. H., Topp, G. C., Eds.; *Methods of Soil Analysis: Part 4 - Physical Methods*; Soil Science Society of America: Madison, WI, 2002; pp 1253−1536.
8. Jury, W. A.; Gardner, W. R.; Gardner, W. H. *Soil Physics*, 5th ed.; John Wiley & Sons, Inc.: New York, 1991.

9. Hillel, D. *Fundamental of soil physics*; Academic Press, Inc.,: San Diego, 1980.
10. van Genuchten, M. T. *Non-equilibrium transport parameters from miscible displacement experiments*; U.S. Salinity Laboratory, USDA, ARS: Riverside, CA, 1981.
11. Chappell, M. A.; Laird, D. A.; Thompson, M. L.; Li, H.; Aggarwal, V.; Teppen, B. J.; Johnston, C. T.; Boyd, S. A. Influence of smectite hydration and swelling on atrazine sorption behavior. *Environ. Sci. Technol.* **2005**, *39*, 3150–3156.
12. USEPA. *Nitroaromatics, nitramines, and nitrate esters by high performance liquid chromatography (HPLC). Method 8330B*; Office of Solid Waste and Emergency Response: Washington, DC, 2006.
13. van Genuchten, M. T. *Determining transport parameters from solute displacement experiments*; U.S. Salinity Laboratory, USDA, ARS: Riverside, CA, 1980.
14. Simunek, J.; van Genuchten, M. T.; Sejna, M.; Toride, N.; Leij, F. J. *The STANMOD computer software for evaluating solute transport in porous media using analytical solutons of convection-dispersion equation*, Versions 1.0 and 2.0; International Ground Water Modeling Center, Colorado School of Mines: Golden, CO, 1999.

Chapter 13

Transport of RDX and TNT from Composition-B Explosive During Simulated Rainfall

Richard A. Price,[1,*] Michelle Bourne,[1] Cynthia L. Price,[1] Jay Lindsay,[2] and Jim Cole[2]

[1]U.S. Army Engineer Research and Development Center (ERDC), 3909 Halls Ferry Road, Vicksburg, MS 39180
[2]Bowhead Technical and Professional Services, 4900 Seminary Road, Suite 1000, Alexandria, VA 22311-1811
[*]Richard A. Price@usace.army.mil

A complete understanding of the fate of munitions constituents (MC) on U.S. Army training lands is needed to develop the fundamental framework for the contaminant transport, transformation and fate (CTT&F) model for predicting the impacts of training activities on the distribution of MC in the environment. Explosive compounds RDX, TNT, and HMX derived from Composition-B explosive are of particular concern due to their toxicity potential and widespread use. This study evaluated distribution of these compounds from particulate Composition-B (Comp-B) following simulated rainfall in soil and plant mesocosms. Initial studies evaluated dissolution of MC from Comp-B with mass of Comp-B to water ratios ranging from 0.0125% to 12.5% and found soluble RDX and TNT was limited to < 5 mg L^{-1}. When Comp-B was agitated in suspended soil particles in runoff elutriates for 30 min, soluble RDX, HMX and TNT generally increased in clay, loam and sandy loam soils except for reduced RDX and no detectable HMX in sandy loam soil. Significantly lower soil calcium and/or higher iron in the sandy loam soil may have contributed to the reduced RDX and HMX. Rainfall simulations were conducted on soil plant mesocosms with bare upland soil, vegetated upland soil, and vegetated wetland soil in a flow

through system to monitor fate and transport of MC from Comp-B placed on the bare upland soil. The purpose of this was to determine effects of vegetated buffer zones on MC transport during rainfall events. Soluble concentrations of RDX and HMX were detected in runoff discharge from the bare upland soil but were significantly reduced following discharge through upland and wetland vegetation. TNT exhibited the greatest reduction in overland flow through upland vegetation with no detectable concentrations in discharge from the wetland. RDX and TNT were distributed in soil following overland flow of simulated rainfall with the higher concentrations remaining near the source zone. Upland plants had RDX and HMX concentrations exceeding soil concentrations indicating the plant uptake was a major route of RDX and HMX removal from the system. Following continued plant interaction with the RDX, HMX and TNT laden soils, dormant vegetation contained higher concentrations of RDX and HMX which was subsequently leached from the tissue to non-detectable concentrations after three rainfall events. These results indicate that the fate and transport of RDX, HMX and TNT in surface water runoff may be controlled by a number of complex, interacting factors including various soil chemical and physical properties, plant uptake and adsorption, and seasonal influences on release from cellulose residues. Further research is needed to quantify kinetics of adsorption, uptake degradation and release in vegetated systems.

Introduction

A complete understanding of the fate of munitions constituents (MC) on U.S. Army training lands is needed to develop the fundamental framework for the contaminant transport, transformation, and fate (CTT&F) model for predicting the impacts of training activities on the distribution of MC in the environment. Explosive compounds RDX (hexahydro-1,3,5-trinitro-1,3,5-triazine), TNT (2,4,6-trinitrotoluene), and HMX (octahydro-1,3,5,7-tetranitro-1,3,5,7-tetrazocine), derived from Composition-B explosive, are of particular concern due to their potential toxicity and widespread use. This study evaluated distribution of these compounds from particulate Comp-B following simulated rainfall in soil-plant mesocosms to determine the combined effects of overland flow, soil surface adsorption, and plant adsorption and uptake on transport of MC to receiving waters.

The distributed watershed CTT&F sub-model was developed to characterized spatial and temporal dynamics of chemicals from both point and non-point sources. CTT&F may be used in conjunction with distributed hydrologic and sediment transport models to quantify contaminant transport processes and certain chemical

reactions in watershed systems. This model can be used to study the environmental impacts of explosive compounds from military installations in surface water and groundwater quality (*1*).

Composition B has been a primary explosive frequently used post-WWII (*2*) in M67 and C-13 fragmentation grenades and a variety of artillery and mortar warheads (*3*), and it consists of 60% military grade RDX, which is composed of 90% RDX and 10% HMX, 39% military grade TNT, and 1% wax. These components can have detrimental health effects. Humans can be exposed to these components by drinking water, breathing air, and coming in contact with soil that is contaminated (*4*). Liver and blood damage, anorexia, anemia, and systemic poisoning affecting bone marrow and the liver are a few of the known health effects associated with exposure to Composition B constituents. In addition, TNT and RDX are considered possible human carcinogens (*4–7*).

Few studies have evaluated the dissolution rates of TNT, RDX, HMX and their associated degradation products from Comp-B explosive exposed to rainfall and surface runoff. Lynch (*4*) measured dissolution rates from molded Comp-B disks in a stirred fixed water volume, while Lever (*8*) collected particles of Comp-B from low-order field detonations and determined effects on surface and mass composition and dissolutions rates by continuous dripping of water onto the particles and described a drop-impingment model for rainfall driven dissolution. Additional laboratory studies using the methods in Lever (*8*) were conducted on Comp-B and other high explosives (*9*), and an outdoor study, using natural precipitation and particle exposure to the elements (*10*), were conducted to validate these models. While these studies determined dissolution rates and particle integrity over time from various exposures to water, they provide little knowledge on the fate of the constituaents of concern during precipitation events in the field. Previous studies by this author (*11–13*) developed rainfall simulation methods to predict surface runoff water quality from contaminated sites. These methods were first applied to explosives contaminated soil (*14*), and they determined significant effects from soil components and vegetation on transport of RDX and TNT in surface runoff water. This study is a result of those findings.

Materials and Methods

Dissolution in Water and Runoff Elutriates

Initial studies evaluated the dissolution of MC from Comp-B with Comp-B mass to water ratios ranging from 0.0125% to 12.5%. Particles of Comp-B were placed in 400 ml of de-ionized water and agitated on a horizontal shaker for 30 minutes at 72 rpm. Solid particles were removed by collection and filtering through 0.7 um glass-fiber filter, and filtered water was analyzed for explosives by USEPA Method 8330 (*15*). Runoff elutriates were prepared using three soil types (clay, loam, and sandy loam) to produce total suspended solid (TSS) concentrations of 50, 500, 5,000, and 50,000 mg L^{-1}. Each elutriate was spiked with 500 mg of particulate Comp-B, shaken, extracted, filtered, and analyzed as described above.

Simulated Runoff from Soil Mesocosms

In a flow-through system, rainfall simulations were conducted on soil-plant mesocosms with bare upland soil, vegetated upland soil, and vegetated wetland soil, to monitor the fate and transport of MC from Comp-B particulate placed on the bare upland soil. The purpose of this was to determine effects of vegetated buffer zones on MC transport in overland flow to receiving waters during rainfall events. Soil mesocosms were prepared with three soil types, clay, loam, and sandy loam, collected from Camp Bullis, TX, Vicksburg, MS, and Camp Shelby, MS, respectively. Three cells measuring 0.38 x 4.6 m were prepared with bare upland soil, upland soil with *Schizachyrium scoparium*, and wetland soil with *Cyperus esculentus,* and sloped at 1% to facilitate runoff flow. After plants reached maturity, the upper quarter surface of bare soil was spiked with 100 g of particulate Comp-B as shown in Figures 1A and 1B. Three replicates of rainfall were applied using a rainfall simulator system described by Price (*12*) at the rate of 5.46 cm hr^{-1} for 30 min. Runoff flowed from the bare upland, through the vegetated upland, and finally through the vegetated wetland before final discharge. Runoff rates were measured at the discharge from each transition, and samples were collected for physical and chemical analysis during each replicate. Soil and plant tissues were also collected before the first rainfall event and following the third rainfall event and analyzed for MC. The process was repeated on dormant vegetation.

Results and Discussion

Dissolution in Water and Elutriates

Most studies evaluating dissolution of Comp-B have involved simple exposure to deionized water. Particles of Comp-B in a training area landscape may be exposed to rainfall striking the particles as well as soil laden runoff water, which theorectically, may provide a more abrasive effect and increasing surface area of exposed Comp-B. It would also be considered, that the dissolution of Comp-B MC in water with increasing suspended soil particles and associated soil chemicals may limit the solubility of MC. The dissolution studies here found that soluble RDX and TNT were limited to < 4 mg L^{-1} in water alone (Figure 2) with TNT consistently higher than RDX and HMX. When Comp-B was agitated in suspended soil particles in runoff elutriates for 30 min, soluble RDX, HMX, and TNT generally increased with increasing TSS. However, in sandy loam soil, RDX significantly decreased to 0.2 mg L^{-1} at the highest TSS concentration and no HMX was detectable. Significantly lower soil calcium and/or higher iron in the sandy loam soil may have contributed to the reduced RDX and HMX. Elutriates prepared with the loam soil exhibited the highest RDX, HMX, and TNT concentrations of 6.2, 0.9, and 8.8 mg L^{-1}, respectively. Based on these results, soluble MC concentrations were not predicted to exceed these levels in rainfall runoff.

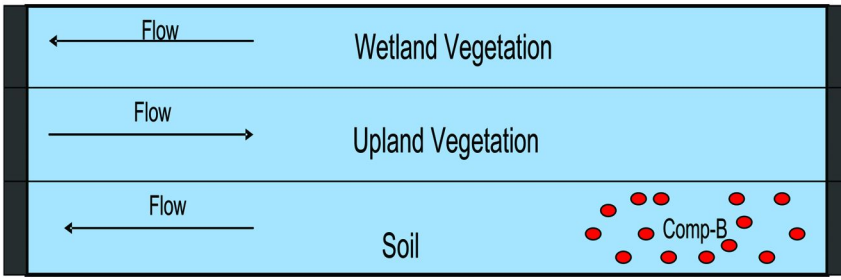

Figure 1A. Schematic of the soil mesocosm setup for simulated flow.

Figure 1B. Photograph showing the different mesocosms aligned in series from left to right. (see color insert)

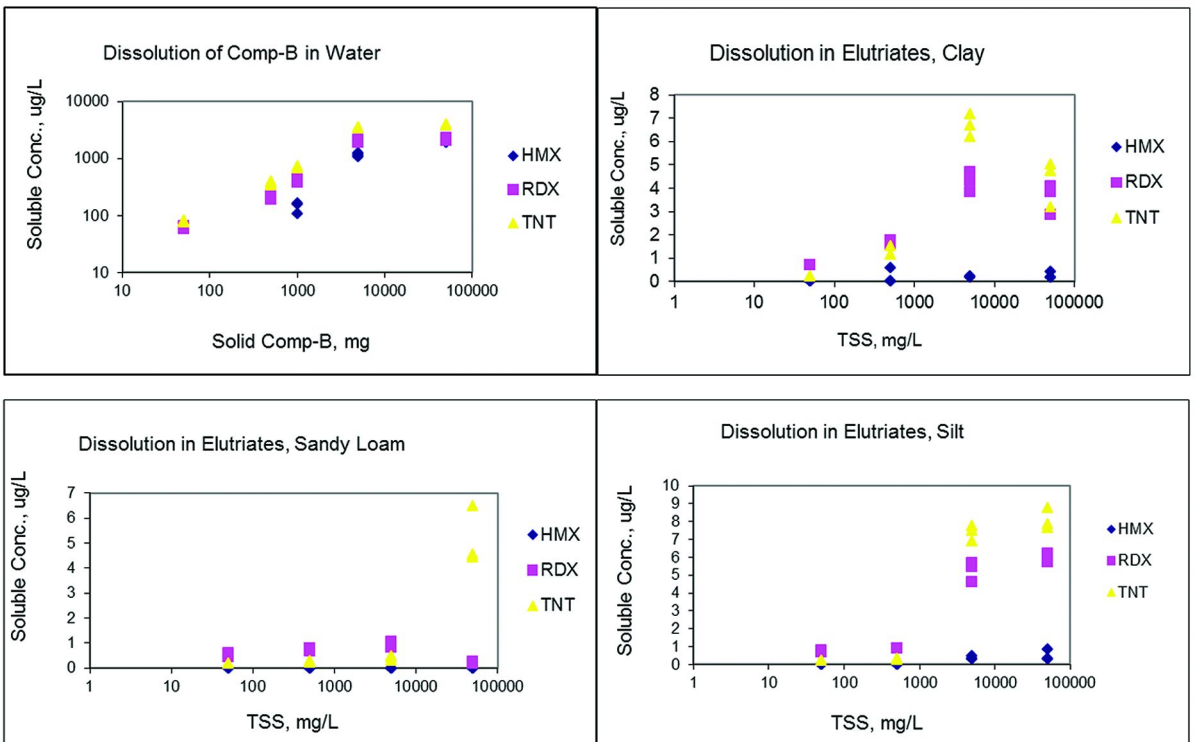

Figure 2. Dissolution of HMX, RDX, and TNT from Comp-B in Water, Clay, Sandy Loam, and Silt.

Simulated Rainfall Runoff

Figure 3 provides soluble and total concentrations of MC in runoff discharged from sandy loam bare upland, vegetated upland, and vegetated wetland during simulated rainfall on live and dormant plant cover. Soluble concentrations of RDX, HMX, and TNT were detected in runoff discharge from the bare upland soil but were significantly reduced following discharge through upland vegetation. Since the point source of Comp-B resided in the bare upland cell, the concentrations of MC should theoretically be reduced by a factor of 0.5 after each pass through the subsequent cell. The overland flow factor through the live vegetated upland cell was 0.43, 0.26, and 0.09 ug L^{-1} for HMX, RDX, and TNT, respectively. TNT exhibited the greatest rate of reduction in overland flow through upland vegetation with near detectable limit concentrations in discharge from the wetland cell. Results indicate a vegetated buffer of 18 and 27 m would be needed to reduce TNT and RDX/HMX to less than detectable limits of 0.4 ug L^{-1}, respectively.

Pre- and post-test analysis of soil and plant tissue for live and dormant rainfall events are shown for RDX in Tables 1 and 2. The highest concentrations of RDX in the soil were found near the source zone following overland flow of simulated rainfall with sporadic occurrences found throughout the entire system, likely transported with floatables (i.e., detritus). Soil loadings of RDX and TNT (Table 3) increased in the bare soil with continued rainfall events. Live upland plants had RDX and HMX concentrations exceeding soil concentrations, indicating the plant uptake was a major route of RDX and HMX migration from the soil and surface water. Following continued plant interaction with the RDX, HMX, and TNT laden soils, dormant vegetation contained higher concentrations of RDX and HMX, which subsequently leached from the dormant tissue to non-detectable concentrations after three rainfall events. TNT exhibited no active plant uptake but has been shown to be readily absorbed by plant detritus (*14*), which is the likely mechanism for TNT measured in the tissue here (Table 4).

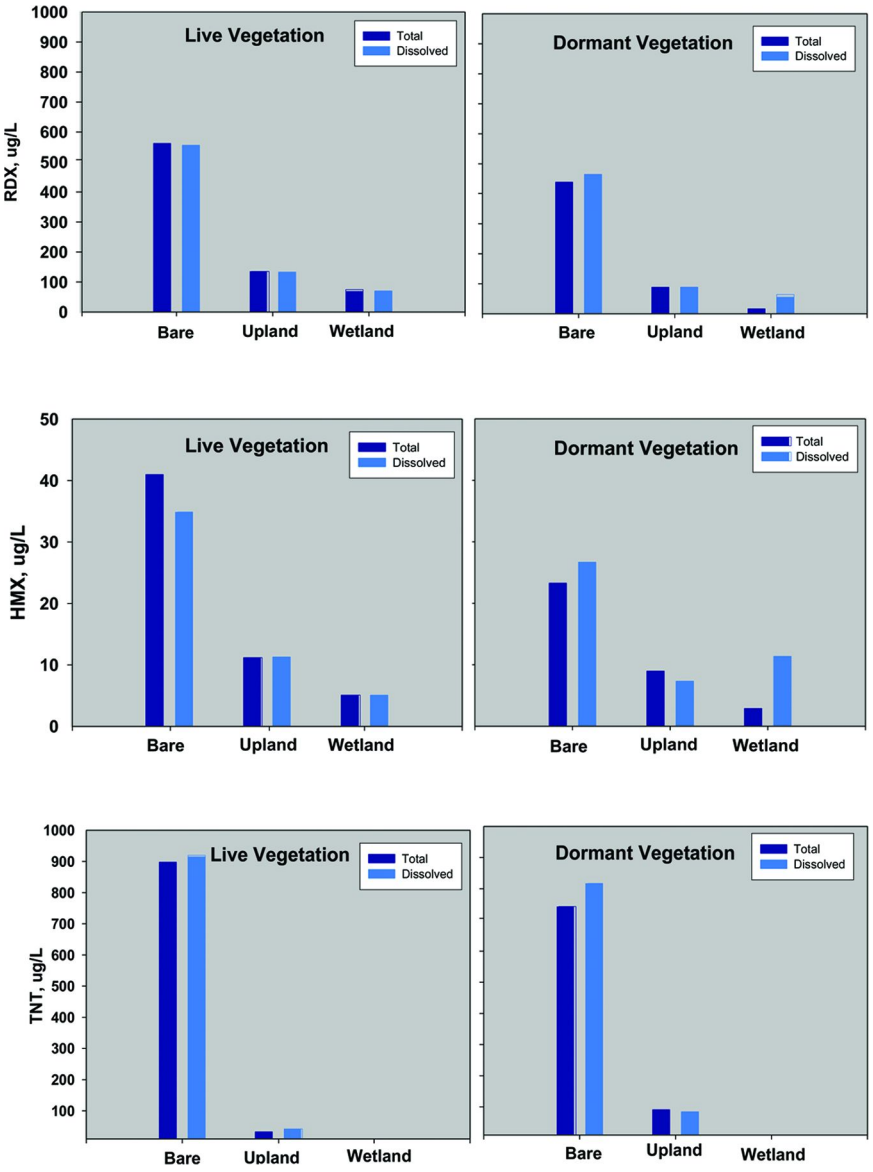

Figure 3. RDX, HMX, and TNT concentrations detected in the runoff of leached composition-B particles through different soil mesocosms connected in series.

Table 1. RDX distribution in soil following rainfall simulations, ug kg^{-1}.

Location	*PRE-LIVE*	*POST-LIVE*	*PRE-DORMANT*	*POST-DORMANT*
Bare 1	75	1340	730	3500
Bare 2	<100	770	1100	1950
Bare 3	<100	160	500	1020
Bare 4	<100	<100	180	185
Upland 1	<100	<100	<100	26
Upland 2	<100	55	<100	<100
Upland 3	55	230	<100	<100
Upland 4	<100	<100	<100	<100
Wetland 1	<100	115	<100	<100
Wetland 2	<100	2715	<100	<100
Wetland 3	<100	165	<100	<100
Wetland 4	<100	<100	<100	NA

Table 2. RDX distribution in plant tissue following rainfall simulations, ug kg^{-1}.

Location	*PRE-LIVE*	*POST-LIVE*	*PRE-DORMANT*	*POST-DORMANT*
Upland 1	<400	2270	3120	<400
Upland 2	<400	1570	1500	<400
Upland 3	<400	1070	1480	<400
Upland 4	<400	<400	<400	<400
Wetland 1	<400	<400	<400	<400
Wetland 2	<400	<400	<400	<400
Wetland 3	<400	755	<400	<400

Table 3. TNT distribution in soil following rainfall simulations, ug kg^{-1}.

Location	*PRE-LIVE*	*POST-LIVE*	*PRE-DORMANT*	*POST-DORMANT*
Bare 1	75 J	1830	650	3580
Bare 2	<100	<100	365	935
Bare 3	<100	105	145	510
Bare 4	<100	<100	<100	330
Upland 1	<100	85 J	<100	<100
Upland 2	<100	<100	<100	<100
Upland 3	80 J	80 J	<100	<100
Upland 4	<100	85 J	<100	<100
Wetland 1	<100	80 J	<100	<100
Wetland 2	<100	<100	<100	<100
Wetland 3	<100	115	<100	<100
Wetland 4	<100	<100	<100	NA

Table 4. TNT distribution in plant tissue following rainfall simulations, ug kg^{-1}.

Location	*PRE-LIVE*	*POST-LIVE*	*PRE-DORMANT*	*POST-DORMANT*
Upland 1	<400	1071	780	<400
Upland 2	<400	<400	<400	<400
Upland 3	<400	<400	<400	<400
Upland 4	<400	<400	820	<400
Wetland 1	<400	<400	<400	<400
Wetland 2	<400	<400	<400	<400
Wetland 3	<400	<400	<400	<400

Conclusions

Dissolution tests using Comp-B and site soil elutriates provided a conservative prediction of discharge of TNT, RDX, and HMX from a Comp-B source zone by rainfall runoff. Rainfall simulations indicate that the fate and transport of RDX, HMX, and TNT in surface water runoff may be controlled by a number of complex interacting factors. These include various chemical and physical soil properties, plant uptake and adsorption, and seasonal influences on release

from cellulose residues. TNT exhibited the greatest rate reduction in overland flow, while RDX and HMX exhibited greater plant uptake. It is expected that a vegetative buffer of at least 27 m in linear distance between the point of runoff exposed to surface distributed Comp-B and receiving waters would reduce surface water concentrations of RDX, HMX, and TNT to below detectable concentrations. Given the known dissolutions rates of toxic components from Comp-B explosive and the results shown here, training range managers can establish exclusion zones to ensure sufficient buffer between target areas and riparian habitats to protect water quality. For the most part, U.S. Army training ranges are already doing this where white phororous munitions are being used. Further research on the fate of Comp-B in runoff to quantify kinetics of soil adsorption and uptake by plants, degradation, and long-term fate in soil rhizospheres can improve contaminant fate models that can be used by installation managers to make sound management decisions based on specific training range soils and landscape characteristics.

References

1. Johnson, B. E.; Zhang, Z. *CTT&F: Distributed sources chemical transport, transformation and fate sub-model*; ERDC TN-EQT-06-1; U.S. Army Engineer Research and Development Center: Vicksburg, MS, 2006.
2. Clausen, J.; Robb, J.; Curry, D.; Korte, N. A case study of contaminants on military ranges: Camp Edwards, Massachusetts, USA. *Environ. Pollut.* **2004**, *129*, 13–21.
3. Jenkins, T. F.; Hewitt, A. D.; Grant, C. L.; et al. Identity and distribtution of residues of energetic compounds at army live-fire training ranges. *Chemosphere* **2006**, *63*, 1280–1290.
4. Lynch, J. C.; Brannon, J. M.; Delfino, J. J. Dissolution rates of three high explosive compounds: TNT, RDX, and HMX. *Chemosphere* **2002**, *47*, 725–734.
5. ATSDR. TNT Fact Sheet, 1996. Available from http://www.atsdr.cdc.gov/tfacts81.html.
6. ATSDR. RDX Fact Sheet, 1996. Available from http://www.atsdr.cdc.gov/tfacts78.html.
7. ATSDR. HMX Fact Sheet, 1997. Available from http://www.atsdr.cdc.gov/tfacts98.html.
8. Lever, J.; Taylor, S.; Perovich, L.; Bjella, K.; Packer, B. *Environ. Sci. Technol.* **2005**, *39*, 8803–8811.
9. Taylor, S.; Lever, J.; Fadden, J.; Collins, P.; Perron, N.; Packer, B. *Chemosphere* **2009**, *77*, 1338–1345.
10. Taylor, S.; Lever, J. H.; Fadden, J.; Perron, N.; Packer, B. *Chemosphere* **2009**, *75*, 1074–1081.
11. Skogerboe, J. G.; Lee, C. R.; Price, R. A. Rainfall-Runoff Water Quality From a Contaminated Upland Dredged Material Disposal Site. *Proceedings of the International Conference, Heavy Metals in the Environment*; 1985; Vol. 2, p 30−32.

12. Price, R. A.; Skogerboe, J. G.; Lee, C. R. *Predicting surface runoff water quality from upland disposal of contaminated dredged material*; Dredging Research Tech. Note EEDP-02-25; 1998.
13. Price, R. A.; Skogerboe, J. G. *Simplified Laboratory Runoff Procedure (SLRP): Procedure and Application*; Dredging Research Tech. Note EEDP-02-29; 1999.
14. Price, R. A.; Larson, S. L. *Mobility of Explosives During Bioreclamation Processes*; Agronomy Abstracts, 1999 Annual Meeting; 1999; p 13.
15. USEPA. *Nitroaromatics and nitramines by HPLC. Second Update SW846, Method 8330*; Office of Solid Waste and Emergency Response: Washington, DC,1994.

Chapter 14

The Contaminant Transport, Transformation, and Fate Sub-Model for Predicting the Site-Specific Behavior of Distributed Sources (Munitions Constituents) on U.S. Army Training and Testing Ranges

Zhonglong Zhang*,[1] and Billy E. Johnson[2]

[1]BTS, Environmental Laboratory, U.S. Army Engineer Research and Development Center, CEERD-EP-W, 3909 Halls Ferry Road, Vicksburg, MS 39180

[2]Environmental Laboratory, U.S. Army Engineer Research and Development Center, CEERD-EP-W, 3909 Halls Ferry Road, Vicksburg, MS 39180

***zhonglong.zhang@usace.army.mil**

Contaminant Transport, Transformation and Fate (CTT&F) sub-model was developed for coupling with existing watershed hydrological modeling systems to predict the site-specific behavior of distributed sources (munitions constituents) on U.S. Army training and testing ranges. Physical transport and transformation processes across the land surface are simulated using distributed approach and routed through channels to the watershed outlet. The CTT&F sub-model includes the ability to represent explosive contaminant processes at the watershed scale including: partitioning of contaminants to solid particles, freely dissolved, dissolved organic carbon (DOC) bound dissolved, and sediment sorbed particulates, erosion and settling of particle associated contaminants, diffusive and mixing exchanges across the water column and upper soil (sediment) interface. CTT&F has the capability to simulate biodegradation, hydrolysis, oxidation, photolysis, volatilization, dissolution, and other transformation processes. To demonstrate model capabilities, CTT&F was coupled with

a Gridded Surface Subsurface Hydrologic Analysis (GSSHA) model, then tested and validated to simulate RDX and TNT transport and transformation using two experimental plots. These experiments examined dissolution of solid contaminants into the dissolved phase and their subsequent transport to the plot outlet. Model results were in close agreement with measured data. Such model can be used to forecast the fate of munitions constituents within and transported from training ranges and to assess range management strategies to protect human and environmental health.

Introduction

The U.S. military operates munitions test and training ranges covering tens of millions of acres of land and waters throughout the United States (*1*). Many active and formerly used Defense sites (FUDS) have soil, sediment, surface water, and groundwater environments contaminated with explosives as a result of munitions fired, dropped, and disposed of on those ranges (*2*, *3*). When a conventional explosive munitions detonates, it releases a large variety of chemical compounds and metals into the environment. Solid particles ranging in size from small to large (up to the diameter of the projectile) may be deposited on the soil surface (*4*, *5*). At open burn/open detonation and explosive, ordnance, and demolition sites, RDX, HMX, TNT, NG, aDNT, and DNT can be found (*6*), which are of particular concern due to their potential toxicity to aquatic organisms and risk to human health. A discussion of explosive compounds expected for different types of ranges can be found in Clausen et al. (*7*). Another concern is heavy metals such as lead, cadmium, chromium, nickel, copper, and barium (*1*). Clausen and Korte (*8*) reported that small arms firing ranges at military training facilities can have enormous heavy metal burdens in soils.Once introduced into the environment, rainfall encountering these chemical compounds and metals can partially dissolve and thus may migrate with the infiltrating water deeper into the soil or as surface runoff. Any remaining dissolved materials may react with the soil matrix and adsorb onto soil particles and/or adsorb to dissolved organic carbon (DOC). In select range assessment detection of one component of Comp B, RDX, has been observed in groundwater on military training ranges (*9*) and thus necessitates the continued vigilance in regards to monitoring and assessing the potential for constituent migration.

Assessing watershed-scale impacts of contaminated sites on water quality is a major component towards determining long-term military installation sustainability. Correspondingly, it is also necessary to estimate those quantities and attempt to determine where they all migrate. Such needs are increasingly achieved with the development of mathematical models that incorporate the processes of contaminant transport and transformations and the degree to which they are affected by human activities. One of the main characteristics of live fire training range munitions constituent (MC) loading is the spatial variability and its relation to landuse. On these sites, contaminant simulation models require a

distributed modeling approach because distributed models can account for spatial heterogeneity and allow for more accurate predictions due to changes in the landscape (e.g., topographic, landuse, MC distribution, soil texture, etc).

A distributed modeling approach, as part of watershed management to meet water quality goals, is not new. Considerable advances have been made in hydrologic modeling in recent years (*10–13*). However, modeling the transport and fate of distributed sources and the phase distribution of contaminants is complex and has not received much attention for military installations and relevant contaminants. In particular, less effort has been devoted to studies simulating dissolution of solid contaminants and their associated multiphase partitioning transport at the watershed scale. The limitations of existing watershed models motivated development of a physically based, distributed source Contaminant Transport, Transformation and Fate (CTT&F) sub-model by the U.S. Army Engineer Research and Development Center (ERDC).

Specifically, the CTT&F sub-model describes transport and transformation of contaminants through the various landscape media in a watershed. It operates on a cell by cell basis, allowing analyses at each cell within a watershed. Further, CTT&F can be linked to spatially distributed hydrologic models such as GSSHA (Gridded Surface Subsurface Hydrologic Analysis) (*11*), CASC2D (CASCade of planes in 2-Dimensions) (*14–16*), TREX (Two-Dimensional Runoff Erosion and Export) (*13*), and others, assuming that the underlying watershed model provides required hydrological and sediment transport fluxes. In grid-based models, landscape features and other characteristics can be varied spatially among cells and contaminants routed from each source cell and through down-gradient cells from the watershed divide to the outlet. The distributed, process-oriented structure of the CTT&F sub-model facilitates identification of critical source areas within the watershed and can give insight to contaminant fate and persistence (*10*, *13*, *17–19*).

The objectives of this research were to: (1) describe the movement and redistribution of contaminants across the overland plane or through a channel network throughout a watershed and the algorithms of the spatially distributed contaminant transformations; (2) develop the CTT&F sub-model; and (3) validate the performance of the CTT&F sub-model by calibration to test plot measurements of RDX and TNT concentrations in runoff.

This development effort differs from previous efforts in that it focuses on transport and transformation of contaminants rather than runoff and sediment erosion caused by rainfall events. The model was designed to simulate four distinct contaminant phases, three of which are equilibrium (dissolved, bound, and particle-sorbed) and one of which is non-equilibrium (solid granular phase). The expectation is that a model of this type can quantify important transport and transformation processes for multiple contaminants and facilitate assessment of distributed sources, leading to better management of watersheds associated with military installations. The dissolution and transport capabilities are demonstrated by plot studies supported by the U.S. Army Corps of Engineers (USACE) Environmental Quality Technology (EQT) Research Program. Contaminants of concern in this study were TNT and RDX. Although applied for military

explosives, CTT&F formulations are general and are applicable to other contaminants as well.

Watershed Modeling Framework

Flow water is the primary mechanisms for movement of distributed contaminants in watersheds. To simulate the contaminant transport and fate, it is necessary to estimate beforehand the watershed flow and sediment transport driven by the hydrological processes. The hydrological variables required to drive the CTT&F sub-model can be calculated using any physically based distributed watershed model capable of producing a reasonable simulation of the watershed flow and sediment transport fields. These include, (1) for surface transport: overland flow depth, flow in the coordinate directions, sediment load, and sediment concentration and (2) for subsurface transport: soil moisture and hydraulic head at various depths in the soil.

The major components of the fully distributed modeling framework are hydrology, sediment transport, and contaminant transport. Each of the major components can be viewed as sub-models within the overall framework. The calculations for each process at any time level are independent and information is carried forward from hydrology to sediment transport to contaminant transport in order to generate a concentration solution. At any time level, flow is assumed to be unaffected by sediment and chemical transport, and sediment transport is unaffected by contaminant transport, so calculations for these three components (sub-models) have a natural hierarchy (Figure 1).

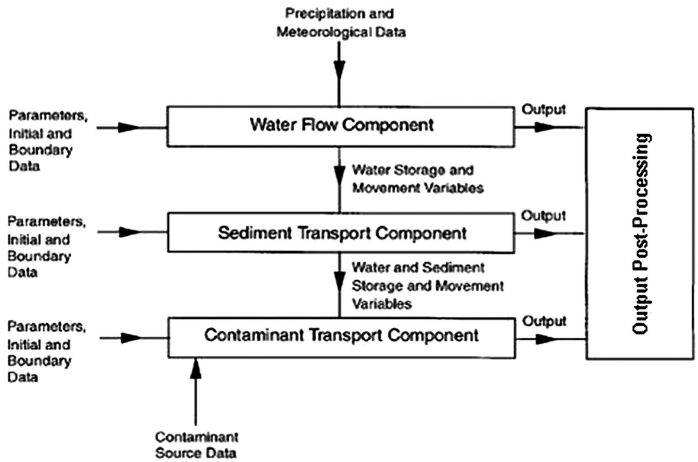

Figure 1. CTT&F modeling system framework (12).

The U.S. Army Corps of Engineer's Gridded Surface Subsurface Hydrologic Analysis (GSSHA) is a physically-based, distributed-parameter, structured grid, hydrologic model that simulates the hydrologic response and sediment transport of a watershed subject to given hydrometeorological inputs. The watershed is divided into grid cells that comprise a uniform finite difference grid. GSSHA is a reformulation and enhancement of the CASC2D (Figure 2). The model incorporates 2D overland flow, 1D stream flow, 1D unsaturated flow and 2D groundwater flow components. Within GSSHA, sediment erosion and transport processes take place both on the land and within the channel. The GSSHA model employs mass conservation solutions of partial differential equations and closely links the hydrologic components to assure an overall mass balance. GSSHA had already been tested and applied for hydrologic response and sediment transport in several watersheds and achieved satisfactory results (*20*). Following is a brief introduction to GSSHA. Details of the GSSHA model can be found in Downer and Ogden (*11*). A review of hydrologic and sediment erosion and transport process descriptions is informative to illustrate the physics behind individual process representations and specific to those needed to drive a full CTT&F sub-model.

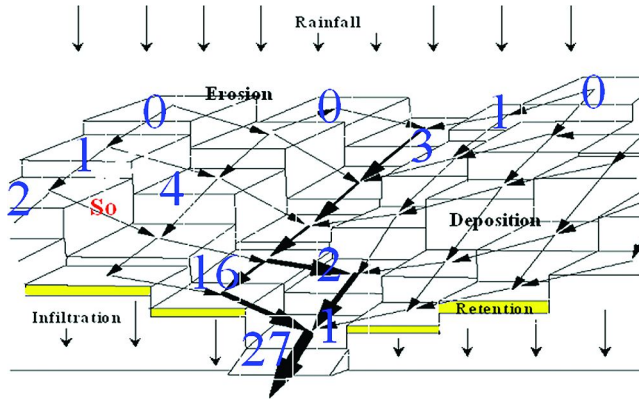

Figure 2. Topographical representation of overland flow and channel routing schemes within a watershed.

Hydrologic Processes

Modeling hydrologic process begins with rainfall being added to the watershed, some of which is intercepted by the canopy cover, evapotranspirated or infiltrated. Hydrologic processes that can be simulated and methods used to approximate the processes with the GSSHA model are listed in Table 1.

Table 1. Processes and approximation techniques in the GSSHA model

Process	*Approximation*
Precipitation distribution	Thiessen polygons (nearest neighbor) Inverse distance-squared weighting
Snowfall accumulation and melting	Energy balance
Precipitation interception	Empirical two parameter
Overland water retention	Specified depth
Infiltration	Green and Ampt (GA) Multi-layered GA Green and Ampt with Redistribution GAR) Richard's equation (RE)
Overland flow routing	2-D diffusive wave
Channel routing	1-D diffusive wave
Evapo-transpiration	Deardorff Penman-Monteith with seasonal canopy resistance
Soil moisture in the vadose zone	Bucket model RE
Lateral groundwater flow	2-D vertically averaged
Stream/groundwater interaction	Darcy's law
Exfiltration	Darcy's law

GSSHA uses two-step, finite-volume schemes to route water for both 2D overland flow and 1D channel flow where flows are computed based on heads and volumes are updated based on the computed flows. Several modifications were made to both the GSSHA channel routing and the overland flow routing schemes to improve stability, and allow interaction between the surface and subsurface components of the model. The combination of improvements in the stability of the overland and channel routing schemes has allowed significant increases in model computational time steps over CASC2D.

Overland Flow Routing

Water flow across the land surface is shallow, unsteady, and non-uniform. This flow regime can be described by the Saint-Venant equations which are derived from physical laws regarding the conservation of mass and momentum. Overland flow routing in GSSHA employs the 2D diffusive wave equation, which allows for backwater and reverse flow conditions. The 2D (vertically integrated) continuity equation for gradually-varied flow over a plane in rectangular (x, y) coordinates is (*16*):

$$\frac{\partial h}{\partial t} + \frac{\partial q_x}{\partial x} + \frac{\partial q_y}{\partial y} = i_e \tag{1}$$

where h = surface water depth [L], q_x, q_y = unit discharge in the x- or y-direction = Q_x/B_x, Q_y/B_y [L^2/T], Q_x, Q_y = flow in the x- or y-direction [L^3/T], B_x, B_y = flow width in the x- or y-direction [L], i_e = excess net precipitation rate [L/T].

The diffusive wave momentum equations for the x- and y-directions are written as:

$$S_{fx} = S_{0x} - \frac{\partial h}{\partial x} \tag{2a}$$

$$S_{fy} = S_{0y} - \frac{\partial h}{\partial y} \tag{2b}$$

where S_{fx}, Sf_y = friction slope (energy grade line) in the x- or y-direction, $S0_x$, $S0_x$ = ground surface slope in the x- or y-direction.

Channel Flow Routing

Channel flow routing in GSSHA employs the 1D diffusive wave equation. The 1D (laterally and vertically integrated) continuity equation for gradually-varied flow along a channel is (*16*):

$$\frac{\partial A}{\partial t} + \frac{\partial Q}{\partial x} = q_l \tag{3}$$

where A = cross sectional area of channel flow [L^2], Q = total discharge [L^3/T], and q_l = lateral flow into or out of the channel [L^2/T].

Sediment Transport

Sediment erosion and transport are potentially very important processes in water quality modeling. Excess sediment affects water quality directly by itself. Sediment transport also influences chemical transport and fate. Suspended sediments act as carriers of chemicals in the watershed flow. Many chemicals sorb strongly to sediment and thus undergo settling, scour, and sedimentation. Sorption also affects a chemical's transfer and transformation rates. The amount of chemicals transported by the sediments depends on the suspended sediment concentration and the sorption coefficient. Both sediment transport rates and concentrations must be estimated in most toxic modeling studies. The sediment algorithm is included as a sub-model in the GSSHA and invoked only when sediment simulation is required. The sediment sub-model is designed for estimating sediment delivery and channel transport in watersheds. It consists of four primary components: (1) sediment transport; (2) erosion; (3) deposition; and (4) bed processes (bed elevation dynamics).

Sediment Transport

The sediment transport models are based on the suspended sediment mass conservation equation (advection-diffusion equation with the sink-source term describing sedimentation resuspension rate) and the equation of bottom deformation. For the overland plane in 2D, the concentration of particles in a flow is governed by conservation of mass (sediment continuity) (*21*):

$$\frac{\partial C_{ss}}{dt} + \frac{\partial \hat{q}_{tx}}{\partial x} + \frac{\partial \hat{q}_{ty}}{\partial y} = \hat{J}_e - \hat{J}_d + \hat{W}_s = \hat{J}_n \tag{4}$$

where C_{ss} = concentration of sediment particles in the flow [M/L^3], $\hat{q}_{tx}$, $\hat{q}_{ty}$ = total sediment transport areal flux in the x- or y-direction [M/L^{2}T], $\hat{J}_e$ = sediment erosion volumetric flux [M/L^{3}T], $\hat{J}_d$ = sediment deposition volumetric flux [M/L^{3}T], $\hat{W}_s$ = sediment point source/sink volumetric flux [M/L^{3}T], $\hat{J}_n$ = net sediment transport volumetric flux [M/L^{3}T].

The total sediment transport flux in any direction has three components, advection, dispersion (mixing), and diffusion, and may be expressed as (*21*):

$$\hat{q}_{tx} = u_x C_{ss} - \left(R_x + D\right)\frac{\partial C_{ss}}{\partial x} \tag{4a}$$

$$\hat{q}_{ty} = u_y C_{ss} - \left(R_y + D\right)\frac{\partial C_{ss}}{\partial y} \tag{4b}$$

where u_x, u_y = flow (advective) velocity in the x- or y-direction [L/T], R_x, R_y = dispersion (mixing) coefficient the x- or y-direction [L^2/T], D = diffusion coefficient [L^2/T].

Note that both dispersion and diffusion are represented in forms that follow Fick's Law. However, dispersion represents a relatively rapid turbulent mixing process while diffusion represents a relatively slow Brownian motion, random walk process (*22*). In turbulent flow, dispersive fluxes are typically several orders of magnitude larger than diffusive fluxes. Further, flow conditions for intense precipitation events are usually advectively dominated as dispersive fluxes are typically one to two orders smaller than advective fluxes. As a result, both the dispersive and diffusive terms may be neglected.

Similarly, the suspended sediment transport in channels is described by the 1-D advection-diffusion equation that includes a sink-source term describing sedimentation and resuspension rates and laterally distributed inflow of sediments. The concentration of particles in flow is governed by the conservation of mass (*21*):

$$\frac{\partial C_{ss}}{\partial t} + \frac{\partial \hat{q}_{tx}}{\partial x} = \hat{J}_e - \hat{J}_d + \hat{W}_s = \hat{J}_n \tag{5}$$

Individual terms for the channel advection-diffusion equation are identical to those defined for the overland plane. Similarly, the diffusive flux term can be neglected. The dispersive flux is expected to be larger than the corresponding term

for overland flow. However, the channel dispersive flux still may be neglected relative to the channel advective flux during intense runoff events.

Sediment Erosion and Deposition

In the overland plane, sediment particles can be detached from the bulk soil matrix by raindrop impact and entrained into the flow by hydraulic action when the exerted shear stress exceeds the stress required to initiate particle motion (*23*). The overland erosion process is influenced by many factors including precipitation intensity and duration, runoff length, surface slope, soil characteristics, vegetative cover, exerted shear stress, and sediment particle size. In channels, sediment particles can be entrained into the flow when the exerted shear stress exceeds the stress required to initiate particle motion. For non-cohesive particles, the channel erosion process is influenced by factors such as particle size, particle density and bed forms. For cohesive particles, the erosion process is significantly influenced by inter-particle forces (such as surface charges that hold grains together and form cohesive bonds) and consolidation. The surface erosion algorithm represents the mechanisms by which sediment is eroded from hillslopes and transported to the stream or channel network. Entrainment rates may be estimated from site-specific erosion rate studies or, in general, from the difference between sediment transport capacity and advective fluxes:

$$\begin{aligned} v_r &= \frac{J_c - v_a C_{ss}}{\rho_b} \qquad J_c > v_a C_{ss} \\ v_r &= 0 \qquad\qquad\quad J_c \le v_a C_{ss} \end{aligned} \tag{6}$$

where v_r = resuspension (erosion) velocity [L/T], J_c = sediment transport capacity areal flux [M/L^2/T], v_a = advective (flow) velocity (in the x- or y-direction) [L/T].

The rate of sediment deposition is proportional to the sediment concentration and settling velocity. If the sediment transport capacity is lower than the sediment load, sediment deposition occurs. The process of sediment deposition is highly selective, the settling velocity of an aggregate or particle being a function of its size, shape, and density. Coarse particles (*>62 μm*) are typically non-cohesive and generally have large settling velocities under quiescent conditions. Numerous empirical relationships to describe the non-cohesive particle settling velocities are available. For non-cohesive (fine sand) particles with diameters from *62 μm* to *500 μm*, the settling velocity can be computed as (*24*):

$$v_{sq} = \frac{\nu}{d_p}\left[\left(25 + 1.2{d_*}^2\right)^{0.5} - 5\right]^{1.5} \tag{7a}$$

$$d_* = d_p\left[\frac{(G-1)g}{\nu^2}\right]^{1/3} \tag{7b}$$

where v_{sq} = quiescent settling velocity [L/T], ν = kinematic viscosity of water [L^2/T], and d_* = dimensionless particle diameter.

Fine particles often behave in a cohesive manner. If the behavior is cohesive, flocculation may occur. Floc size and settling velocity depend on the conditions under which the floc was formed (*25*, *26*). As a result of turbulence and other factors, not all sediment particles settling through a column of flowing water will necessarily reach the sediment-water interface or be incorporated into the sediment bed. Beuselinck et al. (*27*) suggested this process also occurs for the overland plane. When flocculation occurs, settling velocities of cohesive particles can be approximated by relationship of the form (*28*):

$$v_s = a \cdot {d_f}^m \tag{8a}$$

$$v_{se} = P_{dep} v_s \tag{8b}$$

where v_s = floc settling velocity [L/T], a = experimentally determined constant, d_f = median floc diameter [L], m = experimentally determined constant, v_{se} = effective settling (deposition) velocity [L/T], and P_{dep} = probability of deposition.

Upper Sedimentation Processes

The upper soil and sediment bed play important roles in the transport of contaminants. Once a particle erodes, it becomes part of the flow and is transported downstream within the watershed. The fluxes of the channel erosion and sedimentation control the dynamics of the uppermost contaminated layer. Particles and associated contaminants in the surficial sediments may enter deeper sediment layers by burial or be returned to the water column by scour. Whenever burial/scour occurs, particles and associated contaminants are transported through each subsurface sediment segment within a vertical stack.

In response to the difference between bed form transport, erosion, and deposition fluxes, the net addition (burial) or net loss (scour) of particles from the bed causes the bed surface elevation to increase or decrease. The rise or fall of the bed surface is governed by the sediment continuity (conservation of mass) equation, various forms of which are attributed to Exner equation (*29*). Julien (*21*) presents a derivation of the bed elevation continuity equation for an elemental control volume that includes vertical and lateral (x- and y-direction) transport terms. Neglecting bed consolidation and compaction processes, and assuming that only vertical mass transport processes (erosion and deposition) occur, the sediment continuity equation for the change in elevation of the soil or sediment bed surface may be expressed as:

$$\rho_b \frac{\partial z}{dt} + v_{se} C_{ss} - v_r C_{sb} = 0 \tag{9}$$

where z = elevation of the soil surface [L], ρ_b = bulk density of soil or bed sediments [M/L^3], C_{sb} = concentration of sediment at the bottom boundary [M/L^3].

Contaminant Transport, Transformation and Fate Sub-Model

In a watershed, contaminants may be transferred between phases and may be degraded by any of a number of chemical and biological processes. CTT&F uses physically based governing equations that describe the major physical transport and biochemical processes affecting contaminants in a watershed. The governing equations are based on mass conservation for a differential control volume. Mathematical modeling of contaminant transport processes involves simultaneous solution of governing equations for the water column and the underlying bed. An overview of processes in the CTT&F sub-model is presented in Figure 3, where the system is represented as two compartments: water column (runoff or surface water) and surface soil or sediment.

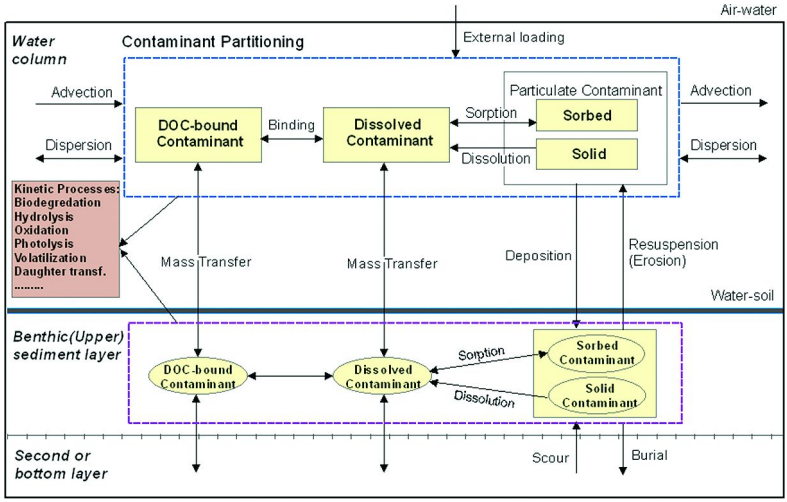

Figure 3. Schematic chart of the key processes simulated by CTT&F sub-model (13).

Four Phase Partitioning and Distribution of Contaminants

Explosive contaminants on training ranges are commonly present as crystalline solids (*30*). For purposes of realistic contaminant transport modeling and range assessment, four contaminant phases are modeled: solid particles, freely dissolved, dissolved organic carbon (DOC) bound dissolved, and sediment sorbed particulates:

$$C_{TT} = C_s + C_T = C_s + C_d + C_b + C_p \tag{10}$$

where C_s = solid particle concentration [M/L^3], C_d = free dissolved phase concentration [M/L^3], C_b = DOC bound phase concentration [M/L^3], C_p = sediment sorbed phase concentration [M/L^3], C_T = total non-solid phase concentration [M/L^3], and C_{TT} = total contaminant concentration [M/L^3].

Solid particle contaminants are treated as a separate, non-equilibrium phase and then are represented in the sediment sub-model as reactive particles that can dissolve over time and enter into water by a kinetic (rate limited) dissolution process. Once dissolved into water, the contaminant is subject to redistribution among the other three phases.

In order to model the three phases, distribution coefficients are used to describe the fraction of total non-solid contaminant associated between freely dissolved, DOC-bound dissolved, and sediment sorbed particulates. Partitioning reactions are usually fast relative to other environmental processes, and local equilibrium may be assumed to exist between the freely dissolved (aqueous), DOC-bound phases, and sediment particle-sorbed. Equilibrium partitioning of contaminants between phases is described by the partition (distribution) coefficient, concentration and effectiveness of binding agents, and concentration of particles or organic carbon. Using the equilibrium partitioning approach, the fraction of the total non-solid contaminant in dissolved, bound, and sorbed phases can be expressed as (*31*):

$$f_d = \frac{1}{1 + k_b C_{DOC} + \sum k_{pn} C_{pn}} \tag{11a}$$

$$f_b = \frac{k_b C_{DOC}}{1 + k_b C_{DOC} + \sum k_{pn} C_{pn}} \tag{11b}$$

$$f_{pn} = \frac{k_{pn} C_{pn}}{1 + k_b C_{DOC} + \sum k_{pn} C_{pn}} \tag{11c}$$

where f_d = fraction of total non-solid contaminant in dissolved phase; f_b = fraction of total non-solid contaminant in DOC-bound phase; f_{pn} = fraction of total non-solid contaminant in sorbed phase associated with particle n; k_b = DOC binding coefficient [L^3/M]; k_{pn} = distribution coefficient [L^3/M]; C_{DOC} = DOC concentration [M/L^3]; and C_{pn} = concentration of particle n [M/L^3].

The fractions in Equations (11a - c) sum to unity: $f_d + f_b + \sum f_{pn} = 1$. Adsorption data usually conform to the linear assumption of the distribution coefficient expression over a very restricted solution concentration range. For the soils or bed sediments, the fractions associated with dissolved, DOC, and sorbed phases, respectively, are derived by considering water content and porosity. Given the total non-solid concentration and the three phase fractions, the dissolved, bound, and sorbed concentrations at equilibrium are uniquely determined as follows:

$$C_d = f_d C_T \tag{11d}$$

$$C_b = f_b C_T \tag{11e}$$

$$C_p = \sum_{n=1}^{N} C_{pn} = \sum_{n=1}^{N} f_{pn} C_T \tag{11f}$$

Contaminant Transport

Within a watershed, contaminant transport processes can be divided into those acting in upland areas (the overland plane) and those in streams (the channel network). These processes are described using the advection-dispersion equation (ADE). For runoff and surface water, the most important transport processes are advection, dispersion, infiltration, erosion, deposition, and mass transfer between the water column and underlying surface soil or sediment (the bed). Additional terms are included to account for mass transfer and transformation processes as well as point sources and sinks. Lateral inflow and outflow terms are added to account for mass transfer when runoff and surface water move between the overland plane and channel network.

The upper soil and bed play important roles in contaminant transport because contaminants can be eroded, migrate through the bed by infiltration, transmission loss, or other porewater gradient-driven processes. The upper layer gains mass through sedimentation, but loses it through erosion as well as further burial. For surface soil and sediment, the most important transport processes are erosion, deposition, and mass transfer between overlying water and the bed. Similar to water column, CTT&F modeled contaminant kinetics include partitioning, mass transfer and transformation processes in the bed. Interactions of surface water and the upper bed are illustrated in Figure 4.

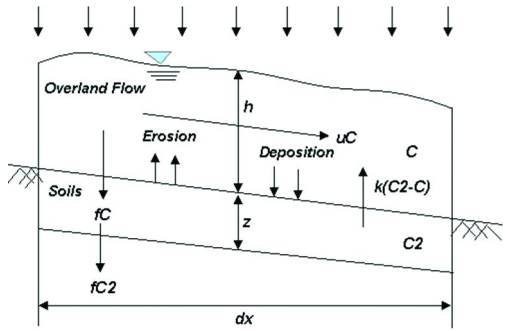

Figure 4. Conceptual transport processes in overland flow and upper soil layer.

Governing equations for the total concentration of contaminants are expressed in 2-dimensional (2D) form for the overland plane and in 1-dimensional (1D) form for stream channels as follows (*32*):

Overland runoff

$$\frac{\partial C_T^r}{\partial t}+u_x\frac{\partial C_T^r}{\partial x}+u_y\frac{\partial C_T^r}{\partial y}-\frac{1}{h}\frac{\partial}{\partial x}\left(hD_x\frac{\partial C_T^r}{\partial x}\right)-\frac{1}{h}\frac{\partial}{\partial y}\left(hD_y\frac{\partial C_T^r}{\partial y}\right) \quad (12)$$
$$=-\frac{f}{h}(f_d+f_b)C_T^r+\frac{k_e}{h}(f_d+f_b)(C_{T2}^r-C_T^r)+\frac{1}{h}\sum_1^N f_{pn}\left(v_r C_{T2}^r-v_{se}C_T^r\right)+\sum S_k$$

Upper soil

$$\frac{\partial C_{T2}^r}{\partial t} = \frac{f}{\Delta z}(f_d + f_b)(C_T^r - C_{T2}^r) - \frac{k_e}{\Delta z}(f_d + f_b)(C_{T2}^r - C_T^r) - \frac{1}{\Delta z}\sum_1^N f_{pn}\left(v_r C_{T2}^r - v_{se} C_T^r\right) + \sum S_k \tag{13}$$

Channel flow

$$\frac{\partial C_T^w}{\partial t} + \frac{Q}{A}\frac{\partial C_T^w}{\partial x} - \frac{1}{A}\frac{\partial}{\partial x}\left(AD_x \frac{\partial C_T^w}{\partial x}\right) = \frac{q_l}{A}\left(C_T^r - C_T^w\right) \tag{14}$$
$$+ \frac{1}{h}\sum_1^N f_{pn}\left(v_r C_{T2}^w - v_{se} C_T^w\right) + EA_s(f_d + f_b)\left(C_{T2}^w - C_T^w\right) + \sum S_k$$

Upper sediment

$$\frac{\partial C_{T2}^w}{\partial t} = \frac{1}{\Delta z}\sum_1^N f_{pn}\left(v_{se} C_T^w - v_r C_{T2}^w\right) - EA_s(f_d + f_b)\left(C_{T2}^w - C_T^w\right) + \sum S_k \tag{15}$$

where C_T^r, C_T^w = total non-solid contaminant concentration in surface water [M/L^3]; C_{T2}^r, C_{T2}^w = total non-solid contaminant concentration in the bed [M/L^3]; D_x, D_y = contaminant dispersion coefficient in the x- or y-direction [L^2/T]; k_e = effective mass transfer coefficient between surface water and the bed [L/T]; E = vertical diffusion coefficient [L^2/T]; A_s = interfacial area [L^2]; and Δz = depth of upper surficial [L]; and ΣS_k = total contaminant transformation flux, positive indicates a source and negative a sink [M/L^3/T]. The superscripts "*r*" and "*w*" denote overland runoff and channel surface water, respectively.

Previous transport equations assume that contaminants either attach to soil particles or partition to water and DOC when wet. Contaminants can be deposited from the air and applied on the surface in a solid form. As such, contaminant solid particles are carried by runoff and surface water and transported through erosion and deposition processes. It is necessary to track mass of contaminant solids within the watershed. The sediment transport equation assumes the types of "solids" variables are conservative, which indicates that no existing kinetic functions are available or applicable. Therefore, mineralization, dissolution, or other transformation processes need to be considered and apply to contaminant solids. CTT&F sub-model performs a mass balance for the concentration of contaminant solids on grid cells based upon specified transport processes, along with special kinetics processes. Mass balance computations are performed in soil/sediment layers as well as the water columns.

Particulate Erosion and Deposition

The flux of contaminants between the upper soil (sediment) and the overlying water needs to be quantitatively understood and modeled. The flux is primarily due to sediment erosion, deposition, and dissolved mass transfer. Each of these

processes acts in different ways, and hence each must be modeled in a different approach. As upper soils (sediments) erode, the contaminants associated with these sediments are transported into the water column, where they may adsorb or desorb, depending on conditions in the overlaying water. Because erosion rates are highly variable in space and time, contaminant fluxes due to erosion and deposition are also highly variable in space and time. Particulate contaminant erosion fluxes by overland flow and channel flow are estimated based on sediment erosion rates provided from the sediment sub-model. The deposition fluxes of sorbed contaminant particulates in overland flow and channel flow are computed from the effective settling velocities.

Dissolved Mass Transfer

In water quality models, a common approach to modeling the dissolved contaminant mass transfer flux between the upper soil and the overlying water is to use a lumped mass transfer coefficient. Gao et al. (*33*) developed a model that combined the chemical transfer associated with the raindrop impacts and diffusion by assuming raindrop and diffusion processes could be coupled by superposition. This model captured soil-runoff chemical transfer behavior more realistically than either mixing-layer models or diffusion-based models. From this model, the mass transfer flux of the dissolved contaminant between the overland flow and the soil water can be expressed:

$$k_e = k_m + \frac{a i_e \theta}{\rho_b} \tag{16}$$

where a = soil detachability [M/L^3], θ = volumetric water content, and k_m = diffusive mass transfer coefficient [L/T].

In above equation, k_m was derived by the concentration gradient across the hydrodynamic boundary layer (*34*, *35*). Diffusion between the upper soil and surface runoff may be neglected since the diffusivity is much smaller than the rainfall induced mass transfer rate (*33*).

Contaminant Transformations

Beyond partitioning and transport, the fate of many contaminants is influenced by biogeochemical transformation processes, including biodegradation, hydrolysis, oxidation (or reduction), photolysis, volatilization, and dissolution. Contaminants may also be linked through sequences of reactions. The importance of these processes depends on the contaminant of interest and the environmental setting. CTT&F can simulate any combination of processes, including reaction sequences and yields where one contaminant undergoes a reaction and is converted to a daughter product. Mass transfer and transformation processes are represented as source or sink terms (ΣS_k) as noted in Equations (12) - (15). In

their most basic reaction rate form, they are represented as first-order processes that depend only on the concentration of the contaminant undergoing reaction:

$$\frac{\partial C_T}{dt} = \sum S_k = \left(K_{bio} + K_{hyd} + K_{oxi} + K_{pht} + K_{vol} + K_{dsl} + K_k\right) C_T \qquad (17)$$

where K_{bio} = biodegradation rate [1/T]; K_{hyd} = hydrolysis rate [1/T]; K_{oxi} = oxidation rate [1/T]; K_{pht} = photolysis rate [1/T]; K_{vol} = volatilization rate [1/T]; K_{dsl} = dissolution rate [1/T] and K_k is reaction rate coefficient for reaction "k," [1/T].

As shown below, transformations can also be described as second-order processes in conjunction with parameters to describe environmental conditions such as oxidant or microorganism concentrations, pH, or solubility, allowing greater specificity with respect to contaminant phases and conditions controlling a reaction. In the CTT&F sub-model, transformation algorithms of contaminants are handled in the same manner in the upper soil or sediment bed as in the water column. The description of water column transformation algorithms provided in the following applies for transformation in the upper soil or sediment bed.

Biodegradation

Biodegradation is transformation of contaminants by microbial activity and can be described as a second-order process in which the overall (first-order) rate is computed from rates for each contaminant phase (e.g. dissolved or particle-sorbed) and the concentration of microorganisms:

$$K_{bio} = \sum_j k_{bio\,j} \left[C_{m,j}\right]_j f_j \qquad (18a)$$

where k_{bio} = second-order biodegradation rate for phase j [L^3/M/T]; f_j = fraction of total chemical in phase j [dimensionless], and C_{mj} = concentration of microorganisms acting on phase j [M/L^3].

When dealing with first-order biodegradation reactions, the use of a half-life rather than a rate is often convenient. If a half-life is specified for the transformation processes, then it is converted to first-order rate constant in the CTT&Fsub-model:

$$k_{bio} = \frac{\ln 2}{t_{1/2}} \qquad (18b)$$

Hydrolysis

Hydrolysis is contaminant transformation by reaction with water and can be described as second-order processes for acidic and basic conditions and a first-order process for neutral conditions for each contaminant phase:

$$K_{hyd} = \sum_j \left(k_{acid\,j} \left[H^+ \right] f_j + k_{neutral\,j} f_j + k_{base\,j} \left[OH^- \right] f_j \right) \tag{19}$$

where $k_{acid\,jj}$ = second-order acid hydrolysis rate for contaminant in phase *j* [L^3/M/T]; $k_{base\,j}$ = second-order base hydrolysis rate for contaminant in phase *j* [L^3/M/T]; k_{nj} = first-order neutral hydrolysis rate for contaminant in phase *j* [1/T]; and [H^+], [OH^-] = concentration of hydronium and hydroxide ions, respectively [M/L^3].

Oxidation

Oxidation (or reduction) is transformation of contaminants by electron exchange and can be described as second-order processes for acidic and basic conditions and a first-order process for neutral conditions for each contaminant phase:

$$K_{oxi} = [RO_2] \sum_j k_{oj} f_j \tag{20}$$

where k_{oj} = second-order net oxidation rate for contaminant in phase j [L^3/M/T]; [RO_2] = oxidant (or reductant) concentration [M/L^3].

Photolysis

Photolysis is the transformation or degradation of a contaminant that results directly from the adsorption of light energy. It is a function of the quantity and wavelength distribution of incident light, the light adsorption characteristics of the contaminant, and the efficiency at which absorbed light produces a contaminant reaction.The first order rate coefficient for photolysis can be calculated from the absorption rate and the quantum yield for a contaminant in each phase:

$$K_{pht} = \sum_j k_{aj} \phi_j f_j \tag{21}$$

where k_{aj} = specific sunlight absorption rate for contaminant in phase j, E/mol-day [E/M/T], and ϕ_j = reaction quantum yield for contaminant in phase j, mol/E [M/E].

Volatilization

Volatilization is the gradient-driven transfer of a contaminant across the air-water interface. The model assumes that only dissolved contaminants can be transported across the interface, and sorption to particulate or DOC reduces volatilization. Volatilization is commonly modeled based on the well-known two-film theory of a gas-liquid transfer velocity. Volatile contaminant concentrations in the atmosphere are often much lower than partial pressures equilibrated with water concentrations. If this concentration is *0*, then

volatilization will always cause a loss of contaminant from the water body. In such case, volatilization reduces to a first-order process with a rate proportional to the conductivity and surface area divided by volume:

$$k_{vlt} = k_v \frac{1}{h} = k_v \frac{A_s}{V_w} \tag{22a}$$

where k_v = mass transfer rate (conductivity) [L/T], and V_w = volume of water column [L^3].

Volatilization from soil is a more complex process, requiring the balancing of several processes. A contaminant in soil will partition between the soil water, soil air, and the soil constituents. In the CTT&F sub-model, the volatilization from soils is assumed to proceed through a surface stagnant air boundary layer and involves desorption of the contaminant from soil, movement to the soil surface in the water or air phase, and vaporization into the atmosphere. Assuming zero vapor concentration above the surface, using Fick's Law, the volatilization rate from soil can be estimated by:

$$k_{vlt} = k_H \frac{D_a A_s}{d}\left(\frac{1}{V_s}\right) \tag{22b}$$

where $D_a = 1.9 \cdot 10^{-4}/MW_C^{2/3}$ is diffusivity of contaminant in air, cm^2/s [L^2/T], V_s = volume of upper soil layer [L^3], d = thickness of stagnant air boundary layer [L]. Jury et al. (*36*) suggested a value of 0.5 cm for d, which in general varies with both evaporation and relative humidity.

Dissolution

Dissolution is the mechanism by which solid contaminants like explosives are transferred to the aqueous phase as dissolved contaminants. Once dissolved, the contaminant is available for redistribution and the full range of applicable transport and transformation processes. The maximum aqueous concentration that a solid phase contaminant can attain is defined by the solubility limit. Inclusion of contaminant aqueous dissolution improves model accuracy and has the potential to aid prediction of hazard persistence and assessment of remediation alternatives affected by dissolution of explosives or other granular contaminants (*37*). Dissolution of a solid particle in water can be described as a diffusion process (*38*, *39*) driven by the concentration gradient around a solid particle, which is expressed as

$$\frac{\partial C_s}{dt} = \frac{k_{dsl}\alpha}{V}\left[S - \left(f_d + f_b\right)C_T\right] \tag{23a}$$

where V = bulk volume (water and particles) [L^3]; k_{dsl} = dissolution mass transfer coefficient [L/T]; α = area available for mass transfer between the solid and liquid [L^2]; and S = aqueous solubility of the contaminant [M/L^3].

The average specific surface area of the solid phase mass depends on the distribution of the size and shape of the solid phase particles and the constituent solid phase density. Assuming solid phase contaminant particles are spherical, the surface area available for mass transfer can be expressed as a function of the contaminant concentration, particle diameter, and particle density (*32*):

$$\alpha = \frac{6C_s V}{d_p \rho_p} \tag{23b}$$

where d_p = particle diameter [L]; and ρ_p = particle density of pure solid phase chemical [M/L^3].

Reaction Products

The contaminants simulated by the CTT&F sub-model may be linked in sequences through reaction yields. When two or more contaminants are simulated, linked transformations that convert one chemical state variable into another may be implemented by specifying a reaction yield coefficient for each process. Reaction yields for transformation processes are useful in transport models to estimate the persistence of contaminants, including their degradation products.

$$K_k = \sum_j \sum_k k_{kj} Y_{kj} (C_T)_j \tag{24}$$

where k_{kj} is reaction rate coefficient for reaction "k" [1/T], and Y_{kj} is effective yield coefficients for reaction production from chemical "j" undergoing reaction "k" [M/M].

Numerical Solutions

The coupled set of governing equations from (9) to (13) can be solved using a number of numerical techniques. In this effort, the general procedure uses a finite difference (FD) control volume solution scheme. A watershed system is discretized into a mesh of square grids ($\Delta x = \Delta y$), which corresponds to digital elevation model (DEM) grids, the locations of which are described in terms of rows, columns, and layers as illustrated in Figure 5. DEM-derived local drainage directions are used as the basis for channel routing.

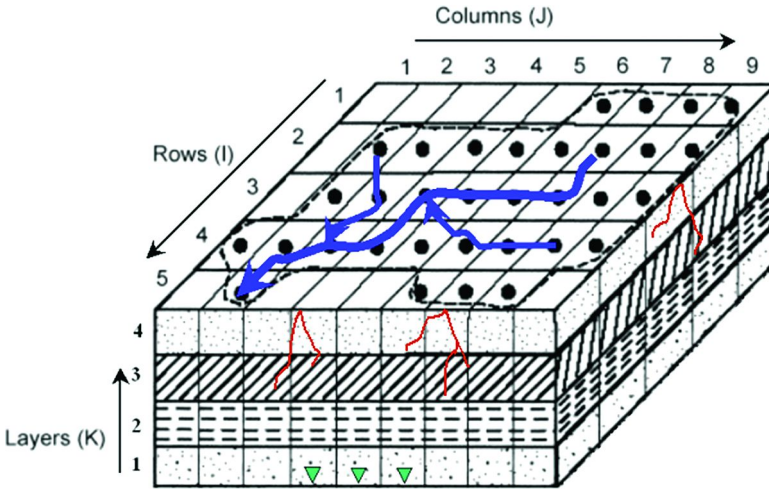

Figure 5. Finite difference computational mesh of the watershed discretization.

An explicit FD method was used to solve the differential equations. In this method the previous values are used to calculate a single unknown for the new time increment. The numerical solution is developed by substituting FD approximations for the derivatives of the governing equations. The solution for discretizing in time and space any of the governing equations presented in this work is obtained by using a forward-time FD. CTT&F also features a "semi-Lagrangian" soil (sediment bed) layer equation to account for the vertical distribution of the physical and contaminant properties of the overland soil and channel sediment columns. Applying a central-in-space explicit FD scheme, overland governing equations (12) and (13) at any FD cell (*i, j*) can be expressed as follows:

$$\frac{C_{i,j}^{n+1}-C_{i,j}^{n}}{\Delta t}=\frac{1}{w}\left\{\begin{array}{l}-u_{xi,j}^{n}\left(C_{i,j+1/2}^{n}-C_{i,j-1/2}^{n}\right)+\dfrac{1}{h_{i,j}^{n}}\left[\left(hD_x\dfrac{\partial C}{\partial x}\right)_{i,j+1/2}^{n}-\left(hD_x\dfrac{\partial C}{\partial x}\right)_{i,j-1/2}^{n}\right]\\ -u_{yi,j}^{n}\left(C_{i+1/2,j}^{n}-C_{i-1/2,j}^{n}\right)+\dfrac{1}{h_{i,j}^{n}}\left[\left(hD_y\dfrac{\partial C}{\partial x}\right)_{i+1/2,j}^{n}-\left(hD_y\dfrac{\partial C}{\partial x}\right)_{i-1/2,j}^{n}\right]\end{array}\right\}$$
$$-\frac{f}{h_{i,j}^{n}}(f_d+f_b)\left[(C_T^r)_{i,j}^{n}-(C_{T2}^r)_{i,j}^{n}\right]+\frac{k_e}{h_{i,j}^{n}}(f_d+f_b)\left[(C_{T2}^r)_{i,j}^{n}-(C_T^r)_{i,j}^{n}\right]$$
$$+\frac{1}{h_{i,j}^{n}}\sum_{1}^{N}f_{pn}\left[(v_rC_{T2}^r)_{i,j}^{n}-(v_{se}C_T^r)_{i,j}^{n}\right]+\Sigma(S_k)_{i,j}^{n} \tag{25}$$

$$\frac{(C_{T2}^r)_{i,j}^{n+1}-(C_{T2}^r)_{i,j}^{n}}{\Delta t}=\frac{f}{\Delta z}(f_d+f_b)\left[(C_T^r)_{i,j}^{n}-(C_{T2}^r)_{i,j}^{n}\right] \tag{26}$$
$$-\frac{k_e}{\Delta z}(f_d+f_b)\left[(C_{T2}^r)_{i,j}^{n}-(C_T^r)_{i,j}^{n}\right]-\frac{1}{\Delta z}\sum_{1}^{N}f_{pn}\left[(v_rC_{T2}^r)_{i,j}^{n}-(v_{se}C_T^r)_{i,j}^{n}\right]+\Sigma(S_k)_{i,j}^{n}$$

where $\Delta x = \Delta y = w$ = grid cell size [L]; j-½ and j+½ denote the left and right interfaces of cell (i, j), respectively; i-½ and i+½ denote the upper and lower interfaces of cell (i, j), respectively.

Channel governing equations (14) and (15) at any FD cell (j) can be expressed as follows:

$$\frac{C_j^{n+1} - C_j^n}{\Delta t} = -\frac{1}{\Delta x_j} u_{xj}^n \left((1-\alpha_{xj+1/2}) C_j^n + \alpha_{xj+1/2} C_{j+1}^n - (1-\alpha_{xj-1/2}) C_{j-1}^n - \alpha_{xj-1/2} C_j^n \right)$$
$$+ \frac{1}{\Delta x_j} \frac{1}{A_j^n} \left((AD_x)_{j+1/2}^{n+1} \frac{C_{j+1}^n - C_j^n}{0.5(\Delta x_j + \Delta x_{j+1})} - (AD_x)_{j-1/2}^{n+1} \frac{C_j^n - C_{j-1}^n}{0.5(\Delta x_{j-1} + \Delta x_j)} \right) \quad (27)$$
$$+ EA_s (f_d + f_b) \left[(C_{T2}^w)_{i,j}^n - (C_T^w)_{i,j}^n \right] + \frac{1}{h_{i,j}^n} \sum_1^N f_{pn} \left[(v_r C_{T2}^w)_{i,j}^n - (v_{se} C_T^w)_{i,j}^n \right] + \Sigma (S_k)_{i,j}^n$$

$$\frac{(C_{T2}^w)_{i,j}^{n+1} - (C_{T2}^w)_{i,j}^n}{\Delta t}$$

$$= -\frac{1}{\Delta z} \sum_1^N f_{pn} \left[(v_r C_{T2}^w)_{i,j}^n - (v_{se} C_T^w)_{i,j}^n \right] - EA_s (f_d + f_b) \left[(C_{T2}^w)_{i,j}^n - (C_T^w)_{i,j}^n \right] + \Sigma (S_k)_{i,j}^n \quad (28)$$

where

$$\alpha_{xj+1/2} = \frac{\Delta x_j}{\Delta x_j + \Delta x_{j+1}} \quad (29a)$$

$$\alpha_{xj-1/2} = \frac{\Delta x_{j-1}}{\Delta x_{j-1} + \Delta x_j} \quad (29b)$$

To generate solutions, the model computes dynamic mass balances for each state variable and accounts for all material that enters, accumulates within, or leaves a control volume through precipitation excess, external loads, transport and transformation. Overland flow transport calculations precede channel transport calculations (for the current time step) and the channel calculations start at the top link of the stream system and progress downstream. Thus the only unknowns for each channel link calculation are the contaminant concentration at the downstream end of the link at the end of the time step. The behavior of the numerical solution depends on the contaminant, the relative importance of the processes occurring, and the value of the Courant number. Small time steps are used in the beginning of each simulation because of the highly nonlinear nature of the equations.

Model Testing and Validation

Experimental Design

To validate the general performance of the model, the CTT&F sub-model was evaluated by means of a test plot study of explosives transport and transformation

processes. The experimental procedure was designed to mimic rainfall-driven surface runoff and transport of explosives residuals deposited on surface soils at firing ranges. The experimental plot was 9.0 ft x 7.5 ft. The plot had a bed slope 2% and was designed to collect runoff water and sediment. Experiments were conducted to simulate two different surface roughness conditions: (1) "disturbed" (unvegetated); and (2) "undisturbed" (vegetated). The soils for these experiments were obtained from the Camp Shelby, Mississippi military firing range. The physical properties of the soils and initial contaminant concentrations before rainfall were measured as presented in Table 2. Rainfall was introduced through a rainfall simulator. The intensity and uniformity of the simulator were calibrated prior to field investigations. The simulated rainfall intensity for the overall plot area averaged 2.8 in/hr (7.1 cm/hr) and ranged from 2.7 to 2.9 in/hr (6.8 to 7.4 cm/hr). The simulated rainfall event lasted 30 ± 60 ± 90 min. Runoff and suspended sediment samples were collected at the downstream end of each plot. Runoff rates and volumes were determined by collecting samples every minute of a 30 minute rainfall simulation and every minute after rainfall was discontinued until it was noted that runoff had ceased. Total suspended sediment (TSS) samples were collected every minute for the first 15 minutes of runoff, then every five minutes during the 30 minutes rainfall simulations and every minute afterward.

Table 2. Physical characteristics of Camp Shelby fire range soils

Sand (%)	*Silt (%)*	*Clay (%)*	*CEC*[a] *(meq/100g)*	*TOC*[b]	*PH*	*Ks*[c] *(in/hr)*
60	20	20	11.6/9.8	1.1	5.2	0.55

[a] *CEC* = cation exchange capacity [b] *TOC* = total organic carbon [c] *Ks* = hydraulic conductivity

For the contaminant transport and transformation experiments, this study focused on Comp B, one of the primary explosive formulations used in munitions since World War II for its high explosive yield (*40*). Range activities can result in locally scattered chunks of Comp B on the soil surface with particles having a variety of surface textures and RDX/TNT ratios (*4*). 500 grams of Comp B in particles of various sizes (less then 1 cm in diameter and 2 mm in thickness to 3.5 cm in diameter and 2.5 cm thickness) was applied onto the soil surface. The Comp B used for this study was a 60/39 mixture of RDX and TNT with 1% wax and in the form of crystalline solids.

Table 3 shows the average explosive contaminant concentrations for three Comp B samples. The physical and chemical properties of RDX and TNT are summarized in Table 4. After Comp B application to the soil surface, the test plot was subjected to a simulated rainfall event, which induced overland flow and contaminant transport. Once in the water, the main factor affecting fate and transport of RDX and TNT is advection with contributing factors being adsorption and transformation (*2*). The rainwater was pre-tested for RDX and TNT to insure

no additional contaminant was entering the system. The contaminant reaction and transport caused by each rainfall event was measured by collecting samples. During each rainfall event, 4-liter runoff samples were collected every 5 minutes (for 30 minutes after initiation of runoff) for chemical analysis and concentration of explosives.

Table 3. Analysis for three Comp B particles

Comp B	*HMX (mg/kg)*	*RDX (mg/kg)*	*TNT (mg/kg)*
1	59424	562798	350955
2	68039	637121	393580
3	71505	672170	422214

Table 4. Physical and chemical characteristics of RDX and TNT[a]

Parameter	*RDX*	*TNT*
Empirical formula	$C_3H_6N_8O_6$	$C_7H_5N_3O_6$
Molecular weight (g/mol)	222.15	227.13
Density (g/cm^3)	1.82	1.654
Solubility in water (mg/L)	28.9 – 75.7	100 – 200
Diffusion coefficient in water (cm^2/s)	7.15×10^{-6}	6.71×10^{-6}
Octanol-water partition coefficient *Log* k_{ow}	0.81, 0.87	2.06, 1.86
Organic carbon partition coefficient *Log* k_{oc}	0.89 – 2.13	2.72
Soil-water partition coefficient k_d (mL/g)	0.0 – 7.8	0.0 – 56.0
Henry constant k_H (atm m^3/mol)	1.96×10^{-11}, 2.6×10^{-11}	1.1×10^{-8}

[a] from McGrath (*30*)

The experimental plot was modeled using a domain consisting of 30 grid cells with a grid cell resolution of 1.5 ft by 1.5 ft (0.46 m by 0.46 m). In this study various transformation parameters for RDX and TNT were calibrated empirically to reproduce the measured concentrations of RDX and TNT from the experiment based on their ranges in previous studies. Parameters included the following: dissolution rate, adsorption kinetics, soil to water partition coefficients, and transformation rate coefficients. Given the small scale of the test plot and the short duration of simulated rainfall, the focus of this study was the dissolution of Comp B, sorption with sediments, and associated multiphase transport of the contaminants.

Model Calibration and Validation

The CTT&F sub-model parameters subject to calibration were the diffusion coefficient, first order transformation rate, and partitioning coefficients. Calibrated model parameter values for RDX and TNT are summarized in Table 5. With one exception, parameter values for the validation simulation were identical to those for calibration. The exception was that the surface roughness values for unvegetated and vegetated plots were different during hydrologic and sediment simulations. RDX and TNT degradation kinetics were not addressed in this study due to short simulation times.

Table 5. Summary of model used parameter values for RDX and TNT

Parameter	*RDX*	*TNT*
Density (g/cm^3)	1.82	1.654
Aqueous solubility (25°C) (g/cm^3)	4.6 x 10^{-5}	1.3 x10^{-4}
Diffusion coefficient (25°C) (cm^2/s)	2.2 x 10^{-6}	6.7 x 10^{-6}
1st order transformation rate (1/hr)	0 – 1.0 x 10^{-1}	-
Soil-water partition coefficient (L/kg)	6.75	56.0

The model was calibrated by comparing simulated and measured runoff, sediment concentration, and contaminant concentrations and iteratively adjusting model parameters to minimize differences between simulated and measured conditions. Numerous performance statistics have been advocated for determining the validity or accuracy of a model, e.g., Kottegoda and Rosso (*41*) and Legates and McCabe (*42*). They include goodness-of-fit or relative error measurements, statistics that quantify the error in units of the process being modeled, and graphical plots. Following statistical performance criteria used for estimating quantitative performance of the CTT&F model were calculated and given in Table 6.

$$RE = \frac{\left| \sum_i SV_i - \sum_i MV_i \right|}{\sum_i MV_i} * 100 \tag{30a}$$

$$RMSE = \sqrt{\frac{1}{n} \sum_i (SV_i - MV_i)^2} \tag{30b}$$

$$R^2 = \frac{\left(\sum_i (MV_i - \overline{MV})(SV_i - \overline{SV}) \right)^2}{\sum_i (MV_i - \overline{MV})^2 \sum_i (SV_i - \overline{SV})^2} \tag{30c}$$

$$NSE = 1.0 - \frac{\sum_i (MV_i - SV_i)^2}{\sum_i (MV_i - \overline{MV})^2} \quad (30d)$$

where MV = measured value, $\overline{MV}$ = mean measured value, SV = simulated value, $\overline{SV}$ = mean simulated value, RE = relative error (%), $RMSE$ = root mean squaree error, R^2 = square of the correlation coefficient, and NSE = Nash and Sutcliffe efficiency.

Table 6. Summary of hydrologic, sediment and contaminant transport model performance

Parameter	*Simulated*	*Measured*	*RE (%)*	R^2	*RMSE*	*NSE*
Unvegetated plot						
Surface runoff (L/min)	189.72	201.75	5.96	0.723	1.195	0.685
Total suspended sediment (mg/L)	20917.60	30653.33	31.76	0.166	719.47	0.231
Dissolved RDX (mg/L)	2.805	2.782	0.84	0.995	0.012	0.994
Dissolved TNT (mg/L)	3.806	3.776	0.79	0.997	0.012	0.997
Vegetated plot						
Surface runoff (L/min)	151.20	139.83	8.13	0.944	0.641	0.923
Total suspended sediment (mg/L)	726.02	2106.67	65.53	0.04	134.00	0.247
Dissolved RDX (mg/L)	1.155	1.207	4.32	0.687	0.052	0.532
Dissolved TNT (mg/L)	0.443	0.417	6.34	0.895	0.014	0.865

The important parameters in terms of the RDX and TNT loads are the physical and chemical characteristics of RDX and TNT. Besides these parameters, flow and soil erosion, including the surface roughness, the USLE practice factor, soil composition and layer depth, also control RDX and TNT fate in overland flow. During the calibration processes, the most sensitive parameters identified for dissolved chemical concentration in overland flow were the dissolution rate and the partition coefficient.

Model Results and Discussion

Numerical results were obtained from running the CTT&F sub-model. In this experiment, overland flow causes erosion and dissolution of the solid Comp B, a fraction of which infiltrates into the soil while the remainder is transported downstream. Even though distributed observations for RDX and TNT concentrations were not measured in this study, we can infer and trace the migration of distributed RDX and TNT sources using the model. As expected, the onset of rainfall results in dissolution of the solid contaminant, with infiltration and wash-off resulting in removal of the solid within a short period of time.

The graphical representation of the spatial variation of dissolved RDX and TNT concentration as a function of time also confirms the generally expected behavior that with increasing time, the peak concentration decreases as it migrates downstream. During this movement, infiltration also occurs so that contamination of the surrounding subsurface area occurs. The model results can provide quantitative information on the amount of contaminant infiltrating into the subsurface. These are important in investigating the loss of contaminants due to the transport and transformation of distributed sources. Obviously, some modifications to these results are to be expected when other transformation effects are incorporated into the model.

The calibration and validation results and the statistics for total flow volume, TSS, dissolved RDX and TNT concentrations are summarized in Table 5. With respect to hydrology, model performance was good for both the unvegetated and the vegetated plots and the simulated values compared reasonably well with the measurements. The flow volume, peak flow, and time to peak are all accurately simulated. The event averaged percent errors of both simulated total surface discharges which were less than 10% of its corresponding measured value. The RMSE and R^2 values between simulated and measured results for the unvegetated plot were 1.195 and 0.723, respectively. For the vegetated plot the RMSE and R^2 values between simulated and measured results were 0.641 and 0.944, respectively.

With respect to sediment transport, the model did not fully capture the initial wash-off of sediments for both simulations, the event averaged percent error of simulated TSS concentration from both unvegetated and vegetated plots was 31.76% and 55.22, respectively. The RMSE was considered to be high and the R^2 value was low. The model performance for suspended sediment concentration was strongly affected by the initial six samples collected and the extremely high sediment concentrations that were measured from these samples.

The errors are suspected to be associated with an error in the sample concentration measurements and/or raindrop splash erosion which is not accounted for within the model. In spite of this, the model was capable of capturing the general trends of TSS concentration over time, the TSS concentrations for both simulations were considered to be satisfactory after the initiation of the event. The Error, RMSE, R^2, and NSE values are greatly improved without the inclusion of the first six samples. Surface runoff and sediment volumes from the unvegetated conditions were greater than those from the vegetated conditions. These finding were expected because reduced runoff volumes from the vegetated surface were

associated with more resistance to overland flow and more infiltration opportunity time.

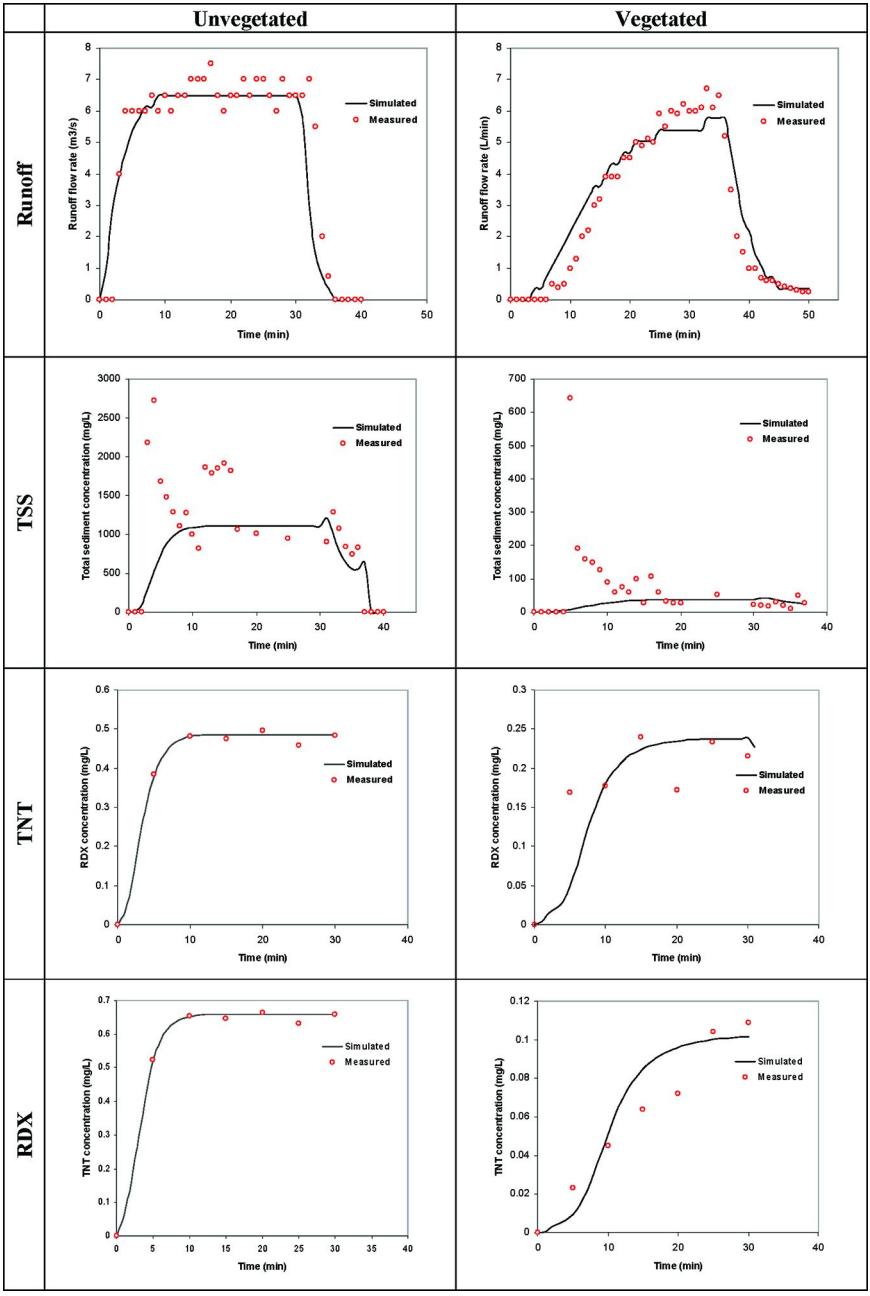

Figure 6. Comparison of simulated and measured surface runoff discharge, TSS, RDX, and TNT for unvegetated and vegetated test plots.

With respect to contaminant transport, RDX and TNT concentration errors for both simulations were very small (within 7%). The R^2 values between simulated and measured concentration results from the unvegetated plot were 0.995 and 0.997 for RDX and TNT, respectively. The R^2 values between simulated and measured results from the vegetated plot were 0.687 and 0.895 for RDX and TNT, respectively. Further, the model performed well for two different data sets. Comparisons of the overall shape of simulated and measured results over time for surface runoff discharge, TSS concentration, dissolved RDX and TNT concentrations in surface runoff are shown in Figure 6. These figures are representative of the results for both unvegetated and vegetated plots. The agreement of model simulations and measurements for the experimental test plots explosive contaminants from the field is satisfactory thus showing that the CTT&F sub-model is able to capture the essence of explosive fate controlled by dissolution, partitioning and overland flow transport processes. While the data set used in this study is satisfactory for model validation, deficiencies in the data set, which are common to most watersheds, prevent validation of the appropriateness of the other processes.

From above discussions, the CTT&F model results can be used to address questions of management interest to guide watershed contamination mitigation efforts by examining the load of material transported through different areas of the landscape. Bare-ground conditions produced higher concentrations of RDX and TNT than the vegetated conditions for all experimental conditions. Therefore vegetated surfaces are effective in reducing the overall transport of contaminants in overland flow. The vegetation can act as an effective barrier allowing for possible contaminant entrapment within the vegetation, adsorption to the plant material, and infiltration through the soil profile. This study also helps in the understanding of the relative transport of RDX and TNT in the overland flow regime from bare and vegetated soil surfaces.

In summury, this experiment illustrates how the CTT&F sub-model can be used to assess the relative impacts that upland source areas have on downstream water quality. Unfortunately, plot limitations inhibited investigation of other scenarios. Because of the limitations in experiment design, further field applications are needed to fully assess the model formulations.

Conclusions

The CTT&F sub-model is a significant contribution to multiphase contaminant transport modeling at the watershed scale in that, a physically based, spatially distributed approach is used which combines the upland and channel components of transport and transformation. A coupled CTT&F sub-model with watershed hydrological model is particularly suitable for simulating the impacts of land-use and climate changes on contaminant transport and transformation, and for identifying watershed management strategies which minimize distributed source effects on water quality and ecosystem. The CTT&F equations are comprehensive, physically based, and fully compatible with various distributed watershed hydrologic models which provide the required hydrological and

sediment variables. The model computes on a grid basis for considering spatially varied soils, land uses, and other hydrologic characteristics. The physical basis is important because it provides the link between the simulations and physical property measurements. Contaminant transformations are add-on and easily modified to account for more complicated processes. The CTT&F sub-model not only generates time series outputs of contaminant state variables at specified cells in space over time, but also provides the temporal spatial distribution results of contaminant sources in different phases.

CTT&F sub-model was tested to demonstrate its performance in describing such processes as solid dissolution, partitioning and overland flow transport using an experimental plot. Comparisons between simulated and measured results for hydrologic, sediment and contaminant variables of the model have been described. The comparisons showed that the model was capable of simulating the explosive contaminants from the field with reasonable accuracy. Contaminants released from surface sources were generally simulated within 10% of observed measurements. Overall comparisons were encouraging, and showed promise for the potential use of the CTT&F sub-model for predicting the fate of distributed sources in watersheds. CTT&F sub-model is an important contribution to the ability to simulate the transport and fate of solid particles, contaminants adsorbed to sediment particles and bound DOC and dissolved into water at the watershed scale.

It is recognized that further work on validating the model capabilities to simulate contaminant transport and transformation has to be done with additional field data. More tests are needed to assess the variability in the model parameters, to confirm the predicted time sequences, and to improve confidence in predicted concentrations. Accurate modeling of distributed sources on training ranges is complicated by the need to select the correct transformation process description and then select the appropriate coefficient for each variable supporting the model. Although there exists literature describing munitions constituents transformations, far less data are available for transformation rates to be used in watershed scale modeling. Field studies and further research remain to be conducted to measure the values of these parameters in order to accurately predict and know the importance of these processes. The CTT&F algorithms and integration with existing hydrologic models will be further validated directly against range monitored data.

Acknowledgments

This work was supported by the U.S. Army Corps of Engineers Environmental Quality Technology (EQT) Research Program. We greatly acknowledge and appreciate the laboratory experiment work conducted by Ms. Cynthia Price and her team.

References

1. Center for Public Environmental Oversight (CPEO). Toxic ranges. http://www.cpeo.org/, 2002.
2. Brannon, J. M.; Myers, T. E. Review of fate and transport processes of explosives. *U.S. Army Engineer Waterways Experiment Station Technical Report IRRP-97-21*; Vicksburg, MS, 1997.
3. Brannon, J. M.; Pennington, J. C. Environmental fate and transport process descriptors for explosives. *U.S. Army Engineer Research and Development Center ERDC/EL TR-02-10*; Vicksburg, MS, 2002.
4. Jenkins, T. F.; Topp, G. C.; Hewitt, A. D.; Grant, C. L.; Thiboutat, S.; Ampleman, G.; Walsh, M. E.; Ranney, T. A.; Ramsey, C. A.; Palazzo, A. J.; Pennington, J. C. Identity and distribution of residues of energetic compounds at army live-fire training ranges. *Chemosphere* **2006**, *63*, 1280–1290.
5. Simons, D. B.; Sentürk, F. *Sediment Transport Technology – Water and Sediment Dynamics (Revised Edition)*; Water Resources Publications, Littleton, CO: 1992.
6. Clausen, J. L. Range Assessment Lessons Learned. *Federal Facilities Environmental Journal*; **2005** (*Summer*), 49−62.
7. Clausen, J. L.; Robb, J.; Curry, D.; Gregson, B.; Korte, N. Contaminants on military ranges: A case study of Camp Edwards, Massachusetts, USA. *Environ. Pollut.* **2004**, *129*, 13–21.
8. Clausen, J.; Korte, N. The distribution of metals in soils and porewater at three U.S. military training facilities. *Soil Sediment Contam.* **2009**, *18*, 546–563.
9. USEPA. *Administrative order for response action EPA SDWA-1-97-1030, USEPA Region 1 in the matter of training range and impact area, Massachusetts military reservation*; USEPA: Washington, DC, 1997. http://groundwaterprogram.army.mil/groundwater/admin/orders/Ao1.pdf.
10. Birkinshaw, S. J.; Ewen, J. Nitrogen transformation component for SHETRAN catchment nitrate transport modelling. *J. Hydrol.* **2000**, *230* (2000), 1–17.
11. Downer, C. W.; Ogden, F. L. GSSHA: A model for simulating diverse streamflow generating processes. *J. Hydrol. Eng.* **2004**, *9* (3), 161–174.
12. Ewen, J.; Parkin, G.; O'Connell, P. E. SHETRAN: distributed river basin flow and transport modeling system. *J. Hydro. Eng.* **2000**, *5* (3), 250–258.
13. Velleux, M. Spatially distributed model to assess watershed contaminant transport and fate. Ph.D. thesis, Colorado State University, Fort Collins, CO,2005.
14. Johnson, B. E.; Julien, P. Y.; Molnár, D. K.; Watson, C. C. The two-dimensional upland erosion model CASC2D-SED. *J. Am. Water Resour. Assoc.* **2000**, *36* (1), 31–42.
15. Julien, P. Y.; Saghafian, B. CASC2D user's manual - a two dimensional watershed rainfall-runoff model; *Department of Civil Engineering, Colorado State University Report CER90-91PYJ-BS-12*; Fort Collins, CO, 1991.

16. Julien, P. Y.; Saghafian, B.; Ogden, F. L. Raster-based hydrologic modeling of spatially-varied surface runoff. *Water Resour. Bull.* **1995**, *31* (3), 523–536.
17. Hjelmfelt, A. T.; Wang, M. Modeling hydrologic and water quality responses to grass waterways. *J. Hydrol. Eng.* **1999**, *4* (3), 251–256.
18. Yan, M.; Kahawita, R. Modeling the fate of pollutant in overland flow. *Water Res.* **2000**, *34* (13), 3335–3344.
19. Young, R. A.; Onstad, C. A.; Bosch, D.; Anderson, W. P. AGNPS: A nonpoint-source pollution model for evaluating agricultural watersheds. *J. Soil & Water Conserv.* **1989**, *44* (2), 168–173.
20. Coastal and Hydraulics Laboratory (CHL). GSSHA bibliography.http://gsshawiki.com/gssha/GSSHA_Bibliography, 2010.
21. Julien, P. Y. *Erosion and Sedimentation*; Cambridge University Press: Cambridge, UK, 1998.
22. Holley, E. R. Unified view of diffusion and dispersion. *J. Hydraul. Div., Am. Soc. Civ. Eng.* **1969**, *95* (2), 621–631.
23. Julien, P. Y; Simons, D. B. Sediment transport capacity of overland flow. *Trans. ASAE* **1985**, *28*, 755–762.
24. Cheng, N. S. Simplified settling velocity formula for sediment particle. *J. Hydraul. Eng.* **1997**, *123* (2), 149–152.
25. Haralampides, K.; McCourquodale, J. A.; Krishnappan, B. G. Deposition properties of fine sediment. *J. Hydraul. Eng.* **2003**, *129* (3), 230–234.
26. Krishnappan, B. G. In situ distribution of suspended particles in the Frasier River. *J. Hydraul. Eng.* **2000**, *126* (8), 561–569.
27. Clausen, J. L. Range Assessment Lessons Learned. *Federal Facilities Environmental Journal*; **2005** (*Summer*), 49−62. Beuselinck, L.; Govers, G.; Steegen, A.; Quine, T. A. Sediment transport by overland flow over an area of net deposition. *Hydrol. Processes* **1999**, *13* (17), 2769–2782.
28. Burban, P. Y.; Xu, Y.; McNeil, J.; Lick, W. Settling speeds of flocs in fresh and sea waters. *J. Geophys. Res., [Oceans]* **1990**, *95* (C10), 18213–18220.
29. Pennington, J. C.; Silverblatt, B.; Poe, K.; Hayes, C. A.; Yost, S. Explosive residues from low-order detonations of artillery munitions. *Distribution and fate of energetics on DoD test and training ranges: Report 5. ERDC TR-05-2*;U.S. Army Engineer Research and Development Center: Vicksburg, MS, 2005; pp 34–54.
30. McGrath, C. J. Review of formulations for processes affecting the subsurface transport of explosives. *U.S. Army Engineer Waterways Experiment Station Technical Report IRRP-95-2*; Vicksburg, MS, 1995.
31. Chapra, S. C. *Surface Water-Quality Modeling*; McGraw-Hill: New York, 1997.
32. Johnson, B. E.; Zhang, Z. Development of a distributed sources Contaminant Transport, Transformation and Fate (CTT&F) sub-model for military installations; *U.S. Army Engineer Research and Development Center ERDC/EL TR-07-10*; Vicksburg, MS, 2007.
33. Gao, B.; Walter, M. T.; Steenhuis, T. S.; Hogarth, W. L.; Parlange, J.-Y. Rainfall induced chemical transport from soil to runoff: theory and experiments. *J. Hydrol.* **2004**, *295* (1−4), 291–304.

34. Wallach, R.; Jury, W. A.; Spencer, W. F. Transfer of chemicals from soil solution to surface runoff: a diffusion-based model. *Soil Sci. Soc. Am. J.* **1988**, *52* (3), 612–618.
35. Wallach, R.; Jury, W. A.; Spencer, W. F. The concept of convective mass transfer for prediction of surface-runoff pollution by soil surface applied chemicals. *Trans. ASAE* **1989**, *32* (3), 906–912.
36. Jury, W. A.; Spencer, W. F.; Farmer, W. J. Behavior assessment model for trace organics in soil: I. model description. *J. Environ. Qual.* **1983**, *12* (4), 558–564.
37. Lynch, J. C.; Brannon, J. M.; Hatfield, K.; Delfino, J. J. An exploratory approach to modeling explosive compound persistence and flux using dissolution kinetics. *J. Contam. Hydrol.* **2004**, *66* (3−4), 147–159.
38. Cussler, E. L. *Diffusion Mass Transfer in Fluid Systems*, 2nd ed.; Cambridge Press: New York, 1997.
39. Lynch, J. C.; Brannon, J. M.; Delfino, J. J. Dissolution rates of three high explosive compounds: TNT, RDX, and HMX. *Chemosphere* **2002**, *47* (2002), 725–734.
40. Lever, J. H.; Taylor, S.; Perovich, L.; Bjella, K.; Packer, B. Dissolution of composition B detonation residuals. *Environ. Sci. Technol.* **2005**, *39* (22), 8803–8811.
41. Kottegoda, N. T.; Rosso, R. *Statistics, Probability, and Reliability for Civil and Environmental Engineers*; McGraw-Hill: New York, 1997.
42. Legates, D. R.; McCabe, G. J. Evaluating the use of 'goodness-of-fit' measures in hydrologic and hydroclimatic model validation. *Water Resour. Res.* **1999**, *35* (1), 233–241.

Chapter 15

Fate and Transport of Energetics from Surface Soils to Groundwater

J. L. Clausen*,[1] and Nic Korte[2]

[1]US Army Corps of Engineers, Engineer Research and Development Center, Cold Regions Research and Engineering Laboratory, 72 Lyme Road, Hanover, NH 03257
[2]Nic Korte LLC, 1946 Clover Court, Grand Junction, CO 81506
***jay.l.clausen@us.army.mil**

The principal energetic compounds found at military ranges include hexahydro-1,3,5-trinitro-1,3,5-triazine (RDX), octahydro-1,3,5,7-tetranitro-1,3,5,7-tetrazocine (HMX), and perchlorate. These are found in rocket, artillery, grenade, and mortar Impact Areas as well as Open Burn/Open Detonation (OB/OD) and Explosive and Ordnance Disposal (EOD) sites. RDX, HMX, and perchlorate are persistent and mobile in aerobic aquatic environments with the primary fate-and-transport mechanisms being advection, dispersion, and dilution. Other compounds frequently detected in soil but less frequently in groundwater include 2-amino-4,6-dinitrotoluene (2a-DNT), 4-amino-2,6-dinitrotoluene (4a-DNT), 2,4-dintrotoulene (2,4-DNT), 2,6-dinitrotoluene (2,6-DNT), nitroglycerin (NG), and 2,4,6-trinitrotoluene (TNT). These compounds are more susceptible to phototransformation, biotransformation, and adsorption than HMX, RDX, and perchlorate, and with the exception of TNT, are typically released in much smaller amounts. TNT and the amino-DNTs are typically found in Impact Areas, OB/OD, and EOD sites. In contrast, DNTs and NG are found principally at artillery and mortar and small arms firing positions while NG is most common at anti-tank rocket firing positions.

Introduction

The fate-and-transport of energetic compounds from munitions is of considerable interest to the US Department of Defense (DoD) because of the potential for groundwater impacts (*1*). For instance, the US Environmental Protection Agency (USEPA) issued Administrative Order #2 in 1997, requiring the cessation of military training with ordnance containing energetic compounds at Camp Edwards, MA (*2*). Training at the Navy bombing range in Vieques, Puerto Rico was discontinued in 2003 largely because of concerns of environmental impacts. Given the current geopolitical climate, the DoD needs military ranges to train soldiers and must balance military training requirements with environmental impacts.

A typical military installation training area consists of a central impact area surrounded by a number of training ranges or firing points (Figure 1). The training ranges are aligned such that firing is directed towards the impact area. Ordnance employed at Army installations includes projectiles from small arms, machine guns, hand grenades, artillery, mortar, and rockets. Pre-World War II munitions primarily contained TNT as the principal explosive. The predominant explosive used in post World War II artillery and mortar munitions is Composition B (Comp B), composed of RDX and TNT. Anti-tank rocket warheads consist primarily of an explosive mixture called Octol which contains HMX and TNT. Tetryl (2,4,6-trinitro-phenylmethylnitroamine) was used in some munitions but was discontinued in the 1950s. Propellants primarily consist of 2,4-DNT, nitrocellulose (NC), NG, and nitroguanidine (NQ). Most energetic residues identified at military ranges, therefore, are nitro-substituted molecules used in explosives and propellants. These nitro-substituted compounds fall into three categories:

- Nitroaromatics such as TNT, 2a-DNT, 4a-DNT, 2,4-DNT, 2,6- DNT, tetryl, and 2,4,6-trinitrophenol (picric acid or PA);
- Nitroamines such as RDX and HMX; and
- Nitrate esters such as pentaerythritol tetranitrate (PETN), NG, and NC.

The energetic residues identified in soil at various artillery and mortar Impact Areas include RDX, HMX, TNT, 2a-DNT, and 4a-DNT (Table I) (*1*, *4–14*). The compounds identified at artillery and mortar firing points are primarily NG and 2,4-DNT (*1*, *3–9*, *12–18*). NG and NC are the primary propellants for anti-tank rockets and have been found in surface soils at firing positions (*1*, *4–9*, *14*, *19–21*). The energetic compounds TNT, 2a-DNT, 4a-DNT, RDX, HMX, 2,4-DNT, and perchlorate have been detected in groundwater at several installations associated with impact areas and OB/OD sites (*16*, *17*, *22–24*). Laboratory and field studies have been conducted over the past several decades such that a good understanding of the fate and transport behavior of HMX, RDX, TNT, perchlorate, DNTs, and NG is available for a variety of environments. Physical and chemical properties have been measured by a variety of researchers and have been summarized by Clausen and co-workers (*22*).

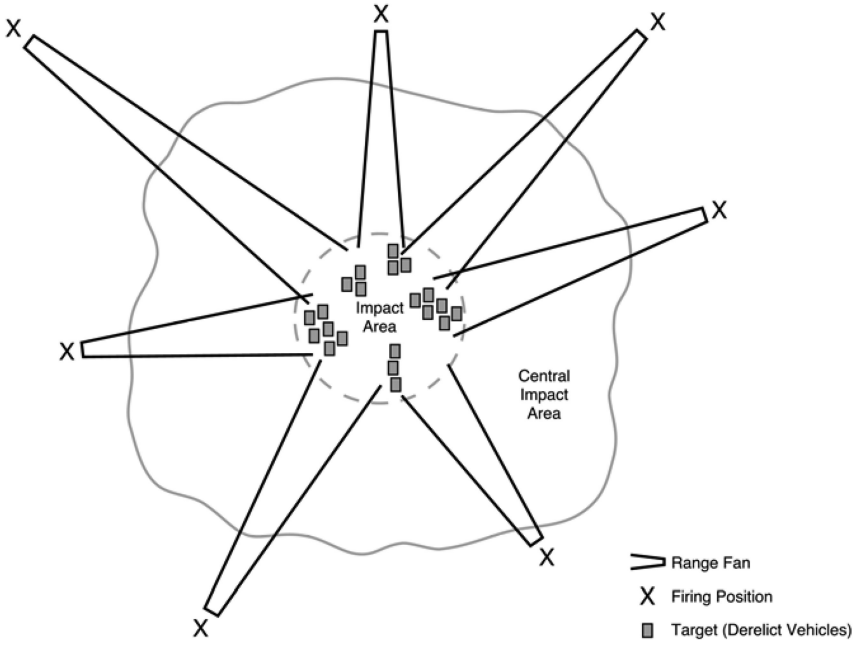

Figure 1. Generic military range layout.

Depositional Conceptual Model

Studies from the detonation of munitions on snow have demonstrated that high-order detonations contribute a very small mass of unburnt energetic residue to the environment, even over decades of use. This residue is not believed sufficient to cause groundwater contamination (*25–27*). Thus, the most likely contamination sources of real significance on ranges are energetic particulates (Fig 2) introduced from low-order detonations (Fig 3), and – to a lesser extent – ruptured unexploded ordnance munitions (*5*, *6*, *25–28*). Contamination may also result from blow-in-place (an activity for elimination of UXO hazard) of unexploded ordnance (UXO). The type of detonation charge (RDX shape charge, RDX penetrator, TNT block, or Composition (C4) [mixture of RDX and plasticizers]) affects the amount of energetic residue produced.

The conceptual model for ranges begins with the deposition of particulates onto the soil surface from low-order detonations or rounds that have cracked open through sympathetic detonation (Fig 4). The energetic material is released as a distributed source—a low-concentration, non-random pattern of widely dispersed residues on soil (*5*, *6*, *25*, *29*). The resulting pattern of deposition is a consequence of the random nature of targeting, inaccuracy of indirect fire weapon systems, multiple firing locations with overlapping firing fans, multiple targets, possible movement of targets over time, and randomness of low-order detonations and secondary detonation of UXO.

Table I. Energetic residues expected at military ranges by training activity.

Training Area	*Range Type*	*Potential Contaminants of Concern*	
		Surface Soil	***Groundwater***
Firing Point	Artillery and Mortar	2,4-DNT, 2,6-DNT, NC	None
	Anti-Tank	NG, NC	None
	Small Arms	2,4-DNT, NG, NC	None
Impact Area	Artillery and Mortar	HMX, RDX, TNT, Perchlorate (limited) Transformation products for TNT and RDX	HMX, RDX, TNT (limited), Perchlorate Transformation products for TNT
	Anti-Tank	HMX, RDX, TNT Transformation products for TNT and RDX	HMX, RDX, TNT (limited) Transformation products for TNT and RDX
	Aerial Bombing Ranges	HMX, RDX, TNT, Perchlorate Transformation products for TNT and RDX	HMX, RDX, Perchlorate
Other	Grenade Courts	HMX, RDX, TNT Transformation products for TNT and RDX	RDX, TNT Transformation products for TNT and RDX
	OB/OD	HMX, RDX, TNT, 2,4-DNT, 2,6-DNT, NG, NC Transformation products for TNT and RDX	HMX, RDX, TNT (limited), Perchlorate Transformation products for TNT and RDX

Figure 2. Example of 2,4,6-trinitrotolune (TNT) particulates found in military impact areas from a low-order detonation.

Figure 3. Example of an artillery 155mm round that underwent a low-order detonation.

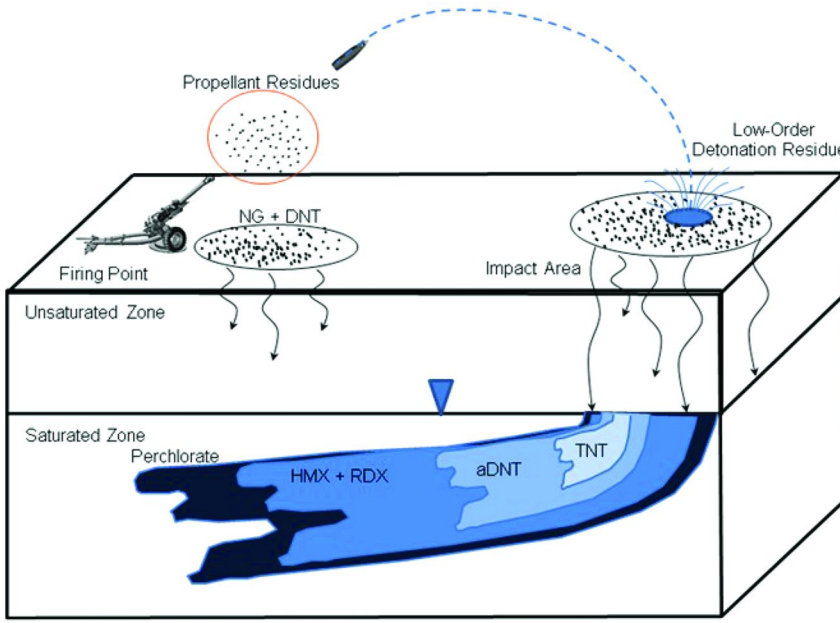

Figure 4. Conceptual model of fate and transport of energetic compounds based on work at the Massachusetts Military Reservation, USA (22).

Fate-and-Transport Conceptual Model

For a given precipitation event, a small portion of the energetic residue can be dissolved. The particulates originating from low-order detonations are dissolved by precipitation passing through the upper half-meter of so of the soil profile (i.e.; 1 to 2 ft). Under appropriate hydrogeochemical conditions, the nitroamines (RDX and HMX) and perchlorate are relatively conservative and are rapidly transported through the unsaturated zone with little or incomplete sorption to the soil (Table II). As a result, there is little tailing effect because RDX, HMX, and perchlorate behave somewhat like tracers. The longer and more intense the precipitation event, the deeper the slug of elevated RDX-, HMX-, and perchlorate-contaminated water moves vertically through the soil. Once the wetting front has migrated below the zone of soil containing source material; RDX, HMX, and perchlorate are typically not detected—both because contaminant particulates are not present at depth, and the mass of the contaminant dissolved in the soil pore-water is small in comparison to the total mass of soil analyzed. The fraction dissolved is controlled by many factors: identity and composition of the energetic material, the size (i.e. surface area), shape, and type of the particulate (neat explosive, soot containing energetic compounds, energetic compound impregnated metal), intensity and duration of the precipitation event, temperature, soil characteristics, and drainage patterns. A detailed summary of the physical and chemical properties of energetic compounds with references cited is provided by Clausen and co-workers (*22*).

In contrast, the nitroaromatics are susceptible to transformation processes such as photodegradation, phytodegradation, and biodegradation (*22*). In addition, this class of compounds can be strongly sorbed onto soil surfaces. The degradation of TNT is often apparent from the presence of degradation products 2a-DNT, 4a-DNT, and 2,4-diamino-6-nitrotoluene (2,4-DANT) in the upper few feet of soil.

Once energetic compounds such as RDX, HMX, and perchlorate reach the water table, they will migrate downgradient towards discharge points. Perchlorate moves essentially at the velocity of groundwater; while RDX, HMX, aDNT, TNT, and DNTs, are attenuated to some extent. Adsorption is the predominant attenuation mechanism for RDX, and HMX whereas adsorption and transformation processes are important for the aDNTs, TNT, and DNTs. This is apparent at the Camp Edwards, MA Demolition Area 1 plume where RDX, HMX, aDNTs, DNTs, and TNT are retarded in groundwater relative to perchlorate (*16*). In the Impact Area at Camp Edwards, only perchlorate, RDX and HMX are consistently observed in the groundwater, with occasional detections of 2a-DNT and TNT at two locations immediately downgradient of targets (*15*). Further downgradient the 2a-DNT and TNT are no longer detectable.

Table II. Fate-and-transport attenuation mechanisms of importance for energetic compounds.

	HMX	*RDX*	*TNT*	*aDNT*	*DNT*	*DANT*	*NG*	*Perchlor-ate*
Adsorption			√	√	√	√	√	
Biotransforma-tion			√	√	√	√	√	
Dissolution	√	√	√	√	√	√	√	√
Phototransforma-tion			√		√		√	
Phytotransforma-tion		√	√				√	

Hexahydro-1,3,5-trinitro-1,3,5-triazine (RDX)

Hexahydro-1,3,5-trinitro-1,3,5-triazine (RDX, Royal Demolition Explosive or cyclonite) is a crystalline solid at room temperature with a molecular weight of 222 g/mol. RDX has a low water solubility (42 mg/L) (*30*) and vapor pressure and its K_{ow} indicates a low affinity for hydrophobic substances. There is no significant effect on solubility over the pH range 4.2-6.2 (*31*). Volatilization is not an important fate-and-transport mechanism for RDX (*30*, *33*, *34*).

The dissolution rate of RDX is slow; therefore, high concentrations can persist in near-surface soils for decades (*35*). For example, a study was conducted in Nevada at an explosives test facility used for one year and abandoned in the

mid 1950's (*36*). Solid chunks of RDX and HMX were visible on the soil in the 1990s. Similarly, field studies conducted at numerous sites across the US often observed remnants of energetic residues on the soil surface or within UXO that had undergone low-order detonation such as at OB/OD sites (Scofield Barracks, Pohakuloa Training Center, Camp Shelby, Camp Edwards and Fort Richardson) and Impact Areas (Fort Hood, Fort Bliss, Fort. Carson, Ft. Polk, Cold Lake Air Weapons Range, Holloman AFB, Yakima Training Center, Scofield Barracks, Canadian Forces Base (CFB)-Valcartier, CFB-Gagetown, Eglin AFB, Camp Edwards and Fort Richardson). In some cases, it was known that the UXO item was introduced decades in the past.

Laboratory column experiments have demonstrated RDX's slow dissolution in a variety of soils ranging from silt to sand. Typically, RDX migration was observed as water was applied, but some always remained in the surface (*37*). These experiments indicated particulate RDX residues are slow to dissolve even in humid environments. More recently, Taylor and co-workers (*38*) conducted a laboratory study on a single Composition B (Comp B) particulate, approximately 5 inches in length, collected from an active artillery and mortar firing range. Water was dripped on the particulate for 60 days before the experiment was terminated. The results suggested complete dissolution of the particulate would take decades to centuries.

Solubility and dissolution rates have also been determined for RDX in the formulations Octol, Comp B, and LX-14 as well as mixtures of the three individual compounds comprising these formulations (*31*). In addition, Lynch and co-workers (*39*) examined the solubility and dissolution rate of RDX as a function of temperature, surface area, and energy input. RDX had the slowest dissolution rate as compared to HMX and TNT, although the data demonstrated dissolved concentrations could exceed the USEPA health advisory limit (0.002 mg/L). The solubilities of the individual compounds from formulations and mixtures were comparable to those of the individual compounds as measured independently. Other observations included; 1) the fact that military grade RDX had sufficient HMX for the latter to attain its solubility limit in solution and; 2) Octol contained detectable quantities of RDX and TNB.

Most studies indicate sorption of RDX is not a significant process, although a few have reported some retention on sediments and clays (*40–42*). For example, McGrath (*32*) reported RDX and HMX passed through laboratory columns with minimal retardation and reduction. Partition coefficients of 0.05 to 0.38 L/kg were determined for coarse-textured soils (*43*), 0.72 L/kg for RDX in a clay soil (*44*), less than 1 L/kg for 15 soils ranging from clay to clayey sand (*45*), 0 to 6.75 L/kg (*46*), and 1 to 3 L/kg (*37*). Similarly, Checkai and co-workers (*47–49*) reported RDX and HMX were highly mobile in soils with low clay content and low CEC (cation exchange capacity). Ainsworth and co-workers (*45*) reported the sorbed mass of RDX ranged from 0.64 to 36 percent of the total mass applied. Similar to research with TNT, these investigators found only a poor correlation between partitioning coefficients (K_d) and fraction of organic carbon (f_{oc}) suggesting the amount of organic matter in the soil is of limited importance. A study of the effects of Eh and pH (*50*) demonstrated no effect of pH for neutral or acid conditions. Eh also had little effect except under highly reducing conditions (-150 mv). Even in

the latter case, however, K_ds were near to or less than 1 L/kg when the pH was between 5 and 7. Most studies report when RDX is sorbed, it is fully reversible (*40*, *41*, *44–46*). Similarly, laboratory investigations employing a variety of soils ranging from clay to sandy loam found less than two percent of the RDX was bound as a non-extractable residue (*33*). Occurrence of RDX sorption has been variously or in combination attributed to CEC, pH, clay content, organic carbon, and extractable iron.

Several studies indicate RDX is susceptible to biodegradation under some conditions. Natural removal of RDX from soil was observed in a study at the Iowa Army Ammunition Plant (AAP) (*51*, *52*). Although the mechanism was not identified, the authors concluded removal appeared to be the result of adsorption and biodegradation. Other research (*53*) showed transformation of RDX in laboratory and field lysimeter studies but redox conditions were not specified. Rodacy and Leslie (*54*) determined the half-life of RDX in soil to be 36 years based on work (*55*) from an arid site using powdered RDX as the starting material. Jenkins and co-workers (*56*) found the half-life of pre-dissolved RDX in moist unsaturated soil to range between 94 and 154 days. These observations indicate RDX may degrade readily in an anaerobic environment (*50*, *57*), with only limited aerobic degradation. Apparently, at low contaminant concentrations (less than 20 mg/kg), the bioavailability of RDX, HMX, TNT, and their degradation products is controlled by desorption from the soil matrix (*58*).

An evaluation of RDX degradation at three redox potentials and four pH levels, employing a solution spiked with 10 mg/L RDX (*59*) demonstrated RDX was unstable under highly reducing conditions, but relatively stable over the short-term under oxidizing and moderately reducing conditions, irrespective of the pH. The authors concluded RDX would not persist in areas where reduction is intense, but would be mobile and persistent in oxidizing or moderately reducing environments. The pH did have a significant effect on anaerobic degradation with 80 percent mineralization at pH 7 compared to 18 percent at pH 5 and 8.

Anaerobic transformation products of RDX are hexahydro-1-nitroso-3,5-dinitro-1,3,5-triazine (MNX), hexahydro-1,3-dinitroso-5-nitro-1,3,5-triazine (DNX), and hexahydro-1,3,5-trinitroso-1,3,5-triazine (TNX) when the soil pH is greater than 8 (*50*). The latter study used high performance liquid chromatography (HPLC) to confirm the loss of RDX and the formation of MNX, DNX, and TNX as transient intermediates. In addition, by using liquid chromatography mass spectrophotometry (LC/MS), this series of experiments produced the first experimental evidence for the formation of hydroxylamino-dinitroso-1,3,5-triazine. Other reported transformation products include formaldehyde, methanol, hydrazine, 1,1-dimethylhydrazine, and 1,2-dimethylhydrazine (*60*, *61*). In general, when RDX is degraded anaerobically, hydroxylamines are formed initially. Eventually ring cleavage occurs resulting in a series of hydrazines. Nitrosamine intermediates formed in this process are believed to be genotoxic carcinogens (*62*). The hydrazines may be short-lived. One set of experiments indicated the hydrazines rapidly disappeared under aerobic, anaerobic, and methanogenic conditions with half-lives ranging from 4.1 to 6 hours (*50*). Nevertheless, a clear conclusion from current work is once the ring in a cyclic nitroamine cleaves the degradation products are thermally

unstable and hydrolyze readily in water. Such abiotic reactions compete with biotic reactions during biodegradation making it very difficult to evaluate the mechanisms at the microbial level. Hence, the actual fate of RDX (and HMX) in terms of phytoremediation and natural attenuation remains uncertain and laboratory studies may not be applicable to the field because there will be more complex conditions including the presence of other organic and inorganic contaminants (*63*).

As noted above, mixed results have been reported with respect to aerobic environments. Several researchers (*33*, *50*) reported no degradation while others (*45*, *60*) observed limited degradation. Still others (*40*) reported degradation for both aerobic and anaerobic environments. Also, under aerobic conditions, experiments with the strain *Cornyebacterium* showed cometabolic degradation of RDX contaminated soils (40 to 60 mg/L in effluent) with more than 90 percent degraded within 1 to 3 days. These experiments showed the presence of ammonium inhibited the microbial degradation of RDX because organisms used RDX as a nitrogen source (*64*).

Thermal and chemical degradation of RDX resulting in the formation of methylenenitroamine may also occur. Methylenenitroamine undergoes spontaneous degradation to produce formaldehyde and nitrous oxide (*63*).

Photodegradation of RDX can occur in water and provides the basis for a wastewater treatment process employing ultraviolet radiation and ozonation. However, phototransformation of RDX in soil is not significant (*65*). Various photolytic half-lives have been reported for field conditions: 1.2 to 5.0 days (*66*), 10.7 hours (*67*), and 7 days (*68*, *69*). Phototransformation products include nitrate, nitrite, ammonia, formaldehyde, nitrous oxide, formamide, and N-nitroso-methylenediamine (*70*, *71*). Nitrate, nitrite, and ammonia have been reported at Camp Edwards, MA but the observed concentrations do not appear to be elevated (*13–16*, *72*, *73*). Formamide and N-nitroso-methylenediamine have not been detected.

Thompson and co-workers (*74*) reported that information was lacking regarding the fate and transformation of RDX in plants. Their study using hydroponic solutions containing RDX to grow Poplar trees, however, is representative of other recent work. The study demonstrated 60 percent of the RDX uptake went into leaf tissue. Over a 7-day period, there was no significant transformation of RDX in the plant tissue, suggesting both RDX accumulation and stability. Similarly, another study (*75*) found "undeniable evidence for plant bioaccumulation of RDX." In the latter investigation, bush bean plants were grown in 10 mg/L RDX hydroponic solutions. The results demonstrated that the RDX was rapidly taken up and that it accumulated in the plant tissue, particularly in the leaves. Over a 7-day exposure period, limited evidence of plant metabolism of RDX was observed. The authors concluded bioconcentration by plants may be a significant mode of transfer of RDX from soils into the food chain.

In summary, under intense anaerobic conditions (e.g. approximately -150 mv) and a near-neutral pH, RDX biodegradation can be an efficient removal mechanism, although toxic intermediates (nitrosamines) are formed during the process (*59*). Migration to groundwater is limited by a relatively slow dissolution, which is a function of the contact time between the HE particulate and infiltrating

precipitation (*22*). However, once dissolved in aerobic aquatic environments RDX is persistent and mobile (*22*).

Octahydro-1,3,5,7-tetranitro-1,3,5,7-tetrazocine (HMX)

Octahydro-1,3,5,7-tetranitro-1,3,5,7-tetrazocine (HMX or High Melting Explosive) is a nitroamine like RDX. HMX is a crystalline solid at room temperature with a molecular weight of 296 g/mol. HMX has a low water solubility (6.6 mg/L) (*76*, *77*) and vapor pressure and its octanol-water partitioning coefficient (K_{ow}) indicates a low affinity for hydrophobic substances. There is no significant effect on solubility over the pH range 4.2-6.2 (*31*). Jenkins and others (*78*) reported a K_{ow} value of 1.15 L/kg for HMX, indicating greater partitioning to water than is typically observed. Apparently, strong intermolecular bonds within the crystalline structure explain the inconsistency of low aqueous solubility and the tendency not to partition out of solution. Rosenblatt and co-workers (*79*) reported an organic carbon adsorption coefficient (K_{oc}) of 3.47 L/kg, which suggests a moderate propensity to adsorb to organic matter.

Dissolution experiments (*39*) showed only a small effect of mixing rate as dissolution varied by a factor of less than two as the mixing rate was doubled. Solubility at 2 to 4^{o}C, however, was less than 1 mg/L, increasing to approximately 4 mg/L as the temperature was raised to 22 to 24^{o}C. Only at temperatures exceeding 30^{o}C did the solubility exceed 7 mg/L. Solubility and dissolution rates have also been determined for HMX, TNT and RDX in the formulations Octol, Comp B, and LX-14 as well as mixtures of the three individual compounds comprising these formulations (*31*). The solubilities of the individual compounds from formulations and mixtures were comparable to those of the individual compounds as measured independently. Similarly, the dissolution rates for HMX and TNT were slightly higher and RDX slightly lower from the mixtures, but the rates were comparable to those of the individual compounds. Dissolution rates were suppressed somewhat in Octol but not in the other formulations as compared to the individual compounds. Other observations included: 1) as noted above, military grade RDX had sufficient HMX for the latter to attain its solubility limit in solution; and 2) Comp B contained sufficient HMX for the compound to attain saturation in solution and also contained detectable quantities of TNB, DNB, and 2,4-DNT. Recent work examined HMX dissolution from Octol collected in the field. The investigation demonstrated that the specific surface area of Octol and HMX from different sources may be the main parameter controlling the dissolution process. The specific surface area of HMX may vary by four orders of magnitude depending on Octol origin; the result being HMX dissolution varying by more than two orders of magnitude (*80*).

Most studies indicate sorption of HMX is not a significant process. McGrath (*32*) reported HMX passed through laboratory columns with minimal retardation and Checkai and co-workers (*47–49*) reported HMX was highly mobile in soils with low clay content and low CEC. Such results are consistent with studies by Pennington and co-workers (*58*) who found HMX to be entirely leached from clay-loam soils from several sites. Distribution coefficients range from as low

as 0 to as high as 13.25 L/kg (*46*) and indicate little retardation under typical conditions. Price and co-workers (*50*) examined the effects of Eh and pH on sorption and demonstrated little or no effect. Although, lowering the Eh to highly reducing conditions (-150 mv) decreased the measured K_ds by a factor of 10. HMX adsorption is reversible according to laboratory work (*40*, *46*) for the several soils studied. However, others (*81*) have reported that desorption is a slow process.

A few studies employing bioreactors with isolates and controlled conditions have shown some aerobic utilization (*82*), but degradation of HMX apparently does not occur in the field under aerobic conditions (*83*). Rodacy and Leslie (*54*) determined the half-life of HMX to be 39 years based on work by DuBois and Baytos (*55*) in an arid environment. In contrast, HMX degradation is observed anaerobically (*50*, *61*). Spanggord and co-workers (*68*) identified the anaerobic end products as nitrite, nitrate, and formaldehyde. Nitroso derivatives were observed in batch experiments but not in column experiments (*61*, *83*). HMX also was biotransformed in an anaerobic sludge with a glucose carbon source to yield octahydro-1-nitroso-3,5,7-trinitro-1,3,5,7-tetrazocine, octahydro-1,3-dinitroso-5,7-dinitro-1,3,5,7-tetrazocine, and its isomer octahydro-1,5-dintroso-3,7-dinitro-1,3,5,7-tetrazocine and the tentatively identified compounds methylenedinitroamine and *bis*(hydroxymethyl)nitroamine (*84*, *85*). The intermediates did not accumulate and were further degraded to nitrous oxide, formaldehyde, and formic acid. The formaldehyde degraded to carbon dioxide and the nitrous oxide rapidly degraded to nitrogen in the absence of glucose. Methane was formed by mineralization. Hydrazine and dimethylhydrazine were not detected. HMX degradation has also been reported under sulfate-reducing conditions and by fungi (*82*).

HMX (as does RDX) undergoes ring cleavage and extensive mineralization (60 percent with anaerobic sludge). However, the biodegradation pathway with respect to microbial populations and the enzymes involved has not been identified with certainty. Nevertheless, it is clear that once the ring cleaves, the degradation products are thermally unstable and hydrolyze readily in water. The latter abiotic reactions compete with biotic reactions during attempted biodegradation and complicate evaluations of the degradation process at the microbial level. Hence, the actual fate of HMX in terms of natural attenuation remains uncertain and laboratory studies may not be applicable to the field where conditions are more complex (*84*, *85*).

Phototransformation of HMX in soil is not significant (*65*), although dissolved HMX does photodegrade with reported half-lives ranging from 1 week (*69*) to 17 days (*68*). Reported degradation products include nitrite, nitrate, and formaldehyde (*68*).

The limited numbers of studies that evaluated phytoremediation of HMX do not indicate a useful role. *Kenaf* was exposed to HMX in soil and irrigation water (*86*). Little growth was observed in soil containing HMX, but normal growth occurred when irrigated with HMX-containing water. HMX was not taken up significantly and what was taken up was found in the aboveground portion of the plants. When the exposed plants were permitted to humify in the soil, HMX was still present (*86*). Other investigators (*76*) examined selected terrestrial and aquatic plants for their capacity to accumulate and degrade HMX and reported

similar results. Plants grown in a controlled environment and plants from a firing range (CFB Wainwright, Central Alberta, Canada) were assessed. HMX accumulated in leaves of most of the selected species to levels significantly above the soil concentration but there was no direct evidence of plant-mediated HMX transformation.

In summary, HMX undergoes anaerobic degradation resulting in the formation of mono and dinitroso products with retention of the ring system. Similar to RDX, HMX does not undergo significant transformations in an aerobic environment nor is adsorption to soil particles an important process at most sites. Migration of HMX to groundwater is limited by slow dissolution of particulates, which is a function of contact time between the HE (high-explosive) particulate and infiltrating precipitation - slower even than RDX.

2,4,6-Trinitrotoluene (TNT)

Trinitrotoluene is a single-ring nitroaromatic compound, a crystalline solid at room temperature with an empirical formula of $C_7H_5N_3O_6$, and a molecular weight of 227 g/mol. TNT's water solubility (approximately 150 mg/L) and vapor pressure are relatively low but greater than those of RDX and HMX. Measurements (*87*) have demonstrated no significant effect of pH on solubility, but temperature exerts a large influence with the solubility being approximately 50 mg/L near 2°C, approximately 100 mg/L near 20°C, and approximately 210 mg/L near 36°C. Volatilization of TNT from surface water to air or from soil moisture to soil gas is not a significant fate-and-transport mechanism (*30*, *34*, *88*). This conclusion is supported by TNT's low vapor pressure (10^{-6} to 10^{-8} mm Hg) and low Henry's law constant (10^{-7} to 10^{-9} atm-m^3/mol). Lack of volatilization is supported by an experiment in which only 8 to 10 percent of the TNT was volatilized over an 18-day stripping experiment in which wastewater from a TNT manufacturing process was aerated (*89*).

The first step in the fate-and-transport process for TNT is dissolution from the energetic residue into solution. At 10°C the dissolution rate of TNT varied from approximately 0.03 to 0.09 mg/min as the mixing rate varied by a factor of slightly more than two (*87*). Under the same mixing conditions, but at 30°C, TNT's dissolution rate varied from approximately 0.14 to approximately 0.34 mg/min. Similarly, varying TNT's surface area from approximately 6 to 9 cm^2 with a constant temperature at 10°C yielded dissolution rates varying from approximately 0.05 to approximately 0.07 mg/min. However, at 30°C and otherwise the same conditions, the dissolution rate varied from approximately 0.23 to approximately 0.31 mg/min.

Other relevant dissolution data comes from column experiments conducted to evaluate dissolution from HE particles at Camp Edwards, MA (*43*). Experiments were performed with two different flow conditions using the explosive formulations Composition 4 (C4) and Composition B (Comp B) in 2-inch diameter glass columns. The observed TNT dissolution rates for the continuous flow conditions ranged from 0.00009 to 0.00062 mg/hr/cm^2. For the flow/no-flow conditions observed dissolution rates ranged from 0.0003 to

0.00038 mg/hr/cm^2. These values are approximately 0.01 percent of a much larger value, 4.16 mg/hr/cm ^{2}, reported for a study which employed stirring in an aqueous solution to measure the dissolution rate (*90*).

Partition coefficients reported by most investigators indicate soils have a high capacity for rapid sorption of TNT (*22*). Varying redox conditions have little effect on TNT sorption (*37*, *40*, *44*, *91*, *92*). Most studies report the inorganic components of soil (clay, iron oxyhydroxides, base saturation) are more important than the organic matter content in predicting sorption (*91*, *93*, *94*, *96*, *97*). Irreversibly-bound TNT and degradation products have been reported (*58*, *91*, *98–101*). Some investigators (*45*, *96*) found TNT sorption reversible under certain conditions. The difference in results may be attributable to degradation products which compete with the parent compound for sorption sites (*92*) and may be irreversibly bound (*102*).

The study of Weissmahr and co-workers (*93*) provides the most comprehensive examination of the competing processes affecting TNT sorption. TNT sorption to NOM (natural organic matter) was low compared to clays although the interaction with clays depended strongly on the type of exchangeable cations (i.e.; base saturation). The authors did acknowledge reports of TNT and the aDNTs being removed from aqueous solution by colloidal NOM, but the nature of these interactions had not been described. According to this study (*93*), the dominant sorption mechanism to clay is an electron-donor complex formation between siloxane oxygens (sigma-donors) and the nitroaromatics (pi-acceptors). High surface densities of strongly hydrated cations (sodium and calcium) reduce the accessibility of siloxane sites for nitroaromatics, whereas weakly hydrated and less bulky ions such as potassium or ammonium promote inner sphere complexes at siloxane sites. The singular feature of this work is it evaluated mixed ionic conditions and complex natural matrices. Aquifer material with less than 1 percent natural occurring organic matter and 3 to 5 percent clays had similar sorption features as pure clay minerals, suggesting sorption to the bulk aquifer matrix was dominated by complex formation at the clays.

TNT not sorbed onto soil is usually transformed rapidly. TNT transformation is reported to occur in any aerobic environment and many organisms are capable of aiding transformation (*46*, *66*, *103*). TNT is biotransformed to the aDNTs, which are transformed to several other products including azo, azoxy, acetyl, and phenolic derivatives. All biotransformations leave the aromatic ring intact (*84*, *85*). Transformation products identified in TNT "pink water" (usual color of wastewater from TNT manufacturing plants) were 2a-DNT, 4a-DNT, 2,4-DANT, and 2,6-diamino-4-nitrotoluene (2,6-DANT) before culminating in the formation of triaminotoluene (TAT) (*104*). Some aerobic bacteria and numerous bacterial strains can degrade daughter products of TNT, but one investigation (*82*) concluded "the scope for complete mineralization of TNT" by aerobic systems "may be of limited use" because of the "formation of dead-end metabolites." Hydroxylamines and the mono and di-amino-nitrotoluenes are the principal microbial transformation products. Hydroxylamines are reactive unstable compounds, which are not typically observed in natural environments. Formation of unknown transformation products or products not extractable

without destruction of the molecule have been observed by several researchers (*94*, *105*, *106*) and accounted for 50 percent of the mass loss with a clay soil (*107*).

In anaerobic systems, complete transformation of TNT to byproducts is common (*105*). The predominant byproducts are 2a-DNT (*47–49*, *53*, *91*, *94*, *105–110*), as well as 4a-DNT, 2,4-DANT (*111*), and 2,6-DANT (*91*, *111*). Several workers (*91*, *111*, *112*) observed a preponderance of 4a-DNT over 2a-DNT. Townsend and Myers (*46*) also report the preferred reduction pathway as TNT→4a-DNT→2,4-DANT. Other transformation products observed include TNB, 2,4,6-trinitrobenzaldehyde (TNBa), and 3,5-dinitroaniline (3,5-DNA) (*108*). 2,4-DNT, 2,6-DNT, and 3,5-DNA have also been reported (*111*). Triaminotoluene (TAT) formation in "pink water" has been reported (*104*) but has not been observed in waters from military ranges. Under anaerobic conditions, TNT undergoes step-wise reduction to TAT wherein the formation of 2,4-DANT is the rate-limiting step. TAT is sometimes considered a dead-end byproduct, which binds irreversibly in the soil.

Abiotic reduction of TNT has also been observed with the following transformation products identified: 4,4′,6,6-Tetranitro-2,2′ azoxytoluene (4,4AZOX) and 2,2,6,6′-tetranitro-4,4′ azoxytoluene (2,2AZOX) (*113*). Price and co-workers (*103*) observed the transformation products 4a-DNT, 2a-DNT, and 4,4AZOX with the 4,4AZOX disappearing within 24 hours in surface soils.

Previous research had considered photodegradation of TNT as possible if standing water was present for any length of time and TNT present in the soil dissolved into the water (*57*, *66*, *114–117*). TNT photodegradation is reportedly faster than biodegradation by a factor of 1,000 (*66*). The reaction is presumed to occur via a triplet-sensitized mechanism which either permits a weak nucleophile to attack and remove a NO_2 or X- group, or allows the formation of a complex with humic acid increasing the favorability of ultraviolet absorbance and, therefore, photodegradation (*66*, *79*, *118*). Photocatalytic degradation, however, was not believed to be an effective method for TNT removal because end products are often as toxic and mobile, if not more so, than the parent compound (*114*). Burlinson and co-workers (*119*) identified a number of photolytic byproducts including TNBa, TNB, and trace amounts of 2,2AZOX, 4,4AZOX, and 2,4′-dimethyl-3,3′,5,5′-tetranitro-ONN-azoxybenzene. Apparently, fewer byproducts are produced with less exposure time (*57*, *66*, *116*). The compound 3,5-DNA (*114*) was observed when both TNT and RDX were present (*115*). Additionally, Andrews and Osmon (*117*) reported unidentifiable volatile products.

A recent field experiment with chunks of TNT under range conditions, however, indicates that photodegradation is, indeed, a significant removal mechanism (*119*). Mass balance data revealed that TNT that dissolved in precipitation accounted for only about one-third of the TNT lost from the chunks. The creation of photo-transformation products on the solid chunks, and their subsequent dissolution or sublimation, was believed to account for the remaining two-thirds.

TNT bioaccumulates in plants with uptake inversely proportional to soil organic matter content indicating TNT bound to humic acids is no longer available (*86*, *121*, *122*). These studies reported that TNT was found mostly in the roots.

In addition, one study (*123*) demonstrated both 2a- and 4a-DNT accumulation in plant tissues indicating the TNT was being transformed as well. On roots and leaves, highly polar and non-extractable TNT metabolites dominated with the aDNT isomers accounting for less than 20 percent of the residues present. Only a few percent of the residues were present as the parent TNT.

In summary, TNT is rapidly degraded in most soil and aquifer systems and, therefore, its presence is typically restricted to areas near its introduction to the environment. The major fate-and-transport processes for TNT in soil and groundwater are dissolution, adsorption, abiotic transformation, biotransformation, diffusion, advection, and hydrodynamic dispersion (*32*, *46*). The transformation rates are sufficiently fast at most sites, for TNT to be attenuated fully in the surface soil thereby preventing contamination of the vadose zone or groundwater. In the case of Impact Areas, the majority of the TNT will be degraded in the surface soil but small quantities can reach shallow groundwater. At OB/OD areas, the mass of TNT may be sufficient to overwhelm the attenuation mechanisms resulting in TNT reaching groundwater. However, TNT usually continues to undergo transformation in groundwater limiting its mobility. Clausen and co-workers in Appendix A (*22*) provide a detailed summary table of the physical and chemical properties of the energetic compounds with references cited.

Dinitrotoluenes (DNT)

The DNTs are nitro-aromatic compounds differing from TNT only in their lack of a third NO_2 group attached to the aromatic ring. The isomers of environmental importance are 2,4- and 2,6-DNT. Both compounds are byproducts in the TNT manufacturing process and are typically found in a 4:1 ratio of 2,4 to 2,6-DNT (*124*). Besides their presence as manufacturing impurities, 2,4-DNT has been used as a binder in some single-base propellants (*125*). The latter study includes a summary of propellant physical and chemical characteristics collected from a wide variety of sources (*125*). These data show that the DNTs have higher water solubilities (approximately 180 mg/L for 2,6-DNT and 270 mg/L for 2,4-DNT) than TNT. Solubility was measured in one experiment by direct sampling of a crystalline suspension in deionized water (*126*). The 2,4-DNT solubility measured in this study, however, was different from that reported by the US Army Material Command (*127*), the historical reference for 2,4-DNT. The 2,4-DNT solubility from this study was 30 percent less at 22^{o}C and 65 percent greater at 50^{o}C.

Vapor pressures for the DNTs are low and their K_{ow}s indicate a moderate affinity for hydrophobic substances (*22*). Despite the low vapor pressure, volatilization of 2,4-DNT is twenty times that of TNT (*91*) and rapid enough it may be useful for UXO detection (*126*). Nonetheless, volatilization is still too slow to be an important fate and transport process (*34*). As an example, depletion of a DNT source was not observed even after 30 years (*88*). Photodegradation of DNTs is possible once dissolved in water, however, this mechanism is limited in

the field because, similar to TNT (*22*, *90*, *92*), their dissolution rate is expected to be slow.

DNT embedded within NC fibers is deposited primarily on the soil surface near artillery firing positions (Fig. 4) as a result of particulate and gaseous deposition from the use of single-base propellants (*10*, *125*). DNT mobility is not significant (Fig. 5), consistent with various research demonstrating strong retention in surface soil (*47–49*, *127*). Sorption experiments were conducted specifically for Camp Edwards, MA to determine the partitioning of 2,4-DNT for various experimental conditions and site soils (*43*). The average K_d value for the shallow soil experiments was 3.2 L/kg, a value indicating significant sorption to soil at the surface. The retention in the surface soils is probably a consequence of increased organic matter or protection of the DNT from environmental exposure via the NC casing. The latter conclusion is consistent with studies showing relatively high levels of 2,4-DNT (0.01 to 100 mg/kg) remaining on the soil surface near active firing points (*10*, *27*) and with studies showing how slowly DNT is leached from the NC matrix (*125*). In the latter investigation, only approximately 0.4% of the available DNT leached after 216 hours of stirring single-base propellant in an aqueous solution. DNT's association with NC is also demonstrated by sampling experience showing that samples must be carefully collected from the top 1 cm of soil, without the vegetation removed, to accurately measure DNT surface concentration. In summary, DNT's strong retention by both NC and the soil matrix precludes significant migration (*127*), although one disposal site at the Massachusetts Military Reservation has had detectable DNTs in associated groundwater (*16*).

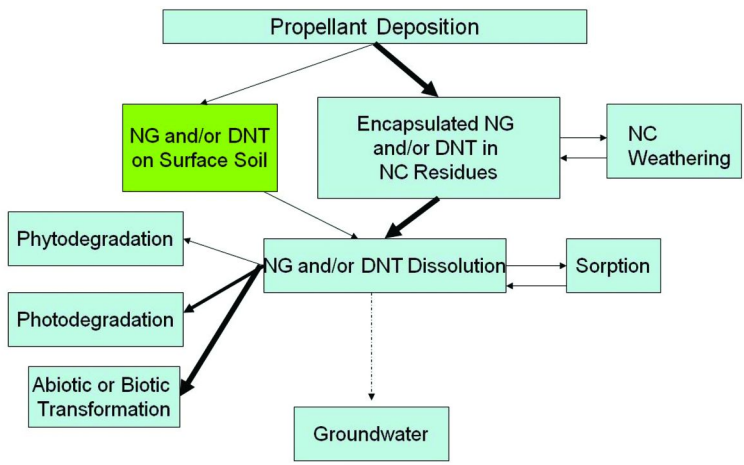

Figure 5. Fate-and-transport conceptual model for the deposition of fired propellant containing nitrocellulose (NC), nitroglycerin (NG), and dinitrotoluene (DNT).

Several researchers have identified biodegradation as the key fate-and-transport mechanism for DNTs in the vadose zone (*66*, *91*) and some of the work has provided ample evidence for aerobic transformation (*128*). Degradation pathways for 2,4-DNT and 2,6-DNT have been elucidated for aerobic systems (*129*). Individual bacteria have been identified capable of growing on a single DNT isomer (*129*, *130*) and have been isolated at contaminated sites (*129*). Any dissolved DNT, therefore, has a high potential to degrade biologically.

A scheme for the aerobic biotransformation of DNT has been presented (*95*). The mechanism included some postulated intermediates as well as some identified in other research. The products of microbial transformation of 2,4-DNT by *Mucrosporium* sp. as identified by thin-layer chromatography and by gas chromatography-mass spectrophotometry (GC/MS) were 2-amino-4-nitrotoluene (2a-4-NT), 4-amino-2-nitrotoluene (4a-2-NT), 2,2′-dinitro-4,4′azoxytoluene, 4,4′-dinitro-2,2′azoxytoluene, and 4-acetamido-2-nitrotoluene. Another compound, possibly a mixed type, was isolated but not identified. Other studies (*131*) reported similar results, identifying the microbial transformation products as 2a-4-NT, 4a-2-NT, 2-nitroso-4-nitrotoluene, and 4-nitroso-2-nitrotoluene. The latter compound was only tentatively identified. Liu and co-workers (*131*) wrote that the biological reduction of 2,4-DNT proceeded through the nitroso hydroxylamine compounds. More recent work (*128*) suggested the aerobic degradation pathway for 2,4-DNT is initially to 4-methyl-5-nitrocatechol then to 2-hydroxy-5-methylquinone, to 2,4,5-trihydroxytoloune, and to 2,4-dihydroxy-5-methyl-6-oxo-2,4-hexadienoic acid. Similarly, research (*127*, *128*) identified the 2,6-DNT degradation pathway to be: 2,6-DNT to 3-methyl-4-nitrocatechol to 2-hydroxy-5-nitro-6-oxo-2,4-heptadienoic acid to 2-hydroxy-5-nitro-2,4-pentadienoic acid to nitrite.

Work performed with microbial isolates has usually not resulted in so many intermediates. For instance, one study demonstrated DNT in liquid cultures could be completely degraded without the production of amino-nitrotoluenes (aNTs) (*94*). When 2,4-DNT and 2,6-DNT-degrading microbial strains were added to a mixture of 2,4-DNT and 2,6-DNT in a soil slurry, disappearance of DNT was accompanied by the release of carbon dioxide and stoichiometric appearance of nitrite. When the experiment was performed with historically contaminated soil, 99 percent of the DNT was removed. Although traces of extractable DNT remained, soil toxicity was low. After an extended acclimation period first the 2,4-DNT and then the 2,6-DNT were degraded in an un-inoculated control. Thus, 2,4-DNT is preferentially consumed relative to 2,6-DNT and high concentrations of 2,4-DNT can inhibit the transformation of 2,6-DNT.

Thus, aerobic biodegradation of the DNTs can occur rapidly in surface water with reported half-lives of 2.7 hours to 1.7 days (*133*). The compound 2,4-DNT was biodegraded to 4A-A-2-NT and 2A-4-NT and 2,6-DNT to 2A-6-NT at the Weldon Springs site (*134*). Transformations are typically sufficiently rapid to prevent groundwater contamination. The reason for the apparent persistence of 2,4-DNT at some sites (*10*, *14*, *27*) is probably a consequence of being embedded within a matrix of NC (*10*, *132*). Being bound in NC, the DNTs are protected from microbial attack until the NC is weathered. (NC is not susceptible to dissolution processes.)

Evidence for anaerobic degradation is mixed. According to one study (*128*), anaerobic degradation processes have not been identified for the DNTs. However, co-metabolic anaerobic degradation processes have been described (*131*, *135*, *136*) and transformation rates for 2,4-DNT ranging from 0.0017 to 0.017/hr in anaerobic aquifer soils have been reported (*137*). As discussed below, evidence has also been presented for anaerobic degradation by *Clostridium acetobutylicum.* Anaerobic activated sludge typically transforms 2,4- and 2,6-DNT to 2a-4-NT or 2-amino-6-nitrotoluene (2a-6-NT), which often accumulate with no further degradation (*129*). This research identified 30 additional isolates (e.g. *Burkholderia* sp. strain DNT) with the ability to mineralize 2,4-DNT by the same pathway. Intermediates and products of 2,4-DNT and 2,6-DNT anaerobic metabolism by *Clostridium acetobutylicum* have also been isolated and identified. *Clostridia* are important because of their ability to reduce aryl nitro groups, but before this study, the examination of 2,4-DNT and 2,6-DNT had not been rigorously performed. The initial products were hydroxylaminonitrotoluenes. Subsequent transformation favored the formation of dihydroxylaminotoluenes with a limited reduction to amino nitrotoluene (aNT) isomers. Nitroso products were not observed. In cell cultures, metabolism beyond dihydroxylaminotoluene was not observed. In cell extracts, where activity could be maintained beyond that in cell cultures, further transformation yielded amino-hydroxylaminotoluenes and eventually diaminotoluenes. These findings further demonstrate the potential for hydroxylamines to be significant intermediates of nitroaromatic transformation under anaerobic fermentative conditions. In contrast to previous studies, rearrangement of dihydroxylaminotoluenes was not observed. Dihydroxylaminotoluenes were found to be quite unstable decomposing rapidly under exposure to oxygen (*129*).

Photodegradation of DNTs is possible if standing water is present for any length of time and DNT present in the soil dissolves into the water. However, photodegradation is not an important mechanism if there is no ponded water because of a presumed slow dissolution rate. DNT is readily photolyzed with up to 50 percent loss of 2,4-DNT in 5 days and 2,6-DNT in 1-day. Other studies have indicated a photodegradation half-life of less than 10 hours with the photodegradation rate accelerated by the presence of humic materials (*66*). The photodegradation product of 2,4-DNT is 2,4-dinitrobenzoic acid, which itself is photodegradable to carbon dioxide, water, and nitric acid. Phytotransformation studies of the DNTs are lacking.

In summary, the DNTs are adsorbed rapidly onto soil and are subject to rapid aerobic biodegradation (Fig 5). The DNTs are not persistent and mobile in an aerobic environment. The principal fate-and-transport mechanisms in soil are adsorption and abiotic and biotic transformation (*22*).

Nitroglycerine (NG)

Reagent-grade NG (227 g/mol) is soluble in water at approximately 1,250 to 1,950 mg/L (*79*, *138*). Consequently, when transport models such as SESOIL are used without considering factors other than solubility, the calculated results

suggest rapid movement of NG through the soil horizon. However, NG is susceptible to adsorption, rapid photodegradation, and biodegradation (Fig. 5). Moreover, NG initially must be released from an insoluble NC matrix because virtually all use is as a gelatinizer in double- and triple-base propellants (*125*). Dissolution from a propellant relies upon the physical weathering of the NC or, perhaps, other mechanisms such as diffusion.

The extent to which release from NC delays environmental cycling of NG has been examined by stirring propellant in aqueous solution (*125*) and by column experiments (*132*). The former experiments indicated as much as 40% or more of the NG could be leached during a 216 hour period of stirring. Much less NG was released during the column experiments. Consequently, field measurements consistently indicate NG concentrations remain well below saturation. More recent work, employing batch equilibration studies with both fired and unfired propellant, has also demonstrated that dissolution is the rate-limiting step in NG migration (*139*).

Untransformed NG is readily susceptible to soil sorption processes having a high affinity for organic matter (log K_{ow} = 41-59 mL/g) (*79*). Batch adsorption experiments with reagent-grade NG with organic-poor soils from Camp Edwards, MA suggested an average K_d value of approximately 2 L/kg (*43*). In contrast, no desorption was observed to occur in batch desorption tests with weathered contaminated soils (*43*). Although nothing was detected in the final solution, desorption K_d > 71 L/kg was estimated based on an initial soil concentration of 7,120 µg/kg, assuming it was present at the detection limit (100 µg/L). Subsequent work under more controlled conditions indicated a desorption K_d of 1.6 L/kg (*139*).

Aerobic biodegradation studies utilizing static batch tests (*56*) found the half - life of NG to be less than 1 day; which was so rapid that the loss rate could not be quantified. Stirred batch reactor studies with a clay-loam soil and organic carbon content of 0.2%, yielded a half- life for NG of 1.5 days (*140*). Another study (*141*) found NG to have a half-life of 2 to 7 days while recent work employing batch equilibration studies demonstrated that degradation was so rapid that sorption processes could not be quantified unless biocide was added to the solutions (*139*).

Nitroglycerin degradation follows successive denitration to produce glycerol 1,2- and 1,3-dinitrate (1,2-GDN and 1,3-GDN), and glycerol 1- and 2-mononitrate (1-GMN and 2-GMN). The GDN and GMN isomers further breakdown into glycerol and carbon dioxide (*142*). However, these metabolites were not found in another study from which the investigators speculated that the rate of transformation of these metabolites was so rapid that they do not accumulate (57)—GDN isomers have explosive properties similar to the NG parent compound (*143*). Spanggord and co-workers (*57*) showed 96% conversion of NG to nitrite, and that microorganisms can utilize NG as a sole carbon source. Studies by other investigators (*144–146*) have identified a variety of bacterium NG degraders. Earlier work (*147*) suggested NG photodegradation was possible and subsequent studies (*148*) suggested the rate of loss via this mechanism was insignificant. Spanggord and co-workers (*57*) suggested a slow rate of photolysis yielding a half life of 57 to 73 days.

To summarize, although NG can be readily dissolved from the NC matrix in which it was deposited; dissolution remains the dominant factor regarding its

environmental availability. Once dissolved, NG is so rapidly biodegraded that its low propensity for sorption does not result in significant migration.

Perchlorate

Perchlorate (ClO_4^-) is introduced into the environment as the solid salt of ammonium, potassium, or sodium perchlorate. Ammonium and potassium perchlorate are used as the oxidizer component and primary ingredient in solid propellants for rockets, missiles, and fireworks. Perchlorates are also used in flares, smokes, tracers, and other pyrotechnics as well as in automobile air bags, as an additive in lubricating oils, and in some batteries. Perchlorate is principally found at OB/OD sites, especially those sites where fireworks have been burned. There is some evidence from Camp Edwards, MA (*15*) that the use of artillery and mortar-spotting charges containing perchlorate can contribute enough mass resulting in groundwater impacts. Perchlorates are highly soluble, non-volatile, and typically mobile in the environment

Based on a comprehensive review (*149*), perchlorate should behave as a conservative tracer. The latter conclusion has been supported by recently-described fieldwork as well (*80*). A K_d of 0.32 L/kg, as reported by the Texas Natural Resource Conservation Commission, is indicative of most measurements (*150*). The perchlorate ion is large with a single negative charge; the resulting low charge density reduces its affinity for positively charged ions and makes it a very poor complexing agent. Because there are no strong binding forces at work, dissolution of perchlorate from soil to water occurs readily. The aqueous solubility of common perchlorate salts can achieve 25% or more on a mass/mass basis in water.

Perchlorate's solubility varies by the salt present and is far higher than the other energetic compounds most frequently detected at ranges. The solubility of ammonium perchlorate is reported to be 20,000 mg/L while potassium perchlorate is 15,000 mg/L at 25°C (*151*). Sodium perchlorate's solubility is reported to be 17,000 mg/L at 25°C (*152*). For comparison, the solubility of TNT has been reported as 115 mg/L at 23°C (*153*), while the solubility of RDX is only 64 mg/l at 25°C (*154*). Perchlorate salts are essentially non-volatile at ambient temperatures, so losses through the vapor pathway are not significant.

Perchlorate salts are persistent in the environment and are not readily degraded by either chemical or biological means. This persistence is a consequence of kinetics not because of a lack of thermodynamic favorability (*147*). Recent research does indicate bacteria capable of perchlorate degradation are widely distributed in nature, but this degradation is usually not a viable path in soil or groundwater under normal environmental conditions (*155*, *156*). Microbial reduction of perchlorate, when it does occur, results in ultimate transformation to chloride and oxygen, with degradation intermediates including chlorate (ClO_3^-) and chlorite (ClO_2^-). The slowest step, however, is the initial reduction of the perchlorate ion; consequently no intermediates accumulate during perchlorate biodegradation. Perchlorate does not undergo phototransformation (*149*).

Studies with bulrushes, crabgrass, goldenrod, and cup grass have demonstrated perchlorate may accumulate in tissues of plants. Bulrushes growing in ponds with perchlorate contamination at 30 to 31 mg/kg were found to accumulate perchlorate in tissues, 7 mg/kg, both above and below the waterline and in roots, with the highest accumulation in tissues above the waterline (*157*). Crabgrass seeds contained perchlorate at a concentration of 1,880 mg/kg. For goldenrod, perchlorate concentrations were highest in leaves (1,030 mg/kg) but it also was present in stems, roots, and seeds (*157*). Tobacco grown in soils treated with Chilean caliche fertilizers accumulated perchlorate in leaves (*158*).

In some instances, perchlorate can be reduced by higher plants without involvement of facultative anaerobic microorganisms (*159*). Ammonium perchlorate was exposed to hydroponically grown trees and plant nodules. The work was performed under sterile conditions to ensure microbial activity did not contribute to perchlorate reduction. No toxic effects were noted and uptake was still occurring at the end of 30 days. Approximately 50 percent of the labeled perchlorate was removed from solution by Poplar trees and plant nodules in 30 days with 27.4 percent translocated in the leaves of the trees. Of the radioactivity remaining in solution, 68 percent had remained with the perchlorate ion. Both in solution and in the leaves, labeled chlorine was associated with unmetabolized perchlorate, chlorate ($Cl0_3^-$), chlorite (ClO_2^-) and chloride. The authors reviewed other work involving perchlorate uptake and concluded that Poplar trees are midway in the range of the performances reported for other terrestrial trees. Willow trees have also proven capable of perchlorate degradation, with two distinctly different phyto-processes at work. Perchlorate can be taken up and degraded in the leaves and branches while degradation can occur in the rhizosphere by perchlorate-degrading microorganisms (*160*). The presence of competing terminal electron acceptors, such as nitrates and other nutrients interfered with the rhizodegradation of perchlorate.

In summary, although perchlorate is readily soluble, it's chemically stability limits natural chemical reduction in the environment. Further, the ion has a limited tendency to interact with other dissolved chemical species or to adsorb to aquifer materials under typical environmental conditions. Once dissolved in water, perchlorate is not significantly retarded by sorption and migrates at essentially the same rate as water. Reduction of the chlorine in perchlorate from the +7 oxidation state to the chloride ion (-1 oxidation state) does not occur readily (*148*). A high input of energy (e.g.; heat, light, or physical shock) or the presence of a catalyst is necessary to initiate significant reduction. This high activation energy is an advantage in munitions and fireworks, but such chemical stability also results in environmental persistence. Consequently, the fate-and-transport of perchlorate released to soils and water is controlled primarily through physical rather than chemical or biological processes. Because of perchlorate's high solubility and mobility, it is not expected to remain in soil at significant concentrations.

Other Explosive Compounds

Other explosive compounds present to a lesser degree at military ranges include 2a-DNT, 4a-DNT, 2,4-DANT, 2,6-DANT, PA, tetryl, TNB, and PETN. These compounds are not likely to be found in impact areas or firing points but may be present at OB/OD sites with concentrated demolition activity. Tetryl, PA, TNB, and PETN were infrequently observed in surface soil at an OB/OD site at Camp Edwards, MA and when present the concentrations were low, less than 10 mg/kg. There is a paucity of data regarding the fate and transport properties of these compounds and, unlike those already discussed, available research has not investigated all possible topics.

A few studies have identified the presence of PA, tetryl, TNB, and PETN, but none have identified these compounds as major contaminants at military sites (*1*, *3–9*). Further, the fate-and-transport properties of these compounds suggest limited mobility if introduced into the natural environment (*22*). For example, the compound 4a-DNT, a prominent degradation product of TNT and a groundwater contaminant at some ranges, has been infrequently evaluated. One study (*132*) used soil columns to evaluate release from weathered Comp B source material. The amount leached was only approximately 1% of what was possible based on solubility alone. In addition, both a-DNTs decreased rapidly after achieving a maximum, apparently a consequence of increasing microbial activity as the experiment proceeded. Over the course of the experiment, however, the quantity of a-DNT appearing in the effluent far exceeded the measured amount in the starting material; the TNT leached was much less. These results clearly support the formation of a-DNT from TNT as described previously. These results further explain why a-DNTs are not found far from source zones (*1*). Some of the a-DNT may biodegrade to 4-amino-6-nitrotoluene (4a-6-NT). It has also been reported that 4a-DNT degrades to 2,6-DANT and that 2a-DNT degrades to 2,4-DANT, although not in significant quantities (*91*).

Of the other compounds listed in this subsection, tetryl was widely employed as a booster and was used in some munitions as an explosive until discontinued in 1979 (*161*). (Tetryl may have been used after 1979 as old stock was used up.) Studies have shown extensive heating of tetryl at 120^{o}C yields picric acid (*161*). The source of TNB is TNT-containing mixtures such as Comp B which contain detectable quantities of TNB as an impurity. In addition, TNT exposed to sunlight can undergo photo-catalyzed oxidation of the methyl carbon to form a carboxylic acid. Subsequent decarboxylation forms TNB. Hence, as noted by Walsh and Jenkins (*109*), when TNT is present in soil TNB can also be present. Similarly, the DANTs are intermediate degradation products of TNT. The latter compounds are much more soluble and, therefore, more mobile than TNT. PETN is an explosive commonly found in detonation cord and high-efficiency blasting caps, as well as pentolite booster charges, used for blow-in-place detonations of UXO. Pentolite is a 50:50 mixture of TNT and PETN. PETN is a nitrate ester unlike the nitroaromatics DANTs, PA, tetryl, and TNB. PETN is not volatile and has low solubility in water. PETN has a solubility of 1 mg/L at 25^{o}C, whereas PA is relatively soluble (10,000 mg/L at an unspecified temperature) (*139*). Tetryl's solubility was reported as 80 mg/L at an unspecified temperature and the solubility

of TNB was reported as 3500 mg/L also at an unspecified temperature. As reported by McGrath (*32*) volatilization is not a significant mechanism for NG, PA, tetryl, TNB, and PETN due to their low vapor pressures.

Some insight into the mobility of tetryl and TNB can be obtained from a study of bioremediation in soil. Valsaraj and co-workers (*162*) measured relative flux from a soil bed and reported the following compounds in decreasing order: TNT, tetryl, DNT, and TNB. Humic substances and other organic materials can adsorb ammonium picrate (AP) and PA, but if absent; PA and picrate can be mobile (*53*, *163–165*). Apparently, solutions containing calcium ions or calcium clays cause rapid flocculation resulting in the removal of picrate from solution (*165*). Picric Acid is expected to be mobile if dissolved and if it reaches groundwater. PETN mobility is inferred from case studies which suggest it is retained in soil.

Biological reduction of one or more of TNB's nitro groups can occur in both aerobic and anaerobic environments with the reaction rate increasing as conditions become more reducing. For example, TNB is subject to biotransformation to 3,5-DNA, which has been recommended as an additional target analyte at ranges (*166*). The compound 3,5-DNA has been added to the explosive analyte suite used at Camp Edwards, MA, however; it has been infrequently detected elsewhere (*13–16*, *72*, *73*).

Picric Acid is rapidly degraded in surface soils. Degradation of PA to picramic acid (2-amino-4,6-dinitrophenol) is possible under anaerobic conditions (*165*). Several investigators have reported tetryl as biologically degradable to picrate (*53*, *165*, *167*). Walsh and co-workers (*168*), however, reported no success identifying degradation products, but did acknowledge tetryl was environmentally unstable. Natural biodegradation of picrate does not occur but may be possible using adapted organisms (*169*).

Mechanisms of biological degradation of nitrate esters such as PETN are not fully understood, but it is known that the cleavage of the ester linkage is required prior to degradation of the organic skeleton of the molecule (*170*). Rodacy and Leslie (*54*) determined the half-life of PETN to be 92 years based on work by DuBois and Baytos (*55*) who reported little disappearance of PETN in an arid soil environment over a three-year period. Other researchers (*81*) reviewed the degradation of nitrate esters including PETN and concluded it was unlikely bacteria will be discovered satisfying all of the requirements needed to degrade this compound.

Little information was found regarding the photodegradation of PA, tetryl, TNB, and PETN. Tetryl is photodegradable yielding picrate, N-methylpicramide, methylnitroamine, nitrate, and nitrite, but the half-life is rather long (*167*). Moreover, picrate does not photodegrade.

Among the many studies examining soil-plant relationships of energetic compounds, no specific studies examining PA, and PETN were found. Only limited work with tetryl was available (*118*, *119*). After 60 days, only 8 percent of the tetryl remained unchanged in the soil. The study reported the order of plant availability was RDX > tetryl ≥ TNT with the extent of plant uptake being dependent on soil type (sand > silt > organic soil) and plant species. Explosive and propellant residues were found mostly in the roots. Tetryl was metabolized to N-methyl-2,4,6-trinitroaniline and a variety of polar metabolites.

Trinitrobenzen biotransforms to 3,5-DNA (*166*). Although finding the compounds and byproducts in the roots is a positive consideration, more research is needed regarding the fate and toxicity of the metabolites (*171*).

In summary, the a-DNTs, formed from TNT, degrade rapidly and are unlikely to be persistent. TNB is another degradation product of TNT and is less mobile than tetryl. Tetryl in turn is less mobile than TNT, and typically degrades rapidly to picrate. Picric acid may degrade to picrate, as does tetryl. Picric acid and picrate are adsorbed if humic materials are present, but can be water soluble and mobile in a sandy environment. Picrate itself is not biodegradable (*164*). The nitrate ester, PETN, is very persistent in soil due to lack of degradation, however; it is strongly adsorbed. Further, PETN migration is inhibited by its low water solubility. In general, 2a-DNT, 4a-DNT, 2,4-DANT, 2,6-DANT, PA, tetryl, TNB, and PETN are not likely to be found at military ranges except in the presence of much higher concentrations of the more abundantly used explosives (e.g. TNT, RDX, and HMX) and their primary metabolites or impurities (e.g. DNT and aDNTs).

Case Studies

Investigations of energetic compounds in the environment have been conducted at many locations. Two extensive case studies are at Camp Edwards on the Massachusetts Military Reservation in the USA and at Canadian Forces Base Valcartier, Quebec, Canada. Those two sites provide excellent overviews of the current state-of-the-science for fate and transport of energetics.

Camp Edwards Artillery and Mortar Impact Area

Camp Edwards, MA on the Massachusetts Military Reservation (MMR) has a broad area of RDX groundwater contamination emanating from the impact area (Fig 6) and spanning a width of over 1220 m (4,000 ft) (*12*, *15*). HMX and perchlorate are also detected in the groundwater. The approximate mix of energetic compounds associated with the site's impact area is shown in Fig 7.

The plume of contaminated groundwater encompasses an area approximately 3,350 m (11,000 ft) long by 1500 m (5,000 ft) wide (Fig. 6). Approximately 3331 to 4921 million liters (880 to 1.3 million gallons) of water have been contaminated. The areal extent is 2.5 km^2 (618 acres). The amount of RDX dissolved in this volume of contamination is approximately 13 to 37 kg (30-80 lbs). Within the center of the impact area, RDX is present from the water table to a depth of approximately 27 m (87 ft) below the water table (bwt). Along the western boundary (downgradient) of the impact area, RDX is present from approximately 6.7 to 29 m (22 to 96 ft) bwt. RDX concentrations are highest under the targets even though training activities with high explosive artillery munitions had not been conducted for more than eleven years, nor with high explosive mortars for more than five years. Hence, sufficient contaminant mass must reside in the soil and vadose zone to maintain the RDX levels observed at the water table. The latter conclusion, however, has not been supported by analytical

data because RDX typically is not detected in the vadose zone and the distribution and the measured mass in soil are not consistent with the groundwater plume.

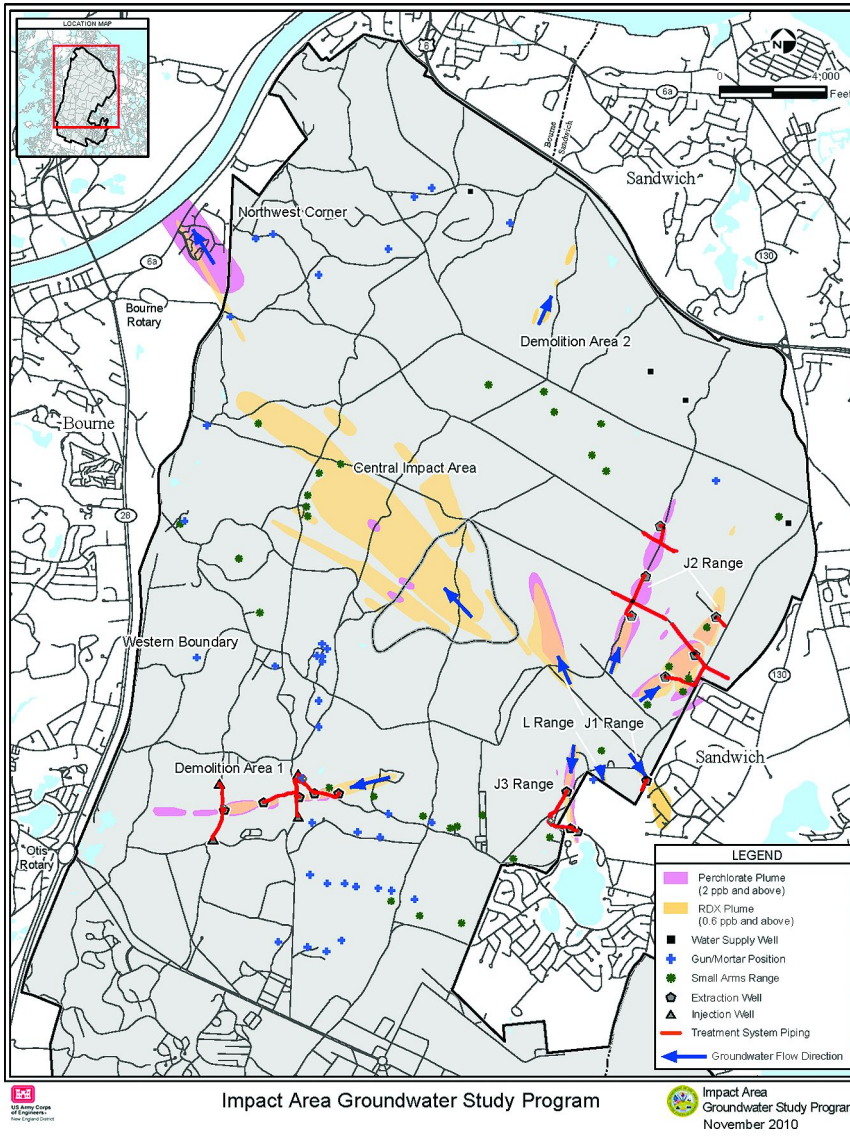

Figure 6. Extent of RDX contamination in the Central Impact Area of Massachusetts Military Reservation as depicted in July 2003 (Impact Area Groundwater Study Program).

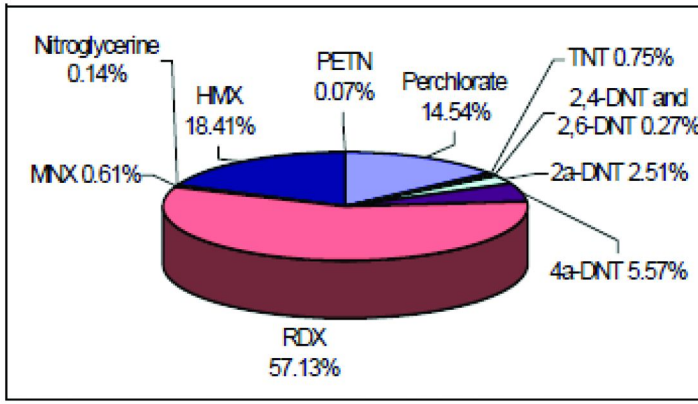

Figure 7. Relative percentage of detections of high explosive compounds found in groundwater associated with the Camp Edwards, MMR, Impact Area (22).

Groundwater flow modeling with particle backtracking for RDX, HMX and perchlorate supports a distributed source Conceptual Model (*15*, *22*). The particle tracks don't converge to a single or limited number of areas but to a large area of approximately 1.3 km^2 (300 acres) (*12*, *15*). This convergence area is coincidental with the known target locations, highest crater density and surface debris, elevated high explosive detections in soil, and largest airborne magnetometry anomalies (*172*, *173*).

The extent of perchlorate contamination is less than RDX, encompassing an area of approximately 2 km^2 (500 acres) (*12*, *15*). The plume orientation is consistent with the groundwater flow direction and measures 1280 m (4,200 ft) at its widest. As observed for RDX and HMX, dissolved perchlorate migrates in the direction of groundwater flow and migrates deeper with increasing distance because of accretion of infiltrating precipitation onto the water table.

There appear to be two source areas for perchlorate: a particular target separate from the Impact Area (CS-19) and the Central Impact Area itself. Perchlorate extends 945 m (3,100 ft) from the CS-19 area and 2286 m (7,500 ft) from the middle of the Central Impact Area. The volume of contaminated water is estimated at 31 to 42 billion liters or 8.3 to 10.6 billion liters (8.2 to 11.1 billion L or 2.2 to 2.8 billion gallons) with the mass of dissolved perchlorate equal to 3 to 4 kg (21-27 lbs). As with RDX, the distribution of perchlorate in groundwater at the Central Impact Area indicates the source may not yet be exhausted (*15*).

The maximum downgradient extent of the HMX plume is approximately 2286 m (7,500 ft) or approximately ¾ the distance of the RDX plume. Based on the groundwater flow calculations, the release dates (~45 years before present) for both RDX and HMX are comparable (*15*). As noted previously, Lynch and co-workers (*31*) reported dissolution studies in which HMX dissolved faster than RDX in formulations such as Octol and Comp B but individual formulations dissolved at nearly the same rate as RDX. Therefore, differences in dissolution kinetics between RDX and HMX cannot account for the differences in plume extent. The

fact that the downgradient extent of HMX is less than that of RDX suggests HMX is attenuated to a greater degree but responsible processes are unknown because the literature indicates the degree of sorption of HMX onto aquifer solids is similar to RDX. A more likely explanation is the low concentrations present. Because HMX is typically reported at values only slightly higher than the minimum detectable level (MDL), the physical processes of dispersion and dilution may be sufficient to reduce the concentration of HMX to levels below the MDL. Therefore, it is possible HMX is co-located with RDX throughout the plume but is not detectable in as large an area because concentrations are below the MDL.

Camp Edwards Firing Positions and Anti-Tank Ranges

Interest in the migration of NG and the DNTs became a greater concern when field studies at several sites reported higher concentrations than previously measured (*175*, *176*). One report described NG as "mobile in soil environments" (*124*). As examples, concentrations to 242 mg/kg were reported in the impact area at Camp Edwards of the MMR and more than 1 mg/kg was found on various other MMR training ranges. At Canadian Forces Base (CFB) Valcartier Arnhem, antitank rocket range surface soils had NG concentrations of nearly 2000 mg/kg five meters behind the rocket firing line and over 100 mg/kg twenty-five meters behind the firing line (*177*, *178*). A rocket firing range at CFB Gagetown was described as having NG concentrations over 1% near the firing location (*177*). Another study reported NG in all composite, and in several discrete samples, collected near the target area of an antitank range (*6*).

Nonetheless, NG apparently has not migrated significantly at Camp Edwards (*139*), a finding consistent with studies conducted at anti-tank and artillery/mortar firing points where NG and DNT migration has been reported as limited to several meters (*179*, *180*). These findings indicate the initial (available) NG, presumably released within the first several precipitation events following firing, is quickly biodegraded. Biodegradation processes appear to be sufficient to remove any NG released—a finding supported by field tension lysimeter studies at Camp Edwards and two other field sites. Data from these sites indicated an absence of NG and DNTs in lysimeters installed 0.6 meters below the firing line and sampled quarterly for one year (*139*).

Canadian Forces Base Valcartier Anti-Tank Target

The long-term record at Arnhem Anti-Tank Range (Garrison Valcartier, Canada, Arnhem Anti-Tank Range (*80*) has permitted a thorough explanation of the migration of several energetic compounds. Contamination was chiefly the result of training with the M-72 Light Anti-Armor Weapon, sometimes referred to as the LAW Rocket. This weapon has a warhead containing Octol (70% HMX and 30% TNT) as the main charge, with a booster containing RDX. The double-based propellant used for this rocket contains 70% nitrocellulose (NC) and 30% nitroglycerin (NG). Based on a study conducted at Western Area Training Center Wainwright, Alberta, Canada; these munitions have a high dud rate (*21*, *174*). Large quantities of HMX can be released. For example, the HMX

concentration in surface soil next to a ruptured LAW rocket at a training range in Yakima, WA was 10,400 mg/kg (*6*).

Sampling at Arnhem conducted within 20 meters of a target in this sandy, well-drained soil (*35*) indicated contamination was principally limited to the surface where concentrations of HMX ranged from 1.8 to more than 2000 mg/kg (Fig 8). There was a pronounced concentration gradient as distance from the target increased with the highest HMX concentrations adjacent to the target. Similarly, HMX, at the 8 to 15 cm (3.0 to 5.9 in) depth, was generally a factor of five less than at 0 to ~ 1 cm. (0 to 0.3 in). Although deeper soil samples were not collected in this study, HMX was found in the shallow groundwater (approximately 3.6 m or 12 ft below ground surface) indicating some component of the original contaminant mass had migrated through the vadose zone. Other investigations at the Arnhem site (*21*, *174*), reported HMX contamination as great as 800 mg/kg with concentrations decreasing 100 fold by 0.3 m (1 ft) in depth. In all, high levels of HMX have been reported for at least five Canadian anti-tank ranges (*21*, *174*). In every case, correlations were evident between soil contaminant concentrations, frequency of use, and the location of the samples relative to the targets.

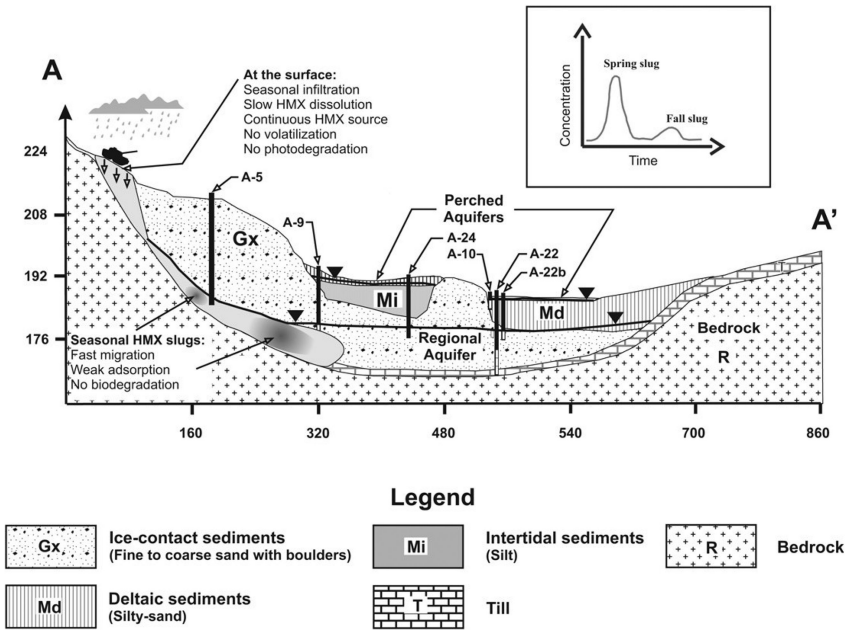

Figure 8. Conceptual model of HMX behavior (profile length and altitude in meters) (from Martel and co-workers (80)).

A recent comprehensive review (*80*) of investigations at Arnhem described most of the crystalline HE mass on the ground surface as HMX (up to 99%). Considering that the HMX/TNT mass ratio in pure Octol is 2.3:1, it is of great

interest that HMX/TNT ratios in surface sediments were 45:1 in May 1995, 186:1 in October 1995, 600:1 in September 1996, and 84:1 in 2003. Thus, compared to TNT, which was preferentially dissolved and transformed, HMX is recalcitrant in surface sediments. This explains why HMX was always detected in groundwater throughout the years, whereas TNT and its metabolites were only occasionally observed. Although, more quickly dissolved and biotransformed under the aerobic conditions of the regional aquifer, the investigators noted that TNT did not seem to be significantly mineralized (*80*).

The TNT groundwater plume was discontinuous because this compound was not always present at the ground surface when infiltration occurred. The plume, therefore, was composed of a series of discontinuous TNT slugs, which were biotransformed, weakly sorbed, and not mineralized. It is also believed that the dissolved HMX plume in ground water was created as a series of slugs, generated at each significant infiltration event and flowing one after another via advective transport in the regional aquifer (*80*). These slugs were weakly retarded by sorption and were neither biotransformed nor mineralized.

The authors also noted that with variable water levels, and substantial portions of the aquifer below the training area changing between saturated and unsaturated conditions: sampling periods have to be chosen with great care because observed ground water contamination varies seasonally. High infiltration rates cause higher mobility of contaminants but may also dilute the contamination. Snow cover and frozen ground inhibit infiltration for several months, causing an accumulation of contaminants at the ground surface, which may be leached just after snowmelt, causing an extreme peak of HE in groundwater (*80*).

The sediment water Kd value of HMX was evaluated from the Arnhem field data (*80*). Assuming a bulk density of 1800 kg/m^3 and an unsaturated water content of 0.045, the Kd value of HMX was between 0.087 and 0.125 L/kg. This means that HMX was weakly sorbed. This observed Kd value for HMX is comparable to one obtained by batch experiments (0.08 L/kg) and to those discussed previously in this chapter.

Perchlorate has also been measured at this site (*80*). Coming from the propellant charges, perchlorate has been detected at varying concentrations in all groundwater samples. The wide distribution of this contaminant can be used as an ongoing tracer experiment, indicating the extension of the contaminated ground water. In 2005, all 17 water samples analyzed for perchlorate contained at least 0.04 µg/L, and six wells (35%) contained more than 1 µg/L. Areal perchlorate distribution in ground water revealed highest levels in the area behind the firing line as predicted from propellant (NG) distribution on the ground.

At Arnhem (*80*), concentrations near 3000 mg/kg (measured NG mass of 54 kg) were found behind the firing line (0–25 m). On a sampled line between the firing position and the central target, NG concentrations were several orders of magnitude lower, resulting in a total mass of 9 kg (*181*). The lowest concentrations were detected in the impact area (0.22 kg).

Other studies at antitank rocket ranges, support the observations at Arnhem (*6*). At the Yakima, WA training range, two samples were collected 5–10 meter in front of the firing line and NG was detected at 1.8 and 3.6 mg/kg. At the Gagetown, Canada, training range, samples were collected at distances 10, 20, and 50 meters

in front of the firing line and 2 and 5 meters behind the firing line. In front of the firing line, the NG concentrations in the surface soil samples ranged from 424 mg/kg at 10 meters to 14.1 mg/kg at 50 meters. The concentrations behind the firing line were even higher, with the highest value being 11,300 mg/kg (1.13%) (*6*).

Conclusions

The major conclusions that can be drawn regarding the fate and transport of energetic compounds are the following:

1. Although based partially on indirect evidence, low-order detonations and cracked or ruptured UXO are likely to be the primary sources of groundwater contamination in impact areas at military training ranges. The contamination is manifested in surface soil as a heterogeneous, diffuse, low-concentration, distributed source term. RDX and HMX will be most frequently detected.
2. High-explosive residues are present on the soil surface as solid particulates and undergo slow dissolution, therefore the source is persistent, remaining in soil for years to come.
3. Trinitrotoluene, NG, 2a-DNT, 4a-DNT, and 2,4-DNT at training ranges typically result in minor impacts to groundwater.
4. The high heterogeneity of energetic compounds on the ground surface around targets on anti-tank ranges and its consequences on sediment sampling methods has been widely described (*177*). The recent examination of data from CFB-Arnhem demonstrates that similar care must be taken to understand the flow regime when characterizing the ground water contamination related to training ranges (*80*). Sampling periods have to be carefully chosen because observed ground water contamination may vary with the seasons.
5. Where present, perchlorate can be used as an ongoing tracer experiment, indicating the extension of the ground water body whose chemistry is altered by the training activity (*80*).

References

1. Clausen, J. L.; Robb, J.; Curry, D.; Korte, N. *Environ. Pollut.* **2004**, *129*, 13–21.
2. USEPA. Administrative Order on Consent; US Environmental Protection Agency, Region 1: Boston, MA, 1997.http://www.epa.gov/ne/mmr/pdfs/448139.pdf.
3. Jenkins, T. F.; Thiboutot, S.; Ampleman, G.; Hewitt, A. D.; Walsh, M. E.; Ranney, T. A.; Ramsey, C. A.; Grant, C. L.; Collins, C. M.; Brochu, S.; Bigl, S. R.; Pennington, J. C. *Identity and Distribution of Residues of Energetic Compounds at Military Live-Fire Training Ranges*; ERDC TR-05-10; US

Army Corps of Engineers, Engineer Research and Development Center: Hanover, NH, 2005.
4. Pennington, J. C.; Jenkins, T. F.; Brannon, J. M.; Thiboutot, S.; Delaney, J. E.; Lynch, J.; Clausen, J. L.; Delfino, J. J. *Distribution and Fate of Energetics on DoD Test and Training Ranges*; SERDP and ESTCP Symposium: Washington, DC, 2001.
5. Pennington, J.; Brannon, J. M.; Mirecki, J. E.; Jenkins, T. F.; Ranney, T. A.; Stark, J. A.; Walsh, M. E.; Hewitt, A. D.; Perron, N. M.; Ampleman, G.; Thiboutot, S.; Lewis, J.; Lynch, J.; Delfino, J. J.; Clausen, J. L.; Hayes, C. A. *Distribution and Fate of Energetics on DoD Test and Training Ranges. Interim Report 1*; TR-01-13; US Army Corps of Engineers, Engineer Research and Development Center: Vicksburg, MS, 2002.
6. Pennington, J. C.; Brannon, J. M.; Mirecki, J. E.; Jenkins, T. F.; Ranney, T. A.; Stark, J. A.; Walsh, M. E.; Hewitt, A. D.; Perron, N. M.; Ampleman, G.; Thiboutot, S.; Lewis, J.; Lynch, J.; Delfino, J. J.; Clausen, J. L.; Hayes, C. A. *Distribution and Fate of Energetics on DoD Test and Training Ranges: Interim Report 2*; ERDC TR-02-8; US Army Corps of Engineers, Engineer Research and Development Center: Arlington, VA, 2002.
7. Pennington, J. C.; Jenkins, T. F.; Ampleman, G.; Thiboutot, S.; Brannon, J. M.; Lewis, J.; DeLaney, J. E.; Clausen, J.; Hewitt, A. D.; Hollander, M. A.; Hayes, C. A.; Stark, J. A.; Marois, A.; Brochu, S.; Dinh, H. Q.; Lambert, D.; Gagnon, A.; Bouchard, M.; Martel, R.; Brousseau, P.; Perron, N. M.; Lefebvre, R.; Davis, W.; Ranney, T. A.; Gauthier, C.; Taylor, S. Ballard, J. *Distribution and Fate of Energetics on DoD Test and Training Range*; ERDC TR-03-2; US Army Corps of Engineers, Engineer Research and Development Center: Arlington, VA, 2003.
8. Pennington, J. C., Jenkins, T. F.; Hewitt, A. D.; Stark, J. A.; Lambert, D.; Perron, N. M.; Taylor, S.; Ampleman, G.; Thiboutot, S.; Lewis, J.; Marois, A.; Gauthier, C.; Brousseau, P.; Martel, R.; Lefebvre, R.; Ballard, J.; Brochu, S.; Clausen, J.; Delaney, J. E.; Hollander, M. A.; Dinh, H. Q.; Davis I.; Ranney, T. A.; Hayes, C. A. *Distribution and Fate of Energetics on DoD Test and Training Ranges: Interim Report 4. Annual Technical Report Prepared for Strategic Environmental Research and Development Program*; ERDC TR-04-4; Arlington, VA, 2004.
9. Pennington, J. C.; Jenkins, T. F.; Thiboutot, S.; Ampleman, G.; Clausen, J.; Hewitt, A. D.; Lewis, J. Walsh, M. R.; Walsh, M. E.; Ranney, T. A.; Silverblatt, B. Marois, A.; Gagnon, A.; Brousseau, P.; Zufelt, J. E.; Poe, K.; Bouchard, M.; Martel, R.; Walker, D. D.; Ramsey, C. A.; Hayes, C. A.; Yost, S. L.; Bjella, K. L.; Trepanier, L.; Berry, T. E.; Lambert, D. J.; Dube, P. Perron, N. M. *Distribution and fate of energetics on DoD test and training ranges. Report 5*; ERDC TR-05-2; US Army Engineer Research and Development Center, Environmental Laboratory: Vicksburg, MS, 2005.
10. Walsh, M. E.; Collins, C. M.; Hewitt, A. D.; Walsh, M. R.; Jenkins, T. F.; Stark, J.; Gelvin, A.; Douglas, T. A.; Perron, N.; Lambert, D.; Bailey, R.; Myers, K. *Range Characterization Studies at Donnelly Training Area, Alaska: 2001 and 2002*; ERDC/CRREL-TR-04-3; US Army Corps of

Engineers, Cold Regions Research and Engineering Laboratory: Hanover, NH, 2004.
11. USCHPPM. *Training Range Site Characterization And Risk Screening Regional Range Study, Jefferson Proving Ground, Madison, Indiana*; Report No. 38-EH-8220-03; US Army Center for Health Promotion and Preventive Medicine: Aberdeen Proving Ground, Maryland, 2003.
12. AMEC. *Draft IAGWSP Technical Team Memorandum 01-13 Central Impact Area Soil Report for the Camp Edwards Impact Area Groundwater Quality Study, Massachusetts Military Reservation, Cape Cod, MA*; MMR.3915; AMEC Earth and Environmental: Westford, MA, 2001.
13. AMEC. *Final IAGWSP Technical Team Memorandum 01-6 Central Impact Area Groundwater Report for the Camp Edwards Impact Area Groundwater Quality Study, Massachusetts Military Reservation, Cape Cod, MA*; MMR-3757; AMEC Earth and Environmental: Westford, MA, 2001.
14. AMEC. *Revised Draft IAGWSP Technical Team Memorandum 01-14 Gun and Mortar Firing Positions Volume I of II for the Camp Edwards Impact Area Groundwater Quality Study, Massachusetts Military Reservation, Cape Cod, MA*; MMR-4425; AMEC Earth and Environmental: Westford, MA, 2001.
15. AMEC. *Draft Addendum to Final IAGWSP Technical Team Memorandum TM 01-6 Central Impact Area Groundwater Report, Camp Edwards Impact Area Groundwater Study Program Massachusetts Military Reservation, Cape Cod, MA*; MMR-8334; AMEC Earth and Environmental: Westford, MA, 2004.
16. AMEC. *Draft Demo 1 Groundwater Report Addendum to TM 01-2, Camp Edwards, Massachusetts Military Reservation, Cape Cod, MA*; MMR-7702; AMEC Earth and Environmental: Westford, MA, 2003.
17. AMEC. *Draft Final IAGWSP Technical Team Memorandum 01-10 Demo 1 Soil Report for the Camp Edwards Impact Area Groundwater Quality Study, Massachusetts Military Reservation, Cape Cod, MA*; MMR-4675; AMEC Earth and Environmental: Westford, MA, 2001.
18. Hewitt, A. D. *Analysis of Nitroglycerine in Soils and on Mortar Fins Using GC-TID*; CRREL Report TR-02-03; US Army Corps of Engineers, Cold Regions Research and Engineering Laboratory: Hanover, NH, 2002.
19. Ogden. *Final IAGS Technical Team Memorandum 99-1 KD & U Ranges for the Camp Edwards Impact Area Groundwater Quality Study, Massachusetts Military Reservation Cape Cod, Massachusetts*; MMR-2071; Ogden Environmental and Energy Services: Westford, MA, 2000.
20. Ogden. *Final Phase I Initial Site Investigation Report KD Range, RTN 4-15033 for the Camp Edwards Impact Area Groundwater Quality Study, Massachusetts Military Reservation Cape Cod, MA*; MMR-2384; Ogden Environmental and Energy Services: Westford, MA, 2000.
21. Thiboutot, S.; Ampleman, G.; Gagnon, A.; Marois, A.; Jenkins, T. F.; Walsh, M. E.; Thorne, P. G.; Ranney, T. A. *Characterization of Antitank Firing Ranges at CFB Valcartier, WATC Wainwright and CFAD Dundrun*; DREV-R-9809; Defence Research Establishment Valcartier: Quebec, Canada, 1998.

22. Clausen, J. L.; Korte, N.; Dodson, M.; Robb, J.; Rieven, S. *Conceptual Model for the Transport of Energetic Residues from Surface Soil to Groundwater by Range Activities*; ERDC-CRREL TR-06-18; US Army Corps of Engineers, Environmental Research and Development Center, Cold Regions Research and Engineering Laboratory: Hanover, NH, 2007.
23. ESE. *1995/1996 Hydrogeological Investigation/Monitoring Results North Post 40 Complex Camp Grayling Training Facility Grayling, MI*; ESE # 47-95076 & 47-95078; Environmental Science and Engineering: Cadillac, MI, 1997.
24. Martel, R.; Hebrt, A.; Lefebvre, R. *Complementary Soil and Groundwater Characterization Study at the Open Burning/Open Detonation Site CFAD Dundurn (Saskatchewan)*; Univerite du Quebec, Defence Research Establishment Valcartier: Quebec, Canada, 1998.
25. Hewitt, A. D.; Jenkins, T. F.; Ranney, T. A.; Stark, J.; Walsh, M. E.; Taylor, S. Walsh, M.; Lambert, D.; Perron, N.; Collins, N. *Estimates for Explosives Residue from the Detonation of Army Munitions*; ERDC/CREEL TR-03-16; US Army Engineer Research and Development Center: Cold Regions Research and Engineering Laboratory, Hanover, NH, 2003.
26. Jenkins, T. F.; Ranney, T. A.; Walsh, M. E.; Miyares, P. H.; Hewitt, A. D.; Collins, N. H. *Evaluating the Use of Snow-Covered Ranges to Estimate the Explosives Residues that Result from Detonation of Army Munitions*; ERDC/CRREL TR-00-15; US Army Corps of Engineers, Engineer Research and Development Center: Hanover, NH, 2000.
27. Jenkins, T. F.; Pennington, J. C.; Ranney, T. A.; Berry, T. E.; Miyares, P. H.; Walsh, M. E.; Hewitt, A. D.; Perron, N. M.; Parker, L. V.; Hayes, C. A.; Wahlgren, E. G. *Characterization of Explosives Contamination at Military Firing Ranges*; ERDC TR-01-5; US Army Corps of Engineers, Engineer Research and Development Center: Hanover, NH, 2001.
28. Jenkins, T. F.; Walsh, M. E.; Miyares, P. H.; Hewitt, A. D.; Collins, N. H.; Ranney, T. A. *Thermochim. Acta* **2002**, *384*, 173–185.
29. Jenkins, T. F.; Ranney, T. A.; Hewitt, A. D.; Walsh, M. E.; Stark, J. A.; Pennington, J. C. *Use of Snow-Covered Ranges to Determine the Amount of Explosives Residues deposited from high-order detonations of army munitions*; Geological Society of America National Meeting: Boston, MA, 2001.
30. McGrath, C. J. *Updated Version of Physical, Chemical, and Environmental Data for Common, Explosive- Associated Compounds (XACs)*; US Army Corps of Engineers, Waterways Experiment Station: Vicksburg, MS, 1966.
31. Lynch, J. C.; Brannon, J. M.; Delfino, J. J. *Chemosphere* **2002**, *47*, 725–734.
32. McGrath, C. J. *Review of Formulations for processes Affecting Subsurface Transport of Explosives*; Report IRRP-95-2; US Army Corps of Engineers, Waterways Experiment Station: Vicksburg, MS, 1995.
33. Cataldo, D. A.; Harvey, S. D.; Fellows, R. J. *An Evaluation of the Environmental Fate and Behavior of Munitions Material (TNT, RDX) in Soil and Plant Systems*; PNL-7529; Pacific Northwest Laboratory, Richland, WA, 1990.

34. Spanggord, R. J.; Mabey, R. W.; Mill, T.; Chou, T. W.; Smith, J. H.; Lee, S. *Environmental Fate Studies on Certain Munition Wastewater Constituents, Phase 3, Part II - Laboratory Studies*; LSU-7934; SRI International: Menlo Park, CA, 1981.
35. Jenkins, T. F.; Walsh, M. E.; Thorne, P. G.; Thiboutot, S.; Ampleman, G.; Ranney, T. A.; Grant, C. L. *Assessment of Sampling Error Associated with the Collection and Analysis of Soil Samples at a Firing Range Contaminated with HMX*; CRREL Special Report 97-22; US Army Corps of Engineers, Cold Regions Research and Engineering Laboratory: Hanover, NH, 1997.
36. Haywood, W.; McRae, D.; Powell, J.; Harris, B. W. *An Assessment of High-Energy Explosives and Metal Contamination in Soil at TA-67 (12), L-Site, and TA-14, Q-Site*; LA-12752-MS; Los Alamos National Laboratory: Los Alamos, NM, 1995.
37. Hale, V. Q.; Stanford, T. B.; Taft, L. G. *Evaluation of the Environmental Fate of Munition Compounds in Soil*; Contract No. DAMD 17-76-C-6065; Battelle Columbus Laboratories: Columbus, OH, 1979.
38. Taylor, S.; Lever, J.; Perovich, L.; Campbell, E.; Pennington, J. *A Study of Composition B Paticles From 81-mm Mortar Detonations*; Battelle Press: Columbus, OH, 2004.
39. Lynch, J. C.; Brannon, J. M.; Delfino, J. J. *J. Chem. Eng. Data* **2002**, *47*, 542–549.
40. Myers, T. E.; Brannon, J. M.; Pennington, J. C.; Davis, W. M.; Myers, K. F.; Townsend, D. M.; Ochman, M. K.; Hayes, C. A. *Laboratory Studies of Soil Sorption/Transformation of TNT, RDX, and HMX*; Technical Report IRRP 98-8; USArmy Corps of Engineers, Waterways Experiment Station: Vicksburg, MS, 1998.
41. Xue, S. K. *Soil Sci.* **1995**, *160*, 317–327.
42. Leggett, D. C. *Sorption of Military Explosive Contaminants on Bentonite Drilling Muds*; CRREL Report 85-18; US Army Corps of Engineers, Cold Regions Research and Engineering Laboratory: Hanover, NH, 1985.
43. Speitel, G. E.; Yamamoto, H.; Autenrieth, R. L.; McDonald, T. *Laboratory Fate and Transport Studies of High Explosives at the Massachusetts Military Reservation. Final Report*; University of Texas: Austin, Texas; Texas A&M University: College Station, Texas, 2002.
44. Selim, H. M.; Iskandar, I. K. *Sorption-Desorption and Transport of TNT and RDX in Soils*; CRREL Report 94-7; US Army Corps of Engineers, Cold Regions Research and Engineering Laboratory: Hanover, NH, 1994.
45. Ainsworth, C. C.; Harvey, S. D.; Szecsody, J. E.; Simmons, M. A.; Cullinan, V. I.; Resch, C. T.; Mong, G. H. *Relationship Between the Leachability Characteristics of Unique Energetic Compounds and Soil Properties*; Project Order No. 91PP1800; Pacific Northwest Laboratory: Richland, WA, 1993.
46. Townsend, D. M.; Myers, T. E. *Recent Developments in Formulating Model Descriptors for Subsurface Transformation and Sorption of TNT, RDX, and HMX*; Technical Report IRRP-96- 1; US Army Corps of Engineers, Waterways Experiment Station: Vicksburg, MS, 1996.
47. Checkai, R. T.; Major, M. A.; Nwanguma, R. O.; Phillips, C. T.; Sadusky, M. C. *Transport and Fate of Nitroaromatic and Nitroamine Explosives in*

Soils from Open Burning/Open Detonation Operations: Anniston Army Depot (AAD); ERDEC-TR-135; Edgewood Research, Development and Engineering Center: Aberdeen Proving Ground, MD, 1993.
48. Checkai, R. T.; Major, M. A.; Nwanguma, R. O.; Phillips, C. T.; Sadusky, M. C. *Transport and Fate of Nitroaromatic and Nitroamine Explosives in Soils from Open Burning/Open Detonation Operations: Milan Army Ammunition Plant (MAAP)*; ERDEC-TR-136; Edgewood Research, Development and Engineering Center: Aberdeen Proving Ground, MD, 1993.
49. Checkai, R. T.; Major, M. A.; Nwanguma, R. O.; Phillips, C. T.; Sadusky, M. C. *Transport and Fate of Nitroaromatic and Nitroamine Explosives in Soils from Open/Open Detonation Operations: Radford Army Ammunition Plant (RAAP)*; ERDEC-TR-133; Edgewood Research, Development and Engineering Center: Aberdeen Proving Ground, MD, 1993.
50. Price, C. B.; Brannon, J. M.; Yost, S. L. *Transformation of RDX and HMX Under Controlled Eh/pH Conditions*; IRRP-98-2; US Army Corps of Engineers, Waterways Experiment Station: Vicksburg, MS, 1998.
51. Best, E. P. H.; Zappi, M. E.; Fredrickson, H. L.; Sprecher, S. L.; Larson, S. L.; Ochman, M. *Ann. N. Y. Acad. Sci.* **1997**, *829*, 179–194.
52. Best, E. P. H.; Zappi, M. E.; Fredrickson, H. L.; Sprecher, S. L.; Larson, S. L.; Miller, J. L. *Screening of Aquatic and Wetland Plant Species for Phytoremediation of Explosives-Contaminated Groundwater from the Iowa Army Ammunition Plant*; Technical Report EL-97-2; US Army Corps of Engineers Waterways Experiment Station: Vicksburg, MS, 1997.
53. Kayser, E. G.; Burlinson, N. *Migration of Explosives in Soil*; NSWC TR 82-566; Naval Surface Weapons Center: Silver Springs, MD, 1982.
54. Rodacy, P.; Leslie, P. *Ion Mobility Spectroscopy as a Means of Detecting Explosives in Soil Samples*; SAND92-13226; Sandia National Laboratories: Albuquerque, NM, 1992.
55. DuBois, F. W.; Baytos, J. F. *Effect of Soil and Weather on the Decomposition of Explosives*; LA-4943; Los Alamos National Laboratory: Los Alamos, NM, 1972.
56. Jenkins, T. F.; Bartolini, C.; Ranney, T. A. *Stability of CL-20, TNAZ, HMX, RDX, NG, and PETN in Moist Unsaturated Soil*; ERDC/CRREL TR-03-7; US Army Corps of Engineers, Engineer Research and Development Center: Hanover, NH, 2003.
57. Spanggord, R. J.; Mill, T.; Chou, T. W.; Mabey, R. W.; Smith, J. H.; Lee, S. *Environmental Fate Studies on Certain Munition Wastewater Constituents, Final Report, Phase 2: Laboratory Study*; LSU-7934; SRI International: Menlo Park, CA, 1980.
58. Pennington, J. C.; Myers, K. F.; Davis, W. M.; Olin, T. J.; McDonald, T. L.; Hayes, C. A.; Townsend, D. M. *Impacts of Sorption on In Situ Bioremediation of Explosives-Contaminated Soils*; Technical Report IRRP-95-1, US Army Corps of Engineers, Waterways Experiment Station: Vicksburg, MS, 1995.
59. Price, C. B.; Brannon, J. M.; Hayes, C. A. *J. Environ. Eng.* **2001**, *127*, 26–31.
60. McCormick, N. G.; Cornell, J. H.; Kaplan, A. M. *The Anaerobic Biotransformation of RDX, HMX, and their Acetylated Derivatives*;

NATICK/85/007; US Army Natick Research and Development Laboratory: Natick, MA, 1984.
61. McCormick, N. G.; Cornell, J. H.; Kaplan, A. M. *The Fate of Hexayhydro-1,3,5-trinitro-1,3,5-triazine (RDX) and Related Compounds in Anaerobic Denitrifying Continuous Culture Systems Using Simulated Wastewater*; NATICK/85/008; US Army Natick Research and Development Laboratory: Natick, MA, 1984.
62. Major, M. A.; Johnson, M. S.; Salice C. J. 2002. *Bioconcentration, bioaccumulation, and biomagnification of nitroaromatic and nitroamine explosives and their breakdown products*; Toxicology Study No. 87-MA-4677-01; US Army Center for Health Promotion and Preventive Medicine: Aberdeen Proving Ground, MD, 2002.
63. Hawari, J. *Microbial Degradation of RDX and HMX: From Basic Research to Field Application*; Biotechnology Research Institute, NRC: Montreal (PQ) Canada, 2000.
64. Yang, Y.; Wang, X.; Yin, P. *Acta Microbiol. Sin.* **1983**, *23*, 251–256.
65. Thiboutot, S.; Ampleman, G.; Hewitt, A. D. *Guide for Characterization of Sites Contaminated with Energetic Materials*; ERDC/CRREL Report TR-02-01; US Army Corps of Engineers, Cold Regions Research and Engineering Laboratory: Hanover, NH, 2002.
66. Spanggord, R. J.; Mill, T.; Chou, T. W.; Mabey, R. W.; Smith, J. H.; Lee, S. *Environmental Fate Studies on Certain Munition Wastewater Constituents, Final Report, Phase 1: Literature Review*; LSU-7934; SRI International: Menlo Park, CA, 1980.
67. Sikka, H. C.; Bannerjee, S.; Pack, E. J.; Appleton, H. T. *Environmental Fate of RDX and TNT*; Report TR-81-538; US Army Medical Research and Development Command: Fort Detrick, MD, 1980.
68. Spanggord, R. J.; Mabey, R. W.; Chou, T. W.; Haynes, D. L.; Alfernese, P. L.; Tse, D. S.; Mill, T. *Environmental Fate Studies of HMX, Screening Studies, Final Report, Phase 2: Laboratory Study*; SRI International: Menlo Park, CA, 1983.
69. Bedford, C. D.; Carpenter, P. S.; Nadler, M. P. *Solid-State Photodecomposition of Energetic Nitroamines (RDX and HMX)*; NAWCPNS TP 8271; Department of the Navy, Naval Air Warfare Center Weapons Division: China Lake, CA, 1996.
70. Glover, D. J.; Hoffsommer, J. C. *Photolysis of RDX in Aqueous Solution with and without Ozone*; NSWC/WOL-TR-78-175; Naval Surface Weapons Center: Silver Spring, MD, 1979.
71. Kubose, D. A.; Hoffsommer, J. C. *Photolysis of RDX in Aqueous Solution, Initial Studies*; NSWC/WOL/TR-77-20; Naval Weapons Surface Center: Silver Spring, MD, 1977.
72. Ogden. *Draft Completion of Work Report Volume 1-5: Camp Edwards Impact Area Groundwater Quality Study, Massachusetts Military Reservation Cape Cod, Massachusetts*; MMR-0050; Ogden Environmental and Energy Services: Westford, MA, 1998.
73. Ogden. *Draft Interim Results Report for the Camp Edwards Impact Area Groundwater Quality Study, Massachusetts Military Reservation Cape Cod,*

Massachusetts; MMR-0025; Ogden Environmental and Energy Services; Westford, MA, 1999.
74. Thompson, P. L.; Ramer, L. A.; Schnoor, J. L. *Environ. Toxicol. Chem.* **1999**, *18*, 279–284.
75. Harvey, S. D.; Fellows, R. J.; Cataldo, D. A.; Bean, R. M. *Environ. Toxicol. Chem.* **1991**, *10*, 845–855.
76. Groom, C. A.; Halasz, A.; Paquet, L.; Morris, N.; Olivier, L.; Dubois, C.; Hawari, J. *Environ. Sci. Technol* **2002**, *36*, 112–118.
77. Talmage, S. S.; Opreska, D. M.; Maxwell, C. J.; Welsh, C. J. E.; Cretella, F. M.; Reno, P. M.; Daniel, F. B. *Rev. Environ. Contam. Toxicol.* **1999**, *161*, 1–156.
78. Jenkins, T. F.; Walsh, M. E.; Schumacher, P. W.; Miyares, P. H. *J - Assoc. Off. Anal. Chem.* **1989**, *72*, 890–899.
79. Rosenblatt, D. H.; Burrows, E. P.; Mitchell, W. R.; Parmer, D. L. In *The Handbook of Environmental Chemistry*; Hutzinger, O., Ed.; Springer: New York, NY, 1989.
80. Martel, R.; Mailloux, M.; Gabriel, U.; Lefebvre, R.; Thiboutot, S.; Ampleman, G. *J. Environ. Qual.* **2009**, *38*, 75–92.
81. Xue, S. K.; Iskandar, I. K.; Selim, H. M. *Soil Sci.* **1995**, *160*, 328–339.
82. Rosser, S.; Basran, A.; Travis, E.; French, C.; Bruce, N. *Adv. Appl. Microbiol.* **2001**, *49*, 1–35.
83. Greene, B.; Kaplan, D. L.; Kaplan, A. M. *Degradation of Pink Water Compounds in Soil - TNT, RDX, and HMX*; NATICK/85/046; US Army Natick Research and Development Center: Natick, MA, 1985.
84. Hawari, J.; Halasz, A.; Beaudet, S.; Paquet, L.; Ampleman, G.; Thiboutot, S. *Environ. Sci. Technol.* **2001**, *35*, 70–75.
85. Hawari, J.; Halasz, A.; Sheremata, T.; Beaudet, S.; Broom, C.; Paquet, L.; Rhofir, C.; Ampleman, G.; Thiboutot, S. *Appl. Environ. Microbiol.* **2001**, *66*, 2652–2657.
86. Thorne, P. G. *Fate of Explosives in Plant Tissues Contaminated During Phytoremediation*; CRREL Special Report 99-19; US Army Corps of Engineers, Cold Regions Research and Engineering Laboratory: Hanover, NH, 1999.
87. Lynch, J. C.; Myers, K. F.; Brannon, J. M.; Delfino, J. J. *J. Chem. Eng. Data.* **2001**, *46*, 1549–1555.
88. Leggett, D. C, Jenkins, T. F.; Murrmann, R. P. *Composition of Vapors Evolved from Military TNT as Influenced by Temperature Solid Composition, Age, and Source*; CRREL Report 77-16; US Army Corps of Engineers, Cold Regions Research and Engineering Laboratory: Hanover, NH, 1977.
89. Howard, P. H. *Handbook of Physical Properties of Organic Compounds*; Lewis Publishers: Chelsea, MI, 1989; Vol 1.
90. Brannon, J. M.; Deliman, P.; Ruiz, C.; Price, C.; Qasim, M. *Conceptual Model and Process Descriptor Formulations for Fate and Transport of UXO*; Technical Report IRRP-99-1; US Army Corps of Engineers, Waterways Experiment Station: Vicksburg, MS, 1999.

91. Pennington, J. C. *Soil Sorption and Plant Uptake of 2,4,6-Trinitrotoluene*; Technical Report EL-88-12; US Army Corps of Engineers, Waterways Experiment Station: Vicksburg, MS, 1988.
92. Brannon, J. M.; Adrian, D. D.; Pennington, J. C.; Myers, T. E.; Hayes, C. A. *Slow Release of PCB, TNT, and RDX from Soils and Sediments*; Technical Report EL-92-38; US Army Corps of Engineers, Waterways Experiment Station: Vicksburg, MS, 1992.
93. Weissmahr, K. W.; Hildenbrand, M.; Haderlein, S. B.; Schwarzenbach, R. P. *Environ. Sci. Technol.* **1999**, *33*, 2596–2600.
94. Myers, T. E.; Townsend, D. M.; Hill, B. C. *Application of a Semianalytical Model to TNT Transport in Laboratory Soil Columns*; Technical report IRRP-98-7, USArmy Corps of Engineers, Waterways Experiment Station: Vicksburg, MS, 1998.
95. McCormick, N. G.; Cornell, J. H.; Kaplan, A. M. *Appl. Environ. Microbiol.* **1978**, *35*, 945–948.
96. Haderlein, S. B.; Weissmahr, K. W.; Schwarzenbach, R. P. *Environ. Sci. Technol.* **1996**, *30*, 612–622.
97. Leggett, D. C. *Role of Donor-Acceptor Interactions in the Sorption of TNT and Other Nitroaromatics from Solution*; CRREL Report 91-13; US Army Corps of Engineers, Cold Regions Research and Engineering Laboratory: Hanover, NH, 1991.
98. Kaplan, D. L.; Kaplan, A. M. *2,4,6-Tinitrotoluene – Surfactant Complexes, Biodegradability, Mutagenicity, and Soil Leaching Studies*; Technical Report NATICK/TR-82/006; US Army Natick Research and Development Laboratories: Natick, MA, 1982.
99. Kaplan, D. L.; Kaplan, A. M. *Environ. Sci. Technol.* **1982**, *16*, 566–571.
100. Kaplan, D. L.; Kaplan, A. M. *Reactivity of TNT and TNT-Microbial Reduction Products with Soil Components*; Technical Report NATICK/TR-83/041; US Army Natick Research and Development Laboratories: Natick, MA, 1983.
101. Comfort, S. D.; Shea, P. J.; Hundal, L. S.; Li, Z.; Woodbury, B. L.; Martin, J. L.; Powers, W. L. *J. Environ. Qual.* **1995**, *24*, 1174–1182.
102. Harvey, S. D.; Fellows, R. J.; Cataldo, D. A.; Bean, R. M. *J. Chromatogr.* **1990**, *518*, 361–374.
103. Price, C. B.; Brannon, J. M.; Yost, S. L.; Hayes, C. A. *Adsorption and Transformation of Explosives in Low-Carbon Aquifer Soils*; ERDC/EL TR-00-11; US Army Corps of Engineers, Engineer Research and Development Center: Vicksburg, MS, 2000.
104. Hwang, P.; Chow, T.; Adrian, N. R. *Environ. Toxicol. Chem.* **1999**, *18*, 836–841.
105. Price, C. B.; Brannon, J. M.; Hayes, C. A. *J. Environ. Eng.* **1997**, *123*, 988–992.
106. Price, C. B.; Brannon, J. M.; Hayes, C. A. *TNT Transformations: An Exhaustible or Continuing Process*; Technical Report; US Army Corps of Engineers, Waterways Experiment Station: Vicksburg, MS, 1997.

107. Brannon, J. M.; Myers, T. E. *Review of Fate and Transport Processes of Explosives*; Technical Report IRRP-97-2; US Army Corps of Engineers, Waterways Experiment Station: Vicksburg, MS, 1997.
108. Thorne, P. G.; Leggett, D. C. *Investigations of Explosives and their Conjugated Transformation Products in Biotreatment Matrices*; CRREL Special Report 99-3; US Army Corps of Engineers, Cold Regions Research and Engineering Laboratory: Hanover, NH, 1999.
109. Walsh, M. E.; Jenkins, T. F. *Identification of TNT transformation products in soils*; CRREL Special Report 92-16; US Army Corps of Engineers, Cold Regions Research and Engineering Laboratory: Hanover, NH, 1992.
110. Craig, H. D.; Sisk, W. E.; Nelson, M. D.; Dana, W. H. *Bioremediation of Explosives-Contaminated Soils: A Status Review*; Proceedings of the 10th Annual Conference on Hazardous Waste Research, Kansas State University: Manhattan, Kansas, 1997.
111. Townsend, D. M.; Myers, T. E.; Adrian, D. D. *2,4,6-Trinitotoluene (TNT) Transformation/ Sorption in Thin-Disk Soil Columns*; Technical Report IRRP-95-4; US Army Corps of Engineers, Waterways Experiment Station: Vicksburg, MS, 1995.
112. Olin, T. J.; Myers, T. E.; Townsend, D. M. *2,4,6-Trinitrotoluene (TNT) Transformation/Sorption in Thin-Disk Soil Columns Under Anaerobic Conditions*; Technical Report IRRP-96-6; USArmy Corps of Engineers, Waterways Experiment Station: Vicksburg, MS, 1996.
113. Brannon, J. M.; Price, C.; Hayes, C. *Chemosphere* **1998**, *36*, 1453–1462.
114. Schmelling, D. C.; Gray, K. A.; Kamat, P. V. *Environ Sci Tech* **1996**, *30*, 2547–2555.
115. LeFaivre, M. H.; Peyton, G. H. *Identification of Reaction By-Products from Oxidative and Photolytic Remediation of Groundwater Contaminated with TNT and RDX*; TM-2028-ENV (CR); Naval Facilities Engineering Services Center: Port Hueneme, CA, 1994.
116. Burlinson, N. E. *Fate of TNT in the Aquatic Environment: Photodegradation versus Biotransformation*; NSWC/TR-79-445; Naval Surface Weapons Center: West Bethesda, MD, 1980.
117. Andrews, C. C.; Osmon, J. L. *The Effects of Ultraviolet Light on TNT in Aqueous Solutions*; WQEC/C 75-197; Naval Weapons Support Center: Crane, IN, 1975.
118. Mabey, W. R.; Tse, D.; Baraze, A.; Mill, T. *Chemosphere* **1983**, *12*, 3–16.
119. Taylor, S.; Lever, J. H.; Fadden, J.; Perron, N.; Packer, B. *Chemosphere* **2009**, *77*, 1338–45.
120. Burlinson, N. E.; Kaplan, L. A.; Adams, C. E. *Photochemistry of TNT: Investigation of the "Pink Water" Problem*; NOLTR-73-173; Naval Ordnance Laboratory: White Oak, Silver Spring, MD, 1973.
121. Cataldo, D. A.; Harvey, S. D.; Fellows, R. J. *The Environmental Behavior and Chemical Fate of Energetic Compounds (TNT, RDX, Tetryl) in Soil and Plant Systems*; 17th Annual Army Environmental Research and Development Symposium and 3rd USACE Innovative Technology Transfer Workshop: Williamsburg, VA, 1993.

122. Cataldo, D. A.; Harvey, S. D.; Fellows, R. J. *The Environmental Behavior and Chemical Fate of Energetic Compounds (TNT, RDX, Tetryl) in Soil and Plant Systems*; PNL-SA-22362; Pacific Northwest Laboratory: Richland, WA, 1993.
123. Larson, S. L.; Jones, R. P.; Escalon, L. *Environ. Toxicol. Chem.* **1999**, *18*, 1270–1276.
124. Popp, J. A.; Leonard, T. B. In *Toxicity of Nitroaromatic Compounds*; Rickert, D. E., Ed.; Hemisphere Publishing: Washington, DC, 1985.
125. Mirecki, J. E.; Porter, B.; Weiss, C. A. *Environmental Transport and Fate Process Descriptors for Propellant Compounds*; ERDC/EL TR-6-7; US Army Corps of Engineers, Waterways Experiment Station: Vicksburg, MS, 2006.
126. Phelan, J.; Barnett, J. L. *J. Chem. Eng. Data* **2001**, *46*, 375–376.
127. Pennington, J. C.; Thorn, K. A.; Hayes, C. A.; Porter, B. E.; Kennedy, K. R. *Immobilization of 2,4- and 2,6-Dinitrotoluenes in Soils and Compost*; ERDC/ELTR-03-02; US Army Corps of Engineers, Engineer Research and DevelopmentCenter: Vicksburg, MS, 2003.
128. Spain, J. C.; Paoli, G. C.; Nishino, S. F. *Aerobic Degradation of Dinitrotoluenes and Pathway for Bacterial Degradation of 2,6-Dinitrotoluene*; Air Force Research Laboratory: Tyndall Air Force Base, FL, 2000.
129. Nishino, S. F.; Paolli, G. C.; Spain, J. C. *Appl. Environ. Microbiol.* **2000**, *66*, 2139–2147.
130. Nishino, S. F.; Spain, J. C.; Lenke, H.; Knackmuss, H. *Environ. Sci. Technol.* **1999**, *33*, 1060–1064.
131. Liu, D. S.; Thomson, K.; Anderson, A. C. *Appl. Environ. Microbiol.* **1984**, *47*, 1295–1298.
132. Hewitt A. D.; Bigl, S. R. *Elution of Energetic Compounds from Propellant and Composition B Residues*; ERDC/CRREL TR-05-13; US Army Engineer Research and Development Center, Cold Regions Research and Engineering Laboratory: Hanover, NH, 2005.
133. Cook, D. M.S. Thesis. Massachusetts Institute of Technology: Cambridge, MA, 1997.
134. Bradley, P. M.; Chapelle, F. H.; Landmeyer, J. E.; Schumacher, J. G. *Ground Water* **1997**, *35*, 12–17.
135. Cerniglia, C. E.; Somerville C. C. *Biodegradation of Nitroaromatic Compounds*; Spain, J. C., Ed. Plenum Publishing: New York, NY, 1995.
136. McCormick, N. G.; Feeherry, F. F.; Levinson, H. *Appl. Environ. Microbiol.* **1976**, *31*, 949–958.
137. Pennington, J. C.; Gunnison, D.; Harrelson, D. W.; Brannon, J. M.; Zakikhani, M.; Jenkins, T. F.; Clarke, J. U.; Hayes, C. A.; Myers, T.; Perkins, E.; Ringelberg, D.; Townsend, D. M.; Fredrickson, H.; Mays, J. H.; *Natural Attenuation of Explosives in Soil and Water Systems at Department of Defense Sites: Interim Report*; Technical Report IRRP-99-8; US Army Corps of Engineers, Waterways Experiment Station: Vicksburg, MS, 1999.
138. Windholz, M. *The Merck Index*, 9th ed.; Merck and Co. Inc.: Rahway, NJ, 1976.

139. Clausen, J. L.; Scott, C.; Osgerby, I. *Soil Sed. Contam.* **2011**, in press.
140. Yost, S. MS Thesis, Louisiana State University and Agricultural and Mechanical College, Baton Rouge, LA, 2004.
141. Lyman, W. J.; Reehl, W. R.; Rosenblatt, D. H. *Handbook of Chemical Property Estimation Methods*; McGraw Hill: New York, NY, 1982.
142. Dacre, J. C.; Rosenblatt, D. H.; *Mammalian Toxicology and Toxicity to Aquatic Organisms of Four Important Types of Waterborne Munitions Pollutants*; TR 7403; US Army Bioengineering Research and Development Laboratory: Aberdeen Proving Ground, MD, 1974.
143. Urbanski, T. *Chemistry and Technology of Explosives*; Pergamon Press: New York, NY, 1965; Vol. 2.
144. Marshall, S. J.; White, G. F. *Appl. Environ. Microbiol.* **2001**, *67* (6), 2622–2626.
145. Bhaumik, S.; Christodoulates, C.; Korfiatis, G. P.; Brodman, B. W. *Water Sci. Technol.* **1997**, *36* (2−3), 139–146.
146. Blehert, D. S.; Knoke, K. L.; Fox, B. G.; Chambliss, G. H. *J. Bacteriol.* **1997**, *179* (22), 6912–6920.
147. Urbanski, T. *Chemistry and Technology of Explosives*; MacMillan Publications: New York, NY, 1964, Vol. 1.
148. Rosseel, M. T.; Bogaert, M. G.; Dekeukelaire, D. *Bull. Soc. Dhim. Belg.* **1974**, *83*, 211.
149. Urbansky, E. T. *Biorem. J.* **1998**, *2*, 81–95.
150. TNRCC. *Texas Risk Reduction Program*; Texas Natural Resource Conservation Commission: Austin, Texas, 2002; Chapter 350 .
151. Ashford, R. D. *Ashford's dictionary of industrial chemicals: Properties, production, uses*; Wavelength Publications Ltd.: London, U.K., 1994.
152. Kim, K.; Logan, B.; Bruce, E. *Water Resour.* **2001**, *35*, 3071–3076.
153. Phelan, J. M. *Measurement and Modeling of Energetic Material Mass Transfer to Pore Water*; Sandia National Laboratories: Albuquerque, NM, 2001.
154. Yalkowsky, S.; Dannenfelser, R. *Aquasol Database of Aqueous Solutions*; College of Pharmacy, University of Arizona: Tucson, AZ, 1992; Vol. 5.
155. Logan, B. E.; Zhang, H.; Mulvaney, P.; Milner, M. G.; Head, I. M.; Unz, R. F. *Appl. Environ. Microbiol.* **2001**, *67*, 2499–2506.
156. Tipton, D. K.; Rolston, D. E.; Scow, K. M. *J. Environ. Qual.* **2003**, *32*, 40–46.
157. Smith, P. N.; Theodorakis, C. W.; Anderson, T. A.; Kendall, R. J. *Ecotoxicology* **2001**, *10*, 305–313.
158. Ellington, J. J.; Wolfe, N. L.; Garrison, A. G.; Evans, J. J.; Avants, J. K.; Teng, Q. *Environ. Sci. Technol.* **2001**, *35*, 3213–3218.
159. Van Aken, B.; Schnoor, J. L. *Environ. Sci. Technol.* **2002**, *36*, 2783–2788.
160. Nzengung, V.; Wang, C.; Harvey, G. *Environ. Sci. Technol.* **1999**, *33*, 1470–1478.
161. US Army. *Military Explosives: Department of the Army Technical Manual*; TM9-1300-214; Department of Army: Washington, DC, 1984.
162. Valsaraj, K. T.; Qaisi, K. M.; Constant, W. D.; Thibodeauz, L. J.; Ro, K. S. *J Hazard. Mater.* **1998**, *59*, 1–12.

163. Goodfellow, W. L.; Burton, D. T.; Graves, W. C.; Hall, L. W.; Cooper, K. R. *Water Res. Bull.* **1983**, *19*, 641–648.
164. Layton, D.; Mallon, B.; Mitchell, W.; Hall, L.; Fish, R.; Perry, L.; Snyder, G.; Bogen, K.; Malloch, W.; Ham, C.; Dowd, P. *Conventional Weapons Demilitarization: A Health and Environmental Effects Data Base Assessment. Explosives and Their Co-contaminants Final Report, Phase II*; Lawrence Livermore National Laboratory: Livermore, CA, 1987.
165. Thorne, P. G.; Jenkins, T. F. *Development of a Field Method for Quantifying Ammonium Picrate and Picric Acid in Soil and Water*; CRREL Special Report 95-20; US Army Corps of Engineers, Cold Regions Research and Engineering Laboratory: Hanover, NH, 1995.
166. Crockett, A. B.; Jenkins, T. F.; Craig, H. D.; Sisk, W. E. *Overview of On-Site Analytical Methods for Explosives*; CRREL Special Report 98-4; US Army Corps of Engineers, Cold Regions Research and Engineering Laboratory: Hanover, NH, 1998.
167. Kayser, E. G.; Burlinson, N.; Rosenblatt, D. H. *Kinetics of Hydrolysis and Products of Hydrolysis and Photolysis of Tetryl*; Technical Report 84-68; Naval Surface Weapons Center: Silver Springs, MD, 1984.
168. Walsh, M. E. *Environmental Transformation Products of Nitroaromatics and Nitroamines. Literature Review and Recommendations for Analytical Method Development*; CRREL Special Report 90-2; US Army Corps of Engineers, Cold Regions Research and Engineering Laboratory: Hanover, NH, 1990.
169. Wyman, J. F.; Guard, H. E.; Eon, W. D.; Quay, J. H. *Appl. Environ. Microbiol.* **1979**, *37*, 222–226.
170. Major, M. A. *Bioremediation of Contaminated Soils; Agronomy Monograph*;American Society of Agronomy: Madison WI, 1999; Vol. 37, pp 112−131.
171. Thompson, P. L.; Ramer, L. A.; Schnoor, J. L. Uptake and Transformation of TNT by Hybrid Poplar Trees. *Environ. Sci. Technol.* **1998**, *32*, 975–980.
172. TT (Tetra Tech Inc.). *Draft Final High Use Target Area Investigation Report Phase I (HUTA I), Volume 1 Text, Figures, and Tables, Massachusetts Military Reservation, Camp Edwards, MA*; MMR-8005; Brookfield, WI, 2003.
173. TT (Tetra Tech Inc.). *Draft Final High Use Target Area Investigation Report Phase II (HUTA II), Massachusetts Military Reservation, Camp Edwards, MA*; MMR-6900; Brookfield, WI, 2002.
174. Thiboutot, S.; Ampleman, G.; Dube, P.; Hawari, J.; Spencer, B.; Paquet, L. *Protocol for the Characterization of Explosive-Contaminated Sites*; DREV-R-9721; Defence Research Establishment Valcartier, Quebec, Canada, 1998.
175. Jenkins, T. F.; Pennington, J. C.; Ampleman, G.; Thiboutot, S.; Walsh, M. R.; Diaz, E.; Dontsova, K. M.; Hewitt, A. D.; Walsh, M. E.; Bigl, S. R.; Taylor, S.; MacMillan, D. K.; Clausen, J. L.; Lambert, D.; Perron, N.; Lapointe, M. C.; Brochu, S.; Brassard, M.; Stowe, M.; Farinaccio, R.; Gagnon, A.; Marois, A.; Gamache, T.; Quémerais, B.; Melanson, L.; Tremblay, R.; Cuillerier, Y.; Gilbert, G.; Faucher, D.; Yost, S.; Hayes, C.; Ramsey, C. A.; Rachow, R. J.; Zufelt, J. E.; Collins, C. M.; Gelvin, A. B.; Saari, S. P. *Characterization and*

Fate of Gun and Rocket Propellant Residues on Testing and Training Ranges: Interim Report 1; ERDC Report TR 07-1; US Army Corps of Engineers, Cold Regions Research and Engineering Laboratory: Hanover, NH, 2007.
176. Brochu, S.; Diaz, E.; Thiboutot, S.; Ampleman, G.; Marois, A.; Gagnon, A.; Hewitt, A. D.; Bigl, S. R.; Walsh, M. E.; Walsh, M. R.; Bjella, K.; Ramsey, C.; Taylor, S.; Wingfors, H.; Qvarfort, U.; Karlsson, R.-M.; Ahlberg, M.; Creemers, A.; van Ham, N. *Environmental Assessment of 100 Years of Military Training at Canadian Forces Base Petawawa; Phase I - Study of the Presence of Munitions-Related Residues in Soils and Vegetation of Main Range and Training Areas*; DRDC Valcartier TR 2008-118; Defence Research Establishment Valcartier, Quebec, Canada, 2009.
177. Jenkins, T. F.; Ranney, T. A.; Hewitt, A. D.; Walsh, M. E.; Bjella, K. *Representative Sampling for Energetic Compounds at an Antitank Firing Range*; ERDC/CRREL TR-04-7; US Army Corps of Engineers, Cold Regions Research and Engineering Laboratory: Hanover, NH, 2004.
178. Reifler, G. R.; Medina, V. *Chemosphere* **2006**, *63*, 1054–1059.
179. Thiboutot, S.; Ampleman, G.; Marois, A.; Gagnon, A.; Bouchard, M.; Hewitt, A. D.; Jenkins, T. F.; Walsh, M.; Bjella, K.; Ramsey, C.; Ranney, T. A. *Environmental Conditions of Surface Soils, CFB Gagetown Training Area: Delineation of the Presence of Munitions-Related Residues* (Phase III, Final Report); DREV-TR-2004-205; Defence Research Establishment Department of National Defence: Valcartier, Quebec, Canada, 2004.
180. Diaz, E.; Brochu, S.; Thiboutot, S.; Ampleman, G.; Marois, A.; Gagnon, A. *Distribution and Fate of Energetics on DoD Test and Training Ranges: Interim Report 6*; Technical Report ERDC TR-06-12; US Army Engineer Research and Development Center: Vicksburg, MS, 2006
181. Jenkins, T. F.; Hewitt, A. D.; Grant, C. L.; Thiboutot, S.; Ampleman, G.; Walsh, M. E.; Ranney, T. A.; Ramsey, C. A.; Palazzo, A. J.; Pennington, J. C. *Chemosphere* **2006**, *63*, 1280–1290.

Chapter 16

Release Rate and Transport of Munitions Constituents from Breached Shells in Marine Environment

Pei-Fang Wang,[1,*] Qian Liao,[2] Robert George,[1] and William Wild[1]

[1]Space and Naval Warfare Systems Center Pacific, San Diego, CA 92152
[2]University of Wisconsin-Milwaukee, Milwaukee, WI 53211
[*]Pei-fang.wang@navy.mil

This study focuses on the information necessary for assessing fate and transport processes associated with munitions constituents (MC) leaching from a single breached shell into a shallow seawater environment for the three scenarios: a breached shell sitting on the bottom, low-order detonation and a breached shell buried in sand. The study includes three components: analytical, empirical and modeling studies. First, a set of specific semi-analytical formulae are developed to describe the release rate of munitions constituents under various conditions of shell integrity and hydrodynamic situations. Specifically, the MC release rate can be explicitly expressed as a function of the following five parameters: ambient current speed (U), hydrodynamic mixing coefficient (D), size of the breach hole (b), cavity radius inside the shell (R), and dissolution rate of MC from the solid to aqueous phase inside the shell (μ). Release rates are governed by the relative magnitudes of the two dimensionless Reynolds Numbers, Ub/D and μR/D. Release rate for low-order detonation is deduced from the general solution. The semi-analytical release rate function is validated by results from both an empirical study and a modeling study for the current controlled release scenarios. For the modeling study, the generic fluid dynamic model, FLUENT was used to simulate the mixing dynamics and release rate through various breach hole sizes and under different ambient

currents. Modeling results were compared with the empirical study results for the same scenarios.

1. Introduction

Releases of munitions constituents (MC) from breached shells in marine environment have been a topic of active research in the past several years. Most of the efforts have been focused on detection and measurement of Unexploded Ordnance (UXO) and MC releases in estuaries and harbors. Due to the complexities involved, these technologies are continuously being evolved. As part of the efforts, MC release from breached shells in marine environment has been studied. This effort directly addresses the amount of MC introduced into the environment from the case of an uncovered single breached round as a baseline scenario. This information can be then used to address the more complex issues implicit for a buried round, and also MC dispersed by a low-order detonation. To address the specific release function and its predictive ability, we conducted three studies, including analytical and numerical modeling studies to predict source release from a breached shell under various hydrodynamic and shell integrity conditions. Results from these two sets of studies were cross-compared and the release rate functions and predictions were verified. The release functions provide source terms for three types of MC, including TNT, HMX and RDX, which are used to drive the fate and transport prediction using the hydrodynamic and transport model, TRIM2D, which has been calibrated for hydrodynamics of San Diego Bay.

With this study, we have developed knowledge and empirical release rate functions to predict rate of MC release into the surrounding environment for each of the scenarios of interest: 1) breached shell lying on top of the sediment, or 2) as exposed solid energetic material released directly to the underwater environment, *e.g.* in a low-order detonation, or 3) breached shell entirely buried in sediment, (Figure 1). For these scenarios, we assume that the release through a breach in a munition casing can be determined by the following five key parameters: 1) the start and growth of the breach or the hole (with a size of b, the radius of the hole); 2) the radius of the cavity formed due to loss of mass released from inside the shell (R); 3) the chemical property (dissolution rate (μ) from solid to aqueous phases of the MC inside the shell casing); 4) the outside ambient current (U) to which the casing hole is exposed; and 5) mass of MC remaining inside (M_c). For scenario 3, low-order detonation contamination, only parameters μ (dissolution), U (ambient current) and M_c (mass remaining) need to be considered as an extreme case where a breach is infinite in size. It is the goal of this effort to define and quantify the MC release rate function, $F(b,R, \mu,U,M_c)$, as a function of the five listed variables, which presumably govern the release rate of MC from the munition casing. Study results of MC release from breached shells in water column (Scenarios 1 and 2) are discussed in this paper. Study results of MC release from breached shells buried in sediment (Scenario 3) can be found in (*10*).

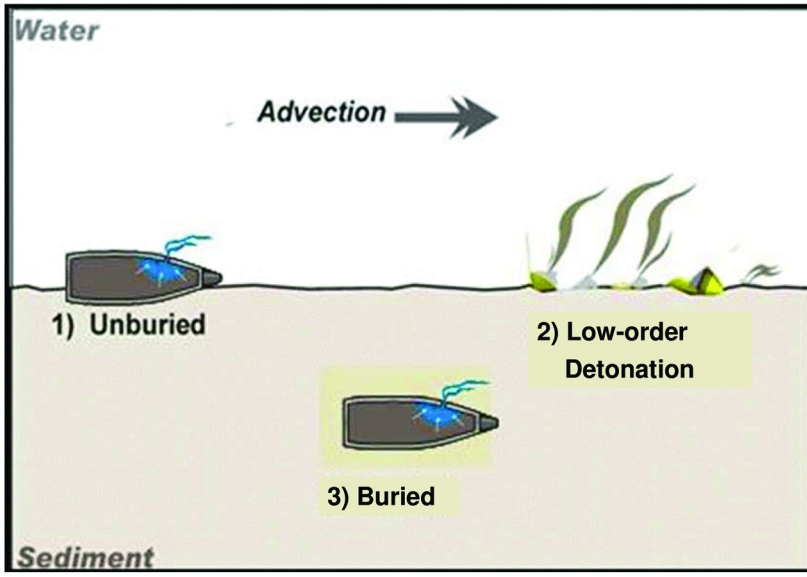

Figure 1. Conceptual model for three scenarios, unburied, low-order detonation in water and buried

We have conducted both analytical and numerical modeling studies on MC release rates under various hydrodynamic and shell integrity conditions. Results from previous studies on the chemical characteristics of MCs in marine water and sediment environments relevant to this study, are evaluated and used for both the release rate solution and subsequent fate and transport modeling study. For example, results on chemical properties, such as solubility and dissolution kinetics for each of the munition constituents of interest, have been used to assist in defining the dependence of the MC release rate function F on the following issues.

Dissolution Rates and Solubility

Both dissolution rates and solubilities of MCs in marine water are used in the release rate formulae (*1*). Solid phase MC dissolves into the aqueous phase at a rate (dissolution rate) that competes with the hydrodynamic diffusivity, created by ambient current and the size of the breached hole, which disperse the MC solution out of the shell through the hole. In the analytical release rate function, the MC-dependent variables include the saturation concentrations (C_S) and the dissolution speed (μ), obtained by dividing the dissolution rate by the saturation concentration. These MC-dependent chemical data are listed in Table 1.

Table 1. Saturation concentrations (C_S), Dissolution rates and Dissolution speed (μ) for TNT, RDX and HMX in Freshwater (*2–6*)

	Saturation Concentration (C_S) (mg/L)	*Dissolution Rate (μg/cm²/s)*	*Dissolution Speed (μ) (cm/s) (Dissolution Rate/Saturation Concentration)*
TNT	88.5[a]	0.20[d]	0.00226
RDX	38.4[b]	0.05[d]	0.00130
HMX	6.6[c]	0.15[d]	0.02272

[a] Ref (*2*). [b] Ref (*3*). [c] Ref (*4*). [d] Refs (*5*) and (*6*).

Dissolution rates for TNT, RDX, and HMX from neat TNT and from two military formulations, Octol and Comp B, have been evaluated under experimentally identical conditions (*1*). These comparisons indicated that dissolution rates were generally in close statistical agreement for comp B and Octol. Neat TNT exhibited a lower rate in saltwater that was independent of the salinities tested. Based on these observations, the dissolution rates for freshwater (Table 1) are used as a conservative measure for the analysis of release rate of MCs into the marine environment from breached shells in the following sections.

2. Technical Approach

2.1. Mixing of MC from Breached Shells

In the MC release problem, it is assumed that MC is released from the shells through a breach or hole in the shell casing, which is exposed to ambient currents. The size of the hole is assumed to be small compared to the overall size of most shells, with curvatures that are small enough not to affect the ambient currents at the outer surface of the shell as in the conceptual model (Figure 2). Under these assumptions, the MC release process can be approximated by a flat plate as in the simplified conceptual model, 3, in which MC is released from a hole on the plate over which ambient current flows.

It is assumed that a majority of the total release occurs during a stage when a relatively large cavity (compared to the breach hole or crack) has formed due to dissolution of the MC matrix. Thus, the overall release rate is governed by the advection and diffusion of MC concentration within the inner cavity, which is in turn determined by the dissolution of MC at the solid-solution interface and the exchange flow at the breach (boundary conditions). The driving force for MC leaching from the inner cavity is the hydrodynamic diffusion caused by ambient current inside the cavity, which generates inner circulation. We also assume that the local shear stress in the vicinity of the breach hole largely determines the inner circulation of the MC solution, *e.g.*, different external flow conditions with similar near-breach/hole hydrodynamic conditions result in a similar inner circulation pattern, resulting in approximately the same mass depletion rate.

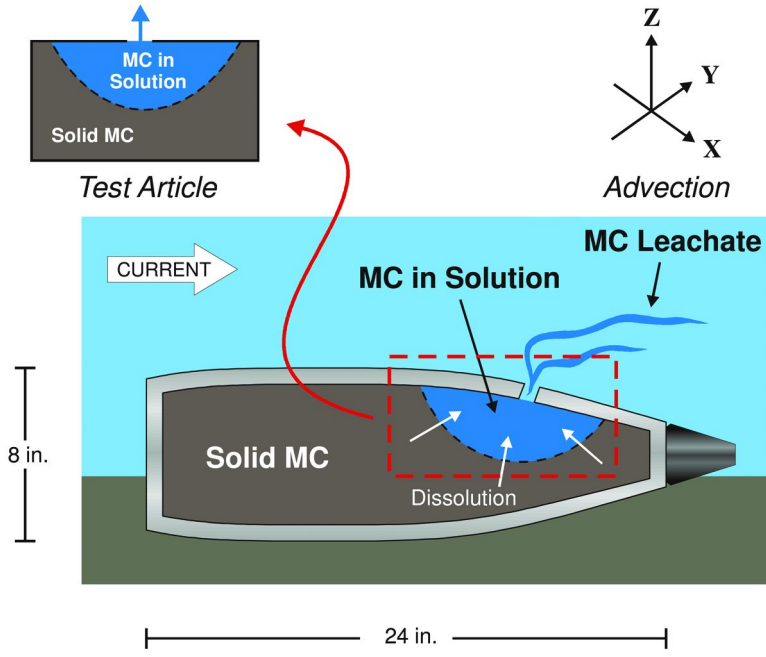

Figure 2. Conceptual model for MC release from a breached shell with a hole. (see color insert)

Based on the above assumptions, the MC flux can be examined with a simplified conceptual model consisting of a uniform ambient fluid flowing over a flat plate that represents the surface of a shell as in Figure 2 and 3. The shell breach is modeled as a circular hole with radius *b*. Water flows over the hole with speed *U*. The typical flow inside the cavity is characterized with 3D structures. However, we assume a cavity with a spherical shape with radius *R*, *i.e.*, diffusion/mixing process (by molecular diffusion and flow-induced stirring) is considered to be homogeneous. The 3-D diffusion/mixing problem inside the casing is thus simplified to a 1-D process. The controlling equation can be written as

$$\frac{\partial C}{\partial t} = D\frac{1}{r^2}\frac{\partial}{\partial r}\left(r^2\frac{\partial C}{\partial r}\right), \tag{1}$$

where C is concentration of MC in the cavity as a function of radial direction, r and time; D is a mixing coefficient, which may include the combined effects of molecular diffusion, D_M, and circulation induced mixing, D_A, (*i.e.*, $D=D_M+D_A$), where D_M is known as a physical property of sea water and MC, and D_A is a hydrodynamic function induced by ambient current speed, U.

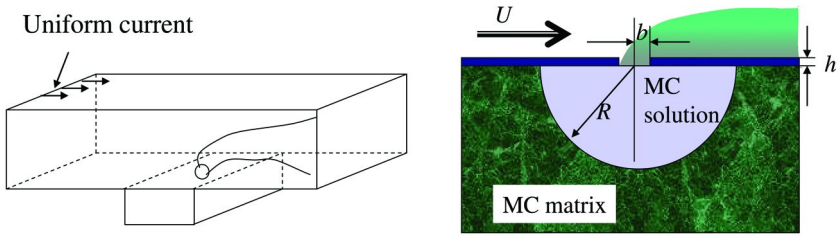

Figure 3. Simplified MC release rate conceptual model configuration.

At an equilibrium state, the general solution to Eq.(1) is

$$C(r) = B - \frac{A}{r}\,, \tag{2}$$

where A and B are constants. The boundary condition at the solid-liquid interface is prescribed as

$$-D\frac{dC}{dr} = \mu(C_s - C) \qquad @\ r = R\,, \tag{3}$$

where μ is the dissolution speed [cm/s], which is obtained by dividing the dissolution rate [mg/cm^2/s] over the saturation concentration, C_S [mg/L]. This boundary condition reflects the fact that flux by diffusion at the solid/liquid interface is in equilibrium with the dissolution process.

At the breach hole, the flux of *C* caused by mean current is considered to be linearly proportional to *U*, the local *C* and the two dimensional (2D) area of the hole, *i.e.*, MC flux is prescribed as $\alpha UC\pi b^2$, which is in equilibrium with diffusive flux from just inside the hole. The coefficient α (approximately equal to 1) is a model parameter which is a function of the local geometry of the breach hole/crack and the thickness of the shell. Thus we can write the boundary condition at the breach hole as:

$$2\pi b^2 D\frac{dC}{dr} = \alpha UC\pi b^2 \qquad @\ r = b\,, \tag{4a}$$

or,

$$\frac{dC}{dr} = \frac{\alpha U}{2D}C \quad @\ r = b\,. \tag{4b}$$

Substituting boundary conditions, Eqs. (3) and (4), into the general solution, Eq.(2), we have obtained the concentration field inside the cavity, as follows:

$$C(r) = \frac{C_s}{\frac{2D}{\alpha U b^2} + \frac{D}{\mu R^2} + \frac{1}{b} - \frac{1}{R}} \left(\frac{2D}{\alpha U b^2} + \frac{1}{b} - \frac{1}{r} \right), \tag{5}$$

The MC release rate can be obtained, by definition, as follows:

$$F = \pi b^2 U C(r = b) = \frac{2\pi D C_s}{\frac{2D}{\alpha U b^2} + \frac{D}{\mu R^2} + \frac{1}{b} - \frac{1}{R}}. \tag{6a}$$

F is the release rate function, which, as depicted in (6a), is a closed-form solution with the five variables, including hydrodynamic diffusivity coefficient (D), current (U), hole size (b), cavity radius (R) and dissolution speed of MC from solid to aqueous phase (μ). The model parameter, α, is defined as a geometry factor (Eq.(4)).

Eq.(6a) can also be expressed in a non-dimensional form as follows:

$$\begin{aligned} \overline{F} &= \frac{F}{\pi b^2 U C_S} \\ &= \frac{\frac{2D}{Ub}}{\frac{2}{\alpha}\left(\frac{D}{Ub}\right) + \frac{b}{R}\left(\frac{D}{\mu R}\right) + 1 - \frac{b}{R}} \\ &\sim \frac{\kappa}{\frac{2}{\alpha}\left(\frac{D}{Ub}\right) + \frac{b}{R}\left(\frac{D}{\mu R}\right) + 1 - \frac{b}{R}} \end{aligned} \tag{6b}$$

The denominator of (6b) includes three non-dimensional parameters, including the current-based Reynolds Number (Ub/D), the model parameter, α, and the number 2, which are both constants, the dissolution-based Reynolds Number (μR/D), and the hole-to-cavity size ratio (b/R). The hydrodynamic properties, D and U, can be described by field data or a numerical fluid dynamic model.

In general, the breached hole is much smaller than the cavity during scenarios where mass flux is most significant. As a result, the 1/R (or b/R) term in the denominator of Eq.(6a) (or 6b) can be neglected, which will help to highlight the behavior of the release rate function for the following two extreme conditions. A third scenario is also addressed for a low order detonation with fully exposed MC, which is accommodated in the model as equivalent to an infinitely large breach.

2.1.1. Current-Controlled Release Function ($\mu R^2 >> \alpha U b^2$)

When the dissolution speed (μ) is much larger than the ambient current (U) or the cavity (R) is much larger than the hole (b), MC solutions inside the cavity are near saturation and the release rate of MC is controlled by the ambient current speed, U and the hole size. The release rate function can be simplified explicitly as:

$$F = \frac{2\pi D C_s}{\frac{2D}{\alpha U b^2} + \frac{1}{b}}. \tag{7}$$

The MC release rate increases with ambient current speed, the area of the hole, and the saturation concentration of the MC.

2.1.2. Dissolution-Rate-Controlled Release Function ($\mu R^2 << \alpha U b^2$)

For this case, release of MC is controlled by the dissolution speed (rate), since ambient current and/or the hole is so large that MC solution dissolved from the solid phase is dispersed out of the breached shell immediately.

$$F = \frac{2\pi D C_s}{\frac{D}{\mu R^2} + \frac{1}{b}} \approx 2\pi R^2 \mu C_S \;; \quad \text{if } \frac{\mu R}{D} << \frac{1}{2}\left(\frac{b}{R}\right) \tag{8}$$

When the hole size is relatively small (compared to the parameter, $\mu R^2/D$), the hole has a damping effect restricting the release rate of MC out of the shell. When the hole size becomes relatively large, (compared to $\mu R^2/D$), the damping effect of the hole diminishes and the release of MC is directly proportional to the surface area of the cavity ($2\pi R^2$) and the dissolved mass rate (μC_S), as indicated in Eq.(8).

2.1.3. Low-Order Detonation Scenario Release

In the case where shells are broken apart and MCs are fully exposed to the ambient current, MC dissolution from the solid phase to the aqueous phase is controlled by the dissolution rate. Once dissolved, the MC plume is advected away by the ambient current. Therefore, under this low-order detonation scenario, MC release follows the dissolution controlled release process. The release function, Eq.(8), derived for release through a hole, can be modified for this scenario:

$$F = A_S \mu C_S \tag{9}$$

where the term 1/b in Eq.(8) is infinitely small (hole is so large that 1/b ~ 0) and the solid-water interfacial area of the semi-sphere, $2\pi R^2$, is replaced by the solid-water surface area (A_S) of MC in water. For this scenario, the solid-water surface area, A_S , may be obtained from field observation/data. Therefore, release of MC under a low-order detonation scenario depends on the integrity of the exposed MC, represented by the total contact surface area between the remaining active MC matrix and the aqueous phase.

3. Model Validation

3.1. Simulation Parameters

The algebraic analytical function for MC release, as discussed in Section 2, has been validated by the numerical simulation results using the FLUENT model. FLUENT (Fluent Inc.) is a general Computational Fluid Dynamic Model (CFD), widely used in automobile and combustion industries. The FLUENT model includes a mesh generating software, GAMIT, which is flexible in generating model configuration and meshes for scenarios designed by the users. For this numerical modeling study, a numerical flume channel is used, which is 1 meter in length, 0.4 meter in width and 0.2 meter in depth. A circular hole (radius = b) is "drilled" into the bottom of the channel. The hole is a representative of the breach hole in the shell, and it connects to a semi-sphere space (radius = R) beneath the flow channel as seen in Figure 4. The flume channel and the semi-sphere are filled with water. The inner surface of the semi-sphere is defined as the MC solid-aqueous interface, through which the MC dissolution occurs. Solution inside the semi-sphere cavity is released through the hole due to the current in the channel. The coordinate system is set such that the center of the hole is the origin, positive x is in the mean flow direction, y is in the cross-channel direction and z is positive upward (normal to flow).

3.2. Validation: Dependence on Current Speed (U) and Radial Direction (r)

In the first validation case, the radius of the breach hole is b = 5 mm. The inside cavity is a semi-sphere with radius R = 0.1 m. Upstream current speed varies from 1 mm/s to 0.5 m/s. Reynolds number based on the hole size and the mean current speed varies from 5 to 2,500.

The circulation enhanced diffusivity, D_A, has a dimension of [Velocity × Length], which in general, should be a function of r; D_A varies with distance r inside the cavity. The velocity scale is modeled as

$$u_A(r) = \frac{\int_{r'=r} \sqrt{[u(r')]^2 + [v(r')]^2 + [w(r')]^2}\, dA}{2\pi r^2}, \tag{10}$$

where u, v, and w are the velocity components in the x-y-z coordinates inside the cavity at the radius, r, over which the surface integral is performed. The value, u_A, is the averaged velocity on a spherical surface with radius r. D_A is modeled as

$$D_A = \beta u_A r, \tag{11}$$

where β is a model parameter.

Based on FLUENT simulation results, D_A/β as a function of r is calculated for different current speed, as shown in Figure 5. In general u_A decreases with r, but $u_A r$ is only weakly dependent on r, except near the breach hole and the solid-liquid interface.

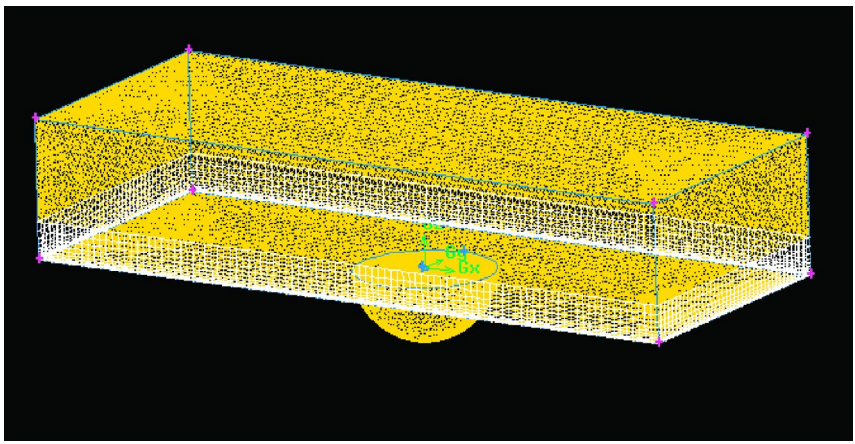

Figure 4. FLUENT model geometry and meshes generated by GAMIT. (see color insert)

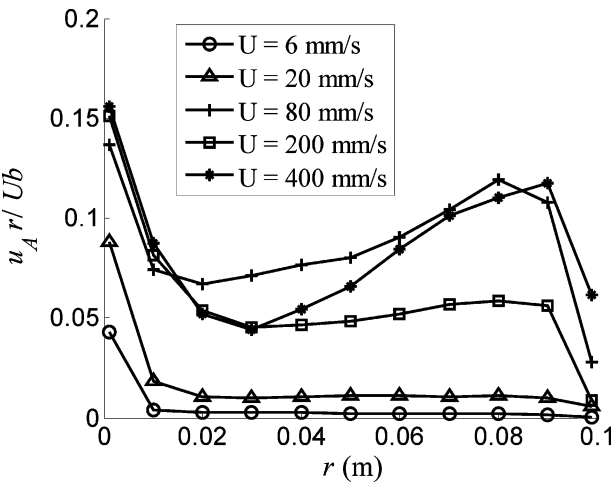

Figure 5. Distribution of $u_A r$ / Ub as a function of r for different current speed

As a first order approximation, we assume D_A is homogenous inside the breach hole and we take the average of D_A/β calculated at different r (except for $r=b$ and $r=R$) as the effective advection induced diffusivity, as defined in Eq.(11), and plot it with respect to current speed U times the hole radius b, as shown in Figure 6.

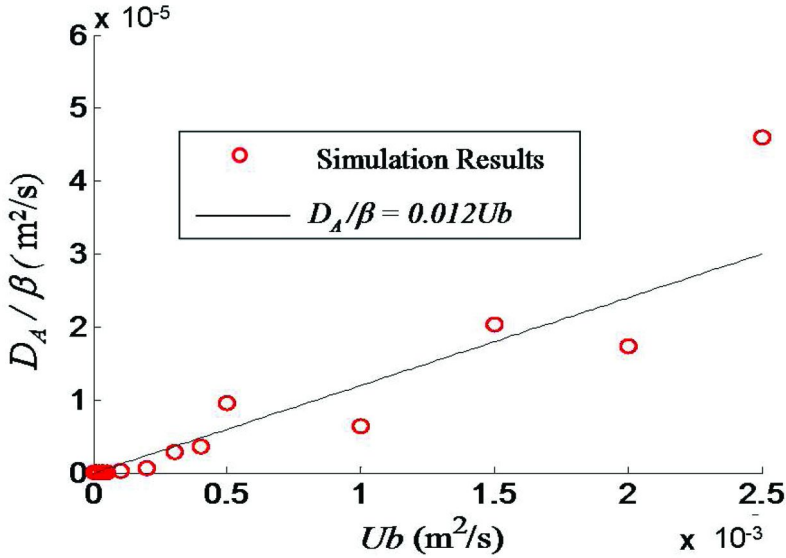

Figure 6. Modeled relationship between the effective diffusivity D_A and the current speed U.

Again, as a first order approximation, we assume there is a linear relationship between D_A/β and Ub. By linearly fitting the simulation result (Figure 6, we can propose a model for D_A:

$$\frac{D_A}{\beta} = 0.012Ub\,. \tag{12}$$

It can be shown that D_A is much greater than the molecular diffusivity D_M except for very small current speed. According to this argument, Eq.(7) for the MC flux rate is

$$F \approx \frac{2\pi \times 0.012\beta UbC_s}{\dfrac{2\times 0.012\beta Ub}{\alpha Ub^2} + \dfrac{1}{b}} \approx \theta U\left(\pi b^2\right)C_S\,, \tag{13}$$

where $\theta = 0.024\alpha\beta/(0.024\beta + \alpha)$, *i.e.*, the flux is linearly proportional to the current speed, the saturated MC concentration and the radius of the breach hole.

The above model is validated with the simulation results, as shown in Figure 7. The above linear relation fits well with simulation results and the model coefficient θ is ~ 0.023. It should be noted that the linear growth of F with U is only valid for large Reynolds number values. As shown in Figure 7, the inset plot for small U's, the effect of molecular diffusion is at the same order of magnitude as that of advection, thus linear dependency is not valid in this regime.

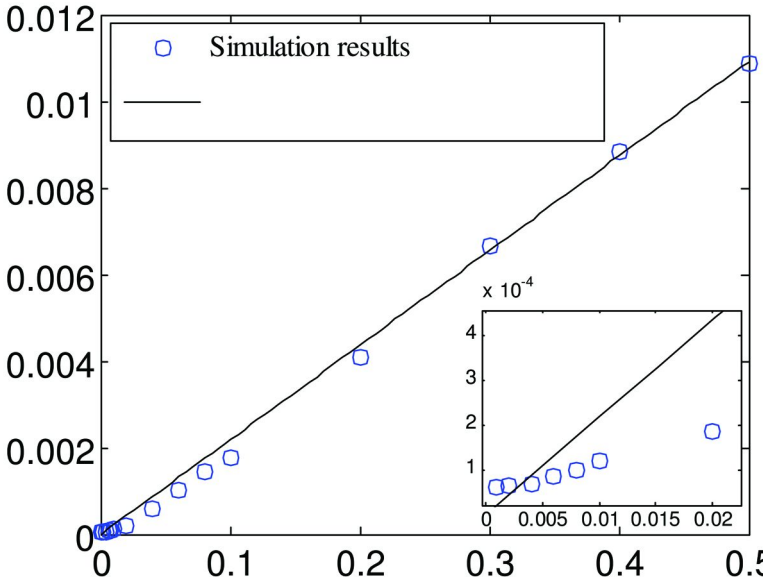

Figure 7. Variation of MC flux rate with respect to current speed.

With the fitted parameter θ, we can substitute the modeled D_A into the equation of concentration profile Eq.(7) and compare it with simulation results. Figure 8 shows both the analytical solution as a function of r, and simulation results for different current speed. There are generally good agreements, especially for smaller current speed. However, for U > 100 mm/s, differences between simulation and analytical solutions become apparent. This is due, in part, to the circulation-induced diffusivity becoming more inhomogeneous, which invalidates our analytical solution.

3.3. Effects of Shell Thickness

In our previous analysis, the shell thickness (hereafter denoted as h) has been ignored. Shell thickness is generally smaller compared to the inner cavity radius R, thus its effects on the overall flux rate can be considered secondary, *i.e.*, it may result in a slightly different coefficient β in the boundary condition of our analytical model (*i.e.*, Eq.(4)), but the general equation of inner scalar transport should not be affected by nominal shell thickness.

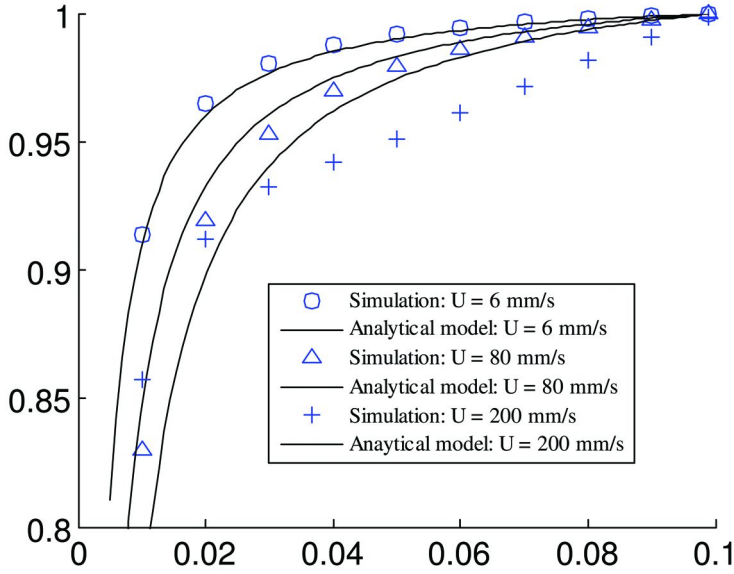

Figure 8. Radial distribution of concentration in the casing. Simulation results compared with analytical solution (Eq. (7)).

Due to the limitation of grid size, details of circulation patterns smaller than h are not easily resolved by simulation. We will, however, present the empirical relation between the release rate and the shell thickness. Three breach radii are selected for simulation, b = 2.5, 5 and 10 mm, respectively. The shell thickness varies from 4 mm to 24 mm and the current velocity is allowed to change from 4 cm/s to 45 cm/s. In most cases, a linear increase of release rate (flux) with the mean current U can be observed. This agrees with the analytical solution Eq.(11). However, the proportionality ($\theta\lambda$) differs from case to case. For the purposes of comparison, the empirical solution for validation case I, Eq.(12), is also shown. The normalized release rate $[F/(C_S U(\pi b^2))]$ as a function of the shell thickness is shown in Figure 9. The normalized release rate fluctuates when h and b are of the same order of magnitude. When $h>>b$, the normalized F seems to be independent of h and becomes a constant. This constant varies between 0.015~0.035, compared to 0.023 demonstrated in the previous validation case. Therefore, future efforts will select an appropriate value that lies within the range of 0.015~0.035.

3.4. Release Time

The general analytical release rate function (Eq.(6a)), which has now been validated by the FLUENT model, can be used to predict the release rates of MC, under various hydrodynamic and shell integrity conditions. For a single shell with known MC mass, the predicted release rates can be further used to estimate time to deplete all MC in the shell under these conditions. Here we use Eq.(6a), for the

calculations of release time for TNT, RDX and HMX under various hydrodynamic and shell integrity conditions.

For analysis of the following scenario, we use a typical round with the following shell dimensions: length = 24″, diameter = 8″, and MC weight = 8 kg. Shell thickness is not included for problem simplification purposes.

For different realistic combinations of the 5 variables in (Eq.(6a)), release time can vary by several orders of magnitude. For example, under an ambient current of 45cm/s (fast flow), release time ranges from 300 years for a hole with radius of 0.05 cm to 1 year for a hole with radius of 0.95 cm, illustrating the importance of hole size. The sensitivity to ambient current is also apparent in Figure 10, where the release time varies by one order of magnitude between slow flow (5 cm/s) and fast flow (45 cm/s). For example, for a hole with a radius of 0.5 cm, it takes about 25 years to deplete the MC inside the shell under ambient current of 5 cm/s. The release time is much shorter, less than 3 years, if the ambient current increases to 45 cm/s.

Figure 11 compares the release time for TNT, RDX, and HMX under the same conditions. TNT release time is fast, followed by RDX and HMX. Although HMX has the highest dissolution speed, its low saturation concentration (Table 1) and interactions with other parameters, including current speed, hole size and cavity size, make the mass release from the shell the slowest of the three MCs for this scenario. For the scenario in Figure 11, saturation concentrations dictate the release time (and rate) for the three MCs.

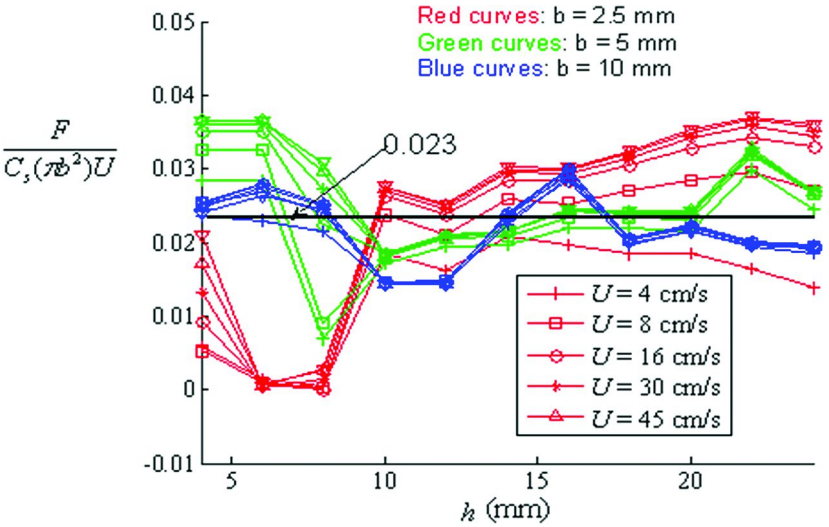

Figure 9. Effects of shell thickness on the normalized release rate. (see color insert)

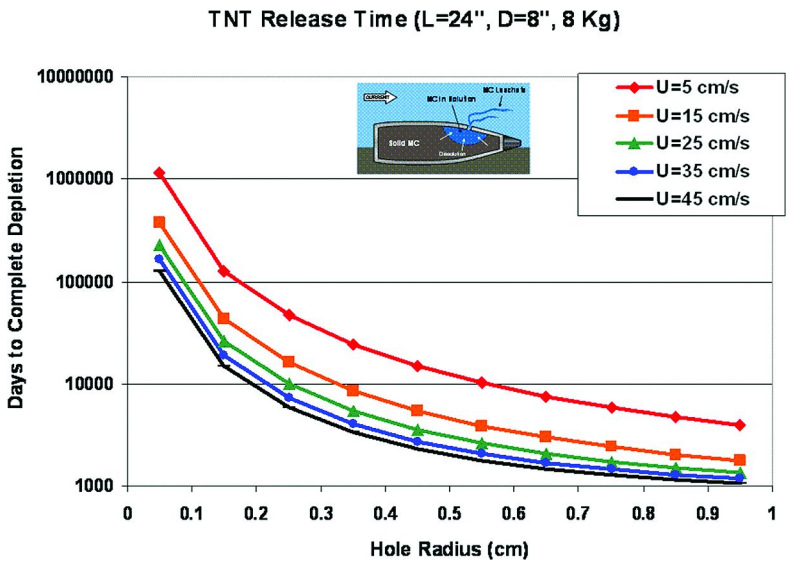

Figure 10. Days to complete release of TNT inside the shell with dimension of L=24", D=8", MC mass=8 kg. Release time are plotted as functions of ambient velocity (U) and hole radius (b).

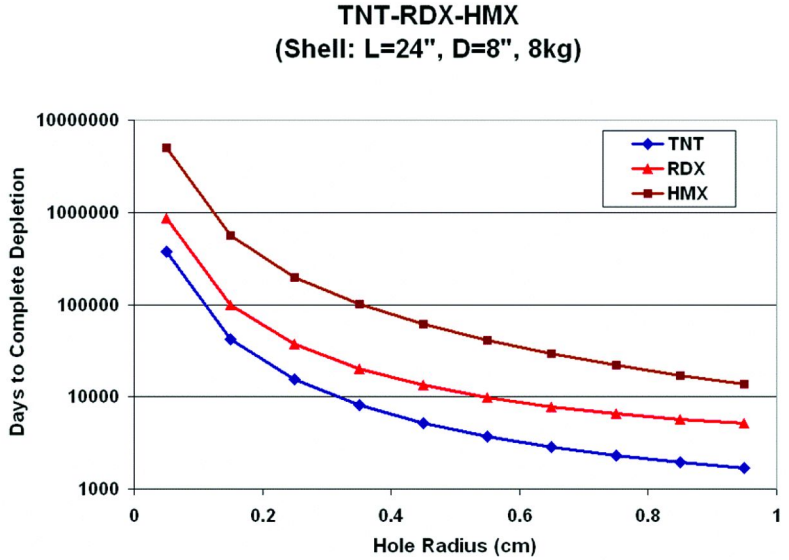

Figure 11. Release time for TNT, RDX and HMX, under the same conditions (U=15 cm/s).

In a natural coastal setting, tidal cycles dictate the flow behavior. Release rates during tidal cycles with tidal current speed ranging from 5 – 45 cm/s are shown in Figures 12 and 13. For small hole size (b=0.1 cm, Figure 12), release rates for TNT, RDX and HMX vary with tidal currents over the entire current speed range. For this scenario, the current-based Reynolds Number (Ub/D) is much smaller than the dissolution-based Reynolds Number (μR/D) and release rates are limited by current speed. For larger holes (*i.e.*, b=2.5 cm, Figure 13), release rate of TNT is limited primarily by current speed when the current is low (<15 cm/s). When the current becomes strong (speed ~15-45 cm/s), release rate of TNT is only weakly dependent on current speed; it is limited primarily by dissolution rate. For RDX, Figures 12 and 13 show that release rate is primarily limited by current speed for small hole size (*i.e.*, b=0.1 cm), but it is primarily limited by dissolution rate for larger hole size (*i.e.*, b=2.5 cm) over the entire range of current speed. The release rate for HMX is limited by current speed for both small and large hole sizes over the entire range of current speed.

From these analyses, it has been shown that release rates for TNT, RDX and HMX are governed by five variables, including current speed, hole size, cavity volume, dissolution rates, and hydrodynamic diffusivity coefficient. Release rates of MC in a dynamic estuarine environment are limited by two overall conditions: current-controlled release and dissolution controlled release. Ultimately, the release rate function can be linked with a hydrodynamic and fate/transport model to simulate the dynamic release and subsequent fate/transport of MCs in the estuarine receiving water.

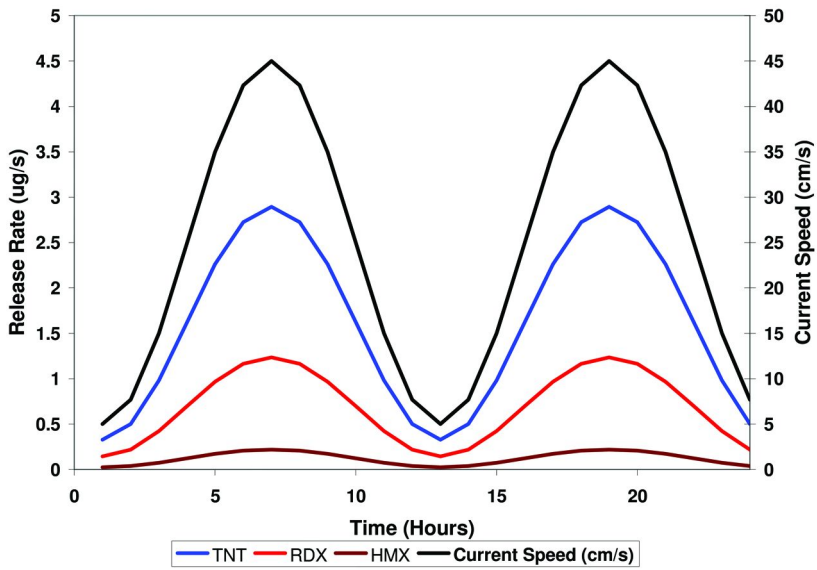

Figure 12. Release rates and current speeds over two tidal cycles (~24 hours) for TNT, RDX, and HMX (b=0.1 cm, R=10 cm). (see color insert)

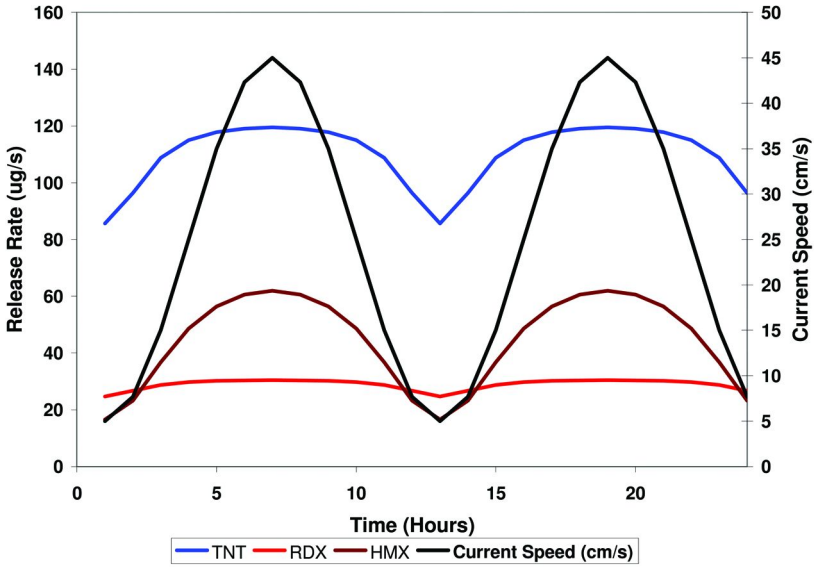

Figure 13. Release rates and current speeds over two tidal cycles (~24 hours) for TNT, RDX, and HMX (b=2.5 cm, R=10 cm) . (see color insert)

3.5. Modeling Fate and Transport of TNT, RDX and HMX

The release rate function, developed and validated by FLUENT previously, is used to provide release rates for a single shell under various hydrodynamic and shell integrity conditions. Since we do not have adequate information about the quantity and magnitude of breached shells in DoD coastal and estuarine waters, the following assumptions are made

The release rate function, developed for this study, can be used to predict release rate for any single breached shell. For multiple breached shells, the total release rates can be obtained by summing the release rates of each individual beached shell. Assuming that such an estimate can be provided.

In the following example, we used TRIM2D to simulate the fate and transport of MCs released from a breached shells hypothetically placed in San Diego Bay, CA (Figure 14) with the following dimensions (Table 2):

Table 2. Sizes and dimensions of the test breached shell.

Length (inches)	*Diameter (inches)*	*Hole radius (mm)*	*Average current (cm/s)*	*MC Mass (kg)*
24	8	20	8	8

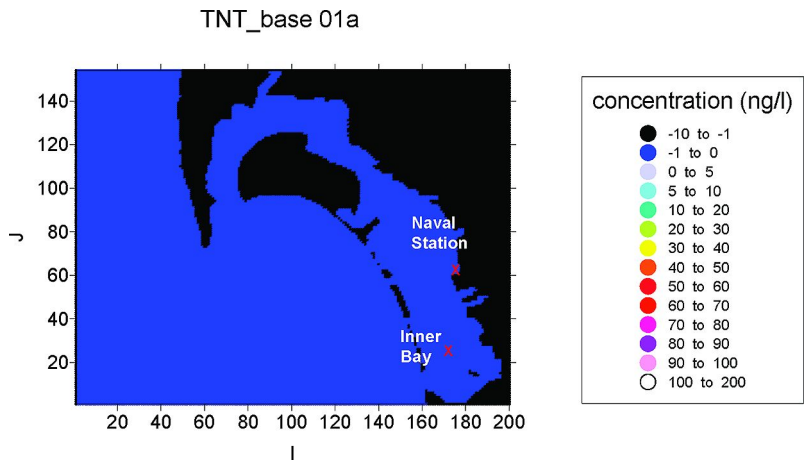

Figure 14. Location (X) of MC release from a single breached shell, inner San Diego Bay and Naval Station, respectively (no loading scenario). (see color insert)

TRIM2D is a depth-averaged tidal and residual circulation model with a finite-difference numerical grid and scheme. TRIM2D has been previously applied to simulate time-varying water surface elevation and averaged water-column currents and associated transport of contaminants for several estuarine systems, including San Francisco Bay, CA, Boston Harbor, MA, Charleston Harbor, SC, and Venice Lagoon, Italy (*7*, *8*). Over the recent years, SSC San Diego has applied TRIM to several water-resource and water quality studies for San Diego (*9–11*).

The use of a two-dimensional (2D), depth-averaged model, such as TRIM, is justified because field data show that the flow in San Diego Bay exhibits strong uniformity in the water column (*12*). Such uniformity of flow in the water column results from the fact that San Diego Bay is shallow and flow in the bay is primarily driven by tides from the Pacific Ocean.

From a rest condition, we ran TRIM for 2 days (48 hours) to ensure that a steady-state flow condition was reached before the constant-load effluent entered into the bay. This initial 2-day run was necessary to eliminate transient flows that should not exist under the steady-state, quasi-repetitive tidal conditions. We used a 6-minute time-step in the model and simulated tidal height and tidal currents. Simulation for 1 year (365 days) was executed and results at the end of 365 days were analyzed. The Modeling Results sections of this report discuss the findings from this modeling study.

3.5.1. Model Setup

A 2D rectangular numerical grid system (of dimensions 100m x 100m) was used for TRIM. These numerical grids cover the entire San Diego Bay and portions of the ocean outside the mouth, consisting of 30,845 grid cells with 21,563 water cells. Measured tides are prescribed along the west, south, and north boundaries of the model domain.

Two simulation scenarios for TRIM were evaluated. The first case explores the release of MCs from a shell located at the end of the inner bay (Figure 14). The second simulation case assumes that MC release occurs near the Naval Station near the middle of the bay. For both simulation cases, current speeds at both locations simulated by TRIM2D are used for estimating release rate. Therefore, the release rates are time-varying.

3.5.2. Model Results

Case #1

Simulated single shell source release steady-state TNT concentrations are also shown in 22 and 23 under an ebb and flood tide, respectively. In general, steady-state concentrations decrease from the source to the mouth of the bay, resulting from hydrodynamic transport and diffusivity in the bay. Under the steady-state conditions, transport of TNT released from the breached shell gradually reaches a balance with the hydrodynamic flushing of the bay water, which is driven by ocean tides mixed with diurnal and semi-diurnal tidal cycles. Simulated steady-state TNT concentrations (ignoring any degradation processes) range from ~30-50 ng/L in the inner bay to10-30 ng/L in the mid-bay areas and to about 1-2 ng/L near the bay mouth.

For this simulation, it is assumed that TNT is released into the water column totally as aqueous solution (dissolved). No net loss of TNT from the water column exists, except the hydrodynamic dispersion and tidal flushing through the mouth of the bay. Hydrodynamic dispersion disperses and redistributes TNT concentrations and tidal flushing through the mouth of the bay provides a net mass loss of TNT out of the bay. When a steady state condition is reached, mass loss rate of TNT by flushing through the mouth should be balanced by the net release rate of TNT from the breached shell. Therefore, results shown in Figures 15 and 16 can be considered to be conservative estimates of TNT exposure from the single-shell source releases.

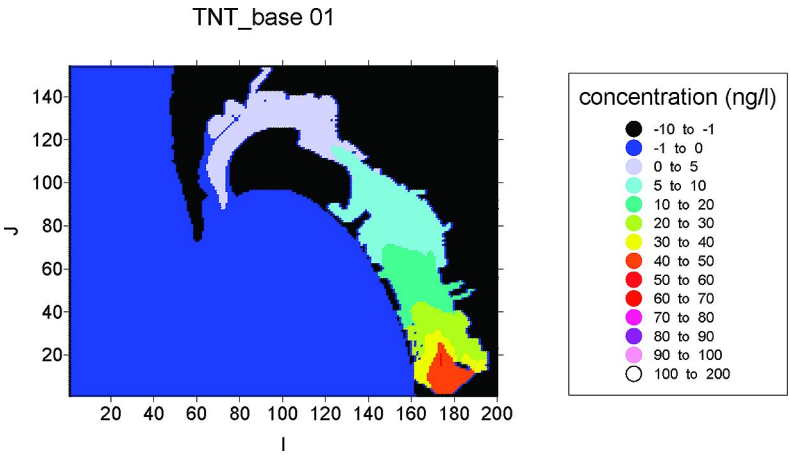

Figure 15. Steady-state TNT concentration during ebb tide (release from inner bay) (x-y coordinates are distances with I, J indices multiplied by 100 meters, the same convention hereafter). (see color insert)

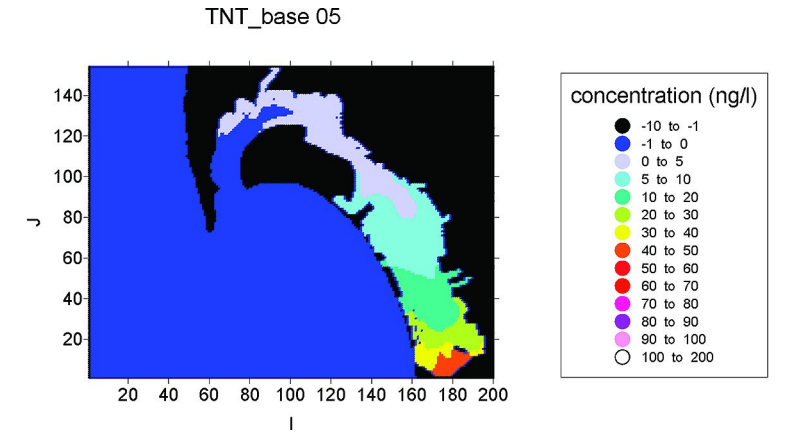

Figure 16. Steady-state TNT concentration during flooding tide (release from inner bay). (see color insert)

Case #2

Simulated steady-state TNT concentrations are shown in Figures 17 and 18 for an ebb and flood tide, respectively. In general, steady-state concentrations decrease from the source, resulting from hydrodynamic transport and dispersion in the bay. Simulated steady-state TNT concentrations range from ~ 8 ng/L in the inner bay to ~4 ng/L in the mid-bay areas and to about ~ 1 ng/L near the bay mouth. Highest TNT concentrations (~15 ng/L) occur near the source region, the Naval Station. Due to the weaker current speed, annual release of TNT from the breach

shell at Naval Station is only about 5 kg/year, in comparison with the larger release rate of about 8.4 kg/year in the southern inner bay (Case #1) (Figures 15 and 16).

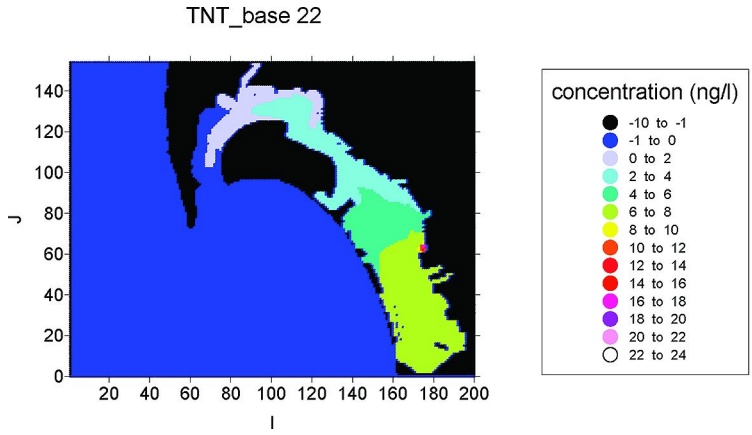

Figure 17. Steady-state TNT concentrations during ebb tide (release from Naval Station). (see color insert)

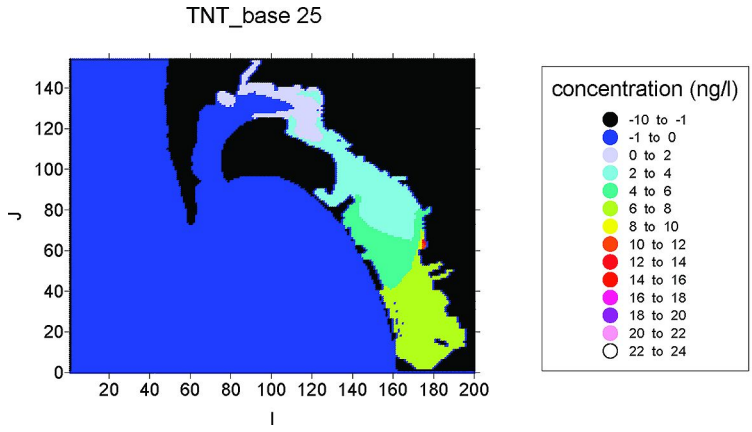

Figure 18. Steady-state TNT concentrations during flooding tide (release from Naval Station). (see color insert)

For the simulations with TRIM2D, it is assumed that all TNT released from the breached shells is in the form of dissolved species (aqueous TNT concentrations). The only TNT mass loss term included is a result of flushing dissolved TNT out of the bay by currents and hydrodynamic dispersion. No loss to the sediment is assumed. Therefore, model simulated dissolved TNT concentrations from TRIM2D can be considered to be upper-bound (conservative) estimates for steady-state TNT concentrations in the water column.

4. Discussion and Summary

Theoretical and numerical studies have been conducted for the release of munitions compounds from a breached shell under various hydrodynamic and shell integrity conditions. Analytical solutions are derived for the release rate based on the assumptions that ambient currents are tangential over the shell surface, and that the hole is small in size compared to the cavity inside the shell. These theoretical analyses and numerical simulations have demonstrated that the flux of MC solution can be expressed explicitly as a function of five primary variables: current speed U, hole area A, saturated concentration C_S , dissolution speed (μ) and hydrodynamic dispersion coefficient, D (Eq.(7)). The analytical release rate solutions have been validated by the model results using FLUENT for the current controlled release scenarios.

The validated results show that, in a dynamic estuarine water body, release rates can experience processes that cover wide regimes including two extreme limiting conditions. For the first condition, $ub^2 << \mu R^2$, the release rate is limited by the ambient current speed. MC dissolution in the cavity occurs at a faster rate than the ability of MC to escape through the hole as a function of the ambient current (hydrodynamic dispersion). As a result, the solution in the cavity is always near saturation. For the condition, $ub^2 >> \mu R^2$, where the release rate is limited by dissolution speed, MC dissolution in the cavity is much slower than the transport of MC solution through the hole. For this case, the solution in the cavity is not near saturation and the retention time of the MC solution inside the breached shell (cavity) is small, resulting in more mass per unit time escaping from the shell.

When the thickness of the shell (h) is considered, the general release rate retains the same functional dependence on the five variables above. However, the shell thickness imposes an effect on the release rate, which can be expressed explicitly as,

$$F = \kappa U\left(\pi b^2\right)C_S \tag{14}$$

where κ is a coefficient which assimilates the effect of the geometry of the breach and shell thickness. If the breach has a circular shape, the value of κ is between 0.015 and 0.035 according to numerical simulations, in comparison with value of 0.023 when the thickness is ignored. This empirical model suggests that the MC release rate grows linearly with U, A and C_s, while it is independent of the cavity size R. This model is only valid if the breach size is relatively small compared to the cavity inside the shell ($b<<R$) and the shell thickness is large compared to the hole radius ($h>b$).

To fully validate the release rate function, further studies are needed, including further modeling studies using FLUENT, and selected laboratory experiments are required to fully validate the model and its parameters.

Transport processes for TNT have been simulated using a fine-scaled hydrodynamic and transport model, TRIM2D. For the conservative scenario, where TNT release loads enter the inner bay water column with no decay or exchange of mass with the sediment, model results provide conservative estimates of TNT in San Diego Bay.

Although much understanding has been obtained about the fate and transport of MC leached from breached shells, the issues described below will require further consideration:

- When multiple shells exist, each with a different shell integrity (different breach hole sizes), and shell sizes, and each under potentially different hydrodynamic conditions, how to best integrate the accumulated effects from the group of shells into the model should be determined. For this, probability-based modeling approaches, such Monte-Carlo methodology, may be able to adequately quantify the accumulative effects from the multiple breaches shells (*10*).
- When the shell is buried in sediment, fate and transport of MC released from the shell would be slowed, occurring on a time scale much longer than the modeled transport in the water column (*10*). This slow, long-term process needs to be considered in conjunction with the possibility of accumulated effects from multiple buried shells. A quantitative, model-based treatment of these factors will be required in order to better understand the significance of fate and transport for these scenarios, which may be reflective of a more realistic or real-world scenario.
- Future experimental studies are needed to further understand the behavior of TNT in marine waters, in particular the ability to evaluate dynamic exchange and transformations of TNT and degradation products specific to known decay pathways appear to be limited. This type of effort should include a systematic sensitivity/uncertainty evaluation and selective experimental validation of critical model components developed in these modeling studies.

References

1. Brannon, J. M.; Price, C. B.; Yost, S. L.; Hayes, C.; Porter, B. Comparison of environmental fate and transport process descriptors of explosives in saline and freshwater systems. *Mar. Pollut. Bull.* **2005**, *50*, 247–252.
2. Ro, K. S.; Venugopal, A.; Adrian, D. D.; Constant, D.; Qaisi, K.; Valsaraj, K. T.; Thibodeaux, L. J.; Roy, D. Solubility of 2,4,6-trinitrotoluene (TNT) in water. *J. Chem. Eng. Data* **1996**, *41*, 758–761.
3. Spanggord, R. J.; Mabey, R. W.; Mill, T.; Chou, T. W.; Smith, J. H.; Lee, S.; Roberts, D. *Environmental fate studies on certain munitions wastewater constituents: Phase IV – Lagoon model studies*; AD-A133987; SRI International, Menlo Park, CA, for U.S. Army Medical Research and Development Command, Ft. Detrick, MD, 1983.
4. McLellan, W. L.; Hartley, W. R.; Brower, M. E. *Health advisory for octahydro-1,3,5,6-tetranitro-1,3,5,6-tetrazocine (HMX)*; Criteria and Standards Division, Office of Drinking Water, U.S. Environmental Protection Agency, Washington, DC, 1988.

5. Lynch, J. C.; Brannon, J. M.; Delfino, J. J. Dissolution rates of three high explosive compounds: TNT, RDX, and HMX. *Chemosphere* **2002**, *47*, 725–734.
6. Lynch, J. C.; Brannon, J. M.; Delfino, J. J. Effects of component interactions on the aqueous solubilities and dissolution rates of the explosive formulations octol, composition B, and LX-14. *J. Chem. Eng. Data* **2002**, *47* (3), 542–549.
7. Cheng, R. T.; Casulli, V.; Gartner, J. W. Tidal, Residual, Intertidal Mudflat (TRIM) Model and Its Annplications to San Francisco Bay, California. *Estuarine, Coastal Shelf Sci.* **1993**, *36*, 235–280.
8. Cheng, R. T. Personal communication.
9. Chadwick D. B.; Leather, J.Richter, K.; Apitz, S.; Lapota; D.Duckworth, D.; Katz, C.; Kirtay, V.; Davidson, B.; Patterson, A.; Wang, P.; Curtis, S. *Sediment Quality Characterization Naval Station San Diego: Final Summary Report*; Technical Report 1777; SSC San Diego, CA, 1999.
10. Wang, P.-F.; Liao, Q.; George, R.; Wild, B. *Defining Munition Constituent (MC) Source Terms in Aquatic Environments on DoD Ranges (Phase IV): MC Release in Sediment*; SSC PAC's Draft Technical Report, 2011
11. Wang, P.-F.; Liao, Q.; George, R.; Wild, B. *Defining Munition Constituent (MC) Source Terms in Aquatic Environments on DoD Ranges (Phase III)*; SSC PAC's Draft Technical Report, 2010.
12. Wang, P. F.; Sutton, D.; Richter, K.; Chadwick, B. *Modeling Migration of Sediment and Sorbed Contaminants Resuspended by Ship Docking in San Diego Bay*; Proceedings in the 4th International Conference on Hydroscience & Engineering, Seoul, Korea, 2000
13. Wang, P. F.; Chadwick, D. B.; Johnson, C.; Grovhoug, J. *Modeling Copper and Biocide Concentrations from Hull Paint Leachate in San Diego Bay*; Technical Report 1935; SSC SD, 2006.
14. Wang, P. F.; Cheng, R. T.; Richter, K.; Gross, E. S.; Sutton, D.; Gartner, J. W. Modeling tidal hydrodynamics of San Diego Bay, California. *J. Am. Water Res. Assoc.* **1998**, *34* (5), 1123–1140.

Chapter 17

Degradation Products of TNT after Fenton Oxidation in the Presence of Cyclodextrins

Curt W. Jarand,[1] Kan Chen,[1] Boguslaw Pozniak,[1] Richard B. Cole,[1] Duc-Truc Pham,[2] Stephen F. Lincoln,[2] and Matthew A. Tarr*,[1]

[1]Department of Chemistry, University of New Orleans, 2000 Lakeshore Drive, New Orleans, LA 70148
[2]Department of Chemistry, University of Adelaide, Adelaide S.A. 5005, Australia
***mtarr@uno.edu**

Contamination of soil and water by 2,4,6-trinitrotoluene (TNT) poses a significant environmental threat in locations where TNT has been produced, stored, or used in military training activities. Fenton chemistry (Fe^{2+} catalyzed production of hydroxyl radicals) has demonstrated utility in the remediation of TNT but it suffers from a lack of specificity and low pH requirements. In the current study we have examined the ability of two commercially available and two synthetic cyclodextrins (CDs) with metal chelating functionalities to enhance Fenton degradation of TNT through formation of TNT/Fe/CD complexes. All CDs examined demonstrated a significant enhancement of TNT degradation rates compared to identical conditions with no CDs present. Analysis of degradation products found both oxidative and reductive pathways to be present.

Introduction

Environmental Impact of TNT

The global production of TNT over the last century and its use in numerous armed conflicts has led to significant contamination of soils and groundwater in many locations. In the United States, the U.S. army reports that at least 1.2 million tons of soils at various facilities exceed the established remediation goal of 17.2

mg/kg of TNT in soils set by the U.S. Environmental Protection Agency (USEPA) for the Nebraska Ordnance Plant (NOP) (*1*, *2*). The NOP was one of a number of US Army ordnance plants to produce TNT and was the first ordnance facility to be listed under the USEPA's national priority listing (NPL), more commonly referred to as 'superfund' sites (*3*). The U.S. Agency for Toxic Substances and Disease Registry (ATSDR) lists 23 US Army munitions facilities responsible for TNT production and storage with TNT contamination (*4*).

In addition to production and storage facilities, numerous training and live-fire ranges have considerable levels of TNT contamination from low-order (incomplete) detonations and unexploded ordinances (UXOs) (*5*, *6*). A recent study of 23 live fire ranges in the United States and Canada found widespread contamination of soils by TNT and other energetic materials and these 23 sites represent only a fraction of the total number of live-fire ranges operated by the United States and Canada (*2*). In total, the United States Department of Defense (USDOD) has identified over 1000 sites with significant levels of contamination by explosives . Significant levels of TNT contamination from low-order detonations, and UXOs can also be expected in areas of the world which have suffered from serious armed conflict over the last several decades, such as many parts of the Middle East, Africa, and South Asia.

Another potentially serious problem with UXO contamination in many parts of the world is the uptake of TNT and its metabolites by both domestic crops and wild plants in contaminated soils (*7*). Uptake of TNT and its metabolites by plants can have a broad-ranging impact on agriculture through direct ingestion of food crops by humans and through livestock exposure in feed produced from contaminated grains and grasses. In addition to the impact on humans and domesticated animals, TNT poses a threat to wildlife feeding on contaminated crops and plants.

Contamination of soils by TNT can pose a threat to groundwater and serious concerns exist about the movement of TNT and its various metabolites into the water table, and ultimately, into drinking water supplies. The USEPA has established a limit of 2 µg/L of TNT in residential water supplies, based on lifetime risk factor for chronic oral dosing (*8*). Other studies have recommended even lower levels, in the 0.1-0.2 µg/L range, based on extrapolated risk from no-observed-effect levels/lowest-observed-adverse-effect levels (NOAELs / LOAELs) in a number of animal studies (*9*). Of the sites identified by the USDOD as having significant levels of explosives contamination, over 95% of the sites contained TNT above permissible levels in soil and 87% contained TNT levels above permissible levels in groundwater (*10–14*).

The fate of TNT varies greatly between contaminated soils, groundwater and surface waters. TNT has very low water solubility (approximately 80 mg/L at 25 ºC), though migration of TNT into groundwater can occur and is highly dependent on soil and groundwater conditions, pH, organic content of the soils, the presence or lack of nitro reducing bacterium, as well as the concentration of TNT in the soils (*15*). In surface waters, TNT can undergo photolytic reduction to yield a variety compounds. The rate of the photolytic reduction is heavily dependent on the biological content of the water as well as the water chemistry (*10*, *13*, *16*). In general, contamination of soils by TNT is considered to pose the most significant

threat due to its recalcitrance and potential for migration into groundwater and remediation efforts have focused heavily on soils.

A number of studies have examined the fate of TNT in soil and groundwater through either direct analysis of the materials present at contaminated sites or through lab-scale studies modeling different site conditions. Under most conditions, transformation of TNT occurs slowly and typically proceeds along a reductive pathway, yielding amino substituted and azoxy products. The reductive pathway typically occurs due to the presence of nitrogen reducing bacteria or fungi in the soils or through the presence of iron containing minerals (*17*).

Remediation of TNT by Fenton Chemistry

In recent years, remediation using advanced oxidative processes (AOPs) have received a great deal of interest as an effective means to treat systems containing oxidizable pollutants, such as TNT. AOPs consist of a variety of different techniques capable of generating radical species which act as the oxidant in these systems. These processes have shown application for the remediation of pollutants in a variety of matrices and many of the methods can be performed in-situ. Of the AOPs studied for application in environmental remediation, Fenton chemistry and closely associated methods such as photo-Fenton and Fenton-like reactions have garnered interest due to the low cost, availability and safety of needed reagents and the strength of the oxidizing agent, the hydroxyl radical, that is produced (*18*).

Fenton chemistry uses a mixture of Fe^{2+} and hydrogen peroxide (H_2O_2) to generate hydroxyl radicals ($\cdot OH$) which are capable of reacting at or near diffusion controlled rates (10^8-10^{10} M^{-1} s^{-1}) with both organic and inorganic oxidizable species (*19*). The generated $\cdot OH$ is an extremely powerful oxidant, second only to fluorine, with an oxidation potential of approximately 2.8 V versus a normal hydrogen electrode (NHE) at pH 7.0 (*20*). The first description of the use of Fe^{2+} and H_2O_2 to create an oxidizing environment was reported by Henry J. Fenton in 1894, when he noted that a solution of ferrous salts and H_2O_2 could be utilized to oxidize tartaric acid (*21*). The mechanism underlying the Fenton reaction was given by Haber and Weiss in 1934 when they proposed that the active oxidant species in the reaction was $\cdot OH$ (*22–24*). Barb et al. further expanded the mechanism leading to $\cdot OH$ generation in a series of papers in which they proposed a 7 step sequence of reactions (*17*):

$$Fe^{2+} + H_2O_2 \rightarrow Fe^{3+} + OH^- + \cdot OH \quad (1.1)$$

$$Fe^{3+} + H_2O_2 \rightarrow Fe^{2+} + \cdot O_2H + H^+ \quad (1.2)$$

$$\cdot OH + H_2O_2 \rightarrow \cdot O_2H + H_2O \quad (1.3)$$

$$\cdot OH + Fe^{2+} \rightarrow Fe^{3+} + OH^- \quad (1.4)$$

$$Fe^{3+} + \cdot O_2H \rightarrow Fe^{2+} + O_2H^+ \quad (1.5)$$

$$Fe^{2+} + \cdot O_2H + H^+ \rightarrow Fe^{3+} + H_2O_2 \quad (1.6)$$

$$\cdot O_2H + \cdot O_2H \rightarrow H_2O_2 + O_2 \quad (1.7)$$

Equations 1.1 through 1.7 have been extensively examined since first being proposed and are well understood and accepted for systems in which no other redox species or strongly coordinating ligands are present (*25–27*).

Overall, reactions 1.1 through 1.7 sum to yield:

$$2\ H_2O_2 \rightarrow O_2 + H_2O \quad (1.8)$$

As can be readily seen through the summed reactions of the Fenton system, the end products of the reaction are benign. In addition to O_2 and H_2O produced, $Fe^{2+/3+}$ is typically converted to ferrous iron hydroxides which will precipitate from the reaction medium unless the matrix is acidified.

A number of studies have examined the Fenton oxidation of TNT in aqueous waste streams and lab-scale ex-situ treatment of aqueous systems obtained through soil flushing (*28*). More recently, Ayoub and co-workers wrote a review of the application of AOP processes for removal of TNT from contaminated soils and waters (*29*). Their review included a number of other AOPs in addition to Fenton chemistry which have been examined for TNT remediation. Overall, studies have found that complete mineralization of TNT is possible under certain conditions of pH and low total organic content (TOC) for aqueous wastes. The complete removal of TNT from soils has proven significantly more problematic for a number of reasons. Firstly, the hydroxyl radical is an aggressive and non-selective oxidant. In matrices with a high TOC, scavenging of the hydroxyl radical occurs through interactions with other components of the matrix besides the target compound (*17*). This is particularly problematic in most soils, but can also be a significant hurdle to overcome in heavily contaminated water. Additionally, the Fenton reaction requires conditions of low pH, 3.0-3.5, to be most effective (*30*). This is often difficult or impractical to achieve for in-situ remediation of soils and many water systems.

Due to the aggressive and non-selective nature of the hydroxyl radical oxidant generated in the Fenton reaction, numerous reaction products are commonly observed for target pollutants. The toxicity of nitroaromatic compounds generally decreases as the degree of nitration decreases (*31*). However, mobility of the degradation products may be increased, leading to the possibility of broader exposure if products enter the water table. Therefore, a comprehensive understanding of the reaction products occurring from the application of Fenton and other AOP reaction systems is required in order to assure that the generated waste products pose less of an environmental and health threat than the target compound being treated.

The oxidation products of TNT in a pure aqueous Fenton reaction system have been studied and described by Hess and coworkers (*25*, *32*, *33*). The initial oxidative pathway they proposed consisted of either direct oxidation of TNT to trinitrobenzene (TNB) followed by subsequent conversion to a TNB-hydroperoxyl radical intermediate or conversion of TNT to TNT-hydroperoxyl radical

intermediate. The proposed TNB-hydroperoxyl and TNT-hydroperoxyl radical intermediates then undergo denitration to form 3,5-dinitrophenol (3,5-DNP) or 4,6-dinitro-*o*-cresol (4,6-DNC) and 3,5-dinitrophenyl-methylene-1-one (3,5-DNPMO), respectively. Following these steps, a series of successive denitrations leads to 1,3,5-trihydroxybenzene and eventual mineralization.

Use of Cyclodextrins in Fenton Chemistry

Past studies by our research group and others have demonstrated the ability of cyclodextrins to increase the efficiency of Fenton degradation of aromatic pollutant species (*34*). Cyclodextrins (CDs) are cyclic oligosaccharides typically composed of 6, 7, or 8 α-D-glucopyranose units joined through an α-1,4 glycosidic bond and are referred to as α-, β-, and γ-cyclodextrins, respectively. CDs are water soluble, yet the annulus of the ring provides a hydrophobic environment, giving CDs their ability to complex small non-polar molecules in aqueous enviroments. CDs are non-toxic, environmentally benign, inexpensive to produce and commercially available, and can be synthetically tailored with a variety of different functional groups attached to the CD ring. They are widely used in industrial, pharmaceutical, food, agricultural and environmental applications. For application in the Fenton reaction of TNT, the increase in degradation efficiency observed in reaction systems has been credited to the formation of a pollutant/CD/Fe^{2+} ternary complexes which have the ability to produce hydroxyl radicals at the site of bound Fe^{2+} during Fenton reactions (*30*). This results in an increase in hydroxyl radical concentration near the target guest molecule relative to the bulk solution, leading to a targeted degradation of the complexed guest molecule.

While the reaction products of TNT in an aqueous Fenton reaction have been well described by Hess and co-workers, no comprehensive studies of the impact of CDs on the product distribution have been undertaken. In order to assess the viability of CD assisted Fenton reactions for the remediation of TNT, a thorough knowledge of these degradation products is required in order to assess both their toxicity and potential for mobility in soils.

Current Study

This current study examined: 1) the kinetics of TNT degradation in CD ternary complexes for a Fenton reaction system, and 2) the products of these reactions through chromatographic (HPLC-UV-Vis) and mass spectrometric (ESI-MS/MS and FTICR-MS) methods. The CDs used in the study include two commercially available CDs, β-cyclodextrin (βCD) and carboxymethyl-β-cyclodextrin (cmβCD), and two synthetic CDs containing a metal chelating group, 6^A-[bis(carboxymethyl)amino]-6^A-β-cyclodextrin (6βCDidaH$_2$) and 6^A-[tri(carboxymethyl)(2-aminoethyl)amino-6^A-deoxy-β-cyclodextrin (6βCDedtaH$_3$) (Figure 1). The application of 6βCDidaH$_2$ and 6βCDedtaH$_3$ in the current study was chosen due to the ability of these CDs to effectively chelate Fe^{2+} at neutral pH. Control reactions conducted in pure water

and in the presence of d-glucose and ethylenediaminetraacetic acid (EDTA) were also conducted.

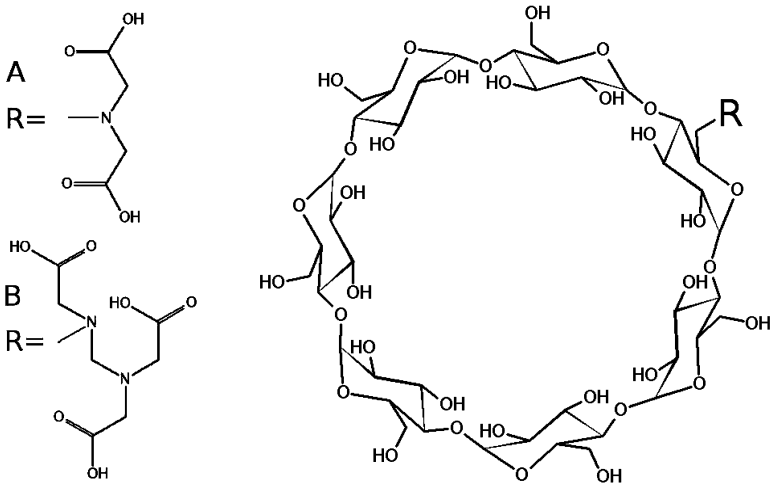

Figure 1. Structure of 6βCDidaH$_2$ (A) and 6βCDedtaH$_3$ (B).

Materials and Methods

Kinetics Studies

Fenton reactions of TNT were conducted by preparing 10 mL aqueous solutions of 0.1 mM TNT, 1 mM CD, and 5 mM $FeSO_4$•$7H_2O$, pH adjusted by addition of H_2SO_4 for reactions run under acidic conditions. Control experiments replacing the CD with either 1 mM EDTA or differing concentrations of d-glucose were also conducted. Reaction solutions were added to a round bottom flask with continuous magnetic stirring. Addition of H_2O_2 was accomplished via syringe pump using a 150 mM aqueous solution added at a flow rate of 2 mL/h for the TNT systems. Sampling of the reaction was accomplished by removing a 300 µL aliquot of the reaction mixture and adding it to a sample vial containing 300 µL of 1% v:v 1-propanol in water (kinetics studies) or 300 µL of methanol (ESI-MS/MS studies) to quench the Fenton reaction through hydroxyl radical scavenging by the alcohol. Aliquots were removed at 2 minute intervals for a total of 10 minutes for each reaction. Samples were centrifuged and filtered through 0.22 µm syringe filters prior to analysis.

The concentration of TNT in the reaction mixtures was measured by HPLC on a Hewlett-Packard Agilent 1100 HPLC with a diode array absorbance detector. An Alltech Econosphere C18, 150 x 4.6 mm i.d., (5 µm particle size) reversed phase column was used for separation. The mobile phase gradient for TNT analysis consisted of 30:70 ACN:water, isocratic from 0 to 3 minutes followed by a linear

gradient from 3 to 13 minutes to 100% ACN and holding at 100% ACN until all analytes had eluted. Quantitation of TNT was carried out based on absorbance at 230 nm.

Determination of Products

Degradation products of TNT were initially identified by HPLC-UV-Vis by comparison of retention times and UV absorbance spectra of known compounds. A searchable spectral library of potential degradation products was constructed in Hewlett-Packard Chemstation Software through injection of single component standards with monitoring from 200-400 nm. Mass spectrometric analysis of the products was done by electrospray mass spectrometry using an Applied Biosystems 3200 Q Trap LC/MS/MS and a Bruker Apex II 7.0 T Fourier transform ion cyclotron resonance mass spectrometer with direct sample introduction into the electrospray ionization source of the mass spectrometer. Samples were introduced to the electrospray source at 10 μL/min flow rate by syringe pump. Ionization was conducted in both positive and negative mode.

Results

All of the cyclodextrin systems used in this study demonstrated a significant increase in rates of TNT degradation by Fenton reaction at both pH 3.1 and without pH adjustment (Table 1). A small increase in the reaction rate was also observed with the addition of 7 mM d-glucose to the Fenton reaction, though TNT reaction rates were suppressed by the addition of either 1 mM d-glucose or 1 mM EDTA to the system. Initial mechanistic studies using HPLC-UV-vis with spectral and retenetion time macting found TNB to be to the major component observed for reactions conducted without the presence of CDs or glucose. No additional products were identified for these reactions. In the presence of CDs and glucose a second major product, 4-amino-2,6-dinitrotoluene, was identified. This product has not been previously observed in Fenton reactions of TNT and is indicative that a reductive pathway for TNT degradation exists in addition to the oxidative pathway for systems with dextrins present.

ESI-MS/MS analysis of the TNT Fenton reaction systems revealed a number of products not observed in the HPLC-UV-Vis study. All the systems studied showed trinitrobenzene as a primary degradation product. For the TNT Fenton reaction in water, 4,6-DNC, 3,5-DNMPO and 3,5-DNP, and dinitrobenzoic acid (DNBA) were observed in addition to TNB. These results are in agreement with the previous study by Hess and co-workers, with the exception of the finding of DNBA. Reactions conducted with 6βCDidaH$_2$ and 6βCDedtaH$_3$ had an additional product, 2,4,6-trinitrobenzyl alcohol (2,4,6-TNBOH), which was not observed for the reactions conducted with βCD and cmβCD. A number of unidentified products were also observed in the TNT/CD reaction systems with several products being common to all TNT/CD reaction systems.

Table 1. Measured pseudo first order rate constants for TNT degradation during Fenton reactions in the presence of cyclodextrins, D-glucose, and EDTA. Relative rate constants (k/k_o) were obtained by normalizing to the rate constant observed for reaction in water with no additives (k_o)

	Enhancement over pure water (k/k_o), pH 3.1	*Enhancement over pure water (k/k_o), no pH adjustment*
6βCDidaH$_2$ (1 mM)	2.0 ± 0.2	1.4 ± 0.1
6βCDedtaH$_3$ (1 mM)	1.4 ± 0.2	ND[a]
cmβCD (1 mM)	3.8 ± 0.5	4.1 ± 0.6
βCD (1 mM)	7.0 ± 2.0	5.1 ± 0.9
D-glucose (1 mM)	ND[a]	0.51 ± 0.06
D-glucose (7 mM)	ND[a]	1.3 ± 0.1
EDTA (1 mM)	ND[a]	0.27 ± 0.04

[a] Not determined.

FTICR-MS analysis of the CD assisted Fenton reactions yielded further evidence of reductive products. Peaks observed at m/z of 210.0166 and 195.9987 correspond to molecular ion formulas of $C_7H_4N_3O_5$ and $C_6H_2N_3O_5$, respectively. Ions at these m/z values were observed in a number of the CD assisted Fenton reaction samples analyzed by ESI-MS/MS but had not been positively identified, with exception of m/z 196 corresponding to ADNT in some reaction systems. The proposed structures for these molecular ions are [nitrosodinitrotoluene-H]$^-$ and [nitrosodinitrobenzene-H]$^-$, respectively. These reductive products were observed in all of the CD assisted Fenton reaction systems examined but were not observed in the control reactions. The presence of 2,4,6-TNBOH in the 6βCDidaH$_2$ and 6βCDedtaH$_3$ and assisted Fenton reactions was confirmed by the presence of an ion at m/z 242.00387 corresponding to $C_7H_4N_3O_7$. A potential oxidation product of 2,4,6-TNBOH was observed at m/z 213.10643 corresponding to $C_7H_5N_2O_6$ is assumed to occur via denitration to yield [hydroxydinitrobenzyl alcohol-H]$^-$.

Conclusions

The results of the kinetic studies clearly demonstrate the ability of some CDs to enhance degradation rates of TNT during Fenton reactions. All CD assisted reactions exhibit a significant enhancement of TNT reaction rates relative to controls without CDs. The initial mechanistic studies demonstrated the existence of both an oxidative and reductive pathway as indicated by the presence of both TNB and 4-ADNT in the CD and d-glucose containing reactions. The higher TNT degradation rates observed in the presence of CDs, compared to d-glucose, likely occur due to pre-association of TNT with the secondary CD radicals formed during the Fenton reaction. Therefore, increased degradation rates of TNT in the presence of CDs is likely due to a combination of: (i) formation of

ternary TNT-CD-Fe^{2+} complexes which facilitate (ii) an increase in localized concentration of hydroxyl radicals near complexed TNT relative to the bulk solution and (iii) efficient formation of secondary CD radicals that effectively reduce the complexed TNT.

The analysis of reaction products by ESI-MS/MS and FTICR-MS showed the presence of a number of both oxidative and reductive products formed during the Fenton reaction. A number of these products, such as 2,4,6-trinitrobenzyl alcohol, hydroxydinitrobenzyl alcohol, 4-ADNT, nitrosodinitroluene, and nitrosodinitrobenzene have not been previously observed in Fenton reactions of TNT. The reductive products generated have a lower toxicity than the trinitro precursors, TNT and TNB (*35*). However, they also have an increased water solubility which would increase mobility in soils with a low TOC. In high TOC soils, the amine functionalities have been shown to bind irreversibly to quinone and other carbonyl groups in the humic fraction of these soils . Therefore, while CD assisted Fenton reactions can significantly increase the kinetics of nitroaromatic degradation compared to typical Fenton systems, they also increase the complexity of the product distribution. The increased complexity of the product distribution, due to the presence of both an oxidative and reductive pathway, must be carefully evaluated before using CD assisted Fenton reactions as a remediation technology.

References

1. Lewis, T.; Newcombe, D.; Crawfold, R. Bioremediation of soils contaminated with explosives. *J. Environ.l Manage.* **2004**, *70*, 291–307.
2. Liou, M. J.; Lu, M. C.; Chen, J. N. Oxidation of TNT by photo-Fenton process. *Chemosphere* **2004**, *57* (9), 1107–1114.
3. USEPA. *Former Nebraska Ordnance Plant* [cited]. Available from: http://www.epa.gov/region7/cleanup/npl_files/ne6211890011.pdf, 2009.
4. ATSDR. *Toxicological Profile of 2,4,6-Trinitrotoluene*; ATSDR, Ed.; U.S. Department of Health and Human Services: 1995.
5. Walsh, M. E.; Ramsey, C. A.; Jenkins, T. F. The effect of particle size reduction by grinding on subsampling variance for explosives residues in soil. *Chemosphere* **2002**, *49* (10), 1267–1273.
6. Bordeleau, G.; et al. Environmental Impacts of Training Activities at an Air Weapons Range. *J. Environ. Qual.* **2008**, *37* (2), 308–317.
7. USEPA. *Integrated Risk Information System (IRIS) - 2,4,6-Trinitrotoluene*; [cited]. Available from: http://www.epa.gov/iris/subst/0269.htm, 2002.
8. Wollin, K. M.; Dieter, H. H. Toxicological Guidelines for Monocyclic Nitro-, Amino- and Aminonitroaromatics, Nitramines, and Nitrate Esters in Drinking Water. *Arch. Environ. Contam. Toxicol.* **2005**, *49* (1), 18–26.
9. Rogers, J. D.; Bunce, N. J. Treatment methods for the remediation of nitro aromatic explosives (Review). *Water Res.* **2001**, *35*, 2101–2111.
10. Achtnich, C.; et al. Stability of Immobilized TNT Derivatives in Soil as a Function of Nitro Group Reduction. *Environ. Sci. Technol.* **2000**, *34* (17), 3698–3704.

11. Achtnich, C.; et al. Reductive Transformation of Bound Trinitrophenyl Residues and Free TNT during a Bioremediation Process Analyzed by Immunoassay. *Environ. Sci. Technol.* **1999**, *33* (19), 3421–3426.
12. Ro, K. S.; et al. Solubility of 2,4,6-Trinitrotoluene (TNT) in Water. *J. Chem. Eng. Data* **1996**, *41*, 758–761.
13. Weis, M.; et al. Fate and Metabolism of [15N]2,4,6-Trinitrotoluene In Soil. *Environ. Toxicol. Chem.* **2004**, *23* (8), 1852–1860.
14. Eriksson, J.; et al. Binding of 2,4,6-Trinitrotoluene, Aniline, and Nitrobenzene to Dissolved and Particulate Soil Organic Matter. *Environ. Sci. Technol.* **2004**, *38* (11), 3074–3080.
15. Douglas, T. A.; et al. A time series investigation of the stability of nitramine and nitroaromatic explosives in surface water samples at ambient temperature. *Chemosphere* **2009**, *76* (1), 1–8.
16. Bandstra, J. Z.; et al. Reduction of 2,4,6-Trinitrotoluene by Iron Metal: Kinetic Controls on Product Distributions in Batch Experiments. *Environ. Sci. Technol.* **2005**, *39* (1), 230–238.
17. Pignatello, J. J.; Oliveros, E.; MacKay, A. Advanced oxidation processes for organic contaminant destruction based on the Fenton reaction and related chemistry. *Crit. Rev. Environ. Sci. Technol.* **2006**, *36* (1), 1–84.
18. Morelli, R.; et al. Fenton-Dependent Damage to Carbohydrates: Free Radical Scavenging Activity of Some Simple Sugars. *J. Agric. Food Chem.* **2003**, *51* (25), 7418–7425.
19. Kavitha, V.; Palanivelu, K. The role of ferrous ion in Fenton and photo-Fenton processes for the degradation of phenol. *Chemosphere* **2004**, *55* (9), 1235–1243.
20. Fenton, H. J. H. Oxidation of tartaric acid in the presence of iron. *J. Chem. Soc.* **1894**, *65*, 899–910.
21. Haber, F.; Weiss, J. The catalytic decomposition of of hydrogen peroxide by iron salts. *Proc. R. Soc., A* **1934**, *134*, 332–351.
22. Barb, W. G.; Baxendale, J. H.; George, P. Reactions of ferrous and ferric ions with hydrogen peroxide. *Nature* **1949**, *163*, 692–694.
23. Barb, W. G.; et al. Reactions of ferrous and ferric ions with hydrogen peroxide. Part I.- The ferrous reaction. *Trans. Faraday Soc.* **1951**, *47*, 462–500.
24. Barb, W. G.; et al. Reaction of ferrous and ferric ions with hydrogen peroxide. Part II.- The ferric ion reaction. *Trans. Faraday Soc.* **1951**, *47*, 591–616.
25. Murati, M.; et al. Electro-Fenton Treatment of TNT in Aqueous Media in Presence of Cyclodextrin. Application to Ex-situ Treatment of Contaminated Soil. *J. Adv. Oxid. Technol.* **2009**, *12* (1), 29–36.
26. Chen, W.-S.; Juan, C.-N.; Wei, K.-M. Mineralization of dinitrotoluenes and trinitrotoluene of spent acid in toluene nitration process by Fenton oxidation. *Chemosphere* **2005**, *60* (8), 1072–1079.
27. Li, Z. M.; Comfort, S. D.; Shea, P. J. Destruction of 2,4,6-Trinitrotoluene by Fenton Oxidation. *J. Environ. Qual.* **1997**, *26* (2), 480–487.
28. Ayoub, K.; et al. Application of advanced oxidation processes for TNT removal: A review. *J. Hazardous Mater.* **2010**, *178* (13), 10–28.

29. Goi, A.; Kulik, N.; Trapido, M. Combined chemical and biological treatment of oil contaminated soil. *Chemosphere* **2006**, *63* (10), 1754–1763.
30. Neuwoehner, J.; et al. Toxicological Characterization of 2,4,6-Trinitrotoluene, its Transformation Products, And Two Nitramine Explosives. *Environ. Toxicol. Chem.* **2007**, *26* (6), 1090–1099.
31. Hess, T.; et al. Studies on nitroaromatic compound degradation in modified Fenton reactions by electrospray ionization tandem mass spectrometry (ESI-MS-MS). *The Analyst* **2003**, *128*, 156–160.
32. Yardin, G.; Chiron, S. Photo-Fenton treatment of TNT contaminated soil extract solutions obtained by soil flushing with cyclodextrin. *Chemosphere* **2006**, *62*, 1395–1402.
33. Lindsey, M. E.; et al. Enhanced Fenton degradation of hydrophobic organics by simultaneous iron and pollutent complexation with cyclodextrins. *Sci. Total Environ.* **2002**, *307* (1−3), 215–229.
34. Zheng, W.; Tarr, M. A. Evidence for the Existence of Ternary Complexes of Iron, Cyclodextrin, and Hydrophobic Guests in Aqueous Solution. *J. Phys. Chem. B* **2004**, *108*, 10172–10176.
35. Thorn, K. A.; Kennedy, K. R. 15N NMR Investigation of the Covalent Binding of Reduced TNT Amines to Soil Humic Acid, Model Compounds, and Lignocellulose. *Environ. Sci. Technol.* **2002**, *36* (17), 3787–3796.

Chapter 18

Potential Anaerobic Bioremediation of Perchlorate-Contaminated Soils through Biosolids Applications

Cynthia L. Price,[1,*]* Mark A. Chappell,[1] Brad A. Pettway,[2] and Beth E. Porter[2]

[1]U.S. Army Engineer Research and Development Center, (ERDC), 3909 Halls Ferry Road, Vicksburg, MS 39180
[2]SpecPro, Inc., 4815 Bradford Drive, Huntsville, AL 35805
***Cynthia.L.Price@usace.army.mil**

The enzyme-mediated degradation of perchlorate has been show to occur by the following pathway; perchlorate to chlorate to chlorite to chloride. The typically low sorptive retention promotes the traditional view that perchlorate degradation is strictly a solution phase, biotic phenomenon. Yet, little is known about the potential interaction chemistry of perchlorate with the soil surface. For this study we incubated an Fe-rich soil at 30% moisture. Replicates were sacrificed with time and extracted with dilute sodium nitrate. Results show that perchlorate was significantly reduced over the 10-week incubation period and was accompanied by increase in chloride concentrations. No perchlorate decrease was seen in controls that contained no biosolids, indicating perchlorate removal in the treated soils may be attributed to biodegradation.

Background

Ammonium and potassium perchlorate are classical oxidizers used in solid rocket propellants. They are also used in pyrotechnics, fuses, spotting charges, and some explosive munitions, as well as in non-military applications. Perchlorate has been detected in groundwater throughout the Unites States and extensive contamination by perchlorate was observed on military installations (*1*, *2*). Contamination on Massachusetts Military Reservation has been exhaustively

studied since 1997, showing that perchlorate was the most commonly found military-related compound in ground water and the second most common in soil. Concentrations in soils were as high as 7560 μg kg^{-1}, with mean detected concentration of 431 μg kg^{-1}, while for ground water, the highest and mean concentrations were 500 μg L^{-1} and 6.7 μg L^{-1}, respectively.

Perchlorate has been shown to cause toxicity in humans due to iodide uptake inhibition in the thyroid (*3*, *4*). United States EPA established Drinking Water Equivalent Level (concentration of a contaminant in drinking water that will have no adverse effect) of 24.5 μg L^{-1}. Perchlorates are highly soluble salts with reported aqueous solubilities of 200-220 g L^{-1} for ammonium perchlorate and 7.5-16.8 g L^{-1} for potassium perchlorate (*5*–*7*). Dissolution of perchlorate salts yields the perchlorate anion (ClO_4^-). Given the predominantly negative character of most soil's permanent charge, perchlorate is expected to undergo repulsive interactions with negatively charged sorption sites, typically moving at the head of the solute front (*8*). Anion exclusion processes can result in solute retardation factors of < 1 for anions in soils.

While anion exclusion processes are common in higher-charged soils, such as those in temperate regions of the U.S., perchlorate has been shown to be retained in the soils developed under intensive weathering conditions prevalent in many tropical or subtropical climates (*9*). Typically, soils developed under these climates are dominated by kaolinitic clay mineralogy and contain relatively high levels of Fe-, Mn-, and Al-oxides. Total soil charge in these systems is substantially less than soils in more temperate areas, yet, the source of the charge is highly pH dependent, meaning that in particularly acid soils, the surface can reverse charge and develop significant net positive charge. This positive charge gives rise to what is known as Anion Exchange Capacity (AEC), which is an empirical parameter describing the soil's potential to adsorb anions like perchlorate. Presence of a significant AEC can notably alter perchlorate's mobility through soil.

While perchlorate is believed to move quickly through the soil with flowing water, perhaps by way of macropores, the bulk soils rarely achieve full saturation. During unsaturated conditions only the smallest pores participate in transport and thus, advection can be greatly slowed. In this situation, perchlorate residence time increases, enhancing opportunities for close-range interactions with the soil mineral surfaces.

Several strains of facultative anaerobic bacteria capable of reducing perchlorate have been isolated from soil, water, and other environmental samples (*10*, *11*). By serving as an electron acceptor to enzymatic systems, perchlorate may potentially be reduced to chloride (Cl^-) through a number of intermediate steps (*12*):

$$\underset{\text{perchlorate}}{ClO_4^-} \rightarrow \underset{\text{chlorate}}{ClO_3^-} \rightarrow \underset{\text{chlorite}}{ClO_2^-} \rightarrow \underset{\text{chloride}}{Cl^-} + O_2$$

Thus, perchlorate reduction kinetics is linked to the presence of microbial populations capable of reducing perchlorate (*13*) and the residence time of the solute in the soil (which depends on soil water content and CEC).

Perchlorate reduction also varies depending on the presence of solutes requiring less energy (lower activation energy) to act as an electron acceptor. One important example is the nitrate anion (NO_3^-). Nitrate is a common anion in soil typically produced by nitrifying enzymatic reactions oxidizing ammonium salts and ammonium-containing biological residues. The lower activation energy of nitrate has been shown to act as a competitor to biotic perchlorate reduction (*13*). However, perchlorate reduction can be readily stimulated by the addition of acetate or lactate, so that nitrate and perchlorate appear to be reduced simultaneously (*13–15*).

However, the possibility exists that perchlorate could be readily reduced by abiotic mechanisms to Cl in soils through coupling to the Fe (II)/(II) redox system. A mechanism of this kind would potentially exhibit much faster kinetics than that conducted by enzymatic means, particularly under water-unsaturated soil conditions. If evidence for this behavior can be demonstrated, then it would represent an important piece of information for consideration in predicting perchlorate environmental fate.

Similar to denitrification, perchlorate bioreduction requires a locally reductive environment and a source of carbon. Typically, reductive conditions in soil are obtained under water-saturated conditions or deep within the soil profile (far from the surface given that gas diffusion is limited in the soil profile). Yet, in the former, water saturating conditions promote perchlorate dissolution and movement in the soil, while in the latter, soil horizons deep within the profile are typically limited in organic carbon. Microanaerobic zones do occur within the soil rhizosphere, but this would require penetration of the perchlorate into the root zones, resulting in potential toxic effects. The alternative to such approaches is to apply an amendment that will induce reductive or anaerobic conditions in soil without promoting perchlorate movement. Ideally, the amendment should be in a solid form yet should be rich in carbon for promoting heterotrophic activity. Also, practical considerations require the amendment to be obtained locally and inexpensively, easily applied, and require minimal management. For this we propose the use of waste-water residuals (WWR) to promote the reductive degradation of perchlorate in soils.

WWR are organic carbon-rich solids obtained from the waste-water treatment process. During water treatment, suspended solids are removed through a combination of chemical flocculants and centrifugation. These residuals then undergo an extensive anaerobic digestion, which is designed to consume harmful chemicals and organics. The resultant high bacterial populations from the digestions provide extremely high organic carbon concentrations in biosolids, up to 30% of the total solids. The benefits of the high organic carbon and plant nutrients contained in biosolids have been realized in the agricultural sector for the last two decades. In addition, biosolids have been shown to be effective in immobilizing toxic metals such as Zn, Cd, and Pb due to their relatively high iron-oxide content (*16*).

The purpose of this chapter is to demonstrate the potential for this simple technology to be used as a field remediation strategy for soil perchlorate.

Methods

A Wahiawa silty clay (Very-fine, kaolinitic, isohyperthermic Rhodic Haplustox) soil was selected for this study. It was expected that the volcanic origin of the material (from Oahu, Hawai'i) would contain a considerable anion exchange capacity for potentially adsorbing the perchlorate anion. Selected physical and chemical characteristics are given in Table 1.

Table 1. Elemental composition and selected physical properties of the Wahiawa soil and Vicksburg biosolids material

Metals (Total Acid Digestion) mg/kg										
Al	*Ca*	*Cd*	*Cr*	*Fe*	*K*	*Mg*	*Mn*	*Na*	*Ni*	*Other*
53590	1303	18.98	251.2	116000	1320	1258	398	150.8	47.4	1854.2

Soil Type	*pH*	*CEC (meq/100g)*	*% Sand*	*% Silt*	*% Clay*	*Total Carbon %*
Silty clay	5.13	9.71	10	12	78	3.44

For these experiments, the Wahiawa soil was combined with a predigested biosolids sludge (Class B, collected at the Vicksburg Wastewater treatment plant) at a 1:1 mass ratio. Fifty-gram, mixture samples were placed in 250 ml polypropylene centrifuge tubes and perchlorate solution (~700 mg kg^{-1} in the form of potassium perchlorate) was added to the mixtures to adjust total sample moisture to 30 % total mass.mass. Centrifuge tubes were then loosely capped. Samples were prepared in triplicate and incubated undisturbed at 37^{o}C over a 10 week period. Additional sets of triplicate controls containing no biosolids were also incubated for the same time period. Samples were weighed over the sample period in order to adjust for evaporative moisture loss if needed.

After each week of incubation, triplicate sets of samples and controls were "sacrificed" and temperature and Eh were measured. Soils were extracted with 50 mL of 5 mM sodium nitrate, centrifuged, and filtered prior to analysis for perchlorate, chlorate, chlorite, chloride and nitrate using ion chromatography (*17*).

Results and Discussion

Figure 1 shows how chemically the system was modified both by the addition of biosolids and over the extended incubation time. The data show that the addition of biosolids resulted in increased pH and decreased Eh in the soil systems.

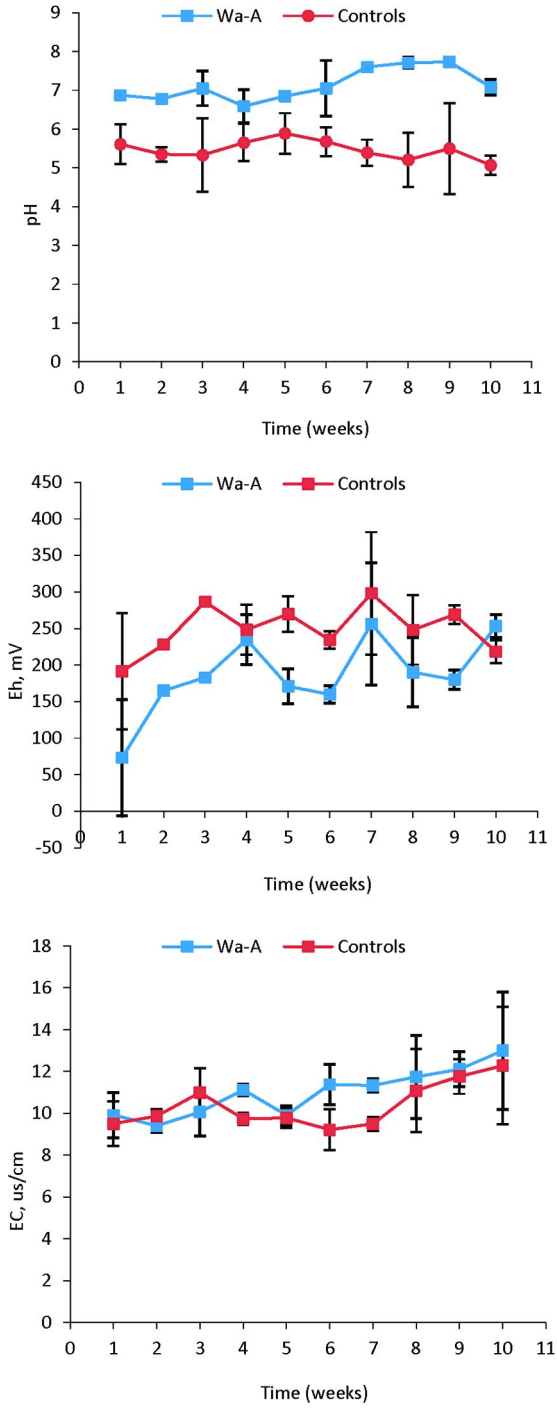

Figure 1. pH, Eh, and EC over time

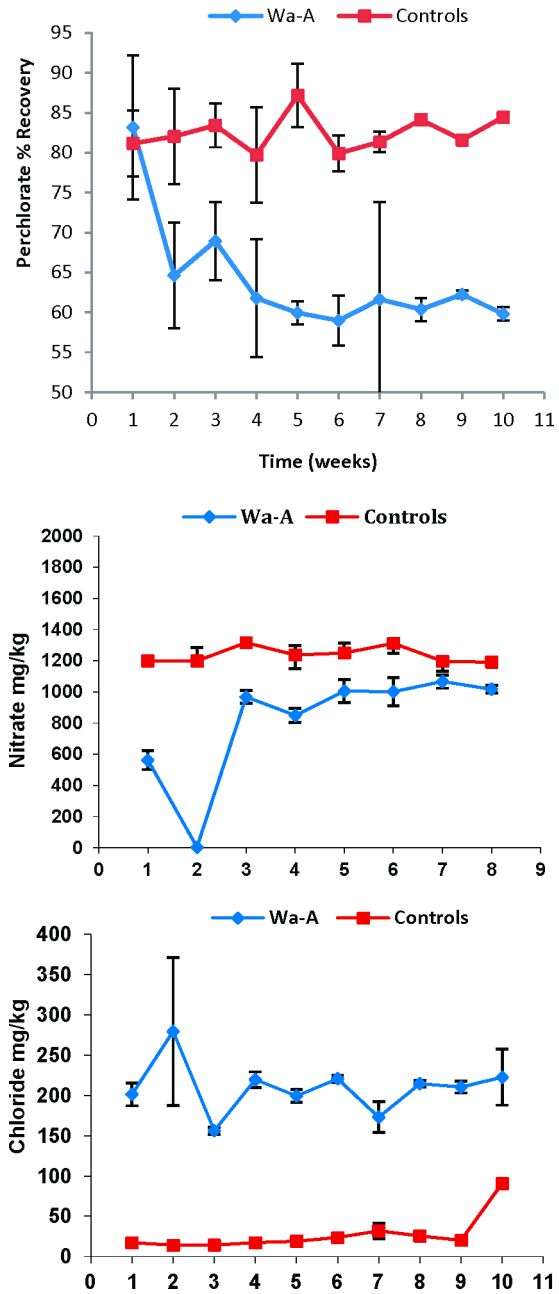

Figure 2. Perchlorate recovery (%) and chloride and nitrate concentrations with time as affected by the addition of biosolids.

Figure 2 shows the effect of biosolids and incubation times on the concentration of soil perchlorate. The data shows that soil perchlorate was significantly reduced over the 10-week period. Approximately 60% of the added perchlorate remained after 10 weeks of incubation for all three soils. In contrast, perchlorate recovery in the controls remained steady at approximately 80 %. The relative stability of the controls as compared to the treated soil suggests that perchlorate removal in the treated soils may be attributed to biodegradation.

Data show that the decrease in perchlorate over time was accompanied by a significant increase in chloride concentrations by week 10, suggesting *in-situ* degradation of the propellant. No evidence of the other intermediate products, chlorate and chlorite, were found. These intermediates would typically be seen when biological degradation is the driving force for the process. However, some reports have shown perchlorate reduction to chloride with no accumulation of intermediates (*10*, *12*) suggesting a very rapid kinetics of transformation.

Nitrate extracted from the soils increased over the 10 week time period with the addition of biosolids while nitrate concentration in the control soil (containing no biosolids) remained relatively stable over time at 1225 mg kg^{-1}. The presence of nitrate in soils has been show to inhibit or compete with perchlorate reduction by acting as an alternate electron acceptor (*11*, *18*, *19*). Others, however, have shown that perchlorate degradation was not inhibited by the presence of nitrate (*10*, *12*). Results show decreased redox conditions in the treated soils which may indicate that the increase in nitrate is a result of nitrification.

These investigations demonstrate that the addition of waste-water residuals to unsaturated soils can significantly influence the degradation of perchlorate. The results of this research have implications for cost-effective *in-situ* remediation of perchlorate in surface soils.

References

1. Clausen, J.; Robb, J.; Curry, D.; Korte, N. A case study of contaminants on military ranges: Camp Edwards, Massachusetts, USA. *Environ. Pollut.* **2004**, *129*, 13–21.
2. Pennington, J. C.; Jenkins, T. F.; et al. *Distribution and fate of energetics on DoD test and training ranges: Interim report 4*; U.S. Army Engineer Research & Development Center (ERDC): Vicksburg, MS, 2004.
3. Renner, R. Perchlorate rockets to US national attention. *J. Environ. Monit.* **1999**, 37–38.
4. Office of Environmental Health Hazard Assessment (OEHHA) of the California Environmental Protection Agency (EPA). *Public health goals for perchlorate in drinking water*; California EPA: Sacramento, CA, USA, 2004.
5. Grayson, M., Ed. *Kirk-Othmer concise encyclopedia of chemical technology*, 3rd ed.; John Wiley & Sons, Inc.: New York, 1985.
6. Ashford, R. D. Ashford's dictionary of industrial chemicals. *Wavelength*; London, 1994.

7. Motzer, W. E. Perchlorate: problems, detection, and solutions. *Environ. Forensics* **2001**, *2*, 301–311.
8. Nielsonand, D. R.; Biggar, J. W. Miscible displacement in soils: I. Experimental information. *Soil Sci. Soc. Proc.* **1961**, *25*, 1–5.
9. Ji, G.; Kong, X. Adsorption of chloride, nitrate, and perchlorate by variable charge soils. *Pedosphere* **1992**, *2*, 317–326.
10. Coates, J. D.; Michaelidou, U.; Bruce, R. A.; O'Connor, S. M.; Crespi, J. N.; Achenbach, L. A. Ubiquity and diversity of dissimilatory (per)chlorate-reducing bacteria. *Appl. Environ. Microbiol.* **1999**, *65*, 5234–5241.
11. Yu, X.; et al. Perchlorate Reduction by Autotrophic Bacteria Attached to Zerovalent Iron in a Flow-through Reactor. *Environ. Sci. Technol.* **2007**, *41*, 990–997.
12. Rikken, G. B.; Kroon, A. G. M.; van Ginkel, C. G. Transformation of (per)chlorate by a newly isolated bacterium: reduction and dismutation. *Appl. Microbiol. Biotechnol.* **1996**, *45*, 420–426.
13. Tipton, D. K.; Rolston, D. E.; Scow, K. M. Transport and biodegradation of perchlorate in soils. *J. Environ. Qual.* **2003**, *32*, 40–46.
14. Wu, J.; Unz, R. F.; Zhang, H.; Logan, B. E. Persistence of perchlorate and the relative numbers of perchlorate- and chlorate-respiring microorganisms in natural waters, soils, and wastewater. *Biorem. J.* **2001**, *5*, 119–130.
15. Schaefer, C. E.; Fuller, M. E.; Condee, C. W.; Lowey, J. M.; Hatzinger, P. B. Comparison of biotic and abiotic treatment approaches for co-mingled perchlorate, nitrate, and nitramine explosives in groundwater. *J. Contam. Hydrol.* **2007**, *89*, 231–250.
16. Hettiarchachchi, G. M.; Scheckel, K. G.; Ryan, J. A.; Sutton, S. R.; Newville, M. m-XANES and m-XRF investigations of metal binding mechanisms in biosolids. *J. Environ. Qual.* **2006**, *35*, 342–351.
17. US EPA. Method 314: Determination of perchlorate in drinking water using ion chromatography. *Test Methods for Evaluating Solid Waste, Physical/ Chemical Methods*; Office of Solid Waste and Emergency Response, SW-846: Washington, DC, 1999.
18. Gal, H.; Ronen, Z.; Weisbrod, N.; Dahan, O.; Nativ, R. Perchlorate biodegradation in contaminated soils and the deep unsaturated zone. *Soil Biol. Biochem.* **2008**, *40*, 1751–1757.
19. Tan, K.; et al. Degradation kinetics of perchlorate in sediments and soils. Water, Air, & Soil Pollution. *Water, Air, Soil Pollut.* **2004**, *151*, 245–259.

Chapter 19

Effects of Wildfire and Prescribed Burning on Distributed Particles of Composition-B Explosive on Training Ranges

Richard A. Price* **and Michelle Bourne**

U.S. Army Engineer Research and Development Center (ERDC), 3909 Halls Ferry Road, Vicksburg, MS 39180
***richard.a.price@usace.army.mil**

Residual ordnance compounds may exist on artillery training areas after low-order detonations. Particles of Composition-B (Comp-B) explosives distributed on training ranges could potentially be a source of RDX, TNT, HMX and their degradation products in various migration pathways such as leaching, surface runoff and biological exposure. Several studies have been conducted to identify toxicity and potential risks of munitions compounds to human and ecological receptors. However, little research has been conducted to quantify the effects of natural processes on the persistence of these and other materials used in military training activities. One such process is the occurrence of incidental or controlled burning of vegetation on training lands that theoretically could provide a remedial effect on residual Comp-B explosive on surface soils. Battelle Memorial Institute (under SERDP Work Unit CP-1305) evaluated effects of fire on subsurface concentrations of RDX and TNT in soil and found that under normal burn conditions on training ranges, thermal degradation did not occur a couple centimeters below the soil surface. This study evaluated the effects of fire on the fate of surface-distributed particulate Comp–B explosive that would result from low-order detonations on training ranges. Initial tests were conducted in a wind tunnel by placing pre-weighed 1 to 2-g particles of Comp-B explosive on the soil surface of vegetated test cells measuring 1.2 x 4.8 m. Vegetation was then

ignited and burned under various vegetation moisture and wind speed conditions. Loss of Comp-B particles was determined both by weight loss of recovered particles and chemical analysis of surface soil. Soil surface temperatures were measured at the soil surface and generally peaked at less than 176 deg C. Most Comp-B particles were easily ignited in the wind tunnel burns, and where complete ignition of particles occurred, chemical analysis confirmed residual Comp-B parent and degradation compounds were less than 3% of original mass. Plot-scale studies were conducted on unconfined 12 x 12 m plots following procedures describe above and confirmed wind tunnel results. Field evaluations were conducted during controlled burns at Forts McCoy, Pickett, Stewart, and Camp Shelby,and resulted in reductions ranging from 79-to 100%. Variations in vegetative biomass, moisture conditions, wind speeds, and other factors affected burn temperature and duration, ultimately controlling exposure of Comp-B particles to sufficient heat/spark for ignition. However, these tests verified that controlled or incidental burns can significantly remove residual Comp-B from training ranges, minimizing potential adverse impacts these materials can pose to the environment.

Introduction

The distribution and transport of munitions compounds on training lands for live-fire artillery training is a concern. Unexploded ordnance (UXO) or low-order detonations (LOD) can result in particles of explosive materials, particularly Composition-B explosive (Comp-B), being distributed within training area ecosystems (*1–3*). The primary components of Comp-B, 2,4,6-trinitrotoluene (TNT), hexahydro-1,3,5-trinitro-1,3,5-triazine (RDX), and octahydro-1,3,5,7-tetranitro-1,3,5,7-tetrazocine (HMX) may potentially migrate into groundwater and surface water. Dissolution rates have been described (*4*, *5*) for Comp-B, and aquatic toxicity studies (*6*, *7*) have shown aquatic toxicity and bioaccumulation of Comp-B constituents to aquatic organisms. While research has shown this potential to exist, widespread occurrences and adverse impacts on US Army training lands are not well documeneted. Simmers (*8*) found that while evidence of considerable UXO existed on an artillery training range at Fort McCoy, Wisconsin, sampling and analysis of sediments and surface waters did not detect any explosive residues. Several studies have evaluated plant uptake of RDX and TNT (*9–13*) demonstrating biotransformation of TNT in plant tissue and significant accumulation of RDX into leafy tissues. There are a number of factors potentially responsible for significant migration of Comp-B constituents in training areas that have not been thoroughly evaluated.

Wildfires are natural events that once were considered destructive to ecological habitats. We now know that many native plant ecosystems require occasional wildfires to sustain native plant communities while inhibiting the

establishment of adventive vegetation. Keane (*14*) summarizes the effects of large fires in various regional ecosystems where most benefit from occasional fires as both a possible tool for the efficient restoration of fire-dominated ecosystems and an effective treatment for reducing fuel hazards. Many resource agencies, including US Army Natural Resource Offices, have pro-active prescribed fire programs to manage natural diversity on public lands. Fires that occur on an artillery impact area (AIA), as a result of munitions detonation, are generally allowed to burn and are simply contained within the boundaries of the AIA.

The lack of interference has unintentionally resulted in high-quality native plant ecosystems on many U.S. Army training ranges, leading to establishment of critical habitat for many threatened and endangered species that appear to coexist with training activities. Fort Bragg, NC and Fort McCoy, WI are good examples of places where the existence of native plant ecosystems in artillery impact areas are sustained by incidental fires resulting from training activities.

However, the occurrence of distributed UXO and their explosive components in training land soils serve as potential sources for contaminant migration into ground and surface waters, as well as potential impacts in foodwebs. A study conducted by Simmers et al. (*15*) and numerous field evaluations (*16–19*) observed that frequent burning of the training range vegetation resulted in high quality native flora, and authors concluded that migration of explosive compounds to surface waters or wetland and aquatic sediments did not occur at active artillery training ranges where UXO was present and wildfires frequently occurred. It is theorized, that residual sources of Comp-B in artillery impact areas exist mainly as particle forms of Comp-B distributed on the soil surface during low order detonations and that these particles are subsequently ignited during the occurrence of wildfire. The significance of this theory is that the continual introduction of residual Comp-B from training activities is mitigated by the thermal effects of wildfire.

Comp-B is currently the most widely used explosive in the U.S. Army arsenal. These high explosive munitions are used in mortars, howitzers, and tanks on U.S. Army AIA. Comp-B is composed of approximately 59.9% RDX, 39.9% TNT, and 1% paraffin wax. In many cases, the percentages may vary and 1 to 7 % of HMX may exist as a byproduct of RDX production. The release of these compounds and their degradation products into the environment can have adverse effects on water quality, biota, and human health once these compounds migrate through groundwater, surface water and food chain pathways. A quantitative assessment of the fate of Comp-B during wildfire events was needed and is the basis of this study. This study evaluated the potential for thermal combustion of Comp-B particles and reduction in total mass of RDX, TNT and their transformation products to determine the efficacy of prescribed or incidental burning as an effective mitigation tool.

Materials and Methods

Bench-scale, plot-scale, and pilot-scale studies were conducted to address both controlled and field conditions. Comp-B was obtained as Hexolite, reclaimed military grade B from a demil facility in Indiana and used throughout the study.

Comp-B was obtained in a 2.5 lb cylindrical shape. It was necessary to reduce the cylinder of Comp-B into smaller pieces for use in the needed studies. Pennington et al. (*20*) suggested that for modeling purposes, particle size should range from >12.5 mm up to the diameter of the ordnance round. This was based on studies that indicated the majority of distributed particles from LOD were >12.5 mm.

The cylinders were determined to be brittle and capable of breakage by light impact. Each 2.5 lb cylinder was carefully tapped with a non-sparking hammer until cracks formed and large pieces were broken loose. These pieces were further reduced in size until all were less than 2.5 cm in diameter. Samples of the particles were submitted for chemical analysis by USEPA Method 8330 (*21*) to confirm the percentages of the parent compounds RDX, TNT and HMX.

Bench-Scale Tests

Weighed particles of Comp-B explosive were placed in a pre-weighed pan of soil and covered with increasing weights of wheat straw and pines needles. The vegetation fuel was ignited with a hand torch and allowed to burn freely. Combustion of particles was noted, and residual Comp-B residues in the soil following burning were determined by chemical analysis of the soil. Additional tests were conducted to determine effects of weathering on combustion of Comp-B when exposed to heat and flame. Comp-B particles were placed in an outdoor test facility and exposed to climatic conditions for a full year. These particles were compared to unweathered particles in a specially designed propane combustion column equipped with temperature probes to determine effects of temperature on melting and combustion of Comp-B particles.

Wind Tunnel Tests

These tests were conducted at the ERDC Big Black Test Site (BBTS) near Vicksburg, MS in a wind tunnel designed for this purpose. The purpose of these tests was to determine fate of Comp-B particles on a vegetated soil surface under different wind speeds and soil types. Soils were collected from near Camp Shelby, MS, Camp Bullis, TX, and Vicksburg, MS representing a sandy clay loam, clay, and loam classifications, respectively. Soils were placed in aluminum soil boxes each measuring 1.2 x 4.9 m and were seeded with *Schizachyrium scoparium*, a native perennial grass distributed over most of North America. After maturation and dormancy of the vegetated soils, 0.5, 1 and 2 g particles of Comp-B were placed at the soil surface, and the vegetation was burned under wind speeds of 1 and 4 mph and two plant moisture conditions (9 and 20%) to produce different burning characteristics (rate of spread, heat per unit area, fireline heat intensity). Temperature was monitored at the soil surface where Comp-B particles were placed and the fate of the particles (combustion, migration into the soil surface) was determined. Residual Comp-B was determined by weight loss of recoverable particles and chemical analysis of surface soil after each burn.

Plot-Scale Tests

Three replicate plots measuring 12 x 12 m were established at the BBTS on indigenous vegetation (primarily *Paspalum notatum*). After vegetation became dormant, pre-weighed particles (approximately 0.5 g each) of Comp-B was randomly placed at eight sample points within the plots. Each sample point was marked with a 40.6 cm length of 1.3 cm diameter steel rebar. Three replicate particles were placed in three 5.08 cm diameter x 2.54 cm high stainless steel rings driven into the soil flush with the soil surface. Temperature probes were placed at each of the eight sample locations, and soil surface temperatures were measured and recorded on a data logger. In order to measure flame height, two 2.4 meter lengths of 1.3 cm steel rebar were placed 1.8 m apart. A 15 cm diameter cotton string was tied between the two rebar at heights of 30 cm up to 150 cm. The plots were burned following established techniques (*22*) for prescribed burning to control excess vegetative fuel.

Burning occurred when climatic and fuel moisture conditions suitable for prescribed burning were present as determined by field measurements and as provided by the National Oceanic and Atmospheric Administration's (NOAA) Fire Weather Website. Following burning of *Paspalum notatum*, a second test was performed on pine straw purchased from a local nursery and placed on the plots at a rate of 1360Kg/ha to replicate a natural evergreen forest floor. After allowing for a 4 month period of weathering, the process above was repeated.

Field Tests

ERDC personnel coordinated with personnel at U.S. Army installations at Forts McCoy, WI, Pickett, VA, Stewart, GA, and Camp Shelby, MS to schedule field evaluations during prescribed burning at each installation. Since climatic conditions are critical in planning the execution of a prescribed fire, 1-3 day notices were the best lead-time available for ERDC personnel to mobilize to the field site. Particles of pre-weighed Comp-B were placed at various locations within the target prescribed fire area. Eight sample points were marked with a steel rebar, and three pre-weighed Comp-B particles were placed at each point. Temperature probes were placed in selected locations when time allowed. Flame height was determined as described in the previous section. Personnel from each installation executed the prescribed fire following established protocols at each installation. Following the conclusion of each prescribed fire, ERDC personnel entered the burn zone and recovered any unburned particles, exposed soil and documented observations.

Project Note: In the initiation of the field tests, changes in the Department of Transportation (DOT) regulations severely restricting the transport of explosive materials made it necessary to investigate a substitute energetic material not classed as an explosive for DOT purposes. Several military propellants were investigated and compared to Comp-B for effects of temperature and flame exposure on combustion response. Laboratory tests determined that M10 propellant exhibited the same burning response to temperature and exposure to

fire, and was used as a surrogate for Comp-B in field tests at Fort Stewart, Fort Pickett and Camp Shelby.

Results and Discussion

Bench-Scale Tests

Chemical analysis by USEPA Method 8330 verified the Comp-B used in these tests contained HMX, RDX and TNT at 6, 57, and 36%, of the total mass, respectively, with approximately 1% desensitizing wax. Both aged (1-year) and un-aged Comp-B began to melt at 200 deg F and combusted at 340 deg F. This is consistent with Material Safety Data Sheets (MSDS) for Comp-B which provide a melting point for TNT and the wax at 174-176 deg F and RDX at 374 - 392 deg F. The MSDS provides a boiling point of 464 deg F, a point which TNT explodes. In our testing, boiling of Comp-B initiated around 320 – 330 deg F at which point no solid Comp-B remained and combustion quickly followed. These observations are exhibited in Figures 1 and 2, with the aged Comp-B on the left. When solid Comp-B was exposed directly to flames, combustion was immediate at normal air temperatures.

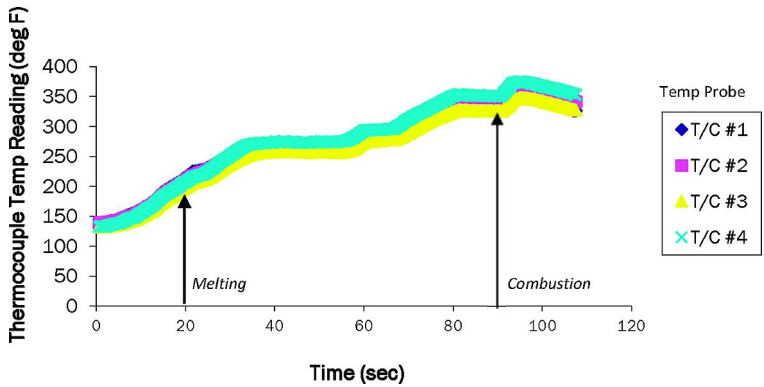

Figure 1. Effects of temperature on melting combustion of aged and un-aged Comp-B. (see color insert)

Figure 2. (Left) Initial melting, (Middle) Liquid state, (Right) Combustion. (see color insert)

Wind Tunnel Tests

Figures 3 and 4 show wind tunnel results comparing temperature profiles to loss of solid Comp-B under two windspeeds and moisture conditions. Temperature probe (T/C) numbers for the temperature plots correspond to the pole numbers in the % reduction graph. As these figures show, there is no clear correlation to peak temperature on the complete combustion of Comp-B. Length of elevated temperatures indicates greater potential exposure to burning vegetation and embers that quickly result in combustion of Comp-B. Increasing wind speed decreases heat exposure time but can increase temperature depending on the amount and characteristics of vegetative fuel. As shown in bench-scale tests, exposure to elevated temperatures (340°F) results in combustion of Comp-B. In wind tunnel tests, these temperatures were often not reached at the soil surface and direct exposure to flame and embers from burning vegetation was necessary for combustion of Comp-B. As shown in Figure 5, burn patterns may be affected by various factors, resulting in incomplete burns and lack of Comp-B combustion.

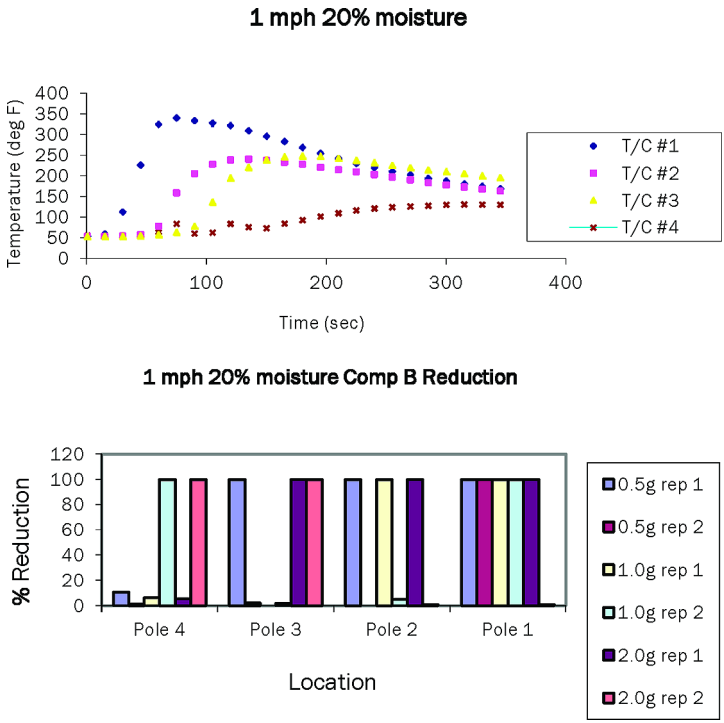

Figure 3. Temperature profiles and effects on Comp-B combustion (see color insert)

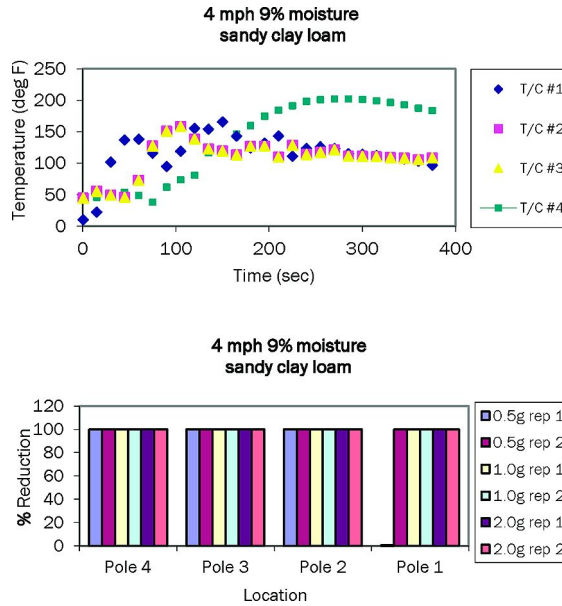

Figure 4. Temperature profiles and effects on Comp-B combustion. (see color insert)

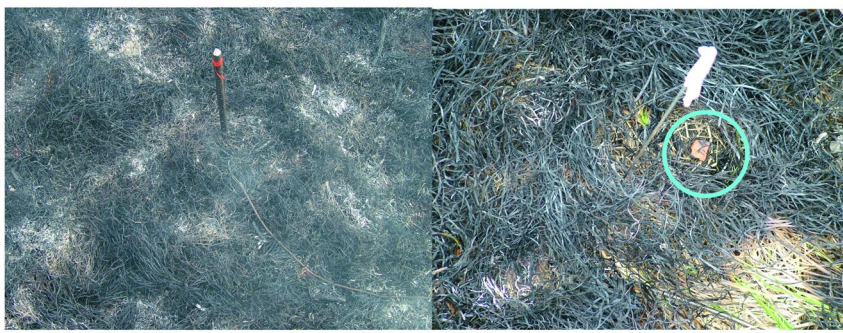

Figure 5. Complete burn (left) and incomplete burn (right) with Comp-B particle (circle). (see color insert)

Soil analysis indicated that parent compounds of RDX, TNT and HMX were present in soil where exposure of Comp-B particles to heat only resulted in slight melting of the particle (Table 1). Where combustion of Comp-B was 100%, residual concentrations of Comp-B parent compunds RDX, TNT, HMX and degradation products DNX, MNX and 2-A-DNT were also present. Migration of TNT to soil tends to be higher where combustion fails to occur as it has a lower melting point, while RDX is the prevalent constituent following combustion.

Table 1. Comp-B constituents in soil following burning, mg kg^{-1}.

Solid Reduced	*HMX*	*DNX*	*MNX*	*RDX*	*TNT*	*2-A-DNT*
1.2 %	1.5	<MDL	<MDL	3.5	10.9	<MDL
100 %	1.6	0.6	1.2	35.9	3.4	0.2

Table 2 shows the fate of Comp-B in wind tunnel plots for three soils and two wind speeds and two fuel moisture conditions. Overall, simulated wildfire burning in the wind tunnel resulted in an 80% loss of solid Comp-B, 8% of which remained as residual constituents of Comp-B in the soil surface for a total net loss of 72%. As previously discussed, effectiveness appeared to be driven by burn patterns, affected by multiple, interacting factors including wind speed, fuel moisture and density of vegetation. While the tests were not designed to clearly identify significance of these factors, it is recognized that these variables may not be used reliably to establish criteria for effective field application.

Table 2. Fate of Comp-B in wind tunnel simulated wildfire.

Soil Type	*Wind Speed, mph*	*Fuel H_2O, %*	*Pre-burn Solid, mg*	*Post-burn Solid, mg*	*Solid Loss, %*	*Post-burn Soil, mg*	*Residual in Soil, %*	*Net Loss, %*
SCL	1	20	28355	10060	65	292	1	36
SCL	4	9	28162	500	98	1932	**7**	**9**
Clay	1	20	27944	12305	56	2597	9	53
Clay	4	9	28395	4265	85	3936	14	29
Loam	1	20	29665	570	98	1689	6	8
Loam	4	9	29034	6487	78	3116	11	33
Average Loss/Residual, %					80		8	72

Plot Scale Tests

Prescribed burning under open-air conditions usually generated lower peak temperatures on indigenous *Paspalum notatum* compared to prescribed burning on pine straw (Figure 6), which peaked as high as 1000 deg F. Hotter, longer burning fire generally ensured complete burning of vegetation and exposure of Comp-B to heat, flame and embers. Overall, results were 62 and 92% combustion of Comp-B in *Paspalum notatum* and pine straw test plots respectively. This indicates that under field conditions effective reduction can be achieved.

- Wind Speed=2-3 mph
- Temperature= 21°C
- Relative Humidity= 40%
- Fuel = *P. notatum*
- Fuel moisture= 12%
- Flame Height=2 ft
- **Loss of Comp-B=79%**

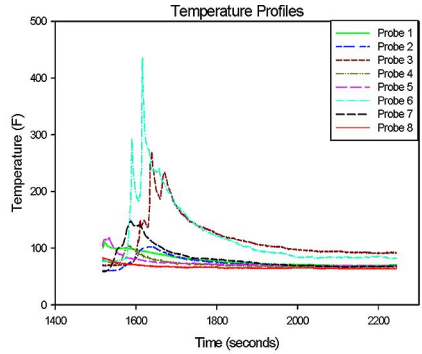

% Reduction of Comp-B	
Probe 1	100
Probe 2	100
Probe 3	100
Probe 4	66.66
Probe 5	33.33
Probe 6	100
Probe 7	100
Probe 8	33.33

- Wind Speed= 2-3 mph w/ 5 mph gusts
- Temperature= 27.6°C
- Relative Humidity= 44.7%
- Fuel = pine straw
- Fuel Moisture= 4%
- Flame Height ≥ 5',
- **Loss of Comp-B= 100%**

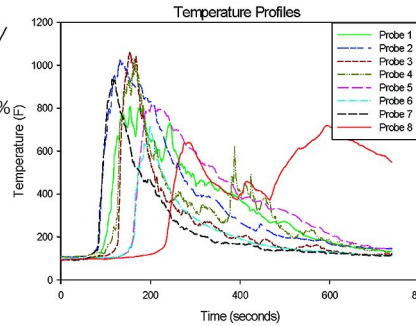

% Reduction of Comp-B	
Probe 1	100
Probe 2	100
Probe 3	100
Probe 4	100
Probe 5	100
Probe 6	100
Probe 7	100
Probe 8	100

Figure 6. Temperature profiles in plot-scale tests and effects on combustion of Comp-B. (see color insert)

Field Tests

Table 3 shows the results of field tests at Forts McCoy, Pickett, Stewart and Camp Shelby. These tests included the various vegetative cover types, typical variation in plant densities and ground fuel (biomass) that can be expected in most Army training lands where fire managed ecosystems occur. The lowest fuel biomass shown in Table 3 did not always result in less combustion of Comp-B or M-10 propellant. Temperature profiles collected at Fort Pickett (Figures 7, 8 and 9) show the typical variation of peak temperatures at each location and maximum temperature yields observed previously in plot scale tests. As indicated previously, direct exposure to burning vegetation or embers generally results in combustion of Comp-B, despite low biomass or lower peak temperatures produced. Overall, field results from 10 prescribed fires resulted in an average reduction of 94% of the Comp-B/M-10 placed on the soil surface. Results indicate that under weather and vegetation conditions suitable for prescribed fire, the average reduction in Comp-B will exceed 90%.

Table 3. Combustion of Comp-B/M10 during prescribed fire on training lands.

Location	*Fuel/Vegetation Type*	*Biomass, g/m²*	*Material*	*Combustion, %*
Fort McCoy	Grassland	50	Comp-B	79
	Hardwood Litter	254	Comp-B	96
	Pine Litter	462	Comp-B	92
Camp Shelby	Grassland	42	M10	88
Fort Pickett	Pine Litter	88	M10	96
	Pine Litter - Grassland	98	M10	88
	Grassland	51	M10	100
Fort Stewart	Pine Litter - Palmetto	309	M10	100
	Pine/Hardwood Litter	147	M10	100
	Pine Litter - Grassland	104	M10	100
		Field Results Average		**94**

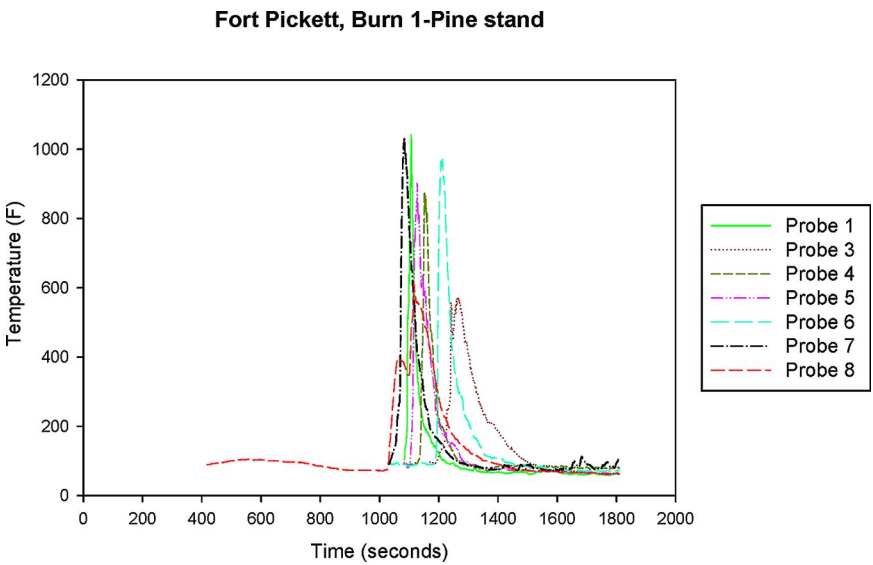

Figure 7. Temperature profiles collected at Fort Pickett pine stand burn. (see color insert)

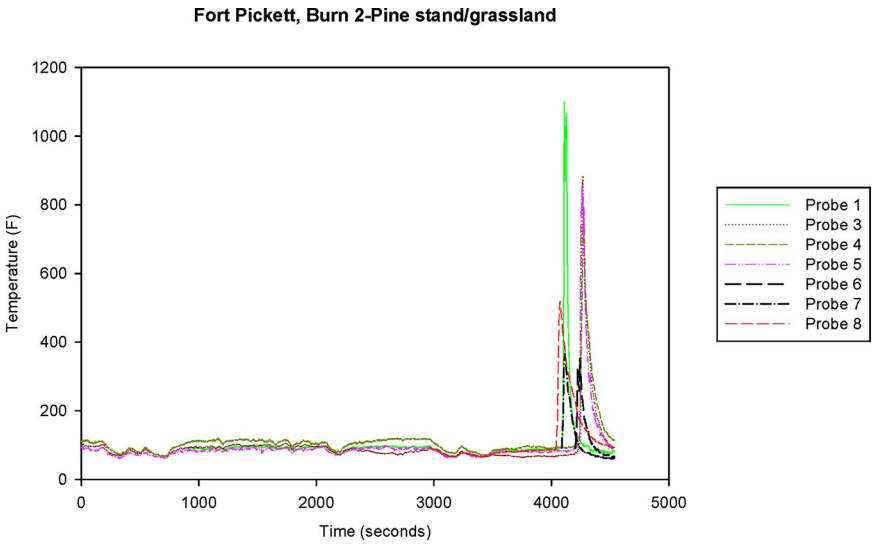

Figure 8. Temperature profiles collected at Fort Pickett pine stand and grassland burn. (see color insert)

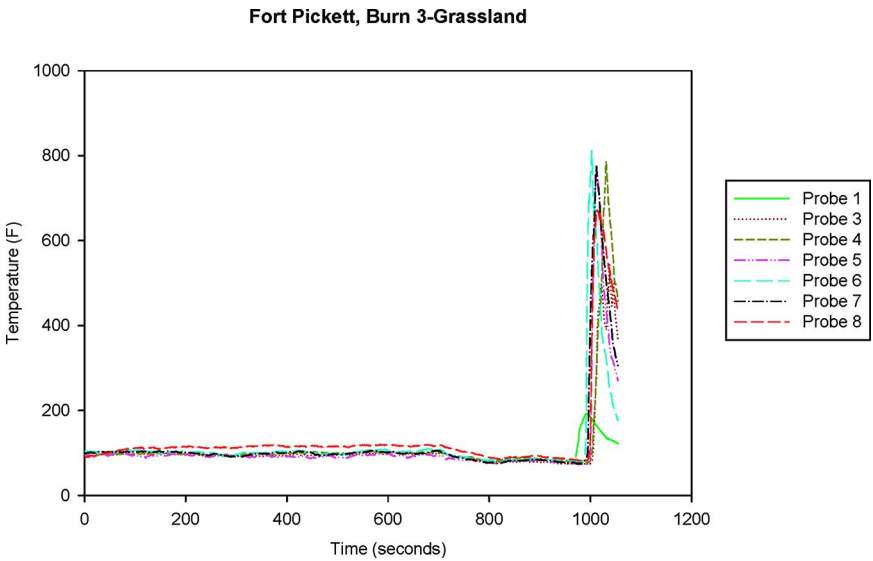

Figure 9. Temperature profiles collected at Fort Pickett grassland burn. (see color insert)

Conclusions

Comp-B was shown to readily burn when exposed to heat of 340 deg F or when in contact with flames or embers. When residual particles are distributed on soil surfaces as a result of low-order detonations of munitions, Comp-B may be exposed to incidental or prescribed fire on training lands. Lab and wind tunnel tests concluded that exposure to heat can melt Comp-B at temperatures of 200 deg F, and such temperatures at soil surfaces may occur and result in slight melting of parent compounds TNT, RDX and HMX into soil surfaces. Fires that produce soil surface temperatures above 340 deg F or flame/ember contact with Comp-B will result in combustion. Combustion was shown to leave residual amounts of mostly RDX followed by TNT, HMX, MNX, DNX and 2-A-DNT. Fires in wind tunnel tests results in an average loss of 80% of solid Comp-B with 8% remaining as residual in the soil surface for a net loss of 72%. Under plot scale conditions, grass and pine straw fires averaged a loss of 62% and 92% solid Comp-B, respectively. Field validation was conducted at four installations during prescribed fire operations on training lands. Reduction of Comp-B (or surrogate M10) ranged from 79% to 100% with an average of 94% across ten different vegetation cover types. The results of this study conclude that under climatic and vegetative cover conditions suitable to support prescribed fire on training lands, 80% or greater of distributed particulate Comp-B will be consumed and pose no further threat to the environment.

References

1. Pennington, J. C.; Jenkins, T. F.; Thiboutot, S.; Ampleman, G.; Clausen, J.; Hewitt, A. D.; Lewis, J.; Walsh, M. R.; Walsh, M. E.; Ranney, T. A.; Silverblatt, B.; Marois, A.; Gagnon, A.; Brousseau, P.; Zufelt, J. E.; Poe, K.; Bouchard, M.; Martel, R.; Walker, D. D.; Ramsey, C. A.; Hayes, C. A.; Yost, S. L.; Bjella, K. L.; Trepanier, L.; Berry, T. E.; Lambert, D. J.; Dubé, P.; Perron, N. M. *Distribution and Fate of Energetics on DoD Test and Training Ranges: Interim Report 5*; ERDC TR-05-2; U.S. Army Engineer Research and Development Center: Vicksburg, MS, 2005.
2. Pennington, J. C.; Jenkins, T. F.; Ampleman, G.; et al. *Distribution and fate of energetics on DoD test and training ranges: Interim Report 6*; Technical Report ERDC TR-06-12; U.S. Army Engineer Research and Development Center: Vicksburg, MS, 2006. http://el.erdc.usace.army.mil/elpubs/pdf/tr06-12.pdf.
3. Jenkins, T. F.; Hewitt, A. D.; Grant, C. L.; Thiboutot, S.; Ampleman, G.; Walsh, M. E.; Ranney, T. A.; Ramsey, C. A.; Palazzo, A. J.; Pennington, J. C. Identity and distribution of residues of energetic compounds at Army live-fire training ranges. *Chemosphere* **2006**, *63*, 1280–1290.
4. Lynch, J. C. *Dissolution Kinetics of High Explosive Compounds (TNT, RDX, HMX)*; ERDC/EL TR-02-23; U.S. Army Engineer Research and Development Center: Vicksburg, MS, 2002.

5. Dontsova, K. M.; Yost, S. L.; Simunek, J.; Pennington, J. C.; Williford, C. W. Dissolution and Transport of TNT, RDX, and Composition B in Saturated Soil Columns. *J. Environ. Qual.* **2006**, *35*, 2043–2054.
6. Belden, J. B.; Ownby, D. R.; Lotufo, G. R.; Lydy, M. J. Accumulation of trinitrotoluene (TNT) in aquatic organism: Part 2 - Bioconcentration in aquatic invertebrates and potential for trophic transfer to channel catfish (Ictalurus punctatus). *Chemosphere* **2005**, *58*, 1161–1168.
7. Rosen, G.; Lotufo, G. R. Toxicity of two munitions constituents to the estuarine amphipod Eohaustorius estuarius in spiked sediment exposures. *Environ. Toxicol. Chem.* **2005**, *24* (11), 2887–2897.
8. Simmers, J. W.; Price, R. A.; Myers, K. F.; Karn, R. A.; Kress, R.; Tatem, H. E.; Jensen, K. C. *Impact area contaminant inventory: Fort McCoy*; Miscellaneous Paper EL-97-4; U.S. Army Engineer Waterways Experiment Station: Vicksburg, MS, 1997.
9. Palazzo, A. J.; Leggett, D. C. Effect and disposition of TNT in a terrestrial plant. *J. Environ. Qual.* **1986**, *15*, 49–52.
10. Pennington, J. C. *Soil sorption and plant uptake of 2, 4, 6-trinitrotoluene*; Technical Report EL-88-12; U.S. Army Engineer Waterways Experiment Station: Vicksburg, MS, 1988; NTIS No. AD A200 502.
11. Pennington, J. C. *Plant uptake of 2,4,6-trinitrotoluene, 4-amino-2, 6-dinitrotoluene, and 2-amino-4,6-dinitrotoluene using 14Clabeled and unlabeled compounds*; Technical Report EL-88-20; U.S. Army Engineer Waterways Experiment Station, Vicksburg, MS, 1988; NTIS No. AD A203 690.
12. Harvey, S. D.; Fellows, R. J.; Cataldo, D. A; Bean, R. M. Fate of the explosive hexahydro-1,3,5-trinitro-1,3,5-triazine (RDX) in soil and bioaccumulation in bush bean hydroponic plants. *Environ. Toxicol. Chem.* **1991**, *10*, 845–855.
13. Price, R. A.; Pennington, J. C.; Larson, S. L.; Neumann, D.; Hayes, C. Uptake of RDX and TNT by agronomic plants. *Soil Sediment Contam.* **2002**, *11* (3), 307–326.
14. Keane, R. E.; Agee, J.; Fule, P.; Keeley, J.; Key, C.; Kitchen, S.; Miller, R.; Schulte, L. Effects of large fires in the United States: benefit or catastrophe. *Int. J. Wildland Fire* **2008**, *17* (6), 696–712.
15. Simmers, J. W.; Price, R. A.; Myers, K. F.; Karn, R. A.; Kress, R.; Tatem, H. E.; Jensen, K. C. *Impact area contaminant inventory: Fort McCoy*; Miscellaneous Paper EL-97-4; U.S. Army Engineer Waterways Experiment Station: Vicksburg, MS, 1997.
16. Simmers, J. W.; et al. *White phosphorus wetland storage installation assessment report: Fort Ord*; Miscellaneous Paper EL-93-11; U.S. Army Engineer Waterways Experiment Station: Vicksburg, MS, 1993.
17. Simmers, J. W.; et al. *White phosphorus wetland storage installation assessment report: Fort Pickett*; Miscellaneous Paper EL-93-12; U.S. Army Engineer Waterways Experiment Station: Vicksburg, MS, 1993.
18. Simmers, J. W.; et al. *White phosphorus wetland storage installation assessment report: Fort Jackson*; Miscellaneous Paper EL-93-15; U.S. Army Engineer Waterways Experiment Station: Vicksburg, MS, 1993.

19. Simmers, J. W.; et al. *White phosphorus method storage installation assessment report: Fort Bragg*; Miscellaneous Paper EL-93-6; U.S. Army Engineer Waterways Experiment Station: Vicksburg, MS, 1993.
20. Pennington, J. C.; Jenkins, T. F.; Ampleman, G.; et al. *Distribution and fate of energetics on DoD test and training ranges: Interim Report 6*; Technical Report ERDC TR-06-12; U.S. Army Engineer Research and Development Center: Vicksburg, MS, 2006. http://el.erdc.usace.army.mil/elpubs/pdf/tr06-12.pdf.
21. United States Environmental Protection Agency. Nitroaromatics and Nitramines by HPLC, SW846 Method 8330; 1996.
22. United States Department of Agriculture, Forest Service Southern Region. Technical Publication R8-TP 11; February 1989.

Chapter 20

Remediation of Surface Soils Contaminated with Energetic Materials by Thermal Processes

Isabelle Poulin*

Energetic Materials Section, Defence Research & Development Canada - Valcartier, 2459 Pie-XI Blvd North, Quebec (Qc) G3J 1X5, Canada
***isabelle.poulin@drdc-rddc.gc.ca**

As a result of military training, many range and training areas are contaminated with energetic material. For many characterized sites in Canada,, more than 70% of the overall contamination was found in the first 10 cm of the surface soil for the propellant residues at firing positions. Military personnel can be exposed to these compounds, which may eventually be transported to surface and ground water. At this moment, there is no protocol for routinely removing propellant residues from surface soils. Various remediation strategies are currently being studied (phytoremediation, fire ecology, etc.) in order to address the problem of surface soils contamination by EMs. This chapter will present the results of laboratory studies and field trials aimed at evaluating the combustion of selected liquid and gelled fuels that could be used as a remediation method for the thermal decomposition of propellant in surface soils.

Introduction

To ensure a high degree of preparedness for any potential mission, training with live weapons is an important part of military activities. As a result of this training, many ranges and training areas (RTAs) are contaminated with energetic materials (EM). Propellant residues accumulate at firing positions due to incomplete combustion in guns, whereas the EM fill in projectiles may be spread across target areas, for example when an unexploded ordnance (UXO) is fractured after being hit by shrapnel of other fragments.

Published 2011 by the American Chemical Society

The environmental characterization of many Canadian and United States bases (*1–14*) showed that the firing positions of many ranges are contaminated with residues of unburned EM from gun propellant. The concentrations of nitroglycerin (NG), one of the main constituents of the double base propellant used in the antitank rockets, detected at firing positions of antitank rocket ranges, are often in the thousands of mg kg^{-1} at distances of 1 to 10 m behind the firing position (antitank rockets spread propellant residues behind them; the residues are ejected with the back-blast). These high concentrations of NG near the firing position decrease with distance behind the firing line, to tens of mg kg^{-1} at a distance of 50 m. For many RTAs studied, the bulk of the EM contamination was present on the soil surface (*4*). On some Canadian bases, contamination was found up to 60 cm deep, but for all sites studied, more than 70% of the overall contamination was found in the first 10 cm of soil (*15*).

It is also well known that NG is highly persistent in the environment. A former antitank range that had been left unused for over a quarter of a century was studied by Defence Research & Development Canada – Valcartier (DRDC Valcartier) scientists in 2009 (*16*) to gather data and develop an understanding of the long-term fate of nitrocellulose (NC)-based propellant residues in soils. Soil was sampled at various depths behind the firing position and the analysis for residues of NG was performed. The results showed that NG, when deposited on the ground as propellant residue in a NC matrix is still detected at levels of 4,000 mg kg^{-1} behind the firing position, even after more than 25 years of inactivity. Most of the NG is still present at the soil surface, while soil penetration of NG can be detected up to 1 m depth. The NG concentrations decrease with depth as observed in active antitank firing ranges. The vertical migration of NG is likely due to the migration of small particular propellant grains or colloidal migration, which have contributed to a low level of NG over time (as desorption from NG-rich NC surfaces). The firing positions of legacy ranges may still contain high concentrations of NG in the surface soils, which, depending of the future uses of these sites, could represent a threat to human health.

In the case of NG, the main residue present at antitank firing positions, signs and symptoms of acute exposure are headaches, nausea, vomiting, occasionally diarrhea, sweating, and lightheadedness, whereas symptoms of chronic exposure are development of a physiological tolerance to exposure, wherein sudden withdrawal from exposure can result in angina-like chest pains, which may be accompanied by malaise, weakness, vomiting, dizziness, headache, or impaired vision (*17*). Chronic exposure may also result in severe headache, hallucinations, and skin rashes. Allergic contact dermatitis can occur secondary to topical NG exposure.

In Canada, these findings represent a concern for the Department of National Defence (DND) since military personnel can be exposed to these compounds, which eventually may be transported to surface and ground waters. The potential migration of EM to waters is not only a hypothetical risk. In 1997, the U.S. Environmental Protection Agency (USEPA) issued Administrative Order No. 2 to the National Guard Bureau and the Massachusetts National Guard requiring that certain training activities (artillery and mortar firing) cease, pending the completion of environmental investigations at the training ranges and impact

area. In January 2000, the USEPA, Region I, issued Administrative Order 3, which, required the suspension of military training because of environmental contamination of soils and groundwater at Massachusetts Military Reservation (MMR) Training Range and Impact Area. The contaminants of concern detected in soils were lead, explosives, explosives-related compounds, pesticides and other organic contaminants, whereas cyclo-1,3,5-trimethylene-2,4,6-trinitramine (RDX), trinitrotoluene (TNT), cyclotetrametylenetetranitramine (HMX) and some other compounds such as perchlorates were found in groundwater (*18*). Currently, there is no protocol for routinely removing explosive residues from surface soils. If such a procedure were validated and implemented, the future impacts on groundwater would likely be reduced. Maintenance operations are planned for a limited number of sites, such as the clearance of UXOs and the cleaning of sand-filled bullet catchers (*19–21*). There are also no standard protocols for maintenance activities for removal of contamination by EM at firing positions and target areas. The work reported here was designed to investigate a potential technique for regular decontamination of EM residues at firing positions.

There are various remediation strategies currently being evaluated to address the issue of surface soil contamination by EM. However, in Canada, none of these activities are used on a regular basis for soil remediation. Two potential remediation strategies include biological treatment or bioremediation (e.g. aqueous-phase bioreactor treatment, composting, land farming, phytoremediation, white rot fungus treatment) (*22*) and thermal treatment technologies (hot gas decontamination and incineration). A chemical approach, the use of lime to induce alkaline hydrolysis of explosives in soils, is also being studied as a remediation strategy (*23*).

Fire ecology, the science of using fire to manage vegetation and ecosystems, has also been investigated as an innovative approach to destroy explosives residues on soil surfaces (*24*). For target areas, where vegetation is present, the use of controlled or prescribed burning as a management technique can be used for a variety of purposes: safety clearance prior to detection and destruction of UXO, wildfire avoidance, and plant and wildlife management. These fires have the potential to destroy energetic compounds - which are either associated with the vegetation that is burned or are in or on the soil surfaces that are heated by the fire. An important criterion for using this approach is that these compounds are exposed to temperatures above their thermal decomposition temperature as the flames propagate. Since many of the contaminated firing positions are not covered with vegetation, alternative burning procedures, in the absence of dry grass or other vegetation, must be considered.

Controlled burning tests were performed both in the laboratory and on military training ranges by US scientists (*25*). From the laboratory testing, several conclusions were drawn: i) the thermal decomposition of TNT and RDX is a function of temperature, concentration, soil moisture, soil chemistry and other physical properties; overall, temperatures near 250°C resulted in rapid decomposition of both TNT and RDX; ii) generally, higher temperatures and lower soil concentrations result in more rapid decomposition of TNT and RDX; iii) oxygen is required to support thermal decomposition; and iv) soil-associated TNT and RDX decompose at temperatures consistent with those observed in

the field (175°C for RDX and 250°C for TNT). The field testing was comprised of prescribed burning of a bed of pine needles spread over a large area as a combustible material. It was demonstrated that during controlled burning, temperatures at and above the ground surface can reach levels that support rapid thermal decomposition, but heat generated during the controlled burn did not penetrate more than a few centimeters into the ground. For example, at two different test areas, temperatures at the ground surface approached 600°C while the maximum temperatures observed at 2.5 cm below were 96°C and 52.5°C. It was also found that there was no temperature effects at 8.5 cm below the ground surface at any of the test area locations. Pine straw burns hot, is effective for fueling a burn, but is not effective at heating the subsurface soil. Previous research has shown that heat penetration into soil is a function of both the intensity and duration of the fire. The pine straw burned too rapidly (less than 10 minutes in most cases), which was not long enough for deep heat penetration into the soil. Temperature data support the suggestion that thicker beds of needles acted as an insulator as the flames propagate. An increased fuel loading also appeared to lower the temperature of the burn on the underside of the needle bed.

The work of Hubbard et al. (*26*) on prescribed burnings in an oak-pine forest also demonstrated that heat penetration in soil was low: during a burning of maximum flame temperature of 344°C, the temperature at 2.0 and 1.0 cm below the soil surface was 45°C and 59°C, respectively. Other authors (*27*) inferred the temperature beneath the surface during burnings using the temperature histories reported by Frandsen and Ryan (*28*), which show a decrease in peak temperature of approximately 200°C between thermocouples positioned at and 2 cm below the mineral soil surface.

Hubbard et al. (*26*) also demonstrated that neat TNT can migrate downward into the soil if temperatures are not sufficiently high, i.e. if TNT melts instead of rapidly decomposing. Neat RDX does not have the same propensity as TNT to melt and migrate into the soil. The melting point temperature for RDX is closer to its decomposition point, 204°C versus 260°C, respectively (*29*).

The natural remedial properties of opportunistic fires that result from exploding ordnance, or as a result of land management activities was studied by Price (*30*). Tests conducted in a wind tunnel and in the field have demonstrated that as much as 90% of Composition B chunks on the surface of vegetated training ranges can be consumed by fire. This study did not address the contaminated soil below the surface, but the overall conclusion from the investigation was that using prescribed burning on ranges has potential for destroying a significant amount of explosives residual in surface soils and plant tissues. It was acknowledged that additional work is needed to better understand different parameters and improve the design of the burn to increase the transfer of heat to the soil profile.

Objectives

This chapter presents the results of laboratory testing and field trials performed for evaluating alternative methods for prescribed burnings of vegetation that are sufficient to heat the soil enough to decompose the EM in the surface and sub-

surface soil layers. The goal was to determine whether the combustion of applied fuels on the soil surface would be sufficient to raise temperature above the thermal decomposition temperature of the energetic materials present as contaminants. Laboratory tests on contaminated soils from an antitank firing position as well as tests on an active firing site were conducted. The soils behind the antitank firing points, where most of the contamination is present, were thermally treated and samples were analyzed for their EM content both before and after combustion of different types of fuels at the surface.

Materials and Methods

Heat Propagation Tests

The first phase of the effort was to determine the heat propagation in soils during the combustion of various fuels (solid, liquid and gel). Thermocouples were used to record the temperature in the soil at different depths (1, 2, 5 and 8 cm below the surface).

In this study, uncontaminated sand (Silica sand, Temiska Inc.) was used. This sand does not contain organics and was chosen for this first step because it represents what is often found in Canadian training ranges. Aluminium containers (20cm x 20cm x 20cm) were used to hold the sand, which was dried in an oven at 100°C before the experiments. A line was drawn at 14 cm from the bottom of the container to indicate the target sand level. Type J thermocouples were placed in the container at 1, 2, 5 and 8 cm below the top of the sand. One aluminium container was filled with dried, room temperature sand, and the thermocouples were inserted into the sand parallel to the bottom of the container until the sensing end was centered in the box. The thermocouples were then connected.

The choice of the fuels was dictated by the following criteria: i) any unburned material should be non-toxic to the environment (humans, wildlife and plants); ii) material should be easy to manipulate; iii) it should be possible to spread and easily ignite the fuel material. This last criterion would become important in an active range situation where it may be necessary for security reasons to ignite the fuel remotely. Propane gas was thus eliminated. The tested fuels were gelled ethanol, gelled methanol, pine wood shavings, and liquid ethanol, methanol and isopropyl alcool. The product referred as “gelled ethanol” is a commercial product called “Gelled Fuel”, manufactured by the Home Presence by Trudeau Company. This product was sold to be used in fondue burners. The product referred as “gelled methanol” in this report was a commercial product called “Magic Flame”, manufactured by Scientific Utility Brands International Inc. It was sold to be used for cooking and/or heating, for example in recreational activities such as camping.

The combustible fuel was first spread or poured on the sand surface prior to starting the data acquisition, which was controlled remotely with a Labview-based software. Once data acquisition commenced, the fuel was ignited using a propane torch. The data were collected continuously throughout the experiment and also continued for at least 10 minutes after the end of the burning. The data collected were evaluated and the maximum temperature reached for each thermocouple

was recorded for comparative fuel analysis and use in contaminated soil burning evaluation.

Small-Scale Test on Contaminated Soil

The objective of the second experimental phase was to use the most promising fuels determined in phase one, and ignite them on contaminated soil to determine the efficiency of EM destruction. The fuels that exhibited the highest temperatures from the heat propagation test were the gelled ethanol and gelled methanol.

The soil used for these tests came from the firing position on Liri Range, an active anti-tank firing range, which is known to be contaminated with EM, primarily NG at the firing position and HMX and TNT at the target area (*31*). Liri Range is situated within the Canadian Forces Base Valcartier, near Quebec City. The soil was collected in autumn 2008 and dried at room temperature in the dark. The soil was stored in closed plastic pails until needed for experimental trials. Prior to use, the soil was sieved to remove the large (> 4 mm) debris and rocks.

In order to determine baseline (initial) NG concentrations in soils, pre-burn samples comprised of 15 multi-increments were collected. The total mass of the multi-increment sample was between 10g and 40g. The collected samples were located at the surface (0cm to 1cm depth) and also at a depth of 2 cm. Once pre-burn samples were acquired, the fuel was then poured over the sand and ignited. In a subset of experiments, the fuel was mixed with the soil. After the end of the burning, the soil was allowed to cool to ambient conditions and post-burn multi-increment sampling was performed in the same manner as pre-burn sampling. The samples were processed and analyzed using HPLC analysis, using an in-house method derived from current EPA analysis methods (US EPA SW846 method 8330b (*32*). As the sample was composed of soil that had been sieved, it was not sieved again before analysis. Also, due to small sample size, the soil samples were not homogenized with acetone as is commonly done with other samples (*33*). Rather, the soil samples were directly and completely mixed with acetonitrile in a glass jar, using a proportion of 2 mL of solvent for 1 g of soil. The jar was placed on a vortex shaker for 1 min, followed by sonication in a cooled ultrasonic bath (4°C) for 18 h. The solutions were then allowed to settle for 30 min before preparation of the sample for HPLC analysis. Dilutions were made when necessary, but the final solution had a composition of 1:1 v/v acetonitrile and water, which was filtered (0.45 μm) prior to HPLC analysis. The injection volume was 20 μL and the column used was a Supelcosil LC-8 column 25 cm × 3 mm × 5 μm eluted with 15:85 isopropanol/water (v/v) at a flow rate of 0.75 mL/min. The column temperature was maintained at 25°C during all analyses. The analysis was performed with an HPLC Agilent HP 1100 equipped with a degasser model G1322A, a quaternary pump model G1311A, an autosampler model G1313A, and an ultraviolet (UV) diode array detector model G1315A monitoring the following wavelengths: 210 nm, 220 nm, and 254 nm.

Field Test on Contaminated Ranges

The goal of the third phase was to evaluate the effect of a controlled first burn on EM present on an active range. The influence of the soil compaction on the efficiency of burning was the main parameter investigated in this test. For burning performed in the laboratory, the soil was sieved and aerated first. This provided the soil with additional oxygen, especially critical when the soil was actively mixed with the gel. In the case of burnings on the range, the soil might have been there for many years, with military activities leading to high compaction of the soil.

This test involved the ignition of a gelled ethanol fuel over an area of 8 m^2 of at an antitank firing position at on the Canadian Forces Base (CFB) Gagetown (Wellington Range). This range is an active antitank range where 84-mm weapons (Carl Gustav) and M-72 (66-mm) light antitank weapons are fired on a regular basis. This range has been active for more than 40 years (*34*). The Carl Gustav is a recoilless weapon which is known to spread a significant quantity of unburned propellant residues behind the firing point, due to the back blast. A study carried out during a live firing exercise in 2007 (*35*) demonstrated that 14 % w/w of nitroglycerin was unburned and dispersed on the ground, with the highest levels having been found between from 5 and to 15 m behind the gunner. The compaction of the soil was studied, while the influence of the conditions of humidity, wind, and soil composition were not studied. Soil samples were collected before and after the thermal treatment and were analyzed for their NG content in nitroglycerin.

The firing position was first examined by an explosive ordnance disposal (EOD) technician. This examination was to ensure that no past activities had not led to the presence of unexploded ordnance (UXO) at the test location. Once the site was deemed safe, the section on the ground that would be burned was identified and parsed into 1 m^2 areas. The first series of burnings was performed behind firing position #1 (FP1) and a second series of burnings was performed behind firing position #2 (FP2). The schematic of the sampling strategy is presented in Figure 1 (the gray squares were sampled before and after the burning).

The sampling areas (squares) behind FP1 and FP2 were identified by their distances from the firing point. The first 1 m2 (Figure 1), was at a distance of 5 to 6 m, therefore identified as FP1-5-6. The second area was identified as FP1-7-8 and so on. Sampling of surface soil was performed using a stainless steel scoop, cleaned between samplings (washed sequentially with water and acetone and wiped dry with a paper towel). For FP1, two squares (FP1-5-6 and FP1-7-8) were sampled as they were, and the two others (FP1-9-10 and FP1-11-12) were first tilled 3 to 4 cm deep using a shovel to aerate the soil and to determine if the treatment was more efficient on uncompacted soil. For the undisturbed areas, surface soil samples (up to 2 cm deep) were comprised of 30 increments collected in a 1 m2 area. The subsurface samples were comprised of 10 increments of soil collected at 2 to 4 cm deep. The samples for the surface soil were identified as “A”, while the subsurface samples were identified as “B”. For tilled areas, only one sample was collected before the burning and it was comprised of 30 increments of soil (up to 4 cm deep). These samples were identified as “A+B”. For all samples, the note “before” was added to the sample name to indicate that they were collected before the burning. All samples were placed in a plastic bag, tightly closed and

placed in a cooler. Samples were brought back to the laboratory and kept in a refrigerator at 4°C prior to treatment and analysis. The same sampling procedure was performed for soils collected after burning. The complete list of samples collected is presented in Table I.

Once the pre-burn "before" soil samples were collected, the remaining soil was prepared for burning. A total quantity of 9 L of ethanol-based gel (Gelled fuel, Home Presence by Trudeau, Montreal, QC) was spread as evenly as possible on the 1m^2 area. As the terrain was not perfectly flat, a minimal quantity of gel occasionally escaped from the 1 m^2 area. In the case of FP1-9-10 and FP1-10-11, the gel was mixed slightly with the soil (up to 4 cm deep). The burnings lasted for 10 to 15 minutes. Fire extinguishers were kept closeby during the burning. For squares where the surface soil was tilled and where gel was mixed with the soil, the burning lasted approximately 8 minutes longer. If, after the burning, a clear black-marked soot area was visible where the burning took place, this was considered indicative of incomplete fuel combustion.

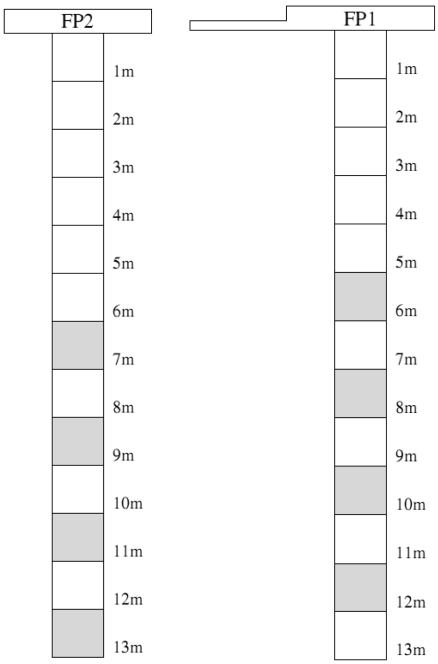

Figure 1. Schematic of the sampling setup (gray squares were sampled)

Table I. Samples taken before and after thermal treatment

Sample #	*FP*	*Distance from FP*	*Burning*	*Sample position*	*Comment*
FP1-5-6-A-before	1	5 to 6 m	before	surface	Gel poured directly on soil.
FP1-5-6-A-after			after		
FP1-5-6-B-before			before	subsurface	
FP1-5-6-B-after			after		
FP1-7-8-A-before		7 to 8 m	before	surface	Gel poured directly on soil.
FP1-7-8-A-after			after		
FP1-7-8-B-before			before	subsurface	
FP1-7-8-B-after			after		
FP1-9-10-A+B-before		9 to 10 m	before	surface	Soil tilled (5 cm deep). Gel was added and mixed in the softened soil.
FP1-9-10-A-after			after		
FP1-9-10-B-after			after	subsurface	
FP1-11-12-A+B-before		11 to 12 m	before	surface	Soil tilled (5 cm deep). Gel was added and mixed in the softened soil.
FP1-11-12-A-after			after		
FP1-11-12-B-after			after	subsurface	
FP2-6-7-A+B-before	2	6 to 7 m	before	surface	Soil tilled (5 cm deep). Gel was poured on top.
FP2-6-7-A-after			after		
FP2-6-7-B-after			after	subsurface	
FP2-8-9-A+B-before		8 to 9 m	before	surface	Soil tilled (5 cm deep). Gel was poured on top.
FP2-8-9-A-after			after		
FP2-8-9-B-after			after	subsurface	
FP2-10-11-A-before		10 to 11 m	before	surface	Gel poured directly on soil.
FP2-10-11-A-after			after		
FP2-10-11-B-before			before	subsurface	
FP2-10-11-B-after			after		
FP2-12-13-A-before		12 to 13 m	before	surface	Gel poured directly on soil.
FP2-12-13-A-after			after		
FP2-12-13-B-before			before	subsurface	
FP2-12-13-B-after			after		

The multi-increment samples were placed in a Pyrex® vessel (21cm x 21cm x 5cm) and homogenized using acetone before sub-sampling for EM extraction. Each sample was covered with acetone and mixed to form a slurry. The acetone was then allowed to evaporate and the entire sample was then sieved (2 mm). For some samples, a crust of NC had formed and was broken up using a mortar and pestle before sieving. After sieving, the homogeneous sample was ready for the extraction procedure. Approximately 10 g of soil (multi-increment sampling of the larger homogenized sample) was placed in a 30 mL amber vial and mixed with 20 mL of acetonitrile. The jars were vortexed for 1 minute, followed by sonication in a cooled ultrasonic bath (4°C) for 18 hours in the dark. The solutions were then allowed to settle for 30 minutes before preparation of the sample for analysis. Dilutions were made when necessary, making sure that the final solution for HPLC analysis had a composition of 1:1 v/v acetonitrile:water. A 2% $CaCl_2$ aqueous solution was used to force the precipitation of NC and the solution was then filtered through a 0.45-µm filter. Soil extracts were maintained at 4°C until analyzed by HPLC as previously described for the small-scale analyses.

Results/Discussion

Heat Propagation Tests

This section presents the results of temperature measurements at different depths in the sand during combustion of various fuels. The results are summarized in Table II.

Gelled Ethanol

For the first test, 500 mL of gelled ethanol was spread on the sand to a thickness of approximately 1.25 cm thick. The burning lasted for approximately 12 minutes. The maximum temperature measured at 1 cm below the surface was approximately 130°C. The maximum temperatures recorded deeper in the sand were much lower than the temperature at 1 cm: 63, 50 and 49°C at 2, 5 and 8 cm, respectively. This indicated that most of the heat is directed upwards and that sand acts as an insulation barrier. The thicker this barrier, the lower and slower the heat penetration, as can be observed by the slight temperature change from room temperature (before ignition) for deeper thermocouples.

Another test was carried out with gelled ethanol, but this time with twice the amount of gel (1 L vs 500 mL), giving a thickness of 2.5 cm over the sand surface. The burning lasted for approximately 27 minutes. The maximum temperature obtained at 1 cm below the surface was approximately 80°C, while maximum temperatures of 68, 61 and 57°C were obtained at 2, 5 and 8 cm below the surface. As compared with the first experiment with only a 1.25 cm thick of gel, the increase in temperature at 1 cm below the surface was lower because the thicker layer of gel acted as an insulating barrier. There is thus no gain in using a higher load of gel for surface decontamination.

Table II. Maximum temperature obtained during the burning of various fuels on sand

Fuel	*Maximum temperature at various depths (°C)*			
	1 cm	*2 cm*	*5 cm*	*8 cm*
Gelled ethanol (1.25 cm thick)[a]	131	63	50	49
Gelled ethanol (2.5 cm thick)[a]	80	68	61	57
Gelled methanol (1 cm thick)[b]	90	57	53	53
Pine wood shavings (3.8 cm thick)	25	22	22	22
Pine wood shavings (3.8 cm thick) soaked with ethanol	80	57	54	52
Ethanol (500 mL)	63	50	38	36
Isopropyl alcool (500 mL)	33	29	27	33
Methanol (500 mL)	28	28	27	33
1st cm of sand mixed with gelled ethanol (~ 1:1 v/v)	191	92	65	62
Home-made ethanol gel (with calcium acetate) (1.25 cm thick)	65	58	31	21
1st cm of sand mixed with home-made ethanol gel (with calcium acetate) (~ 1:1 v/v)	85	69	48	28

[a] Gelled fuel, Home Presence by Trudeau, Montreal, QC. [b] Cooking gel fuel, Magic Flame, Scientific Utility Brands International Inc. London, ON.

Gelled Methanol

For this test, 400 g of gel was poured on the sand. This resulted in gel thickness of approximately 1 cm on the sand. The burning lasted for approximately 15 minutes. The maximum temperature measured at 1 cm below the surface was near 90°C. The temperatures recorded deeper in the sand were much lower than at 1 cm: 57, 53 and 53°C at 2, 5 and 8 cm below the surface, respectively. As for the gelled ethanol, this indicated clearly that much of the heat was directed upwards and that sand acts as an insulation barrier. The highest temperature recorded at 1 cm below the surface (90°C) was lower than the one recorded for the gelled ethanol (130°C). This could be explained by the fact that methanol produces less energy during combustion as compared to ethanol (calculated using the enthalpy of reaction).

Wood Shavings

For this test, a 1-L beaker was filled with pine wood shavings and then poured over the sand thus giving a thickness of 3.8 cm on the sand. The fuel was then ignited with a propane torch, but in this case, at multiple ignition points instead of a single ignition point as with the previous tests. Even with multiple ignition points, the fire only lasted for less than 5 minutes, and did not burn all of the wood, More than 2 cm of wood was observed to remain intact under the soot layer. The increase in temperature at 1 cm below the sand surface was negligible.

Ethanol Soaked Wood Shavings

To enhance the ignition and burning, wood shavings were soaked with ethanol prior to spreading (500 mL of ethanol for 1 L of wood shavings, approximately 3.8 cm thick of shavings). Ignition with propane torch was done at only one position, and the fire lasted for about 20 minutes. When the fire ended, there was about 0.5 cm of unburned wood below the soot in the middle of the container, and even more (between 1 and 2 cm) closer to the edges. The highest temperature recorded was 80°C, at 1 cm below the surface.

Ethanol, Isopropanol, Methanol

The liquid solvents, ethanol, isopropanol and methanol were tested. For each test, 1 L of solvent was used. In the case of ethanol, the fire lasted for 3 minutes, and the maximum temperature measured at 1 cm below the surface was 63°C. As expected, most of the solvent percolated into the sand and pooled at the bottom of the aluminum container. The sand remained moist at the end of the burning.

The other solvents tested, isopropanol and methanol, were observed to behave in the same manner as ethanol: the fire did not last for a long time (3 min for isopropanol, and about 2 min for methanol) and the temperature increase in the sand was lower than for the ethanol (Table II).

Sand/Gelled Ethanol Mix

Because the results for the ethanol gel appeared most promising (the temperature at 1 cm below the surface was higher than 100°C), a separate test was performed to determine if the temperature in the soil would be higher if the fuel was first mixed with the top layer of sand. The top 1 cm of sand (~300 mL) was removed from the aluminium container and mixed in a separate vessel with 500 mL of gelled ethanol. This mixture was then returned into the container, so that the thermocouple at 1 cm below the sand surface was at the interface between the 13 cm of sand (below) and the 1 cm of sand-gel mixture (above). The fire burned for approximately 20 minutes and almost no residue was observed. The maximum temperature at 1 cm below the surface was 191°C. The temperatures

recorded for deeper thermocouples were: 92, 65 and 62°C at 2, 5 and 8 cm, respectively. The temperature at 1 cm below the surface was the highest recorded for this phase of the work. Thus, the procedure of mixing sand with fuel seems the most promising for energetics remediation.

Synthetic Ethanol Gel

As the commercial ethanol gel used contained water (% unknown), a gel with a known small proportion of water was sythetically prepared using calcium acetate. Calcium acetate was dissolved in water, and then ethanol was added incrementally, thus forming a gel *in situ*. After each increment, the gel was mixed with an electric blender to ensure good homogenization. The proportions were 17 g of calcium acetate, 50 mL of water and 800 mL of ethanol. This gel was stable, but tended to harden after a couple of hours. Brief mixing in the blender was sufficient to return the gel to its original state.

A volume of 500 mL of sythetic gel was spread over the soil, to a thickness of approximately 1.25 cm on the sand. Two tests were made, and upon ignition, the maximum temperature at 1 cm below the surface was observed to be 52°C for the first test, and 65°C for the second. These temperatures were lower than the temperature reached with the same volume of commercial gelled ethanol (130°C).

Sand/Synthetic Ethanol Gel Mix

The same setup employed for the sand/gelled ethanol mix was used for the tests involving synthetic ethanol gel. The top 1 cm of sand (~300 mL) was removed from the aluminium container and mixed in a separate vessel with 500 mL of synthetic ethanol gel. This mixture was then returned in the container, so that the thermocouple at 1 cm below the sand surface was at the interface between the 13 cm of sand (below) and the 1 cm of sand-gel mixture (above). The fire burned for approximately 19 minutes. The maximum temperature at 1 cm below the surface was 85°C while maximum temperatures recorded for deeper thermocouples were: 69, 47 and 28°C at 2, 5 and 8 cm, respectively. These temperatures are much lower that that obtained from burning the commercial gelled ethanol under the same conditions.

Summary

Our experimental results of these thermal studies confirm that much of the heat of combustion is directed upwards and that sand acts as an insulation barrier. The thicker this barrier, the lower and slower the heat penetration, as can be observed by the slight temperature change from initial room temperature for deeper thermocouples. The use of a thicker layer of combustible did not increase the temperature as the unburned fuel itself acted as an insulation barrier. The most promising fuel tested was the commercial gelled ethanol (Gelled fuel, Home

Presence by Trudeau, Montreal, QC). Mixing the first cm of soil with gel in a 1:1 v/v proportion resulted in a temperature of > 190°C at 1 cm below the sand surface.

Small-Scale Test on Contaminated Soil

Sampling of the contaminated soil surface (0-1 cm depth) and at a depth of 2 cm, was performed before and after the burning. The NG concentrations as determined by HPLC are presented in Table III. The soils showed a significant reduction in NG for the thermal treatments involving gelled ethanol, but the burning of gelled methanol over the soil was not efficient. The temperature during the burning of gelled methanol did not increase enough or burn for a sufficient duration.

Table III. Nitroglycerine (NG) concentration in surface (0-1 cm deep) soil samples before and after various burnings

Thermal process	*[NG] (mg kg^{-1}) before*	*[NG] (mg kg^{-1}) after*	*Reduction (%)*
Gelled ethanol (1 cm thick)	2537	1190	53
Gelled ethanol (1.25 cm thick)	2365	557	76
1st cm of sand mixed with gelled ethanol (~ 1:1 v/v)	2548	152	94
1st cm of sand mixed with gelled ethanol (~ 1:1 v/v) duplicate	2947	235	92
Gelled methanol (1 cm thick)	2075	1847	11

The commercial gelled ethanol provided the most interesting results. When placed directly over the soil, the combustion of gelled ethanol resulted in a decrease of 53% and 76% in NG concentration. When the gel was mixed with the first layer of soil, the reduction in NG concentration was over 90% (mean of two trials). These results are promising, but to provide an increased level of confidence, future trials should include the analysis of more samples before and after burning to determine the amount of variance associated with the decreasing NG concentrations. Presently, these values served as qualitative indicators that the best results were obtained with commercial gelled ethanol.

It should be realized that the systems employed in this study are simplistic, and not precisely representative of conditions that would occure during outdoor tests on an active range or legacy site. The contaminated soil will not exhibit the same conditions as the soil used in the small-scale preliminary test. The presence of humidity, heterogeneous composition (i.e. not only sand), vegetation, a non-uniform particle size distribution, and potentially compacted soil may influence the burning. The influence of these parameters still needs to be investigated.

Field Test on Contaminated Ranges

Results of the HPLC analyses are presented in Table IV. The thermal treatment was observed to decrease the concentration of NG in all samples, except one of the 4 subsurface samples for gel poured directly on the soil. As expected from the large variation in the results, the standard deviations on the average percent NG reduction is very large. This could be related to the fact that each 1 m^2 of soil has potentially different characteristic humidity, presence of vegetation, proportions of small boulders vs. sand, and degree of soil compaction. In the case of samples where the soil was tilled (homogenized) before burning, the standard deviation is significantly lower.

Table IV. Reduction of the NG concentration in soil samples after the thermal treatment

Setup	*Reduction of the NG concentration (dry soil)*		
	%	*Average*	*Standard deviation*
Surface (0-1 cm deep) samples			
Gel poured directly on soil.	26	50	30
	25		
	80		
	60		
Soil tilled (5 cm deep). Gel was added and mixed in the softened soil.	89	87	3
	85		
Soil tilled (5 cm deep). Gel was poured on top.	83	84	2
	86		
Subsurface (2 cm deep) samples			
Gel poured directly on soil.	56	20	30
	1		
	49		
	-14[a]		
Soil tilled (5 cm deep). Gel was added and mixed in the softened soil.	31	40	10
	51		
Soil tilled (5 cm deep). Gel was poured on top.	21	21	3
	25		

[a] indicates an increase in the measured concentration

The decrease in NG concentration was observed to be greatest for the surface samples. This is a consistent observation for all results of other tests presented herein. Heat propagation is not efficient down the soil profile. Results in Table IV also indicate that tilling the soil aids in increasing the efficiency of NG destruction. For the top 1 cm of soil, NG concentration was reduced by 80% when the soil was tilled. Tilling leads to aeration of the soil and oxygen incorporated into the soil helps to sustain combustion, resulting in more heat produced closer to the soil. For the surface soil, there was no clear evidence that mixing with the fuel contributes to increased NG decomposition. For the subsurface samples, there was a small increase NG removal when the gel was mixed with the soil. It should be noted that other EM compounds were also analyzed for by the HPLC method, but only NG was detected. During laboratory tests, soot was not observed on the post-burning samples, but for field tests, soot was observed on the ground after burning. This indicates that the surface remained relatively cool during the field tests and the fuel did not burn completely. This is consistent with the observed reduction in NG concentration being higher for the laboratory tests.

It has now been demonstrated that burning is easily performed on a range, as compared to laboratory tests, which were carried out in the first phases of this work (*36*, *37*), the next step will focus on measurements to evaluate details of the burning process. The temperature at various depths below the burning will again be measured using thermocouples. However, the following properties of soil will be studied prior to burning: humidity, void fraction, soil granulometry and soil type (organic content). Conditions during burning will also be recorded, such as wind speed and air temperature. The analysis of NG metabolites will be performed to complement the NG analysis in the pre- and post-burning soil. Finally, the combustion gases will be sampled and analyzed in the smoke plume over the burning. For a perfect combustion (high temperature and sufficient oxygen), the products should be carbon dioxide and water, but it is likely that the incomplete combustion on the ground will lead to the production of other compounds, such as nitrogen oxides. Taking all of these soil and combustion parameters into account will likely reveal important behaviors and trends that will allow for explanation of our experimental results in a more quantitative manner. This future trial is anticipated to occur over the next year and the results will be available shortly after.

Conclusion

Nitroglycerin (NG) is one of the main contaminants among energetic materials (EM) found at antitank firing positions. An *in situ* thermal treatment was performed directly on a firing position in order to evaluate decreases in the concentration of NG in the surface soil. The burning of an ethanol gel under unknown conditions (humidity, wind, inhomogeneous soil, compaction, presence of vegetation and small boulders), was evaluated as a preliminary qualitative to determine soil decontamination efficacy. The most efficient procedure tested was decompacting the soil by tilling it (5 cm depth) and spreading the ethanol gel on top. Mixing the gel with the top soil only slightly increased NG reduction

for surface soil, but greatly increased the NG reduction for subsurface soil (2 cm deep).

Reduction of more than 80% NG was observed for the surface soil. This procedure was simple and fast to execute. Since decontamination is more significant for surface soil, the best management practice would be to perform decontamination on a regular basis. We recommend regularly implementing this buring strategy on active impact areas. Such a practice should limit NG migration down the soil profile. Such a procedure could be particularly useful for new ranges, where the firing position is free from contamination at deeper layers. In the case of older or former ranges, this procedure would not decontaminate the soil efficiently, unless repeated cycles of deep soil mixing and burnings could be implemented.

Future Work

The decontamination treatment using the burning of an ethanol gel is promising, but it is strongly recommended, before the implementation of the thermal treatment described herein as a regular maintenance activity, that a future study be completed to better quantify and document the burning process. Soil properties (*e.g.* humidity, organic content, heat propagation) and atmospheric conditions (*e.g.* winds, temperature) should be measured during burning experiments. Air sampling and analyses should be performed to determine if toxic gases are emitted during burning. Potential increases in NG metabolites should also be evaluated in the soil samples after burning.

References

1. Jenkins, T. F.; Pennington, J. C.; Ranney, T. A.; Berry, T. E., Jr.; Miyares, P. H.; Walsh, M. E.; Hewitt, A. D.; Perron, N.; Parker, L. V.; Hayes, C. A.; Wahlgren, E. *Characterization of Explosives Contamination at Military Firing Ranges*; ERDC TR-01-5; U.S. Army Engineer Research and Development Center, Cold Regions Research and Engineering Laboratory: Hanover, NH, 2001.
2. Jenkins, T. F.; Thiboutot, S.; Ampleman, G.; Hewitt, A. D.; Walsh, M. E.; Ranney, T. A.; Ramsey, C. A.; Grant, C. L.; Collins, C. M.; Brochu, S.; Bigl, S. R.; Pennington, J. C. *Identity and Distribution of Residues of Energetic Compounds at Military Live-Fire Training Ranges*; ERDC TR-05-10; U.S. Army Engineer Research and Development Center, Cold Regions Research and Engineering Laboratory: Hanover, NH, 2005.
3. Brochu, S.; Diaz, E.; Thiboutot, S.; Ampleman, G.; Marois, A.; Gagnon, A.; Hewitt, A. D.; Bigl, S.; Walsh, M. E.; Walsh, M. R.; Bjella, K.; Ramsay, C.; Taylor, S.; Wingfors, H.; Qvarfort, U.; Karlsson, R.-M.; Ahlberg, M.; Breemers, A.; van Ham, N. *Environmental Assessment of 100 Years of Military Training at Canadian Forces Base Petawawa: Phase 1 – Study of the Presence of Munitions-Related Residues in Soils and Vegetation of*

Main Ranges and Training Areas; DRDC Valcartier TR 2008-118; Defence Research and Development Canada – Valcartier: Quebec, QC, 2009.
4. Jenkins, T. F.; Hewitt, A. D.; Grant, C. L.; Thiboutot, S.; Ampleman, G.; Walsh, M. E.; Ranney, T. A.; Ramsey, C. A.; Palazzo, A. J.; Pennington, J. C. Identity and Distribution of Residues of Energetic Compounds at Army Live-Firing Training Ranges. *Chemosphere* **2006**, *63*, 1280–1290.
5. Hewitt, A. D.; Jenkins, T. F.; Ramsey, C. A.; Bjella, K. I.; Rannay, T. A.; Perron, N. M. *Estimating Energetic Residue Loading on Military Artillery Ranges: Large Decision Units*; ERDC/CRREL TR-05-7; U.S. Army Engineer Research and Development Center, Cold Regions Research and Engineering Laboratory: Hanover, NH, 2005.
6. Pennington, J. C.; Jenkins, T. F.; Ampleman, G.; Thiboutot, S.; Brannon, J. M.; Lynch, J.; Ranney, T. A.; Stark, J. A.; Walsh, M. E.; Lewis, J.; Hayes, C. H.; Mirecki, J. E.; Hewitt, A. D.; Perron, N. M.; Lambert, D. J.; Clausen, J.; Delfino, J. J. *Distribution and Fate of Energetics on DoD Test and Training Ranges: Report 2*; ERDC TR-02-8; U.S. Army Engineer Research and Development Center, Environmental Laboratory: Vicksburg, MS, 2002.
7. Pennington, J. C.; Jenkins, T. F.; Ampleman, G.; Thiboutot, S.; Brannon, J. M.; Clausen, J.; Hewitt, A. D.; Brochu, S.; Dubé, P.; Lewis, J.; Ranney, T. A.; Faucher, D.; Gagnon, A.; Stark, J. A.; Brousseau, P.; Price, C. B.; Lambert, D. J.; Marois, A.; Bouchard, M.; Walsh, M. E.; Yost, S. L.; Perron, N. M.; Martel, R.; Jean, S.; Taylor, S.; Hayes, C. H.; Ballard, J. M.; Walsh, M. R.; Mirecki, J. E.; Downe, S.; Collins, N. H.; Porter, B.; Karn, R. *Distribution and Fate of Energetics on DoD Test and Training Ranges: Interim Report 4*; ERDC TR-04-4; U.S. Army Engineer Research and Development Center, Environmental Laboratory: Vicksburg, MS, 2004.
8. Pennington, J. C.; Jenkins, T. F.; Ampleman, G.; Thiboutot, S.; Brannon, J. M.; Hewitt, A. D.; Lewis, J.; Brochu, S.; Diaz, E.; Walsh, M. R.; Walsh, M. E.; Taylor, S.; Lynch, J. C.; Clausen, J.; Ranney, T. A.; Ramsey, C. A.; Hayes, C. A.; Grant, C. L.; Collins, C. M.; Bigl, S. R.; Yost, S.; Dontsova, K. *Distribution and Fate of Energetics on DoD Test and Training Ranges: Final Report*; ERDC TR-06-13; U.S. Army Engineer Research and Development Center, Environmental Laboratory: Vicksburg, MS, 2006.
9. Thiboutot, S.; Ampleman, G.; Marois, A.; Gagnon, A.; Bouchard, M.; Hewitt, A.; Jenkins, T.; Walsh, M.; Bjella, K. *Environmental Condition of Surface Soils and Biomass Prevailing in the Training Area at CFB Gagetown, New Brunswick*; DRDC Valcartier TR 2003-152; Defence Research and Development Canada – Valcartier: Quebec, QC, 2004.
10. Thiboutot, S.; Ampleman, G.; Marois, A.; Gagnon, A.; Bouchard, M.; Hewitt, A.; Jenkins, T.; Walsh, M.; Bjella, K.; Ramsey, C.; Ranney, T. A. *Environmental Conditions of Surface Soils, CFB Gagetown Training Area: Delineation of the Presence of Munitions Related Residues (Phase III, Final Report)*; DRDC Valcartier TR 2004-205; Defence Research and Development Canada – Valcartier: Quebec, QC, 2003.
11. Jenkins, T. F.; Ranney, T. A.; Hewitt, A. D.;Walsh, M. E.; Bjella, K. L. *Representative Sampling for Energetic Compounds at an Antitank*

Firing Range; ERDC/CRREL TR-04-7; US Army Engineer Research and Development Center: Hanover, NH, 2004.
12. Pennington, J. C.; Jenkins, T. F.; Ampleman, G.; Thiboutot, S.; Brannon, J. M.; Lewis, J.; Delaney, J. E.; Clausen, J.; Hewitt A. D.; Hollander, M. A.; Hayes, C. A.; Stark, J. A.; Marois A.; Brochu, S.; Dinh, H. Q.; Lambert, D.; Gagnon, A.; Bouchard, M.; Martel, R.; Brousseau, P.; Ranney, T. A.; Gauthier, C.; Taylor, S.; Ballard, J. M. *Distribution and Fate of Energetics on DoD Test and Training Ranges: Interim Report 3*; ERDC TR-03-2; US Army Engineer Research and Development Center: Vicksburg MS, 2003.
13. Walsh, M. E.; Ramsey, C. A.; Collins, C. M.; Hewitt, A. D.; Walsh, M. R.; Bjella, K. L.; Lambert, D. J.; Perron, N. M. *Collection Methods and Laboratory Processing of Samples from Donnelly Training Area Firing Points, Alaska, 2003*; ERDC/CRREL TR-05-6; US Army Engineer Research and Development Center: Hanover, NH, 2005.
14. Diaz, E.; Brochu, S.; Thiboutot, S.; Ampleman, G.; Marois, A.; Gagnon, A. *Energetic Materials and Metals Contamination at CFB/ASU Wainwright, Alberta, Phase l*; DRDC Valcartier TR 2007-385; Defence Research and Development Canada – Valcartier: Quebec, QC, 2008.
15. Thiboutot, S. Personnal communication, Defence Research and Development Canada – Valcartier, QC, Canada, 2008.
16. Thiboutot, S.; Ampleman, G.; Gagnon, A.; Marois, A.; Martel, R.; Bordeleau, G. *Persistence and Fate of Nitroglycerin in Legacy Antitank Range*; DRDC Valcartier TR 2010-059, Defence Research and Development Canada – Valcartier: Quebec, QC, 2010.
17. United States Department of Labor, Occupational Safety & Health Administration, Occupational Safety and Health Guideline for Nitroglycerin. http://www.osha.gov/SLTC/healthguidelines/nitroglycerin/recognition.html.
18. Pennington, J. C.; Clausen, J.; Jenkins, T. F. *Introduction, Chapter 1 in Distribution and Fate of Energetics on DoD Test and Training Ranges: Interim Report 3*; ERDC TR-03-2; U.S. Army Engineer Research and Development Center, Environmental Laboratory: Vicksburg, MS, 2003.
19. National Defence, Operational Training, Volume 3, Part 2. *Range Construction and Maintenance*; B-GL-381-002/TS-000; Ottawa, ON, 2005.
20. National Defence, Operational Training, Part 3. *Range and Unexploded Explosive Ordnance (UXO) Clearance Handbook*; B-GL-381-003/TS-000; Ottawa, ON, 2008.
21. National Defence, Operational Training. *Range Construction and Maintenance (Draft)*; B-GL-381-002/TS-000; Ottawa, ON, 2008.
22. Federal Remediation Technologies Roundtable. *Remediation Technologies Screening Matrix and Reference Guide*, Version 4.0; USA, 2008. http://www.frtr.gov/matrix2/top_page.html.
23. Martin, A.; Larson, S.; Davis, J.; Felt, D.; Fabian, G.; O'Connor, G. *Open Burn/Open Detonation (OB/OD) Management Using Lime for Explosives Transformation*; SERDP & ESTCP's Partners in Environmental Technology Technical Symposium & Workshop, Washington D.C., USA, 2008.

24. Fact sheet, project CP-1305, Strategic Environmental Research and Development Program (SERDP). http://www.serdp.org/Research/upload/CP-1305.pdf.
25. Battelle, Integrated Science & Technology, Inc., and University of Rhode Island. *Technical Report for Impacts of Fire Ecology Range Management (FERM) on the Fate and Transport of Energetic Materials on Testing and Training Ranges*; Contract No. DACA72-02C-0038; SERDP Environmental Restoration Program – 1305, 2006.
26. Hubbard, R. M.; Vose, J. M.; Clinton, B. D.; Elliott, K. J.; Knoepp, J. D. Stand Restoration Burning in Oak-Pine Forests in the Southern Appalachians: Effects on Aboveground Biomass and Carbon and Nitrogen Cycling. *For. Ecol. Manage.* **2004**, *190*, 311–321.
27. Hartford, R. S.; Frandsen, W. H. When It's Hot, It's Hot… Or Maybe It's Not! (Surface Flaming May Not Portend Extensive Soil Heating). *Int. J. Wildland Fire* **1992**, *2* (3), 103–144.
28. Frandsen, W. H.; Ryan, K. C. Soil Moisture Reduces Below Ground Heat Flux and Soil Temperatures Under a Burning Fuel Pile. *Can. J. For. Res.* **1986**, *16*, 244–248.
29. Hussain, G.; Rees, G. J. Thermal Decomposition of RDX and Mixtures. *Fuel* **1995**, *74* (2), 273–277.
30. Price, R. A. *Thermal Treatment of Composition B Residues by Wildfire and Managed Burns*; The 237th ACS National Meeting, Salt Lake City, UT, March 22−26, 2009.
31. Marois, A.; Gagnon, A.; Thiboutot, S.; Ampleman, G.; Bouchard, M. *Caractérisation des sols de surface et de la biomasse dans les secteurs d'entraînement, Base des Forces canadiennes, Valcartier*; DRDC Valcartier TR 2004-206; Defence Research and Development Canada – Valcartier: Quebec, QC, 2004.
32. United States Environmental Protection Agency. Method 8330b, Nitroaromatics, Nitramines and Nitrate Esters by High Performance Liquid Chromatography (HPLC), United States, October 2006. http://www.epa.gov/waste/hazard/testmethods/pdfs/8330b.pdf.
33. Jenkins, T. F.; Hewitt, A. D.; Walsh, M. R.; Walsh, M. E.; Bailey, R. N.; Ramsey, C.; Bigl, S. R.; Lambert, D. J.; Brochu, S.; Diaz, E.; Lapointe, M.-C.; Poulin, I.; Faucher, D. Accumulation of Propellant Residues at Small Arms Firing Points. *Characterization and Fate of Gun and Rocket Propellant Residues on Testing and Training Ranges: Final Report*; ERDC Technical Report 08-1; US Army Engineer Research and Development Center, Cold Regions Research and Engineering Laboratory: Hanover, NH, 2008; Chapter 8.
34. Dubé, P.; Ampleman, G.; Thiboutot, S.; Gagnon, A.; Marois, A. *Characterization of Potentially Explosives-Contaminated Sites at CFB Gagetown, 14 Wing Greenwood and CFAD Bedford*; DREV-TR-1999-137; Defence Research Establishment Valcartier: Val-Belair, QC, 1999.
35. Thiboutot, S.; Ampleman, G.; Marois, A.; Gagnon, A.; Gilbert, D.; Tanguay, V.; Poulin, I. *Deposition of Gun Propellant Residues from 84-mm Carl*

Gustav Rocket Firing; DRDC Valcartier, TR 2007-408; Defence Research and Development Canada – Valcartier: Quebec, QC, 2008.
36. Poulin, I.; Nadeau, G.; Gagnon, A. *Development of a Remediation Strategy for Surface Soils Contaminated with Energetic Materials by Thermal Processes*; DRDC Valcartier, TR 2009-150; Defence Research and Development Canada – Valcartier: Quebec, QC, 2009.
37. Poulin, I.; Marois, A. *In-Situ Nitroglycerin Decontamination of an Antitank Firing Position: Development of a Remediation Strategy for Surface Soils Contaminated with Energetic Materials by Thermal Process, Phase 4*; DRDC Valcartier, TM 2010-194; Defence Research and Development Canada – Valcartier: Quebec, QC, in press.

Chapter 21

Residual Dinitrotoluenes from Open Burning of Gun Propellant

Emmanuela Diaz,* Sylvie Brochu, Isabelle Poulin, Dominic Faucher, André Marois, and Annie Gagnon

Energetic Materials Section, Defence Research and Development Canada-Valcartier, 2459 Pie-XI Blvd North, Quebec (Qc) G3J 1X5, Canada
***Emmanuela.diaz@drdc-rddc.gc.ca**

Following military live fire artillery training, excess propellant bags are routinely open-burned at the firing site. Combustion of these propellants are typically incomplete under these conditions in the field, resulting in residues deposited on the soil surface, such as nitroglycerine and dinitrotoluenes. To better assess the amount of contaminants released during this process, burning tests were conducted with propellant bags from 105- and 155-mm munitions used for howitzer guns. Three different "activities" or burning tests were performed to achieve this study, which are described here. Residual 2,4- and 2,6-dinitrotoluene (DNTs) were analysed in all collected samples.

Introduction

At the end of most military exercises involving large caliber ammunition, such as 105- and 155-mm howitzers, trainees are usually left with a surplus quantity of unused gun propellant. Propellant charges for various large caliber ammunition are supplied in bags of known propellant quantity, from which a certain number are chosen for selective targeting at various distances. Propellant bags not used during the training exercise are destroyed on-site by open burning. For example, the firing of 30,000 rounds of 105-mm ammunition results in the burning of approximately 20,000 kg of single base propellant. If the propellant used were designated with bag numbers 6 and 7, this results in 641 g per round or 50 % in mass of the propelling charge (given that the single base propellant formulation contains 10 %

Published 2011 by the American Chemical Society

of dinitrotoluene compounds (DNTs) (*1*), resulting in 2000 kg of DNTs burned). As the combustion is not complete during open burning of surplus propellant stocks, this quantity is considered a potential source of pollution for ranges and training aeas (RTAs).

In Canada, open burning of excess gun propellant was prohibited in 2010. Prior to this policy (and when this study was executed), excess propellant bags were routinely disposed of through open burning. Although outlawed in Canada, nevertheless, this method of disposal continues to be employed in other countries. Figure 1 shows the visual trace of this disposal technique when conducted on ice, snow and on bare soil.

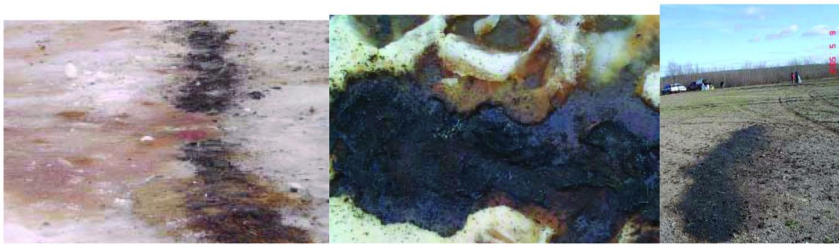

Figure 1. Residual contamination from open burning on ice, snow and soil.

The main pollutants released from burned propellants are 2,4- and 2,6-DNT, nitroglycerine (NG) and Pb. Soil contamination by DNTs and Pb are legislatively controlled by limit thresholds (see Table 1). Past studies have demonstrated that open burning of gun propellant can serve as a source of contamination and, consequently, potentially impact the environment (*2–4*). In fact, concrete burning pads were constructed for burning excess gun propellant at fixed locations in training areas to avoid deposition of unburned residues on soil. Pb and 2,4- and 2,6-DNT were measured in the soil as 60,000, 490 and 30 mg kg^{-1}, respectively (*4*). In another study, 40 burning points were sampled for propellants in soil over a 50 x 100 m area (*3*) with special care taken to remove all unburned propellant grains before analysis as to not affect the measurements. Concentrations of 770 and 30 mg kg^{-1} soil for 2,4- and 2,6-DNT were measured, respectively.

Badger Army Ammunition Plant was used intermittently over a 33-year period to produce single and double base propellants for gun, rocket and small arms ammunition. The disposal area used between 1942 and 1983 to burn waste propellant and as well as other process chemicals, created a point source of 2,4-, 2,6-DNT and Pb that resulted in a three-mile long plume of contaminated groundwater. This plume has migrated offsite of the facility and has been detected in private drinking water wells. Currently, a decontamination process is underway by the U.S. government to cleanup this disposal site, at an estimated cost of $250 million U.S. dollars (*5*).

Table 1. Soil contaminant standards from U.S. Environmental Protection Agency (EPA), Quebec, Ontario and Canada.[a]

Soil standards					
Residential/Parkland, mg/kg					
	Quebec	*Ontario*	*Canada (CCME[b])*	*Maryland*	*Region 3[c] USA*
2,4-DNT	0.04	1.1	N.A.	16	1.6
2,6-DNT	2×10^{-4}	N.A.	N.A.	7.8	61
Dibutylphtalate	6	N.A.	N.A.	780	6.1×10^{3}
Lead	500	200	140	400	400
Industrial, mg/kg					
2,4-DNT	1.7	N.A.	N.A.	200	5.5
2,6-DNT	3×10^{-2}	N.A.	N.A.	100	620
Dibutylphtalate	7×10^{4}	N.A.	N.A.	1.0×10^{4}	6.2×10^{4}
Lead	1000	1000	600	1000	800

[a] N.A. = not available. [b] CCME for Canadian Council of Ministers of the Environment.
[c] Region 3 corresponds to the mid-Altantic states (Delaware, District of Columbia, Maryland, Pennsylvania, Virginia, and West Virginia).

The objective of this study was to measure the residual concentration of 2,4- and 2,6-DNT after open burning of single base gun propellant. Three activities were performed: (1) February 2005 at Canadian Forces Base (CFB) Valcartier; (2) March 2005 at CFB Valcartier (DRDC experimental test site) and; (3) May 2005 at CFB Gagetown. Activities 1 and 3 consisted of collecting samples after the burning of an unknown number of bags during live firing events, while Activity 2 was a trial planned by DRDC where various experimental tests were performed on snow-covered ground to evaluate the mass of residues generated. Activities 1 and 2 were performed over snow-covered ground while sampling during Activity 3 was performed on the soil surface (*6*).

Experimental

Propellant Charges

The gun propellant used in 105- and 155-mm munitions during soldier training exercises was a single base formulation named M1, which is composed of 85 % nitrocellulose, 10 % 2,4-DNT, approximately 5 % dibutlyphtalate and 1 % potassium sulphate. M1 also contains 2,6-DNT, a by-product of 2,4-DNT synthesis. For both gun calibers, the propellant is separated into charges of various weight and loaded into a polyester-viscose rayon cloth bag marked with the

increment or charge number (*1*). This system allows the soldier to withdraw one or more bags to adjust the charge depending on the target position. The propelling charge for the 105-mm munitions was M67, which consists of approximately 1.28 kg of gun propellant divided into 7 increment charges. Increment charge 5 incorporates a piece of Pb foil as a decoppering agent for the barrel of the Howitzer. The propelling charge for the 155-mm caliber was the M4A1 (M4 series), which is divided in 5 bags (numbers 3 to 7) and their total weight is 6.098 kg (*7*). No Pb is added to bags for the 155-mm munitions.

Experimental Design and Sampling Approach

Three main "activities" defined as propellant burn tests were performed in this study: burn tests for Activities 1 and 2 were conducted over snow-covered ground while Activity 3 was conducted over bare soil. Burn tests in Activities 1 and 3 (described in the following paragraphs) were conducted in conjunction with pace and tempo of live-fire training exercises. Thus, the exact number of propellant bags was not known, but estimated from a photography taken before burning commence. In contrast, Activity 2 was carried out by the DRDC team under more controlled conditions, where the exact quantity of propellant burned was known.

Activities 1 and 3

Activity 1 took place during an artillery exercise where 105-mm munitions were fired. Sample collection was adapted to interfere as little as possible with military training. For this reason, it was not possible to exactly count the number of propellant bags they were burned by the soldiers.

However, the number of bags were estimated from a digital image of the propellant stacks taken before the burning. From this image, we estimated that approximately 45 bags of charges numbers 5, 6 and 7 were placed along the ground in a line or row of approximately 1.8 m before burning, equaling a total gun propellant mass of 11.7 kg. After the propellant burn, and active training was concluded, the DRDC team divided the disposal "line" into three segments of 60 cm length for sampling. Snow cover remaining in each 60-cm segment after the propellant burn was collected in plastic bags and sealed until further processing (see Figure 2).

For Activity 3, propellant was burned following active artillery training with 105-mm howitzer ammunition (*8*). Images of the stacked propellant bags before and after burning are shown in Figure 3. Propellant residue grains were collected by sampling at 25 to 30 increments along the length of the burned row, taking great care to collect only residues and avoid incorporating soil into the sample.

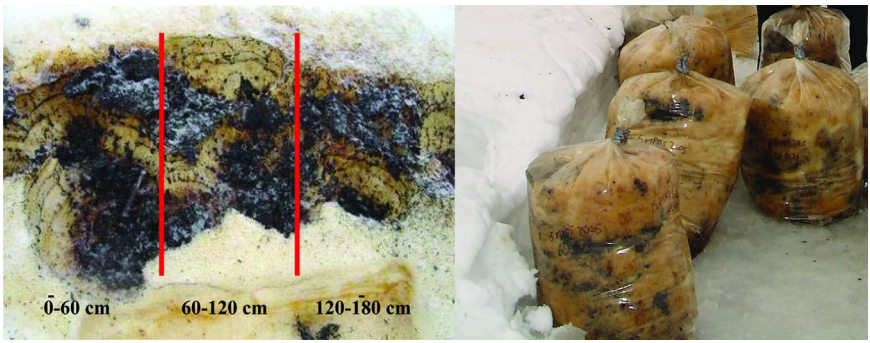

Figure 2. Row of gun propellant bags residues (left) and sampling in plastic bags (right).

Figure 3. Line of bags before (left) and after (right) the burning on the ground.

Activity 2

Activity 2 involved burning tests of stacks of propellant which were placed by the DRDC team over areas of snow cover. Since these tests were not performed as part of a military training exercise, we were better able to control experimental conditions and parameters related to testing. For these tests, we had available sixty complete cartridges of propellant for 155-mm munitions to study the effect of different patterns of burning on the quantity of residual material. All burnings were conducted on pristine snow cover. Although the sampling team attempted to exhaustively collect the majority of residual material on the test area, a yellow color was still apparent in the snow afterwards.

Activity 2 was conducted in two parts: first, tests were conducted with individual bags of propellant, as shown in Figure 4a. We performed one burning per bag (number 3, 4, 5, 6 and 7) totalling five burnings.The second part of Activity 2 involved the simultaneous burning of multiple propellant bags placed in line as shown in Figure 4b, similar to what is done following live-fire exercises. For this part of Activity 2, five replicate rows containing 15 bags of gun propellant each were burned, while only one row composed of 30 propellant bags and

another row composed of 60 propellant bags were burned, with the length of each row ranging from 5 to 8 m.

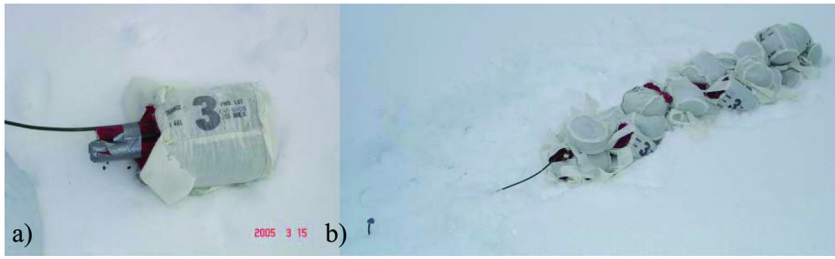

Figure 4. a) Individual bag; b) Row of 30 bags before their burning.

Burning the propellant over the snow-covered ground presented some unique challenges. The burning area was easily noticeable in the snow by its yellow color. However, sampling this clearly visible area provided difficulties since the heat of the reaction melted the overlying snow cover. This resulted in the ready leaching of propellant contaminants into the underlaying soil material. This yellow color was visually apparent to a depth of 65 cm below the soil surface, therefore samples were collected down to this depth as well. The yellow color is observed after propellant burning over ice and in snow, arising from the incomplete combustion of the gun propellant. This color was not observed when burning was performed over bare soil.

As burning tests for the rows of propellant containing 15 bags was replicated five times, we were able to calculate meaningful statiscial parameters. Calculations showed that the variance of the mean residual 2,4-DNT can be calculated to estimate the error associated with the mean percentage of residual 2,4-DNT. The result obtained is 0.0003 as the variance on the mean percentage that is 0.08%. However, this error is underestimated since the area of contamination was not completely collected. Thus, a significant error can be associated to the residues left on the snow after the collection of samples. We concluded to not provide an estimated error to this work for these reasons. Yet, this problem does not detract from the larger aim of this study, which is to determine if open burning of gun propellant leaves residual contamination. The contamination was probably more underestimated for the burning of several bags as compared to the individual bag burnings, since the extent of the burn area was more significant in this first case. In fact, the extent of contamination, i.e. the yellow contamination trace, was lower for individual bag burning than for the burning of several bags.

The percentage of residual 2,4-DNT reported in the following tables were calculated by dividing the mass of residual 2,4-DNT by the initial mass of gun propellant burned. This percentage allows an easy calculation of the mass of 2,4-DNT left in snow after the burning of a known quantity of single base gun propellant.

Sample Processing, Extraction, and Analysis

For soil samples, residues were air-dried in the dark, and then homogenized by adding acetone until a slurry was formed after which the acetone was evaporated. For snow samples, the collected snow was melted and the water was evaporated in a pail to recuperate the residues from the burning. The estimated mass loss from the evaporation of sample water and from the collection and transfer of residues from the pail to the extraction media ranged from 2 to 15%. Propellant residues recovered from snow and soil samples were sieved using a 25-mesh sieve (< 710 µm). Afterwards, an 8 g composite subsample was generated by randomly collecting several increments from the entire processed sample. This incremental samping approach was used in order to provide the greatest homogeneity in the subsample. This composite subsample was then placed in an amber vial and mixed with acetonitrile (10 to 20 mL) for 1 min, and then extracted using an ultrasonic water bath for 18 h. The vials were then centrifuged for 60 min at 2000 rpm and the supernatant was collected. The supernatant was diluted with a 1:1 acetonitrile to water mixture. Afterwards, a 2-mL volume of the mixture was removed and then diluted with another 2-mL volume of 1% calcium chloride. This mixture was then filtered through a 0.45 µm filter and the filtrate analyzed by high performance liquid chromatography (HPLC).

High Performance Liquid Chromatography (HPLC) (8)

All extracts were maintained at 4°C in the dark until analyzed by HPLC according to an in-house procedure based on EPA method 8330B (1994) (*9*). Dissolved propellant concentrations were determined using an Agilent HP 1100 HPLC system equipped with an ultraviolet (UV) diode array detector, which was set for simultaneously monitoring absorbances at 210, 220, and 254 nm during the chromatographic separation. During the separation, a 20 µL was injected into 15:85 isopropanol/water (v/v) mobile phase pumped at a flow rate of 0.75 mL min^{-1}. The separation was conducted across a Supelcosil LC-8 column (25 cm x 3 mm x 5 µm) stationary phase. The column temperature was maintained at 25 °C during the analysis. Standards and solvents were diluted 1:1 acetonitrile to water. Sample elutions were compared to a set of 14 standard energetic and propellant compounds, including HMX, RDX, 1,3,5-trinitrobenzene (TNB), 1,3-dinitrobenzene (DNB), nitrobenzene (NB), trinitrotoluene (TNT), tetryl, NG, 2,4-DNT, 2,6-DNT, 2-A-DNT, 2-nitrotoluene (NT), 3-NT, and 4-NT.

Results

Activity 1

Table 2 shows the total mass of 2,4-DNT obtained after burning propellant for 105-mm ammunition over snow following a live-fire training event. In some cases, evaporation of the water from the snow resulted in residue particles that were strongly agglomerated at the bottom of the pail. This made it extremely

difficult to pass these particles through the 25-mesh sieve as described in experimental methods section. For this reason, some sample collected along the 1.8 m row of propellant bags was not analyzed. In the first 60 cm segment, the two samples of snow collected were analyzed, while for 60-120 cm segment, two of the three samples of snow collected were analyzed. Finally, one of the three samples collected from the 120-160 cm was analyzed.

Table 2. Residual 2,4-DNT quantites detected after burning over pristine snow cover during Activity 1. Distances indicate specific segments collected along the 1.8 m row of stacked propellant bags as described previously.

Sample	*2,4-DNT*	*residual 2,4-DNT*
	g	*%*
0-60 cm bag 1	0.53	0.07
0-60 cm bag 2	2.15	0.07
60-120 cm – bag 1	4.07	0.1
60-120 cm – bag 3	0.13	0.1
120-180 cm	4.94	0.13

When duplicate samples were collected from the same area, it was observed that the mass of 2,4-DNT was greater for the first collected sample (4.07 g) than that collected in the second duplicate (0.13 g). Obviously, this represented the fact that exhaustive sampling for the first duplicate greatly reduced the quantity of residue left for the second duplicate sample.

The calculated total mass of 2,4-DNT found in the propellant residues was 12 g. It was estimated that this mass represented approximately 45 bags of gun propellant that were burned. Assuming that 15 bags per row were burned, i.e. 3900 g of gun propellant with a homogeneous distribution of bags # 5, 6 and 7 (*1*), then we calculate that on average, the burned residue contained 0.1 % 2,4-DNT (i.e., 0-60 cm contained 0.07 %; 60-120 cm: 0.1 % and 120-180 cm: 0.13 %). Note that this calculation of the mass of 2,4-DNT in the burning residues was normalized by the initial mass of gun propellant, multiplied by 100. It was calculated that the proportion of 2,6-DNT in the residues varied from 0 to 4 %.

Activity 2

Activity 2 involved burning tests of 155-mm ammunition on snow cover under more controlled conditions than Activities 1 and 3, since the number of bags burned was known exactly and different strategies of burning conditions were experimented. The first stage of this test was to burn the individual bags of propellant (bags # 3, 4, 5, 6 and 7) on a pristince snow cover (see Figure 4a). The results obtained for each charge are presented in Table 3. The quantity of 2,4-DNT recovered ranged from 0.04 to 0.13% (or an average 0.08%) of the total

residue mass. We attempted to relate the quantity of 2,4-DNT remaining in the burned residues to the initial quantity of propellant contained in each particular bag (e.g., # 3, 4, 5, 6, 7), but in the end, found no relationship between these parameters. Therefore, the quantity of 2,4-DNT contained within the residual material collected over the snow cover cannot be statistically correlated with the initial quantity of propellant before burning. Measurements of 2,6-DNT (data not shown) demonstrated that the quantity of this compound ranged from 2 to 3 %.

Table 3. Quantity of residue and 2,4-DNT recovered following burning of individual bags of propellant over a pristine snow cover.

Charge number (mass of the bag)	*solid residues*	*solid residues*	*2,4-DNT*	*residual 2,4-DNT*
	g	*%*	*g*	*%*
4 (0.524 kg of gun propellant)	91.8	17	0.40	0.08
5 (0.779 kg of gun propellant)	12.5	2	0.28	0.04
6 (1.261 kg of gun propellant)	54.2	4	0.48	0.04
7 (1.530 kg of gun propellant)	36.3	2	2.01	0.13
3 (1.814 kg of gun propellant)	37.9	2	1.59	0.09

Our inability to correlate initial mass of DNT with residual quantity left in unburned propellant particles suggests a link between the different scenarios in which propellant bags are stacked and oriented before burning. Thus, the second stage of Activity 2 involved determining the quantity of residue material and the concentration of 2,4-DNT remaining with that material under different burning scenarios. In particular, propellant bags are typically stacked in a row by soliders after live-fire exercises and burned all at once, as opposed to burned individually as performed in the first stage of Activity 2. For this work, three different scenarios were tested. First, five replicate rows consisting of 15 bags of propellant each were burned. Afterwards, these rows were sampled and analyzed as previously described. The data (Table 4) shows that quantity of 2,4-DNT measured within the residue material was statiscially reproducible. Measured quantities of 2,4-DNT ranged from 0.04 to 0.09% total mass of the burned residue material.

The second scenario involved burning one row consisting of 30 bags of propellant, while the third experimental scenario involved burning of one row consisting of 60 propellant bags. The quantity of residual 2,4-DNT (Table 4) after burning the row with 30 bags of propellant was 36.3 g (0.1% total residue mass), while the residual 2,4-DNT concentration from the row with 60 bags was 22.1 g (0.03% total residue mass). The lower quantity of 2,4-DNT recovered from the row with 60 propellant bags may be in part explained by the fact that the residue material was spread out over a larger area than expected, making it more difficult to exhaustively sample the site. Thus, this difficulty must be resolved before a more extensive interpretation of the data can be offered. In addition, we again

did not observe any correlation between the initial and final concentrations of 2,4-DNT remaining in the residue material.

Table 4. Quantity of total residue material and 2,4-DNT recovered after burning bags of propellant over a pristine snow cover.

Scenario (initial mass of gun propellant)	*solid residue*	*2,4-DNT*	*residual 2,4-DNT*
	g	*g*	*%*
15 bags, burn 1 (18.294 kg)	406.0	11.5	0.06
15 bags, burn 2 (18.294 kg)	427.0	16.8	0.09
15 bags, burn 3 (18.294 kg)	394.3	13.4	0.07
15 bags, burn 4 (18.294 kg)	538.6	12.2	0.07
15 bags, burn 5 (18.294 kg)	275.7	7.3	0.04
30 bags (36.588 kg)	808.7	36.3	0.10
60 bags (73.176 kg)	1681.0	22.1	0.03

From the mean percentage, i.e. 0.07 %, it is possible to estimate the amount of 2,4-DNT left on snow after the burning of a known mass of single base gun propellant. For example, if 10 kg of gun propellant is burned on snow, approximatively 7 g of 2,4-DNT will be released in the environment. As we failed to exhaustively recover the residue from the burn area, , we believe the results are underestimated as mentioned earlier in the text. The proportion of 2,6-DNT of the total DNTs recovered varied from 1 to 3 %.

Activity 3

Activity 3 consisted of the open burning of gun propellant bags during live fire exercises, where the exact number of propellant bags that were burned was unknown. However, burns were conducted over bare soil as opposed to pristine snow cover . Two different sites were sampled following live-fire exercises. For this particular test, soil samples were collected from the burn area in duplicate, processed, and anlayzed as described previously, however, care was taken to remove the propellant residue from the collected soil sample. The results from these tests are presented in Table 5. The mean concentrations of 2,4-DNT detected at the two sites were 700 ± 100 and 345 ± 5 mg kg^{-1} soil, respectively, This can be explained by the fact that a larger number of propellant bags were burned at Site 1 than Site 2, which, of course, is a sensible result. Also, we measured for the first time, quantities of 1,3-DNB in the soil samples – something not found in the tests over pristine snow cover. . The proportion of 2,6-DNT of the total DNTs in the soil ranged from 4 to 5 %.

Table 5. Energetic materials detected in samples collected at Sites 1 and 2 during Activity 3.[a]

Sample	*1,3-DNB*	*2,4-DNT*	*2,6-DNT*
	mg/kg	*mg/kg*	*mg/kg*
Gun propellant burning-Site 1	1.7	740	39
Gun propellant burning-Site 1 DUP	1.2	550	25
Gun propellant burning-Site 2	1.0	340	14
Gun propellant burning-Site 2 DUP	1.0	350	13

[a] DUP = field duplicate

Discussion

Alternative Methods to the Burning of Gun Propellant

DRDC Valcartier studied the effect of burning composition M1 single base propellant directly over soil and a pristine snow cover. Burning of the propellant material was overwhelmingly incomplete, as demonstrated by Activities 1 and 2, leaving behind significant quantities of residue particles, and relatively high concentrations of dintrotoluene compounds. Incomplete combustion of the propellant over the snow cover seemed to be in part, attributed to the melting and subsequent consumption of the energy by the resulting water, resulting in a less complete combustion. The following discussion explains briefly the different approaches suggested by DRDC Valcartier to minimize the accumulation of toxic compounds, such as 2,4-DNT and NG (if double base propellant is used) in the environment from propellant burning.

Incorporation of Modular Charge Artillery System

The Modular Charge Artillery System (MACS) was developed to increase the efficiency of propellant use for weapons, while minimizing the excess left over after training. "MACS uses a "build-a-charge" concept in which all M231 and M232 increments are identical in the lot, eliminating the need to dispose of unused increments. Unused increments are retained for future use. MACS propellants are transported and handled in the same manner as other conventional propellants" (*10*). This system has been available for 155-mm howitzer guns since 2003. Military personnel confirmed to DRDC scientists that no burning of excess propellant occurs with the use of the MACS.

Recycling of the Excess of Gun Propellant

Excess bags of propellant following live firing exercises can be returned from the field and placed in a secure magazine, for later collection, reprocessing, and use as new gun propellant.

A New Burning Scenario

It is obvious that the current scenario of open burning does not promote the complete combustion of the propellant compounds. A new scenario should be designed to ensure more complete combustion. For example, the propellants could be burned using a field reactor, engineered for more complete combusion under higher temperature and pressure. However, such an engineering solution is probably not feasible or conducive to field situations, where the warfighter may be required to stringently follow a particular protocol or require additional equipment to achieve this. Moreover, with such an approach, no detonation will occur if the mass of gun propellant bags burned does not exceed the critical mass needed to obtain a deflagration to detonation transition.

Burning Gun Propellant in Metal Pans Placed in the Field

In some installations, excess of gun propellant after live-fire exercise are burned after placing the material in large metal pans (*11*). Under this scenario, propellant residues after the burn are concentrated in a single location, avoiding the potential for dispersing the materials onto the soil or surface waters. Althought deployed on a number of military bases, burning propellant on concrete pad is not recommended since the concrete can fracture with seasonal fluctuations, allowing for leaching of the residues with rainfall, and migration into the environment.

Incinerator

The excess of gun propellant could also be simply burned in an incinerator. Such conditions could ensure more complete control of burn conditions, while catching residue material and prevent spread into the environment. Moreover, an incinerator can reduce the gaseous or particulate emissions during the burning process when equipped with the proper gaseous emissions scrubbers (*12*).

Conclusion

Activity 1 demonstrated that open burning of excess gun propellant bags was incomplete, resulting in leftover residue material containing relatively high concentrations of dinitrotoluenes. 2,4-DNT quantities were on average 0.1 %. In Activity 2, different scenarios of burning were tested, showing that there was little

difference in the quantity of residue and dinitrotoluenes whether the propellant bags were burned or in stacks or rows. Activity 3 represented a sampling event following live-fire exercises, where propellant burning was tested over bare soil as opposed to a pristine cover of snow.

In general, burning the excess bags of propellant over the pristine snow cover seemed to result in greater concentrations of residual dinitrotoluene than when burned over bare soil. It was hypothesized that this was a result of the energy loss attributed to the absorption and metling of the snow during the burn. Thus, less energy was available to combust the propellant itself. This melting, coupled with the permeation of the snow melt into the soil, made complete sampling of the snow material impossible. Thus, we expect that dinitrotoluene concentrations measured from open burning over snow are underestimates.

A similar study, conducted by Walsh et al. (*13*), showed that the burning of single base propellant over bare soil (wet and dry moisture conditions) of single base propellant left approximately 0.9 % of residual 2,4-DNT relative to the initial mass of 2,4-DNT present in the formulation (note that in this study, the percentage is calculated by dividing the mass of 2,4-DNT detected with the total mass of gun propellant burned). Given that the proportion of 2,4-DNT in single base propellant is 10%, a similar percentage was obtained if our result is converted to obtain the residual 2,4-DNT over the initial 2,4-DNT (0.8%), as Walsh et al. reported. However, this similarity is surprising since in this study the burning was performed on snow while their tests were performed over clean sand. No reason was found to explain why the residual 2,4-DNT is similar in both cases, as the combustion was supposed to be affected by the snow and, consequently, the water produced during the melting of the snow. This reaction should decrease the rate of the combustion inducing a less complete combustion.

Future work should be carried out with known quantities of gun propellant bags burned over bare soil to obtain more accurate estimates of dinitrotoluenes remaining in the residual material. In this study, the unburned residues seemed less dispersed on the soil than on the pristine snow cover. We hypothesized that the snow covered absorbed the heat energy intended for burning the excess propellant by melting the snow, thus reducing the efficiency of combustion of the propellant bags.

Finally, we recommend that in order to avoid or limit the residual contamination due to the burning of excess propellant, some important alternatives should be considered, as discussed previously. These alternatives include: 1) employing modular charges (e.g., MACS) for weapons, such as the 155-mm munitions; 2) establish recycling programs allowing for the reuse of excess of gun propellant; 3) burning of gun propellant over metal pans either carried out by the soliders or placed strategically in the field; 4) develop more efficient burning scenarios, such as possibly a field-portable reactor, and ; 5) collection and transport of excess propellant to be burned in a base incinerator. It is to be noted that solutions 1 and 2 would be ideal, for not only decreasing waste and enhancing efficiency, but also does not rely on the burning at all.

References

1. Ammunition for 105-mm Howitzer, Ammunition and Explosives Technical Information; C-74-315-H00; National Defence, 2004.
2. Ampleman, G.; Thiboutot, S.; Gagnon, A.; Marois, A. *Study of the Impacts of OB/OD Activity on Soils and Groundwater at the Destruction Area in CFAD Dundurn*; DREV-R-9827; Defence Research Establishment:,Valcartier, Quebec, December 1998.
3. Marois, A.; Gagnon, A.; Thiboutot, S.; Ampleman, G.; Bouchard, M. *Caractérisation des sols de surface et de la biomasse dans les secteurs d'entraînement*; TR 2004-206; Base des Forces canadiennes, Valcartier, Defence Research and Development Canada-Valcartier, October 2004.
4. Thiboutot, S.; Ampleman, G.; Marois, A.; Gagnon, A.; Bouchard, M.; Hewitt, A.; Jenkins, T.; Walsh, M.; Bjella, K.; Ramsey, C.; Ranney, T.A. *Environmental conditions of surface soils, CFB Gagetown training area: delineation of the presence of munitions related residues (Phase III, final report)*; TR 2004-205; Defence Research and Development Canada - Valcartier, October 2004.
5. Badger Army Ammunition Plant, Midwest Hazardous Substance Research Center Outreach Programs for Communities. http://www.egr.msu.edu/tosc/Summaries/BAAP.shtml.
6. Diaz, E.; Brochu, S.; Poulin, I.; Faucher, D.; Marois, A.; Gagnon, A. *Residual Dinitrotoluenes from Open Burning of Gun Propellant*; Defence Research and Development Canada – Valcartier, to be published.
7. *Ammunition for 155-mm Howitzer, Ammunition and Explosives Technical Information*; C-74-320-BAO; National Defence, 2006.
8. Diaz, E.; Gilbert, D.; Faucher, D.; Marois, A.; Gagnon, A. *Gun Propellant Residues Dispersed from Static Artillery Firings of LG1 Mark II and C3 105-mm Howitzers*; TR 2007-282; Defence Research and Development Canada – Valcartier, October 2008.
9. EPA Method 8330B. http://www.epa.gov/epawaste/hazard/testmethods/pdfs/8330b.pdf.
10. Pearson, J. S. *Modular Charge Artillery System*; Field Artillery, March-June 2004. http://sill-www.army.mil/FAMAG/2004/MAR_JUN_2004/PAGE55-56.pdf.
11. Thiboutot, S.; Ampleman, G.; Kervarec, M.; Cinq-Mars, A.; Gagnon, A.; Marois, A.; Poulin, I.; Boucher, F.; Lajoie, R.; Legault, K.; Withwell, S.; Sparks, T.; Eng, J.; Cartier, M.; Archambault, P. *Development of a Table for the Safe Burning of Excess Artillery Propellant Charge Bags*; unclassified, DRDC Valcartier TR 2010-254, December 2010.
12. Stratta, J.; Schneider, R.; Adrian, N. R.; Weber, R. A.; Donahue, B. A. *Alternatives to Open Burning/Open Detonation of Energetic Materials*; Technical Report 98/104; US Army Corps of Engineers Construction Engineering Research Laboratories (USACERL), August 1998. http://www.cecer.army.mil/techreports/klo_bod.ult/KLO_BOD.ULT.post.pdf.
13. Walsh, M. R.; Walsh, M. E.; Hewitt, A. D. Energetic residues from field disposal of gun propellants. *J. Hazard. Mater.* **2009**, *173*, 115–122.

Disclaimer

The material contained in this book has been compiled from sources believed to be reliable and to have expertise in the topic. It does not purport to cover all related issues, specify minimum legal standards, or represent the policy of the American Chemical Society (ACS). All warranties (both express and implied), guarantees, and representations as to the accuracy or sufficiency of the information contained herein are hereby disclaimed, and the ACS and its members assume no responsibility in connection herewith. Because of the rapidity with which the law changes and the many different laws to be found in various geographic areas, users of this book should consult pertinent local, state, and federal laws and regulations, and consult with legal counsel.

Editors' Biographies

Mark A. Chappell

Dr. Mark Chappell is a research physical scientist and leader of the Soil & Sediment Geochemistry Team at the US Army Engineer Research & Development Center. He holds a Ph.D. in soil science, with his research focusing on the solid-phase chemistry of natural systems. His research involves a number of projects investigating the solid-phase speciation of soil metals, explosives, humic organic carbon phases, and nanomaterial interactions in complex environmental systems. He is an expert in soil chemistry with various publications on the interaction, fate, and transport of contaminants in soil and sediments.

Cynthia L. Price

Cindy Price is a research physical scientist with the US Army Engineer Research & Development Center located in Vicksburg, MS. Research activities have included support for civil and military missions under the US Army Corps of Engineers and US Department of Defense for over 20 years; with a focus on contaminant mobilization from sediments and soils into air, surface water, ground water and aquatic organisms. Primary recent research activities are in the areas of fate and transport of munitions in soils and sediments; and in contaminated dredged materials assessment and management.

Robert D. George

Rob George is a senior chemist at SSC-Pacific in the Advanced Systems & Applied Sciences Division, and group leader for Detection, Sensors, and Systems Technology in the Environmental Sciences branch. His research interests are broadly focused on materials in the environment, including detection/sensing, paints/coatings, contaminant release, and environmental forensics. Prior to SSC-Pacific, he conducted research (optical materials/thin-films) at the Naval Research Laboratory as a National Research Council (NAS) post-doctoral appointee. He received a Ph.D. from Arizona State University performing cross-disciplinary research (organic/organometallic materials/chemical sensors) in the Departments of Chemistry & Biochemistry and Chemical, Bio, & Materials Engineering.

Subject Index

D

E

F

G

H

I

K

L

M

N

O

P

R

S

T

U

V

W

Z